# VI. INTERNATIONAL ICONTECH CONFERENCE ON INNOVATIVE SURVEYS IN POSITIVE SCIENCES

December 4-5, 2022 Rijeka, Croatia- Amadria Park Hotel Milenij

### **FULL TEXT BOOK**

Editor:

Prof. Dr. Gamze GENÇ

ISBN: 978-625-6380-59-2



# VI.INTERNATIONAL ICONTECH CONFERENCE ON INNOVATIVE SURVEYS IN POSITIVE SCIENCES

December 4-5, 2022 Rijeka, Croatia- Amadria Park Hotel Milenij

### **FULL TEXT BOOK**

### **Editor:**

Prof. Dr. Gamze GENÇ

All rights of this book belong to Iksad Global -2022©.

Without permission can't be duplicate or copied.

Authors of chapters are responsible both ethically and juridically.

Issued: 15.12.2022

WWW.ICONTECHSURVEYS.ORG

ISBN: 978-625-6380-59-2

### **CONFERENCE ID**

### TITLE OF CONGRESS

VI.International ICONTECH CONFEERENCE on Innovative Surveys in Positive Sciences

**DATE - PLACE** 

December 4-5, 2022 Rijeka, Croatia- Amadria Park Hotel Milenij

### **ORGANIZATION**

Institute of Economic Development and Social Researches



EDITED BY

Prof. Dr. Gamze GENÇ

### COORDINATOR

Alina AMANZHOLOVA

### **EVALUATION PROCESS**

All applications have undergone a double-blind peer review process

### **PARTICIPATING COUNTRIES**

Croatia, Türkiye, Azerbaijan, Saudi Arabia, Romania, Pakistan, Iraq, Algeria, Hungary, Poland, Brazil, India, Morocco, Serbia, Albania, South Africa, North Macedonia, Kosovo, China

TOTAL NUMBER OF PAPERS: 80
THE NUMBER OF PAPERS FROM TURKEY: 38
OTHER COUNTRIES: 42



### **HEAD OF CONFERENCE**

### Samir LADACI

Full Professor (Automatics & Control Engineering)

\* Chairman of the Scientific Committee of the E.E.A. Department,\* Head of the Doctoral Committee on Automatics,\* Member of the Administration Council of the Polytechnic School National Polytechnic School of

Council of the Polytechnic School National Polytechnic School of Constantine, Department of Electronic, Electrotechnic and Automatic, Constantine, Algeria

### **ORGANIZING COMMITTEE MEMBER(S)**

Dr. Muhammad Imran - Department of Food Science, Faculty of Life Sciences Government College University, Faisalabad, Punjab, Pakistan

Dr. Betul APAYDIN YILDIRIM - Ataturk University

Dr. Hülya ÇİÇEK - Gaziantep University

Dr. Shaukat Aref Mohammed - University of Zakho

Dr. Kenes JUSUPOV - M. Tinisbaev Kazakh Communication Academy

Dr. Guguli DUMBADZE- Batumi Shota Rustaveli State University

Dr. Almaz AHMETOV - Ministry of Health of Azerbaijan

Dr. Yıldırım İsmail TOSUN -Sirnak University

Dr. Seyithan SEYDOŞOĞLU -Siirt University

Dr. Nilgün ULUTAŞDEMİR- Gümüşhane University

Dr. D. Bria - Faculty of Sciences, UMP, Oujda, Morocco

Dr. Smaail RADI- Dean of Faculty of Sciences, UMP

M. El Malki - Faculty of Sciences, UMP, Oujda, Morocco

Dr. F. Jeffali - Superior School of Technology, UMP, Oujda, Morocco

Dr. Z. Tahri - National School of Applied Sciences, UAE, Al Hoceïma, Morocco

Dr. R. Benkaddour - Superior School of Technology, UMP, Oujda, Morocco

Dr. A. Khaled - National School of Applied Sciences, UAE, Al Hoceïma, Morocco

Dr. A. Nasser - Superior School of Technology, UMP, Oujda, Morocco

 $\label{eq:continuous} \mbox{Dr.\,A.\,Ghadban-National\,School\,of\,Applied\,Sciences,\,UAE,\,Al\,Hoce\"{i}ma,\,Morocco}$ 

Dr. Seyithan Seydosoglu - Siirt University, Turkey

Dr. Nilgun Ulutasdemir - Gumushane University, Turkey

Dr. Murat KIRANŞAN-Gumushane University, Turkey

F. Z. Elamri - Faculty of Sciences, UMP, Oujda, Morocco

Dr. Y. Ben-Ali - Faculty of Sciences, UMP, Oujda, Morocco

Dr. A. Bakdid - Faculty of Sciences, UMP, Oujda, Morocco

Dr. Elvan CAFEROV -ADPU



### **SCIENTIFIC & REVIEW COMMITTEE**

Dr. Melike (YÖNDER) ERTEM-İzmir Kâtip Çelebi University, Faculty of Health Sciences Dr. M.Meena - Department of Science and Humanities (Chemistry), R.M.K.Engineering College Kavaraipettai, India

Dr. ANURADHA THAKARE - Pimpri Chinchwad College of Engineering Pune, India

Dr. Nilay ÖZDEMİR-Ege University

Dr. Hülya ÇİÇEK - Gaziantep University

Dr. Adem AKPINAR - Uludağ University

Dr. Ahmet Hanifi ERTAŞ - Bursa Technical University

Dr. M. Özgün KORUKÇU- Bursa Uludağ University

Dr. Duygu İNCİ-Kocaeli University, Faculty of Applied Sciences

Dr. Emine GUL CANSU-ERGUN-Baskent University, Department of Electrical and Electronics Engineering,
Dr. Sevfi ŞEVİK-Hitit University

Dr. Betul APAYDIN YILDIRIM - Ataturk University

Dr. Fatih YILDIRIM - Ataturk University

Dr. Ramazan İLGÜN-Aksaray University, Veterinary Faculty

Dr. A. El Moussaouy - Regional Center for Education and Training, UMP, Oujda, Morocco

Dr. A. Kerkour El Miad - Superior School of Technology, UMP, Oujda, Morocco

Dr. M. El Ghorba - National School of Electricity and Mechanics, UH2, Cassablanca, Morocco

Dr. Mourad GHARBI - Faculty of Sciences, M5U, Rabat, Morocco

Dr. Kenes JUSUPOV - M. Tinisbaev Kazakh Communication Academy

Dr. Lille TANDIVALA- Shota Rustavelli State University

Dr. Guguli DUMBADZE- Batumi Shota Rustaveli State University

Dr. Maha Hamdan ALANAZI - Riyad King Abdulaziz Technology University

Dr. N.N. KERMANOVA - Al - Farabi Kazakh National University

Dr. Sudabe SALİIHOVA - Azerbaijan State University

Dr. Rovshan ALIYEV - Bakü State University

Dr. Avetül GELEN- Bursa Technical University

Dr. Muharrem Kemal ÖZFIRAT -Dokuz Eylül University

Dr. A.Vijayalakshmi - Asst. Professor, Science & Humanities (Chemistry), R.M.K. Engineering College

Dr. Mustafa Kemal BİLİCİ -Marmara University

Dr. Rahşan KOLUTEK -Nevşehir Hacı Bektaş Veli University

Dr. Hilal KILINÇ- Dokuz Eylül University

Dr. Esra LAKOT ALEMDAĞ -Recep Tayyip Erdoğan University

Dr. Özlem ÖZDEMİR -Gazi University

Dr. Alpay Tamer ERTÜRK- Kocaeli University

Dr. Gülden ELEYAN - Avrasya University

Dr. Derya ÜNLÜ - Bursa Technical University

Dr. Murat EYVAZ -Gebze Technical University



### **SCIENTIFIC & REVIEW COMMITTEE**

Dr. Cengiz MORDENİZ - Tekirdağ Namık Kemal University Dr. Aslı KÖSE- Gümüşhane University Dr. Neslihan AYDIN - Uludağ University Dr. Tülay ÖNCÜ ÖNER - Manisa Celal Bayar University Dr. Mert GULUM - Karadeniz Technical University

Dr. F. Tayeboun - Djillali Liabes University, Sidi-Bel-Abbes, Algeria

Dr. K. A. Meradi - Institute of Technology, University of Ain Temouchent, Algeria Dr. Muhammad Imran - Department of Food Science, Faculty of Life Sciences Government College University, Faisalabad, Punjab, Pakistan

Dr. Karim Sellami - Military Technological College Muscat, Sultanate of Oman

Dr. Adnane Benzirar - Faculty of Medicine and Pharmacy, UMP, Oujda, Morocco

Dr. Najib Abdeljaouad - Faculty of Medicine and Pharmacy, UMP, Oujda, Morocco

Dr. Madani Hamid - Faculty of Medicine and Pharmacy, UMP, Oujda, Morocco

Dr. H. BOUALI, Superior School of Technology, UMP, Oujda, Morocco

Dr. A. Kerkour El Miad - Faculty of Sciences, UMP, Oujda, Morocco

Dr. R. Malek - National School of Applied Sciences, UMP, Oujda, Morocco

Dr. J. Barkani - Multidisciplinary Faculty, TAZA, Morocco

Dr. I. Zorkani - Faculty of Sciences Dhar El Mahraz, SMBA University, Fez, Morocco

Dr. M. I. Sedra - Sciences and technologies Faculty, Errachidia, Morocco

Dr. F. Dimane - National School of Applied Sciences, UAE, Al Hoceïma, Morocco

Dr. B. Tidhaf - National School of Applied Sciences, UMP, Oujda, Morocco

Dr. Nilgun Ulutasdemir - Gumushane University, Turkey

Dr. M. Serhini - Faculty of Sciences, UMP, Oujda, Maroc

Dr. K. Ghoumid - National School of Applied Sciences, UMP, Oujda, Maroc

Dr. H. Bekkay - National School of Applied Sciences, UMP, Oujda, Maroc

Dr. Mustafa Kemal Bilici - Marmara University

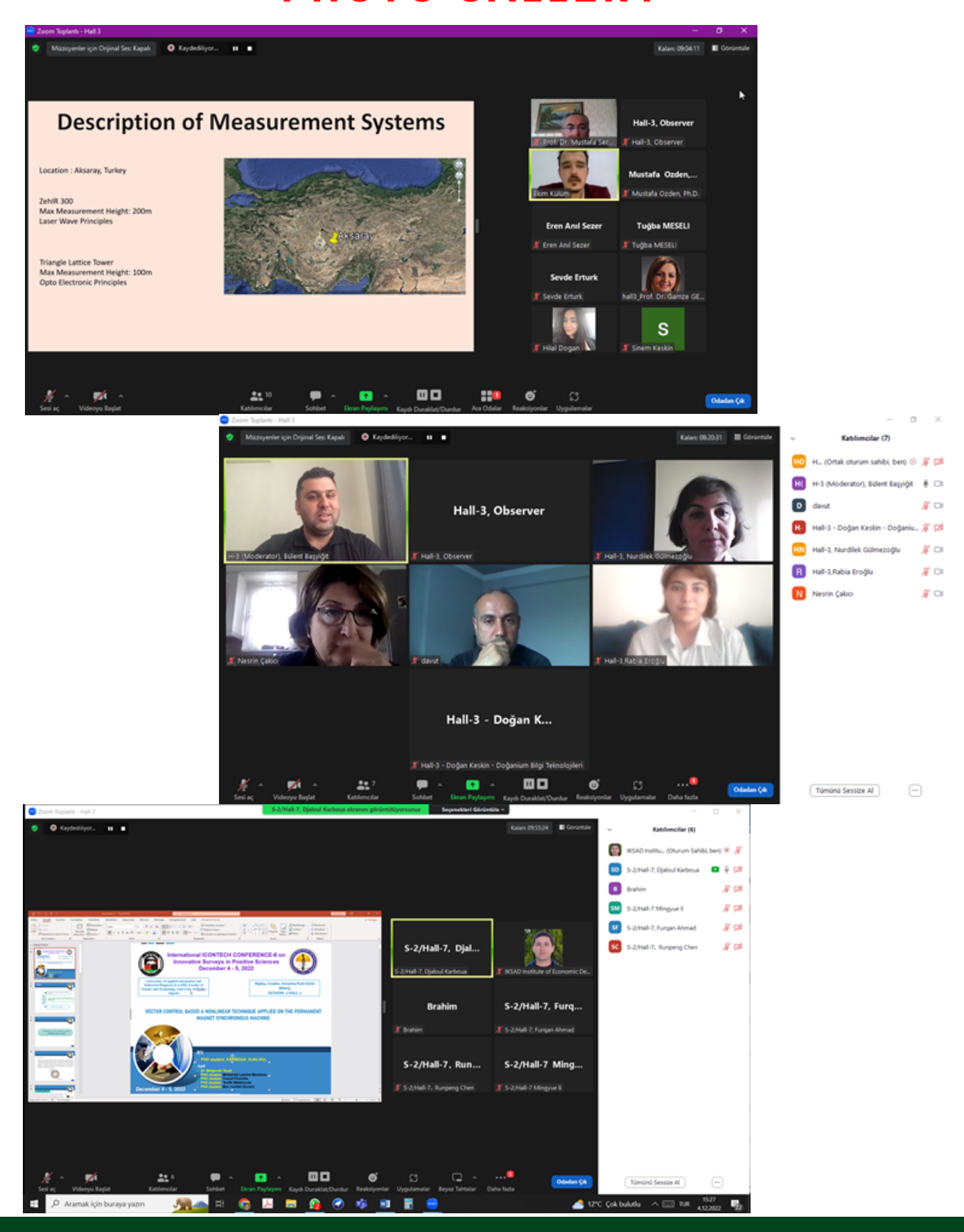
Dr. Mehmet Cemal Adiguzel - Ataturk University

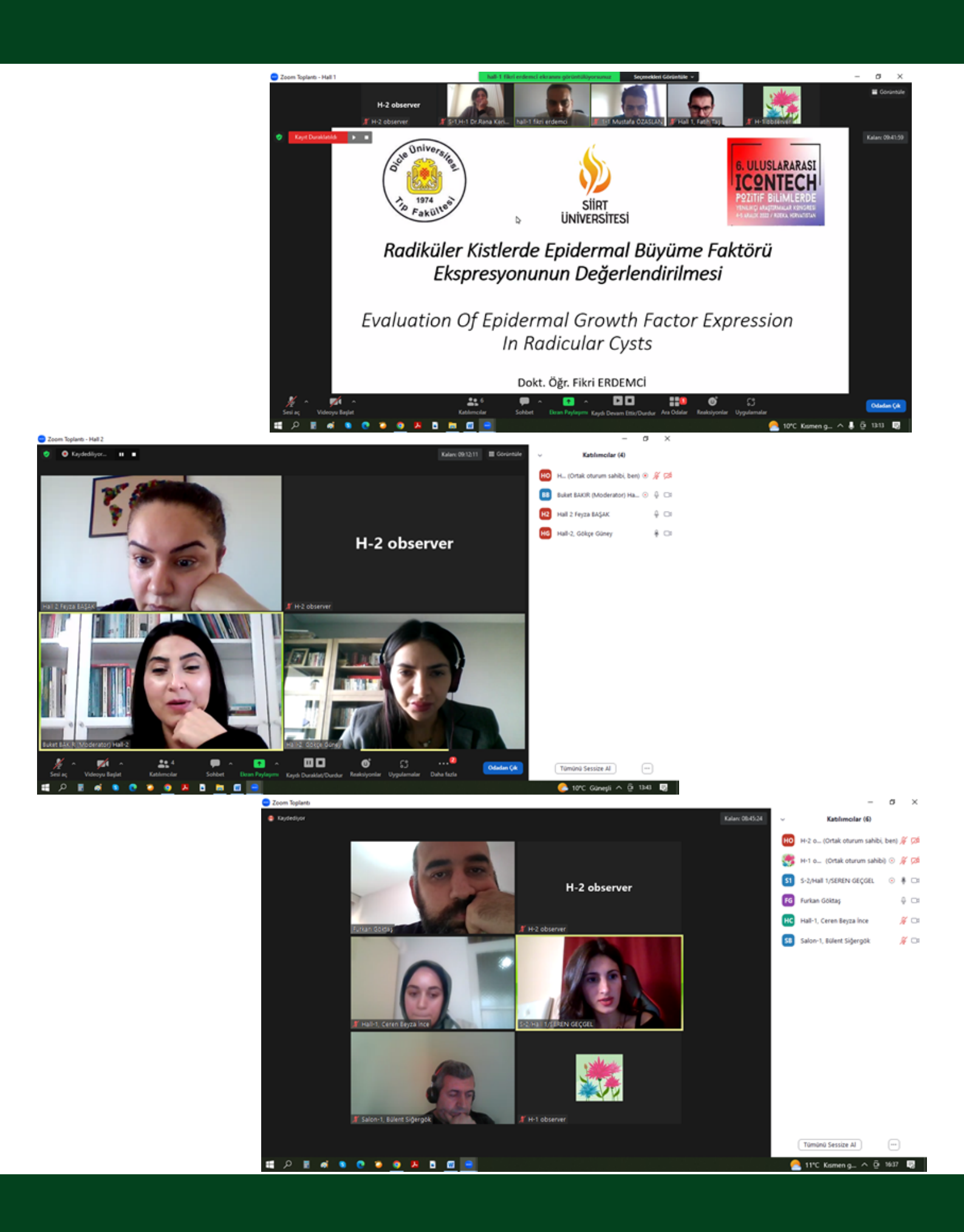
Dr. J. JASMINE HEPHZIPAH M.E. - Asst Professor in ECE Dept, R.M.K Engineering College, Chennai

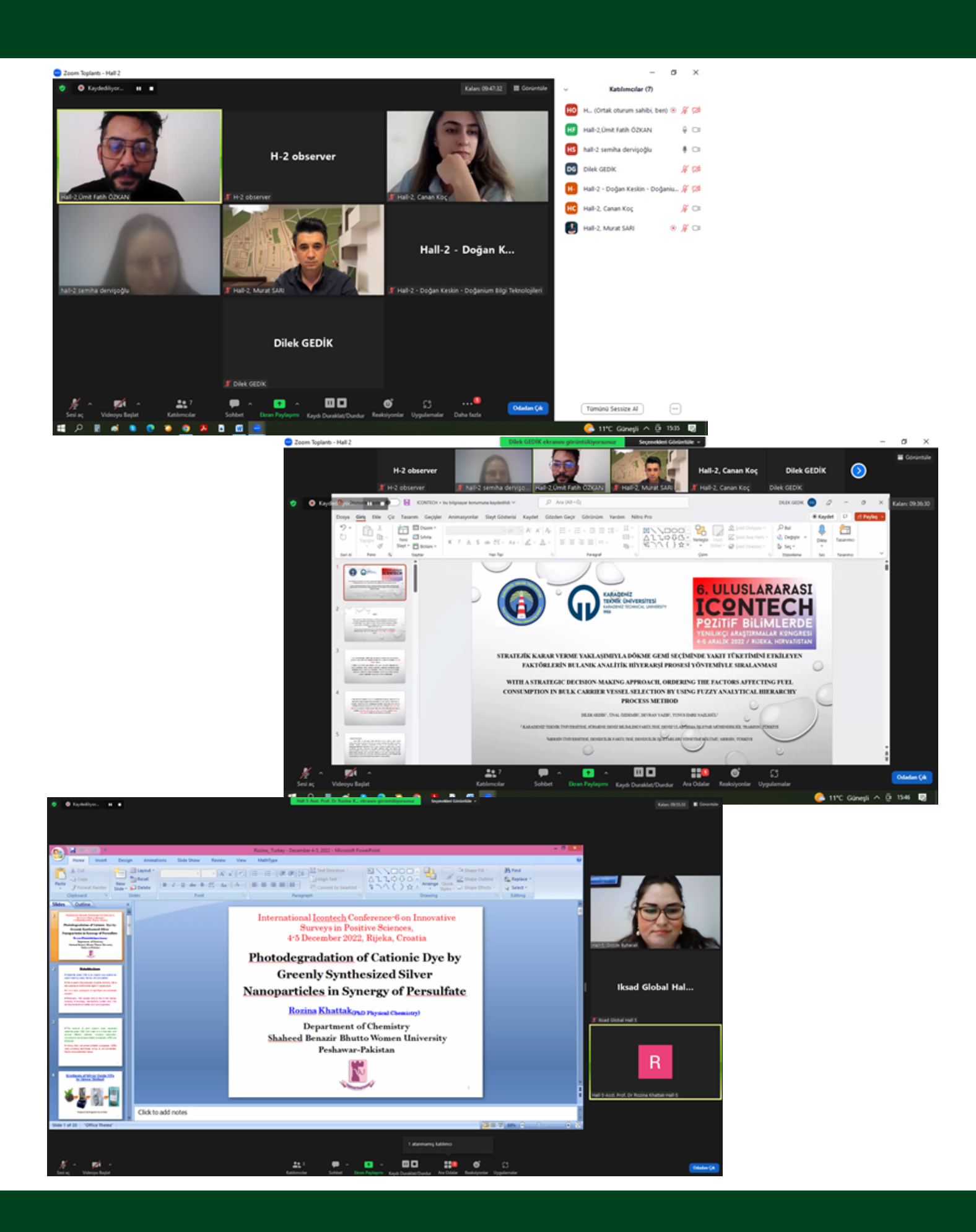
> Dr. Ghanshyam Barman - Uka Tarsadia University, India Dr. Kader DAĞCI KIRANŞAN -Ataturk University

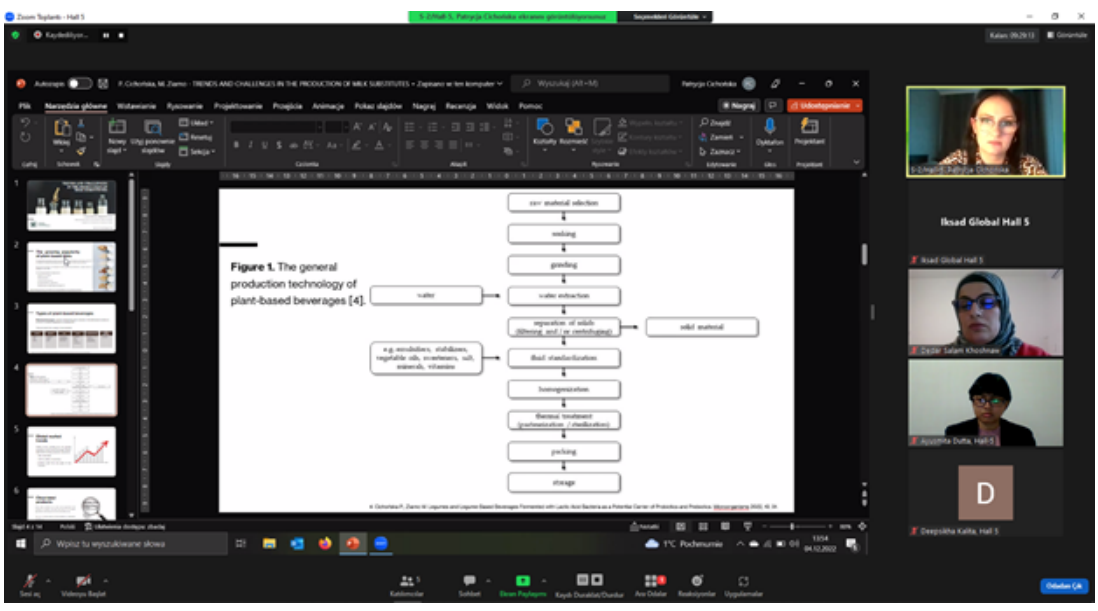
Dr. Muhammad Faisal - Director Ministry of Human Rights, Pakistan

### **PHOTO GALLERY**

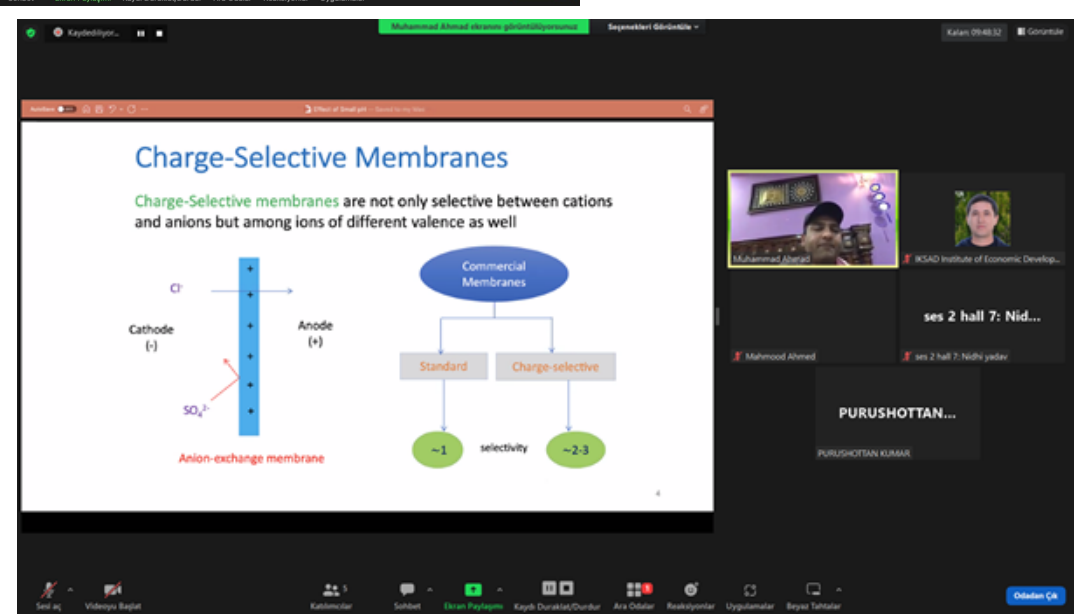
















# International ICONTECH CONFERENCE-6

on Innovative Surveys in Positive Sciences

December 4-5, 2022

Rijeka, Croatia- Amadria Park Hotel Milenij

# **CONGRESS PROGRAM**

**ONLINE PRESENTATIONS** 

Meeting ID: 851 3167 6152 Passcode: 060606

### **ZOOM LINK:**

https://us02web.zoom.us/j/85131676152?pwd=UlBNZ1RickxvcUNSUE9aZDJkcnpTUT09

### IMPORTANT, PLEASE READ CAREFULLY

- To be able to make a meeting online, login via https://zoom.us/join site, enter ID instead of "Meeting ID
- or Personal Link Name" and solidify the session.
- The presentation will have 15 minutes (including questions and answers).
- The Zoom application is free and no need to create an account.
- The Zoom application can be used without registration.
- The application works on tablets, phones and PCs.
- Speakers must be connected to the session 10 minutes before the presentation time.
- All congress participants can connect live and listen to all sessions.
- During the session, your camera should be turned on at least %70 of session period
- Moderator is responsible for the presentation and scientific discussion (questionanswer) section of the session.

### TECHNICAL INFORMATION

- Make sure your computer has a microphone and is working.
- You should be able to use screen sharing feature in Zoom.
- Attendance certificates will be sent to you as pdf at the end of the congress.
- Moderator is responsible for the presentation and scientific discussion (questionanswer) section of the session.

Before you login to Zoom please indicate your name surname and hall number, exp. Hall-1, Shahla Tahirgizi

### ÖNEMLİ, DİKKATLE OKUYUNUZ LÜTFEN

- ➤ Kongremizde Yazım Kurallarına uygun gönderilmiş ve bilim kurulundan geçen bildiriler icin online (video konferans sistemi üzerinden) sunum imkanı sağlanmıstır.
- Sunumlar için 15 dakika (soru ve cevaplar dahil) süre ayrılmıştır.
- Online sunum yapabilmek için https://zoom.us/join sitesi üzerinden giriş yaparak "Meeting ID or Personal Link Name" yerine ID numarasını girerek oturuma katılabilirsiniz.
- > Zoom uygulaması ücretsizdir ve hesap oluşturmaya gerek yoktur.
- Zoom uygulaması kaydolmadan kullanılabilir.
- Uygulama tablet, telefon ve PC'lerde çalışıyor.
- Her oturumdaki sunucular, sunum saatinden 10 dk öncesinde oturuma bağlanmış olmaları gerekmektedir.
- > Tüm kongre katılımcıları canlı bağlanarak tüm oturumları dinleyebilir.
- Moderatör oturumdaki sunum ve bilimsel tartışma (soru-cevap) kısmından sorumludur.

### **TEKNIK BILGILER**

- > Bilgisayarınızda mikrofon olduğuna ve çalıştığına emin olun.
- Zoom'da ekran paylaşma özelliğine kullanabilmelisiniz.
- Katılım belgeleri kongre sonunda tarafınıza pdf olarak gönderilecektir
- Kongre programında yer ve saat değişikliği gibi talepler dikkate alınmayacaktır

Zoom'a giriş yaparken önce lüffen adınızı, soyadınızı ve SALON numaranızı yazınız Örnek: Salon-1, Shahla Tahirgizi

### **PARTICIPANT COUNTRIES: (19)**

Croatia, Türkiye, Azerbaijan, Saudi Arabia, Romania, Pakistan, Iraq, Algeria, Hungary, Poland, Brazil, India, Morocco, Serbia, Albania, South Africa, North Macedonia, Kosovo, China

	Session 1	Session 2
Croatia	11:00-13:00	13:30-15:30
Turkiye	13:00-15:00	15:30-17:30
Azerbaijan	14:00-16:00	16:30-18:30
Saudi Arabia	13:00-15:00	15:30-17:30
Romania	12:00-14:00	14:30-16:30
Pakistan	15:00-17:00	17:30-19:30
Poland	11:00-13:00	13:30-15:30
India	15:30-17:30	18:00-20:00
Morocco	10:00-12:00	12:30-14:30
Albania	11:00-13:00	13:30-15:30
Iraq	13:00-15:00	15:30-17:30
Algeria	11:00-13:00	13:30-15:30
Hungary	11:00-13:00	13:30-15:30
Brazil	07:00-09:00	09:30-11:30
Serbia	11:00-13:00	13:30-15:30
South Africa	12:00-14:00	14:30-16:30
North Macedonia	11:00-13:00	13:30-15:30
Kosovo	11:00-13:00	13:30-15:30
China	18:00-20:00	20:30-22:30
France	11:00-13:00	13:30-15:30

# 04.12.2022

# Session-1 / Hall-1

Rijeka Time: 1100-1300

Ankara Time: 1300-1500

### HEAD OF SESSION: Assist. Prof. Dr. Fatih TAŞ

TOPIC TITLE	AUTHORS	AFFILIATION
CHEMICAL AND PHYSIOLOGICAL PROPERTIES SHOWN BY GOLD IN THE HUMAN ORGANISM	Dr. Kərimova Rəna Cabbar kızı Rzayeva Sürəyya Cabbar kızı Əzizova Əsmət Nizami kızı Bayramov Adil Allahyar oğlu Yusifova Mətanət Yusif kızı	Azerbaijan Medical University, Azerbaijan
LIVER DAMAGE, PHYSIOLOGICAL CHARACTERISTICS AND ITS RELATIONSHIP WITH THE ENDOCRINE SYSTEM	Dr. Kərimova Rəna Cabbar kızı Ağayeva Asiya Hacı kızı Həsənova Xumar Əliövsət kızı Cəfərova Zemfira İbrahim kızı Şahməmmədova Sevinc Osman kızı Dr. Məşədiyeva Bayramova Səbinə Ənvər kızı	Azerbaijan Medical University, Azerbaijan
EVALUATION OF EPIDERMAL GROWTH FACTOR EXPRESSION IN RADICULAR CYSTS	Fatih TAŞ Fırat AŞIR Fikri ERDEMCİ	Siirt University, Türkiye Dicle University, Türkiye
SUBACUTE SUBDURAL HEMATOM BLEEDING INTO ARACHNOID CYST: OUR CLINICAL RESULTS	Mustafa OZASLAN Sedat YASİN Necati UCLER	Gaziantep University, Türkiye Elazığ Şehir Hastanesi, Türkiye
THE EVALUATION OF LOCALIZATION, SURGICAL RESECTION AND RADIOTHERAPY RESULTS OF ATYPIC MENINGIOMAS	Mustafa OZASLAN Serdal ALBAYRAK Necati UCLER	Gaziantep University, Türkiye Elazığ Şehir Hastanesi, Türkiye
THE VALIDITY OF ESTIMATED HEART BEAT PARAMETERS ON ESTABLISHING EXERCISE INTENSITY IN HEALTHY MALES	Şevval Yurtoğlu Ahmet Ayyıldız Sermin Algül Oğuz Özçelik	Kastamonu University, Türkiye Van Yüzüncü Yıl University, Türkiye

# 04.12.2022

# Session-1 / Hall-2

Rijeka Time: 1100-1300

Ankara Time: 1300-1500

### **HEAD OF SESSION: Assoc. Prof. Buket BAKIR**

TOPIC TITLE	AUTHORS	AFFILIATION
THE EFFECTS OF APPLICATION OF HAWTHORN VINEGAR ON CD4 AND CD8 T LYMPHOCYTES EXPRESSION IN SPLEEN OF RATS	Assoc. Prof. Buket BAKIR Assoc. Prof. Nilay SEYİDOĞLU	Tekirdag Namik Kemal University, Türkiye
HISTOMORPHOMETRIC EVALUATION OF THE EFFECTS OF CAPSAICIN APPLICATION ON SMALL INTESTINE OF RATS	Assoc. Prof. Buket BAKIR Prof. Dr. Ebru KARADAĞ SARI	Tekirdag Namik Kemal University, Türkiye
COMPARISON OF GENERAL HISTOLOGICAL FEATURES IN TONGUE TISSUES OF PUPPY AND ADULT NEW ZEALAND RABBIT	Feyza BAŞAK Tansu KUŞAT Emine Ümran ÖRSÇELİK	Karabük University, Türkiye Kırıkkale University, Türkiye
ADVANCED TREATMENT OF SOME EMERGING MICROPOLLUTANTS BY PHOTOCATALYTIC AND MEMBRANE PROCESSES FROM RAW HOSPITAL WASTEWATER AND COST ANALYSIS	Gokce GUNEY Delia Teresa SPONZA	Dokuz Eylül University, Türkiye
PLIOCENE DEPOSITIONAL STAGES IN ERZURUM BASIN; AN EXAMPLE OF BASIN INVERSION. EASTERN ANATOLIA . TURKIYE	Mehmet Salih BAYRAKTUTAN	Ataturk University, Türkiye

# 04.12.2022

# Session-1 / Hall-3

Rijeka Time: 1100-1300

Ankara Time: 1300-1500

# HEAD OF SESSION: Assist. Prof. Dr. Bülent BAŞYİĞİT

TOPIC TITLE	AUTHORS	AFFILIATION
IMPACTS OF HUMIC ACID PRACTICES ON NITROGEN, PHOSPHORUS AND POTASSIUM UPTAKE OF BEANS IN SALINE CONDITIONS	Prof. Dr. Nurdilek GÜLMEZOĞLU İmren KUTLU	Eskişehir Osmangazi University, Türkiye
THE POINTS TO BE CONSIDERED IN THE PRESERVATIVE SOLUTION UPTAKE, PENETRATION, AND RETENTION DETERMINATION STUDIES BEFORE AND AFTER PERMEABILITY IMPROVEMENT PRETREATMENTS IN WOOD	Davut BAKIR	Artvin Çoruh University, Türkiye
INVESTIGATION OF ESBL AND CARBAPENEMASE POSITIVE ENTEROBACTERIACEAE STRAINS AND GENOTYPES IN MUSSELS CAUGHT IN THE ÇANAKKALE STRAIT	Nesrin ÇAKICI	Çanakkale Onsekiz Mart University, Türkiye
MICROBIOLOGICAL HAZARDS IN POULTRY	Nesrin ÇAKICI Rabia EROĞLU	Çanakkale Onsekiz Mart University, Türkiye
BENEFICIAL EFFECT OF MAILLARD CONJUGATION ON EMULSIFYING BEHAVIOR OF PEA PROTEIN	Bülent BAŞYİĞİT	Harran University, Türkiye

# 04.12.2022

# Session-1 / Hall-4

Rijeka Time: 1100-1300

Ankara Time: 1300-1500

# HEAD OF SESSION: Major Gheorghe Giurgiu

TOPIC TITLE	AUTHORS	AFFILIATION
NUTRACEUTICALS DENIPLANT IN THE NEUROPATHIC PAIN IN DOG WITH SPINAL CORD INJURY	Major Gheorghe Giurgiu, Prof. Dr. Manole Cojocaru	Deniplant-Aide Sante Medical Center, Biomedicine, Bucharest, Romania Titu Maiorescu University, Faculty of Medicine, Bucharest, Romania
IN VIVO TOXICITY OF CADMIUM CHLORIDE IN ALBINO RATS AND PROTECTIVE EFFECTS OF VITAMIN B1 AND NUTRIENTS HEMATOBIOCHEMICAL EFFECTS OF CADMIUM INTOXICATED ALBINO RATS WITH ZN, VITAMIN B1 AND NUTRIENTS	Shivani Yadav, D.K Chauhan	Chaudhary Charan Singh University, Meerut, Uttar Pradesh
EFFECTS OF THE COVID-19 PROCESS ON FARM ANIMAL HUSBANDRY AND NUTRITION	Ayşe ŞEN Kadir ERTEN	Tekirdag Namik Kemal University, Türkiye
EFFECTS OF TANIN ON RUMINANT ANIMAL BEHAVIORS	Ayşe ŞEN Kadir ERTEN	Tekirdag Namik Kemal University, Türkiye
ACUTE AND SUBACUTE TOXICITY ASSESSMENT MODEL OF FERULA GROWING IN NORTHERN MOROCCO	NOUIOURA Ghizlane, TOURABI Maryem, LYOUSSI Badiaa, DERWICH EI houssine	Université sidi Mohammed ben Abdellah, Fès, Maroc.
IMPORTANCE AND APPLICATIONS OF ENGINEERING PROPERTIES IN FOOD INDUSTRIES	Simple Sharma, Barinderjit Singh	I. K. Gujral Punjab Technical University, Jalandhar - Kapurthala Highway, Punjab 144603, India

# 04.12.2022

# Session-1 / Hall-5

Rijeka Time: 1100-1300

Ankara Time: 1300-1500

### HEAD OF SESSION: Assist. Prof. Dr. Rozina Khattak

TOPIC TITLE	AUTHORS	AFFILIATION
PHOTODEGRADATION OF CATIONIC DYE BY GREENLY SYNTHESIZED SILVER NANOPARTICLES IN SYNERGY OF PERSULFATE	Assist. Prof. Dr. Rozina Khattak	Department of Chemistry, Shaheed Benazir Bhutto Women University, Pakistan
PHYTOCHEMICAL AND ANTIOXIDANT POTENCIAL OF PARKIA BIGLOBOSA HUSK METHANOL EXTRACT IN ALBINO RATS	Jude Nwaoga, Sanusi Ahmad Jega, Shafiu Shehu Anka, Ibrahim Abdullahi	Kebbi State University of Science and Technology Aleiro, Kebbi State, Nigeria. Usmanu Danfodiyo University Sokoto, Nigeria. Federal Polytechnic Kaura Namoda, Zamfara State, Nigeria
FAILURE ANALYSIS OF ACRYLONITRILE BUTADIENE STYRENE (ABS) MATERIALS AND DAMAGE MODELING BY FRACTURE	Hassan Bouhsiss, A. En-naji, A. Wahid , S. Lasfar, Abdekarim Kartouni, Mohamed El Ghorba	Hassan II University of Casablanca, Casablanca, Morocco
STRUCTURE-BASED DRUG REPURPOSING TO INHIBIT THE DNA GYRASE OF Mycobacterium tuberculosis	Balasubramani G L, Rinky Rajput, Manish Gupta, Pradeep Dahiya, Jitendra K Thakur, Rakesh Bhatnagar, Abhinav Grover	Jawaharlal Nehru University, New Delhi National Institute of Plant Genome Research, New Delhi Banaras Hindu University, Banaras, India
THE PREVALENCE OF URINARY TRACT INFECTION STRAINS AMONG PREGNANT WOMAN WITH Escherichia coli IN LAGOS STATE, NIGERIA	OLAITAN Abiodun Josiah, BAJULAYE Albert Ajayi, Ass Prof. BANJO Temitope Temitayo,, OLAJUWON Mistura Ojuolape, AKINOLA Christiana Boluwatife	Lagos State University, Ojo Lagos State. Lagos State University of Education Oto/Ijanikin Lagos State. Crawford University Igbesa, Ogun State. Louisiana State University, United State of America.
INVESTIGATION OF BURST STRENGTH, ABRASION RESISTANCE AND PILLING RESISTANCE PROPERTIES OF KNITTED FABRICS PRODUCED FROM 100% CARDED COTTON RING AND PROSPIN® YARNS	Gözde BUHARALI Sunay ÖMEROĞLU	Bartin University, Ulus Vocational School, Department of Textile, Clothing, Footwear and Leather Bursa Uludag University, Engineering Faculty, Department of Textile Engineering

# 04.12.2022

# Session-1 / Hall-6

Rijeka Time: 1100-1300

Ankara Time: 1300-1500

### **HEAD OF SESSION: Dr. Mahmood Ahmed**

TOPIC TITLE	AUTHORS	AFFILIATION
ANTIUREASE EFFECT OF BENZENESULFONOHYDRAZIDES, IN VITRO AND IN SILICO STUDIES	Dr. Mahmood Ahmed	University of Education, Lahore, Pakistan
EFFECT OF SMALL PH ALTERATIONS ON THE TRANSPORTATION PROPERTIES OF IONS AND LIMITING CURRENTS THROUGH POLYELECTROLYTE MULTILAYERS DEPOSITED ON MEMBRANES	Muhammad Ahmad	University of Education, Township, Lahore, Pakistan
PRESCRIBING PATTERN OF ANTIBACTERIAL AGENTS IN ADULT POPULATION: ASSESSMENT OF EFFICACY AND HARMS ASSOCIATED WITH IRRATIONAL PRACTICES	Dr. Huma Ali, Dr. Anum Tariq	Institute of Pharmaceutical Sciences Jinnah Sindh Medical University Karachi
DYE REMOVAL BY WASTE-DERIVED SULFONATED POLYSTYRENE	Mohammed el amine ZENNAKI, Lahcene TENNOUGA, Brahim BOURAS, Kouider MEDJAHED	Tlemcen University, Algeria
ASSESSEEMNT OF PHYSICO-CHEMICAL GROUNDWATER QUALITY OF THE GHISS- NEKOR AQUIFER (CENTRAL RIF, MOROCCO)	Saida Assouik Fouad Mourabit M'hamed Ahari	Abdelmalek Essaadi university, Faculty of Sciences and Technologies of Al Hoceima, Department of chimestry, Al Hoceima, Morocco
IN SILICO EVALUATION OF THE ANTIMALARIAL POTENTIAL OF THE PHYTOCONSTITUENTS OF THE AZADIRACHTA INDICA PLANT	Ekundayo T. AREH, Olubunmi ATOLANI, Learnmore KAMBIZI	Confluence University of Science and Technology, Nigeria University of Ilorin, Nigeria Cape Peninsula University of Technology, South Africa

# 04.12.2022

# Session-2 / Hall-1

Rijeka Time: 13<sup>30</sup>-15<sup>30</sup>

Ankara Time: 15<sup>30</sup>-17<sup>30</sup>

HEAD OF SESSION: Seren GEÇGEL

TOPIC TITLE	AUTHORS	AFFILIATION
ECONOMIC ANALYSIS OF SOLAR POWER PLANT FOR MERSIN PROVINCE	Seren GEÇGEL Fatih ÜNAL	Mersin University, Türkiye
WALLETGATE: A SERVICE-BASED OPEN WALLET APPROACH	Semih MUŞABAK Zeynep Nur SANDIKCI Elçin YILMAZ Ediz ŞAYKOL	Sipay Elektronik Para ve Ödeme Hizmetleri A.Ş. Beykent University, Türkiye
MAKING PROPELL SPEED CONTROL OF THE DRON DESIGNED IN SOLIDWORKS IN V-REP ROBOTIC SIMULATOR ENVIRONMENT WITH CODES PREPARED IN MATLAB	Bülent SİĞERGÖK Mehmet ÇAVAŞ	Fırat University, Türkiye
EFFECTS OF SODIUM HYDROXIDE ON THE UNCONFINED COMPRESSIVE STRENGTH OF CLAY-SAND SOILS	Tacettin GEÇKİL Özge Nur ÇETKİN Ceren Beyza İNCE	Inonu University, Türkiye
INVESTIGATION OF THE USAGE OF FERROCHROME SLAG AS FILLERS IN BITUMINOUS HOT MIXTURES	Tacettin GEÇKİL Sena KOÇ Ceren Beyza İNCE	Inonu University, Türkiye
MAXIMUM LOSS AND CONDITIONAL EXPECTED VALUE ANALYSES FOR THE MULTIVARIATE QUADRATIC QUALITY LOSS FUNCTION	Furkan GÖKTAŞ	Karabuk University, Türkiye
INTERVAL VALUED MEAN -VARIANCE ANALYSIS: AN APPLICATION ON BIST 30 HOLDING STOCKS	Furkan GÖKTAŞ	Karabuk University, Türkiye

# 04.12.2022

# Session-2 / Hall-2

Rijeka Time: 13<sup>30</sup>-15<sup>30</sup>

Ankara Time: 15<sup>30</sup>-17<sup>30</sup>

# HEAD OF SESSION: Ümit Fatih ÖZKAN

TOPIC TITLE	AUTHORS	AFFILIATION
REVIEW OF EVALUATION METRICS FOR GENERATIVE ADVERSARIAL NETWORKS	Canan KOÇ Fatih ÖZYURT	Firat University, Türkiye
AN OPTIMIZATION-BASED VIDEO STABILIZATION APPROACH	Semiha Dervişoğlu Mehmet Sarıgül Levent Karacan	Iskenrun Technical University, Türkiye
EVALUATION OF THE IMPACT OF THE CORONAVIRUS (COVID-19) PANDEMIC ON THE WORKING CONDITIONS OF COMPUTER ENGINEERS IN TURKIYE	Murat Sarı Ümit Fatih ÖZKAN Doğan Ömer KESKİN	Kütahya Dumlupınar University, Türkiye Computer Engineer, Doğanium Technology, Gebze, Kocaeli, Türkiye
WITH A STRATEGIC DECISION-MAKING APPROACH, ORDERING THE FACTORS AFFECTING FUEL CONSUMPTION IN BULK CARRIER VESSEL SELECTION BY USING FUZZY ANALYTICAL HIERARCHY PROCESS METHOD	Dilek Gedik Ünal Özdemir Devran Yazır Yunus Emre Nazlıgül	Karadeniz Teknik University, Türkiye Mersin University, Türkiye
AN EXAMPLE OF LITERATURE REVIEW WITH NATURAL LANGUAGE PROCESSING (NLP) TECHNIQUES ON THE USE OF GAMIFICATION METHODOLOGY IN MARITIME EDUCATION	Emin Serkan ERDÖNMEZ Cenk ŞAKAR	Dokuz Eylül University, Türkiye

# 04.12.2022

# Session-2 / Hall-3

Rijeka Time: 13<sup>30</sup>-15<sup>30</sup>

Ankara Time: 15<sup>30</sup>-17<sup>30</sup>

# HEAD OF SESSION: Dr. Mustafa Serdar GENÇ

TOPIC TITLE	AUTHORS	AFFILIATION
TRANSITION MODELLING	Mustafa Serdar GENÇ	Erciyes University, Türkiye
FSI ANALYSIS OF CARBON REINFORCED RECYCLABLE COMPOSITE WIND TURBINE BLADE	Eren Anıl SEZER, Sinem KESKİN, Mustafa Serdar GENÇ, Berkay AYDOĞAN	Erciyes University, Türkiye
FLOW CHARACTERISTICS ON NACA2415 AIRFOIL AT LOW REYNOLDS NUMBER	Mustafa ÖZDEN, Mustafa Serdar GENÇ, Halil Hakan AÇIKEL, Kemal KOCA	Erciyes University, Türkiye
NUMERICAL ANALYSIS OF BICYCLE HELMET	Zeynel Turan, Sinem KESKİN, Halil Hakan AÇIKEL	Erciyes University, Türkiye
CASE STUDY ON THE EVALUATION OF WIND MEASUREMENTS PERFORMED BY LIDAR AND CUP ANEMOMETER	Ekim KÜLÜM, Mustafa Serdar GENÇ	Erciyes University, Türkiye
EVALUATION OF GREENGROCER WASTES IN KAYSERI FOR BIOGAS PRODUCTION	Gamze GENÇ, Hatice Büşra PEKER, Hilal DOĞAN	Erciyes University, Türkiye
EXPERIMENTAL STUDY ON THE EFFECT OF GRAPHENE IN FLAT-PLATE COLLECTORS	Gamze GENÇ, Rumeysa URAL, Merve ATİK, Hilal DOĞAN	Erciyes University, Türkiye

# 04.12.2022

# Session-2 / Hall-4

Rijeka Time: 13<sup>30</sup>-15<sup>30</sup>

Ankara Time: 15<sup>30</sup>-17<sup>30</sup>

### HEAD OF SESSION: Dr. Ouail MJAHED

TOPIC TITLE	AUTHORS	AFFILIATION
NEW DENIAL OF SERVICE ATTACKS DETECTION APPROACH USING HYBRIDIZED NEURAL NETWORKS AND BALANCED DATASET	Ouail MJAHED Salah EL HADAJ El Mahdi EL GUARMAH Soukaina MJAHED	Faculty of Sciences and Technology, Department of Computer Sciences, L2IS, Marrakech, Morocco.
CLASSIFICATION OF CHEST X-RAY IMAGES OF LUNG DISEASES USING DEEP CONVOLUTIONAL NEURAL NETWORK	Joy Oluwabukola OLAYIWOLA Joke A. BADEJO Kikelomo Adetola Omotoye Jamiu Rotimi OLASINA	Covenant University, College of Engineering, Department of Electrical and Information Engineering, Ota, Nigeria
VISUALIZING THE WORLD'S HAPPINESS ACROSS THE WORLD AND ANALYZING ITS CONTRIBUTING FACTORS	Edona Krasniqi Bashkim Çerkini Dhuratë Hyseni	South East European University, Tetova, North Macedonia University of Applied Sciences in Ferizaj, Ferizaj, Kosovo University of Prishtina, Prishtina, Kosovo
COMPARISON BETWEEN PROFESSIONAL 3D SCANNING AND FREE SCANNING	Marigona Bajrami Bashkim Çerkini Fakije Zejnullahu	University of Applied Sciences in Ferizaj, Ferizaj, Kosovo
DESIGNED AND IMPLEMENTATION OF MAJOR NIGERIAN LANGUAGES TRANSLATION MOBILE APP, USING THE DEEP-TRANSLATE APPROACH	OLASINA Jamiu Rotimi AFUWAPE Oluwabukola Dorcas	Federal Polytechnic Ilaro, Nigeria
AN OVERVIEW OF FACE RECOGNITION METHODS	Abderrahmane Aqachtoul Karam Khaoula El mejdi Asma Youssef Ait khouya	Moulay Ismail University, Morocco
THE PROMISE AND LIMITATIONS OF ALGORITHMS IN ARTIFICIAL INTELLIGENCE FOR HEALTHCARE	Dr. Ritu	Prof NDIM, Delhi

# 04.12.2022

# Session-2 / Hall-5

Rijeka Time: 13<sup>30</sup>-15<sup>30</sup>

Ankara Time: 15<sup>30</sup>-17<sup>30</sup>

### HEAD OF SESSION: dr Ljiljana Simonović Grujić

TOPIC TITLE	AUTHORS	AFFILIATION
RELATION BETWEEN MOTIVATION AND PERFORMANCE AT NURSES OF SHKODER	Dr. Irena Shala, Dr. Kilda Gusha, Elizabeta Koçeku	University of Shkodra "Luigj Gurakuqi", Shkodra
HEALTH DISTRICT GOVERNANCE AND POWER RELATIONS IN BURKINA FASO	Issa Sombié, Ph D	Institut des Sciences des Sociétés- CNRST/Burkina Faso
USING OF GREEN SPACES IN HEALTHCARE FACILITIES AND ITS IMPACT ON HUMAN HEALTH	Parween Karim Dedar S. Khoshnaw Zana F. Ali	Consultant Architect, Directorate of Health – Erbil, Kurdistan Region, Iraq University of Pécs, Boszorkány u. 2, 7624 Pecs, Hungary
A QUALITATIVE STUDY ON THE EFFECTS OF MINDFULNESS ON PSYCHOLOGICAL WELL- BEING	Ayusmita Dutta Deepsikha Kalita, Dr. Suantak Demkhosei Vaiphei	Assam Downtown University, Guwahati
SCHOOL ACHIEVEMENT AND LEARNING DIFFICULTIES OF ADOLESCENTS FROM VIOLENT FAMILIES	dr Ljiljana Simonović Grujić	Bejgrade, Srbija
TRENDS AND CHALLENGES IN THE PRODUCTION OF MILK SUBSTITUTES	Patrycja Cichońska, Małgorzata Ziarno	Warsaw University of Life Sciences (WULS-SGGW), Institute of Food Science, Department of Food Technology and Assessment, Warsaw, Poland

# 04.12.2022

# Session-2 / Hall-6

Rijeka Time: 13<sup>30</sup>-15<sup>30</sup>

Ankara Time: 15<sup>30</sup>-17<sup>30</sup>

# HEAD OF SESSION: Dr. Raja Mohammad LATIF

TOPIC TITLE	AUTHORS	AFFILIATION
MODELLING THE PREDICTION OF NIGERIAN INSURANCES DATA	Ogundeji, A.A,James, Tolulope. O, Onwuka G.I, Babyemi, A.W, B. Shehu, SU Okeleke	Department of Mathematics Kebbi State University of Science and Technology, Aliero, Nigeria
(r*g*)**-MAPPINGS IN TOPOLOGICAL SPACES	Dr. Raja Mohammad LATIF	Prince Mohammad Bin Fahd University, Kingdom of Saudi Arabia
ANALYSIS OF A NEW THZ GRAPHENE STRUCTURE WITH ELECTROMAGNETICALLY INDUCED TRANSPARENCY	VICTOR DMITRIEV GERALDO MELO İZAİAS GONÇALVES	Federal University of Pará, Department of Electrical Engineering, Belém, Brazil
α(gg*)*-COMPACTNESS IN TOPOLOGICAL SPACES	Dr. Raja Mohammad LATIF	Prince Mohammad Bin Fahd University, Kingdom of Saudi Arabia
A NEW METHOD OF SIMPLIFIED JOHNSON COOK MODEL PARAMETER OPTIMIZATION FOR DP600 AND DP800 STEELS	Labinot Topilla, Serkan Toros, Habip Gökay Korkmaz	UBT – Higher Education Institution, Mechatronics Engineering , 10000, Prishtinë, Kosovo. Nigde Omer Halisdemir University, Mechanical Engineering Department, 51245, Nigde, Turkey
ANALOG LOWPASS FILTER DESIGN USING PASCAL POLYNOMIALS	Assist. Prof. Dr. Atilla Uygur	Gebze Technical University, Engineering Faculty, Electronics Department
DESIGN NEW CYCLOHEXANE-1,3-DIONE DERIVATIVES AS ANTI-NSCLC CANCER AGENTS USING QSAR AND DOCKING STUDIES	Khaoula Mkhayar, Rachid Haloui, Ossama Daoui, Souad Elkhattabi, Samir Chtita, Kaouakeb El khattabi	Sidi Mohamed Ben Abdellah-Fez University, Fez, Morocco. Hassan II University of Casablanca, Casablanca, Morocco
IDENTIFICATION OF SOLANUM NIGRUM (LEAVES EXTRACT) PHENOLIC COMPOUNDS, THEIR EFFECTS ON BEHAVIOR AND BLOOD BIOCHEMISTRY OF ROTENONE INDUCED PARKINSON'S RAT MODEL	Farzana Iftikhar, Shazia Perveen, Sumaira Kanwal, Khawar Ali Shahzad	The Women University Multan, Punjab, Pakistan,61000. Comsats University Islamabad, Punjab, Sahiwal Campus, 57000. Islamia University Bahawalpur. Punjab Pakistan.

# 04.12.2022

# Session-2 / Hall-7

Rijeka Time: 13<sup>30</sup>-15<sup>30</sup>

Ankara Time: 15<sup>30</sup>-17<sup>30</sup>

# HEAD OF SESSION: Runpeng Chen

TOPIC TITLE	AUTHORS	AFFILIATION
BIOLOGICAL SCREENING AND MOLECULAR DOCKING STUDIES OF SULPHUR CONTAINING HETEROCYCLES FOR THE INHIBITION OF $\alpha$ -GLUCOSIDASE ENZYME	Furqan Ahmad Saddique, Matloob Ahmad	Department of Chemistry, Government College University, Faisalabad, Pakistan.
STANDARD METHODS FOR THE EXAMINATION OF WATER AND WASTE WATER AND PRESENT WORK IN SUR SAROVAR BIRD SANCTUARY IN KEETHAM LAKE AGRA UTTAR PRADESH INDIA	Nidhi Yadav, Dr. Vishwakant Gupta	Agra Dr. Bhimrao Ambedkar University, Agra.
VECTOR CONTROL BASED A NONLINEAR TECHNIQUE APPLIED ON THE PERMANENT MAGNET SYNCHRONOUS MACHINE	Djaloul Karboua, Belgacem Toual, Mohamed Lamine Benaissa, Youcef Chouiha, Toufik Mebkhouta, Ben ouadeh Douara	Laboratory of Applied automation and Industrial Diagnosis (LAADI), Algeria Laboratory of Electrical Engineering Biskra (LGEB), Algeria
MAGNETICALLY RECOVERABLE AND HIGHLY EFFICIENT SUN-LIGHT-ACTIVE Clay/CN/M/AgW NANOCOMPOSITES FOR PHOTOCATALYTIC DEGRADATIONS OF GM	Brahim Ennasraoui, Hamza Ighnih, Redouane Haounati, Hassan Ouachtak, Naima Hafid, Amane Jada, Abdelaziz Ait Addi	Ibn Zohr University, Agadir, Morocco. Centre Régional des Métiers de l'Education et de la Formation Souss Massa, Morocco Université de Haute Alsace (UHA), F- 68100 Mulhouse, France
THE PATHOGENESIS AND RISK FACTORS OF LUNG INJURY IN SEVERE ACUTE PANCREATITIS: A SYSTEMATIC REVIEW AND META-ANALYSIS	Runpeng Chen, Dongyang Wang, Qinghua Wang	School of Nursing, Binzhou Medical University, Yantai, China
PREVALENCE AND FACTORS ASSOCIATED WITH WORKPLACE VIOLENCE AMONG NURSING STUDENTS: A SYSTEMATIC REVIEW AND META-ANALYSIS	Mingyue Li, Dongyang Wang, Qinghua Wang	School of Nursing, Binzhou Medical University, Yantai, China
EFFECT OF CORNCOB ASH AS A PARTIAL REPLACEMENT OF CEMENT ON MECHANICAL PROPERTIES OF FIBROUS CONCRETE	Humaira Kanwal, Muhammad Irfan, Muhammad Asim, Muhammad Ahsan, Tayyaba Latif Mughal, Muhammad Tahir, Amna Mahmood, Sadia Mughal, Adil sultan	School of Nursing, Binzhou Medical University, Yantai, China

# **CONTENT**

CONGRESS ID	I
ORGANIZING & SCIENTIFIC COMMITTEE	II
PROGRAM	III
PHOTO GALLERY	IV
ABSTRACTS	V

Author	Title	No
Eren Anıl SEZER Sinem KESKİN Mustafa Serdar GENÇ Berkay AYDOĞAN	FSI ANALYSIS OF CARBON REINFORCED RECYCLABLE COMPOSITE WIND TURBINE BLADE	1
Ekim KÜLÜM Mustafa Serdar GENÇ	CASE STUDY ON THE EVALUATION OF WIND MEASUREMENTS PERFORMED BY LIDAR AND CUP ANEMOMETER	10
Atilla UYGUR	ANALOG LOWPASS FILTER DESIGN USING PASCAL POLYNOMIALS	20
Canan KOÇ Fatih ÖZYURT	REVIEW OF EVALUATION METRICS FOR GENERATIVE ADVERSARIAL NETWORKS	25
Raja MOHAMMAD LATIF	α(gg*)*-COMPACTNESS IN TOPOLOGICAL SPACES	31
Raja MOHAMMAD LATIF	(r*g)** -MAPPINGS IN TOPOLOGICAL SPACES	53
Tacettin GEÇKİL Sena KOÇ Ceren Beyza İNCE	INVESTIGATION OF THE USAGE OF FERROCHROME SLAG AS FILLERS IN BITUMINOUS HOT MIXTURES	76
Labinot TOPILLA Serkan TOROS Habip Gökay KORKMAZ	A NEW METHOD OF SIMPLIFIED JOHNSON COOK MODEL PARAMETER OPTIMIZATION FOR DP600 AND DP800 STEELS	85
Nurdilek GÜLMEZOĞLU İmren KUTLU	IMPACTS OF HUMIC ACID PRACTICES ON NITROGEN, PHOSPHORUS AND POTASSIUM UPTAKE OF BEANS IN SALINE CONDITIONS	92
Gözde BUHARALI Sunay ÖMEROĞLU	INVESTIGATION OF BURST STRENGTH, ABRASION RESISTANCE AND PILLING RESISTANCE PROPERTIES OF KNITTED FABRICS PRODUCED FROM 100% CARDED COTTON RING AND PROSPIN® YARNS	97
Gokce Pehlivaner Guney Delia Teresa Sponza	ADVANCED TREATMENT OF SOME EMERGING MICROPOLLUTANTS BY PHOTOCATALYTIC AND MEMBRANE PROCESSES FROM RAW HOSPITAL WASTEWATER AND COST ANALYSIS	107
Furkan GÖKTAŞ	MAXIMUM LOSS AND CONDITIONAL EXPECTED VALUE ANALYSES FOR THE MULTIVARIATE QUADRATIC QUALITY LOSS FUNCTION	117
Furkan GÖKTAŞ	INTERVAL VALUED MEAN – VARIANCE ANALYSIS: AN APPLICATION ON BIST 30 HOLDING STOCKS	122

Fatih TAŞ Firat AŞİR Firat NALİNE İNFESINE OF APPLICATION OF FIRAT FIRAT FOR MERSÎN PROVÎNCE  THE EFFECTS OF APPLICATION OF HAWTHORN VÎNEĞAR ON CD4 AND CD8 T LYMPHOCYTES EXPRESSION IN SPLEEN OF RATS
Özge Nur ÇETKİN Ceren Beyza İNCE         UNCONFINED COMPRESSIVE STRENGTH OF CLAY-SAND SOILS         134           Ouail MJAHED Salah EL HADAJ El Mahdi EL GUARMAH Soukaina MJAHED         NEW DENIAL OF SERVICE ATTACKS DETECTION APPROACH USING HYBRIDIZED NEURAL NETWORKS AND BALANCED         141           Semiha DERVİŞOĞLU Mehmet SARIĞÜL Levent KARACAN         AN OPTIMIZATION-BASED VIDEO STABILIZATION APPROACH         145           Dilek GEDİK Ünal ÖZDEMİR Devran YAZIR Yunus Emre NAZLIĞÜL         WITH A STRATEĞIC DECISION-MAKING APPROACH, ORDERING THE FACTORS AFFECTING FUEL CONSUMPTION IN BULK CARRIER VESSEL SELECTION BY USING FUZZY ANALYTICAL HIERARCHY PROCESS METHOD         150           Emin Serkan ERDÖNMEZ Cenk ŞAKAR         AN EXAMPLE OF LITERATURE REVIEW WITH NATURAL LANGUAĞE PROCESSINĞ (NLP) TECHNIQUES ON THE USE OF GAMIFICATION METHODOLOĞY IN MARITIME EDUCATION         155           Buket BAKIR Ebru KARADAĞ SARI         HISTOMORPHOMETRIC EVALUATION OF THE EFFECTS OF CAPSAICIN APPLICATION ON SMALL INTESTINE OF RATS         165           Seren GEÇĞEL Fatih ÜNAL         ECONOMIC ANALYSIS OF SOLAR POWER PLANT FOR MERSIN PROVINCE         172           Buket BAKIR Nilay SEYİDOĞLU         HAWTHORN VINEĞAR ON CD4 AND CD8 T LYMPHOCYTES EXPRESSION IN SPLEEN OF         179
Salah EL HADAJ EI Mahdi EL GUARMAH Soukaina MJAHED Semiha DERVİŞOĞLU Mehmet SARIGÜL Levent KARACAN  Dilek GEDİK Ünal ÖZDEMİR Yunus Emre NAZLIGÜL Emin Serkan ERDÖNMEZ Cenk ŞAKAR  Buket BAKIR Ebru KARADAĞ SARI  Seren GEÇGEL Fatih ÜNAL  Buket BAKIR Nilay SEYİDOĞLU  Buket BAKIR NILAY SEMINA DERVİŞOĞLU  Buket BAKIR NİLAY SEYİDOĞLU  NEURAL NETWORKS AND BALANCED NEW NEW NEW NEW NEW NEW NEW NEW NEW NEW
Mehmet SARIĞÜL Levent KARACAN  STABILIZATION APPROACH  WITH A STRATEGIC DECISION-MAKING APPROACH, ORDERING THE FACTORS AFFECTING FUEL CONSUMPTION IN BULK CARRIER VESSEL SELECTION BY USING FUZZY ANALYTICAL HIERARCHY PROCESS METHOD  AN EXAMPLE OF LITERATURE REVIEW WITH NATURAL LANGUAGE PROCESSING (NLP) TECHNIQUES ON THE USE OF GAMIFICATION METHODOLOGY IN MARITIME EDUCATION  Buket BAKIR Ebru KARADAĞ SARI  Seren GEÇGEL Fatih ÜNAL  Seren GEÇGEL Fatih ÜNAL  Buket BAKIR Nilay SEYİDOĞLU  AN OPTIMIZATION-BASED VIDEO STABILIZATION APPROACH  APPROACH, ORDERING THE FACTORS AFFECTING FUEL CONSUMPTION IN BULK CARRIER VESSEL SELECTION BY USING (NLP) TECHNIQUES ON THE USE OF GAMIFICATION METHODOLOGY IN MARITIME EDUCATION  SMALL INTESTINE OF RATS  THE EFFECTS OF CAPSAICIN APPLICATION ON SMALL INTESTINE OF RATS  THE EFFECTS OF APPLICATION OF HAWTHORN VINEGAR ON CD4 AND CD8 T LYMPHOCYTES EXPRESSION IN SPLEEN OF
Dilek GEDİK Ünal ÖZDEMİR Devran YAZIR Yunus Emre NAZLIGÜL  Emin Serkan ERDÖNMEZ Cenk ŞAKAR  Buket BAKIR Ebru KARADAĞ SARI  Seren GEÇGEL Fatih ÜNAL  Buket BAKIR Nilay SEYİDOĞLU  Dilek GEDİK Ünal ÖZDEMİR AFFECTING FUEL CONSUMPTION IN BULK CARRIER VESSEL SELECTION BY USING FUZZY ANALYTICAL HIERARCHY PROCESS METHOD  AN EXAMPLE OF LITERATURE REVIEW WITH NATURAL LANGUAGE PROCESSING (NLP) TECHNIQUES ON THE USE OF GAMIFICATION METHODOLOGY IN MARITIME EDUCATION  HISTOMORPHOMETRIC EVALUATION OF THE EFFECTS OF CAPSAICIN APPLICATION ON SMALL INTESTINE OF RATS  THE EFFECTS OF SOLAR POWER HAWTHORN VINEGAR ON CD4 AND CD8 T LYMPHOCYTES EXPRESSION IN SPLEEN OF
Emin Serkan ERDÖNMEZ Cenk ŞAKAR  NATURAL LANGUAGE PROCESSING (NLP) TECHNIQUES ON THE USE OF GAMIFICATION METHODOLOGY IN MARITIME EDUCATION  HISTOMORPHOMETRIC EVALUATION OF THE EFFECTS OF CAPSAICIN APPLICATION ON SMALL INTESTINE OF RATS  Seren GEÇGEL Fatih ÜNAL  ECONOMIC ANALYSIS OF SOLAR POWER PLANT FOR MERSIN PROVINCE  THE EFFECTS OF APPLICATION OF HAWTHORN VINEGAR ON CD4 AND CD8 T LYMPHOCYTES EXPRESSION IN SPLEEN OF  155  165  172
Seren GEÇGEL ECONOMIC ANALYSIS OF SOLAR POWER PLANT FOR MERSIN PROVINCE  Buket BAKIR  Seren GEÇGEL ECONOMIC ANALYSIS OF SOLAR POWER PLANT FOR MERSIN PROVINCE  THE EFFECTS OF APPLICATION OF HAWTHORN VINEGAR ON CD4 AND CD8 T LYMPHOCYTES EXPRESSION IN SPLEEN OF
Fatih ÜNAL PLANT FOR MERSİN PROVINCE 172  THE EFFECTS OF APPLICATION OF  Buket BAKIR Nilay SEYİDOĞLU HAWTHORN VINEGAR ON CD4 AND CD8 T LYMPHOCYTES EXPRESSION IN SPLEEN OF 179
Buket BAKIR Nilay SEYİDOĞLU  HAWTHORN VINEGAR ON CD4 AND CD8 T LYMPHOCYTES EXPRESSION IN SPLEEN OF  179
Parween Karim Dedar S. Khoshnaw Zana F. Ali USING OF GREEN SPACES IN HEALTHCARE FACILITIES AND ITS IMPACT ON HUMAN HEALTH
Gamze GENÇ Rumeysa URAL Merve ATİK Hilal DOĞAN  EXPERIMENTAL STUDY ON THE EFFECT OF GRAPHENE IN FLAT-PLATE COLLECTORS
Gamze GENÇ Hatice Büşra PEKER Hilal DOĞAN  KAYSERİ'DEKİ MANEVA ATIKLARININ BİYOGAZ ÜRETİMİNDE DEĞERLENDİRİLMESİ  210
Mustafa ÖZDEN  Mustafa Serdar GENÇ Halil Hakan AÇIKEL Kemal KOCA  FLOW CHARACTERISTICS ON NACA2415 AIRFOIL AT LOW REYNOLDS NUMBER Z22
Mustafa Serdar GENÇ TRANSITION MODELLING 229

on Innovative Surveys in Positive Sciences 4-5 December 2022 / Full Text Book

# FSI ANALYSIS OF CARBON REINFORCED RECYCLABLE COMPOSITE WIND TURBINE BLADE

<sup>1,a</sup> Eren Anıl SEZER <sup>1, 2,3 b</sup> Sinem KESKİN <sup>1, 2,3 c</sup> Mustafa Serdar GENÇ <sup>4,d</sup> Berkay AYDOĞAN

<sup>1</sup> Energy Systems Engineering", Erciyes University, 38039, Kayseri, Turkey

<sup>2</sup> "Wind Engineering ve Aerodynamic Research Group", Erciyes University, 38039, Kayseri, Turkey

<sup>3</sup> MSG Technology Co. Ltd., Erciyes Technopark, Techno-1 Building No:61/20, 38039, Kayseri, Turkey

<sup>4</sup> Mechanical Engineering", Ege University, 35040, Bornava, İzmir, Turkey

### **ABSTRACT**

Due to the increasing energy needs, the use of energy resources is increasing day by day. In this context, as a result of  $NO_2$ , CO,  $SO_2$ , and gases released as a result of increased resource use, research and studies have been carried out on clean energy sources in recent years. Considering this development, the use of wind turbines, which enable the conversion of wind energy, which is one of the renewable energy sources, into electrical energy is also becoming widespread. However, since the service life of wind turbine blades is between 20 and 30 years, it becomes essential to make wind turbine blades using recyclable materials, since in such a case, more limited and challenging situations may be encountered, both economically and environmentally, as well as raw materials. Since the structures of the wind turbine blades produced today are made of thermoset resins, it becomes more difficult to recycle. The project aims to recycle the blades by using thermoplastic that is in the same polymer group as them instead of thermoset resins in the wind turbine blade structure. In this study, analyzes were performed on the NACA 4412 airfoil using ANSYS FLUENT software. The CFD simulation was carried out with carbon fiber-reinforced material with a thermoplastic matrix at  $Re = 7 \times 10^4$ . As a result of the calculations, the deformation, stress, and tension conditions of the wind turbine blade made of thermoplastic matrix and carbon fiber material were measured.

**Keywords:** Thermoplastic, Thermoset, Carbon fiber, FSI, Deformation, Stress, Tension

### 1.Introduction

Carbon fiber (CF), glass fiber (GF), or carbon/glass (hybrid) fiber reinforced polymer composites (FRPCs) are used in aircraft, wind turbines (WTs), aerospace and used in automotive. stiffness)[[1], [2], [3], [4], [5], [6] It is an important field polymer in improving the mechanical properties of the matrix, especially the behavior of carbon fibers. [7] In order to improve the mechanical properties of the composite material, it is necessary to optimize the interface between the fiber and the matrix, using certain methods for the modification of the reinforcing fiber.[8] FRPCs also provide high strength-toweight ratio and stiffness. It exhibits remarkable properties such as high damping property, long service life, high hardness, bending strength, abrasion resistance, impact resistance, corrosion and fire resistance. For this reason, it allows the use of wind energy in wind turbines as an efficient, sustainable and continuous source of clean energy. These advantages have led to the worldwide application of wind energy and the development of many fields [[9], [10], [11]]. The current wind energy market exists with around 540 GW of installed RT capacity in various parts of the world [12]. Albers et al. estimate that a significant portion of the installed wind turbines will complete their standard life from 2020 to 2034 [13]. They stated that it would be appropriate to use the turbulence density profile instead of the wind speed profile in obtaining the friction velocity and surface roughness length data, which are two important parameters in the boundary layer flow in their previous research for the deformation situation [14]. In practice one cannot reduce the wind speed to zero, therefore a power factor C<sub>p</sub> is defined as the ratio between the actual power achieved and the maximum usable power and this value is accepted up to  $C_{pmax} = 0.593[15]$ . Modern wind turbines operate and are optimized close to this limit,

on Innovative Surveys in Positive Sciences

4-5 December 2022 / Full Text Book

with up to 0.5 Cp. [16]. In the use of blade profiles for wind turbines, numerical models were created to better determine their properties and examined these models.

In this study, it is aimed to design a recyclable wind turbine blade by using thermoplastic resins instead of thermoset resin. The study is considered as numerical modeling and analysis. The reference wing model length is 77,5 cm, the wing chord length is maximum 18 cm, it has been designed at different twisted angles and analyzed at 40° attack angle by generating 100W electricity.

### 2.Material and Methods

In our study, NACA 4412 and NACA 4424 blades, which are airfoil models determined by the National Advisory Committee for Aeronautics (NACA), were used to obtain the best aerodynamic results in terms of design.

Inputs	Values
Blade Model	NACA 4412, NACA 4424
Turbine Power	100W
Blade Pitch Angle	40°
Blade Tip Speed Ratio (λ)	6
Air Denstiy	1.225 kg/m3
Turbine Pressure Coefficient (Cp)	0.4
Lift Coefficient (CL)	0.8
Velocity	6 m/s
Blade Length	0.775 m
Blade Twist	Twisted

Table 2.1. Limit Conditions

Before the blade design, the number of stations was determined. After the number of stations, the blade length was calculated from the power calculation formula of the blade. After these processes, it was decided to have a wing length of 77,5 cm and 12 stations.

After calculating the wing chord length and twisted angles at each station, optimization processes were made for blade strength during the design phase. NACA 4424 and NACA 4412 blades with the same Cl values were used. In the root section, NACA 4424 was used in the first 3 stations and NACA 4412 was used in the other 9 stations.

Power From The Wing:

$$P_{max} = (C_p)_{max} \frac{1}{2} \rho \pi R^2 V_{\infty}^3$$
 (2.1)

Power Factor:

$$C_p = \frac{P_{\varsigma\iota k\iota\varsigma}}{\frac{1}{2}\rho V^3 A} \tag{2.2}$$

Blade Tip Speed Ratio:

$$\lambda = \frac{\text{Blade Tip Speed}}{\text{Wind Speed}} = \frac{\Omega R}{V}$$
 (2.3)

Court Length Equation:

$$\alpha_{\rm B} = \frac{2}{3} \left( tan^{-1} \frac{R}{\lambda_{diz} r} \right) - \alpha_{diz} \tag{2.4}$$

Wing Torsion Angle Equation (Twist Angle):

$$C == \frac{1}{B} \frac{16\pi}{C_L} r \left( sin^2 \left[ \frac{1}{3} \left( tan^{-1} \frac{R}{\lambda r} \right) \right] \right)$$
 (2.5)

on Innovative Surveys in Positive Sciences

4-5 December 2022 / Full Text Book

Tabla	22	Plada	Infor	mation
i anie	<i>L. L</i>	втапе	mior	manon

Station	Rotor Diameter	Twist Angle	Chord Length
1	0.064629962	36.28996634	0.17613733
2	0.129259924	23.99998875	0.181346117
3	0.193889886	16.46003463	0.154011397
4	0.258519848	11.71002511	0.128286906
5	0.32314981	8.53426523	0.108293885
6	0.387779772	6.28995413	0.093060184
7	0.452409733	4.630257989	0.081304933
8	0.517039695	3.357490349	0.072047761
9	0.581669657	2.352333706	0.064608091
10	0.646299619	1.539950654	0.058517705
11	0.710929581	0.869893685	0.05345021
12	0.775559543	0.308211155	0.049174206

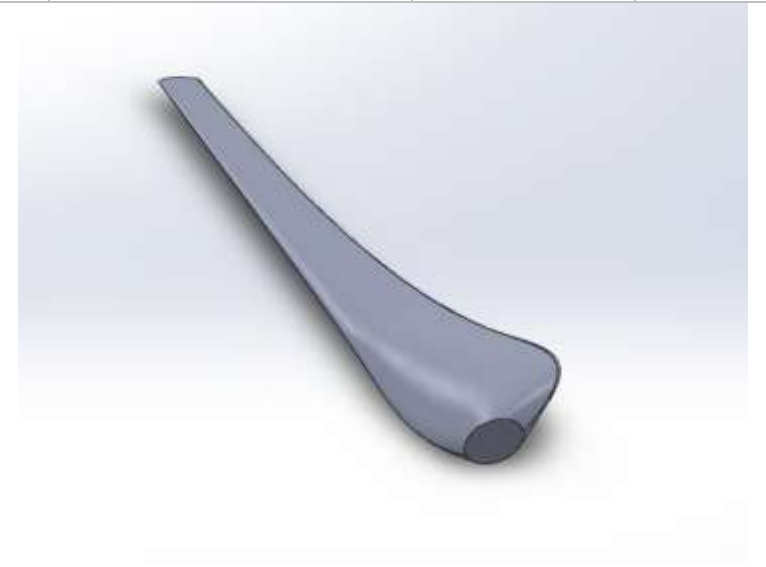


Fig. 1. Blade Model

The necessary parameters for this work were primarily determining the basic wind turbine blade. The relative composition of the composite material components is given as a ratio by weight or ratio by volume. While the ratio by weight is generally used in the production phase, the ratio by volume is used to determine the properties of composite materials. These two values are associated with each other by considering the density value.

For the reinforcement element:

$$W_f = \frac{W_f}{W_c} = \frac{\rho_f}{\rho_c} V_f \tag{2.6}$$

Where W means weight,  $W_f$  means reinforcing element weight,  $W_c$  means composite weight,  $\rho_f$  means reinforcement density,  $\rho_c$  means composite density,  $V_f$  means reinforcing element volume.

For Matrix:

$$W_m = \frac{W_m}{W_c} = \frac{\rho_m}{\rho_c} V_m \tag{2.7}$$

Where  $W_m$  means matrix weight,  $W_c$  means composite weight,  $\rho_m$  means matrix density,  $\rho_c$  means composite density,  $V_m$  means matrix volume.

on Innovative Surveys in Positive Sciences

4-5 December 2022 / Full Text Book

The density of composite materials can be calculated under conditions where the ratio by volume or ratio by weight is known.

$$\rho_c = \rho_f V_f + \rho_m V_m \tag{2.8}$$

$$\frac{1}{\rho_c} = \frac{W_f}{\rho_f} + \frac{W_m}{\rho_m} \tag{2.9}$$

The density equation, based on the ratio by volume, can be written for all properties of composite materials (hardness, modulus of elasticity, etc.) in certain cases.

Mixtures Rule:

$$X_c = X_f V_f + X_m V_m \tag{2.10}$$

Where  $X_C$  means composite poisson ratio,  $X_f$  means poisson's ratio of fiber material,  $X_m$  means volume fraction of matrix material,  $V_m$  means poisson's ratio of matrix material,  $V_f$  means volume fraction of fiber material

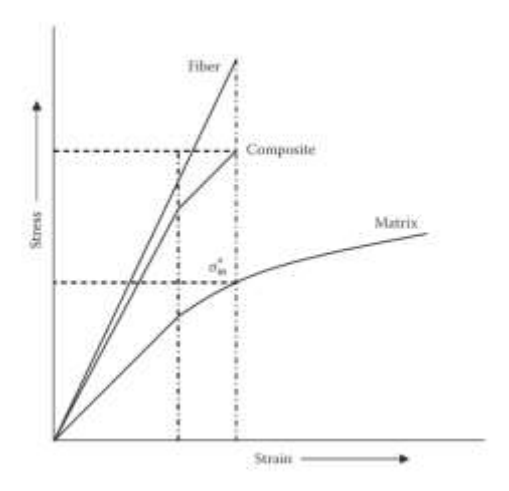


Fig.2. stress-strain plot for fiber-reinforced composites

### 2.2 Fiber Reinforced Composites Under Parallel Load

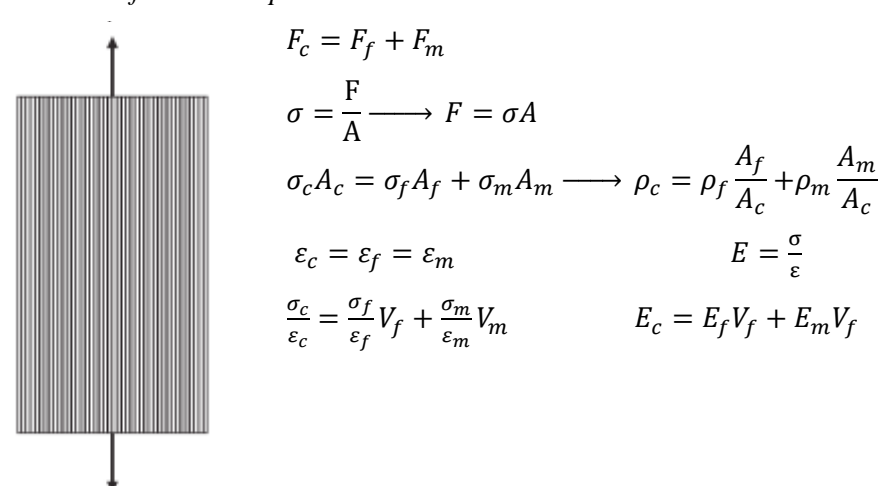


Fig.3. Under parallel load

on Innovative Surveys in Positive Sciences

4-5 December 2022 / Full Text Book

### 2.3 Fiber Reinforced Composites Under Horizontal Load

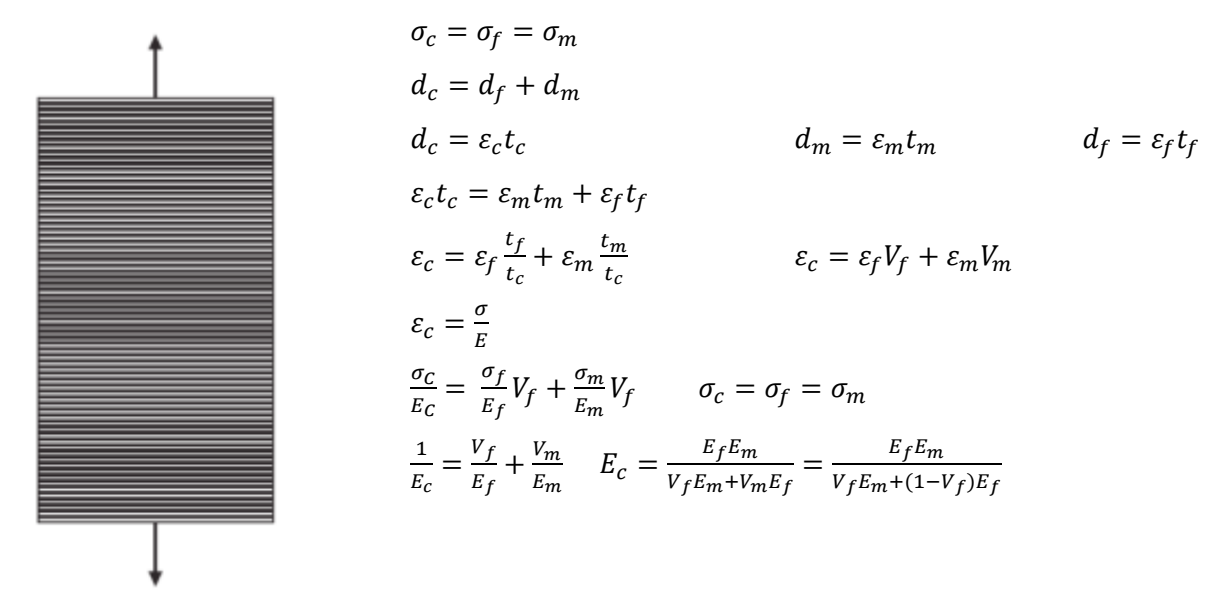


Fig.4. Under Horizontal Load

Poison Rate:

$$X_{C}=X_{f}V_{f}+X_{m}V_{m} \tag{2.10}$$

- The poisson ratio of carbon fiber, which is a composite material, is 0.1,
- Volume fraction of composite material 0.1,
- The poisson ratio of the matrix material, polypropylene, is 0.43,
- The volume fraction of the matrix material is 0.9,

As a result of the calculations according to 2.10, the poisson ratio of the polypropylene matrix carbon fiber reinforced material is 0.397. The polypropylene was chosen as the thermoplastic owing to it has very good resistance to fatigue and high impact strength.

The standard analysis was performed in 5000 iterations with the sst-k omega turbulence model under Re 70000. During the calculation of Reynolds number, the maximum court length of the wing was taken as a basis. Afterwards, one-way fluid structural interaction is completed.

### 3. Results

In this section, the results of the deformation, stress and strain values on the wing as a result of the FSI analysis are included.

on Innovative Surveys in Positive Sciences 4-5 December 2022 / Full Text Book

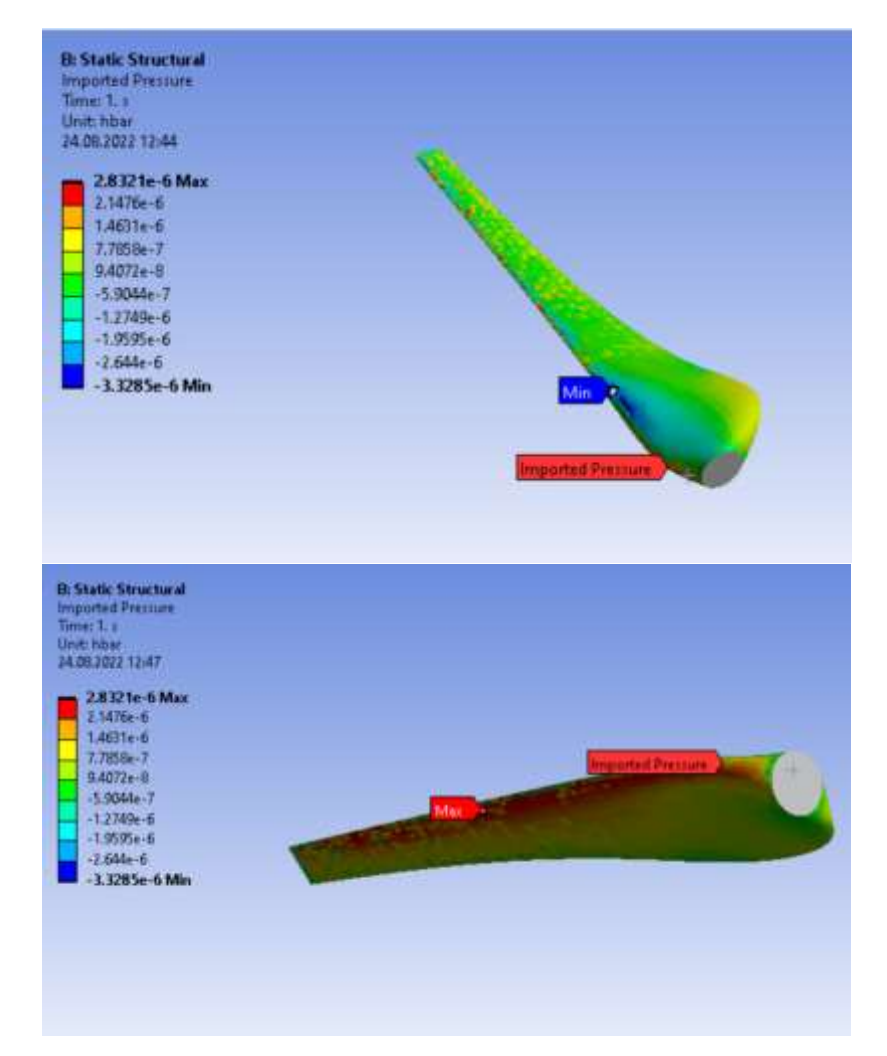


Fig.5. a) Subregion imported pressure b) Upper zone imported pressure

Afterwards the pressure values measured on the fluid flow (fluent) were transferred to the static structural, the deformed areas on the wing were measured.

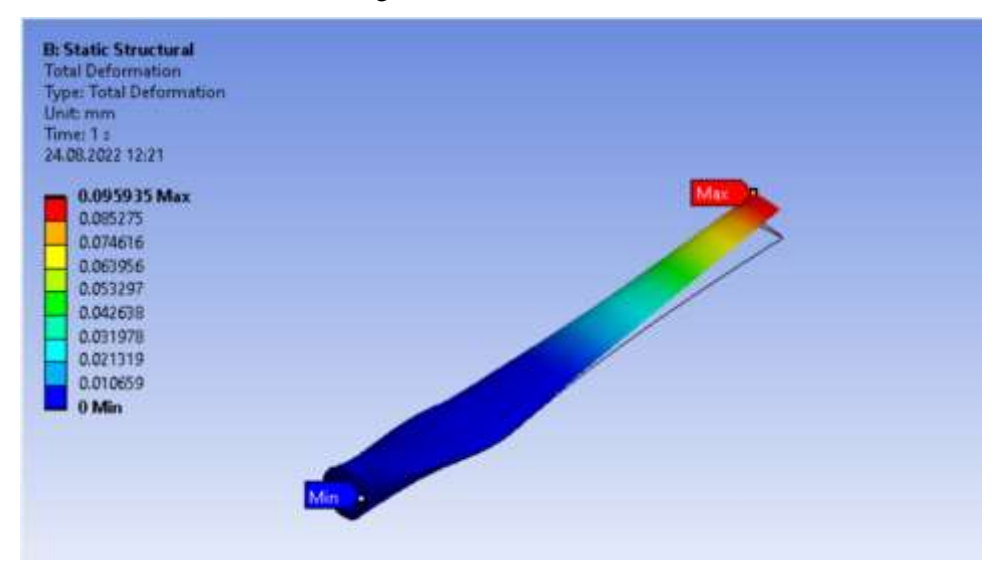


Fig.6. Total Deformation

The maximum deformation of the wing is 0.096 mm. It occurs mostly at the wingtips in this deformed region.

on Innovative Surveys in Positive Sciences 4-5 December 2022 / Full Text Book

The deformation values on the wing are at a tolerable level.

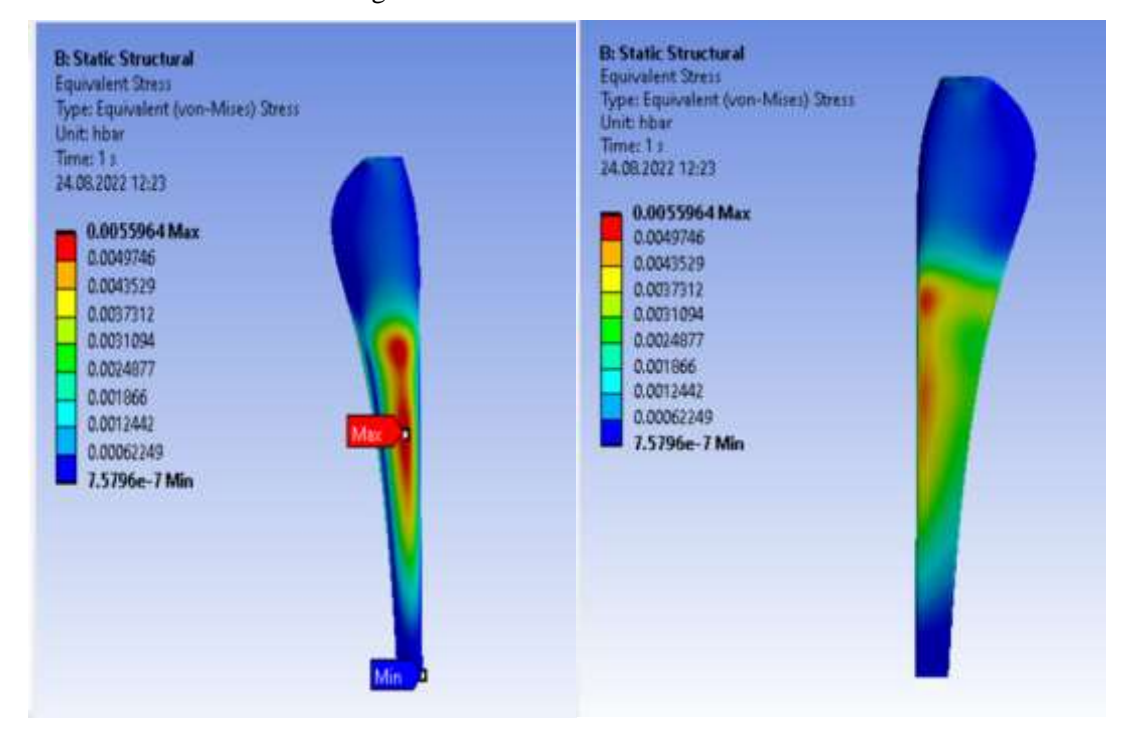


Fig.7. Equivalent Stress

When we look at the von misses stresses of the materials we use, the measured values are measured to have high efficiency and strength of the material.

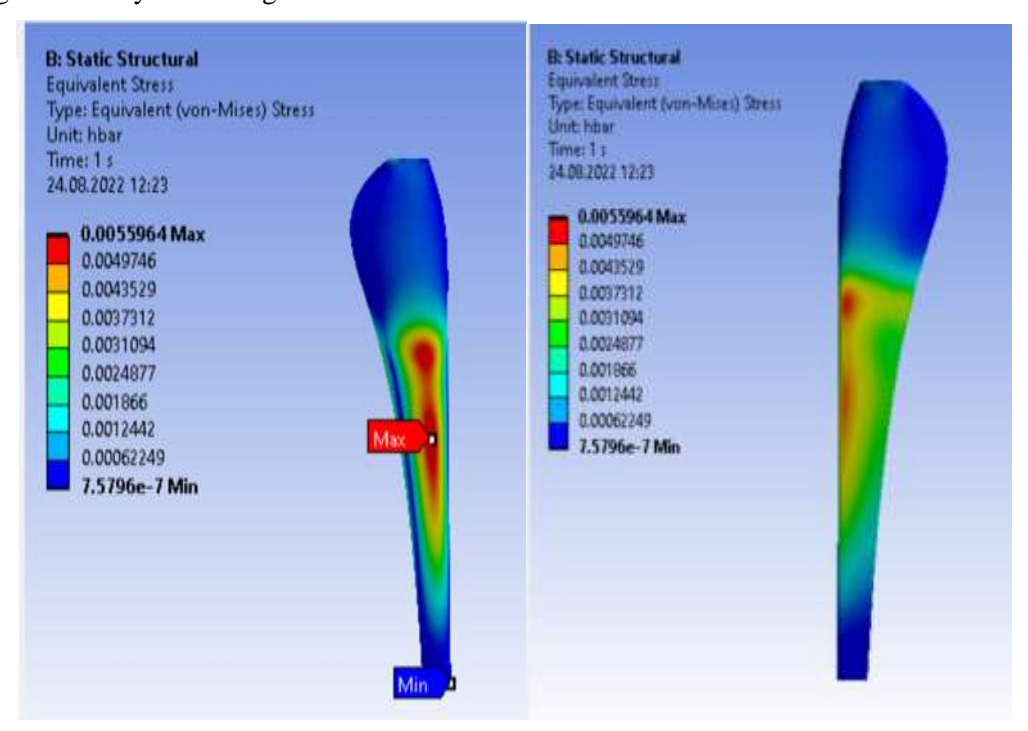


Fig.6 Equivalent Elastic Strain

Measured strain and stress values are at a tolerable level. Any object can be lengthened and shortened when force is applied on it. Since the strain value in the analysis is also a very low value, it can be ignored under normal conditions.

on Innovative Surveys in Positive Sciences 4-5 December 2022 / Full Text Book

### 4.Summary and Conclusion

In this experiment, the analysis of the polypropylene matrix and carbon fiber reinforced NACA 4412 wing model was made. The air volume was first given to the NACA4412 wing model designed in the ANSYS interface. The mesh suitable for CFD analysis was applied to the air volume above the wing. Air inlet, outlet, etc. to the program after meshing. can be added, regions have been added and introduced. Subsequently these processes, the wing was transferred to the Fluent medium and pressure analysis was performed. As a result of this analysis, it was transferred to the Static Structural program to measure the deformations caused by the pressure value. In addition, the wing deformations were measured by applying the pressures in the Fluent environment to the determined point on the wing. In the researches and as in this study, it has been determined that the deformation conditions are generally at the end points of the wings. The purpose of this experiment is to produce reversible wind turbine blades and to calculate the deformation, strength and strain values of the material used before blade production. As a result of these researches and analyzes, it is aimed to create long-term wind turbine blades in daily life.

### Acknowledgements

The authors thank the Scientific and Technological Research Council of Turkey (TÜBİTAK) for the Scholarship for University Students Industry-Oriented Research Projects Support Program 2209/B under the contract number: 1139B412103236 for the author Eren Anıl SEZER.

### References

- [1] Bishop G. UK polymer composites sector study and competitive analysis. ISSN 1473 2734 NPL Rep MATC 80 Natl 2001:1–56.
- [2] L. Mishnaevsky, K. Branner, H.N. Petersen, J. Beauson, M. McGugan, B.F. Sørensen,

Materials for wind turbine blades: an overview Materials, 10 (2017), pp. 1-24.

- [3] A. Ding, S. Li, J. Wang, A. Ni A new analytical solution for spring-in of curved composite parts Compos Sci Technol, 142 (2017), pp. 30-40.
- [4] A. Ding, J. Wang, A. Ni, S., Li A new analytical solution for cure-induced spring-in of L-shaped composite parts, Compos Sci Technol, 171 (2019), pp. 1-12.
- [5] M.R. Sanjay, P. Madhu, M. Jawaid, P. Senthamaraikannan, S. Senthil, S. Pradeep, Characterization and properties of natural fiber polymer composites: a comprehensive review, B.V., 172 (2018).
- [6] D.K. Singh, A. Vaidya, V. Thomas, M. Theodore, S. Kore, U. Vaidya Finite element modeling of the fiber-matrix interface in polymer composites J Compos Sci, 4 (2020), p. 58.
- [7] Miller, T. C., Chajes, M. J., Mertz, D. R., Hastings, J. N., 2001, Strengtheningof a steel bridge girder using CFRP plates, J. Bridge Eng. 6(6),pp. 514–522.
- [8] Dobreva, D., Nenkova, S., and Vasileva, St., 2005, Investigation of themicrostructure of polypropylene composites filled with wood flour modified with monochloroacetic acid, NATO Science Ser. II 223,pp.177-180.
- [9] D.J. Willis, C. Niezrecki, D. Kuchma, E. Hines, S.R. Arwade, R.J. Barthelmie, et al. Wind energy research: state-of-the-art and future research directions Renew Energy, 125 (2018), pp. 133-154.
- [10] Q. Wang, H. Ning, U.S.P. Vaidya Mechanical behavior of long carbon fiber reinforced polyarylamide at elevated temperature J Mater Sci Eng (2016).
- [11] N. Hiremath, S. Young, H. Ghossein, D. Penumadu, U. Vaidya, M. Theodore, Low cost textile-grade carbon-fiber epoxy composites for automotive and wind energy applications, Compos B Eng, 198 (2020).
- [12] J. Chen, J. Wang, A. Ni Recycling and reuse of composite materials for wind turbine blades: an overview J Reinforc Plast Compos, 38 (2019), pp. 567-577.

on Innovative Surveys in Positive Sciences 4-5 December 2022 / Full Text Book

- [13] . Kamoun, B., Afungchui, D., Chauvin, A, 2005. A wind turbine blade profile analysis code based on the singularities method. Renewable Energy, 30, pp. 339–352.
- [14] . Merabet, A., Necib, B., 2003. Characterisation of wings with NACA 0012 airfoils. Renewable and Sustainable Energy Rewievs, 131-137.
- [15] What does "cp.max" actually mean? cp.max Rotortechnik GmbH & Co. KG [en] (cpmax.com)
- [16] GA harmain et al/Int.J.ChemTech Res.2013,5

on Innovative Surveys in Positive Sciences 4-5 December 2022 / Full Text Book

# CASE STUDY ON THE EVALUATION OF WIND MEASUREMENTS PERFORMED BY LIDAR AND CUP ANEMOMETER

#### Ekim KÜLÜM

Kirsehir Ahi Evran University, Department of Electronics and Automation, Kirsehir, Turkiye, 40300
Wind Engineering and Aerodynamics Research Laboratory, Department of Energy
Systems Engineering, Erciyes University, 38039, Kayseri, Turkiye

## Mustafa Serdar GENÇ

Wind Engineering and Aerodynamics Research Laboratory, Department of Energy
Systems Engineering, Erciyes University, 38039, Kayseri, Turkiye
Energy Conversions Research and Application Center, Erciyes University, 38039, Kayseri, Turkiye

#### **ABSTRACT**

The use of remote sensing devices are increasing in the wind energy sector. Reason of this aim that remote sensing devices are more mobile than conventional measurement stations and can measure wind speed at hub height. However, considering the working principle of remote sensing devices and difference in measurements made in different sites, the use of remote sensing deices alone in wind measurement has not yet become widespread. In this context, there are many studies in worldwide on the comparison of anemometer and remote sensing devices. Since the use of remote sensing devices is not widespread in Turkiye yet. So number of such studies is quite low. The presented study is a comparative analysis of wind measurements carried out in Turkiye performed by LIDAR and cup anemometer. Measurements began in Feb 2018, took 363 days for LIDAR and 312 days for anemometers. The average wind speed, Daily wind speeds, hourly average wind speeds, wind power densities and statistical distributions have made comparatively analyzed with different methods. The analyzes have prepared for wind measurements at 9 different heights with LIDAR and for 5 wind measurements at 4 different heights with anemometers. When the average wind speeds of the measurements evaluate at the same heights, it have observed that the LIDAR and anemometer wind speeds have good fit. However the hourly values are examined, it have observed that the average wind speeds measured by LIDAR are higher between 08:00-13:00. Furthermore, when the average wind speeds of the anemometers have examined, it have observed that the measurement performed at 58m is higher than the performed at 75m. Although the cause of this situation can not be estimated precisely, it is thought to be caused by wind shear. Finally, Weibull scale and shape parameters have found by 4 different methods. Weibull parameters obtained by WAsP and Openwind methods have found acceptable with measured data distribution.

**Keywords:** Wind Energy, LIDAR, Wind Resource Assessment

#### ÖZET

Uzaktan algılama cihazlarının kullanım payı rüzG3ar enerjisi sektöründe gün geçtikçe artarak devam etmektedir. Bu durumun sebebi uzaktan algılama cihazlarının klasik ölçüm istasyonlarına göre daha mobil olması ve türbin göbek yüksekliğinde ölçüm gerçekleştirebilmesidir. Ancak uzaktan algılama cihazlarının çalışma prensibi ve farklı sahalarda yapılan ölçümler dikkate alındığında uzaktan algılama cihazlarının rüzgâr ölçümü konusunda tek başına kullanımı henüz yaygınlaşmamıştır. Bu kapsamda literatürde çeşitli anemometre türleri ve uzaktan algılama cihazlarının karşılaştırılmasına dair birçok çalışma söz konusudur. Bu çalışmalarda farklı saha ve farklı analiz yöntemleri kullanılmıştır. Türkiye'de ise uzaktan algılama cihazlarının kullanımı yaygın olmadığı için bu tür çalışmaların sayısı oldukça azdır. Söz konusu çalışma, LIDAR ve kepçe anemometre kullanılarak Türkiye'de gerçekleştirilmiş rüzgâr ölçümlerinin karşılaştırmalı analizidir. Subat 2018'de başlayan ölçümler, LIDAR için 12

on Innovative Surveys in Positive Sciences 4-5 December 2022 / Full Text Book

ay (363 gün) ve anemometre için 10 ay (312 gün) sürmüştür. Çalışmada iki ölçüme dair, ortalama rüzgâr hızı, günlük ortalama rüzgâr hızları, saatlik ortalama rüzgâr hızları, güç yoğunlukları ve farklı yöntemler ile gerçekleştirilen istatiksel dağılımları karşılaştırmalı olarak analiz edilmiştir. Belirtilen analizler LIDAR ile gerçekleştirilen 9 farklı yükseklikteki ölçümler için ve anemometre ile gerçekleştirilen 4 farklı yükseklikte 5 ölçüm için hazırlanmıştır. Aynı yüksekliklerde yapılan ölçümlerin ortalama rüzgâr hızları incelendiğinde Saatlik ortalama incelendiğinde, ortalama rüzgâr hızının düşük olduğu 08:00 – 13:00 saatleri arasında LIDAR ile ölçülen ortalama hızların daha yüksek olduğu gözlemlenmiştir. Ek olarak anemometreler ile alınan verilerin ortalama hızları değerlendirildiğinde 58m gerçekleştirilen ölçümün 75m ile gerçekleştirilen ölçümden yüksek olduğu gözlemlenmiştir. Bu durum sebebi kesin olarak tahmin edilememek ile birlikte doğal rüzgâr kesmesi kaynaklı olduğu düşünülmektedir. Weibull parametreleri 4 farklı metot ile bulunmuş olup. WAsP ve Openwind yöntemleri ile elde edilen şekil ve ölçek parametreleri oluşturulan dağılımlar uygun bulunmuştur.

# 1. GİRİŞ

Dünyada ve ülkemizde enerji ihtiyacı artan bir ivmeye sahiptir. Fosil yakıtların çevreye zararları ve kaynakları tükeniyor olması göz önünde bulundurulduğunda yenilenebilir enerji kaynaklarına olan ihtiyaç kaçınmaz hale gelmektedir. Belirli zaman aralıkları gerçekleşen enerji krizleri de ülkeleri yenilebilir enerji kaynaklarına geçişi hızlandırma konusunda teşvik etmektedir.

Başta Türkiye olmak üzere birçok ülke rüzgâr enerjisi kurulu gücünü attırma eğilimindedir. Halihazırda dünya geneli rüzgâr enerjisi kurulu gücü 837GW'tır. Bu durum dünya genelinde 1.1 milyar ton CO<sub>2</sub> salınımı engellenmiştir[1]. Haziran 2022 tarihi itibari ile Türkiye'nin kurulu rüzgâr enerjisi gücü 10.976GW'a ulaşmıştır. Bu değer Türkiye'de toplam kurulu gücün 10.81%'ine tekabül etmektedir. Son 10 yılda Türkiye'nin kurulu rüzgâr enerjisi gücü 6.35 kat artmakla birlikte 2022'nin ilk yarısında 369MW'lık artış olmuştur. Ek olarak son 10 yılda Türkiye'nin kurulu rüzgâr enerjisi gücü sürekli artış eğilimindedir[2]. YEKA ihalelerinin sayılarının artması ve son olarak 450MW kapasiteli YEKA (3) RES 14 Haziran tarihinde gerçekleştirilmesi ile Türkiye'nin rüzgâr enerjisi kurulu gücü artarak devam edecektir.

Rüzgâr enerji santralleri proje geliştirme ve işletme aşamasında kuşkusuz ki en kritik parametrelerden biri anemometrelerdir. Anemometrelerin doğruluğu ve diğer başarım parametreleri enerji üretimi hesaplamaları için büyük öneme sahiptir. Ek olarak fizibilite çalışmalarını da etkilemektedir. Dolayısıyla rüzgâr hızı değerlerinin değerlendirilmesi ve analizi önemli bir hale gelmektedir. Rüzgâr ölçüm kampanyası planlanırken ölçüm istasyonlarının sayısı ve üzerine yerleştirilecek meteorolojik ölçüm cihazlarının sayısı yönetmelikler ve teknik değerlendirmeler sonucu belirlenir. Alternatif ve yardımcı ölçüm olarak uzaktan algılama cihazları rüzgâr ölçüm projelerinde sıkça kullanılmaktadır.

Birçok uzaktan algılama cihazlarından yaygın olarak LIDAR (Light Detection And Ranging) ve SODAR (Sonic Detection And Ranging) en çok tercih edilenler arasındadır. Çalışma prensipleri ve rüzgâr enerjisi marketinde ölçmenin rolü sebebi ile uzaktan algılama cihazlarının ölçüm sonuçları sık sık diğer anemometreler ile karşılaştırılmaktadır. Jakobsen ve arkadaşları Güney-Batı Norveç'te bir fiyort girişindeki rüzgâr koşullarını LIDAR ve sonik anemometre kullanarak değerlendirmişlerdir. Çalışmada 1 adet WindCube 100S LIDAR, 1 adet WXT520 2D anemometre ve 4 adet Gill 1561-PK-020 3D anemometre kullanılmıştır. Veriler arasında çapraz korelasyon gerçekleştirilmiş olup, sonik anemometre ile LIDAR korelasyon katsayılarının uyumlu olduğu gözlemlenmiştir. Farklı çalışma modlarında ve farklık yükseklik, güney açılarında test edilen LIDAR cihazı ile anemometreler arasında 1.7km'lik mesafe mevcuttur. Ortalama hız değerleri incelendiğinde en hız değeri WXT520 cihazı 11.5m/s olarak vermiştir. LIDAR ve diğer 2 anemometrenin ortalama hız değerleri 10.4 ile 10.6m/s arasında değişmektedir. Ek olarak çalışmada 2 adet kısa mesafeli WindScanner cihazları kullanılmıştır. Araştırmada uzun menzilli LIDAR'ların karmaşık arazilerde kullanımının uygunluğu gösterilmiştir. Ancak tarama süresinin uzunluğunun iyileştirilmesi gerektiği vurgulanmıştır[3].

Bir diğer çalışma ise WindCube V2LIDAR ve meteorolojik ölçüm direği kullanılarak 11-14 gün arası değişen sürelerde 3 farklı sahada yapılan ölçümler karşılaştırılmıştır. Ölçüm yapılan sahalar farklı arazi koşullarına sahiptir. Sumang ölçüm noktası 362.2m yükseklik ve orta sınıf dağlık alan, Gangjeong

on Innovative Surveys in Positive Sciences 4-5 December 2022 / Full Text Book

ölçüm noktası sahil alanı ve 2.63m yüksekliğinde ve Susan ölçüm noktası 113.58m yüksekliğinde orta sınıf dağlık alandır. Meteorolojik ölçüm istasyonu üzerinde 40,50,60,70 ve 80m yüksekliklerde NRG ve Thies marka anemometreler ile rüzgâr hız değerleri toplanmıştır. Karşılaştırma yapmak amacı ile sahaların karmaşıklık sınıflandırması Ruggedness Index (RIX) yöntemi ile belirlenmiştir[4]. RIX değerleri Sumang, Gangjeong ve Susan için sırasıyla 2.91%, 0% ve 2.05% çıkmıştır. Ek olarak power law yöntemi kullanılarak sahaların LIDAR ve ölçüm istasyonu değerleri için wind shear exponent (WSE) değerleri hesaplanmıştır. Sonuçlar RIX oranları ile benzerlik göstermektedir. Ancak Gangjeong için LIDAr ve anemometre WSE değerleri arasındaki fark beklenenden fazladır. Ortalama rüzgâr hızları ise Sumang, Gangjeong ve Susan için sırasıyla 0.29m/s, 0.18m/s ve 0.13m/s LIDAR ölçümleri daha azdır[5]. Bu durum LIDAR ve anemometre ölçümlerinin karşılaştırmalarında genel olarak görülen bir durumdur.

Bu çalışmada Aksaray, Türkiye'de gerçekleştirilen ZephIR 300 LIDAR ve üzerinde Thies ve NRG anemometreler ile ölçüm yapan meteorolojik istasyonun verileri ile gerçekleştirilmiştir. Gerçekleştirilen vaka çalışması ile uzaktan algılama cihazları ve anemometre karşılaştırma çalışmalarına katkı sağlamaktadır. Ölçümler sonucu elde edilen veriler WindGrapher programı demo versiyonu ile edilmiş ve değerlendirilmiştir.

## 2. Ölçüm ve Analiz Bilgileri

Ölçümler Şubat 2018'de başlamış olup, LIDAR (Fig 1a) için 363 gün ve meteoroloji istasyonu(Fig 1b) için 312 gün sürmüştür. LIDAR ile 185,165,145,125,101,93,85,75 ve 58m yüksekliklerin rüzgâr hız ve yön bilgisi ölçülmüştür. Ek olarak sıcaklık, nem, basınç, yağış ve eğim sensörleri ile bu değerler ölçülmüştür. Meteorolojik istasyonda ise 101m'de 2 adet, 93,75 ve 58m'de rüzgâr hızı değerleri anemometreler ile ölçülmüştür. Ayrıca istasyon üzerinde 2 adet rüzgâr yön sensörü, sıcaklık/nem sensörü ve basınç sensörü bulunmaktadır. Ölçümler sistemlerinin aralarında 43m mesafe bulunmaktadır. Bu durumun sebebi hem ölçüm istasyonlarının sabitleme halatlarının bulunması hem de LIDAR dikey ölçümü esnasında ölçüm direğinin etkisinden kaçınılmasıdır. Ölçüm sistemleri arası yükseklik farkı 3m'dir.





Fig 1: a)ZephIR 300 LIDAR[6] b)Meteorological mast and LIDAR location on Google Earth Pro. Çalışmada ilk olarak ölçümlerin ortalama rüzgâr hızları ve 16 sektör yön dağılımları incelenmiştir.

on Innovative Surveys in Positive Sciences

4-5 December 2022 / Full Text Book

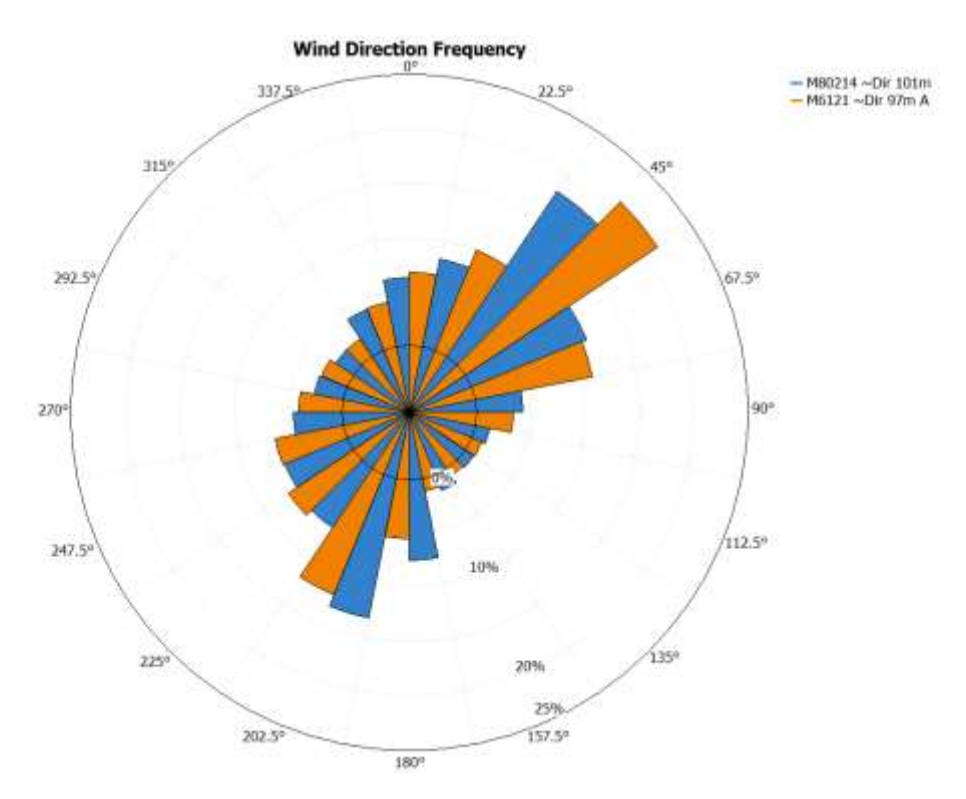


Fig 2: Rüzgâr yön frekans dağılımı

Her iki ölçüm sistemi içinde hakim rüzgâr yönü Fig 2'de görüldüğü gibi ilk olarak 45<sup>0</sup> olarak belirlenmiştir. Ancak 202.5<sup>0</sup> yönünde de yüksek frekansta rüzgâr akışı mevcuttur. Ancak LIDAR ve meteorolojik istasyon birlikte değerlendiğinde bu yönlerin frekans ağırlıkları birbirlerine göre farklıdır. Bir diğer aşamada ortalama hız değerleri karşılaştırılmıştır. Öncelikli olarak her bir cihazın farklı yüksekliklerde olan ölçümleri kendi içerisinde değerlendirilmiştir. Ardından farklı cihazların aynı yüksekliklerdeki ortalama rüzgâr hızları eşitlik 1'deki formülden yola çıkılarak karşılaştırılmıştır.

$$\bar{x} = \frac{1}{N} \sum_{i=1}^{N} x_i$$
 Eşitlik 1

Farklı ölçüm metotlarına sahip cihazların karşılaştırılmasına dair vaka çalışmaları gerçekleştirilirken saatlik ortalama hızların birlikte değerlendirilmesi önemli bir yere sahiptir.

Rüzgâr verisi incelemelerinde bir diğer kritik incelemelerden bir tanesi de frekans dağılımlarının incelenmesidir. Frekans dağılımlarını hesaplanması için birçok yöntem mevcuttur. Söz konusu çalışmada Maximum likelihood, Least squares, WAsP ve Openwind yöntemleri ile Weibull parametreleri dağılımlar 101m yüksekliğinde bütün ölçümler için analiz edilmiştir.

Maiximum Likelihood

$$k = 1 / \left( \frac{\sum_{i=1}^{N} \bigcup_{i}^{k} ln(U_{j})}{\sum_{i=1}^{N} \bigcup_{i}^{k}} - \frac{\sum_{i=1}^{N} ln(\cup i)}{N} \right)$$

Ui rüzgâr hızı

N veri sayısı

k sahpe parametresi

A scale parametresi

on Innovative Surveys in Positive Sciences

4-5 December 2022 / Full Text Book

$$A = \left(\frac{\sum_{i=1}^{N} U_i^k}{N}\right)^{\frac{1}{k}}$$

Least squares

$$ln\left\{ln\left[\frac{1}{1-F(U)}\right]\right\} = k ln U - k ln A$$

Openwind A

$$A = \sqrt[3]{\frac{\frac{1}{N} \sum_{i=1}^{N} U_i^3}{\Gamma\left(\frac{3}{k} + 1\right)}}$$

Openwind k

$$\sqrt[3]{\frac{1}{N}\sum_{i=1}^{N}U_{i}^{3}} = \frac{1}{N}\sum_{i=1}^{N}U_{i}$$

$$\Gamma\left(\frac{3}{k}+1\right) = \frac{1}{N}\left(\frac{1}{k}+1\right)$$

WAsP A

$$A = \sqrt[3]{\frac{1}{N} \sum_{i=1}^{N} U_i^3} \frac{1}{\Gamma(\frac{3}{k} + 1)}$$

WAsP k

$$\left(\frac{\frac{1}{N}\sum_{i=1}^{N}U_{i}}{\left|\frac{1}{N}\sum_{i=1}^{N}U_{i}^{3}\right|}\right)^{k} = -\ln(X)$$

$$\left(\frac{3}{k} + 1\right)$$

Weibull

$$f(v) = \frac{k}{A} \left(\frac{v}{A}\right)^{k-1} \cdot \exp\left[-\left(\frac{v}{A}\right)^{k}\right]$$
$$F(U) = 1 - \exp\left[-\left(\frac{U}{A}\right)^{k}\right]$$

Son olarak 101m, 93m, 75m ve 58m için rüzgâr güç dağılımları (WPD) bütün ölçüm yöntemleri için analiz edilmiş ve karşılaştırılmıştır. WPD değerlendirmesi rüzgâr enerji santrallerinde rüzgâr sınıfının belirlenmesinde kullanılmaktadır. Hava yoğunluğu hesaplanırken sıcaklık, nem ve basınç değerleri için ölçüm bilgileri dikkate alınmıştır.

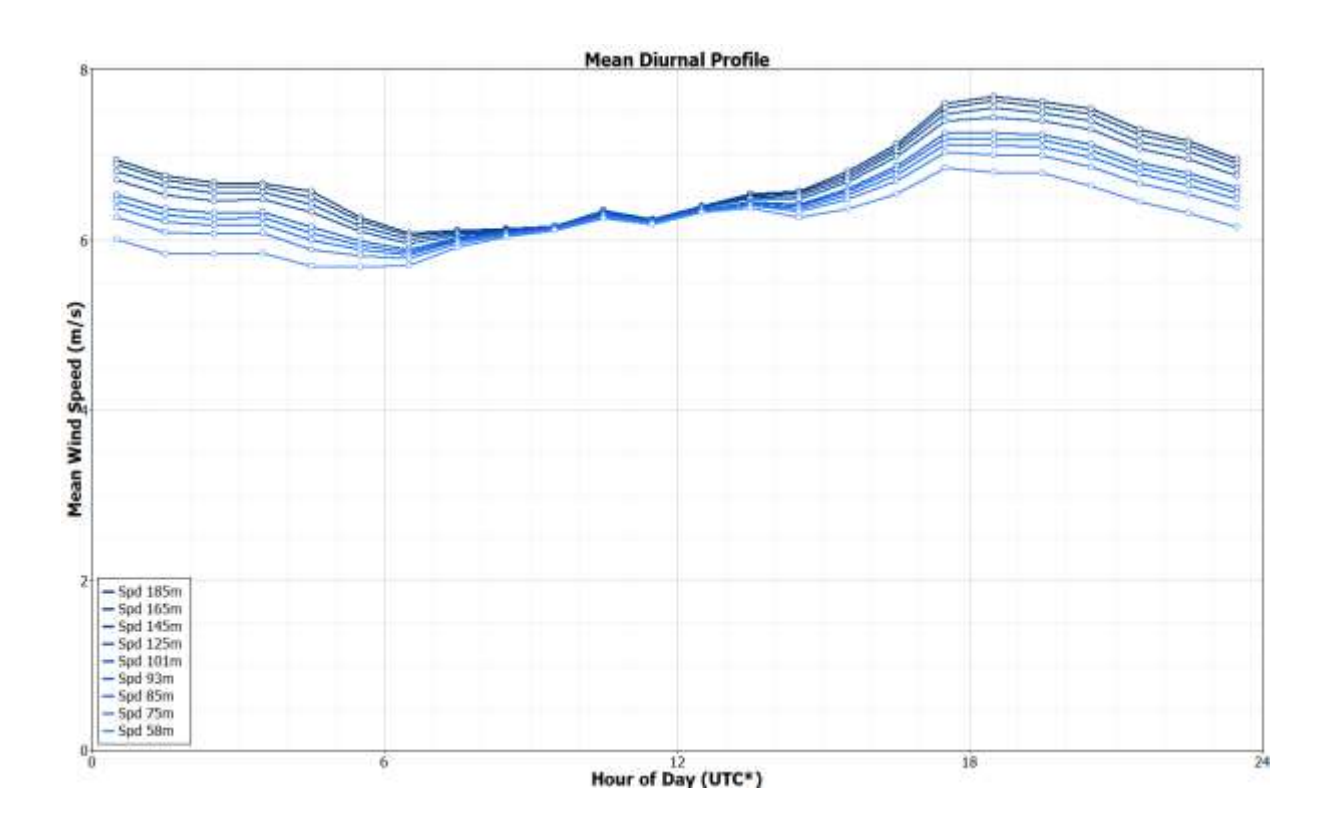
on Innovative Surveys in Positive Sciences

4-5 December 2022 / Full Text Book

$$\rho = \frac{1}{T} \left[ \frac{p}{R_d} - \phi \, p_{sat} \left( \frac{1}{R_d} - \frac{1}{R_v} \right) \right]$$

## 3. Sonuçlar

Çalışmada birçok yöntem LIDAR (Fig 3a) ve anemometrelerin (Fig 3b) rüzgâr ölçümleri değerlendirilmiştir. LIDAR saatlik ortalama incelendiğinde 08:00 - 13:00 saatleri arasında ortalama rüzgâr hızları birbirlerine yakındır. Bu durum sebebi o saatlerde rüzgâr akışının düşük düzeyde olmasıdır. Ancak diğer saatlerde beklenildiği gibi ölçüm yüksekliği arttıkça ortalama hız artmaktadır. Anemometrelerin saatlik ortalama hızları incelendiğinde ise benzer bir durum gözlenmiştir ancak 75m yükseklik için ortalama rüzgâr hızı durgun saatlerde 58m'den daha düşük ortalamaya sahiptir. Kesin olmamakla birlikte bu durum kurulum hatası veya rüzgâr kesmesi olduğu düşünülmektedir. 101m'de yapılan ölçümler karşılaştığında ise 06:00 – 18:00 saatleri arasında LIDAR ölçümü anemometreden yüksek iken diğer saatlerde anemometre ortalama değeri daha yüksektir. Cihazlarda arasında saatlik paralel olarak değisen rüzgâr hızı ortalaması gözlemlenmemistir. Bu durumun cihazların calısma prensipleri, bulutluluk durumu gibi birçok sebebi olabilmektedir.



on Innovative Surveys in Positive Sciences

4-5 December 2022 / Full Text Book

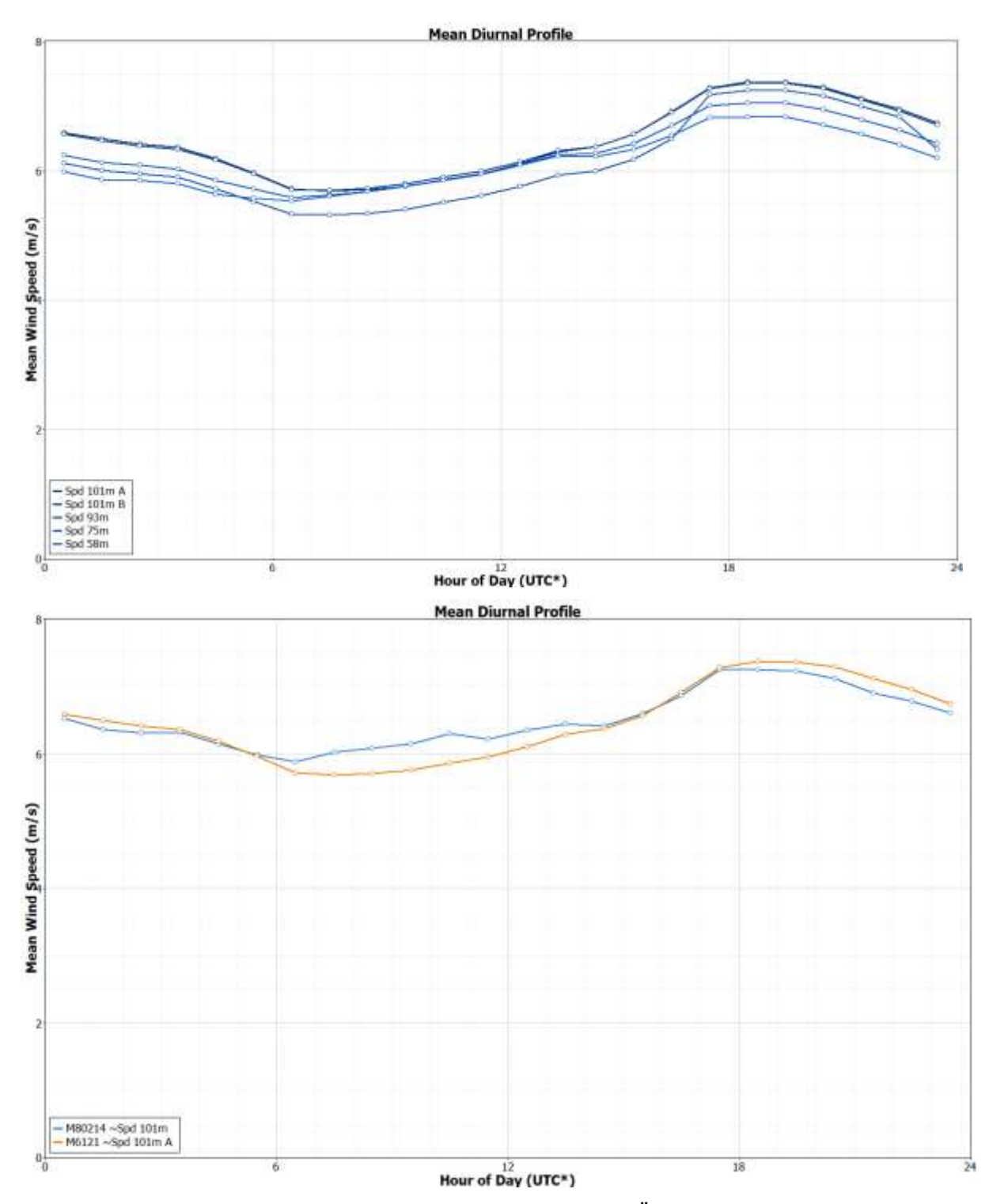
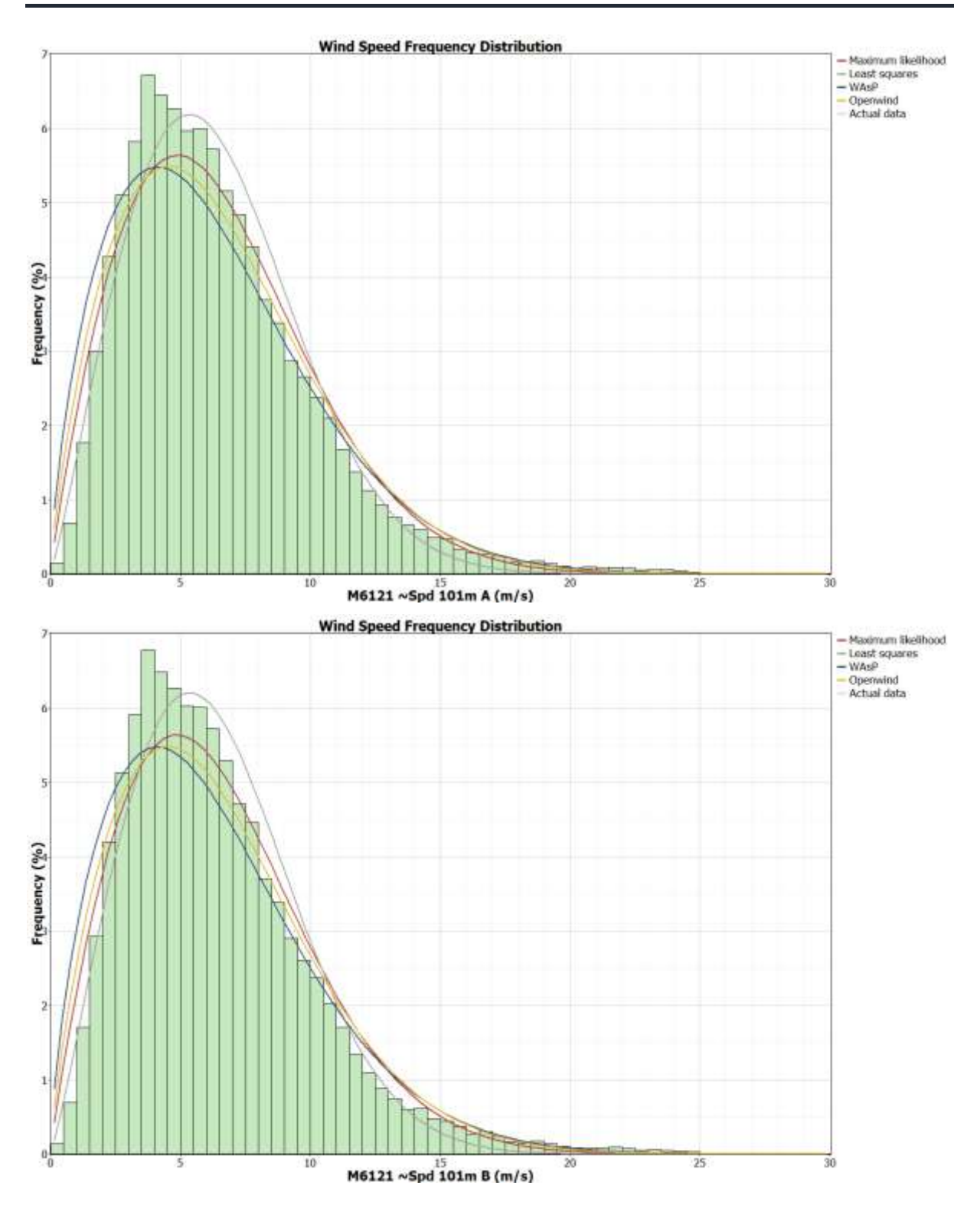


Fig 3: a) LIDAR ölçümlerinin saatlık rüzgâr hızı ortalaması b) Ölçüm istasyonu saatlık rüzgâr hızı ortalaması c)101m'de gerçekleştirilen ölçümlerin karşılaştırılması

Frekans dağılımları incelendiğinde ise WAsP ve Openwind yaklaşımları ile elde edilen dağılımlarda bu çalışma için daha uygun olduğu gözlemlenmiştir(Fig 4).

on Innovative Surveys in Positive Sciences

4-5 December 2022 / Full Text Book



on Innovative Surveys in Positive Sciences

4-5 December 2022 / Full Text Book

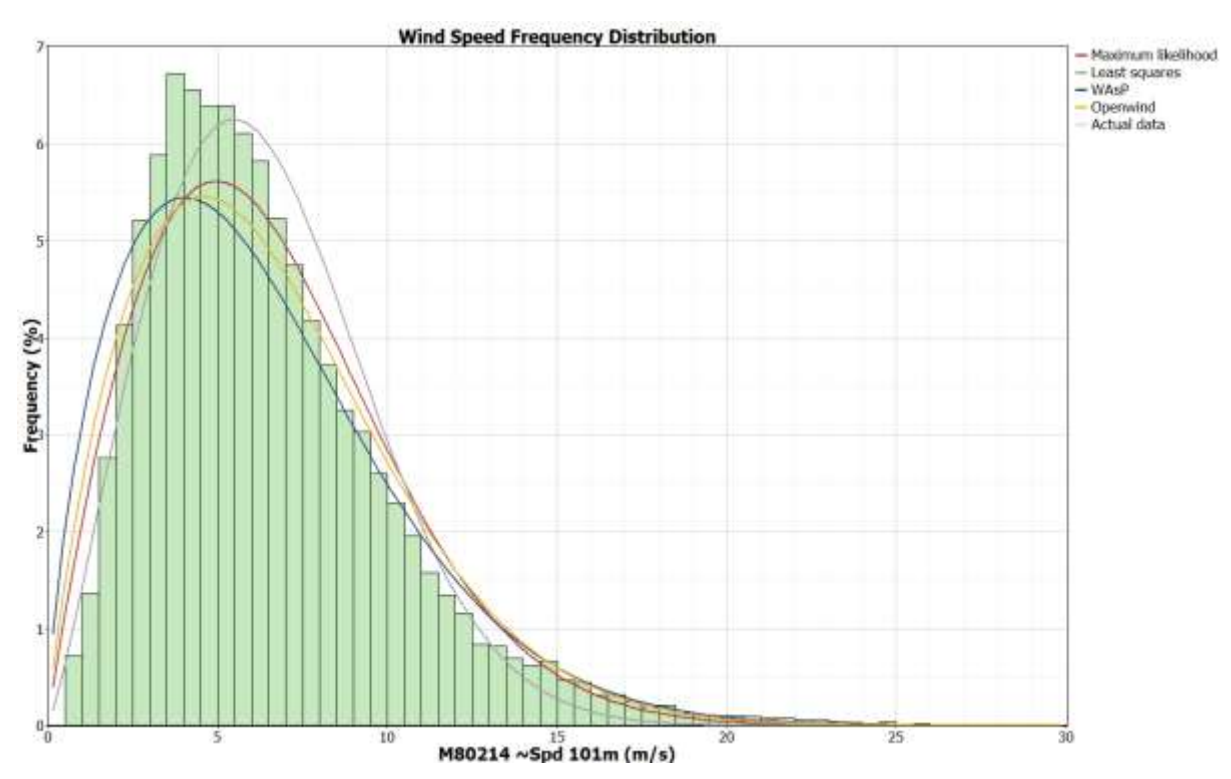


Fig 4:a) Ölçüm istasyonu 101m A ölçümü rüzgâr hızı frekans dağılımı b) Ölçüm istasyonu 101m B ölçümü rüzgâr hızı frekans dağılımı c)LIDAR 101m ölçümü rüzgâr hızı frekans dağılımı

Rüzgâr güç yoğunluğu karşılaştırıldığında ise LIDAR WPD değerinin 101m'de(Fig 5) aylara göre dağılımları incelendiğinde paralellik göstermektedir. Ancak LIDAR ile gerçekleştirilen 101m'de WPD değeri aylık ortalamalarda anemometrelere göre düşük çıkmıştır. Bu durum sebebi rüzgâr hızının düşük olmasından kaynaklanmamaktadır. LIDAR ve ölçüm istasyonunda ölçülen diğer meteorolojik parametrelerin ölçümlerinin farklılık göstermesinden kaynaklanmaktadır.

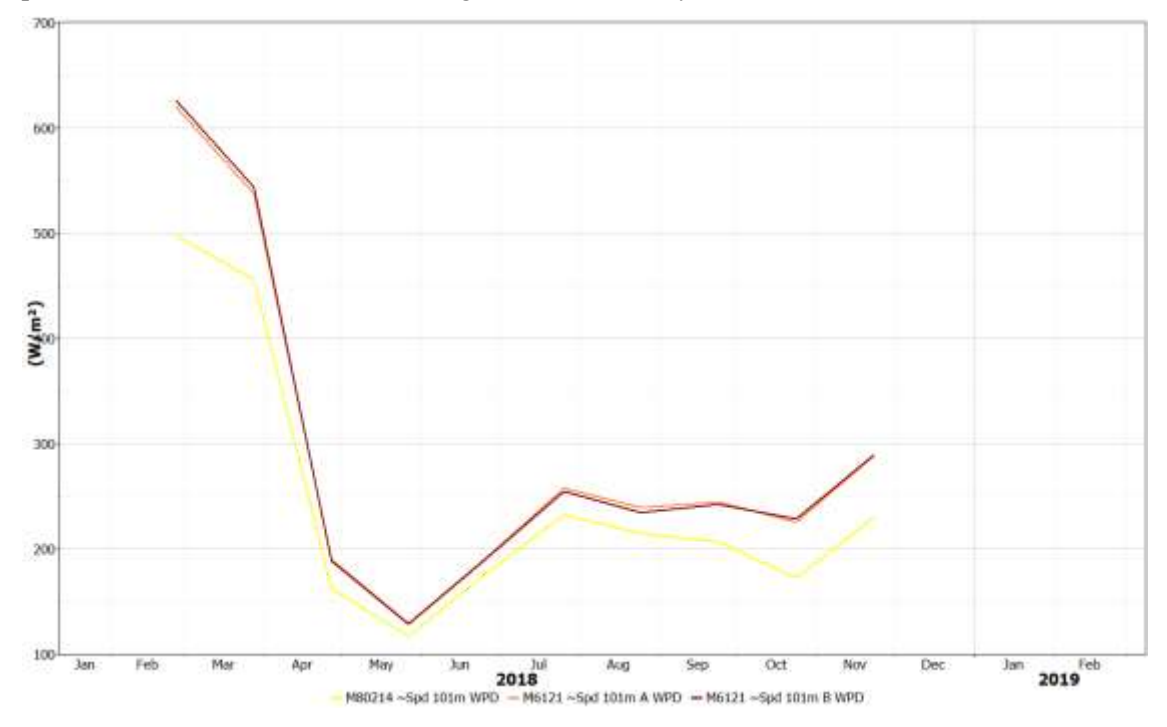


Fig 5: 101m'de gerçekleştirilen LIDAR ve anemometre ölçümlerinin WPD değerlerinin karşılaştırılması

on Innovative Surveys in Positive Sciences 4-5 December 2022 / Full Text Book

#### 4. Sonuç

LIDAR ve anemometre ölçümleri karşılaştırılması ve RSD cihazlarının güvenilirliğinin ortaya konulması amacı birçok araştırma yapılmamıştır ve yapılmaya devam etmektedir. RSD ve anemometre karşılaştırması bir kritere bağlı olmakla birlikte saha özelinde değerlendirmesi gereken bir durumdur. Söz konusu çalışmada aynı koşullarda ve lokasyonda ölçüm yapan LIDAR ve anemometreler birçok yönden karşılaştırılmış ve sonuç olarak;

- Her iki cihazda da aynı yükseklikte gerçekleştirilen rüzgâr hızı değerlerinin ortalamaları kabul edilebilir derecede yakındır.
- Ancak aynı koşullarda ve eş zamanlı yapılan ölçümlerde saatlik ortalamalar farklılık göstermektedir.
- Rüzgâr hız frekans dağılımları karşılaştırıldığında ise yaygın yöntemlerin aksine iki cihaz içinde WAsP ve Openwind yaklaşımları uygunluk sağlamıştır. Bu durum bu tür vaka incelemelerinde saha özelinde farklı yöntemlerinin denenmesinin önemini göstermiştir.
- RSD ve anemometre ölçümlerinin karşılaştırıldığı vakalarda yapılan incelemelerin sadece rüzgâr verileri üzerinde sınırlı kalmaması gerektiği anlaşılmıştır. Bu durum ilerleyen çalışmalarda diğer meteorolojik parametrelerin daha detaylı analiz edilmesi zorunluluğunu ortaya çıkarmıştır.

#### Referanslar

- 1. Lee, J. and F. Zhao, GWEC Global Wind Report-2021. 2021.
- 2. Resources, R.o.T.M.o.E.a.N. *Wind*. 2022 [cited 2022; Available from: https://enerji.gov.tr/eigm-yenilenebilir-enerji-kaynaklar-ruzgar.
- 3. Jakobsen, J.B., et al., Assessment of Wind Conditions at a Fjord Inlet by Complementary Use of Sonic Anemometers and Lidars. Energy Procedia, 2015. **80**: p. 411-421.
- 4. Bowen, A.J. and N.G. Mortensen, *WAsP prediction errors due to site orography*. Riso National Laboratory, 2004: p. 28-29.
- 5. Kim, D., et al., A comparison of ground-based LiDAR and met mast wind measurements for wind resource assessment over various terrain conditions. Journal of Wind Engineering and Industrial Aerodynamics, 2016. **158**: p. 109-121.
- 6. LIDARS, Z. *ZephIR 300*. 2022 [cited 2022; Available from: <a href="https://www.zxlidars.com/new-offshore-wind-lidar-launched-zephir-300m-for-marine/">https://www.zxlidars.com/new-offshore-wind-lidar-launched-zephir-300m-for-marine/</a>.

on Innovative Surveys in Positive Sciences 4-5 December 2022 / Full Text Book

## ANALOG LOWPASS FILTER DESIGN USING PASCAL POLYNOMIALS

## Atilla Uygur

Gebze Technical University, Faculty of Engineering, Electronics Engineering Department, Kocaeli, Turkey.

ORCID ID: 0000-0001-5220-5188

#### **ABSTRACT**

In this study, Pascal polynomials have been utilized in the design of a lowpass filter approximation. Necessary steps to be taken for reaching the approximation has been shown in the paper. The used transfer function is a stopband edge optimized, third order Pascal-type lowpass. It is based on numerical results because no known analytical solutions are possible for the overall design of filters using Pascal polynomial method. The stability criteria for the transfer function have been considered in terms of bounded-input bounded-output (BIBO) stability. The characteristics of some of the Pascal polynomials have also been reviewed with figures. Since the original polynomials in their standart form are not suitable for actual filter design, the required modifications to them have been shown. In the actual circuit implemantation, the scaled and shifted versions of the original polynomials have been used and necessary relations have been shown to satisfy the realizable filter transfer function requirements. Finally, the consequent filter approximation that is based on modified Pascal polynomials have been given with its magnitude and phase characteristics in figures. Its features for the third order lowpass design have been discussed. Although there are some passive filter implementations, active filter realizations are very limited in the literature. In order to further investigate the aspects of the method, using SPICE program, the proposed circuit realization of the transfer function has been given using operational transconductance amplifier (OTA) blocks. The related simulation results and figures have also been added to the paper. It is found that the method of the modified Pascal polynomials and the proposed design of the third order Pascal lowpass filter circuit have performed well. It can be said that according to the simulation figures and the mathematical results, this method is suitable for analog filter realizations, and it can be used as promising alternatives to the classical analog filter approximations.

**Keywords:** Pascal polynomials, analog filters, filter approximation.

#### INTRODUCTION

Filtering in continuous time depends on polynomial approximations due to fact that the ideal response is unreachable by real circuits. There are some well-known approximations used in analog filters such as Butterworth, Chebyshev, etc. They are sometimes called as polynomial approximations because of their transfer functions consisting of only poles without zeros. The approximations that have both poles and zeros are usually called as rational approximations such as inverse Chebyshev or Cauer filters (Van Valkenburg, 2001). One relatively recent addition to these polynomial approximations is the Pascal filter that has some interesting and promising properties such as relatively low, pole Q factors and favorable group delay performance in comparison to the filters utilizing Chebyshev approximation (Dimopoulos, 2012).

Pascal filters were first proposed in (Goodman and Aburdine, 2008). The name comes from the polynomial type used in the filter approximation. Pascal polynomials, in fact, are the basis functions of Discrete Pascal Transform (DPT). This method basically utilizes slighty modified binomial coefficients of the Pascal triangle in the transformation matrix (Aburdene, 2005).

#### RESEARCH AND FINDINGS

Pascal polynomials can be generated by using the equation in (1) where n shows the order.

on Innovative Surveys in Positive Sciences

4-5 December 2022 / Full Text Book

$$P_n(x) = (-1)^n (n!)^{-1} x(x-1)(x-2) \dots (x-n+1)$$
 (1)

Due to the asymmetry, these polynomials are not suitable for analog filtering in their original form, and they should be modified. Fortunately, this modification requires a simple shifting step of changing the variable x by x+(n-1)/2 and this results in the following equation

$$P_n(x) = (-1)^n (n!)^{-1} \left(x + \frac{n-1}{2}\right) \left(x + \frac{n-1}{2} - 1\right) \left(x + \frac{n-1}{2} - 2\right) \dots \left(x + \frac{-n+1}{2}\right)$$
(2)

According to the equation in (2), some of the Pascal polynomials are found and summarized in (3a-f).

For 
$$n = 0$$
,  $P_0(x) = 1$  (3a)

For 
$$n = 1$$
,  $P_1(x) = -x$  (3b)

For 
$$n = 2$$
,  $P_2(x) = \frac{1}{2}x^2 - \frac{1}{8}$  (3c)

For 
$$n = 3$$
,  $P_3(x) = -\frac{1}{6}x^3 + \frac{1}{6}x$  (3d)

For 
$$n = 4$$
,  $P_4(x) = \frac{1}{24}x^4 - \frac{5}{48}x^2 + \frac{3}{128}$  (3e)

For 
$$n = 5$$
,  $P_5(x) = -\frac{1}{120}x^5 + \frac{1}{24}x^3 - \frac{1}{30}x$  (3f)

These polynomials can be used for analog filtering using the conventional squared magnitude transfer function relation as shown in (4) where  $\varepsilon$  is a parameter based on the filter design.

$$|T(j\omega)|^2 = \frac{1}{1+\varepsilon^2 |P_n(j\omega)|^2} \tag{4}$$

It is possible to scale these polynomials for the resulting transfer functions to have the value of 0 dB at unit frequency. Additional scalings can also be done according to the preferences of the designer as detailed in (Dimopoulos, 2012). To investigate the characteristics of the polynomials in (3a-f), four figures for low and high values of variable x for the orders n=2, 3 and n=4, 5 are plotted in Fig. 1a-b and Fig. 2a-b respectively.

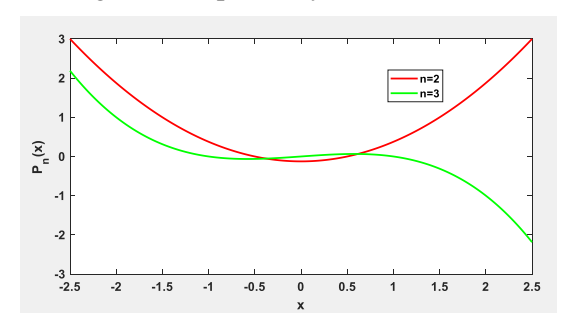


Fig. 1a. Pascal polynomials (n=2, 3 and -2.5<x<2.5) 25<x<25)

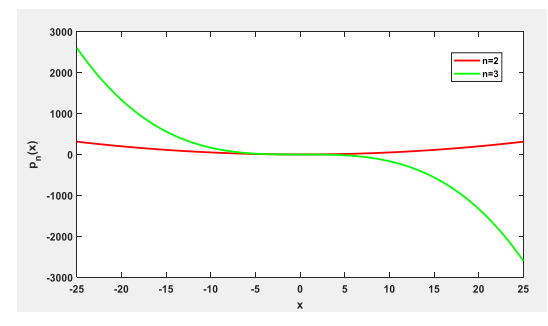


Fig. 1b. Pascal polynomials (n=2, 3 and -

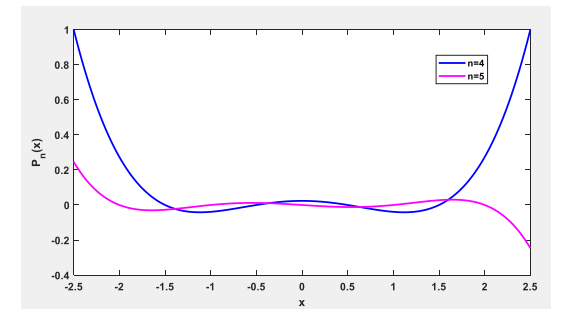


Fig. 2a. Pascal polynomials (n=4, 5 and -2.5<x<2.5) -25<x<25)

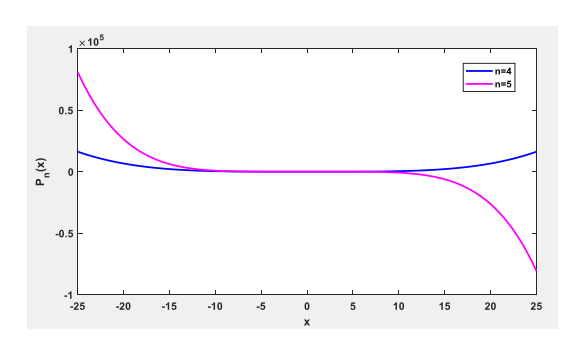


Fig. 2b. Pascal polynomials (n=4, 5 and

on Innovative Surveys in Positive Sciences 4-5 December 2022 / Full Text Book

As it is seen from the figures, polynomials behave oscillatory and they don't change much for low values of x, similar to Chebyshev polynomials, however, when the variable x increases in value, they rapidly get larger values. In particular, this can be said for relatively higher order polynomials as seen in Fig. 2b. In filter approximations, this characteristic can be exploited by some ways. For instance, in low pass filters, the polynomial approximation is desired to have less ripples at the passband, but at the same time, it is required to swifly change its value in the transition band to achieve a steep fall to mimic the behaviour of the ideal "brick wall" low pass filter representation.

Using Pascal polynomials as described in (Dimopoulos, 2012). with proper scaling, the following third order transfer function in (5) is obtained for the stopband edge optimized filter with the parameter  $\alpha_{max}$ =1.5 dB. The denominator is a Hurwitz polynomial. All poles are on the left half plane which is also the condition for BIBO stability.

$$T(s) = \frac{0.38923}{s^3 + 0.84022s^2 + 1.10299s + 0.38923}$$
 (5)

This transfer function is realized by using the following OTA-C filter from the reference (Sun and Filder, 1996) by slightly modifying the circuit as shown in Fig. 3. for the third order response. Additionally, for actual circuit implementation, it is suitably frequency normalized. Its transfer function in terms of capacitor values and OTA transconductances is given in (6) where gm shows OTA transconductances.

$$T(s) = \frac{gm_{a1}}{gm_r} \frac{1}{\frac{c_1c_2c_3}{gm_1gm_2gm_3}s^3 + \frac{c_2c_3}{gm_2gm_3}s^2 + \frac{c_3}{gm_3}s + 1}$$
(6)

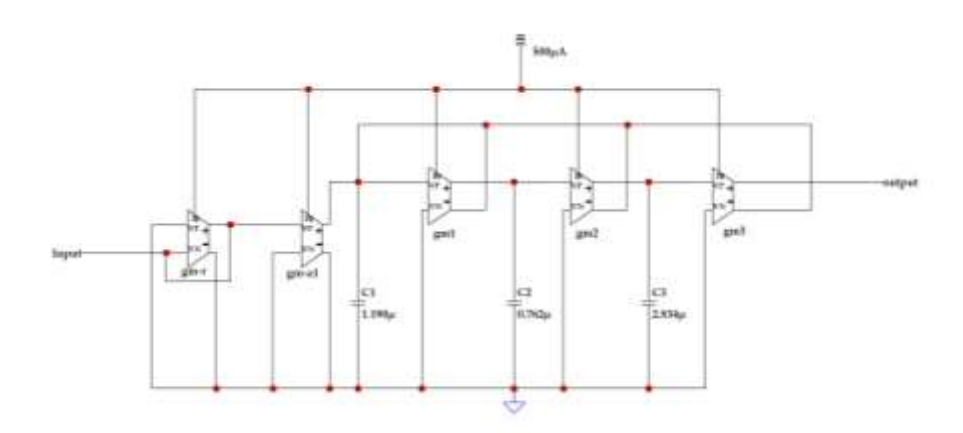
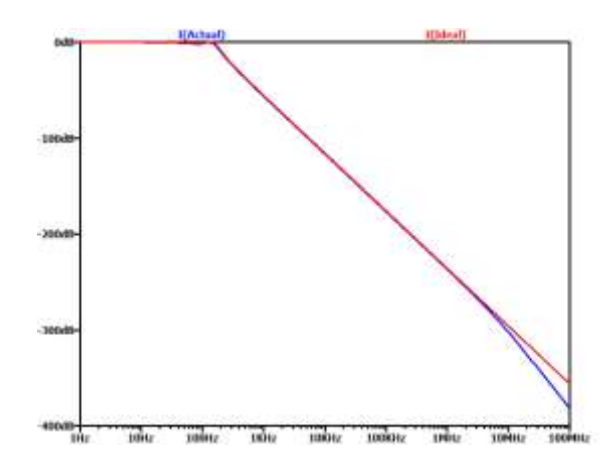


Fig. 3. Third order lowpass active Pascal filter

In the simulations, dual output OTAs are realized by commercially available LM13700 OTAs from Texas Instrument. To obtain dual outputs, two of them are used to generate one dual output OTA. The similar connections can be found in (Taskiran et al, 2019). In SPICE, foundry PSPICE model from Texas Instrument (Texas Instrument, 2022) is used in simulations. However, input offset current model using POLY has caused significant convergence problems in LTSPICE, so it has changed with a B source appropriately. For the biasing currents of OTAs, total current of  $500\mu A$  is used as shown in the figure. It has found that this value helps to roughly tune the filter and alleviate the effects of parasitics of LM13700s. Magnitude and phase responses of the actual filter is given in Fig. 4a and Fig. 4b respectively.

on Innovative Surveys in Positive Sciences

4-5 December 2022 / Full Text Book



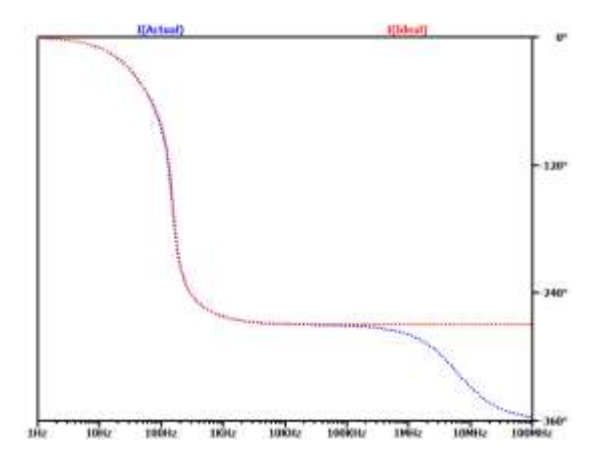


Fig. 4a. The magnitude response

Fig. 4b. The phase response

In addition to AC simulations, the transient response of the actual filter and the ideal one has been given together in Fig. 5. The applied input sinusoidal signal has the amplitude of  $20\mu A$  and the frequency of 100 Hz.

According to SPICE simulations, the filter has behaved very close to the ideal one, particularly after setting a proper current level for IB bias of OTAs. The deviations have started when the frequency has increased. This has definitely expected due to limited bandwidths of the OTA stages. It is also seen from the figure of the transient response below, for the applied sinusoidal signal, the actual circuit response is close to the ideal one.

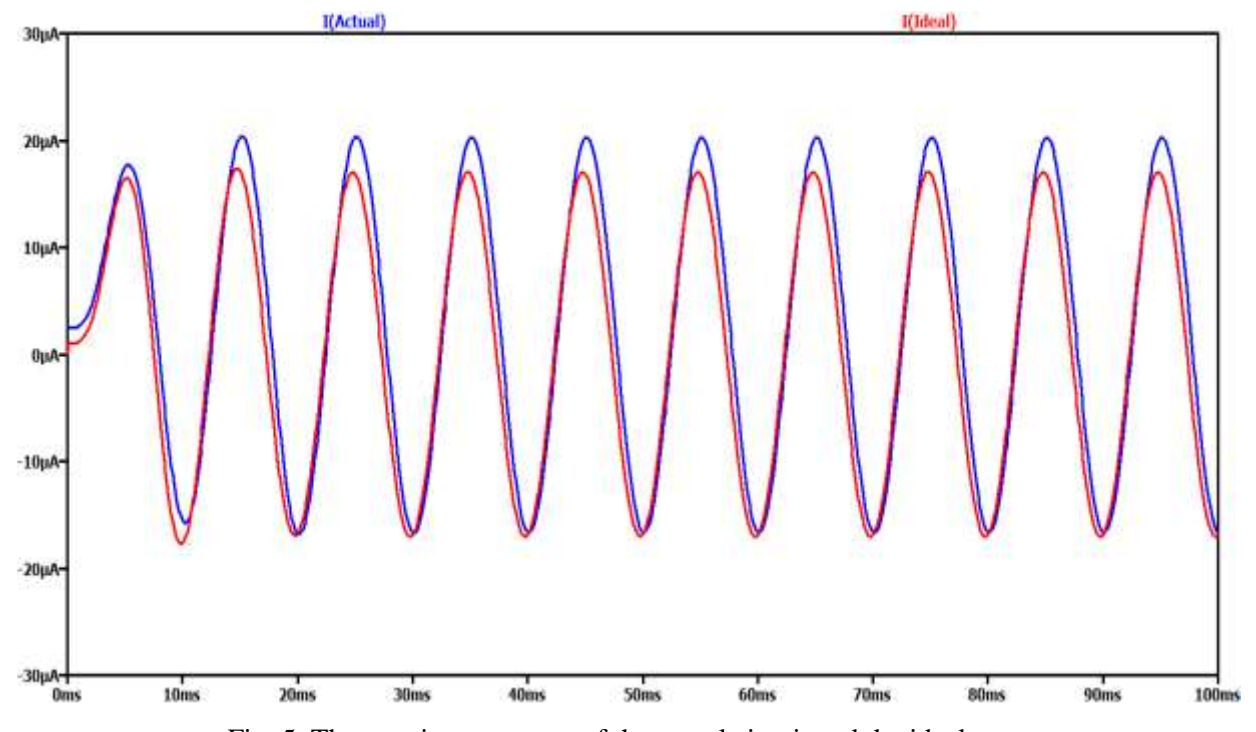


Fig. 5. The transient response of the actual circuit and the ideal one

## **RESULTS**

In this study, the theory of Pascal polynomials that are suitable for analog filter applications has been discussed. A third order lowpass Pascal filter is designed using operational transconductance amplifiers as the active building blocks. For validation, SPICE simulations have been carried out with the model of LM13700 OTA from Texas Instrument. The related AC and transient simulations have been added

on Innovative Surveys in Positive Sciences 4-5 December 2022 / Full Text Book

to the paper. The simulations show that the designed circuit has performed significantly close to the ideal results.

#### REFERENCES

Aburdene, M. F., 2005. The Discrete Pascal Transform and Its Applications, IEEE Signal Processing Letters, vol. 12, no. 7, pp. 493–495.

Dimopoulos, H.G., 2012. Analog electronic filters: theory, design and synthesis, Springer.

Goodman, J. T., and Aburdine, M. F., 2008. Pascal filters. IEEE Transactions on Circuits and Systems—I: Regular Papers, vol. 55. no. 10, pp. 3090–3094.

Sun, Y. and Fidler J.K., 1996. Current-mode OTA-C realization of arbitrary filter characteristics, Electronic Letters, vol. 32, no. 13, pp. 1181–1182.

Taskiran, Z. G. C, Ayten, U. E., and Sedef, H., 2019. Dual-output operational transconductance amplifier-based electronically controllable memristance simulator circuit. Circuits, Systems, and Signal Processing, vol. 38, pp. 26–40.

Texas Instrument, 2022. LM13700 Dual transconductance amplifier with linearizing diodes and buffers. https://www.ti.com/product/LM13700

Van Valkenburg, M. E, 2001. Design of analog filters, Oxford: Oxford University Press.

on Innovative Surveys in Positive Sciences 4-5 December 2022 / Full Text Book

# ÇEKİŞMELİ ÜRETİCİ AĞLAR İÇİN DEĞERLENDİRME METRİKLERİNİN GÖZDEN GEÇİRİLMESİ

#### REVIEW OF EVALUATION METRICS FOR GENERATIVE ADVERSARIAL NETWORKS

#### Canan KOC1

<sup>1</sup> Firat University, Engineering Faculty, Software Engineering, Elazig, Turkey. <sup>1</sup>ORCID ID: 0000-0002-2651-9471

Doç. Dr. Fatih ÖZYURT<sup>2</sup>

 $^2\ First\ University,\ Engineering\ Faculty,\ Software\ Engineering,\ Elazig,\ Turkey.$ 

<sup>2</sup>ORCID ID: 0000-0002-8154-6691

#### **ABSTRACT**

Data sets are a key place for academic studies to be carried out today. At the heart of all of these academic studies, data sets of areas that are difficult to access and difficult to find, especially in the field of health, are sometimes impossible. There are many situations that can be encountered and difficult to overcome, such as the ethics board report or the rare data on diseases. The proposed solution to help eliminate these types of problems is the deep neural network architecture called the Generative Adversarial Networks (GANs). Using the GAN architecture, called the Generator and Discriminator, which consists of two cross-border networks that are in conflict with each other, synthetic data is produced and used data sets of these data in academic and scientific studies, to cover this deficiency. Some quantitative and qualitative metrics are needed to assess the success of synthetic images produced by GANs, which are such an important place in academic studies. In this study, a number of sample-based assessment metrics have been reviewed for GAN. In these metrics reviewed, it was first determined that the manual evaluation of the images generated was a good starting point. Another result was the result that quantitative measurements such as the Start score and the Frechet starting distance could be combined with qualitative evaluation to ensure a strong assessment of the GAN models. Finally, the most important part of the reviews has been concluded that models should be evaluated using the quality of synthetic images produced.

Keywords: Generative Adversarial Networks, synthetic data, evaluation criteria

#### ÖZET

Günümüzde akademik çalışmaların yapılabilmesi için veri setleri önemli bir yer tutmaktadır. Bütün bu akademik çalışmaların temelinde, özellikle sağlık alanında erişilmesi ve bulunması zor olan alanların veri setlerinin oluşturulması çok zor hatta bazen imkânsızdır. Etik kurul raporu ya da nadir hastalıkların az bulunan verileri gibi karşılaşılabilecek ve aşılması güç birçok durum mevcuttur. Bu tarz sorunların ortadan kaldırılmasına yardımcı olmak için önerilen çözüm önerisi ise Çekişmeli Üretici Ağlar (GANs) isimli derin sinir ağları mimarisidir. Üretici ve Ayırıcı olarak adlandırılan ve birbiriyle çekişme halinde olan iki sinir ağından oluşan GAN mimarisi kullanılarak sentetik veriler üretilip, bu verilerden oluşan veri setlerini akademik ve bilimsel çalışmalarda kullanmak bu eksiği kapatmaktır. Akademik çalışmalarda bu kadar önemli bir yer tutan GAN'ların ürettiği sentetik görüntülerin başarısını değerlendirmek için bazı nicel ve nitel metriklere ihtiyaç duyulmaktadır. Bu çalışmada GAN için birkaç örnek tabanlı değerlendirme metriği incelenmiştir. İncelenen bu metriklerde ise oluşturulan görüntülerin manuel olarak değerlendirilmesinin ilk olarak iyi bir başlangıç noktası olduğu saptanmıştır. Sonrasında varılan bir başka sonuçta ise Başlangıç puanı ve Frechet başlangıç mesafesi gibi nicel ölçülerin, GAN modellerinin güçlü bir değerlendirmesini sağlamak için nitel değerlendirme ile birleştirilebileceği sonucu elde edilmiştir. Son olarak ise incelemelerin en önemli kısmı olan modellerin, üretilen sentetik görüntülerin kalitesi kullanılarak değerlendirilmesi gerektiği sonucuna varılmıştır.

Anahtar Kelimeler: Çekişmeli Üretici Ağlar, Sentetik Veri, Değerlendirme Kriterleri

on Innovative Surveys in Positive Sciences 4-5 December 2022 / Full Text Book

#### 1. Introduction

From today's technological perspective, the subject of artificial intelligence is the foundation of work in many different fields. Artificial intelligence technology imitates the human brain to do what needs to be done. Thus, based on the information obtained, it is known as AI, which is defined as a system that can improve itself repeatedly. With the help of artificial intelligence technology, computers process large amounts of data. This allows them to be trained to perform specific tasks by recognizing patterns in the data. For many reasons, such as automating repetitive learning and data discoveries, analyzing more and deeper data using boundary networks with many layers of hidden layers, and getting the most out of data, AI is a key part of scientific studies.

The concept of machine learning came from the question of Alan Turing's "can machines think" in the early 1950 years. The AI concept was initially used by John McCarthy at the Dartmouth Conference in 1956 [1]. In the field of AI, data sets are the basis for the study to train the model. The presence of required tagged or unlabeled data or the presence of sufficient data is an important part of the model's training. In June 2014, Ian Goodfellow developed a deep neural network approach called Generative Adversarial Networks (GANs) to solve the problem of missing or missing data from datasets by producing false data similar to actual data. The GANs consist of two neural networks, called Generator and Discriminator, which are in constant conflict with each other. The main purpose of these two neural networks is to produce the closest false data to reality. The example given in Figure 1 is one of the clearest examples of the GAN approach. From cats, a real cat on the right is a fake cat image on the left. This cat image was created by an artificial intelligence model developed entirely synthetic by researchers at the NVIDIA firm [2].



Figüre 1. Fake and Real Cat Images [2]

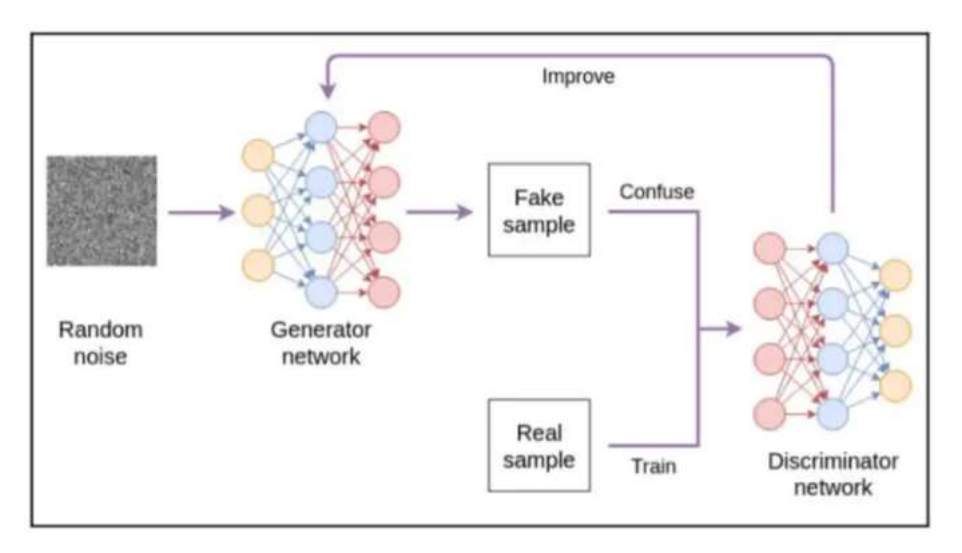
#### 2. Generative Adversarial Networks (GANs)

The Generative Adversarial Networks, which is an unsupervised learning model, or the GANs approach, is one of the latest models to begin their work in the field of manufacturer networks. It is used to create or extract new examples that can be closest to the truth from real data. In addition, it includes finding and learning the layouts or patterns in input data automatically. Since its initial release in 2014, several different variants have been introduced, including DCGAN [3], StackGAN [4], CycleGAN [5], InfoGAN [6], and Age-cGAN [7]. It consists mainly of two neural networks in the event of a conflict. The purpose of these two neural networks, called Generator and Discriminator, is to produce the most realistic false pictures. It's a neural network that tries to produce a fake image, as the name Generator suggests. It receives a simple noise vector as input and produces a false output as a result. The Discriminator, as its name suggests, is trying to distinguish the fake image produced by the Generator from the actual image.

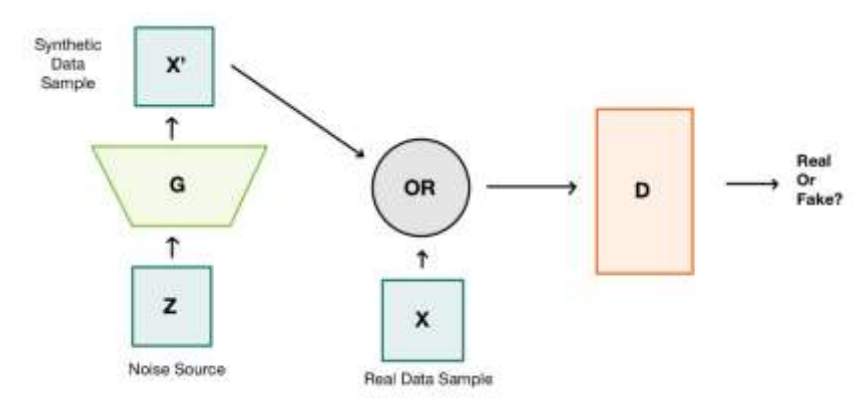
The GAN architecture is similar to a forger and a police officer. The forger tries to generate the closest money to the truth every time, while the police try to identify the counterfeit money. While the forger is the Generator here, the police represent the Discriminator network [8]. In this way, there is an ongoing conflict between both networks. As the training continues, the Generator network acquires images that are closest to actual images. Figure 2 illustrates the structure of a conventional GAN architecture. In Figure 3, "z" represents a noise vector, "x" represents false data, "x" represents actual data, while "G" represents the Generator network and "D" represents a Discriminator network in the GAN structure.

on Innovative Surveys in Positive Sciences

4-5 December 2022 / Full Text Book



Figüre 2. Classic GANs Structure [9]



Figüre 3. Classic GANs Structure (detailed)

The training of neural networks in the GAN model is essentially expressed as a simple MinMax game. This is formulated as the MinMax game below.

Min Max V(D, G) = 
$$[E_{x \sim pdata(x)} [logD(x)]] + [E_{x \sim pz(z)} [log (1 - D(G(z)))]]$$
 [10]  
G D (2)

D(G(z)) possible that the Discriminator network is a fake image

When the part defined in the formula given (1) tries to maximize the output, the part defined as (2) tries to minimize the output. The Discriminator network calculates the possibility that the images coming to it are real and gives them a value between 0 and 1. Here, the probability that the actual image is real is 1, but the possibility that the fake image is real is 0. The educator network is trained using the Loss value, which is the difference between the probability values given and the values it should be.

The values of the Discriminator network are updated in each iteration during the training to draw the value of the actual image to 1 and the value of the fake image to 0. The generator network is trained to evaluate the fact that the fake images it produces are true-to-life, i.e. 1. Therefore, it wants to reduce this error to 0 per iteration. For this error value to be 0, the D (G(z)) must be 1 on the Generator network, so that the Generator network error value is 0. In this way, as the training process progresses, the Discriminator network is more successful in differentiating real and fake images, while the Generator network is successful in producing more realistic fake images.

on Innovative Surveys in Positive Sciences 4-5 December 2022 / Full Text Book

#### 3. Evaluation Metrics

Data generated with GAN must be evaluated for the data setup and reliable use of the data generated. However, there is no Loss function to evaluate a GAN's Generator. Therefore there is no way to continue the training and evaluate the quality of the model only from Loss. Qualitative and quantitative techniques have been developed to assess the performance of an GAN model rather than the Loss function.

## 3.1. Qualitative Metrics

The quality of the counterfeit image produced as a measure is used for the evaluation of the counterfeit images produced. Evaluation of quality is to manually review and evaluate these counterfeit images produced from different iteration steps. This method is one of the most common methods for evaluating GANs. There are some disadvantages to this, as well as the benefits of helping to review and adjust models and being a quick and intuitive way[11]. A review of the quality of the image produced may include the prejudices of the critic. It can also be limited to the number of images. To qualitatively assess, review and explore the hidden area of the images produced by a model, there are methods in the literature such as researching and visualizing network internals, finding the nearest neighbor of the fabricated images, and evaluating the crash of the mode[11]. When applying an assessment and preference decision, the person who evaluates the image is presented with different examples and asked which examples they prefer. As Denton and his friends use, fake images generated for the person who evaluated the image during fast stage categorization are shown shortly. As a result, he is asked to be classified as real or fake [12].

#### 3.2. Quantitative Metrics

The basis of quantitative metrics is based on mathematical expressions and are the methods by which the results are most clearly evaluated. This method is trying to capture quantitative differences between actual and generated images. The greatest benefit of quantitative methods is to ensure accurate evaluation of results. There are multiple quantitative evaluation methods, but the most popular quantitative assessment methods for the GAN approach are the Inception Score (IS) and the Frechet Inception Distance (FID) [13].

#### 3.2.1. Inception Score (IS)

Inception Score was recommended by Salimans and friends in 2016 in the article entitled "Improved Techniques for Training GANs" [13]. The main reason for developing this score is to eliminate subjective human vision for images. There are two main objectives, such images resembling a specific object and producing various objects. Includes the use of a deep learning boundary network model, called a pre-trained Inception V3 model, to classify the images created [14]. The process is to estimate the probability of which class each image is created briefly and then summarize it in Inception Score. The probability mentioned here is a conditional probability, such as class labels. Compared to all other classes, the false images that are produced are classified into a class that has the most powerful properties of the real image, indicating high quality. Therefore, all generated images in the collection must have a less conditional entropy [13].

#### **3.2.2.** Frechet Inception Distance (FID)

This metric used to measure the property distance between the actual image and the images created is defined as a measure of the similarity between the curves [15]. It is used to measure the distance between the two distributions while taking into account the position and sequence of points along the curves. The Inception V3 model is used in this evaluation method as used in the Inception Score. The use of activations from the Inception V3 model to summarize each image is called FID. This activation is taken from the penultimate collection layer. Since the Inception V3 model used here is trained with the ImageNet dataset of various real images, it can be deceptive to apply THE FID to very different datasets [16]. However, THE FID evaluation method was shown to be similar to human decisions and to perform well in terms of discrimination, robustness, and computing efficiency [11].

on Innovative Surveys in Positive Sciences 4-5 December 2022 / Full Text Book

#### 4. Conclusion

The lack of data in the field of AI is resolved by Generative Adversarial Networks (GANs). With the GAN approach, real-life synthetic data is produced, supporting the work. Measuring the proximity and similarity of this counterfeit data produced to the truth is important for the work being carried out. In this study, the methods used to evaluate the counterfeit images produced are mentioned. These evaluation methods are divided into quantitative and qualitative. Qualitative methods are often used to evaluate the quality of images, as finding precise and precise results will also cause problems. The result is that quantitative measurements can be combined with qualitative evaluation to ensure a strong assessment of the GAN models. The most important part of the investigation has been concluded that models should be evaluated using the quality of synthetic images produced.

#### REFERENCES

- [1] *Yapay Zekâ*. Boğaziçi Üniversitesi Yayınevi. (2020, December 17). Retrieved November 28, 2022, from https://www.bounyayin.com/yayin/yapay-zekâ/
- [2] Analyzing and improving the image quality of stylegan. (n.d.). Retrieved November 28, 2022, from https://www.openaccess.thecvf.com/content\_CVPR\_2020/papers/Karras\_Analyzing\_and\_Improving\_t he\_Image\_Quality\_of\_StyleGAN\_CVPR\_2020\_paper.pdf
- [3] Radford, A., Metz, L., & Chintala, S. "Unsupervised representation learning with deep convolutional generative Adversarial Networks". *CoRR*, abs/1511.06434, 2015
- [4] Zhang, H., Xu, T., Li, H., Zhang, S., Wang, X., Huang, X., & Metaxas, D. "Stackgan: Text to photorealistic image synthesis with stacked generative adversarial networks". <u>Institute of Electrical and Electronics Engineers Inc.</u>, 5908-5916, 2017
- [5] Zhu, J.-Y., Park, T., Isola, P., & Efros, A. A. "Unpaired image-to-image translation using cycle-consistent adversarial networks". *IEEE International Conference on Computer Vision (ICCV)*, 2242-2251, 2017
- [6] Chen, X., Duan, Y., Houthooft, R., Schulman, J., Sutskever, I., & Abbeel, P. "Infogan: Interpretable representation learning by information maximizing generative adversarial nets". , *Advanced in Neural Information Processing Systems*, 2016
- [7] Antipov, G., Baccouche, M., & Dugelay, J.-L. "Face aging with conditional generative adversarial networks". , *IEEE Conference on Image Processing (ICIP)*, 2089-2093, 2017
- [8] I. J. Goodfellow, J. Pouget-Abadie, M. Mirza, B. Xu, D. Warde-Farley, S. Ozair, A. Courville, and Y. Bengio. "Generative Adversarial Nets," Advances in Neural Information Processing Systems, 2014, pp. 2672-2680.
- [9] Gunduz, O. (2021, August 23). *Gan (generative adversarial networks)*. Medium. Retrieved November 30, 2022, from https://gnoguz.medium.com/gan-generative-adversarial-networks-75b0c1d0c658
- [10] Generative Adversarial Networks (Gans): An overview of ... (n.d.). Retrieved December 1, 2022, from
- $https://www.researchgate.net/publication/341699736\_Generative\_Adversarial\_Networks\_GANs\_An\_Overview\_of\_Theoretical\_Model\_Evaluation\_Metrics\_and\_Recent\_Developments$
- [11] Ali Borji. Pros and Cons of GAN Evaluation Measures. Oct. 23, 2018. arXiv: 1802.03446 [cs]. URL: http://arxiv.org/abs/1802.03446
- [12] Emily Denton, Soumith Chintala, Arthur Szlam, and Rob Fergus. Deep Generative Image Models Using a Laplacian Pyramid of Adversarial Networks. June 18, 2015. arXiv: 1506. 05751 [cs]. URL: http://arxiv.org/abs/1506.05751
- [13] Salimans, T., Goodfellow, I., Zaremba, W., Cheung, V., Radford, A., & Chen, X. (2016, June 10). *Improved techniques for training gans*. arXiv.org. Retrieved December 2, 2022, from https://arxiv.org/abs/1606.03498

on Innovative Surveys in Positive Sciences 4-5 December 2022 / Full Text Book

- [14] Szegedy, C., Vanhoucke, V., Ioffe, S., Shlens, J., & Wojna, Z. (2015, December 11). *Rethinking the inception architecture for computer vision*. arXiv.org. Retrieved December 2, 2022, from https://arxiv.org/abs/1512.00567
- [15] Wikimedia Foundation. (2022, October 21). *Fréchet distance*. Wikipedia. Retrieved December 2, 2022, from <a href="https://en.wikipedia.org/wiki/Fr%C3%A9chet\_distance">https://en.wikipedia.org/wiki/Fr%C3%A9chet\_distance</a>
- [16] Shaohui Liu, Yi Wei, Jiwen Lu, and Jie Zhou. An Improved Evaluation Framework for Generative Adversarial Networks. July 19, 2018. arXiv: 1803.07474 [cs]. URL: http://arxiv.org/abs/1803.07474

on Innovative Surveys in Positive Sciences 4-5 December 2022 / Full Text Book

# α(gg)\*COMPACT SPACES IN TOPOLOGICAL SPACES

Asst. Prof. Dr. Raja Mohammad LATIF

Department of Mathematics and Natural Sciences

Prince Mohammad Bin Fahd University

Al Khobar, Kingdom of Saudi Arabia

ORCID NO: 0000-0003-3140-9581

#### **ABSTRACT**

In 2022, T. Shyla Isaq Mary and G. Abhirami introduced and studied basic properties of a new class of sets in topological spaces namely alpha generalization of generalized star closed  $(\alpha(gg)*-closed)$  sets. We will extend the concept of compactness via  $\alpha(gg)*-open$  sets by introducing  $\alpha(gg)*-compactness$  in topological spaces and will investigate their relationships among them as well as their characterizations by making use of generalized mappings including  $\alpha(gg)*-continuous$  functions and  $\alpha(gg)*-irresolute$  functions. The objective of this chapter is to introduce the new concepts called  $\alpha(gg)*-compact$  space,  $\alpha(gg)*-Lindelof$  space, countably  $\alpha(gg)*-compact$  space, almost  $\alpha(gg)*-compact$  space, and mildly  $\alpha(gg)*-compact$  space in topological spaces and investigate their fundamental properties.

2020 AMS Subject Classification. Primary: 54B05, 54D20, 54D30.

**Key Words and Phrases:** Topological space,  $\alpha(gg)$ \*-closed set,  $\alpha(gg)$ \*-open set,  $\alpha(gg)^*$ -compact space,  $\alpha(gg)^*$ -Lindelof space, countably  $\alpha(gg)^*$ -compact space, almost  $\alpha(gg)^*$ -compact space, mildly  $\alpha(gg)^*$ -compact space.

#### 1. INTRODUCTION

The concept of supra topology was introduced by A. S. Mashhour et al [20] in the year 1983. They studied s-continuous functions and s\*continuous functions. In 2008, R. Devi et al [8] introduced the concept of supra  $\alpha$ -open sets and supra  $\alpha$ -continuous mappings. Jamal M. Mustafa [24] studied supra b-compact and supra b-Lindelof spaces. Vidyarani et al [40] introduced the concept of supra N-compact, countably supra N-compact, supra N-Lindelof and investigated their relationships using the concept of continuity. In 2013, Missier and Rodrigo [22] introduced new class of sets in general topology called  $\alpha$ -open (supra  $\alpha$ -open) sets. In 2019, Amir A. Mohammed and Beyda S. Abdullah [23] introduced a new class of open sets in a topological space called ii-open sets and investigated its fundamental properties and studied some properties and several characterizations of this class including the relation of ii-open sets with many other classes of open sets. They showed that the family of ii-open subsets of a topological space (X,  $\tau$ ) forms a topology on X which is finer than  $\tau$ . In 2022,

## on Innovative Surveys in Positive Sciences 4-5 December 2022 / Full Text Book

T. Shyla Isaq Mary and G. Abhirami [19] introduced and studied basic properties of a new class of sets in topological spaces namely alpha generalization of generalized star closed  $(\alpha(gg)*-closed)$  sets. We will extend the concept of compactness via  $\alpha(gg)*-compactness$  by introducing  $\alpha(gg)*-compactness$  in topological spaces and will investigate their relationships among them as well as their characterizations by making use of generalized mappings including  $\alpha(gg)*-continuous$  functions and  $\alpha(gg)*-compact$  functions. The objective of this chapter is to introduce the new concepts called  $\alpha(gg)*-compact$  space,  $\alpha(gg)*-compact$  space, countably  $\alpha(gg)*-compact$  space, almost  $\alpha(gg)*-compact$  space, and mildly  $\alpha(gg)*-compact$  space in topological spaces and investigate fundamental properties.

#### 2. PRELIMINARIES

The  $(X, \tau)$  and  $(Y, \sigma)$  (or simply, X and Y) denote topological spaces on which no separation axioms are assumed unless explicitly stated and  $f:(X,\tau)\to (Y,\sigma)$  means a mapping f from a topological space X to a topological space Y. A subset A of a topological space  $(X,\tau)$  is said to be open if  $A\in \tau$ . A subset A of a topological space X is said to be closed if the set X-A is open. The interior of a subset A of a topological space X is defined as the union of all open sets contained in A. It is denoted by Int(A). The closure of a subset A of a topological space X is defined as the intersection of all closed sets containing A. It is denoted by Cl(A). If U is a set and X is a point in X, then N(X), and  $U^c$  denote respectively, the neighborhood system of X, and the complement of U, respectively. We start with recalling the following definitions and results [19], which are necessary for this study in the sequel.

**Definition 2.1.** A subset A of a topological space  $(X, \tau)$  is said to be *semi-open* set if  $A \subseteq Cl[Int(A)]$  and semi-closed set if  $Int[Cl(A)] \subseteq A$ .

**Definition 2.2.** A subset A of a topological space  $(X, \tau)$  is said to be *regular-open* set if A = Int[Cl(A)] and regular-closed set if Cl[Int(A)] = A.

**Definition 2.3.** A subset A of a topological space  $(X, \tau)$  is said to be regular *semi-open* set if there is a regular open set U such that  $U \subseteq A \subseteq Cl(U)$ .

**Definition 2.4.** A subset A of a topological space  $(X,\tau)$  is said to be an  $\alpha$ -open set if  $A \subseteq Int \lceil Cl(Int(A)) \rceil$  and an  $\alpha$ -closed set if  $Cl \lceil Int(Cl(A)) \rceil \subseteq A$ .

**Definition 2.5.** A subset A of a topological space  $(X,\tau)$  is said to be a generalized closed (briefly g-closed) set if  $Cl(A)\subseteq U$ , whenever  $A\subseteq U$  and U is open in  $(X,\tau)$ .

# on Innovative Surveys in Positive Sciences 4-5 December 2022 / Full Text Book

**Definition 2.6.** A subset A of a topological space  $(X,\tau)$  is said to be generalization of generalized closed (briefly gg-closed) set if  $gCl(A) \subseteq U$  whenever  $A \subseteq U$  and U is regular semi-open.

**Definition 2.7.** A subset A of a topological space  $(X,\tau)$  is said to be generalization star closed (briefly (gg) \*closed) set if  $rCl(A) \subseteq U$ , whenever  $A \subseteq U$  and U is (gg) \*open in  $(X,\tau)$ . The complement of a (gg) \*closed set is called a (gg) \*open set.

**Definition 2.8.** A subset A of a topological space  $(X,\tau)$  is said to be an  $\alpha g$ -closed set if  $\alpha Cl(A) \subseteq U$ , whenever  $A \subseteq U$  and U is open in  $(X,\tau)$ . The complement of an  $\alpha g$ -closed set is called an  $\alpha g$ -open set.

**Definition 2.9.** A subset A of a topological space  $(X,\tau)$  is said to be alpha generalization of **generalization star closed** (briefly  $\alpha(gg) \star closed$ ) set if  $\alpha Cl(A) \subseteq U$ , whenever  $A \subseteq U$  and U is  $(gg) \star open in <math>(X,\tau)$ . The complement of  $\alpha(gg) \star closed$  set is called  $\alpha(gg) \star open set$ . The collection of all  $\alpha(gg) \star open sets$  is denoted by  $\alpha(gg) \star O(X,\tau)$ .

**Theorem 2.10.** Let  $(X, \tau)$  be a topological space. Then, every closed set is  $\alpha(gg) \star closed$  set.

**Proof.** Let A be a closed set in  $(X,\tau)$ . Let  $A \subseteq H$  and H is  $(gg) \star open$ . Since A is closed  $Cl(A) \subseteq H$ . But  $\alpha Cl(A) \subseteq Cl(A) \subseteq H \Rightarrow \alpha Cl(A) \subseteq H$ . Hence A is  $\alpha(gg) \star closed$ 

**Definition 2.11.** The union of (respectively intersection) of all  $\alpha(gg)$ \*open (respectively  $\alpha(gg)$ \*closed) sets, each contained in (respectively containing) a set A of X is called the  $\alpha(gg)$ \*interior (respectively  $\alpha(gg)$ \*closure) of A, which is denoted by  $\alpha(gg)$ \*Int(A) (respectively  $\alpha(gg)$ \*Cl(A)).

**Theorem 2.12.** The arbitrary intersection of any family of  $\alpha(gg) \star closed$  sets is a  $\alpha(gg) \star closed$  set.

**Proof.** Let  $\Gamma = \{A_i : i \in I\}$  be a family of  $\alpha(gg) \star closed$  sets in a topological space  $(X, \tau)$ . Let U be a  $(gg) \star open$  set in X such that  $A_i \subseteq U$  for each  $i \in I$ . Then  $\alpha Cl(A) \subseteq U$  for each  $i \in I$ . This implies that  $\alpha Cl(I_{i \in I}A_i) \subseteq I_{i \in I}\alpha Cl(A_i) \subseteq U$ . Thus  $\alpha Cl(I_{i \in I}A_i) \subseteq U$ . Hence  $I \Gamma = I_{i \in I}A_i$  is  $\alpha(gg) \star closed$ .

**Theorem 2.13.** The arbitrary union of any family of  $\alpha(gg) \star open$  sets is an  $\alpha(gg) \star open$  set.

**Proof.** The proof is easy by using complements and Theorem 2.12 and DeMorgan's Law.

## on Innovative Surveys in Positive Sciences 4-5 December 2022 / Full Text Book

**Theorem 2.14.** Let  $(X, \tau)$  be a topological space. Then every  $\alpha$ -closed set is  $\alpha(gg) \star closed$  set.

**Proof.** Let A be an  $\alpha$ -closed closed set in  $(X, \tau)$ . Let  $A \subseteq U$  and U is (gg) topen. Since A is  $\alpha$ -closed,  $\alpha Cl(A) = A \subseteq U$ . This implies  $\alpha Cl(A) \subseteq U$ . Hence A is  $\alpha(gg)$  tolosed

**Theorem 2.15.** Let  $(X,\tau)$  be a topological space and  $A, B \subseteq X$ . Then the following assertions are true.

- (1)  $\alpha(gg) \star Int(A)$  is the union of all  $\alpha(gg) \star open$  subsets of A.
- (2) A is  $\alpha(gg) \star open$  if and only if  $\alpha(gg) \star Int(A) = A$ .
- (3)  $A \subseteq \alpha(gg) \star Cl(A) \subseteq Cl(A)$ .
- (4)  $Int(A) \subseteq \alpha(gg) \star Int(A) \subseteq A$ .
- (5) If  $A \subseteq B$ , then  $\alpha(gg) \star Cl(A) \subseteq \alpha(gg) \star Cl(B)$ .
- (6) A is  $\alpha(gg) \star closed$  if and only if  $\alpha(gg) \star Cl(A) = A$ .
- $(7) \alpha(gg) \star Cl [\alpha(gg) \star Cl(A)] = \alpha(gg) \star Cl(A).$
- (8) If  $A \subseteq B$ , then  $\alpha(gg) *Int(A) \subseteq \alpha(gg) *Int(B)$ .
- $(9) \alpha(gg) \star Int[\alpha(gg) \star Int(A)] = \alpha(gg) \star Int(A).$
- (10)  $X \lceil \alpha(gg) \star Int(A) \rceil = \alpha(gg) \star Cl(X A)$ .
- (11)  $X \lceil \alpha(gg) \star Cl(A) \rceil = \alpha(gg) \star Int(X A)$ .
- (12)  $x \in \alpha(gg) \star Cl(A)$  if and only if for every  $\alpha(gg) \star open$  set U containing  $x, U \cap A \neq \emptyset$ .
- (13)  $\bigcup_{\lambda \in \Lambda} \alpha(gg) \star Cl(U_{\lambda}) \subseteq \alpha(gg) \star Cl(\bigcup_{\lambda \in \Lambda} U_{\lambda}).$
- $(14) \alpha(gg) \star Int(A \cap B) \subseteq \lceil \alpha(gg) \star Int(A) \rceil \cap \lceil \alpha(gg) \star Int(B) \rceil.$

**Definition 2.16.** A subset A of a topological space  $(X, \tau)$  is called an  $\alpha(gg) \star neighbourhood$  of a point X in X if there exists an  $\alpha(gg) \star open$  set U in X such that  $x \in U \subseteq A$ .

The set of all  $\alpha(gg) \star neighbourhoods$  of an element X in X will be denoted by:  $\alpha(gg) \star N_x = \alpha(gg) \star N_x(X) = \{A \subseteq X : A \text{ is an } \alpha(gg) \star neighbourhood \text{ of } x\}.$ 

## on Innovative Surveys in Positive Sciences 4-5 December 2022 / Full Text Book

**Proposition 2.17.** A subset A of a topological space  $(X, \tau)$  is  $\alpha(gg) \star open$  if and only if it is an  $\alpha(gg) \star neighbourhood$  of each of its points.

**Proof.** If A is  $\alpha(gg) * open$  in X, then  $x \in A \subseteq A$  for each  $x \in A$ . Thus A is an  $\alpha(gg) * neighbourhood$  of each of its points. Conversely, suppose that A is an  $\alpha(gg) * neighbourhood$  of each of its points. Then for each  $x \in A$ , there exists an  $\alpha(gg) * open$  set  $U_x$  in X such that  $x \in U_x \subseteq A$ . Hence  $\bigcup_{x \in A} U_x \subseteq A$ . Since  $A \subseteq \bigcup_{x \in A} U_x$ , therefore  $A = \bigcup_{x \in A} U_x$ . Thus A is an  $\alpha(gg) * open$  set in X, since it is a union of  $\alpha(gg) * open$  sets.

**Definition 2.18.** A mapping  $f:(X,\tau)\to (Y,\sigma)$  is called  $\alpha(gg)$ \*\*irresolute at a point  $x\in X$  if for all  $\alpha(gg)$ \*\*open subsets V in Y containing f(x), there is an  $\alpha(gg)$ \*\*open subset U of X such that  $x\in U$  and f(U) is a subset of V. The function f will be called  $\alpha(gg)$ \*\*irresolute if f is  $\alpha(gg)$ \*\*irresolute at each point  $x\in X$ .

**Theorem 2.19.** Let  $f:(X,\tau)\to(Y,\sigma)$  be a function. Then the following statements are equivalent.

- (1) f is  $\alpha(gg) \star irresolute$ .
- (2) For each  $x \in X$  and each  $\alpha(gg) *neighbourhood V$  of f(x) in Y, there is a  $\alpha(gg) *neighborhood U$  of x such that  $f(U) \subseteq V$ .
- (3) The inverse image of every  $\alpha(gg) \star closed$  subset of Y is an  $\alpha(gg) \star closed$  subset of X.
- (4) The inverse image of every  $\alpha(gg) \star open$  subset of Y is an  $\alpha(gg) \star open$  subset of X.

**Definition 2.20.** A function  $f:(X,\tau)\to (Y,\sigma)$  is called  $\alpha(gg)\star continuous$  if  $f^{-1}(V)$  is  $\alpha(gg)\star open$  set in X for every open set V in Y.

**Proposition 2.21.** A function  $f:(X,\tau)\to (Y,\sigma)$  is called  $\alpha(gg)\star continuous$  if and only if  $f^{-1}(V)$  is  $\alpha(gg)\star closed$  set in X for every closed set V in Y.

**Definition 2.22.** A function  $f:(X,\tau)\to (Y,\sigma)$  is called  $Pre-\alpha(gg)*open$  if and only if the image set f(U) is  $\alpha(gg)*open$  set in Y for every  $\alpha(gg)*open$  set U in X.

**Proposition 2.23.** A bijection function  $f:(X,\tau)\to (Y,\sigma)$  is called  $\alpha(gg)$ \*homeomorphism if f is  $pre-\alpha(gg)$ \*open and  $\alpha(gg)$ \*irreseolute.

# on Innovative Surveys in Positive Sciences 4-5 December 2022 / Full Text Book

**Definition 2.24.** A function  $f:(X,\tau)\to (Y,\sigma)$  is called perfectly  $\alpha(gg)\star continuous$  if the inverse image  $f^{-1}(V)$  of every  $\alpha(gg)\star open$  set V of Y is both open and closed in X.

**Definition 2.25.** A function  $f:(X,\tau)\to (Y,\sigma)$  is called strongly  $\alpha(gg)\star continuous$  if the inverse image  $f^{-1}(V)$  of every  $\alpha(gg)\star open V$  in Y is open in X.

# 3. α(gg)★COMPACT SPACES

**Definition 3.1.** A collection  $\{A_i : i \in I\}$  of  $\alpha(gg) * open$  sets in a topological space  $(X, \tau)$  is called an  $\alpha(gg) * open$  cover of a subset B of X if  $B \subseteq U\{A_i : i \in I\}$  holds.

**Definition 3.2.** A topological space  $(X, \tau)$  is called  $\alpha(gg) \star compact$  if every  $\alpha(gg) \star open$  cover of X has a finite subcover.

**Definition 3.3.** A subset B of a topological space  $(X, \tau)$  is said to be  $\alpha(gg) \star compact$  relative to  $(X, \tau)$  if, for every collection  $\{A_i : i \in I\}$  of  $\alpha(gg) \star open$  subsets of X such that  $B \subseteq U\{A_i : i \in I\}$ , there exists a finite subset  $I_0$  of I such that  $B \subseteq U\{A_i : i \in I_0\}$ .

**Definition 3.4.** A subset B of a topological space  $(X, \tau)$  is said to be  $\alpha(gg) \star compact$  if B is  $\alpha(gg) \star compact$  as a subspace of X.

**Definition 3.5.** Every  $\alpha(gg) \star compact$  space is compact.

**Proof.** Let  $\{A_i : i \in I\}$  be an open cover of  $(X, \tau)$ . Since every open set in X is  $\alpha(gg) \star open$  in X. So  $\{A_i : i \in I\}$  is an  $\alpha(gg) \star open$  cover of  $(X, \tau)$ . Since  $(X, \tau)$  is  $\alpha(gg) \star compact$ ,  $\alpha(gg) \star open$  cover  $\{A_i : i \in I\}$  of  $(X, \tau)$  has a finite sub cover say  $\{A_i : i = 1, 2, 3, ..., n\}$  for X. Hence  $(X, \tau)$  is a compact space.

**Definition 3.6.** Every  $\alpha(gg) * closed$  subset of an  $\alpha(gg) * compact$  space  $(X, \tau)$  is  $\alpha(gg) * compact$  relative to X.

**Proof.** Let A be an  $\alpha(gg) \star closed$  subset of a topological space  $(X, \tau)$ . Then  $A^c$  is  $\alpha(gg) \star open$  in  $(X, \tau)$ . Let  $\Gamma = \{A_i : i \in I\}$  be an  $\alpha(gg) \star open$  cover of A by  $\alpha(gg) \star open$  subsets of  $(X, \tau)$ . Then  $\Gamma^* = \Gamma \cup \{A^c\}$  is an  $\alpha(gg) \star open$  cover of  $(X, \tau)$ . That is  $X = (\bigcup_{i \in I} A_i) \cup A^c$ . By hypothesis,  $(X, \tau)$  is an  $\alpha(gg) \star compact$  space and hence  $\Gamma^*$  is reducible to a finite subcover of  $(X, \tau)$  say  $X = (\bigcup_{i \in I_0} A_i) \cup A^c$  for some finite subset  $I_0$  of I.

# on Innovative Surveys in Positive Sciences 4-5 December 2022 / Full Text Book

But A and  $A^c$  are disjoint. Hence  $A \subseteq U\{A_i : i \in I_0\}$ . Thus  $\alpha(gg) * open$  cover  $\Gamma = \{A_i : i \in I\}$  of A contains a finite subcover. Hence A is  $\alpha(gg) * compact$  relative to  $(X, \tau)$ .

**Theorem 3.7.** An  $\alpha(gg)$ \*continuous image of an  $\alpha(gg)$ \*compact space is compact.

**Proof.** Let  $f:(X,\tau)\to (Y,\sigma)$  be an  $\alpha(gg)$ \*-continuous mapping from an  $\alpha(gg)$ \*-compact topological space  $(X,\tau)$  onto a topological space  $(Y,\sigma)$ . Let  $\Gamma=\{A_i:i\in I\}$  be an open cover of Y. Therefore  $f^{-1}(\Gamma)=\{f^{-1}(A_i):i\in I\}$  is an  $\alpha(gg)$ \*-copen cover of X, as f is  $\alpha(gg)$ \*-continuous. Since X is  $\alpha(gg)$ \*-compact, the  $\alpha(gg)$ \*-open cover  $f^{-1}(\Gamma)=\{f^{-1}(A_i):i\in I\}$  of X, has a finite subcover say  $\{f^{-1}(A_i):i=1,2,3,...,n\}$ . Therefore  $X=\bigcup_{i=1}^n f^{-1}(A_i)$ , which implies  $Y=f(X)=\bigcup_{i=1}^n A_i$ . That is  $\{A_i:i=1,2,3,...,n\}$  is a finite subcover of  $\Gamma=\{A_i:i\in I\}$ . Hence  $(Y,\sigma)$  is compact.

**Theorem 3.8.** Suppose that a function  $f:(X,\tau)\to (Y,\sigma)$  is  $\alpha(gg)$ \*irresolute and a subset S of X is  $\alpha(gg)$ \*compact relative to  $(X,\tau)$ , then the image f(S) is  $\alpha(gg)$ \*compact relative to  $(Y,\sigma)$ .

**Proof.** Let  $\Gamma = \{A_i : i \in I\}$  be a collection of  $\alpha(gg) \star open$  subsets of  $(Y, \sigma)$ , such that  $f(S) \subseteq \mathbf{U}\{A_i : i \in I\}$ . Since f is  $\alpha(gg) \star irresolute$ . So  $S \subseteq \mathbf{U}\{f^{-1}(A_i) : i \in I\}$ , where  $\{f^{-1}(A_i) : i \in I\} \subseteq \alpha(gg) \star O(X, \tau)$ . Since S is  $\alpha(gg) \star compact$  relative to  $(X, \tau)$ , there exists a finite sub collection  $\{f^{-1}(A_1), f^{-1}(A_2), \ldots, f^{-1}(A_n)\}$  such that  $S \subseteq \mathbf{U}\{f^{-1}(A_1), f^{-1}(A_2), \ldots, f^{-1}(A_n)\}$ . That is  $f(S) \subseteq \mathbf{U}\{A_1, A_2, \ldots, A_n\}$ . Hence f(S) is  $\alpha(gg) \star compact$  relative to  $(Y, \sigma)$ .

**Theorem 3.9.** Suppose that a mapping  $f:(X,\tau)\to (Y,\sigma)$  is strongly  $\alpha(gg)\star continuous$  mapping from a compact space  $(X,\tau)$  onto a topological space  $(Y,\sigma)$ . Then  $(Y,\sigma)$  is  $\alpha(gg)\star compact$ .

**Proof.** Let  $\{A_i : i \in I\}$  be an  $\alpha(gg) \star open$  cover of  $(Y, \sigma)$ . Since f is strongly  $\alpha(gg) \star continuous$ ,  $\{f^{-1}(A_i) : i \in I\}$  is an open cover of  $(X, \tau)$ . Again, since  $(X, \tau)$  is compact, the open cover  $\{f^{-1}(A_i) : i \in I\}$  of  $(X, \tau)$  has a finite sub cover say  $\{f^{-1}(A_i) : i = 1, 2, 3, ..., n\}$ . Therefore  $X = U\{f^{-1}(A_i) : i = 1, 2, 3, ..., n\}$ , which implies  $f(X) = U\{A_i : i = 1, 2, 3, ..., n\}$ , so that

# on Innovative Surveys in Positive Sciences 4-5 December 2022 / Full Text Book

 $Y = U\{A_i : i = i = 1, 2, 3, ..., n\}$ . Thus  $\{A_1, A_2, ..., A_n\}$  is a finite subcover of  $\{A_i : i \in I\}$  for  $(Y, \sigma)$ . Hence  $(Y, \sigma)$  is  $\alpha(gg) \star compact$ .

**Theorem 3.10.** Suppose that a mapping  $f:(X,\tau)\to (Y,\sigma)$  is perfectly  $\alpha(gg)\star continuous$  mapping from a compact space  $(X,\tau)$  onto a topological space  $(Y,\sigma)$ . Then  $(Y,\sigma)$  is  $\alpha(gg)\star compact$ .

**Proof.** Let  $\{A_i : i \in I\}$  be an  $\alpha(gg) \star open$  cover of  $(Y, \sigma)$ . Since f is perfectly  $\alpha(gg) \star continuous$ ,  $\{f^{-1}(A_i) : i \in I\}$  is an open cover of  $(X, \tau)$ . Again, since  $(X, \tau)$  is compact, the open cover  $\{f^{-1}(A_i) : i \in I\}$  of  $(X, \tau)$  has a finite sub cover say  $\{f^{-1}(A_i) : i = 1, 2, 3, ..., n\}$ . Therefore  $X = U\{f^{-1}(A_i) : i = 1, 2, 3, ..., n\}$ , which implies  $f(X) = U\{A_i : i = 1, 2, 3, ..., n\}$ , so that  $Y = U\{A_i : i = 1, 2, 3, ..., n\}$ . That is  $\{A_1, A_2, ..., A_n\}$  is a finite subcover of  $\{A_i : i \in I\}$  for  $(Y, \sigma)$ . Hence  $(Y, \sigma)$  is  $\alpha(gg) \star compact$ .

**Theorem 3.11.** Suppose that a function  $f:(X,\tau)\to (Y,\sigma)$  is an  $\alpha(gg)\star irresolute$  mapping from an  $\alpha(gg)\star compact$  space  $(X,\tau)$  onto a topological space  $(Y,\sigma)$ . Then  $(Y,\sigma)$  is  $\alpha(gg)\star compact$ .

**Proof.** Let  $f:(X,\tau)\to (Y,\sigma)$  be an  $\alpha(gg)$ \*irresolute mapping from an  $\alpha(gg)$ \*compact space  $(X,\tau)$  onto a topological space  $(Y,\sigma)$ . Let  $\{A_i:i\in I\}$  be an  $\alpha(gg)$ \*copen cover of  $(Y,\sigma)$ . Then  $\{f^{-1}(A_i):i\in I\}$  is an  $\alpha(gg)$ \*copen cover of  $(X,\tau)$ , since f is  $\alpha(gg)$ \*irresolute. As  $(X,\tau)$  is  $\alpha(gg)$ \*compact, the  $\alpha(gg)$ \*copen cover  $\{f^{-1}(A_i):i\in I\}$  of  $(X,\tau)$  has a finite sub cover say  $\{f^{-1}(A_i):i=1,2,3,...,n\}$ . Therefore  $X=U\{f^{-1}(A_i):i=1,2,3,...,n\}$ , which implies  $f(X)=U\{A_i:i=1,2,3,...,n\}$ , so that  $Y=U\{A_i:i=1,2,3,...,n\}$ . That is  $\{A_1,A_2,...,A_n\}$  is a finite subcover of  $\{A_i:i\in I\}$  for  $(Y,\sigma)$ . Hence  $(Y,\sigma)$  is  $\alpha(gg)$ \*compact.

**Theorem 3.12.** If  $(X, \tau)$  is compact and every  $\alpha(gg) * closed$  set in X is also closed in X, then  $(X, \tau)$  is  $\alpha(gg) * compact$ .

**Proof.** Let  $\{A_i : i \in I\}$  be an  $\alpha(gg) \star open$  cover of X. Since every  $\alpha(gg) \star closed$  set in X is also closed in X. Thus  $\{X - A_i : i \in I\}$  is a closed cover of X and hence  $\{A_i : i \in I\}$  is an open

## on Innovative Surveys in Positive Sciences 4-5 December 2022 / Full Text Book

cover of X. Since  $(X, \tau)$  is compact. So there exists a finite subcover  $\{A_i : i = 1, 2, 3, ..., n\}$  of  $\{A_i : i \in I\}$  such that  $X = U\{A_i : i = 1, 2, 3, ..., n\}$ . Hence  $(X, \tau)$  is  $\alpha(gg) \star compact$ .

**Theorem 3.13.** A topological space  $(X, \tau)$  is  $\alpha(gg) \star compact$  if and only if every family of  $\alpha(gg) \star closed$  sets of  $(X, \tau)$  having finite intersection property has a nonempty intersection.

**Proof.** Suppose  $(X, \tau)$  is  $\alpha(gg) \star compact$ . Let  $\{A_i : i \in I\}$  be a family of  $\alpha(gg) \star closed$  sets with finite intersection property. Suppose  $\prod_{i \in I} A_i = \phi$ , then  $X - \mathbf{I} \left( \{A_i : i \in I\} \right) = X$ . This implies  $\mathbf{U} \left\{ (X - A_i) : i \in I \right\} = X$ . Thus the cover  $\left\{ (X - A_i) : i \in I \right\}$  is an  $\alpha(gg) \star copen$  cover of  $(X, \tau)$ . Then as  $(X, \tau)$  is  $\alpha(gg) \star compact$ , the  $\alpha(gg) \star copen$  cover  $\left\{ (X - A_i) : i \in I \right\}$  has a finite sub cover say  $\left\{ (X - A_i) : i = 1, 2, 3, ..., n \right\}$ . This implies that  $X = \mathbf{U} \left\{ (X - A_i) : i = 1, 2, 3, ..., n \right\}$  which implies  $X = X - \mathbf{I} \left\{ A_i : i = 1, 2, 3, ..., n \right\}$ , which implies  $X = X - \mathbf{I} \left\{ A_i : i = 1, 2, 3, ..., n \right\}$ , which implies  $X = X - \mathbf{I} \left\{ A_i : i = 1, 2, 3, ..., n \right\}$ , which implies  $X = X - \mathbf{I} \left\{ A_i : i = 1, 2, 3, ..., n \right\}$ . This disproves the assumption. Hence  $\mathbf{I} \left\{ A_i : i \in I \right\} \neq \phi$ .

Conversely, suppose  $(X, \tau)$  is not  $\alpha(gg) \star compact$ . Then there exits an  $\alpha(gg) \star open$  cover of  $(X, \tau)$  say  $\{G_i : i \in I\}$  having no finite subcover. This implies for any finite subfamily  $\{G_i : i = 1, 2, 3, ..., n\}$  of  $\{G_i : i \in I\}$ , we have  $U\{G_i : i = 1, 2, 3, ..., n\} \neq X$ , which implies  $X - (U\{G_i : i = 1, 2, 3, ..., n\}) \neq X - X$ , therefore  $I\{X - G_i : i = 1, 2, 3, ..., n\} \neq \emptyset$ . Then the family  $\{X - G_i : i \in I\}$  of  $\alpha(gg) \star closed$  sets has a finite intersection property. Also by assumption  $I\{X - G_i : i \in I\} \neq \emptyset$  which implies  $X - (U\{G_i : i \in I\}) \neq \emptyset$ , so that  $U\{G_i : i \in I\} \neq X$ . This implies  $\{G_i : i \in I\}$  is not a cover of  $\{X, \tau\}$ . This disproves the fact that  $\{G_i : i \in I\}$  is a cover for  $\{X, \tau\}$ . Therefore an  $\alpha(gg) \star open$  cover  $\{G_i : i \in I\}$  of  $\{X, \tau\}$  has a finite sub cover  $\{G_i : i = 1, 2, 3, ..., n\}$ . Hence  $\{X, \tau\}$  is  $\alpha(gg) \star compact$ .

**Theorem 3.14.** Let A be an  $\alpha(gg) \star compact$  set relative to a topological space X and B be an  $\alpha(gg) \star closed$  subset of X. Then AI B is  $\alpha(gg) \star compact$  relative to X.

**Proof.** Let A be  $\alpha(gg) \star compact$  relative to X. Let  $\{A_i : i \in I\}$  be a cover of AIB by  $\alpha(gg) \star open$  sets in X. Then  $\{A_i : i \in I\} \cup \{B^c\}$  is a cover of A by  $\alpha(gg) \star open$  sets in X, but A is  $\alpha(gg) \star compact$  relative to X, so there exists a finite subset  $I_0 = \{i_1, i_2, i_3, \ldots, i_n\} \subseteq I$  such

## on Innovative Surveys in Positive Sciences 4-5 December 2022 / Full Text Book

that  $A \subseteq \left( \mathbf{U} \left\{ A_{i_k} : k = 1, 2, 3, \dots, n \right\} \right) \mathbf{U} B^C$ . Then  $A \mathbf{I} B \subseteq \mathbf{U} \left\{ A_{i_k} \mathbf{I} B : k = 1, 2, 3, \dots, n \right\} \subseteq \mathbf{U} \left\{ A_{i_k} : k = 1, 2, 3, \dots, n \right\}$ . Hence  $A \mathbf{I} B$  is  $\alpha (gg) \star compact$ .

**Theorem 3.15.** Suppose that a function  $f:(X,\tau)\to (Y,\sigma)$  is  $\alpha(gg)$ \*-irresolute and a subset B of X is  $\alpha(gg)$ \*-compact relative to X. Then f(B) is  $\alpha(gg)$ \*-compact relative to Y.

**Proof.** Let  $\{A_i: i \in I\}$  be a cover of f(B) by  $\alpha(gg) *-open$  subsets of Y. Since f is  $\alpha(gg) *-irresolute$ . Then  $\{f^{-1}(A_i): i \in I\}$  is a cover of B by  $\alpha(gg) *-open$  subsets of X. Since B is  $\alpha(gg) *-compact$  relative to X,  $\{f^{-1}(A_i): i \in I\}$  has a finite sub cover say  $\{f^{-1}(A_1), f^{-1}(A_2), ..., f^{-1}(A_n)\}$  for B. Then it implies that  $\{A_i: i=1,2,3,...,n\}$  is a finite subcover of  $\{A_i: i \in I\}$  for f(B). So f(B) is  $\alpha(gg) *-compact$  relative to Y.

**Definition 3.16.** Let  $(X, \tau)$  be a topological space and let E be a subset of X. Let  $\tau_E^{\alpha(gg)^*} = \{AI \ E : A \in \alpha(gg) * O(X, \tau)\}$ . Then  $(E, \tau_E^{\alpha(gg)^*})$  is a topological space.

**Theorem 3.17.** Let  $(X, \tau)$  be a topological space and let E be a subset of X. Then  $(E, \tau_E^{\alpha(gg)^*})$  is compact if and only if for any  $\alpha(gg) * open$  cover  $\Gamma$  of E has a finite subcover of E.

**Proof.** Suppose E is compact. Let  $\Gamma \subseteq \alpha(gg) \star O(X, \tau)$  such that  $E \subseteq U\Gamma$ . Let  $\Gamma_E = \{AI \ E : A \in \Gamma\}$ . Then  $E = U\Gamma_E$  and  $\Gamma_E \subseteq \tau_E^{\alpha(gg)\star}$ . By hypothesis, there exists a finite subset  $\Gamma_E^* = \{A_i \ E : i = 1, 2, 3, ..., n\} \subseteq \Gamma_E$  such that  $E = U\Gamma_E^*$ . Then  $\Gamma^* = \{A_i : i = 1, 2, 3, ..., n\} \subseteq \Gamma$  and  $E \subseteq U\Gamma^*$ .

Conversely, let  $\Upsilon = \{A_i \mid E : i \in I\} \subseteq \tau_E^{\alpha(gg)^*}$  such that  $E = U\Upsilon$ . Then  $\Upsilon^* = \{A_i : i \in A\}$  is an  $\alpha(gg)$ \*-open covering of E. By hypothesis, there exists  $\Upsilon^{**} = \{A_i : i = 1, 2, 3, ..., n\}$  a finite subset of  $\Upsilon^*$  such that  $E \subseteq U\Upsilon^{**}$ . Then  $\Upsilon^{\#} = \{A_i \mid E : i = 1, 2, 3, ..., n\}$  is a finite subset of  $\Upsilon$  such that  $E = U\Upsilon^{\#}$ . This proves that  $E = U\Upsilon^{\#}$  is compact.

# 4. COUNTABLY α(gg)\*COMPACT SPACES

In this section, we present the concept of countably  $\alpha(gg) \star compactness$  and its properties.

**Definition 4.1.** A topological space  $(X, \tau)$  is said to be countably  $\alpha(gg) \star compact$  if every countable  $\alpha(gg) \star open$  cover of X has a finite sub cover.

## on Innovative Surveys in Positive Sciences 4-5 December 2022 / Full Text Book

**Theorem 4.2.** If  $(X, \tau)$  is a countably  $\alpha(gg) \star compact$  space, then  $(X, \tau)$  is countably compact.

**Proof.** Let  $(X, \tau)$  be a countably  $\alpha(gg) \star compact$  space. Let  $\{A_i : i \in I\}$  be a countable open cover of  $(X, \tau)$ . Since  $\tau \subseteq \alpha(gg) \star O(X, \tau)$ . So  $\{A_i : i \in I\}$  is a countable  $\alpha(gg) \star open$  cover of  $(X, \tau)$ . Since  $(X, \tau)$  is countably  $\alpha(gg) \star compact$ , therefore countable  $\alpha(gg) \star open$  cover  $\{A_i : i \in I\}$  of  $(X, \tau)$  has a finite sub cover say  $\{A_i : i = 1, 2, 3, \ldots, n\}$  for X. Hence  $(X, \tau)$  is a countably compact space.

**Theorem 4.3.** If  $(X, \tau)$  is countably compact and every  $\alpha(gg) *closed$  subset of X is closed in X, then  $(X, \tau)$  is countably  $\alpha(gg) *compact$ .

**Proof.** Let  $(X, \tau)$  be a countably compact space. Let  $\{A_i : i \in I\}$  be a countable  $\alpha(gg) * open$  cover of  $(X, \tau)$ . Since every  $\alpha(gg) * closed$  subset of X is closed in X. Thus every  $\alpha(gg) * open$  set in X is open in X. Therefore  $\{A_i : i \in I\}$  is a countable open cover of  $(X, \tau)$ . Since  $(X, \tau)$  is countably compact, so countable open cover  $\{A_i : i \in I\}$  of  $(X, \tau)$  has a finite sub cover say  $\{A_i : i = 1, 2, 3, ..., n\}$  for X. Hence  $(X, \tau)$  is a countably  $\alpha(gg) * compact$  space.

**Theorem 4.4.** Every  $\alpha(gg) \star compact$  space is countably  $\alpha(gg) \star compact$ .

**Proof.** Let  $(X, \tau)$  be an  $\alpha(gg) \star compact$  space. Let  $\{A_i : i \in I\}$  be a countable  $\alpha(gg) \star compact$  cover of  $(X, \tau)$ . Since  $(X, \tau)$  is  $\alpha(gg) \star compact$ , so  $\alpha(gg) \star compact$  cover  $\{A_i : i \in I\}$  of  $(X, \tau)$  has a finite sub cover say  $\{A_i : i = 1, 2, 3, ..., n\}$  for  $(X, \tau)$ . Hence  $(X, \tau)$  is countably  $\alpha(gg) \star compact$  space.

**Theorem 4.5.** Let  $f:(X,\tau)\to (Y,\sigma)$  be an  $\alpha(gg)$ \*continuous onjective mapping. If X is countably  $\alpha(gg)$ \*compact space, then  $(Y,\sigma)$  is countably compact.

**Proof.** Let  $f:(X,\tau)\to (Y,\sigma)$  be an  $\alpha(gg)$ \*continuous mapping from a countably  $\alpha(gg)$ \*compact space  $(X,\tau)$  onto a topological space  $(Y,\sigma)$ . Let  $\{A_i:i\in I\}$  be a countable open cover of Y. Then  $\{f^{-1}(A_i):i\in I\}$  is a countable  $\alpha(gg)$ \*copen cover of X, as f is  $\alpha(gg)$ \*continuous. Since X is countably  $\alpha(gg)$ \*compact, the countable  $\alpha(gg)$ \*copen cover  $\{f^{-1}(A_i):i\in I\}$  of X has a finite sub cover say  $\{f^{-1}(A_i):i=1,2,3,...,n\}$ . Therefore  $X=U\{f^{-1}(A_i):i=1,2,3,...,n\}$ , which implies  $Y=f(X)=U\{A_i:i=1,2,3,...,n\}$ . That is  $\{A_i:i=1,2,3,...,n\}$  is a finite sub cover of  $\{A_i:i\in I\}$  for Y. Hence Y is countably compact.

## on Innovative Surveys in Positive Sciences 4-5 December 2022 / Full Text Book

**Theorem 4.6.** Suppose that a mapping  $f:(X,\tau)\to (Y,\sigma)$  is perfectly  $\alpha(gg)\star continuous$  mapping from a countably compact space  $(X,\tau)$  onto a topological space  $(Y,\sigma)$ . Then  $(Y,\sigma)$  is countably  $\alpha(gg)\star compact$ .

**Proof.** Let  $\{A_i:i\in I\}$  be a countable  $\alpha(gg)*open$  cover of  $(Y,\sigma)$ . Since f is perfectly  $\alpha(gg)*continuous$ ,  $\{f^{-1}(A_i):i\in I\}$  is a countable open cover of  $(Y,\sigma)$ . Again, since  $(X,\tau)$  is countably  $\alpha(gg)*compact$ , the countable open cover  $\{f^{-1}(A_i):i\in I\}$  of  $(X,\tau)$  has a finite subcover say  $\{f^{-1}(A_i):i=1,2,3,...,n\}$ . Therefore  $X=U\{f^{-1}(A_i):i=1,2,3,...,n\}$ , which implies  $f(X)=U\{A_i:i=1,2,3,...,n\}$ , so that  $Y=U\{A_i:i=1,2,3,...,n\}$ . That is  $\{A_1,A_2,...,A_n\}$  is a finite subcover of  $\{A_i:i\in I\}$  for  $(Y,\sigma)$ . Hence  $(Y,\sigma)$  is countably  $\alpha(gg)*compact$ .

**Theorem 4.7.** Suppose that a mapping  $f:(X,\tau)\to (Y,\sigma)$  is strongly  $\alpha(gg)$ \*continuous mapping from a countably compact space  $(X,\tau)$  onto a topological space  $(Y,\sigma)$ . Then  $(Y,\sigma)$  is countably  $\alpha(gg)$ \*compact.

**Proof.** Let  $\{A_i:i\in I\}$  be a countable  $\alpha(gg) \star open$  cover of  $(Y,\sigma)$ . Since f is strongly  $\alpha(gg) \star continuous$ ,  $\{f^{-1}(A_i):i\in I\}$  is a countable open cover of  $(X,\tau)$ . Again, since  $(X,\tau)$  is countably compact, the countable open cover  $\{f^{-1}(A_i):i\in I\}$  of  $(X,\tau)$  has a finite sub cover say  $\{f^{-1}(A_i):i=1,2,3,...,n\}$ . Therefore  $X=U\{f^{-1}(A_i):i=1,2,3,...,n\}$ , which implies  $f(X)=U\{A_i:i=1,2,3,...,n\}$ , so that  $Y=U\{A_i:i=1,2,3,...,n\}$ . That is  $\{A_1,A_2,...,A_n\}$  is a finite subcover of  $\{A_i:i\in I\}$  for  $(Y,\sigma)$ . Hence  $(Y,\sigma)$  is countably  $\alpha(gg) \star compact$ .

**Theorem 4.8.** The image of a countably  $\alpha(gg) * compact$  space under a  $\alpha(gg) * irresolute$  mapping is countably  $\alpha(gg) * compact$ .

**Proof.** Suppose that a mapping  $f:(X,\tau)\to (Y,\sigma)$  is an  $\alpha(gg)$ \*\*irresolute mapping from a countably  $\alpha(gg)$ \*\*compact space  $(X,\tau)$  onto a topological space  $(Y,\sigma)$ . Let  $\{A_i:i\in I\}$  be a countable  $\alpha(gg)$ \*\*compact cover of  $(Y,\sigma)$ . Then  $\{f^{-1}(A_i):i\in I\}$  is a countable  $\alpha(gg)$ \*\*compact, the countable  $\alpha(gg)$ \*\*compact, the countable  $\alpha(gg)$ \*\*copen cover  $\{f^{-1}(A_i):i\in I\}$  of  $(X,\tau)$  has a finite sub cover say  $\{f^{-1}(A_i):i=1,2,3,...,n\}$ . Then it follows that  $X=U\{f^{-1}(A_i):i=1,2,3,...,n\}$ , which implies  $f(X)=U\{A_i:i=1,2,3,...,n\}$ , so that  $Y=U\{A_i:i=1,2,3,...,n\}$ . That is  $\{A_1,A_2,...,A_n\}$  is a

## on Innovative Surveys in Positive Sciences 4-5 December 2022 / Full Text Book

finite subcover of  $\{A_i : i \in I\}$  for  $(Y, \sigma)$ . Hence  $(Y, \sigma)$  is countably  $\alpha(gg) \star compact$ .

**Theorem 4.9.** Let  $(X, \tau)$  be a topological space and  $x \in X$ . A point  $x \in X$  is said to be  $\alpha(gg) \star limit$  point of  $A \subseteq X$  provided that every  $\alpha(gg) \star neighbourhood$  of x contains at least one point of A different from x.

**Theorem 4.10.** Every infinite subset of an  $\alpha(gg) \star compact$  space has an  $\alpha(gg) \star limit$  point.

**Proof.** Let A be an infinite subset of an  $\alpha(gg) \star compact$  space  $(X, \tau)$ . Suppose that A has not an  $\alpha(gg) \star limit$  point. Then for each  $x \in X$ , there exists an  $\alpha(gg) \star open$  set  $G_x$  containing at most one point of A. Now, the collection  $\Lambda = \{G_x : x \in X\}$  forms an  $\alpha(gg) \star open$  cover of X. As X is  $\alpha(gg) \star compact$ , then there exist  $x_1, x_2, \dots, x_n$  in X such that  $X = \bigcup_{i=1}^{i=n} G_{x_i}$ . Therefore X has at most n points of A. This implies that A is finite. But this contradicts that A is infinite. Thus A has an  $\alpha(gg) \star limit$  point.

# 5. α(gg)\*LINDELOF SPACES

In this section, we concentrate on the concept of  $\alpha(gg) \star Lindel\ddot{o}f$  space and its properties.

**Definition 5.1.** A topological space  $(X, \tau)$  is said to be  $\alpha(gg) \star Lindel\"{o}f$  space if every  $\alpha(gg) \star open$  cover of X has a countable subcover.

**Definition 5.2.** Every  $\alpha(gg) \star Lindel\"{o}f$  space  $(X, \tau)$  is  $Lindel\ddot{o}f$  space.

**Proof.** Let  $(X, \tau)$  be an  $\alpha(gg) \star Lindel\"{o}f$  space. Let  $\{A_i : i \in I\}$  be an open cover of  $(X, \tau)$ . Since  $\tau \subseteq \alpha(gg) \star O(X, \tau)$ . Therefore  $\{A_i : i \in I\}$  is an  $\alpha(gg) \star open$  cover of  $(X, \tau)$ . Since  $(X, \tau)$  is  $\alpha(gg) \star Lindel\"{o}f$  space. So there exists a countable subset  $I_0$  of I such that  $\{A_i : i \in I_0\}$  is an  $\alpha(gg) \star open$  subcover of  $(X, \tau)$ . Hence  $(X, \tau)$  is a  $Lindel\"{o}f$  space.

**Theorem 5.3.** Every  $\alpha(gg) \star compact$  space is  $\alpha(gg) \star Lindel\"{o}f$ .

**Proof.** Let  $(X, \tau)$  be an  $\alpha(gg)$ \*-compact space. Let  $\{A_i : i \in I\}$  be an  $\alpha(gg)$ \*-open cover of  $(X, \tau)$ . Since  $(X, \tau)$  is  $\alpha(gg)$ \*-compact space. Then  $\{A_i : i \in I\}$  has a finite sub-cover say  $\{A_i : i = 1, 2, 3, ..., n\}$ . Since every finite sub-cover is always countable sub-cover and therefore  $\{A_i : i = 1, 2, 3, ..., n\}$  is a countable sub-cover of  $\{A_i : i \in I\}$ . Hence  $(X, \tau)$  is  $\alpha(gg)$ \*-Lindelöf space.

# on Innovative Surveys in Positive Sciences 4-5 December 2022 / Full Text Book

**Theorem 5.4.** Every  $\alpha(gg) * closed$  subset of an  $\alpha(gg) * Lindel\"{o}f$  space is  $\alpha(gg) * Lindel\"{o}f$ .

**Proof.** Let F be an  $\alpha(gg) \star closed$  subset of X and  $\{G_i : i \in I\}$  be  $\alpha(gg) \star open$  cover of F. Then  $F^c$  is  $\alpha(gg) \star open$  and  $F \subseteq U\{G_i : i \in I\}$ . Hence  $X = (U\{G_i : i \in I\}) \cup F^c$ . Since X is  $\alpha(gg) \star Lindel\"{of}$ , then  $X = (U\{G_i : i \in I_0\}) \cup F^c$  for some countable subset  $I_0$  of I. Therefore  $F \subseteq U\{G_i : i \in I_0\}$ . Thus F is  $\alpha(gg) \star Lindel\"{of}$ .

**Theorem 5.5.** Let A be an  $\alpha(gg) \star Lindel\"{o}f$  subset of X and B be an  $\alpha(gg) \star closed$  subset of X. Then AIB is  $\alpha(gg) \star Lindel\"{o}f$ .

**Proof.** Let  $\{G_i: i \in I\}$  be an  $\alpha(gg) * open$  cover of AI B. Then  $A \subseteq (\bigcup_{i \in I} G_i) \cup B^c$ . Since A is  $\alpha(gg) * Lindel\"{o}f$ , then there exists a countable subset  $I_0$  of I such that  $A \subseteq (\bigcup_{i \in I_0} G_i) \cup B^c$ . Therefore AI  $B \subseteq \bigcup_{i \in I_0} G_i$ . Thus AI B is  $\alpha(gg) * Lindel\"{o}f$ .

**Theorem 5.6.** A topological space  $(X, \tau)$  is  $\alpha(gg) \star Lindel\"{o}f$  if and only if every collection of  $\alpha(gg) \star closed$  subsets of X satisfying the countable intersection property, has, itself, a non-empty intersection.

Necessity: Let  $\Lambda = \{F_i : i \in I\}$  be a collection of  $\alpha(gg) \star closed$  subsets of X which has the countable intersection property. Assume that  $\mathbf{I}_{i \in I} F_i = \phi$ . Then  $X = \bigcup_{i \in I} F_i^c$ . Since X is  $\alpha(gg) \star Lindel\ddot{o}f$ , then there exists a countable subset  $I_0$  of I such that  $X = \bigcup_{i \in I_0} F_i^c$ . Therefore,  $\mathbf{I}_{i \in I_0} F_i = \phi$  contradicts that  $\Lambda$  has the countable intersection property. Thus  $\Lambda$  has, itself, a non-empty intersection.

**Sufficiency:** Let  $\{G_i: i \in I\}$  be an  $\alpha(gg) \not\sim open$  cover of X. Suppose  $\{G_i: i \in I\}$  has no countable subcover. Then  $X - \bigcup_{i \in I} G_i \neq \emptyset$ , for any countable subset J of I. Now,  $\prod_{i \in I} G_i^c \neq \emptyset$  implies that  $\{G_i^c: i \in I\}$  is a collection of  $\alpha(gg) \not\sim closed$  subsets of X which has the countable intersection property. Therefore  $\prod_{i \in I} G_i^c \neq \emptyset$ . Thus  $X \neq \bigcup_{i \in I} G_i$  contradicts that  $\{G_i: i \in I\}$  is an  $\alpha(gg) \not\sim open$  cover of X. Hence X is  $\alpha(gg) \not\sim Lindel\"{of}$ .

**Theorem 5.7.** An  $\alpha(gg)$ \*-continuous image of an  $\alpha(gg)$ \*-Lindelöf space is a Lindelöf space.

on Innovative Surveys in Positive Sciences 4-5 December 2022 / Full Text Book

**Proof.** Let  $f:(X,\tau)\to (Y,\sigma)$  be an  $\alpha(gg)$ \*continuous mapping from a  $\alpha(gg)$ \*Lindelöf space X onto a topological space Y. Let  $\{A_i:i\in I\}$  be an open cover of Y. Then  $\{f^{-1}(A_i):i\in I\}$  is an  $\alpha(gg)$ \*copen cover of X, as f is  $\alpha(gg)$ \*continuous. Since X is  $\alpha(gg)$ \*Lindelöf space, the  $\alpha(gg)$ \*copen cover  $\{f^{-1}(A_i):i\in I\}$  of X has a countable subcover say  $\{f^{-1}(A_i):i\in I_0\}$  for some countable set  $I_0\subseteq I$ . Therefore  $X=U\{f^{-1}(A_i):i\in I_0\}$ , which implies  $f(X)=U\{A_i:i\in I_0\}$ , then  $Y=U\{A_i:i\in I_0\}$ . That is  $\{A_i:i\in I_0\}$  a countable subcover of  $\{A_i:i\in I\}$  for Y. Hence  $\{Y,\sigma\}$  is a Lindelöf space.

**Theorem 5.8.** The image of an  $\alpha(gg)$ \*Lindelöf space under an  $\alpha(gg)$ \*irresolue mapping is  $\alpha(gg)$ \*Lindelöf space.

**Proof.** Suppose that a mapping  $f:(X,\tau)\to (Y,\sigma)$  is an  $\alpha(gg)$ \*-irresolue mapping from a  $\alpha(gg)$ \*-Lindelöf space  $(X,\tau)$  onto a topological space  $(Y,\sigma)$ . Let  $\{B_i:i\in I\}$  be an  $\alpha(gg)$ \*-open cover of  $(Y,\sigma)$ . Since f is  $\alpha(gg)$ \*-irresolue. Therefore  $\{f^{-1}(B_i):i\in I\}$  is an  $\alpha(gg)$ \*-open cover of  $(X,\tau)$ . As  $(X,\tau)$  is  $\alpha(gg)$ \*-Lindelöf space, the  $\alpha(gg)$ \*-open cover  $\{f^{-1}(B_i):i\in I\}$  of  $(X,\tau)$  has a countable subcover say  $\{f^{-1}(B_i):i\in I_0\}$  for some countable set  $I_0\subseteq I$ . Therefore  $X=U\{f^{-1}(B_i):i\in I_0\}$ , which implies  $f(X)=U\{B_i:i\in I_0\}$ , so that  $Y=U\{B_i:i\in I_0\}$ . That is  $\{B_i:i\in I_0\}$  a countable subcover of  $\{B_i:i\in I\}$  for Y. Hence  $(Y,\sigma)$  is an  $\alpha(gg)$ \*-Lindelöf space.

**Theorem 5.9.** If  $(X, \tau)$  is  $\alpha(gg) \star Lindel\"{o}f$  space and countably  $\alpha(gg) \star compact$  space, then  $(X, \tau)$  is  $\alpha(gg) \star compact$  space.

**Proof.** Suppose  $(X, \tau)$  is  $\alpha(gg) *Lindel\"{o}f$  space and countably  $\alpha(gg) *compact$  space. Let  $\{A_i : i \in I\}$  be an  $\alpha(gg) *compact$  cover of  $(X, \tau)$ . Since  $(X, \tau)$  is  $\alpha(gg) *Lindel\"{o}f$  space,  $\{A_i : i \in I\}$  has a countable subcover say  $\{A_i : i \in I_0\}$  for some countable set  $I_0 \subseteq I$ . Therefore  $\{A_i : i \in I_0\}$  is a countable  $\alpha(gg) *compact$  over of  $(X, \tau)$ . Again, since  $(X, \tau)$  is countably  $\alpha(gg) *compact$  space,  $\{A_i : i \in I_0\}$  has a finite subcover and say  $\{A_i : i = 1, 2, 3, ..., n\}$ . Therefore  $\{A_i : i = 1, 2, 3, ..., n\}$  is a finite subcover of  $\{A_i : i \in I\}$  for  $(X, \tau)$ . Hence  $(X, \tau)$  is an  $\alpha(gg) *compact$  space.

# on Innovative Surveys in Positive Sciences 4-5 December 2022 / Full Text Book

**Theorem 5.10.** If a function  $f:(X,\tau)\to (Y,\sigma)$  is  $\alpha(gg)\star irresolue$  and a subset A of X is  $\alpha(gg)\star Lindel\"{o}f$  relative to X, then f(A) is  $\alpha(gg)\star Lindel\"{o}f$  relative to Y.

**Proof.** Let  $\{B_i: i \in I\}$  be a cover of f(A) by  $\alpha(gg) \not\sim open$  subsets of Y. By hypothesis, f is  $\alpha(gg) \not\sim irresolue$  and so  $\{f^{-1}(B_i): i \in I\}$  is a cover of A by  $\alpha(gg) \not\sim open$  subsets of X. Since A is  $\alpha(gg) \not\sim Lindel\"{o}f$  relative to X,  $\{f^{-1}(B_i): i \in I\}$  has a countable subcover say  $\{f^{-1}(B_i): i \in I_0\}$  for A, where  $I_0$  is a countable subset of I. Now  $\{B_i: i \in I_0\}$  is a countable subcover of  $\{B_i: i \in I\}$  for f(A). So f(A) is  $\alpha(gg) \not\sim Lindel\"{o}f$  relative to Y.

# 6. ALMOST α(gg)\*COMPACT SPACES

**Definition 6.1.** A topological space  $(X, \tau)$  is called almost  $\alpha(gg) \star compact$   $(resp. almost \alpha(gg) \star Lindel\"{o}f)$  provided that every  $\alpha(gg) \star open$  cover of X has a finite (resp. countable) sub-collection, the  $\alpha(gg) \star closure$  of whose members cover X.

The proofs of the following four propositions are straightforward and therefore will be omitted.

**Proposition 6.2.** Every almost  $\alpha(gg) \star compact$  space is almost  $\alpha(gg) \star Lindel\ddot{o}f$  space.

**Proposition 6.3.** Every  $\alpha(gg) \star compact$  space  $(resp. \alpha(gg) \star Lindel\"{o}f space)$  is almost  $\alpha(gg) \star compact$   $(resp. almost \alpha(gg) \star Lindel\"{o}f)$ .

**Proposition 6.4.** Any finite (resp. countable) topological space  $(X, \tau)$  is almost  $\alpha(gg) * compact$  (resp. almost  $\alpha(gg) * Lindel\"{o}f$ ).

**Proposition 6.5.** A finite (resp. countable) union of almost  $\alpha(gg) \star compact$  (resp. almost  $\alpha(gg) \star Lindel\ddot{o}f$ ) subsets of  $(X, \tau)$  is almost  $\alpha(gg) \star compact$  (resp. almost  $\alpha(gg) \star Lindel\ddot{o}f$ ).

**Definition 6.6.** A subset E of  $(X, \tau)$  is called  $\alpha(gg) *clopen$  provided that it is  $\alpha(gg) *open$  and  $\alpha(gg) *closed$ .

**Theorem 6.7.** Let F be an  $\alpha(gg) * clopen$  subset of an almost  $\alpha(gg) * compact$   $(resp. almost \alpha(gg) * Lindel\"{o}f)$  space  $(X, \tau)$ . Then F is almost  $\alpha(gg) * compact$   $(resp. almost \alpha(gg) * Lindel\"{o}f)$ .

# on Innovative Surveys in Positive Sciences 4-5 December 2022 / Full Text Book

**Proof.** Let F be an  $\alpha(gg) \star clopen$  subset of an almost  $\alpha(gg) \star compact$  space X and  $\{G_i: i \in I\}$  be a  $\alpha(gg) \star open$  cover of F. Then  $F^c$  is  $\alpha(gg) \star open$  and  $X \subseteq (U\{G_i: i \in I\}) \cup F^c$ . Since X is almost  $\alpha(gg) \star compact$ , then there exists a finite subset  $I_0$  of I such that  $X = (U\{\alpha(gg) \star Cl(G_i): i \in I_0\}) \cup F^c$ . Thus it follows that  $F \subseteq U\{\alpha(gg) \star Cl(G_i): i \in I_0\}$ . Hence F is almost  $\alpha(gg) \star compact$ .

The proof is similar in the case of almost  $\alpha(gg) \star Lindel\ddot{o}f$ .

**Theorem 6.8.** If A is an almost  $\alpha(gg) \star compact$  (resp. almost  $\alpha(gg) \star Lindel\"{o}f$ ) subset of  $(X, \tau)$  and B is an  $\alpha(gg) \star clopen$  subset of X, then AI B is almost  $\alpha(gg) \star compact$  (resp. almost  $\alpha(gg) \star Lindel\"{o}f$ ).

**Proof.** Let  $\Lambda = \{G_i : i \in I\}$  be an  $\alpha(gg) \not\sim open$  cover of AI B. Then  $A \subseteq (U\{G_i : i \in I\}) \cup B^c$ . Since A is almost  $\alpha(gg) \not\sim compact$ , then there exists a finite subset  $I_0$  of I such that  $A \subseteq (U\{\alpha(gg) \not\sim Cl(G_i) : i \in I_0\}) \cup B^c$ . Hence AI  $B \subseteq U\{\alpha(gg) \not\sim Cl(G_i) : i \in I_0\}$ . Thus AI B is almost  $\alpha(gg) \not\sim compact$ .

The proof is similar in the case of almost  $\alpha(gg) \star Lindel\ddot{o}f$ .

**Theorem 6.9.** Let a mapping  $f:(X,\tau)\to (Y,\sigma)$  be  $\alpha(gg)\star irresolute$ . Suppose that A is almost  $\alpha(gg)\star compact$  (resp. almost  $\alpha(gg)\star Lindel\"{o}f$ ) subset of X. Then f(A) is almost  $\alpha(gg)\star compact$  (resp. almost  $\alpha(gg)\star Lindel\"{o}f$ ).

**Proof.** Suppose that  $\{G_i:i\in I\}$  is  $\alpha(gg)*open$  cover of f(A). Then  $f(A)\subseteq U\{G_i:i\in I\}$ . Now  $A\subseteq U\{f^{-1}(G_i):i\in I\}$ . Since f is  $\alpha(gg)*irresolute$ , then  $\{f^{-1}(G_i):i\in I\}$  is an  $\alpha(gg)*open$  cover of A. By hypothesis, A is almost  $\alpha(gg)*compact$ , then there exists a finite subset  $I_0$  of I such that  $A\subseteq U\{\alpha(gg)*Cl[f^{-1}(G_i)]:i\in I_0\}$ . Since f is  $\alpha(gg)*irresolute$ , then  $\alpha(gg)*Cl(f^{-1}(G_i))\subseteq f^{-1}[\alpha(gg)*Cl(G_i)]$ , for all  $i\in I_0$ . Hence it follows that  $f(A)\subseteq U_{i\in I_0}f[f^{-1}(\alpha(gg)*Cl(G_i))]\subseteq U_{i\in I_0}\alpha(gg)*Cl(G_i)$ , which implies that  $f(A)\subseteq U_{i\in I_0}\alpha(gg)*Cl(G_i)$ . Thus f(A) is almost  $\alpha(gg)*compact$ .

The proof is similar in the case of almost  $\alpha(gg)$ \*Lindelöf.

on Innovative Surveys in Positive Sciences
4-5 December 2022 / Full Text Book

**Theorem 6.10.** Let  $f:(X,\tau)\to (Y,\sigma)$  be an  $\alpha(gg)\star open$  bijective mapping and  $(Y,\sigma)$  is almost  $\alpha(gg)\star compact$ . Then  $(X,\tau)$  is almost compact.

**Proof.** Let  $\{G_i: i \in I\}$  be an open cover of X. Then  $f(X) = f(\bigcup_{i \in I} G_i)$ . Therefore  $Y = \bigcup_{i \in I} f(G_i)$ . Now, Y is almost  $\alpha(gg) \star compact$ , then there exists a finite subset  $I_0$  of I such that  $Y = \bigcup_{i \in I_0} \alpha(gg) \star Cl[f(G_i)]$ . Since f is  $\alpha(gg) \star open$  bijective mapping, then f is  $\alpha(gg) \star closed$  mapping. Therefore, we have  $\alpha(gg) \star Cl[f(G_i)] \subseteq f[Cl(G_i)]$ , for all  $i \in I_0$ . Thus  $Y \subseteq \bigcup_{i \in I_0} f[Cl(G_i)] \subseteq f[\bigcup_{i \in I_0} Cl(G_i)]$ , which implies that  $X = f^{-1}(Y) \subseteq \bigcup_{i \in I_0} Cl(G_i)$ . Thus  $X = \bigcup_{i \in I_0} Cl(G_i)$ . Hence X is almost compact.

**Theorem 6.11.** If every collection of  $\alpha(gg) \star closed$  subsets of  $(X, \tau)$ , satisfying the finite (resp. countable) intersection property, has, itself, a non-empty intersection, then X is almost  $\alpha(gg) \star compact$  (resp. almost  $\alpha(gg) \star Lindel\"{o}f$ ).

**Proof.** Let  $\{G_i:i\in I\}$  be an  $\alpha(gg)$ \*-open cover of X. Suppose  $\{G_i:i\in I\}$  has no finite sub collection such that the  $\alpha(gg)$ \*-closure of whose members cover X. Then  $X-\bigcup_{i=1}^{i=n}\alpha(gg)$ \*- $Cl(G_i)\neq \phi$ , for any  $n\in N$ . Therefore  $X-\bigcup_{i=1}^{i=n}G_i\neq \phi$ . Now,  $\prod_{i=1}^nG_i^c\neq \phi$  implies  $\{G_i^c:i\in I\}$  is a collection of  $\alpha(gg)$ \*-closed subsets of X which has the finite intersection property. Thus  $\prod_{i\in I}G_i^c\neq \phi$  implies  $X\neq \bigcup_{i\in I}G_i$ . But this is a contradiction. Hence X is almost  $\alpha(gg)$ \*-compact.

A similar proof is given in the case of almost  $\alpha(gg)$ \*Lindelöf.

# 7. MILDLY α(gg)\*COMPACT SPACES

**Definition 7.1.** A topological space  $(X, \tau)$  is called mildly  $\alpha(gg) \star compact$   $(resp. mildly \alpha(gg) \star Lindel\"{o}f)$  provided that every  $\alpha(gg) \star clopen$  cover of X has a finite (resp. countable) subcover.

**Definition 7.2.** Every mildly  $\alpha(gg) \star compact$  space is mildly  $\alpha(gg) \star Lindel\"{o}f$ .

**Proof.** It is straightforward.

**Theorem 7.3.** Every almost  $\alpha(gg) \star compact$  (resp. almost  $\alpha(gg) \star Lindel\"{o}f$ ) space  $(X, \tau)$  is mildly  $\alpha(gg) \star compact$  (resp. mildly  $\alpha(gg) \star Lindel\"{o}f$ ).

# on Innovative Surveys in Positive Sciences 4-5 December 2022 / Full Text Book

**Proof.** Let  $\Lambda = \{H_i : i \in I\}$  be an  $\alpha(gg) \star clopen$  cover of  $(X, \tau)$ . Since  $(X, \tau)$  is almost  $\alpha(gg) \star compact$ , then there exists a finite subset  $I_0$  of I such that  $X = \bigcup_{i \in I_0} \alpha(gg) \star Cl(H_i)$ . Now,  $\alpha(gg) \star Cl(H_i) = H_i$ . Thus  $(X, \tau)$  is mildly  $\alpha(gg) \star compact$ .

A similar proof is given when  $(X, \tau)$  is almost  $\alpha(gg) \star Lindel\ddot{o}f$ .

**Corollary 7.4.** Every  $\alpha(gg) \star compact$   $(resp. \alpha(gg) \star Lindel\"{o}f)$  space is mildly  $\alpha(gg) \star compact$   $(resp. mildly \alpha(gg) \star Lindel\"{o}f)$ .

**Theorem 7.5.** If F is an  $\alpha(gg) \star clopen$  subset of a mildly  $\alpha(gg) \star compact$   $(resp. mildly \alpha(gg) \star Lindel\"{o}f)$  space X, then F is mildly  $\alpha(gg) \star compact$   $(resp. mildly \alpha(gg) \star Lindel\"{o}f)$ .

**Proof.** Let F be an  $\alpha(gg) \star clopen$  subset of X and  $\{G_i : i \in I\}$  be an  $\alpha(gg) \star clopen$  cover of F. Then  $F^c$  is an  $\alpha(gg) \star clopen$  set and  $F \subseteq \bigcup_{i \in I} G_i$ . Therefore  $X = (\bigcup_{i \in I} G_i) \cup F^c$ . Since X is mildly  $\alpha(gg) \star compact$ , then there exists a finite subset  $I_0$  of I such that  $X = (\bigcup_{i \in I_0} G_i) \cup F^c$ . So  $F \subseteq (\bigcup_{i \in I_0} G_i)$ . Hence F is mildly  $\alpha(gg) \star compact$ .

The proof is similar in a case of mildly  $\alpha(gg) \star Lindel\ddot{o}f$ .

**Theorem 7.6.** If A is a mildly  $\alpha(gg) \star compact$  (resp. mildly  $\alpha(gg) \star Lindel\"{o}f$ ) subset of X and B is an  $\alpha(gg) \star clopen$  subset of X, then A**I** B is mildly  $\alpha(gg) \star compact$  (resp. mildly  $\alpha(gg) \star Lindel\"{o}f$ ).

**Proof.** Let  $\Lambda = \{G_i : i \in I\}$  be an  $\alpha(gg) \star clopen$  cover of AI B. Then  $A \subseteq (\bigcup_{i \in I} G_i) \cup B^c$ . Since A is mildly  $\alpha(gg) \star compact$ , then there exists a finite subset  $I_0$  of I such that  $A \subseteq (\bigcup_{i \in I_0} G_i) \cup B^c$ . Therefore AI  $B \subseteq \bigcup_{i \in I_0} G_i$ . Thus AI B is mildly  $\alpha(gg) \star compact$ .

The proof is similar in case of mildly  $\alpha(gg)$ \*Lindelöf.

**Theorem 7.7.** If  $f:(X,\tau)\to (Y,\sigma)$  is an  $\alpha(gg)\star open$  bijective mapping and  $(Y,\sigma)$  is mildly  $\alpha(gg)\star compact$ , then  $(X,\tau)$  is mildly compact.

**Proof.** Let  $\{G_i: i \in I\}$  be a clopen cover for X. Then  $f(X) = f(\bigcup_{i \in I} G_i)$ . Hence  $Y = \bigcup_{i \in I} f(G_i)$ . Since f is  $\alpha(gg) \star open$  bijective mapping, then f is  $\alpha(gg) \star closed$ . Therefore  $\{f(G_i): i \in I\}$  is an  $\alpha(gg) \star clopen$  cover of X. Since Y is mildly  $\alpha(gg) \star compact$ , then there

# on Innovative Surveys in Positive Sciences 4-5 December 2022 / Full Text Book

exists a finite subset  $I_0$  of I such that  $Y = \bigcup_{i \in I_0} f(G_i)$ . Therefore  $X = \bigcup_{i \in I_0} G_i$ . Thus X is mildly compact.

**Proposition 7.8.** A subset A of  $(X, \tau)$  is mildly compact  $(resp. mildly \ Lindel\"{o}f)$  if and only if  $(X, \tau_A)$  is mildly compact  $(resp. mildly \ Lindel\"{o}f)$ .

# 8 Conclusions

We have used  $\alpha(gg) \star open$  sets to introduce the new concepts of notions in topological spaces namely  $\alpha(gg) \star compact$  space, countably  $\alpha(gg) \star compact$  space,  $\alpha(gg) \star Lindel\"{o}f$  space, almost  $\alpha(gg) \star compact$  space, and mildly  $\alpha(gg) \star compact$  space and have investigated several properties and characterization of these new concepts.

#### **ACKNOWLEDGEMENT**

The author is highly and gratefully indebted to Prince Mohammad Bin Fahd University, Saudi Arabia, for providing research facilities during the preparation of this research paper.

#### REFERENCES

- [1] Ghufran A. Abbas and Taha H. Jasim, On Supra  $\alpha$ -Compactness in Supra Topological Spaces, Tikrit Journal of Pure Science, Vol. 24(2) (2019), 91 97.
- [2] Beyda S. Abdullah, and Amir A. Mohammed, On Standard Concepts Using ii-Open Sets, Open Access Library Journal, 2019, Volume 6, e5604, 1 12. ISSN Online: 2333 9721, ISSN Print: 2333 9705.
- [3] Baravan A. Asaad and Alias B. Khalaf, On  $P_s$  Compact Space, International Journal Scientific & Engineering Research, Volume 7, Issue 8, August 2016, 809 815.
- [4] S. Balasubramanian, C. Sandhya and P.A.S. Vyjayanthi, On  $\nu$  Compact spaces, Scientia Magna, 5(1) (2009), 78-82.
- [5] Miguel Caldas, Saeid Jafari, and Raja M. Latif, b—Open Sets and A New Class of Functions, Pro Mathematica, Peru, Vol. 23, No. 45 46, pp. 155 174, (2009).
- [6] Sakkraiveeranam Chandrasekar, Velusamy Banupriya and M. Suresh,  $\theta_g *\alpha$ -Closed Sets in Topological Spaces, International Journal of Pure and Applied Mathematics, (In Press).
- [7] Sakkraiveeranam Chandrasekar, Velusamy Banupriya and Jeyaraman Suresh Kumar, Properties and Applications of  $\theta_{\text{g}} \star \alpha$ -Closed Sets in Topological Spaces, Journal of New Theory, Number: 18, (2017), Pages: 1 11.
- [8] R. Devi, S. Sampathkumar and M. Caldas, On supra  $\alpha$  open sets and S-continuous mappings, General Mathematics, 16 (2), (2008), 77 84.
- [9] W. Dunham, A New Closure Operator for non T1 topology, Kyuungpook Math. J., 22(1982), pp. 55 -60.
- [10] H. Z. Hdeib, ω-closed mappings, Rev. Colomb. Mat., 16 (1-2) (1982), 65–78.
- [11] M. Khan, T. Noiri and M. Hussain, On s\*g-closed sets and s\*-normal spaces, CODEN, JNSMAC (April & October 2008) 48, pp. 31 41.

# on Innovative Surveys in Positive Sciences

4-5 December 2022 / Full Text Book

- [12] K. Krishnaveni and M. Vigneshwaran, Some Stronger forms of supra  $bT\mu$  continuous function, Int. J. Mat. Stat. Inv., 1(2), (2013), 84 87.
- [13] K. Krishnaveni, M. Vigneshwaran,  $bT\mu$  compactness and  $bT\mu$  connectedness in supra topological spaces, European Journal of Pure and Applied Mathematics, Vol. 10, No. 2, 2017, 323 334 ISSN 1307-5543 <a href="https://www.ejpam.com">www.ejpam.com</a>.
- [14] Raja M. Latif, Supra-R-Compactness and Supra-R-Connectedness, International Journal of Recent Trends in Engineering and Research, Volume 04, Issue 01, (2018), Pages 426 443.
- [15] Raja M. Latif, Supra-I-Compactness and Supra-I-Connectedness, International Journal of Mathematics Trends and Technology, Volume 53, Number 7 (2018), pages 525 537.
- [16] N. Levine, Semi-open sets and semi-continuity in topological spaces, Amer. Math. Monthly, 70(1963), 36-41.
- [17] Sabiha I. Mahmood and Jumana S. Tareq, On  $S*g-\alpha$ -Open Sets in Topological Spaces, Ibn Al-Haitham Journal for Pure and Applied Sciences, Vol. 27 (3), (2014), 542 555.
- [18] A. S. Mashhour, M. E. Abd El-Monsefand S. N. El-Deed, On Precontinuous and weak precontinuous Mappings, Proc. Math. Phys. Soc. Egypt, 53 (1982), pp. 47 53.
- [19] T. Shyla Isaq Mary and G. Abhirami,  $\alpha(gg)$ \*- Closed Sets in Topological Spaces, International Journal of Mathematics Trends and Technology, Volume 68 Issue 3, 5 10, March 2022.
- [20] A. S. Mashhour, A. A. Allam, F. S. Mohamoud and F. H. Khedr, On supra topological spaces, Indian J. Pure and Appl. Math., No.4, 14(1983), 502 510.
- [21] Shadya M. Mershkhan and Baravan A. Asaad, Some Properties of  $P_p$ -Compact Spaces, General Letters in Mathematics, Vol. 7, Sep. 2019, pp. 13 23.
- [22] S. Pious Missier and P. Anbarasi Rodrigo, Some Notions of Nearly Open Sets in Topological Spaces, Intenational Journal of Mathematical Archive, 4(12)(2013)12 18.
- [23] Amir A. Mohammad and Beyda S. Abdullah, ii-Open Sets in Topological Spaces, International Mathematical Forum, Vol. 14, 2019, no. 1, 41 48.
- [24] Jamal M. Mustafa, supra b-compact and supra  $b-Lindel\ddot{o}f$  spaces, Journal of Mathematics and Applications, No36, (2013), 79-83.
- [25] O. Njastad, Some Classes of Nearly Open sets, Pacific J. Math., 15(3)(1965), pp. 961 970.
- [26] T. Noiri and O. R. Sayed, On  $\Omega$  closed sets and  $\Omega$ s closed sets in topological spaces, Acta Math, 4(2005), 307 318.
- [27] Hakeem A. Othman and Md. Hanif Page, On an Infra  $\alpha$  Open Sets, Global Journal of Mathematical Analysis, 4(3) (2016) 12 16.
- [28] P. G. Patil, w compactness and w connectedness in topological spaces, Thai. J. Mat., (12), (2014), 499 507.
- [29] A. Robert and S. Pious Missier, On Semi\*-Connected and Semi\*-Compact Spaces, International Journal of Modern Engineering Research, Vol. 2, Issue 4, July Aug. 2012, pp. 2852 2856.
- [30] A. Robert and S. Pious Missier, A New Class of Nearly Open Sets, Intenational Journal of Mathematical Archive, 3(7) (2012) 2575 2582.
- [31] A. Robert and S. Pious Missier, Compactness and Compactness via Semi-Star-Alpha-Open Sets, International Journal of Mathematics Trends and Technology, Volume 12, Number 1, Aug. 2014, pp. 1-7.
- [32] O. R. Sayed, Takashi Noiri, On supra b open set and supra b continuity on topological spaces, European Journal of pure and applied Mathematics, 3(2) (2010), 295 –302.
- [33] O. R. Sayed and T. Noiri, Supra b-irresoluteness and supra b-compactness on topological space, Kyungpook Math. J., 53(2013), 341 348.
- [34] T. Selvi and A. Punitha Dharani, Some new class of nearly closed and open sets, Asian Journal of Current Engineering and Maths, 1:5 Sep Oct (2012) 305 307.
- [35] T. M. Al-Shami, Supra semi-compactness via supra topological spaces, Journal of Taibah University for Science, 2018, VOL. 12, NO. 3, 338–343.
- [36] L. A. Steen and J. A. Seebach Jr, Counterexamples in Topology, Holt, Rinenhart and Winston, New York 1970.
- [37] N. V. Velicko, H-closed topological spaces, Amer. Math. Soc. Transl., 78(2) (1968), 103 118.

# on Innovative Surveys in Positive Sciences 4-5 December 2022 / Full Text Book

- [38] L. Vidyarani and M. Vigneshwaran, On Supra N-closed and sN-closed sets in Supra Topological Spaces, International Journal of Mathematical Achieve, Vol-4, Issue-2, (2013), 255 259.
- [39] L. Vidyarani and M. Vigneshwaran, Some forms of N-closed maps in Supra Topological spaces, IOSR Journal of Mathematics, Vol-6, Issue-4, (2013), 13 17.
- [40] L. Vidyarani and M. Vigneshwaran, Supra N-compact and Supra N-connected in SupraTopological spaces, Global Journal of Pure and Applied Mathematics. Volume 11, Number 4 (2015), pp. 2265-2277.
- [41] Albert Wilansky, Topology for Analysis, Devore Phlications, Inc, Mineola New York. (1980).
- [42] Stephen Willard, General Topology, Reading, Mass.: Addison Wesley Pub. Co. (1970).
- [43] Stephen Willard and Raja M. Latif, Semi-Open Sets and Regularly Closed Sets in Compact

on Innovative Surveys in Positive Sciences 4-5 December 2022 / Full Text Book

# (r\*g\*)\*\*MAPPINGS IN TOPOLOGICAL SPACES

#### Prof. Dr. RAJA MOHAMMAD LATIF

Department of Mathematics and Natural Sciences

College of Sciences and Human Studies

Prince Mohammad Bin Fahd University

P.O. Box 1664 Al Khobar, Kingdom of Saudi Arabia

ORCID NO: 0000-0003-3140-9581

#### **ABSTRACT**

In 2020, N. Meena Kumari and T. Indira introduced a new class of closed sets called (r\*g\*)\*\*- closed sets in topological spaces and investigated some basic properties. In this paper, we introduce (r\*g\*)\*\*- continuous function, (r\*g\*)\*\*- irresolute function, (r\*g\*)\*\*- open function, (r\*g\*)\*\*- closed function, pre -(r\*g\*)\*\*- open function, and pre -(r\*g\*)\*\*- closed function, and investigate several properties and characterizations of these new types of mappings in topological spaces.

Mathematics Subject Classification (2020): 54C05, 54C08, 54C10.

**Keywords and Phrases:** Topological space, (r\*g\*)\*\*- open set, (r\*g\*)\*\*- closed set, (r\*g\*)\*\*- interior set, (r\*g\*)\*\*- closure set, (r\*g\*)\*\*- continuous function, (r\*g\*)\*\*- iirresolute function, (r\*g\*)\*\*- open function, (r\*g\*)\*\*- closed function, pre-(r\*g\*)\*\*- open function, pre-(r\*g\*)\*\*- closed function, pre-(r\*g\*)\*\*- closed function.

#### 1. INTRODUVTION

Introducing new versions of open sets in a topological space which may acquire either weaker or stronger properties is often studied. The first attempt was done by Levine [12], where he introduced the concepts of semi-open set, semi-closed set, and semi-continuity of a function. In 2020, N. Meena Kumari and T. Indira introduced a new class of closed sets called (r\*g\*)\*\*- closed sets in topological spaces and investigated some basic properties. In this paper, we introduce (r\*g\*)\*\*- continuous function, (r\*g\*)\*\*- irresolute function, (r\*g\*)\*\*- open function, (r\*g\*)\*\*- closed function, pre -(r\*g\*)\*\*- open function, and pre -(r\*g\*)\*\*- closed function, and investigate several properties and characterizations of these new types of mappings in topological spaces.

on Innovative Surveys in Positive Sciences 4-5 December 2022 / Full Text Book

# 2. BASIC PROPERTIES AND APPLICATIONS OF (r\*g\*) \*\*- OPEN SETS

In this section, we shall define the concept of  $(\mathbf{r} * \mathbf{g} *) * * * - \text{open}$  set and determine its connection to the classical open set and characterize the concepts of  $(\mathbf{r} * \mathbf{g} *) * * * - \text{open}$  sets.

**Definition 2.1.** A subset A of a topological space  $(X, \tau)$  is named  $Re \ gular$  closed if Cl[Int(A)] = A and regular open if Int[Cl(A)] = A.

The regular-closure of a subset A of X denoted by rCl(A) is defined to be the intersection of all regular-closed sets containing A. The regular-interior of A denoted by rInt(A) is defined to be the union of all regular-open sets contained in A.

**Definition 2.2.** A subset A of a topological space  $(X,\tau)$  is called a generalized closed set  $(briefly \ g\text{-}closed\ set)$  if  $Cl(A)\subseteq U$  whenever  $A\subseteq U$  and U is open in X. The complement of g-closed set is called g-open set.

**Definition 2.3.** A subset A of a topological space  $(X,\tau)$  is called a (r\*g\*)-closed set if  $rCl(A) \subseteq U$  whenever  $A \subseteq U$  and U is g-open in X.

**Definition 2.4.** A subset A of a topological space  $(X,\tau)$  is called a (r\*g\*)\*-closed set if  $Cl(A) \subseteq U$  whenever  $A \subseteq U$  and U is (r\*g\*)-open in X.

**Definition 2.5.** A subset A of a topological space  $(X, \tau)$  is called a (r\*g\*)\*\*-closed set if  $Cl(A) \subseteq U$  whenever  $A \subseteq U$  and U is (r\*g\*)\*-open. The complement of (r\*g\*)\*\*-closed set is called a (r\*g\*)\*\*-open set.

**Proposition 2.6.** Every closed set is (r\*g\*)\*\*-closed set.

**Definition 2.7.** A subset A of a topological space  $(X,\tau)$  is called a (r\*g\*)\*\*-open (briefly (r\*g\*)\*\*-open) set if  $A^c$  is (r\*g\*)\*\*-closed set in X. The collection of all (r\*g\*)\*\*-open subsets of  $(X,\tau)$  is denoted by  $(r*g*)**-O(X,\tau)$ .

**Proposition 2.8.** If A and B are (r\*g\*)\*\*-closed sets in X, then  $A \cup B$  is (r\*g\*)\*\*-closed in X.

on Innovative Surveys in Positive Sciences 4-5 December 2022 / Full Text Book

**Proposition 2.9.** If A and B are (r\*g\*)\*\*-open sets in X, then A I B is (r\*g\*)\*\*-open set in X.

**Proposition 2.10.** If A and B are (r\*g\*)\*\*-closed sets in X, then A I B is (r\*g\*)\*\*-closed in X.

**Proposition 2.11.** If A and B are (r\*g\*)\*\*-open sets in X, then AUB is (r\*g\*)\*\*-open in X.

**Definition 2.12.** Let  $(X,\tau)$  be a topological space and  $B \subseteq X$ . We define the (r\*g\*)\*\*- closure of B (briefly (r\*g\*)\*\*- Cl(B)) to be the intersection of all (r\*g\*)\*\*- closed sets containing B which is denoted by (r\*g\*)\*\*- Cl(B)=I  $\{A:B\subseteq A \text{ and } A\in (r*g*)**-$  C $(X,\tau).\}$ . We note that (r\*g\*)\*\*- Cl(B) is the smallest (r\*g\*)\*\*- closed set containing B.

**Definition 2.13.** Let  $(X,\tau)$  be any topological space and B be a subset of X. A point p of X is called a (r\*g\*)\*\*-interior point of B, if there exists a (r\*g\*)\*\*-open set G such that  $p \in G \subseteq B$ . The set of all (r\*g\*)\*\*-interior points of B is said to be (r\*g\*)\*\*-interior of B (briefly (r\*g\*)\*\*-Int(B)) and it is defined by  $(r*g*)**-Int(B) = U\{A: A \subseteq B \text{ and } A \in (r*g*)**-O(X,\tau)\}$ .

**Definition 2.14.** Let  $\mathbb{Y}$  be a subset of a topological space  $(X,\tau)$  and let  $x \in X$ . We say that  $\mathbb{Y}$  is  $(r \star g \star) \star \star - neighborhood$  of x, if there is a  $(r \star g \star) \star \star - open$  set U such that  $x \in U \subseteq \mathbb{Y}$ .

**Proposition 2.15.** If U and V are sets in a topological space  $(X, \tau)$ , then

(1) 
$$(r * g *) * * - Int(\phi) = \phi$$
.

(2) 
$$(r * g *) * * - Int(X) = X$$
.

(3) 
$$(r *g *) **- Int(U) \subseteq U$$
.

$$(4) U \subseteq V \Rightarrow (r *g *) **- Int(U) \subseteq (r *g *) **- Int(V).$$

# on Innovative Surveys in Positive Sciences 4-5 December 2022 / Full Text Book

**Proposition 2.16.** Let G be any subset of a topological space  $(X, \tau)$ . Then  $x \in (r * g *) * * - Cl(A)$  if and only if for every (r \* g \*) \* \* - open set U containing x,  $U \mid G \neq \phi$ .

**Proposition 2.17.** For any subset U of topological space  $(X, \tau)$ ,  $(r * g *) * * - Int(U) \subseteq U \subseteq (r * g *) * * - Cl(U)$ .

**Definition 2.18.** Let A be a subset of a topological space  $(X,\tau)$ . A point  $x \in A$  is said to be a (r \* g \*) \* \* - limit point of A if for each (r \* g \*) \* \* - open set U containing x, U I  $(A - \{x\}) \neq \phi$ . The set of all (r \* g \*) \* \* - limit points of A is called the (r \* g \*) \* \* - derived set of A and is denoted by (r \* g \*) \* \* - D(A).

**Theorem 2.19.** For any subset A of a topological space X, (r\*g\*)\*\*-Cl(A) = AU[(r\*g\*)\*\*-D(A)].

**Proof.** Since  $(r*g*)**-D(A) \subseteq (r*g*)**-Cl(A)$ .  $AU[(r*g*)**-D(A)] \subseteq (r*g*)**-Cl(A)$ . On the other hand, let  $x \in (r*g*)**-Cl(A)$ . If  $x \in A$ , then the proof is complete. If  $x \notin A$ , each (r\*g\*)\*\*-open set U containing x intersects A at a point distinct from x, so  $x \in (r*g*)**-D(A)$ . Thus,  $(r*g*)**-Cl(A) \subseteq [AU((r*g*)**-D(A))]$ , which completes the proof.

**Corollary 2.20.** A subset A of a space X is (r\*g\*)\*\*-closed if and only if it contains the set of all of its (r\*g\*)\*\*-limit points.

**Theorem 2.21.** For subsets A, B of a space X, the following statements are true:

(1) 
$$(r \star g \star) \star \star - Int(A)$$
 is the largest  $(r \star g \star) \star \star - open$  set contained in  $A$ ;

(2) 
$$A$$
 is  $(r*g*)**-open$  if and only if  $A = (r*g*)**-Int(A)$ .

$$(3) (r*g*)**-Int[(r*g*)**-Int(A)] = (r*g*)**-Int(A);$$

$$(4) (r*g*)**-Int(A) = \lceil A - ((r*g*)**-D(X-A)) \rceil;$$

$$(5)\left[X - \left((r * g *) * * - Cl(A)\right)\right] = (r * g *) * * - Int(X - A);$$

$$(6) \left\lceil X - \left( (r \star g \star) \star \star - Int(A) \right) \right\rceil = (r \star g \star) \star \star - Cl(X - A);$$

$$(7) \lceil (r \star g \star) \star \star - Int(A) \rceil U \lceil (r \star g \star) \star \star - Int(B) \rceil \subseteq (r \star g \star) \star \star - Int(A \cup B);$$

on Innovative Surveys in Positive Sciences 4-5 December 2022 / Full Text Book

$$(8) (r *g *) **-Int(A I B) = \lceil (r *g *) **-Int(A) \rceil I \lceil (r *g *) **-Int(B) \rceil;$$

**Proof.** (4) If  $x \in [A - ((r * g *) * * * - D(X - A))]$ , then  $x \notin (r * g *) * * * - D(X - A)$  and so there exists a (r \* g \*) \* \* \* - open set U containing x such that  $U \mid (X - A) = \emptyset$ . Then,  $x \in U \subseteq A$  and hence  $x \in (r * g *) * * * - Int(A)$ , that is,  $[A - ((r * g *) * * * - D(X - A))] \subseteq (r * g *) * * * - Int(A)$ . On the other hand, if  $x \in (r * g *) * * * - Int(A)$ , then  $x \notin (r * g *) * * * - D(X - A)$  since (r \* g \*) \* \* - Int(A) is (r \* g \*) \* \* - open and  $[((r * g *) * * - Int(A))] \in \emptyset$ . Hence, (r \* g \*) \* \* - Int(A) = [A - ((r \* g \*) \* \* - D(X - A))].

$$(6) X - [(r *g *) **- Int(A)] = X - [A - ((r *g *) **- D(X - A))] = (X - A) U[(r *g *) **- D(X - A)] = (r *g *) **- Cl(X - A).$$

**Theorem 2.22.** Let  $(X, \tau)$  be a topological space and  $A, B \subseteq X$ . Then the following statements are true:

- (1)  $x \in (r * g *) * * Cl(A)$  if and only if for every (r \* g \*) \* \* open subset U containing x,  $U \mid A \neq \phi$ .
- (2)  $A \subseteq B$  implies that  $(r * g *) * * Cl(A) \subseteq (r * g *) * * Cl(B)$ .
- (3) A is (r\*g\*)\*\*-closed if and only if (r\*g\*)\*\*-Cl(A) = A.
- (4) (r\*g\*)\*\*-Cl[(r\*g\*)\*\*-Cl(A)] = (r\*g\*)\*\*-Cl(A).
- $(5) \left[ (\texttt{r} \star \texttt{g} \star) \star \star Cl(A) \right] U \left[ (\texttt{r} \star \texttt{g} \star) \star \star Cl(B) \right] = (\texttt{r} \star \texttt{g} \star) \star \star Cl(A \cup B).$
- (6)  $(r *g *) **-Int(X A) = X \lceil (r *g *) **-Cl(A) \rceil$ .
- (7)  $(r*g*)**-Cl(X-A) = X \lceil (r*g*)**-Int(A) \rceil$ .

**Definition 2.23.** (r \* g \*) \* \* - Bd(A) = A - [(r \* g \*) \* \* - Int(A)] is said to be the (r \* g \*) \* \* - border of A.

**Theorem 2.23.** For a subset A of a space X, the following statements hold:

- (1)  $Bd(A) \subseteq (r *g *) **- Bd(A)$  where Bd(A) denotes the border of A;
- (2) A = (r\*g\*)\*\*-Int(A)U(r\*g\*)\*\*-Bd(A);

on Innovative Surveys in Positive Sciences 4-5 December 2022 / Full Text Book

(3) 
$$\lceil (r \star g \star) \star \star - Int(A) \rceil I \lceil (r \star g \star) \star \star - Bd(A) \rceil = \phi;$$

(4) 
$$A$$
 is a  $(r*g*)**-open$  set if and only if  $(r*g*)**-Bd(A) = \phi$ ;

$$(5) (r*g*)**-Bd \lceil (r*g*)**-Int(A) \rceil = \emptyset;$$

(6) 
$$(r*g*)**-Int[(r*g*)**-Bd(A)]=\phi;$$

$$(7) (r \star g \star) \star \star - Bd \lceil (r \star g \star) \star \star - Bd (A) \rceil = (r \star g \star) \star \star - Bd (A);$$

(8) 
$$(r*g*)**-Bd(A) = AI[(r*g*)**-Cl(X-A)];$$

(9) 
$$(r*g*)**-Bd(A) = (r*g*)**-D(X-A)$$
.

**Proof.** (6) If  $x \in (r * g *) * * - Int[(r * g *) * * - Bd(A)]$ , then  $x \in (r * g *) * * - Bd(A)$ . On the other hand, since  $(r * g *) * * - Bd(A) \subseteq A$ ,  $x \in (r * g *) * * - Int[(r * g *) * * - Bd(A)] \subseteq (r * g *) * * - Int(A)$ . Therefore, we get  $x \in [(r * g *) * * - Int(A)]$  I [(r \* g \*) \* \* - Bd(A)], which contradicts (3). Thus,  $(r * g *) * * - Int[(r * g *) * * - Bd(A)] = \emptyset$ .

$$(8) (r*g*)**-Bd(A) = A - [(r*g*)**-Int(A)] = A - [X - ((r*g*)**-Cl(X-A))] = A \cdot [(r*g*)**-Cl(X-A)].$$

$$(9) (r *g *) **-Bd(A) = A - [(r *g *) **-Int(A)] = A - [A - ((r *g *) **-D(X - A))] = (r *g *) **-D(X - A).$$

**Definition 2.24.** (r\*g\*)\*\*-Fr(A) = [(r\*g\*)\*\*-Cl(A)] - [(r\*g\*)\*\*-Int(A)] is said to be the (r\*g\*)\*\*- frontier of A.

**Theorem 2.25.** For a subset A of a space X, the following statements hold:

(1) 
$$Fr(A) \subseteq (r * g *) **- Fr(A)$$
 where  $Fr(A)$  denotes the frontier of  $A$ ;

(2) 
$$(r*g*)**-Cl(A) = [(r*g*)**-Int(A)]U[(r*g*)**-Fr(A)];$$

(3) 
$$\left[\left(r\star g\star\right)\star\star -Int(A)\right]I\left[\left(r\star g\star\right)\star\star -Fr(A)\right]=\phi;$$

$$(4) (r \star g \star) \star \star - Bd(A) \subseteq (r \star g \star) \star \star - Fr(A);$$

on Innovative Surveys in Positive Sciences 4-5 December 2022 / Full Text Book

$$(5) (r *g *) **- Fr(A) = \lceil (r *g *) **- Bd(A) \rceil U \lceil (r *g *) **- D(A) \rceil;$$

(6) A is a 
$$(r*g*)**-open$$
 set if and only if  $(r*g*)**-Fr(A) = (r*g*)**-D(A)$ ;

$$(7) (r*g*)**-Fr(A) = [(r*g*)**-Cl(A)]I [(r*g*)**-Cl(X-A)];$$

(8) 
$$(r \star g \star) \star \star - Fr(A) = (r \star g \star) \star \star - Fr(X - A);$$

(9) 
$$(r*g*)**-Fr(A)$$
 is  $(r*g*)**-closed$ ;

$$(10) (r \star g \star) \star \star - Fr[(r \star g \star) \star \star - Fr(A)] \subseteq (r \star g \star) \star \star - Fr(A);$$

$$(11) (r *g *) **- Fr[(r *g *) **- Int(A)] \subseteq (r *g *) **- Fr(A);$$

$$(12) (r \star g \star) \star \star - Fr[(r \star g \star) \star \star - Cl(A)] \subseteq (r \star g \star) \star \star - Fr(A);$$

$$(13) (r *g *) **- Int(A) = A - [(r *g *) **- Fr(A)].$$

**Proof.** (2) 
$$[(r *g *) **- Int(A)]U[(r *g *) **- Fr(A)] =$$

$$(r*g*)**-Int(A)U[(r*g*)**-Cl(A)-(r*g*)**-Int(A)]=(r*g*)**-Cl(A)$$

$$(3) \left[ (r * g *) **- Int(A) \right] I \left[ (r * g *) **- Fr(A) \right] = \left[ (r * g *) **- Int(A) \right] I \left[ ((r * g *) **- Cl(A)) - ((r * g *) **- Int(A)) \right] = \phi.$$

(5) 
$$Since \left[ (r * g *) * * - Int(A) \right] U \left[ (r * g *) * * - Fr(A) \right] =$$

$$\left[ (r * g *) * * - Int(A) \right] U \left[ (r * g *) * * - Bd(A) \right] U \left[ (r * g *) * * - D(A) \right],$$

$$(r * g *) * * - Fr(A) = \left[ (r * g *) * * - Bd(A) \right] U \left[ (r * g *) * * - D(A) \right].$$

$$(7) (r*g*)**-Fr(A) = [(r*g*)**-Cl(A)] - [(r*g*)**-Int(A)] = [(r*g*)**-Cl(A)]I [(r*g*)**-Cl(X-A)].$$

(9) 
$$(r*g*)**-Cl[(r*g*)**-Fr(A)] =$$

$$(r*g*)**-Cl[((r*g*)**-Cl(A))I((r*g*)**-Cl(X-A))] \subseteq$$

$$(r*g*)**-Cl[(r*g*)**-Cl(A)]I(r*g*)**-Cl[(r*g*)**-Cl(X-A)]$$

$$=[(r*g*)**-Cl(A)]I[(r*g*)**-Cl(X-A)] = (r*g*)**-Fr(A). \text{ Hence}$$

$$(r*g*)**-Fr(A) \text{ is } (r*g*)**-closed.$$

on Innovative Surveys in Positive Sciences 4-5 December 2022 / Full Text Book

$$(10) (r*g*)**-Fr[(r*g*)**-Fr(A)] =$$

$$(r*g*)**-Cl[(r*g*)**-Fr(A)]I (r*g*)**-Cl[X-((r*g*)**-Fr(A))] \subseteq$$

$$(r*g*)**-Cl[(r*g*)**-Fr(A)] = (r*g*)**-Fr(A).$$

(12) 
$$(r*g*)**-Fr[(r*g*)**-Cl(A)]=$$

$$(r*g*)**-Cl[(r*g*)**-Cl(A)]-(r*g*)**-Int[(r*g*)**-Cl(A)]=$$

$$[(r*g*)**-Cl(A)]-[(r*g*)**-Int((r*g*)**-Cl(A))]\subseteq$$

$$[((r*g*)**-Cl(A))-((r*g*)**-Int(A))]=(r*g*)**-Fr(A).$$

(13) 
$$A - \left[ \left( r \star g \star \right) \star \star - Fr(A) \right] = A - \left[ \left( \left( r \star g \star \right) \star \star - Cl(A) \right) - \left( \left( r \star g \star \right) \star \star - Int(A) \right) \right] = \left( r \star g \star \right) \star \star - Int(A).$$

# 3-8: CHARACTERIZATIONS OF MAPPINGS

The purpose of this part is to introduce (r\*g\*)\*\*-continuous, (r\*g\*)\*\*-irresolute, (r\*g\*)\*\*-open, (r\*g\*)\*\*-closed, pre-(r\*g\*)\*\*-open, and pre-(r\*g\*)\*\*-closed functions and explore properties and characterizations of these functions.

# 3. (r\*g\*)\*\*-CONTINUOUS FUNCTIONS

The purpose of this section is to investigate the properties and characterizations of (r\*g\*)\*\*-continuous functions.

**Definition 3.1.** A function  $f:(X,\tau)\to (Y,\sigma)$  is said to be (r\*g\*)\*\*-continuous if  $f^{-1}(V)\in (r*g*)**-\bigcirc (X,\tau)$  for every  $V\in\sigma$ .

**Theorem 3.2.** Let  $f:(X,\tau) \to (Y,\sigma)$  be a function. Then the following statements are equivalent:

- (1) f is (r\*g\*)\*\*-continuous.
- (2) The inverse image of each closed set in Y is a (r\*g\*)\*\*-closed set in X;

(3) 
$$(r *g *) **-Cl [f^{-1}(V)] \subseteq f^{-1} [Cl(V)]$$
, for every  $V \subseteq Y$ ;

(4) 
$$f\lceil (r*g*)**-Cl(U)\rceil \subseteq Cl\lceil f(U)\rceil$$
, for every  $U\subseteq X$ ;

- (5) For any point  $x \in X$  and any open set V of Y containing f(x), there exists  $U \in (r * g *) * * O(X, \tau)$  such that  $x \in U$  and  $f(U) \subseteq V$ ;
- (6)  $(r*g*)**-Bd[f^{-1}(V)]\subseteq f^{-1}[(r*g*)**-d(V)]$ , for every  $V\subseteq Y$ ;

on Innovative Surveys in Positive Sciences 4-5 December 2022 / Full Text Book

(7) 
$$f\lceil (r *g *) **- D(U) \rceil \subseteq Cl\lceil f(U) \rceil$$
, for every  $U \subseteq X$ ;

(8) 
$$f^{-1}[Int(V)] \subseteq (r *g *) **-Int[f^{-1}(V)]$$
, for every  $V \subseteq Y$ ;

**Proof.** (1)  $\Rightarrow$  (2): Let  $F \subseteq Y$  be closed. Since f is (r\*g\*)\*\*-continuous,  $f^{-1}(Y-F)=X-f^{-1}(F)$  is (r\*g\*)\*\*-closed in X.

$$(2) \Rightarrow (3): \text{ Since } Cl(V) \text{ is closed for every } V \subseteq Y, \text{ then } f^{-1} \Big[ Cl(V) \Big] \text{ is } (r * g *) **-closed.$$
 Therefore 
$$f^{-1} \Big[ Cl(V) \Big] = (r * g *) **-Cl \Big[ f^{-1} \Big( Cl(V) \Big) \Big] \supseteq (r * g *) **-Cl \Big[ f^{-1}(V) \Big].$$

(3) 
$$\Rightarrow$$
 (4): Let  $U \subseteq X$  and  $f(U) = V$ . Then  $(r * g *) * * * - Cl[f^{-1}(V)] \subseteq f^{-1}[Cl(V)]$ . Thus  $(r * g *) * * * - Cl(U) \subseteq (r * g *) * * * - Cl[f^{-1}(f(U))] \subseteq f^{-1}[Cl(f(U))]$  and  $f[(r * g *) * * * - Cl(U)] \subseteq Cl[f(U)]$ .

$$(4) \Rightarrow (2): \text{ Let } W \subseteq Y \text{ be a closed set, and } U = f^{-1}(W). \text{ Then } f\Big[\big(\mathtt{r} \star \mathtt{g} \star\big) \star \star - Cl\big(U\big)\Big] \subseteq Cl\Big[f\big(U\big)\Big] = Cl\Big[f\big(f^{-1}(W)\big)\Big] \subseteq Cl(W) = W. \text{ Thus } \Big(\mathtt{r} \star \mathtt{g} \star\big) \star \star - Cl\big(U\big) \subseteq f^{-1}\Big[f\big(\mathtt{r} \star \mathtt{g} \star\big) \star \star - Cl(U\big)\Big] \subseteq f^{-1}(W) = U. \text{ So } U \text{ is } (\mathtt{r} \star \mathtt{g} \star) \star \star - closed.$$

(2)  $\Rightarrow$  (1):Let  $V \subseteq Y$  be an open set. Then Y - V is closed. Then  $f^{-1}(Y - V) = X - f^{-1}(V)$  is (r \* g \*) \* \* - closed in X and hence  $f^{-1}(V)$  is (r \* g \*) \* \* - open in <math>X.

(1) 
$$\Rightarrow$$
 (5): Let  $f:(X,\tau) \rightarrow (Y,\sigma)$  be  $(r*g*)**-continuous$ . For any  $x \in X$  and any open set  $V$  of  $Y$  containing  $f(x)$ ,  $U = f^{-1}(V) \in (r*g*)**-O(X,\tau)$ , and  $f(U) = f[f^{-1}(V)] \subseteq V$ .

(5)  $\Rightarrow$  (1): Let  $V \in \sigma$ . We prove  $f^{-1}(V) \in (r * g *) * * * - O(X, \tau)$ . Let  $x \in f^{-1}(V)$ . Then  $f(x) \in V$  and there exists  $U \in (r * g *) * * * - O(X, \tau)$  such that  $x \in U$  and  $f(x) \in f(U) \subseteq V$ . Hence  $x \in U \subseteq f^{-1}[f(U)] \subseteq f^{-1}(V)$ . It shows that  $f^{-1}(V)$  is a (r \* g \*) \* \* \* - neighborhood of each of its points. Therefore  $f^{-1}(V) \in (r * g *) * * * - O(X, \tau)$ .

(6) 
$$\Rightarrow$$
 (8): Let  $V \subseteq Y$ . Then by hypothesis,  $(r *g *) **- Bd[f^{-1}(V)] \subseteq f^{-1}[Bd(V)]$ 

$$\Rightarrow f^{-1}(V) - \left\lceil \left( \operatorname{r*g*} \right) * * - \operatorname{Int} \left( f^{-1}(V) \right) \right\rceil \subseteq f^{-1} \left[ V - \operatorname{Int} \left( V \right) \right] = f^{-1} \left( V \right) - f^{-1} \left[ \operatorname{Int} \left( V \right) \right]$$

$$\Rightarrow f^{-1}[Int(V)] \subseteq (r *g *) **- Int[f^{-1}(V)].$$

(8) 
$$\Rightarrow$$
 (6): Let  $V \subseteq Y$ . Then by hypothesis,  $f^{-1} \Big[ \mathit{Int} \big( V \big) \Big] \subseteq \big( \texttt{r*g*} \big) **- \mathit{Int} \Big[ f^{-1} \big( V \big) \Big]$ 

on Innovative Surveys in Positive Sciences 4-5 December 2022 / Full Text Book

$$\Rightarrow f^{-1}(V) - \left[ \left( r \star g \star \right) \star \star - Int \left( f^{-1}(V) \right) \right] \subseteq f^{-1}(V) - f^{-1} \left[ Int(V) \right] = f^{-1} \left[ V - Int(V) \right]$$
$$\Rightarrow \left( r \star g \star \right) \star \star - Bd \left[ f^{-1}(V) \right] \subseteq f^{-1} \left[ Bd(V) \right].$$

(1) 
$$\Rightarrow$$
 (7): It is obvious, since  $f$  is  $(r*g*)**-continuous$  and by (4)  $f[(r*g*)**-Cl(U)] \subseteq Cl[f(U)]$  for each  $U \subseteq X$ . So  $f[(r*g*)**-D(U)] \subseteq Cl[f(U)]$ .

 $(7) \Rightarrow (1)$ : Let  $U \subseteq Y$  be an open set, V = Y - U and  $f^{-1}(V) = W$ . Then by hypothesis  $f\left[\left(r * g *\right) * * * - D(W)\right] \subseteq Cl\left[f(W)\right]$ . Thus  $f\left[\left(r * g *\right) * * * - D(f^{-1}(V))\right] \subseteq Cl\left[f\left(f^{-1}(V)\right)$ 

$$(1) \Rightarrow (8): \text{ Let } V \subseteq Y. \text{ Then } f^{-1}\Big[\operatorname{Int}(V)\Big] \text{ is } (r * g *) * * - open in } X. \text{ Thus } f^{-1}\Big[\operatorname{Int}(V)\Big] = (r * g *) * * - \operatorname{Int}\Big[f^{-1}\big(\operatorname{Int}(V)\big)\Big] \subseteq (r * g *) * * - \operatorname{Int}\Big[f^{-1}\big(V\big)\Big]. \text{ Therefore } f^{-1}\Big[\operatorname{Int}(V\big)\Big] \subseteq (r * g *) * * - \operatorname{Int}\Big[f^{-1}(V\big)\Big].$$

(8) 
$$\Rightarrow$$
 (1): Let  $V \subseteq Y$  be an open set. Then  $f^{-1}(V) = f^{-1}[Int(V)] \subseteq (r *g *) **- Int[f^{-1}(V)]$ . Therefore,  $f^{-1}(V)$  is  $(r *g *) **- open$ . Hence  $f$  is  $(r *g *) **- continuous$ .

In the next Theorem, #(r \*g \*) \*\*-c. denotes the set of points x of X for which a function  $f:(X,\tau) \to (Y,\sigma)$  is not (r \*g \*) \*\*-continuous.

**Theorem 3.3.** #(r\*g\*)\*\*-c. is identical with the union of the (r\*g\*)\*\*- frontiers of the inverse images of (r\*g\*)\*\*- open sets containing f(x).

**Proof.** Suppose that f is not (r\*g\*)\*\*-continuous at a point x of X. Then there exists an open set  $V \subseteq Y$  containing f(x) such that f(U) is not a subset of V for every  $U \in (r*g*)**-O(X,\tau)$ . containing x. Hence, we have  $U I f^{-1}(X-f^{-1}(V)) \neq \emptyset$  for every  $U \in (r*g*)**-O(X,\tau)$  containing x. It follows that  $x \in [(r*g*)**-Cl(X-f^{-1}(V))]$ . We also have  $x \in f^{-1}(V) \subseteq (r*g*)**-Cl[f^{-1}(V)]$ . This means that  $x \in (r*g*)**-Fr[f^{-1}(V)]$ . Now, let f be (r\*g\*)\*\*-continuous at  $x \in X$  and  $V \subseteq Y$  any open set containing f(x). Then,  $x \in f^{-1}(V)$  is a (r\*g\*)\*\*-open set of X. Thus,  $x \in (r*g*)**-Int[f^{-1}(V)]$  and therefore  $x \notin (r*g*)**-Fr[f^{-1}(V)]$  for every open set V containing f(x).

**Remarks 3.4.** (1) Every (r\*g\*)\*\*-continuous function is continuous, but the converse may not be true.

# on Innovative Surveys in Positive Sciences 4-5 December 2022 / Full Text Book

(2) If a function  $f:(X,\tau)\to (Y,\sigma)$  is (r\*g\*)\*\*-continuous and a function  $g:(Y,\sigma)\to (Z,\vartheta)$  is (r\*g\*)\*\*-continuous, then  $g\circ f:(X,\tau)\to (Z,\vartheta)$  is (r\*g\*)\*\*-continuous.

- (3) If a function  $f:(X,\tau)\to (Y,\sigma)$  is  $(r\star g\star)\star \star continuous$  and a function  $g:(Y,\sigma)\to (Z,\vartheta)$  is continuous, then  $g\circ f:(X,\tau)\to (Z,\vartheta)$  is  $(r\star g\star)\star \star continuous$ .
- (4) Let  $(X, \tau)$  and  $(Y, \sigma)$  be topological spaces. If  $f: (X, \tau) \to (Y, \sigma)$  is a function, and one of the following

(a) 
$$f^{-1}[Int(B)] \subseteq (r *g *) **-Int[f^{-1}(B)]$$
 for each  $B \subseteq Y$ .

(b) 
$$(r *g *) ** - Cl [f^{-1}(B)] \subseteq f^{-1}[Cl(B)]$$
 for each  $B \subseteq Y$ .

(c) 
$$f[(r*g*)**-Cl(A)] \subseteq Cl[f(A)]$$
 for each  $A \subseteq X$  holds, then  $f$  is continuous.

**Lemma 3.5.** Let  $A \subseteq Y \subseteq X$ , Y is (r \* g \*) \* \* \* - open in X and A is (r \* g \*) \* \* \* - open in Y. Then A is (r \* g \*) \* \* \* - open in X.

**Proof.** Since A is (r\*g\*)\*\*-open in Y, there exists a (r\*g\*)\*\*-open set  $U \subseteq X$  such that  $A = Y \cup U$ . Thus A being the intersection of two (r\*g\*)\*\*-open sets in X, is (r\*g\*)\*\*-open in X.

# 4. (r\*g\*) \*\*- IRRESOLUTE FUNCTIONS

In this section, the functions to be considered are those for which inverses of (r\*g\*)\*\*-open sets are (r\*g\*)\*\*-open. We investigate some properties and characterizations of such functions.

**Definition 4.1.** Let  $(X, \tau)$  and  $(Y, \sigma)$  be topological spaces. A function  $f:(X, \tau) \to (Y, \sigma)$  is called  $(r \star_{\mathcal{G}} \star) \star_{resolute}$  if the inverse image of each  $(r \star_{\mathcal{G}} \star) \star_{resolute}$  set of Y is a  $(r \star_{\mathcal{G}} \star) \star_{resolute}$  set in X.

**Theorem 4.2.** Let  $f:(X,\tau)\to(Y,\sigma)$  be a function between topological spaces. Then the following statements are equivalent:

- (1) f is (r\*g\*)\*\*-irresolute;
- (2) the inverse image of each (r\*g\*)\*\*-closed set in Y is a (r\*g\*)\*\*-closed set in X;
- (3)  $(r*g*)**-Cl[f^{-1}(V)] \subseteq f^{-1}[(r*g*)**-Cl(V)]$  for every  $V \subseteq Y$ ;
- (4)  $f[(r*g*)**-Cl(U)]\subseteq (r*g*)**-Cl[f(U)]$  for every  $U\subseteq X$ ;

on Innovative Surveys in Positive Sciences 4-5 December 2022 / Full Text Book

(5) 
$$f^{-1}[g(r*g*)**-Int(B)]\subseteq (r*g*)**-Int[f^{-1}(B)]$$
 for every  $B\subseteq Y$ .

**Theorem 4.3.** Prove that a function  $f:(X,\tau)\to (Y,\sigma)$  is (r\*g\*)\*\*-irresolute if and only if for each point P in X and each (r\*g\*)\*\*-open set B in Y with  $f(p)\in B$ , there is a (r\*g\*)\*\*-open set A in X such that  $p\in A$ ,  $f(A)\subseteq B$ .

**Proof.** Necessity. Let  $p \in X$  and  $B \in (r * g *) * * * - O(Y, \sigma)$  such that  $f(p) \in B$ . Let  $A = f^{-1}(B)$ . Since f is (r \* g \*) \* \* \* - irresolute, A is (r \* g \*) \* \* \* - open in X. Also  $p \in f^{-1}(B) = A$  as  $f(p) \in B$ . Thus we have  $f(A) = f[f^{-1}(B)] \subseteq B$ .

**Sufficiency**. Let  $B \in (r * g *) * * - O(Y, \sigma)$ , and  $A = f^{-1}(B)$ . We show that A is (r \* g \*) \* \* - open in X. For this let  $x \in A$ . It implies that  $f(x) \in B$ . Then by hypothesis, there exists  $A_x \in (r * g *) * * - O(X, \tau)$  such that  $x \in A_x$  and  $f(A_x) \subseteq B$ . Then  $A_x \subseteq f^{-1}[f(A_x)] \subseteq f^{-1}(B) = A$ . Thus  $A = U\{A_x : x \in A\}$ . It follows that A is (r \* g \*) \* \* - open in X. Hence f is (r \* g \*) \* \* - irresolute.

**Definition 4.4.** Let  $(X, \tau)$  be a topological space. Let  $x \in X$  and  $N \subseteq X$ . We say that N is a (r \* g \*) \* \* - neighborhood of x if there exists a (r \* g \*) \* \* - open set M of X such that  $x \in M \subseteq N$ .

**Theorem 4.5.** Prove that a function  $f:(X,\tau)\to (Y,\sigma)$  is  $(r\star g\star)\star \star -irresolute$  if and only if for each x in X, the inverse image of every  $(r\star g\star)\star \star -neighborhood$  of f(x), is a  $(r\star g\star)\star \star -neighborhood$  of x.

**Proof.** Necessity. Let  $x \in X$  and let B be a (r\*g\*)\*\*-neighborhood of f(x). Then there exists  $U \in (r*g*)**-O(Y,\sigma)$  such that  $f(x) \in U \subseteq B$ . This implies that  $x \in f^{-1}(U) \subseteq f^{-1}(B)$ . Since f is (r\*g\*)\*\*-irresolute, so  $f^{-1}(U) \in (r*g*)**-O(X,\tau)$ . Hence  $f^{-1}(B)$  is a (r\*g\*)\*\*-neighborhood of x.

**Sufficiency.** Let  $B \in (r *g *) **-O(Y, \sigma)$ . Put  $A = f^{-1}(B)$ . Let  $x \in A$ . Then  $f(x) \in B$ . But then, B being (r \*g \*) \*\*-open set, is a (r \*g \*) \*\*-neighborhood of f(x). So by hypothesis,  $A = f^{-1}(B)$  is a (r \*g \*) \*\*-neighborhood of x. Hence by definition, there exists  $A_x \in (r *g *) **-O(X, \tau)$  such that  $x \in A_x \subseteq A$ . Thus  $A = U\{A_x : x \in A\}$ . It follows that A is a (r \*g \*) \*\*-open set in X. Therefore f is (r \*g \*) \*\*-irresolute.

# on Innovative Surveys in Positive Sciences 4-5 December 2022 / Full Text Book

**Theorem 4.6.** Prove that a function  $f:(X,\tau)\to (Y,\sigma)$  is  $(r\star_g\star)\star_{rresolute}$  if and only if for each x in X and each  $(r\star_g\star)\star_{rresolute}$  of f(x), there is a  $(r\star_g\star)\star_{rresolute}$  of f(x), there is a

**Proof.** Necessity. Let  $x \in X$  and let U be a (r \* g \*) \*\*-neighborhood of f(x). Then there exists  $O_{f(x)} \in (r * g *) **-O(Y, \sigma)$  such that  $f(x) \in O_{f(x)} \subseteq U$ . It follows that  $x \in f^{-1} \Big[ O_{f(x)} \Big] \subseteq f^{-1}(U)$ . By hypothesis,  $f^{-1} \Big[ O_{f(x)} \Big] \in (r * g *) **-O(X, \tau)$ . Let  $V = f^{-1}(U)$ . Then it follows that V is a (r \* g \*) \*\*-neighborhood of x and  $f(V) = f\Big[ f^{-1}(U) \Big] \subseteq U$ .

**Sufficiency.** Let  $B \in (r * g *) * * * - O(Y, \sigma)$ . Put  $O = f^{-1}(B)$ . Let  $x \in O$ . Then  $f(x) \in B$ . Thus B is a (r \* g \*) \* \* \* - neighborhood of f(x). So by hypothesis, there exists a (r \* g \*) \* \* \* - neighborhood  $V_x$  of x such that  $f(V_x) \subseteq B$ . Thus it follows that  $x \in V_x \subseteq f^{-1}[f(V_x)] \subseteq f^{-1}(B) = O$ . Since  $V_x$  is a (r \* g \*) \* \* \* - neighborhood of x, so there exists an  $O_x \in (r * g *) * * - O(X, \tau)$  such that  $x \in O_x \subseteq V_x$ . Hence  $x \in O_x \subseteq O$ ,  $O_x \in (r * g *) * * - O(X, \tau)$ . Thus  $O = U\{O_x : x \in O\}$ . It follows that O is (r \* g \*) \* \* - open in X. Therefore, f is (r \* g \*) \* \* - irresolute.

**Theorem 4.7.** Prove that a function  $f:(X,\tau)\to (Y,\sigma)$  is (r\*g\*)\*\*-irresolute if and only if  $f[(r*g*)**-D(A)]\subseteq f(A)U[(r*g*)**-D(f(A))]$ , for all  $A\subseteq X$ .

**Proof.** Necessity. Let  $f:(X,\tau)\to (Y,\sigma)$  be  $(r\star g\star)\star \star - irresolute$ . Let  $A\subseteq X$ , and  $a_0\in (r\star g\star)\star \star - D(A)$ . Assume that  $f(a_0)\not\in f(A)$  and let V denote a  $(r\star g\star)\star \star - neighborhood$  of  $f(a_0)$ . Since f is  $(r\star g\star)\star \star - irresolute$ , so by Theorem 4.6, there exists a  $(r\star g\star)\star \star - neighborhood$  U of  $a_0$  such that  $f(U)\subseteq V$ . It follows that U I  $A\neq \phi$ ; there exists, therefore, at least one element  $a\in U$  I A such that  $f(a)\in f(A)$  and  $f(a)\in f(V)$ . Since  $f(a_0)\notin f(A)$ , we have  $f(a)\neq f(a_0)$ . Thus every  $(r\star g\star)\star \star - neighborhood$  of  $f(a_0)$  contains an element of f(A) different from  $f(a_0)$ , consequently,  $f(a_0)\in (r\star g\star)\star \star - D[f(A)]$ . This proves necessity of the condition.

**Sufficiency.** Assume that f is not (r \* g \*) \* \* \* - irresolute. Then by Theorem 4.6, there exists  $a_0 \in X$  and a (r \* g \*) \* \* \* - neighborhood V of  $f(a_0)$  such that every (r \* g \*) \* \* \* - neighborhood U of  $a_0$  contains at least one element  $a \in U$  for which  $f(a) \notin V$ . Put  $A = \{a \in X : f(a) \notin V\}$ . Then  $a_0 \notin A$  since  $f(a_0) \in V$ , and therefore  $f(a_0) \notin A$ ; also  $f(a_0) \notin (r * g *) * * * - D[f(A)]$  since  $VI\left(V - \{f(a_0)\}\right) = \emptyset.$  Therefore,  $f(a_0) \in f[(r * g *) * * * - D(A)] - [f(A)U((r * g *) * * * - D(f(A)))] \neq \emptyset$ , which is a contradiction

to the given condition. The condition of the Theorem is therefore sufficient, and the theorem is proved.

# on Innovative Surveys in Positive Sciences 4-5 December 2022 / Full Text Book

**Theorem 4.8.** Let  $f:(X,\tau) \to (Y,\sigma)$  be a one-to-one function. Then f is (r\*g\*)\*\*-irresolute if and only if  $f[(r*g*)**-D(A)] \subseteq (r*g*)**-D[f(A)]$ , for all  $A \subseteq X$ .

**Proof. Necessity.** Let f be (r\*g\*)\*\*-irresolute. Let  $A \subseteq X$ ,  $a_0 \in (r*g*)**-D(A)$  and V be a (r\*g\*)\*\*-neighborhood of  $f(a_0)$ . Since f is (r\*g\*)\*\*-irresolute, so by Theorem 4.6, there exists a (r\*g\*)\*\*-neighborhood U of  $a_0$  such that  $f(U) \subseteq V$ . But  $a_0 \in (r*g*)**-D(A)$ ; hence there exists an element  $a \in U$  I A such that  $a \neq a_0$ ; then  $f(a) \in f(A)$  and since f is one to one,  $f(a) \neq f(a_0)$ . Thus every (r\*g\*)\*\*-neighborhood V of  $f(a_0)$  contains an element of f(A) different from  $f(a_0)$ ; consequently  $f(a_0) \in (r*g*)**-D[f(A)]$ . We have therefore  $f[(r*g*)**-D(A)] \subseteq (r*g*)**-D[f(A)]$ .

**Sufficiency.** Follows from Theorem 4.7.

# **5** (r\*g\*)\*\*-**OPEN FUNCTIONS**

The purpose of this section is to investigate some characterizations of (r\*g\*)\*\*-open mappings.

**Definition 5.1.** Let  $(X, \tau)$  and  $(Y, \sigma)$  be topological spaces. A function  $f:(X, \tau) \to (Y, \sigma)$  is called  $(r \star g \star) \star \star - open$  if for every open set G in X, f(G) is a  $(r \star g \star) \star \star - open$  set in Y.

**Theorem 5.2.** Prove that a mapping  $f:(X,\tau)\to (Y,\sigma)$  is (r\*g\*)\*\*-open if and only if for each  $x\in X$ , and  $U\in \tau$  such that  $x\in U$ , there exists a (r\*g\*)\*\*-open set  $W\subseteq Y$  containing f(x) such that  $W\subseteq f(U)$ .

**Proof.** Follows immediately from Definition 5.1.

**Theorem 5.3.** Let  $f:(X,\tau)\to (Y,\sigma)$  be  $(r\star g\star)\star \star -open$ . If  $W\subseteq Y$  and  $F\subseteq X$  is a closed set containing  $f^{-1}(W)$ , then there exists a  $(r\star g\star)\star \star -closed$   $H\subseteq Y$  containing W such that  $f^{-1}(H)\subseteq F$ .

**Proof.** Let H = Y - f(Y - F). Since  $f^{-1}(W) \subseteq F$ , we have  $f^{-1}(Y - F) \subseteq (Y - W)$ . Since f is (r \* g \*) \* \* - open, then H is (r \* g \*) \* \* - closed and  $f^{-1}(H) = X - f^{-1} \lceil f(X - F) \rceil \subseteq X - (X - F) = F$ .

**Theorem 5.4.** Let  $f:(X,\tau)\to (Y,\sigma)$  be a (r\*g\*)\*\*-open function and let  $B\subseteq Y$ . Then  $f^{-1}\Big[(r*g*)**-Cl\Big((r*g*)**-Int\Big((r*g*)**-Cl(B)\Big)\Big]\subseteq Cl\Big[f^{-1}(B)\Big].$ 

**Proof.**  $Cl[f^{-1}(B)]$  is closed in X containing  $f^{-1}(B)$ . By Theorem 5.3, there exists a (r \* g \*) \* \* \* - closed set  $B \subseteq H \subseteq Y$  such that  $f^{-1}(H) \subseteq Cl[f^{-1}(B)]$ . Thus,

on Innovative Surveys in Positive Sciences 4-5 December 2022 / Full Text Book

$$\begin{split} f^{-1}\Big[\big(\mathtt{r}\star\mathtt{g}\star\big)\star\star-Cl\big(\big(\mathtt{r}\star\mathtt{g}\star\big)\star\star-Int\big(\big(\mathtt{r}\star\mathtt{g}\star\big)\star\star-Cl\big(B\big)\big)\big)\Big] \subseteq \\ f^{-1}\Big[\big(\mathtt{r}\star\mathtt{g}\star\big)\star\star-Cl\big(\big(\mathtt{r}\star\mathtt{g}\star\big)\star\star-Int\big(\big(\mathtt{r}\star\mathtt{g}\star\big)\star\star-Cl\big(H\big)\big)\big)\Big] \subseteq f^{-1}\Big[H\Big] \subseteq Cl\Big[f^{-1}(B)\Big]. \end{split}$$

**Theorem 5.5.** Prove that a function  $f:(X,\tau)\to (Y,\sigma)$  is (r\*g\*)\*\*-open if and only if  $f\lceil Int(A)\rceil\subseteq (r*g*)**-Int\lceil f(A)\rceil$ , for all  $A\subseteq X$ .

**Proof. Necessity.** Let  $A \subseteq X$  and  $x \in Int(A)$ . Then there exists  $U_x \in \tau$  such that  $x \in U_x \subseteq A$ . So  $f(x) \in f(U_x) \subseteq f(A)$ . and by hypothesis,  $f(U_x) \in (r * g *) * * - O(Y, \sigma)$ . Hence  $f(x) \in (r * g *) * * - Int[f(A)]$ . Thus  $f[Int(A)] \subseteq (r * g *) * * - Int[f(A)]$ .

**Sufficiency.** Let  $U \in \tau$ . Then by hypothesis,  $f [Int(U)] \subseteq (r *g *) **- Int [f(U)]$ . Since Int(U) = U as U is open. Also,  $(r *g *) **- Int [f(U)] \subseteq f(U)$ . Hence f(U) = (r \*g \*) \*\*- Int [f(U)]. Thus f(U) is (r \*g \*) \*\*- open open in Y. So f is (r \*g \*) \*\*- open.

Remark 5.6. The equality may not hold in the preceding Theorem.

**Theorem 5.7.** Prove that a function  $f:(X,\tau)\to (Y,\sigma)$  is (r\*g\*)\*\*-open if and only if  $Int[f^{-1}(B)]\subseteq f^{-1}[(r*g*)**-Int(B)]$ , for all  $B\subseteq Y$ .

**Proof.** Necessity. Let  $B \subseteq Y$ . Since  $Int[f^{-1}(B)]$  is open in X and f is (r \* g \*) \* \* \* - open,  $f[Int(f^{-1}(B))]$  is (r \* g \*) \* \* \* - open in Y. Also we have  $f[Int(f^{-1}(B))] \subseteq f[f^{-1}(B)] \subseteq B$ . Hence,  $f[Int(f^{-1}(B))] \subseteq (r * g *) * * * - Int(B)$ . Therefore  $Int(f^{-1}(B)) \subseteq f^{-1}[(r * g *) * * - Int(B)]$ .

**Sufficiency.** Let  $A \subseteq X$ . Then  $f(A) \subseteq Y$ . Hence by hypothesis, we obtain  $Int(A) \subseteq Int[f^{-1}(f(A))] \subseteq f^{-1}[(r * g *) * * - Int(f(A))]$ . Thus  $f[int(A)] \subseteq (r * g *) * * - Int[f(A)]$ , for all  $A \subseteq X$ . Hence, by Theorem 5.5, f is (r \* g \*) \* \* - open.

**Theorem 5.8.** Let  $f:(X,\tau)\to (Y,\sigma)$  be a mapping. Then a necessary and sufficient condition for f to be (r\*g\*)\*\*-open is that  $f^{-1}[(r*g*)**-Cl(B)]\subseteq Cl[f^{-1}(B)]$  for every subset B of Y.

**Proof.** Necessity. Assume f is (r\*g\*)\*\*-open. Let  $B \subseteq Y$ . Let  $x \in f^{-1}[(r*g*)**-Cl(B)]$ . Then  $f(x) \in (r*g*)**-Cl(B)$ . Let  $U \in \tau$  such that  $x \in U$ . Since f is (r\*g\*)\*\*-open, then f(U) is a (r\*g\*)\*\*-open set in Y. Therefore, BI  $f(U) \neq \phi$ . Then UI  $f^{-1}(B) \neq \phi$ . Hence  $x \in Cl[f^{-1}(B)]$ . We conclude that  $f^{-1}[(r*g*)**-Cl(B)] \subseteq Cl[f^{-1}(B)]$ .

# on Innovative Surveys in Positive Sciences 4-5 December 2022 / Full Text Book

**Sufficiency.** Let  $B \subseteq Y$ . Then  $(Y-B) \subseteq Y$ . By hypothesis,  $f^{-1} \Big[ (r \star g \star) \star \star - Cl(Y-B) \Big] \subseteq Cl \Big[ f^{-1}(Y-B) \Big]$ . This implies that  $X - Cl \Big[ f^{-1}(Y-B) \Big] \subseteq X - f^{-1} \Big[ (r \star g \star) \star \star - Cl(Y-B) \Big]$ . Therefore  $X - Cl \Big[ X - f^{-1}(B) \Big] \subseteq f^{-1} \Big[ Y - ((r \star g \star) \star \star - Cl(Y-B)) \Big]$ . This implies that  $Int \Big[ f^{-1}(B) \Big] \subseteq f^{-1} \Big[ (r \star g \star) \star \star - Int(B) \Big]$ . Now form Theorem 5.7, it follows that f is  $(r \star g \star) \star \star - open$ .

# 6. (r\*g\*)\*\*-CLOSED FUNCTIONS

In this section, we introduce (r\*g\*)\*\*-closed functions and study certain properties and characterizations of these types of functions.

**Definition 6.1.** A mapping  $f:(X,\tau)\to (Y,\sigma)$  is called (r\*g\*)\*\*-closed if the image of each closed set in X is a (r\*g\*)\*\*-closed set in Y.

**Theorem 6.2.** Prove that a mapping  $f:(X,\tau)\to (Y,\sigma)$  is (r\*g\*)\*\*-closed if and only if  $(r*g*)**-Cl\lceil f(A)\rceil\subseteq f\lceil Cl(A)\rceil$  for each  $A\subseteq X$ .

**Proof.** Necessity. Let f be (r\*g\*)\*\*-closed and let  $A \subseteq X$ . Then  $f(A) \subseteq f[Cl(A)]$  and f[Cl(A)] is a (r\*g\*)\*\*-closed set in Y. Thus  $(r*g*)**-Cl[f(A)] \subseteq f[Cl(A)]$ .

**Sufficiency**. Suppose that  $(r*g*)**-Cl[f(A)] \subseteq f[Cl(A)]$ , for each  $A \subseteq X$ . Let  $A \subseteq X$  be a closed set. Then  $(r*g*)**-Cl[f(A)] \subseteq f[Cl(A)] = f(A)$ . This shows that f(A) is a (r\*g\*)\*\*-closed set. Hence f is (r\*g\*)\*\*-closed.

**Theorem 6.3.** Let  $f:(X,\tau)\to (Y,\sigma)$  be (r\*g\*)\*\*-closed. If  $V\subseteq Y$  and  $E\subseteq X$  is an open set containing  $f^{-1}(V)$ , then there exists a (r\*g\*)\*\*-open set  $G\subseteq Y$  containing V such that  $f^{-1}(G)\subseteq E$ .

**Proof.** Let G = Y - f(X - E). Since  $f^{-1}(V) \subseteq E$ , we have  $f(X - E) \subseteq Y - V$ . Since f is (r \* g \*) \*\*-closed, then G is a (r \* g \*) \*\*-open set and also  $f^{-1}(G) = X - f^{-1}[f(X - E)] \subseteq X - (X - E) = E$ .

**Theorem 6.4.** Suppose that  $f:(X,\tau)\to (Y,\sigma)$  is a (r\*g\*)\*\*-closed mapping. Then  $(r*g*)**-Int[(r*g*)**-Cl(f(A))]\subseteq f[Cl(A)]$  for every subset A of X.

**Proof.** Suppose f is a (r\*g\*)\*\*-closed mapping and A is an arbitrary subset of X. Then f[Cl(A)] is (r\*g\*)\*\*-closed in Y. Then  $(r*g*)**-Int[(r*g*)**-Cl(f(Cl(A)))] \subseteq$ 

on Innovative Surveys in Positive Sciences 4-5 December 2022 / Full Text Book

$$f [Cl(A)]$$
. But also  $(r*g*)**-Int[(r*g*)**-Cl(f(A))] \subseteq (r*g*)**-Int[(r*g*)**-Cl(f(A))] \subseteq f[Cl(A)]$ . So  $(r*g*)**-Int[(r*g*)**-Cl(f(A))] \subseteq f[Cl(A)]$ .

**Theorem 6.5.** Let  $f:(X,\tau)\to (Y,\sigma)$  be a (r\*g\*)\*\*-closed function, and  $B,C\subseteq Y$ .

**Proof.** (1) If U is an open neighborhood of  $f^{-1}(B)$ , then there exists a (r\*g\*)\*\*-open neighborhood V of B such that  $f^{-1}(B) \subseteq f^{-1}(V) \subseteq U$ .

(2) If f is also onto, then if  $f^{-1}(B)$  and  $f^{-1}(C)$  have disjoint open neighborhoods, so have B and C.

**Proof.** (1) Let V = Y - f(X - U). Then  $V^c = Y - V = f(U^c)$ . Since f is (r \* g \*) \* \* - closed, so V is a (r \* g \*) \* \* - open set. Since  $f^{-1}(B) \subseteq U$ , we have  $V^c = f(U^c) \subseteq f[f^{-1}(B^c)] \subseteq B^c$ . Hence,  $B \subseteq V$ , and thus V is a (r \* g \*) \* \* - open neighborhood of B. Further  $U^c \subseteq f^{-1}[f(U^c)] = f^{-1}(V^c) = [f^{-1}(V)]^c$ . This proves that  $f^{-1}(V) \subseteq U$ .

(2) If  $f^{-1}(B)$  and  $f^{-1}(C)$  have disjoint open neighborhoods M and N, then by (1), we have (r\*g\*)\*\*\*-open neighborhoods U and V of B and C respectively such that  $f^{-1}(B) \subseteq f^{-1}(U) \subseteq (r*g*)**-Int(M)$  and  $f^{-1}(C) \subseteq f^{-1}(V) \subseteq (r*g*)**-Int(N)$ . Since M and N are disjoint, so are (r\*g\*)\*\*-Int(M) and (r\*g\*)\*\*-Int(N), hence so  $f^{-1}(U)$  and  $f^{-1}(V)$  are disjoint as well. It follows that U and V are disjoint too as f is onto.

**Theorem 6.6.** Let  $f:(X,\tau)\to(Y,\sigma)$  be a bijection. Then the following are equivalent:

- (a) f is (r\*g\*)\*\*-closed.
- (b) f is (r\*g\*)\*\*-open.
- (c)  $f^{-1}$  is (r\*g\*)\*\*-continuous.

**Proof.** (a)  $\Rightarrow$  (b): Let  $U \in \tau$ . Then X - U is closed in X. By (a), f(X - U) is (r \* g \*) \* \* \* - closed in Y. But f(X - U) = f(X) - f(U) = Y - f(U). Thus f(U) is (r \* g \*) \* \* - open in Y. This shows that f is (r \* g \*) \* \* - open.

(b)  $\Rightarrow$  (c): Let  $U \subseteq X$ . be an open set. Since f is (r \*g \*) \*\*-open. So  $f(U) = (f^{-1})^{-1}(U)$  is (r \*g \*) \*\*-open in Y. Hence  $f^{-1}$  is (r \*g \*) \*\*-continuous.

# on Innovative Surveys in Positive Sciences

4-5 December 2022 / Full Text Book

(c)  $\Rightarrow$  (a): Let A be an arbitrary closed set in X. Then X-A is open in X. Since  $f^{-1}$  is (r \* g \*) \* \* - continuous,  $(f^{-1})^{-1}(X-A)$  (r \* g \*) \* \* - open in Y. But  $(f^{-1})^{-1}(X-A) = f(X-A) = Y-f(A)$ . Thus f(A) is (r \* g \*) \* \* - closed in Y. This shows that f is (r \* g \*) \* \* - closed.

**Remark 6.7.** A bijection  $f:(X,\tau)\to (Y,\sigma)$  may be open and closed but neither (r\*g\*)\*\*-open nor (r\*g\*)\*\*-closed.

# 7. PRE - (r\*g\*) \*\*- OPEN FUNCTIONS

The purpose of this section is to introduce and discuss certain properties and characterizations of pre - (r\*g\*)\*\*-open functions.

**Definition 7.1.** Let  $(X, \tau)$  and  $(Y, \sigma)$  be topological spaces. Then a function  $f:(X, \tau) \to (Y, \sigma)$  is said to be  $pre \cdot (r \star g \star) \star \star \cdot open$  if and only if for each  $A \in (r \star g \star) \star \star \cdot O(X, \tau)$ ,  $f(A) \in (r \star g \star) \star \star \cdot O(Y, \sigma)$ .

**Theorem 7.2.** Let  $f:(X,\tau)\to (Y,\sigma)$  and  $g:(Y,\sigma)\to (Z,\mu)$  be any two pre-(r\*g\*)\*\*-open functions. Then the composition function  $g\circ f:(X,\tau)\to (Z,\mu)$  is a pre-(r\*g\*)\*\*-open function.

**Proof.** Let  $U \in (r * g *) * * * - O(X, \tau)$ . Then  $f(U) \in (r * g *) * * * - O(Y, \sigma)$ . Since f is pre - (r \* g \*) \* \* \* - open. But then  $g(f(U)) \in (r * g *) * * * - O(Z, \mu)$  as g is pre - (r \* g \*) \* \* \* - open. Hence,  $g \circ f$  is pre - (r \* g \*) \* \* \* - open.

**Theorem 7.3.** Prove that a mapping  $f:(X,\tau)\to (Y,\sigma)$  is pre-(r\*g\*)\*\*-open if and only if for each  $x\in X$  and any  $U\in (r*g*)**-O(X,\tau)$  such that  $x\in U$ , there exists  $V\in (r*g*)**-O(Y,\sigma)$  such that  $f(x)\in V$  and  $V\subseteq f(U)$ .

Proof. Routine.

**Theorem 7.4.** Prove that a mapping  $f:(X,\tau)\to (Y,\sigma)$  is pre-(r\*g\*)\*\*-open if and only if for each  $x\in X$  and for any (r\*g\*)\*\*-neighborhood U of x in X, there exists a (r\*g\*)\*\*-neighborhood V of f(x) in Y such that  $V\subseteq f(U)$ .

**Proof.** Necessity. Let  $x \in X$  and let U be a (r \* g \*) \*\*-neighborhood of x. Then there exists  $W \in (r * g *) **-O(X, \tau)$  such that  $x \in W \subseteq U$ . Then  $f(x) \in f(W) \subseteq f(U)$ . But

on Innovative Surveys in Positive Sciences 4-5 December 2022 / Full Text Book

 $f(W) \in (r * g *) * * - O(Y, \sigma)$  as f is pre - (r \* g \*) \* \* - open. Hence V = f(W) is a (r \* g \*) \* \* - neighborhood of f(x) and  $V \subseteq f(U)$ .

**Sufficiency.** Let  $U \in (r * g *) **-O(X, \tau)$  and let  $x \in U$ . Then U is a (r \* g \*) \*\*-neighborhood of x. So by hypothesis, there exists a  $(r * g *) **-neighborhood V_{f(x)}$  of f(x) such that  $f(x) \in V_{f(x)} \subseteq f(U)$ . It follows at once that f(U) is a (r \* g \*) \*\*-neighborhood of each of its points. Therefore f(U) is (r \* g \*) \*\*-open. Hence f is pre-(r \* g \*) \*\*-open.

**Theorem 7.5.** Prove that a function  $f:(X,\tau)\to (Y,\sigma)$  is pre-(r\*g\*)\*\*-open if and only if  $f\lceil (r*g*)**-Int(A)\rceil \subseteq (r*g*)**-Int\lceil f(A)\rceil$ , for all  $A\subseteq X$ .

**Proof.** Necessity. Let  $A \subseteq X$  and  $x \in (r * g *) * * * - Int(A)$ . Then there exists  $U_x \in (r * g *) * * * - O(X, \tau)$  such that  $x \in U_x \subseteq A$ . So  $f(x) \in f(U_x) \subseteq f(A)$  and by hypothesis,  $f(U_x) \in (r * g *) * * * - O(Y, \sigma)$ . Hence  $f(x) \in (r * g *) * * * - Int[f(A)]$ . Thus  $f[(r * g *) * * * - Int(A)] \subseteq (r * g *) * * * - Int[f(A)]$ .

**Sufficiency.** Let  $U \in (r * g *) * * - O(X, \tau)$ . Then by hypothesis,  $f[(r * g *) * * - Int(U)] \subseteq (r * g *) * * - Int[f(U)]$ . Since (r \* g \*) \* \* - Int(U) = U as U is (r \* g \*) \* \* - open. Also  $(r * g *) * * - Int[f(U)] \subseteq f(U)$ . Hence f(U) = (r \* g \*) \* \* - Int[f(U)]. Thus f(U) is (r \* g \*) \* \* - open in Y. So f is pre - (r \* g \*) \* \* - open.

We remark that the equality does not hold in Theorem 7.5 as the following example shows.

**Example 7.6.** Let  $X = Y = \{1, 2\}$ . suppose X is anti-discrete and Y is discrete. Let f = Id.,  $A = \{1\}$ . Then  $\phi = f \lceil (r * g *) * * - Int(A) \rceil \neq (r * g *) * * - Int[f(A)] = \{1\}$ .

**Theorem 7.7.** Prove that a function  $f:(X,\tau)\to (Y,\sigma)$  is pre-(r\*g\*)\*\*-open if and only if  $(r*g*)**-Int[f^{-1}(B)]\subseteq f^{-1}[(r*g*)**-Int(B)]$ , for all  $B\subseteq Y$ .

**Proof.** Necessity. Let  $B \subseteq Y$ . Since  $(r*g*)**-Int[f^{-1}(B)]$  is (r\*g\*)\*\*-open in X and f is pre-(r\*g\*)\*\*-open,  $f[(r*g*)**-Int(f^{-1}(B))]$  (r\*g\*)\*\*-open in Y. Also we have  $f[(r*g*)**-Int(f^{-1}(B))] \subseteq f[f^{-1}(B)] \subseteq B$ . Hence,  $f[(r*g*)**-Int(f^{-1}(B))] \subseteq (r*g*)**-Int(B)$ . Therefore  $(r*g*)**-Int[f^{-1}(B)] \subseteq f^{-1}[(r*g*)**-Int(B)]$ .

# on Innovative Surveys in Positive Sciences 4-5 December 2022 / Full Text Book

**Sufficiency.** Let  $A \subseteq X$ . Then  $f(A) \subseteq Y$ . Hence by hypothesis, we obtain  $(r * g *) * * - Int(A) \subseteq (r * g *) * * - Int[f^{-1}(f(A))] \subseteq f^{-1}[(r * g *) * * - Int(f(A))]$ . This implies that  $f[(r * g *) * * - Int(A)] \subseteq f[f^{-1}((r * g *) * * - Int(f(A)))] \subseteq (r * g *) * * - Int[f(A)]$ . Thus  $f[(r * g *) * * - Int(A)] \subseteq (r * g *) * * - Int[f(A)]$ , for all  $A \subseteq X$ . Hence, by Theorem 7.5, f is pre - (r \* g \*) \* \* - open.

**Theorem 7.8.** Prove that a mapping  $f:(X,\tau)\to (Y,\sigma)$  is pre-(r\*g\*)\*\*-open if and only if  $f^{-1}\lceil (r*g*)**-Cl(B)\rceil \subseteq (r*g*)**-Cl\lceil f^{-1}(B)\rceil$ , for every subset B of Y.

**Proof.** Necessity. Let  $B \subseteq Y$  and let  $x \in f^{-1} [(r * g *) * * * - Cl(B)]$ . Then  $f(x) \in (r * g *) * * * - Cl(B)$ . Let  $U \in (r * g *) * * * - O(X, \tau)$  such that  $x \in U$ . By hypothesis,  $f(U) \in (r * g *) * * * - O(Y, \sigma)$  and  $f(x) \in f(U)$ . Thus  $f(U) I B \neq \emptyset$ . Hence  $U I f^{-1}(B) \neq \emptyset$ . Therefore,  $x \in (r * g *) * * * - Cl[f^{-1}(B)]$ , So we obtain  $f^{-1} [(r * g *) * * * - Cl(B)] \subseteq (r * g *) * * * - Cl[f^{-1}(B)]$ .

**Sufficiency.** Let  $B \subseteq Y$ . Then  $(Y-B) \subseteq Y$ . By hypothesis,  $f^{-1} \Big[ (r * g *) * * - Cl(Y-B) \Big] \subseteq (r * g *) * * - Cl \Big[ f^{-1}(Y-B) \Big]$ . This implies that  $X - \Big[ (r * g *) * * - Cl \Big( f^{-1}(Y-B) \Big) \Big] \subseteq X - f^{-1} \Big[ (r * g *) * * - Cl(Y-B) \Big]$ . Hence  $X - \Big[ (r * g *) * * - Cl \Big[ X - f^{-1}(B) \Big] \subseteq f^{-1} \Big[ Y - \Big( (r * g *) * * - Cl(Y-B) \Big) \Big]$ . Then this implies that  $gsg - Int \Big[ f^{-1}(B) \Big] \subseteq f^{-1} \Big[ (r * g *) * * - Int(B) \Big]$ . Now by Theorem 7.7, it follows that f is pre - (r \* g \*) \* \* - open.

**Theorem 7.9.** Let  $f:(X,\tau)\to (Y,\sigma)$  and  $g:(Y,\sigma)\to (Z,\mu)$  be two mappings such that  $g\circ f:(X,\tau)\to (Z,\mu)$  is (r\*g\*)\*\*-irrsolute. Then

- (1) If g is a pre-(r\*g\*)\*\*--open injection, then f is (r\*g\*)\*\*-irrsolute.
- (2) If f is a pre-(r\*g\*)\*\*-open surjection, then g is (r\*g\*)\*\*-irrsolute.

**Proof.** (1) Let  $U \in (r * g *) **-O(Y, \sigma)$ . Then  $g(U) \in (r * g *) **-O(Z, \mu)$  since g is pre-(r \* g \*) \*\*-open Also  $g \circ f$  is (r \* g \*) \*\*-irrsolute. Therefore, we have  $(g \circ f)^{-1} [g(U)] \in (r * g *) **-O(X, \tau)$ . Since g is an injection, so we have :  $(g \circ f)^{-1} [g(U)] = (f^{-1} \circ g^{-1}) [g(U)] = f^{-1} [g^{-1}(g(U))] = f^{-1}(U)$ . Consequently  $f^{-1}(U)$  is (r \* g \*) \*\*-open in X. This proves that f is (r \* g \*) \*\*-irrsolute.

# on Innovative Surveys in Positive Sciences 4-5 December 2022 / Full Text Book

(2) Let  $V \in (r * g *) **-O(Z, \mu)$ . Then  $(gof)^{-1}(V) \in (r * g *) **-O(X, \tau)$  since gof is (r \* g \*) \*\*-irrsolute. Also f is pre-(r \* g \*) \*\*-open,  $f[(gof)^{-1}(V)]$  is (r \* g \*) \*\*-open in Y. Since f is surjective, we note that  $f[(gof)^{-1}(V)] = [fo(gof)^{-1}](V) = [fo(f^{-1}og^{-1})](V) = [(fof^{-1})og^{-1}(V)] = g^{-1}(V)$ . Hence g is (r \* g \*) \*\*-irrsolute.

# 8. PRE-(r\*g\*)\*\*-CLOSED FUNCTIONS

In this last section, we introduce and explore several properties and characterizations of pre - (r + g + closed) functions.

**Definition 8.1.** A function  $f:(X,\tau)\to (Y,\sigma)$  is said to be  $pre-(\mathbf{r}*\mathbf{g}*)**-closed$  if and only if the image set f(A) is  $(\mathbf{r}*\mathbf{g}*)**-closed$  for each  $(\mathbf{r}*\mathbf{g}*)**-closed$  subset A of X.

**Theorem 8.2.** The composition of two pre-(r\*g\*)\*\*-closed mappings is a pre-(r\*g\*)\*\*-closed mapping.

**Proof.** The straightforward proof is omitted.

**Theorem 8.3.** Prove that a mapping  $f:(X,\tau)\to (Y,\sigma)$  is  $pre-(\mathbf{r}\star\mathbf{g}\star)\star\star-closed$  if and only if  $(\mathbf{r}\star\mathbf{g}\star)\star\star-Cl[f(A)]\subseteq f[(\mathbf{r}\star\mathbf{g}\star)\star\star-Cl(A)]$  for every subset A of X.

**Proof.** Necessity. Suppose f is a pre-(r\*g\*)\*\*-closed mapping and A is an arbitrary subset of X. Then f[(r\*g\*)\*\*-Cl(A)] is (r\*g\*)\*\*-closed in Y. Since  $f(A) \subseteq f[(r*g*)**-Cl(A)]$ , we obtain  $(r*g*)**-Cl[f(A)] \subseteq f[(r*g*)**-Cl(A)]$ .

**Sufficiency.** Suppose F is an arbitrary (r\*g\*)\*\*-closed set in X. By hypothesis, we obtain  $f(F) \subseteq (r*g*)**-Cl[f(F)] \subseteq f[(r*g*)**-Cl(F)] = f(F)$ . Hence f(F) = (r\*g\*)\*\*-Cl[f(F)]. Thus f(F) is (r\*g\*)\*\*-closed in Y. It follows that f is pre-(r\*g\*)\*\*-closed.

**Theorem 8.4.** Let  $f:(X,\tau)\to (Y,\sigma)$  be a pre-(r\*g\*)\*\*-closed function, and  $B,C\subseteq Y$ .

- (1) If U is a  $(\mathbf{r}*\mathbf{g}*)**-open$  neighborhood of  $f^{-1}(B)$ , then there exists a  $(\mathbf{r}*\mathbf{g}*)**-open$  neighborhood V of B such that  $f^{-1}(B) \subseteq f^{-1}(V) \subseteq U$ .
- (2) If f is also onto, then if  $f^{-1}(B)$  and  $f^{-1}(C)$  have disjoint  $(\mathbf{r} * \mathbf{g} *) * * * open$  neighborhoods, so have B and C.

# on Innovative Surveys in Positive Sciences 4-5 December 2022 / Full Text Book

**Proof.** (1) Let V = Y - f(X - U). Then  $V^c = Y - V = f(U^c)$ . Since f is pre - (r\*g\*)\*\*-closed, so V is (r\*g\*)\*\*-open. Since  $f^{-1}(B) \subseteq U$ , we have  $V^c = f(U^c) \subseteq f[f^{-1}(B^c)] \subseteq B^c$ . Hence,  $B \subseteq V$ , and thus V is a (r\*g\*)\*\*-open neighborhood of B. Further  $U^c \subseteq f^{-1}[f(U^c)] = f^{-1}(V^c) = [f^{-1}(V)]^c$ . This proves that  $f^{-1}(V) \subseteq U$ .

(2) If  $f^{-1}(B)$  and  $f^{-1}(C)$  have disjoint (r\*g\*)\*\*\*-open neighborhoods M and N, then by (1), we have (r\*g\*)\*\*\*-open neighborhoods U and V of B and C respectively such that  $f^{-1}(B) \subseteq f^{-1}(U) \subseteq (r*g*)**-Int(M)$  and  $f^{-1}(C) \subseteq f^{-1}(V) \subseteq (r*g*)**-Int(N)$ . Since M and N are disjoint, so are (r\*g\*)\*\*-Int(M) and (r\*g\*)\*\*-Int(N), and hence so  $f^{-1}(U)$  and  $f^{-1}(V)$  are disjoint as well. It follows that U and V are disjoint too as f is onto.

**Theorem 8.5.** Let  $f:(X,\tau)\to(Y,\sigma)$  be a bijection. Then the following are equivalent:

- (1) f is pre-(r\*g\*)\*\*-closed.
- (2) f is pre-(r\*g\*)\*\*-open.
- (3)  $f^{-1}$  is (r\*g\*)\*\*-irresolute.

**Proof.** (1)  $\Rightarrow$  (2): Let  $U \in (r * g *) ** - O(X, \tau)$ . Then X - U is (r \* g \*) \*\* - closed in X. By (1), f(X - U) is (r \* g \*) \*\* - closed in Y. But f(X - U) = f(X) - f(U) = Y - f(U). Thus f(U) is (r \* g \*) \*\* - open in Y. This shows that f is pre - (r \* g \*) \*\* - open.

 $(2) \Rightarrow (3)$ : Let  $A \subseteq X$ . Since f is pre-(r\*g\*)\*\*-open, so by Theorem 7.8,  $f^{-1}[(r*g*)**-Cl(f(A))] \subseteq (r*g*)**-Cl[f^{-1}(f(A))]$ . It implies that  $(r*g*)**-Cl[f(A)] \subseteq f[(r*g*)**-Cl(A)]$ .

Thus  $(r \star g \star) \star \star - Cl \Big[ (f^{-1})^{-1} (A) \Big] \subseteq (f^{-1})^{-1} \Big[ (r \star g \star) \star \star - Cl (A) \Big]$ , for all  $A \subseteq X$ . Then by Theorem 4.8, it follows that  $f^{-1}$  is  $(r \star g \star) \star \star - irresolute$ .

(3)  $\Rightarrow$  (1): Let A be an arbitrary (r\*g\*)\*\*-closed set in X. Then X-A is (r\*g\*)\*\*-open in X. Since  $f^{-1}$  is (r\*g\*)\*\*-irresolute,  $(f^{-1})^{-1}(X-A)$  is (r\*g\*)\*\*-open in Y. But  $(f^{-1})^{-1}(X-A)=f(X-A)=Y-f(A)$ . Thus f(A) is (r\*g\*)\*\*-closed in Y. This shows that f is pre-(r\*g\*)\*\*-closed.

# on Innovative Surveys in Positive Sciences

4-5 December 2022 / Full Text Book

#### **ACKNOWLEDGEMENT**

The author is highly and gratefully indebted to Prince Mohammad Bin Fahd University, Al Khobar, Saudi Arabia, for providing all necessary research facilities during the preparation of this research paper.

#### REFERENCES

- [1] S.P. Arya and M. Deb, On  $\theta$ -continuous mappings, Math. Student 42(1974), 81-89.
- [2] M. Caldas, M. Ganster, D.N. Georgious, S. Jafari and T. Noiri, On  $\theta$ -semipen sets and separation axioms in topological spaces, Carpathian J. Math., 24 (2008), No. 1, 13 22.
- [3] E. Ekici,  $(\delta$ -pre,s)-continuous functions, Bulletin of the Malaysian Mathematical Sciences Society, Second Series 27(2004), no. 2, 237 251.
- [4] E. Ekici, On  $\delta$ -semiopen sets and a generalization of functions, Bol. Soc. Mat. (38) vol. 23 (1-2) (2005), 73-84.
- [5] M. Ganster, T. Noiri, I.L. Reilly, Weak and strong forms of  $\theta$ -irresolute functions, J. Inst. Math. Comput. Sci. 1(1) (1988), 19-29.
- [6] Saeid Jafari, Some properties of  $\theta$ -continuous functions, Far East J. Math. Sci. 6(5) (1998), 689-696.
- [7] Javier A. Hassan, and Mhelmar A. Labendia,  $\theta_s$  open sets and  $\theta_s$  continuity of mapps in the product space, Journal of Mathematics and Computer Science, 25 (2022), 182 190.
- [8] A. Kilicman, Z. Salleh, Some results on  $(\delta$ -pre,s)-continuous functions, International Journal Math. Mat. Sci. 2006(2006), 1-11.
- [9] Raja M. Latif, On Characterizations of Mappings, Soochow Journal of Mathematics, Volume 19, No.4, (1993), pp. 475 495.
- [10] Raja Mohammad Latif, Theta  $-\omega$  Mappings in Topological Spaces, WSEAS Transactions on Mathematics, Volume 19, 2020, Art.#18, pp. 186 207. (Scopus Indexed) (www.scopus.com)
- [11] Raja Mohammad Latif, Properties of Theta Continuous Functions in Topological Spaces, (MACISE 2020: International Conference on Mathematics and Computers in Science and Engineering (MACISE) Madrid Spain 18 20 January 2020), (2020), Volume 1, pages 81 90. (Scopus Indexed) (www.scopus.com)
- [12] N. Levine, Semi-open sets and semi-continuity in topological spaces, Amer. Math. Monthly, 70 (1963), 36-41.
- [13] M. Lellis Thivagar, Nirmala Rebecca Paul and Saeid Jafari, On New Class of Generalized Closed Sets, Annals of the University of Craiova, Mathematics and Computer Sciwnce Series, Vulume 38 (3), (2011), pp. 84 93.
- [14] P.E. Long, L.L. Herrington, The  $\tau_{\theta}$  -topology and faintly continuous functions, Kyungpook Math. J. 22(1982), 7-14.
- [15] N. Meenakumari and T. Indira, (r\*g\*) \*\*- closed sets in topological spaces, European Journal of Moleculer & Clinical Medicine, Volume 7, Issue 11, (2020), 9487 9496.
- [16] T. Noiri, S. Jafari, Properties of  $(\theta,s)$ -continuous functions, Topology and its Applications, 123(1) (2002), 167-179.
- [17] T. Noiri, On δ-continuous functions, J. Korean Math. Soc., 16 (1980), 161-166.
- [18] M. Saleh, On  $\theta$ -closed sets and some forms of continuity, Archivum Mathematicum (On BRNO) 40 (2004), 383 393.
- [19] M. Saleh, On super and  $\delta$ -continuities, Mathematics and Mathematics Education, World Scientific, 2002, 281-291.
- [20] N. V. Velicko, H-closed topological spaces. Mat. Sb. 70 (1966), 98-112, English transl., in Amer. Math. Soc. Transl. (2) 78 (1968), 103-118.
- [21] Albert Wilansky, Topology for Analysis, Devore Phlications, Inc, Mineola New York. (1980).
- [22] Stephen Willard, General Topology, Reading, Mass.: Addison Wesley Pub. Co. (1970)

on Innovative Surveys in Positive Sciences 4-5 December 2022 / Full Text Book

# FERROKROM CÜRUFUNUN BİTÜMLÜ SICAK KARIŞIMLARDA FİLLER OLARAK KULLANILABİLİRLİĞİNİN ARAŞTIRILMASI

# INVESTIGATION OF THE USAGE OF FERROCHROME SLAG AS FILLERS IN BITUMINOUS HOT MIXTURES

## Tacettin GEÇKİL

Doç. Dr., İnönü Üniversitesi ORCID: 0000-0001-8070-6836

#### Sena KOÇ

Yüksek Lisans Öğrencisi, İnönü Üniversitesi ORCID: 0000-0003-1365-9341

#### Ceren Beyza İNCE

Doktora Öğrencisi, İnönü Üniversitesi ORCID: 0000-0002-6385-0964

#### ÖZET

Biyokütle, çanlıların, çeşitli ihtiyaçlarını gidermesi sonucunda meydana gelen atıklardır. Bu atıklar, çok çeşitli olup genellikle tarımsal, ormansal, hayvansal, sanayi, endüstriyel ve evsel atıklar olarak sınıflandırılmaktadır. Hemen hemen her sektörde kullanılarak değerlendirilmeye calısılan bu atıklar, son yıllarda yol mühendisleri tarafından da kullanılmaya başlamıştır. Bu çalışmada, biyokütle esaslı endüstriyel bir atık olan ferrokrom cürufunun bitümlü sıcak karışım (BSK)'larda filler olarak kullanılabilirliği araştırılmıştır. Bunun için, ilk olarak, saf B 50/70 bitümü ve kırmataş kalker agregasının çeşitli karakteristik özellikleri belirlenmiştir. Daha sonra, sıcak karışım numunelerinin hazırlanmasında Marshall karışım tasarım yöntemi kullanılarak BSK'ların optimum bitüm içeriği tespit edilmistir. Optimum bitüm içeriğinin tespit edilmesinden sonra, bu oran esas alınarak ilk olarak saf bağlayıcı ile Marshall briket numuneleri hazırlanmıştır. Ardından, ferrokrom cürufunun filler malzeme olarak sıcak karısımda kullanılabilirliğini belirleyebilmek amacıyla sıcak karısımdaki filler oranı ağırlıkça %25, 50, 75 ve 100 oranlarında azaltılarak bunun yerine aynı oranlarda ferrokrom cürufu ikame edilerek cüruf ilaveli BSK numuneleri hazırlanmıştır. Hazırlanan saf ve cüruf ikameli tüm briket numuneleri Marshall stabilite ve akma deneyine tabi tutulmuştur. Elde edilen deney sonuçları değerlendirildiğinde, cüruf ikamesiyle sıcak karışım numunelerinin stabilite değerlerinin %8,1 kadar artış gösterdiği ve bunun %50 cüruf ikameli numunelerden elde edildiği görülmüştür. Bu sonuç, ferrokrom cürufu ikameli asfalt kaplamaların trafik yükleri altında iken kaplamalarda meydana gelebilecek kalıcı deformasyonlara karşı daha dirençli olduğunu göstermektedir. Sonuç olarak, endüstriyel bir atık olan ferrokrom cürufunun sıcak karışımlarda filler yerine ikame edilerek kullanılabileceği ve bununla birlikte BSK'ların stabilitesi üzerinde olumlu bir etkiye sahip olabileceği görülmüştür.

**Anahtar kelimeler:** Bitümlü sıcak karışım, Biyokütle, Endüstriyel atık, Ferrokrom cürufu, Marshall stabilite, Kalıcı deformasyon.

#### **ABSTRACT**

Biomass is the waste that is formed as a result of meeting the various needs of living things. These wastes are generally classified as agricultural, forestry, animal, industrial and domestic wastes. These wastes, which are tried to be evaluated by using them in almost every sector, have also started to be used by road engineers in recent years. In this study, the usability of ferrochrome slag, a biomass-based

on Innovative Surveys in Positive Sciences 4-5 December 2022 / Full Text Book

industrial waste, as filler in bituminous hot mixtures (BSK) were investigated. For this, firstly, various characteristic properties of aggregate were determined with pure B 50/70 bitumen. Then, the optimum bitumen content of BSKs was determined by using the Marshall mix design method in the preparation of the mix specimens. After determining the optimum bitumen content, Marshall briquette specimens were first prepared with pure binder based on this ratio. Then, in order to determine the usability of ferrochrome slag as filler material in the hot mixture, the filler ratio in the hot mixture was reduced by 25, 50, 75 and 100 wt%, and slag-added BSK specimens were prepared by replacing it with ferrochrome slag in the same proportions. All prepared pure and slag substituted briquette specimens were subjected to Marshall stability and flow test. When the test results obtained were evaluated, it was observed that the stability values of the hot mix specimens increased by 8.1% with the slag substitution, and this was obtained from the specimens with 50% slag substitution. This result shows that asphalt pavements substituted with ferrochrome slag are more resistant to permanent deformations that may occur in pavements under traffic loads. As a result, it has been seen that ferrochrome slag, which is an industrial waste, can be used as a substitute for fillers in hot mixes, and it can have a positive effect on the stability of BSKs.

**Keyword:** Bituminous hot mixture, Biomass, Industrial waste, Ferrochrome slag, Marshall stability, Permanent deformation.

#### 1. GİRİŞ

Dünya üzerindeki bütün canlıların yaşamında ve ekolojik dengenin bozulmasındaki en büyük tehdit unsurlarından biri atık malzemelerdir. Atık malzemeler çok çeşitli olup genellikle tarımsal atıklar (patates, kenevir vb.), ormansal atıklar (odun vb.), endüstriyel atıklar (cüruf atıklar, metaller, artık yağlar vb.), hayvansal atıklar (at, koyun, keçi gibi hayvanların gübreleri vb), evsel atıklar (kağıt, poşet, cam, metal vb.) ve kanalizasyon atıkları olup bu atıklar aynı zamanda birer biyokütlesel kaynaklardır [1-3]. Canlıların sağlığına zarar vermekle birlikte çevresel tahribata neden olan bu atık malzemeler, günümüzde çok geniş alanları işgal etmektedir. Özellikle endüstriyel atıkların açık alanlardaki depolama alanları oldukça daralmaktadır [1,2].

Son yıllarda dünya genelinde endüstriyel atıkların artmasıyla birlikte işletmelerin bu atıkları yok etmeleri yüksek maliyet sebebiyle güçleşmektedir. Bu durum endüstriyel atıkların farklı alanlarda kullanılması ve değerlendirilmesini yaygınlaştırmaktadır. Özellikle endüstriyel bir atık malzeme olan yüksek firin cürufları birçok alanda geri dönüştürülerek kullanılmaktadır [3,4]. Bu cürufların kullanılması depolama alanlarının azalmasına, doğal kaynakların korunmasına ve ülke ekonomisine büyük ölçüde katkı sağlayacaktır. Ülkemizde büyük miktarlarda oluşan uçucu kül, silis dumanı, ferronikel cürufları, ferrokrom cürufu gibi atık malzemeler endüstriyel atıklar olarak örnek verilebilir [5,6]. Hemen hemen her sektörde kullanılarak değerlendirilmeye çalışılan bu atıklar, son yıllarda yol mühendisleri tarafından da kullanılmaya başlamıştır.

Ülkemizde karayolu ağlarında en çok tercih edilen kaplama türü esnek kaplamalardır. Esnek kaplamalar, genellikle sathi kaplama ve bitümlü sıcak karışım kaplama olmak üzere iki şekilde uygulanabilmektedir. Son yıllarda ekonomik şartlarla birlikte kaplamaların hizmet ömürleri ve performansları göz önüne alındığından yapılan yollarda sathi kaplama yerine bitümlü sıcak karışım (BSK) kaplamalar tercih edilmektedir. BSK'lar agrega ve bitüm olmak üzere iki malzemeden oluşmaktadır ve bu iki malzemenin özellikleri kaplama performansını doğrudan etkilemektedir. Yol inşasında ve hazır beton içerisinde hacimsel olarak %60-75 genellikle kadar agrega kullanılır [6-9]. Agregalar, doğal ve yapay olmak üzere iki şekilde temin edilirler. Yapay olarak elde edilen agregalara örnek olarak cüruflardan elde edilen agregalar verilebilir.

Dünya genelinde özellikle ferrokrom cürufu yol inşaatında önemli ölçüde kullanılmaktadır [6-8,10,11]. Ferrokrom cürufu, ferrokrom üretimi yapan tesislerin elektrik-ark fırınlarının işlem sonucunda ortaya çıkan atık malzemedir. Bu atık malzeme depolama tesislerinde depolanamadığı için doğada birikinti halinde bulundurulmaktadır. Bu atık birikintiler çeşitli çevre zararlarına sebep olmaktadır. ferrokrom cürufu havada yavaş yavaş soğumaya bırakılarak üretilmesinden dolayı aktıf değildir ve kristal bir form kazanmaktadır. Bu şekilde üretilen cüruf, yüksek mekanik özelliklere sahip olduğundan, genellikle

on Innovative Surveys in Positive Sciences 4-5 December 2022 / Full Text Book

agrega yerine kullanılmaktadır. Depolama alanlarının azalması ve bu cüruf atıklarının miktarlarının sürekli artmasıyla birlikte farklı alanlarda kullanımı değerlendirilerek çalışmaların başlatılması önem kazanmıştır [12].

Bu çalışmada, biyokütle esaslı endüstriyel bir atık olan ferrokrom cürufunun bitümlü sıcak karışım (BSK)'larda filler malzeme olarak kullanılabilirliği araştırılmıştır.

BSK kaplamalarda, trafik yükü ve çevre şartları nedeniyle zamanla çeşitli bozulmalar meydana gelmektedir. Sıcak asfalt kaplamalarda en sık meydana gelen bozulma türleri; tekerlek izi, düşük sıcaklık çatlağı, yorulma çatlağı ve sudan kaynaklı hasarladır [13]. Bu bozulmalara sebep olan başlıca nedenler, yapım ve tasarım hataları, iklim ve çevre koşulları ve trafik etkileri olarak sıralanabilir [5]. Günümüzde bu bozulmaları minimuma indirmek ya da yok etmek ve kaplamadan beklenen özellikleri iyileştirmek amacıyla çeşitli katkı maddeleri kullanılmaktadır [3]. Fakat çoğu katkı maddelerinin temin edilmesi maliyet açısından yüksek olması sebebiyle, özellikle son zamanlarda araştırmacılar katkı malzemesi olarak atık malzemeleri değerlendirerek kullanmaya başlamışlardır [4].

Bu çalışmada, endüstriyel bir atık olan ferrokrom cürufu'nun, BSK'ların önemli performans özelliklerinden biri olan Marshall stabilitesi üzerindeki etkisi araştırılarak yol kaplamalarının trafik yükü etkilerine karşı dayanımı arttırılmaya çalışılmıştır.

#### 2. MATERYAL VE METOT

#### 2.1. Materyal

Çalışmada, Karayolları 8. Bölge Müdürlüğü asfalt plentinden temin edilen penetrasyon sınıfı B 50/70 olan saf asfalta ait fiziksel özellikler Tablo 1'de verilmiştir.

Deney	Standart	Sınır	Sonuç	
Penetrasyon (0.1mm)	ASTM D5	50-70	50,6	
Yumuşama noktası (°C)	ASTM D36	46-54	53,8	
Düktilite (cm)	ASTM D113	min. 100	>100	
Parlama noktası (°C)	ASTM D92	min. 230	245	
Özgül ağırlık (gr/cm <sup>3</sup> )	ASTM D70	1.0-1.1	1.034	

**Tablo 1.** B 50/70 asfaltın fiziksel özellikleri

Modifikasyonda katkı olarak kullanılan ferrokrom cürufu (FeCR) (Şekil 1), Elazığ ferrokrom işletmesinin elektrik-ark fırınlarından temin edilmiş ve kimyasal özelikleri Tablo 2'de verilmiştir.

**Tablo 2.** Ferrokrom cürufu'nun kimyasal özellikleri [14]

Birleşim (%)	SiO <sub>2</sub>	Al <sub>2</sub> O <sub>3</sub>	Fe <sub>2</sub> O <sub>3</sub>	CaO	MgO	Cr <sub>2</sub> O <sub>3</sub>
FeCR	33,80	25,48	0,61	1,10	35,88	2,12

on Innovative Surveys in Positive Sciences 4-5 December 2022 / Full Text Book

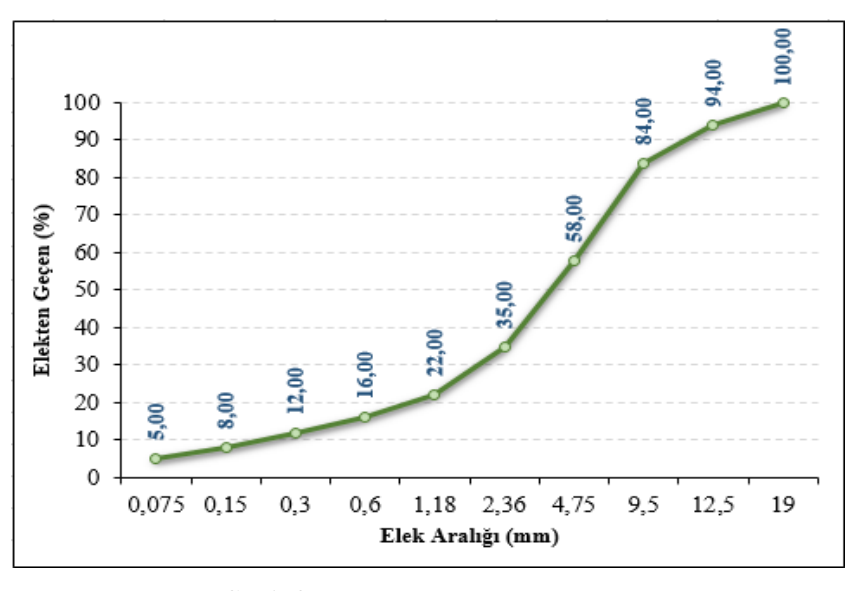


Şekil 1. Endüstriyel bir atık olan Ferrokrom Cürufu

Marshall karışım tasarımında kullanılan kırma taş kalker agregasının fiziksel özellikleri Tablo 3'de, agrega gradasyonu ise Şekil 2'de verilmiştir.

Deney	Standart	Limit	Sonuç
Kaba agrega zahiri özgül ağırlık (gr/cm³)	ASTM C127	-	2,76
İnce agrega zahiri özgül ağırlık (gr/cm³)	ASTM C128	-	2,83
Filler zahiri özgül ağırlık (gr/cm³)	<b>ASTM D 854</b>	-	2,66

Tablo 3. Agreganın fiziksel özellikleri



Şekil 2. Agrega gradasyonu

#### **2.2.** Metot

#### 2.2.1. Sıcak Karışım Numunelerinin Hazırlanması

Ferrokrom cürufu'nun BSK'ların performans özelliklerine etkilerini belirlemek amacıyla, ASTM D 1559'a göre saf asfaltlar ile Marshall dizayn yöntemi ile sıcak karışım numuneleri hazırlanmıştır. Bunun için, ilk olarak saf B50/70 bitüm kullanılarak karışım tasarımı için gerekli olan optimum bitüm içeriği oranı tespit edilmiştir. Bu oran esas alınarak, ilk olarak saf bağlayıcı ile Marshall briket numuneleri hazırlanmıştır. Daha sonra, ferrokrom cürufunun filler malzeme olarak sıcak karışımda kullanılabilirliğini belirleyebilmek amacıyla sıcak karışımdaki filler oranı ağırlıkça %25, 50, 75 ve 100

on Innovative Surveys in Positive Sciences 4-5 December 2022 / Full Text Book

oranlarında azaltılarak bunun yerine aynı oranlarda ferrokrom cürufu ikame edilerek cüruf ilaveli BSK numuneleri hazırlanmıştır. Her bir numunenin hazırlanması için, bitüm ve 1200 gr agrega 170 °C ve 165 °C sıcaklıkta ısıtılmıştır. Bitüm ve agrega karıştırma sıcaklığında karıştırıldıktan sonra, 457 mm yükseklikten serbest olarak düşen tokmak ile her bir yüzeyine 75 vuruş olacak şekilde, toplamda 150 vuruş uygulanarak sıkıştırma sıcaklığında sıkıştırılmıştır.

Çalışmada, saf ve katkılı karışımlar sırasıyla S, S+%25FC, S+%50FC, S+%75FC ve S+%100FC olarak kodlanmıştır.

#### 3. DENEYSEL YÖNTEM

## 3.1. Sıcak Karışımların Marshall Stabilite ve Akma Deneyine Tabi Tutulması

Marshall stabilite ve akma deneyi, ASTM D 1559 standardına göre sıcak karışım asfaltların plastik akmaya karşı gösterdiği mukavemetin belirlenmesi için yapılır. Deneye ön hazırlık olarak, sıcak karışım numunelerinin 3 farklı ağırlıkları ve yükseklikleri belirlenir. Daha sonra numuneler 60±1 °C sıcaklıktaki su banyosunda yaklaşık 30-40 dakika kadar bekletilir. Bu süre bitiminde numuneler sudan çıkarılarak Marshall cihazına yerleştirilir ve briket numunesine 50±2 mm/dakika hızla yükleme yapılır. Deney sonunda briket numunesinin kırıldığı andaki stabilitesi ve akma değeri Marshall cihazına otomatik kaydedilir. Stabilite değeri, sıcak karışımın deformasyonlara karşı gösterdiği en yüksek mukavemeti, akma ise numunede maksimum yüke ulaştığı anda meydana gelen düşey deformasyonu göstermektedir. Standart numune yüksekliği bu deney için 63.5 mm olarak belirlenmiştir. Ancak yükseklikleri farklı olan numuneler için denklem (1) yardımıyla stabilite düzeltme katsayıları hesaplanır [2,15].

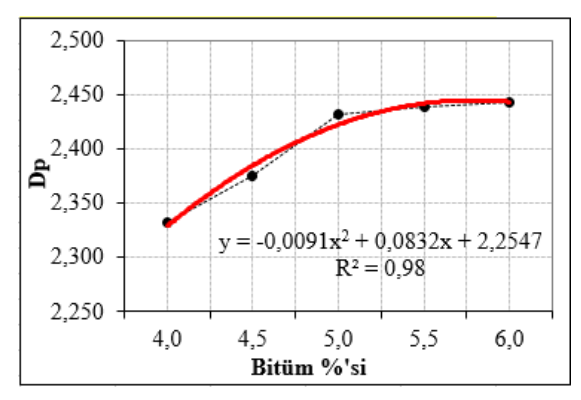
$$c = 5.24 \text{ x } e^{(-0.0258x\text{h})} \tag{1}$$

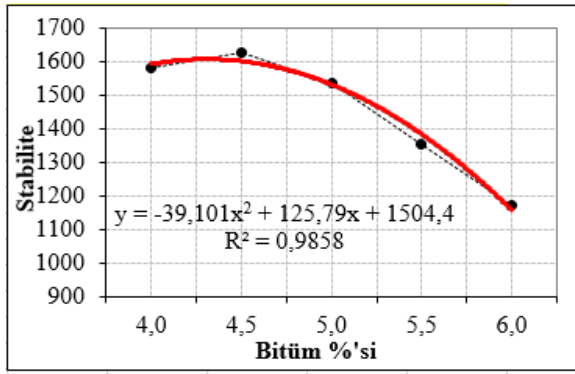
Denklemde c; düzeltme katsayısı, h; numune yüksekliğini göstermektedir. Bulunan stabilite ve akma değerlerinin ortalaması hesaplanarak kaydedilir ve böylece sonuçlar elde edilmiş olur. Aynı zamanda bu deney sonucunda, sıcak karışımların sertliğinin ve deformasyona karşı direncinin bir göstergesi olarak kabul edilen Marshall oranı (MQ) değeri de hesaplanabilmektedir. Marshall oranı (MQ), stabilite değerinin akma değerine oranıdır [2,15].

#### 4. BULGULAR VE DEĞERLENDİRME

#### 4.1. Sıcak Karışımların Marshall Stabilite ve Akma Deney Sonuçları

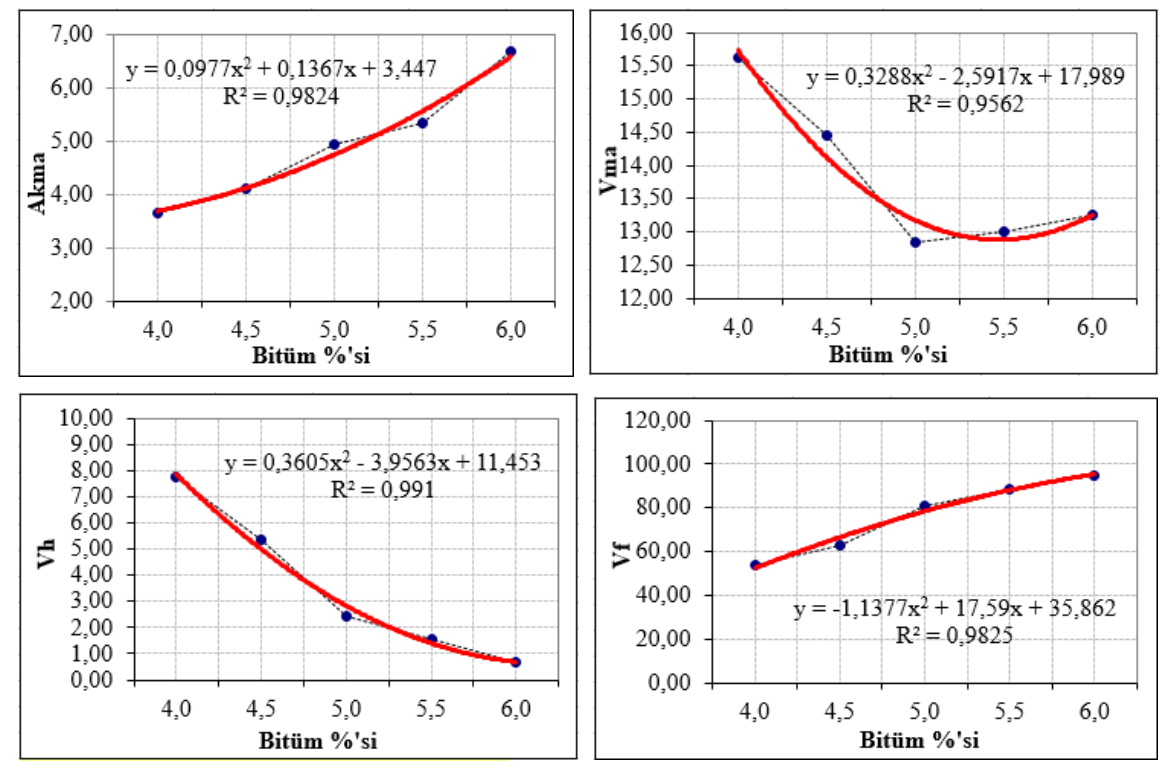
Saf B 50/70 asfalt bağlayıcılı karışım numunesinin optimum asfalt içeriği tespit etmek için, sıcak karışımda kullanılacak olan agrega miktarı sabit tutularak, agrega ağırlığının %4 - %4,5 - %5 - %5,5 - %6 oranlarında asfalt eklenerek her orandan üçer adet olmak üzere toplam 15 adet briket numunesi hazırlanmıştır. Sıcak karışım numunelerinin fiziksel özellikleri belirlendikten sonra, hacim özgül ağırlıkları (Dp), boşluk oranları (Vh), agregalar arası boşluk oranları (VMA) ve asfaltla dolu boşluk oranları (Vf) gibi hacimsel özellikleri tespit edilerek numuneler üzerinde Marshall stabilite ve akma deneyi yapılmıştır. Saf B50/70 asfalt bağlayıcılı karışım numunelerinin bulunan hacimsel ve mekanik özelliklerinin asfalt ile değişim grafikleri Şekil 3'de verilmiştir.





on Innovative Surveys in Positive Sciences

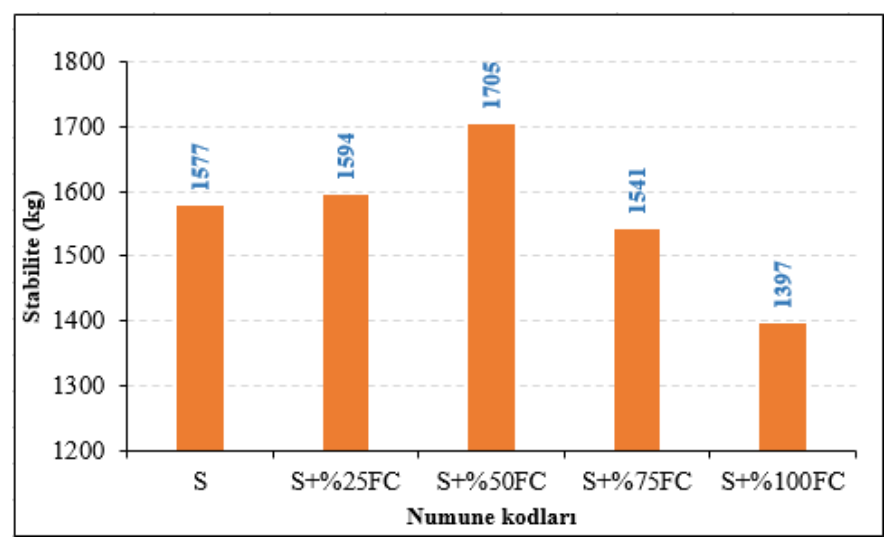
4-5 December 2022 / Full Text Book



**Şekil 3.** Optimum asfalt içeriğinin belirlenmesi için hazırlanan numunelerin hacimsel ve mekanik özellikleri

Şekil 3'de verilen sıcak karışım numunelerinin çeşitli hacimsel ve mekanik özellikleri yardımı ile Dp'nin maksimum (%5) ve stabilitenin maksimum (%4,5), Vh'ın %4 (%4,75) ve Vf'nin %70 (%4,5) olduğu asfalt yüzdelerinin aritmetik ortalaması alınarak optimum bitüm içeriği oranı %4,75 olarak belirlenmiştir. Belirlenen bu oranda saf (kontrol) ve ferrokrom cürufu katkılı karışım numuneleri hazırlanarak Karayolları Teknik Şartname (KTŞ) limitleri ile karşılaştırılarak, bu değerlerin [16] uyumlu olduğu görülmüştür. Hazırlanan ferrokrom cürufu katkılı karışımların, saf karışımla kıyaslanabilmesi için %4,75 oranı sabit tutulmuştur.

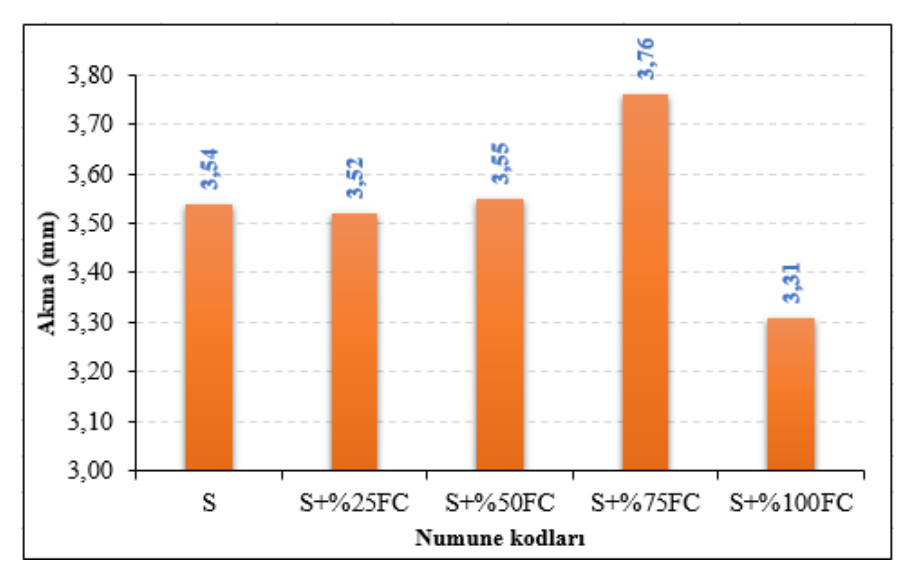
Saf ve ferrokrom cürufu katkılı BSK numunelerinin Marshall stabilite ve akma değerleri sırasıyla Şekil 4 ve Şekil 5'de, karışım numunelerinin MQ değerlerinin ferrokrom cürufu oranı ile değişimi ise Şekil 6'de verilmiştir.



Şekil 4. Karışım numunelerinin stabilite değerleri

on Innovative Surveys in Positive Sciences

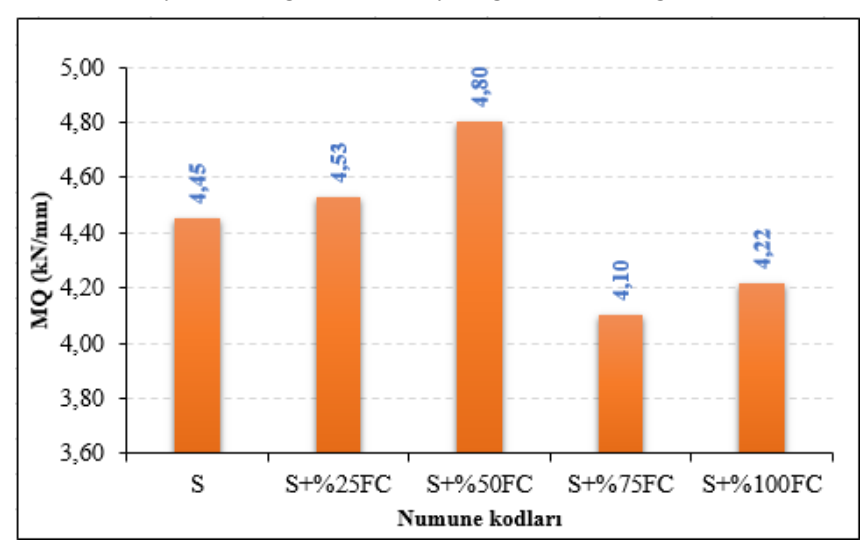
4-5 December 2022 / Full Text Book



Sekil 5. Karışım numunelerinin akma değerleri

Şekil 4'de BSK numunelerinin stabilite değerleri incelendiğinde, ferrokrom cürufu ile karışım numunelerinin stabilite değerlerinde değişiklikler meydana gelmiştir. Meydana gelen bu değişimler saf karışıma kıyasla sırasıyla %1,1 ve %8,1 artış; %2,3 ve %11,4 azalma şeklindedir. Karışım numuneleri arasında en yüksek stabilite değeri ise %50 ferrokrom cürufu katkılı karışım numunesinde görülmektedir. Bu durumda ferrrokrom cürufu katkısının, sıcak asfalt karışım kaplamaların kalıcı deformasyon direncini arttırdığını ifade etmek mümkündür.

Şekil 5 incelendiğinde, ferrokrom cürufu katkılı sıcak karışımların akma değerlerinde değişiklikler göstermiştir. Ancak, bu değişimler saf karışım ile hemen hemen aynı seviyelerdedir. Sıcak karışımın akma değeri, BSK kaplamanın trafik yükleri altındaki plastik veya esnek sıcak karışımların kırılma esnasındaki davranışını ifade eder. Elde edilen sonuç, ferrokrom cüruflu sıcak karışımların kırılma esnasındaki davranışında büyük bir değişiklik olmayacağı şeklinde değerlendirilebilir.



Şekil 6. Karışım numunelerinin MQ değerleri

Şekil 6'da görüldüğü gibi modifiye karışımların MQ değerleri, ferrrokrom cürufu katkı oranı artışı değişiklik göstermiştir. Meydana gelen bu değişimler saf karışıma kıyasla sırasıyla %1,8 ve %7,9 artış; %7,9 ve %5,2 azalma şeklindedir. MQ değeri, sıcak karışımların kayma gerilmelerine karşı direncinin bir ölçüsü olarak değerlendirilmektedir. Elde edilen bu sonuçlara göre, ferrrokrom cürufunun, karışımların kayma gerilmelerine ve kalıcı deformasyonlara karşı direncini arttırdığı ve en yüksek MQ değerinin %50 ferrrokrom cürufu katkılı karışımlarda görüldüğü ifade edilebilir.

on Innovative Surveys in Positive Sciences 4-5 December 2022 / Full Text Book

#### 5. SONUCLAR

Endüstriyel bir atık olan ferrokrom cürufu'nun BSK kaplamalarda kullanılabilirliğinin araştırıldığı bu çalışmada elde edilen sonuçlar aşağıda verilmiştir:

- 1. Marshall stabilite deney sonuçlarına göre, ferrokrom cürufu katkısıyla karışımların kalıcı deformasyonlara karşı gösterdiği direncin %8,1 kadar artış gösterdiği ve bunun %50 ferrokrom cürufu ikameli numunelerden elde edildiği görülmüştür. Bu sonuç, ferrokrom cürufu ikameli asfalt kaplamaların trafik yükleri altında iken kaplamalarda meydana gelebilecek kalıcı deformasyonlara karşı daha dirençli olduğunu göstermektedir.
- 2. Karışım numunelerin akma değerleri incelendiğinde, ferrrokrom cürufu katkılı karışım numunelerinin kırılma anındaki davranışının saf karışım ile benzer olduğu görülmüştür.
- 3. BSK numunelerinin MQ değerleri incelendiğinde ise, en yüksek MQ değeri %50 ferrokrom cürufu katkılı karışımlardan elde edilmiş ve bu nedenle ferrokrom cürufu katkısıyla hazırlanan karışımların kayma gerilmeleri altında daha dirençli olduğu belirlenmiştir.

Sonuç olarak, endüstriyel bir atık olan ferrokrom cürufunun sıcak karışımlarda filler yerine ikame edilerek kullanılabileceği ve bununla birlikte BSK'ların stabilitesi üzerinde olumlu bir etkiye sahip olabileceği görülmüştür.

# TEŞEKKÜR

Bu çalışma, İnönü Üniversitesi Bilimsel Araştırma Projeleri (BAP) Koordinasyon Biriminin İÜ-BAP FBG-2021-2270 numaralı projesi ile desteklenmiştir. Desteklerinden dolayı BAP Koordinasyon Birimine teşekkür ederiz.

#### KAYNAKLAR

- [1] Akyıldız H, Efe H, Önen F. (2020). Baraj Yapımında Atık Malzemelerin Kullanımı: Kadıköy Göleti Örneği, Mühendislik Dergisi, 11(1): 439-445.
- [2] Geçkil T, İnce CB, İssi S. (2021). Pirina Modifiyeli Bitümlerin Yüksek Sıcaklıklardaki İşlenebilirliği ve Kalıcı Deformasyon Direnci, Politeknik Dergisi, 25(2): 745-755.
- [3] Uysal F, Bahar S. (2018). Cüruf Çeşitleri ve Kullanım Alanları, Trakya University Journal of Engineering Sciences, 19(1): 37-52.
- [4] Yılmaz A, Sütaş İ. (2008). Ferrokrom Cürufunun Yol Malzemesi Olarak Kullanımı, İMO Teknik Dergi, 19(93): 4455-4470.
- [5] Yılmaz A, Yıldız AH. (2015). Cüruf Atıklarının Yol İnşaatında Kullanılması Durumunda Çevresel Etkileri, Uluslararası Burdur Deprem ve Çevre Sempozyumu, 267-279.
- [6] Geçkil T. (2008). Siyah Karbonun Bitümlü Sıcak Karışımların Özelliklerine Etkisinin İncelenmesi. Doktora Tezi, Fırat Üniversitesi.
- [7] Tunç A. (2004). Esnek Kaplama Malzemeleri El Kitabı, Asil Yayın Dağıtım, İstanbul, 352s.
- [8] Tunç A. (2007). Yol Malzemeleri ve Uygulamaları, Nobel Yayın Dağıtım, İstanbul, 840s.
- [9] Ahmedzade P, Fainleib A, Günay T, Grygoryeva O. (2014). Modification of Bitumen By Electron Beam İrradiated Recycled Low Density Polyethylene, Construction and Building Materials, 69: 1-9.
- [10] Booysen H. (2008). The Use of The Waste Delisting Process Case Study: The Management of Ferrochrome Slag As A Construction Product in South Africa. MSc Thesis, North-West University.
- [11] Yılmaz A. (2022). Antalya Ferrokrom İşletmesinin Elektrik-Ark Fırını Cüruflarının ve Baca Tozu Atıklarının Asfalt Betonunda Kullanılabilirliğinin Araştırılması. Yüksek Lisans Tezi, Akdeniz Üniversitesi.
- [12] Suhu N, Biswas A, Kapure G. (2016). A Short Review on Utilization of Ferrochromium Slag, Mineral Processing and Extractive Metallurgy Review, 37(4): 211-219.

on Innovative Surveys in Positive Sciences 4-5 December 2022 / Full Text Book

- [13] Huang Y, Wang Q, Shi M. (2017). Characteristics and Reactivity of Ferronickel Slag Powder, Construction and Building Materials, 156: 773-789.
- [14] Kantarcı F. (2013). Elazığ Ferrokrom Cürufundan Alkali Aktivasyon Metoduyla Üretilen Geopolimer Çimentolu Betonların Yangın Dayanımının Araştırılması. Yüksek Lisans Tezi, İnönü Üniversitesi.
- [15] Geçkil T, Önal Y, İnce CB. (2021). Atık PET ile Modifiye Edilmiş Bitümlü Sıcak Karışımların Nem Direnci, Politeknik Dergisi, 24(2): 461-471.
- [16] Karayolları Genel Müdürlüğü, Karayolları Teknik Şartnamesi, 2013.

on Innovative Surveys in Positive Sciences 4-5 December 2022 / Full Text Book

# A NEW METHOD OF SIMPLIFIED JOHNSON COOK MODEL PARAMETER OPTIMIZATION FOR DP600 AND DP800 STEELS

Labinot Topilla<sup>1\*</sup>, Serkan Toros<sup>2</sup>, Habip Gökay Korkmaz<sup>2</sup>

\*1 UBT – Higher Education Institution, Mechatronics Engineering , 10000, Prishtinë, Kosovo.

#### **ABSTRACT**

Dual-phase steels are widely used in the automotive industrial sectors. The main properties of dual-phase steels are strength and ductility, or the ability to form them into the desired shape. The ferrite phase and martensite phase dominate the microstructure of the above-mentioned steels. Due to the mechanical properties that dual-phase steels possess, research on them is still growing. Therefore, this study provides an experimental investigation and a new finite element modeling optimization method for the prediction parameters of the simplified Johnson-Cook model. All investigations are based on the determination of the true flow curves of the DP600 and DP800 steels. Therefore, the uniaxial tensile tests for the experimental and numerical simulations were performed with three different strain rates. The aim was to calibrate or define the Simplified\_Johnson\_Cook\_MAT\_98 parameters known as A, B, n, and C through a finite element modeling optimization procedure; LS-OPT was used for the prediction of the parameters. Since the necessary numerical results were obtained, the results were validated by comparing the numerical simulation results with the experimental results.

**Keywords:** Dual-phase steel, optimization, parameters, strain rate

#### INTRODUCTION

Advanced high-strength steels (AHSL) are widely used in the automotive industry (Terrazas et al., 2017); particularly, dual-phase steels (DP) are widely used as structural parts of automobile bodies (Wicklung, n.d.). DP steels are distinguished by their strength and ductility. Furthermore, during deeper investigations of DP steel up to the microstructural level, it was revealed that DP steels are primarily composed of two main phases, namely the ferrite and martensite phases. While the advantage of the ferrite phase is ductility, on the other hand, the advantage of the martensite phase is strength (Keeler et al., 2017).

In the literature, it was found that DP steels appear to have different volume fractions of phases and different grain sizes, even if they have the same identified name. As a result, studies that have calculated volume fractions based on microstructure area and measured grain sizes in DP600 and DP800 steels support this conclusion. In the study of Sodjit and Uthaisangsuk (2012) it was found that higher amounts of the martensitic phase resulted in a finer ferritic grain size. Wherefore, at DP600 steel with a 35% martensite volume fraction, the average ferrite grain size was 4.98 (um), while at DP800 with a 40% martensite volume fraction, the average ferrite grain size was 3.57 (um). In a table study, Çavuşoğlu et al. (2019) discovered in a table study that a higher amount of martensite phase resulted in finer martensite grain size. Further, at DP600 steel with a 31% martensite volume fraction, the average martensite grain size was 6 (um), while at DP800 steel with a 38% martensite volume fraction average martensite grain size was 4.5 (um).

In the literature, there are different methods and ways through which the parameters of different models are determined, including the model used in this study. Therefore, some of the following studies are presented below: In order to determine strain rate's impact on the strength properties of materials, Stopel and Skibicki (2016) have adopted the methodology for determining constants for Johnson-Cook material models utilizing Charpy impact tests in LS-DYNA modeling programs, Besides that, in the studies conducted by Karkalos and Markopoulos (2018), the fireworks optimization algorithm introduced by Tan and Zhu (2010) was used to calculate and determine the parameters of the Johnson-Cook material

<sup>&</sup>lt;sup>2</sup>Nigde Omer Halisdemir University, Mechanical Engineering Department, 51245, Nigde, Turkey.

on Innovative Surveys in Positive Sciences 4-5 December 2022 / Full Text Book

model for AISI 316L stainless steel. Furthermore, in the work done by Grzesik et al. (2017) for the determination of predicting parameters of the Johnson–Cook constitutive material models for Inconel 718 alloy tested under different strain rates and different temperatures, the Sftool module available in the MATLAB program was used. On the other side, Topilla and Toros (2022)a determined the failure parameters at the microstructural level for the ferrite phase of DP600, DP800, and DP1000. The determined failure parameters were for the Gurson, Gurson Johnson Cook, and Johnson Cook models through LS-OPT.

Within this study, the behavior of the DP600 and DP800 steels at different strain rates was investigated experimentally, on the other side, the material model parameters were optimized and determined using the finite element modeling method, specifically LS-OPT software. During the optimization, only the simulations of the standard specimen's material were run at different strain rates, and the relevant optimization scheme is given in Section 3. Herein, separate simulations for three different tensile velocities were defined for the system, and A, B, n, and C values were tried to be determined together. The yield curve results obtained from the optimization studies and their comparison with the experimental data are shown in Section 3. Finally, a great deal of agreement was found between the optimization studies and the experimental data for the hardening region.

#### MATERIALS AND METHODS

# 1. Experimental Procedure

In this paper, two types of dual-phase steel, namely DP600 and DP800, were investigated. Their chemical composition is shown in Table 1. The uniaxial tensile test of standard specimens (ASTM E8) was performed at room temperature at three different strain rates:  $0.0083 \ s^{-1}$ ,  $0.042 \ s^{-1}$ , and  $0.16 \ s^{-1}$ . The specimens were taken at (0) of the rolling direction; the nominal width was 12.5 mm, the nominal thickness was 0.78 mm, and the nominal gauge length was 50 mm. For both DP steels, three specimens were tested for each strain rate, similar to Topilla and Toros (2022) (b). The tests were carried out to obtain the results of the true stress-strain curves under different strain rates (see Figure 1). As can be seen, from Figure 1. the results in terms of true stress and true strain can vary depending on the strain rate.

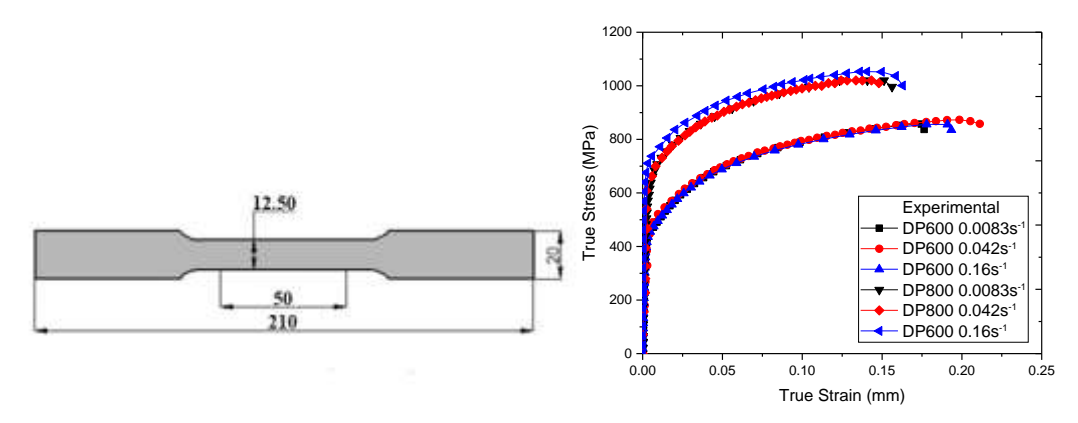


Figure 1. Specimen and true stress-strain results of DP600 and DP800 steels

Table 1. Chemical composition of DP600, and DP800 steels

Steel	P	Si	Cu	Ni	Cr	Mn	C - Ferrite	C - Martensite
DP800	0.015	0.230	0.050	0.030	0.020	1.420	0.006	0.294
DP600	0.015	0.100	0.000	0.000	0.480	1.580	0.006	0.234

on Innovative Surveys in Positive Sciences 4-5 December 2022 / Full Text Book

#### 2. Simplified Johnson-Cook Model

This is model type 98 in the LS-DYNA library. The Johnson-Cook Simplified Model is used for cases where strain rates vary greatly. In this improved model, thermal effects and damage are not taken into account. An iterative plane stress update is used for the solid components; however, due to identified rearrangements with thermal relaxation and damage, this model is half as fast as the full Johnson/Cook iteration. The simplified Johnson-Cook model is given in Eq 1.

$$\sigma_{\nu} = (A + B\overline{\epsilon}^{p^n})(1 + Cln\dot{\epsilon}^*) \tag{1}$$

where A accounted for the yield stress, B and n for the strain hardening effect, C for the influence of th e material under strain rate, and  $\bar{\mathbf{E}}^p$  for the dimensionless effective plastic strain rate defined (Zhang et al., 2022). In general, the experiment's lowest strain rate is taken as a reference in fitting the corresponding equation to the yield curves. The calculation of the expression giving the normalized stress ratio is given in Eq 2.

$$\dot{\mathcal{E}}^* = \frac{\dot{\bar{\varepsilon}}}{EPS0} \tag{2}$$

#### **RESULTS**

### 3. FEM Optimization procedure and results

In this work, a finite element modeling optimization method using LS-OPT is employed to determine the simplified Johnson Cook constitutive model parameters. As a result, this process included a total of six specimens for optimization: three for DP600 and three for DP800 steels. Herein, separate simulations for three different strain rates were defined for the system, and A, B, n, and C values were tried to be determined together. Before beginning to use this optimization method, there are some important steps that must be taken in order to achieve successful optimization.

The first step is the preparation of the main functional modeling key card. The key card contained an ASTM E8 specimen identical to the experimental case, with all geometrical and mechanical dates matching (Figure 1). For this key card, the material chosen was the Simplified Johnson Cook 098 material model Eq 1, which is part of the material library of LS-DYNA software. All mechanical dates, such as p (mass density), E (Young's modulus), PR (Poisson's ratio), VP (formulation of rate effects), and ESPO (effective plastic strain rate), were similar to experimental dates and were placed on the key card.

The second step was the preparation of the optimization process and running the simulations. The optimization was performed in the LS-OPT software (Figure 2). At "setup," arbitrary constitutive material model parameters were placed (see Tables 2 and 3), while "sampling" was divided into three stages corresponding to specimens of each strain rate and their mechanical properties. It is worth noting that the true stress-strain curves of the specimen were placed at this point in history. The optimization of parameters was performed on a normal run followed by 10 iterations. Upon successful completion of the optimization, the results can be seen in Figure 3. and OPT results at Tables 2–3.

on Innovative Surveys in Positive Sciences

4-5 December 2022 / Full Text Book

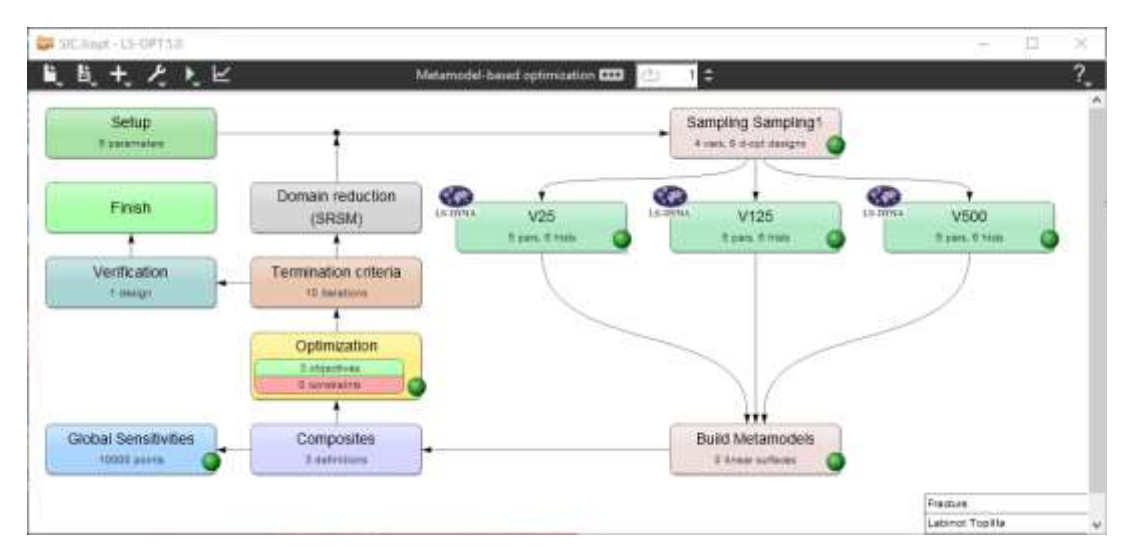


Figure 1. The schematic optimization form is represented by defining the SJC parameters.

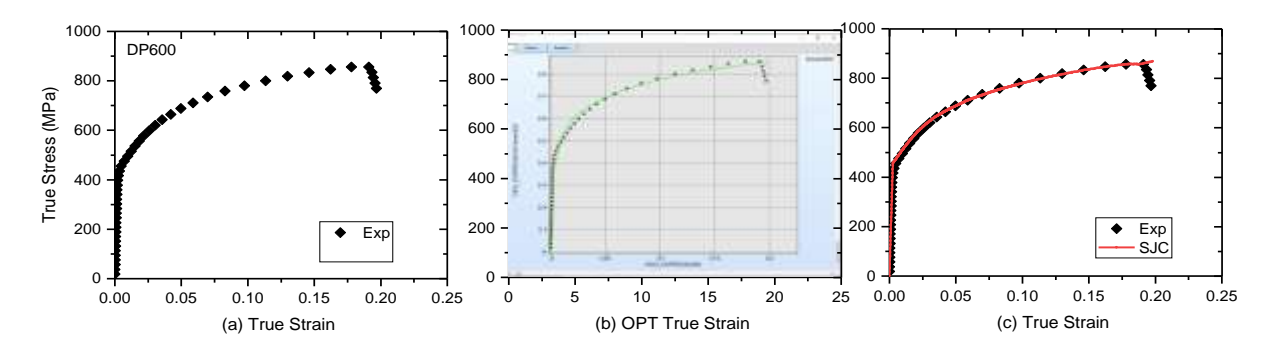


Figure 3. One example of comparing results between experimental, optimization, and simulation results

The optimization results were run separately for both DP600 and DP800. The optimization algorithm chosen for the SJC model is used in this model. The initial, minimum, and maximum values and obtained result values of the optimized material model parameters after optimization processes are given in Tables 2-3.

Specimens	Velocity	Parameters	A (GPa)	B (GPa)	С	n
DP600	v=500mm/s, 0°	Starting	0.415	0.881	0.00816	0.2
	v=125mm/s, 0°	Minimum	0.090	0.6	0.001	0.02
	v=25mm/s, 0°	Maximum	0.550	1.1	0.1	0.5
DP600	All above	Results	0.320	1.050	0.0010174	0.36374

**Table 2.** Optimisations parameters of Simplified Johnson-Cook for DP600 steel.

on Innovative Surveys in Positive Sciences 4-5 December 2022 / Full Text Book

**Table 3.** Optimisations parameters of Simplified Johnson-Cook for DP800 steel.

Specimens	Velocity	Parameters	A (GPa)	B (GPa)	С	n
DP800	v=500mm/s, 0°	Starting	0.585	0.819	0.00821	0.2
	v=125mm/s, 0°	Minimum	0.3	0.65	0.001	0.02
	v=25mm/s, 0°	Maximum	0.700	1.1	0.1	0.5
DP800	All above	Results	0.504173	1.055	0.01275	0.32

When the yield curves obtained from the experiments are controlled, there is no significant change in the yield curves of the material at different strain rates. In this case, it means that the strain rate sensitivity of the material is low. However, a decrease in formability is observed. The yield curves obtained after the optimization processes and their comparison with the experimental data are shown in Figures 4 (a-c) and 5 (a-c) for both materials. When the graphs obtained are examined at the true stress and strain level, the simulation results show a great deal of agreement with the experimental. When the graphs obtained for these two materials are evaluated, the homogeneous deformation zone is quite wide and the necking elongation point is quite short. This allows the results of the analyses to be obtained quickly.

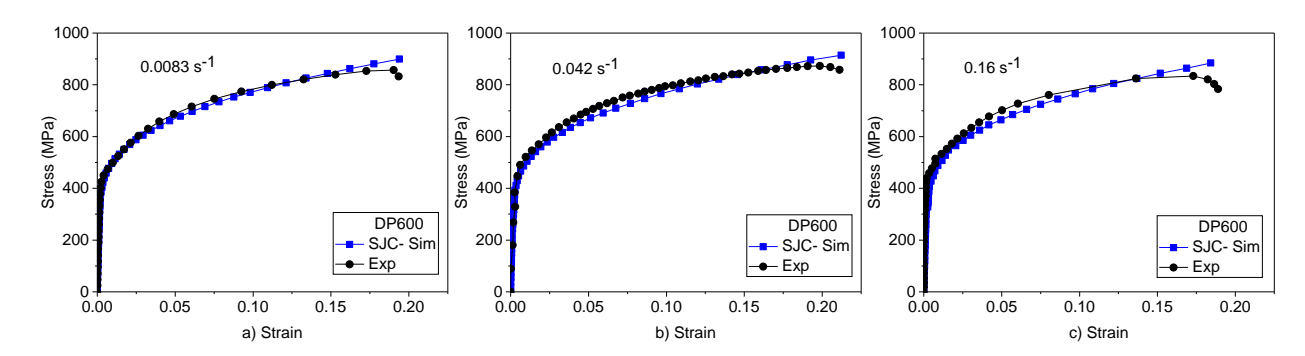
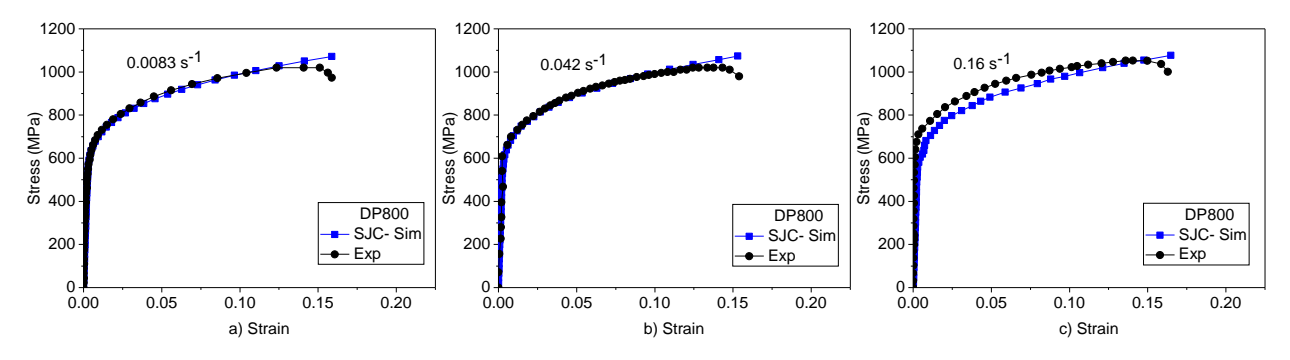


Figure 4. Comparisons between experimental and numerical true stress-strain curves of DO600 steel



**Figure 5.** Comparisons between experimental and numerical true stress-strain curves of DO800 steel **DISCUSSION** 

However, it is worth mentioning that the parameters A, B, n, and C have a large impact on the fitting of curves, while the parameter m (temperature) has no impact in this case. while this case does not contain the temperature. So, parameters A and B should mainly have values that are significantly higher than parameters C, n, and m, but the values of A and B should be positive. In much of the literature, it is stated that the constant parameters C, n, and m vary from these values, ranging from 0 to 1.5 (Kleponis,

on Innovative Surveys in Positive Sciences 4-5 December 2022 / Full Text Book

2001). From the research done so far, we have not come across any papers that show that the optimization of the Johnson Cook constitutive parameters was done through LS-OPT for DP600 steel and DP800 steel and tested with different strain rates. Table X displays the parameters A and B as GPa values because LS-OPT mostly optimized the parameter acceptance curves using these values. In this case, converting these A and B parameters to MPa was done, and then the simulation was run.

In Figure 6. the results of the simulation are presented, from which comparisons of effective plastic strain under different strain6rates can be seen. The purpose of presenting these results is to show to what degree the given material and sample have undergone effective elongation. Therefore, as seen in DP600 steel, effective plastic strain under different strain rates is found to be 1.919 E-01 for  $0.0083 \text{ s}^{-1}$ , 2.054 E-01 for  $0.042 \text{ s}^{-1}$ , and 1.880 E-01 for  $0.16 \text{ s}^{-1}$ , while in DP800 steel, effective plastic strain under different strain rates is found to be 1.577 E-01 for  $0.0083 \text{ s}^{-1}$ , 1.514 E-01 for  $0.042 \text{ s}^{-1}$ , and 1.660 E-01 for  $0.16 \text{ s}^{-1}$ .

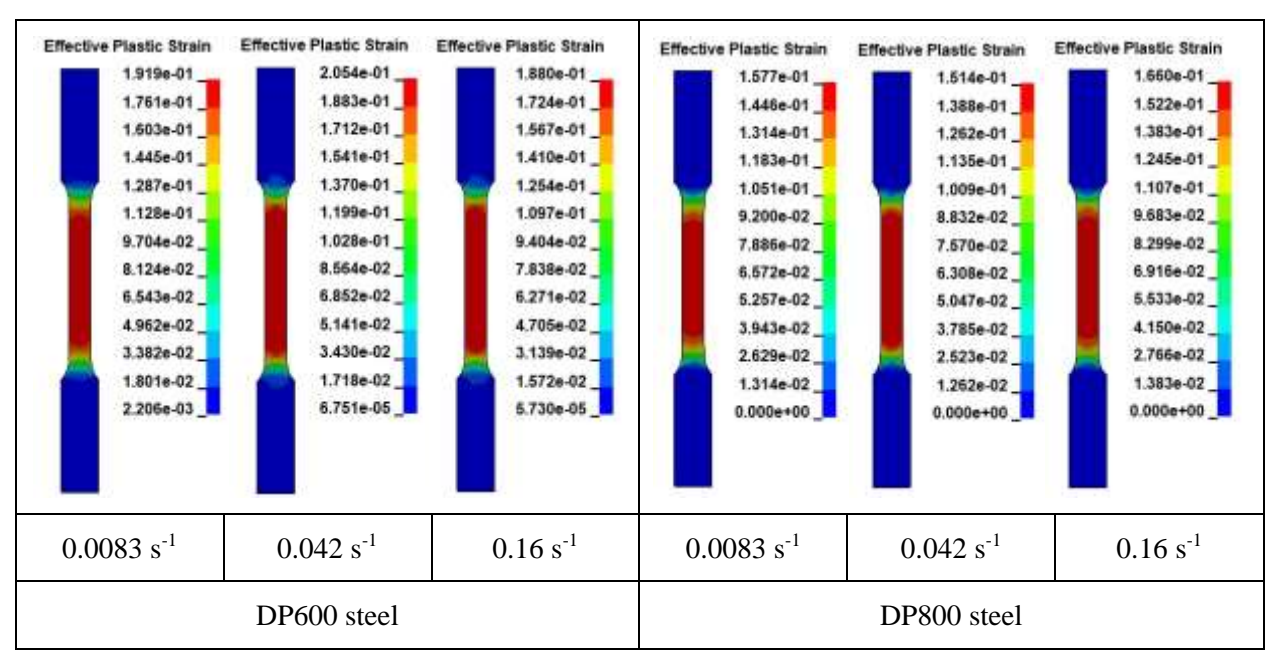


**Figure 6.** Comparisons between numerical FEM results of effective plastic strain results for DO600 and DP800 steels

#### **CONCLUSION**

In this research, numerous uniaxial tensile tests at three different strain rates were carried out to identify the Johnson-Cook constitutive material model parameters for standard specimens of DP600 steel and DP800 steel. In addition, by using the commercial tool LS-DYNA, the numerical simulations were modeled extensively to develop undamaged model parameters for standard specimens at room temperature. The LS-OPT programming solver was used in conjunction with a standard run-based optimization procedure to define parameters of the JC constitutive model while minimizing the relative error between the experimental and numerical simulation curves. When comparing results expressed as true stress-strain curves, the results obtained from the optimized JC model showed good agreement with the experimental observations. Even though more computational time is required to achieve the JC material constants while performing the optimization procedures, the SJC model is an incredible tool to use for future cases to predict the flow curve of ductile materials without damaging

#### REFERENCES

Çavuşoğlu, O., Toros, S., Gürün, H. 2019. Microstructure based modelling of stress—strain relationship on dual phase steels. *Ironmaking and Steelmaking*, 46(4), 313–319. https://doi.org/10.1080/03019233.2017.1371959

on Innovative Surveys in Positive Sciences 4-5 December 2022 / Full Text Book

Grzesik, W., Niesłony, P., Laskowski, P. 2017. Determination of Material Constitutive Laws for Inconel 718 Superalloy Under Different Strain Rates and Working Temperatures. *Journal of Materials Engineering and Performance*, 26(12), 5705–5714. https://doi.org/10.1007/s11665-017-3017-8

Karkalos, N. E., Markopoulos, A. P. 2018. Determination of Johnson-Cook material model parameters by an optimization approach using the fireworks algorithm. *Procedia Manufacturing*, 22, 107–113. https://doi.org/10.1016/j.promfg.2018.03.017

Keeler, S., Kimchi, M., Mooney, P. J. 2017. Advanced High-Strength Steels Guidelines Version 6.0. *WorldAutoSteel*, *September*, 314. https://www.worldautosteel.org/projects/advanced-high-strength-steel-application-guidelines/

Kleponis, D. S. 2001. An Analysis of Parameters for the Johnson-Cook Strength Model for 2-in-Thick Rolled Homogeneous Armor. *Army Research Laboratory Aberdeen Proving Ground, MD 21005-5066*, *Weapons an*(June), 36.

Sodjit, S., Uthaisangsuk, V. 2012. Microstructure based prediction of strain hardening behavior of dual phase steels. *Materials and Design*, *41*, 370–379. https://doi.org/10.1016/j.matdes.2012.05.010

Stopel, M., Skibicki, D. 2016. Determination of Johnson-Cook model constants by measurement of strain rate by optical method. *AIP Conference Proceedings*, 1780(October). https://doi.org/10.1063/1.4965956

Tan, Y., Zhu, Y. 2010. Fireworks algorithm for optimization. *Lecture Notes in Computer Science (Including Subseries Lecture Notes in Artificial Intelligence and Lecture Notes in Bioinformatics)*, 6145 *LNCS*(PART 1), 355–364. https://doi.org/10.1007/978-3-642-13495-1\_44

Terrazas, O. R., Findley, K. O., & Van Tyne, C. J. 2017. Influence of martensite morphology on sheared-edge formability of dual-phase steels. *ISIJ International*, *57*(5), 937–944. https://doi.org/10.2355/isijinternational.ISIJINT-2016-602

Topilla, L., Toros, S. 2022 (a). Stress-strain distribution and failure mechanisms in dual-phase steels investigated with microstructure-based modeling. *Latin American Journal of Solids and Structures*, 19. https://doi.org/10.1590/1679-78257157

Topilla, L., Toros, S. 2022 (b). Gurson-Tvergaard-Needleman (GTN) parameters of DP steels with different rolling directions were determined and investigated at different strain rates . Eurasian Journal of Science Engineering and Technology , , . DOI: 10.55696/ejset.1113577

Wicklung, E. N. T. (). Maßgeschneiderte Dualphasenstähle für Front- und Seiten-Lastfälle. 36–39.

Zhang, H., Hu, D., Ye, X., Chen, X., He, Y. 2022. A simplified Johnson-Cook model of TC4T for aeroengine foreign object damage prediction. *Engineering Fracture Mechanics*, 269(September), 108523. https://doi.org/10.1016/j.engfracmech.2022.108523

on Innovative Surveys in Positive Sciences 4-5 December 2022 / Full Text Book

# IMPACTS OF HUMIC ACID PRACTICES ON NITROGEN, PHOSPHORUS AND POTASSIUM UPTAKE OF BEANS IN SALINE CONDITIONS

# Nurdilek Gülmezoğlu<sup>1</sup>

<sup>1</sup> Eskişehir Osmangazi University, Faculty of Agriculture, Soil Science and Plant Nutrition Department, Eskişehir, Türkiye

<sup>1</sup>ORCID ID: 0000-0002-5756-526X

#### İmren Kutlu<sup>2</sup>

<sup>2</sup> Eskişehir Osmangazi University, Faculty of Agriculture, Field Crops Department, Eskişehir, Türkiye <sup>2</sup> ORCID ID: 0000-0002-3505-1479

#### **ABSTRACT**

Salt causes both osmotic and ionic stresses by inhibiting plant growth and mineral uptake. Humic substances play an important role by controlling the chemical and biological properties of the environment surrounding the plant roots, affecting the nutrient uptake of plants in soil salinity conditions. The positive effects of humic acid (HA) on reducing salt stress in the soil are being investigated in the cultivation of salt-sensitive plants such as beans. In this work, the impacts of several HA application methods (control, soil, foliar and soil+foliar) on nitrogen (N), phosphorus (P), and potassium (K) uptake of bean plants that were exposed to increasing salt (0, 50, 100 and 150 mM) has been aimed. The bean plants were grown in a controlled environment until the flowering period and then, NPK uptake of roots and aboveground parts was determined after harvest. The results showed that NPK uptake in the root and stem of the bean plants was considerably improved when HA is applied especially from the soil and then, from the soil+foliar. We observed that while the amount of salt dose application is increased, NPK uptake descreased in parallel. It was concluded that the application of 50 mM HA directly into the soil improves the NPK uptake as well as protects the plant against the adverse effects of salt.

Keywords: Bean, humic acid, NPK uptake, salt stress.

#### Introduction

One of the most important problems affecting the yield negatively in agricultural activities in arid and semi-arid regions is salinity. Salinity can be caused by excessive and uncontrolled irrigation and insufficient drainage, as well as by intensive agricultural activities, excessive fertilization and the use of poor quality irrigation water (Cullu et al., 2010).

Soil properties need to be improved in order to increase productivity in vegetative production in saline soils, which have a negative effect on plant growth. For this purpose, it is known that soils should be supported by organic matter. Humic substances (humic acid and fulvic acid) are the main components of soil organic matter (Pettit, 2004). For this reason, humic and fulvic acids are used to improve some properties of soils, increase the availability of nutrients and encourage plant growth. Humic substances can form compounds with transition metal cations and this event sometimes has a positive effect on nutrient uptake and sometimes has a negative effect on nutrient uptake by competing with roots (Verlinden et al., 2009). The effects of various humic acid application methods on nitrogen, phosphorus and potassium (K) uptake of salt-exposed bean plants were investigated in this study.

#### **Materials and Methods**

In the experiment, a registered dry bean variety ('Yunus-90') and TKI-Humas from leonardite produced by Turkey Coal Enterprises as humic acid were used. Soil was taken from the Eskisehir Osmangazi University campus at a depth of 0-30 cm. The physical and chemical properties and contents of the soil

on Innovative Surveys in Positive Sciences 4-5 December 2022 / Full Text Book

used are given in Table 1. The study's soil had sandy-loamy textured, non-saline and slightly alkaline. Some mineral nutrient (K, P, Mn, Zn, and Fe) and organic matter contents in soil were low, thought lime and Cu contents were sufficient.

TO 11 1 D				C '1	1	•
Table I D	hazeronla	and chamica	l proportion	01.001	nead in the	avnarimant
LADIC L. F	nvsicar	and chemical	i biobeines	OI SOII	nsea in me	CYDCHIIICH
1 440 14 1	,		Properties	01 0011		0.1001111111

Properties	Unit	Values	Properties	Unit	Values
pН	-	7.67	Organic Matter	(%)	0.65
EC	$(dS m^{-1})$	1.20	K	$(mg kg^{-1})$	136
Lime	(%)	11.83	P	$(mg kg^{-1})$	0.49
Texture			Mn	$(mg kg^{-1})$	0.89
Clay	(%)	10.28	Cu	$(mg kg^{-1})$	1.10
Sand	(%)	67.45	Zn	$(mg kg^{-1})$	0.23
Silt	(%)	22.27	Fe	$(mg kg^{-1})$	1.20

The soil was sieved and filled in pots (4 liter plastic). Before sowing, nitrogen (200 mg), potassium (125 mg kg<sup>-1</sup>) and phosphorus (100 mg kg<sup>-1</sup>), zinc (5 mg kg<sup>-1</sup>) and iron (2.5 mg kg<sup>-1</sup>) were added to soil as basic mineral nutrition.

The experiment was set up in a randomized plot design with three replications under controlled conditions described as previous report (Gulmezoglu and Izci, 2020; Kutlu and Gulmezoglu, 2022). For humic acid applications; (1) control (basic fertilization), (2) humic acid to the soil, (3) humic acid to the foliar and humic acid to both the soil and (4) foliar were applied. For humic acid applications from the soil before sowing, 60 lt humic acid was calculated and mixed into the soil. A 0.2% humic acid solution was prepared and applied foliar when the plants had 5-6 leaves (35 days after planting). Salt applications (0, 50, 100, and 150 mM NaCl) were started when true leaves developed (25 days after planting) and until then the plants were irrigated with deionized water. Salt applications were continued until harvest.

Plants were cut 1 cm above the soil surface 50 days (before blooming) after the bean seeds had germinated. Plant roots were removed from the soil. Leaves and roots washed with deionized water and dried then grounded. For the analysis of phosphorus and potassium in the ground plant parts, wet burning was done in the microwave oven. The amount of phosphorus in the plants was measured according to the vanadomolybdate yellow color method in samples. Potassium concentrations of plant parts were determined in a flame photometer. Nitrogen analysis was performed on plant samples with the Kjeldahl method.

Nitrogen, phosphorus and potassium uptakes of the plants were calculated (g) by multiplying the dry weight with the ratio of the nutrient element (%). Variance analysis was performed on the results by using the SPSS statistical program. The difference between the means was grouped by using the Duncan's new multiple range test at 5% level of significance.

#### **Result and Discussion**

Nitrogen uptake

Humic acid and salt applications had a statistically significant effect on the nitrogen uptake in the leaves, root and whole plant of the bean.  $HA \times S$  interaction had a significant effect only in the root (Table 1).

Table 2. ANOVA of nitrogen, phosphorus and potassium uptakes of bean plants.

	Nitrogen uptake			Phosphorus uptake			Potassium uptake		
	Leaves	Root	Total	Leaves	Root	Total	Leaves	Root	Total
Humic Acid (HA)	**	**	**	**	**	**	ns	**	ns
Salt (NaCl)	*	**	**	ns	**	*	ns	**	*
$HA \times S$	ns	*	ns	ns	ns	ns	ns	ns	ns

\*\*: P<0.01, \*: P<0.05, n.s.: non-significant

on Innovative Surveys in Positive Sciences 4-5 December 2022 / Full Text Book

The application of humic acid from the soil increased the most nitrogen uptake in the leaves, root and whole plant of the bean (Figure 1). As salt doses increased, nitrogen uptake decreased. Nitrogen uptake was found to be lower at 100 and 150 mM NaCl doses, especially in the root.

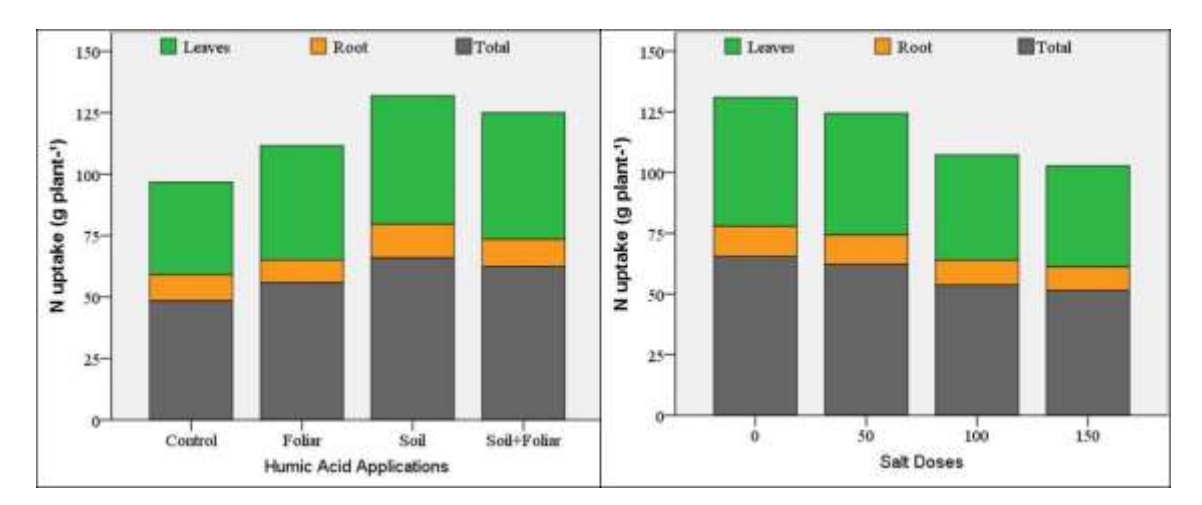


Figure 1. Root, leaf and total nitrogen uptake of bean plants.

#### Phosphorus uptake

Humic acid and salt applications were found to be statistically effective on the root and total plant phosphorus uptake of the leaves and root phosphorus uptake of the plants (Table 2).

Humic acid application from the soil had the highest amount of phosphorus uptake of the bean plant. The 50 mM NaCl application rised the highest phosphorus uptake. Phosphorus uptake in plants decreased with other salt doses.

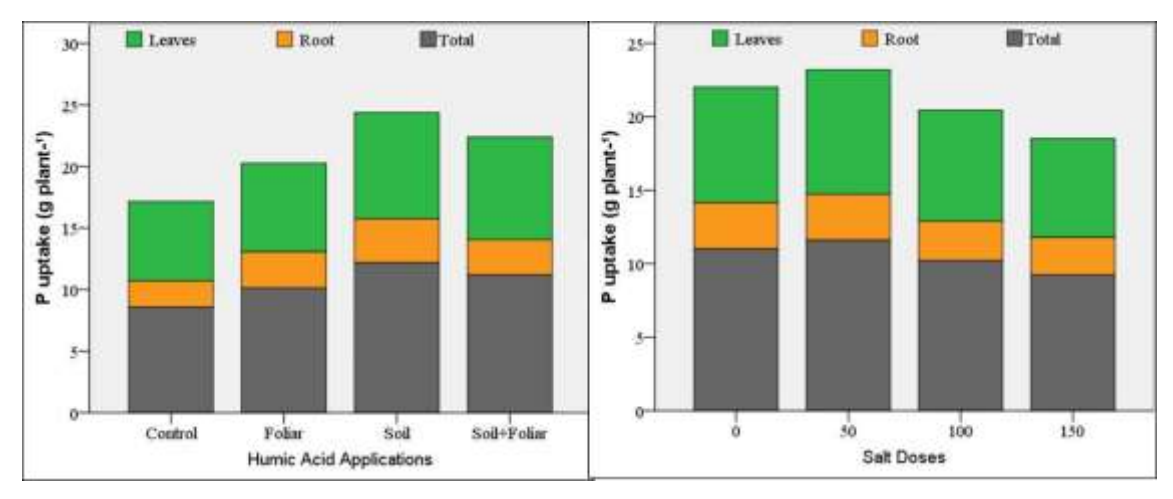


Figure 2. Root, leaf and total phosphorus uptake of bean plants.

#### Potassium uptake

Statistically significant effects of humic acid and salt applications on potassium uptake of plants in root and salt applications on total plant potassium uptake were determined.

on Innovative Surveys in Positive Sciences

4-5 December 2022 / Full Text Book

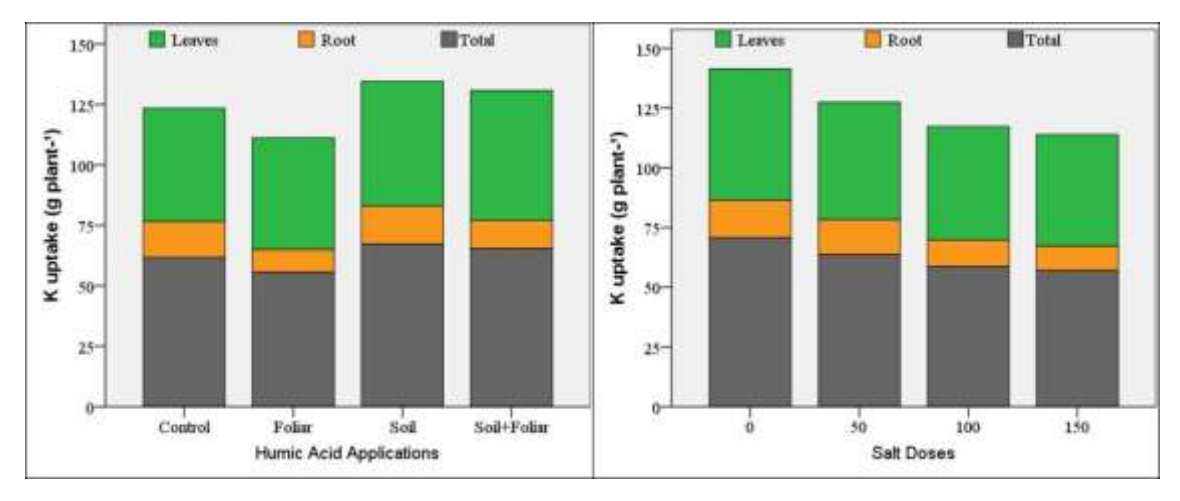


Figure 3. Root, leaf and total potassium uptake of bean plants.

Each NaCl doses affect negatively nitrogen and potassium uptake. Nitrogen and potassium uptakes decreased with salt application in this study. In many experiments, it has been reported that salinity reduces nitrogen accumulation in the plant (Alam, 1999), phosphorus content (Cocozza et al., 2020) and potassium uptake due to their competition with sodium (Wang et al., 2020). However, the responses of phosphorus uptake to NaCl application increased 50 mM NaCl treatment. It can be explained that low salinity could mitigate the negative effects of phosphorus deficiency in plant. Low or moderate salinity stimulates bean phosphorus uptake. Similar results were also reported by Gulmezoglu and Daghan (2017).

It was determined that humic acid applications from the soil increased the nitrogen, phosphorus and potassium uptake of the bean plant. Humic materials are able to complex various cations (pseudochelation) and serve as a sink for cations in the soil. They have a negative surface charge at all pH values where crop growth occurs. Reports of improved cation availability following addition of humic materials are common (Mikkelsen, 2005; Dawood et al., 2019). In conclusion, the humic asit applications had a curative effect from soil on nitrogen, phosphorus and potassium uptakes. Finally, it can be stated that bean will have lower NaCl and humic asit applications from soil will reduce the salt damage.

#### References

Alam, S. M. (1999). Nutrient uptake by plants under stress conditions. Handbook of Plant and Crop Stress, 2, 285-313.

Cocozza, C., Brilli, F., Pignattelli, S., Pollastri, S., Brunetti, C., Gonnelli, C., Loreto, F. (2020). The excess of phosphorus in soil reduces physiological performances over time but enhances prompt recovery of salt-stressed Arundo donax plants. Plant Physiology and Biochemistry, 151, 556-565.

Cullu, M. A., Aydemir, S., Qadir, M., Almaca, A., Öztürkmen, A. R., Bilgiç, A., Ağca, N. (2010). Implication of groundwater fluctuation on the seasonal salt dynamic in the Harran plain, south-eastern Turkey. Irrigation and Drainage, 59, 465-476.

Dawood, M. G., Abdel-Baky, Y. R., El-Awadi, M. E. S., Bakhoum, G. S. (2019). Enhancement quality and quantity of faba bean plants grown under sandy soil conditions by nicotinamide and/or humic acid application. Bulletin of the National Research Centre, 43(1), 1-8.

Gulmezoglu, N., Daghan, H. (2017). The interactive effects of phosphorus and salt on growth, water potential and phosphorus uptake in green beans. Appl. Ecol. Environ. Res, 15(3), 1831-1842.

Gulmezoglu, N., Izci, E. (2020). Ionic responses of bean (Phaseolus vulgaris L.) plants under salinity stress and humic acid applications. Notulae Botanicae Horti Agrobotanici Cluj-Napoca, 48(3), 1317-1331.

Kutlu, I., Gulmezoglu, N. (2022). Suitable Humic Acid Application Methods to Maintain Physiological and Enzymatic Properties of Bean Plants Under Salt Stress. Gesunde Pflanzen, 1-12.

on Innovative Surveys in Positive Sciences 4-5 December 2022 / Full Text Book

Mikkelsen, R. L. (2005). Humic materials for agriculture. *Better Crops*, 89(3), 6-10.

Pettit, R. E. (2004). Organic matter, humus, humate, humic acid, fulvic acid and humin: their importance in soil fertility and plant health. *CTI Research*, *10*, 1-7.

Verlinden, G., Pycke, B., Mertens, J., Debersaques, F., Verheyen, K., Baert, G., Bries, J., Haesaert, G. (2009). Application of humic substances results in consistent increases in crop yield and nutrient uptake. *Journal of Plant Nutrition*, 32(9), 1407-1426.

Wang, L., Yermiyahu, U., Yasuor, H., Ning, S., Tan, J., Ben-Gal, A. (2022). Simulating water and potassium uptake of greenhouse tomato as a function of salinity stress. *Irrigation Science*, 40(6), 873-884.

on Innovative Surveys in Positive Sciences 4-5 December 2022 / Full Text Book

# INVESTIGATION OF BURST STRENGTH, ABRASION AND PILLING RESISTANCE PROPERTIES OF KNITTED FABRICS PRODUCED FROM 100% CARDED COTTON RING AND PROSPIN® YARNS

#### Gozde BUHARALI

Bartin University, Ulus Vocational School, Department of Textile, Clothing, Footwear and Leather, Bartin, Turkey

ORCID ID: 0000-0003-3641-5016

# Sunay OMEROGLU

Bursa Uludag University, Engineering Faculty, Department of Textile Engineering, Bursa, Turkey ORCID ID: 0000-0002-1618-6562

#### **ABSTRACT**

In this study, new and original modified ring yarns called "ProSPIN®" were used together with conventional ring yarns for the production of knitted fabrics. The aim of this study is to comparatively examine the burst strength, abrasion and pilling resistance properties of knitted fabrics produced using ring and their equivalent ProSPIN yarns. For this purpose, single jersey fabrics were produced from 100% carded cotton ring and their equivalent ProSPIN yarns with twist coefficients  $\alpha_e$  3.5 and yarn counts Ne 12, Ne 16, Ne 20 and Ne 28. Burst strength, abrasion resistance and pilling resistance properties of the fabrics produced were investigated. When the test results were examined, it was seen that the burst strength, abrasion resistance and pilling resistance values of single jersey fabrics produced using ProSPIN yarns were higher.

**Keywords:** Ring Yarn, ProSPIN® Yarn, Single Jersey Fabric, Burst Strength, Abrasion Resistance, Pilling Resistance

#### 1. INTRODUCTION

Conventional ring spinning system, first developed by John THORPE in 1828 to spin cotton yarn, took its place in the sector after 1850. The development process of the conventional ring spinning system from past to present has brought this system to an important point in its flexibility and improved yarn quality. Although many alternative spinning systems have emerged, the conventional ring spinning system has managed to maintain its place with its superior yarn structure and flexible application area (Stalder, 1995; Ulku, 2000).

Considering the structure of ring yarns, it is seen that not all fibers are included in the yarn structure. It is known that this situation, which negatively affects yarn structure and breaks, causes various problems in spinning and post-spinning processes. As a result of the researches, it has been revealed that this situation is caused by the spinning triangle that occurs at the nip point of the front rollers in the drafting system, and various compact spinning systems have been developed to eliminate this problem (Yilmaz, 2004; Sezgin, 2005).

In conventional ring spinning (Figure 1), the zone between the nip line (N-N¹) of the pair of delivery rollers and the twisted end of the yarn is called the 'spinning triangle'. The width of the spinning triangle (B) depends mainly on the spinning tension, which varies inversely with the tension. Also it is always narrower than the width of the fibres fed (A), which represents the critical weak spot of the ring spinning process (Buharali and Omeroglu, 2019a).

on Innovative Surveys in Positive Sciences

4-5 December 2022 / Full Text Book

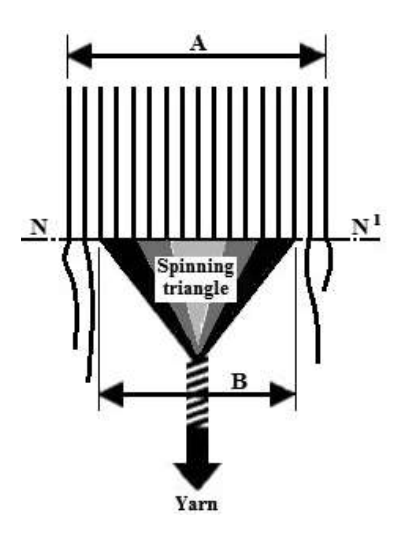


**Figure 1.** Spinning triangle formation in conventional ring spinning (Buharali and Omeroglu, 2019a)

In this region, the fiber assembly is scattered because it is untwisted, and the edge fibers away from the center of the fiber assembly either form fly or poorly participate in the yarn structure. This causes yarn hairiness and a decrease in the contribution of fibers to yarn strength. In addition, most of the yarn breaks originate from this region (Hechtl, 1996; Yilmaz, 2004).

The ProSPIN® spinning system in this study was developed by Ozdilek Inc. in order to solve the spinning triangle problem and improve the yarn properties obtained. In ProSPIN, the roving which is fed into the drafting system of the ring spinning frame is separated into two strands by the use of a specially designed compactor. Later the two separate and compacted fibre strands are unified by the twist to form a yarn (Buharali and Omeroglu, 2019a; Buharali and Omeroglu, 2019b).

With this study, it is aimed to transfer the data, evaluation and results of some basic performance properties of single jersey fabrics produced from ring and their equivalent ProSPIN yarns to the sector and researchers.

# 2. MATERIALS AND METHODS

In this experimental study, 100% cotton raw material, originating from Greece, was used as the starting material. In the yarn production phase of the study, a carded production line was used. Equivalent ProSPIN and ring yarns were produced in four different yarn counts, Ne 12, Ne 16, Ne 20 and Ne 28, with a twist coefficient level of  $\alpha_e$  3.5.

At the end of the yarn production, strength, unevenness and hairiness tests were applied to the sample cops separated to test the yarn properties. Before the measurements were carried out, the prepared samples were kept in standard atmospheric conditions ( $20 \pm 2^{\circ}$ C temperature and  $65 \pm 2\%$  humidity) for 24 hours to ensure their conditioning. The strength tests of the produced yarns were carried out using the Uster Tensojet 3 yarn strength tester. Values evaluated within the scope of the test are the results of breaking strength (cN/tex) and elongation at break (%). The unevenness tests of the produced yarns were carried out using the Uster Tester 3 yarn evenness tester. Values evaluated within the scope of the unevenness test are  $CV_m\%$ , (-50%) thin places, (+50%) thick places and (+200%) neps results. Within the scope of the experimental study, the hairiness tests of the produced yarns were carried out using both the Uster Tester 3 test device (for Uster H values) and the Zweigle G567 hairiness test device (for Class 1 mm, Class 2 mm and S3 values). Table 1 shows the test results of yarns.

on Innovative Surveys in Positive Sciences 4-5 December 2022 / Full Text Book

Table 1. Test results of yarns

Vous Duonouties		Ri	ng			ProS	PIN	
Yarn Properties	Ne 12	Ne 16	Ne 20	Ne 28	Ne 12	Ne 16	Ne 20	Ne 28
Tenacity (cN/tex)	14.60	14.32	13.81	12.97	15.66	16.06	15.83	14.43
Elongation at break	5.06	4.58	4.30	4.02	5.11	4.59	4.57	4.37
CV <sub>m</sub> %	12.11	12.95	13.73	15.45	10.68	11.77	12.76	14.16
Thin places (-50%)	0	1	0	11	0	0	0	3
Thick places (+50%)	29	68	103	274	4	23	45	125
Neps (+%200)	19	54	106	264	13	44	95	232
Uster H	8.24	7.29	6.91	6.32	7.05	5.97	5.55	5.53
Zweigle Class 1 mm	18 570	16 053	15 433	13 481	17 469	13 368	12 363	12
Zweigle Class 2 mm	3 344	2 385	2 440	2 185	2 636	1 706	1 601	1 522
Zweigle S3	953	605	808	1 207	580	330	313	329

Knitted fabrics in single jersey knit structure were produced from the yarns produced under the same conditions. Codes of fabrics and some construction parameters are given in Table 2.

Table 2. Codes of fabrics and some construction parameters

Fabric Code	Yarn Type	Courses (1/cm)	Wales (1/cm)	Brand and Model of Machine	Machine Diameter (inch)	Machine Fineness (gauge)	Number of Systems	
R12	Ring Ne 12	15	8	Monarch	34	12	102	
P12	ProSPIN Ne 12	13	O	VXC-3S	34	12	102	
R16	Ring Ne 16	17	10	Monarch	30	20	84	
P16	ProSPIN Ne 16	17	10	VXC-FLD	30	20	04	
R20	Ring Ne 20	17	9	Monarch	20	20	0.4	
P20	ProSPIN Ne 20	17	9	VXC-FLD	30	20	84	
R28	Ring Ne 28	19	12	Monarch	26	20	70	
P28	ProSPIN Ne 28	19	12	VXC-3S	26	28	78	

The tests applied to fabrics are burst strength, abrasion resistance and pilling resistance tests. The burst strength of the produced knitted fabrics was determined by the Messmer Buchel burst strength tester, which is a diaphragm measuring device shown in Figure 2. For this purpose, using the TS 393 EN ISO 13938-1 standard, samples from all types of fabrics were prepared and measurements were made.



Figure 2. Messmer Buchel burst strength test device used in the experimental study

Determination of the abrasion resistance of the knitted fabrics produced was carried out with the Martindale abrasion and pilling test device shown in Figure 3. For this, three samples were prepared from each type of fabric and the abrasion status of the surfaces was examined by using the TS EN ISO 12947-2 standard and 9 kPa pressure. In the determination of the abrasion resistance of fabrics, photographs of the samples worn at certain cycles were also taken, and in the results and discussion section, the appearance of the fabrics after 20 000 cycles, as well as the period in which the first break in the course or wale direction of the fabrics occurred, is also included.

on Innovative Surveys in Positive Sciences 4-5 December 2022 / Full Text Book

Figure 3. Martindale abrasion and pilling test device used in the experimental study

The pilling resistance determination of the produced knitted fabrics was carried out with the Martindale abrasion and pilling test device shown in Figure 4 (A). For this purpose, using the TS EN ISO 12945-2 standard, samples were prepared from all types of fabrics and the tendency of the surfaces to pile up and pilling was examined. The sample placed on the upper part and the abrasive sample placed on the lower part are of the same fabric, so that the face of the test fabric is rubbed against the same fabric. At the end of 2 000 cycles, samples were taken, and evaluations were made of the pilling conditions of the sample fabrics in the Verivide CAC150 light cabinet (Figure 4 (B)) and D65 daylight. The images of the fabrics after pilling given in the results and discussion section were obtained with the MshOt MS60 stereo microscope with a magnification of 7X.





Figure 4. Martindale abrasion and pilling tester (A), Verivide CAC150 light cabinet (B)

t-Test analysis method was used to evaluate the data obtained as a result of the tests performed on the fabrics produced. t-Test is an analysis method used to compare two means (Eymen, 2007). SPSS 22.0 statistical program was used in the analysis.

#### 3. RESULTS AND DISCUSSION

The average and CV% values of the test results of the fabrics produced are given in Table 3 and Figures 5, 6 and 8. Figure 7 shows the images of the fabrics produced after 20 000 cycles in the abrasion test, and Figure 9 shows the images of the fabrics produced under the microscope after pilling. Table 4 shows the results of the statistical analysis between the properties of single jersey fabrics produced from conventional ring and ProSPIN yarns.

Table 3. Burst strength, abrasion resistance and pilling resistance test results of fabrics

Fabric	Burst Str	ength (kPa)	Abrasion Re	esistance (cycle)	Pilling
Code	Mean	CV%	Mean	CV%	Resistance
R12	363.3	1.59	35 000	5.71	1-2
P12	398.3	4.41	48 667	3.14	2-3
R16	350.0	0	48 000	2.08	3
P16	370.0	0	52 000	0.96	3-4
R20	255.0	3.40	23 333	6.55	2-3
P20	281.7	3.70	35 000	1.43	3-4
R28	226.7	2.55	35 000	2.86	2-3
P28	230.0	0	42 000	1.19	3-4

on Innovative Surveys in Positive Sciences 4-5 December 2022 / Full Text Book

Table 4. t-Test analysis results (significance values)

Eshwia Duamautias	Compared Fabrics							
Fabric Properties	R12-P12	R16-P16	R20-P20	R28-P28				
Burst Strength (kPa)	0.044*	0.001*	0.094	0.423				
Abrasion Resistance (cycle)	0.001*	0.005*	0.003*	0.002*				

<sup>\*:</sup> There are statistically significant differences for  $\alpha = 0.05$ .

# 3.1. Evaluation of burst strength test results

According to Figure 5, it is seen that the burst strength values of fabrics produced from ProSPIN yarns are higher than those of fabrics produced from ring yarns with the same yarn count, varying between 1.5% and 10.5%. When the breaking strength values of the yarns used for the production of fabrics are examined, it is seen that the strength differences between ProSPIN and ring yarns are not fully reflected in the burst strength values of the fabric, considering that the strength differences between ProSPIN and ring yarns are between 7.3% and 14.6%. When the burst strength values are examined, there is no obvious trend of change depending on the yarn count.

According to the results of the t-test analysis performed using the burst strength values of raw single jersey fabrics, it was determined that the differences between the burst strength values of the fabrics produced from ProSPIN and ring yarns for two different fabric groups produced from Ne 12 and Ne 16 yarns were statistically significant at the level of  $\alpha = 0.05$ .

The burst strength results obtained in the study are in line with the results in the literature. In the studies conducted by Ceken and Goktepe (2005), Omeroglu (2005), Mavruz and Ogulata (2008), and Altas and Kadoglu (2009), it was found that the burst strength values of fabrics knitted from compact yarns were higher than those of ring-knitted fabrics. In the study carried out by Omeroglu (2005), it is stated that knitted fabrics produced from compact yarns have a softer handle, as compact yarns can be produced at lower twist coefficients than ring yarns thanks to their high strength properties. In this study, it was concluded that ProSPIN yarns can be produced with lower twist coefficients than ring yarns in order to have the same strength as ring yarns, and thus the fabrics produced from ProSPIN yarns can be softer.

In the study carried out by Unal and Omeroglu (2013), the burst strength values of the fabrics knitted from compact Sirospun yarns are higher than the fabrics knitted from conventional Sirospun yarns, due to the higher strength properties of compact Sirospun yarns, which is in line with the results of this study. Similarly, Kirecci et al. (2011), it has been determined that the knitted fabrics obtained from these yarns have higher burst strength values, thanks to the high strength values of Sirospun yarns. In the study carried out by Demir and Kilic (2017), it was stated that the burst strength values of fabrics made from Sirospun yarns were higher than fabrics made from double-ply yarns.

When the burst strength of the knitted fabrics in the study was examined, as expected, the burst strength of the fabrics produced from thick yarns was higher. Another remarkable result of the study is that the burst strength differences between fabric groups are statistically significant, especially in fabrics produced from thick yarns. Mavruz and Ogulata (2008), Akaydin et al. (2009) and Akkis (2009) reported that burst strength values of fabrics are affected by yarn raw material type, density, yarn count and knitting type.

on Innovative Surveys in Positive Sciences

4-5 December 2022 / Full Text Book

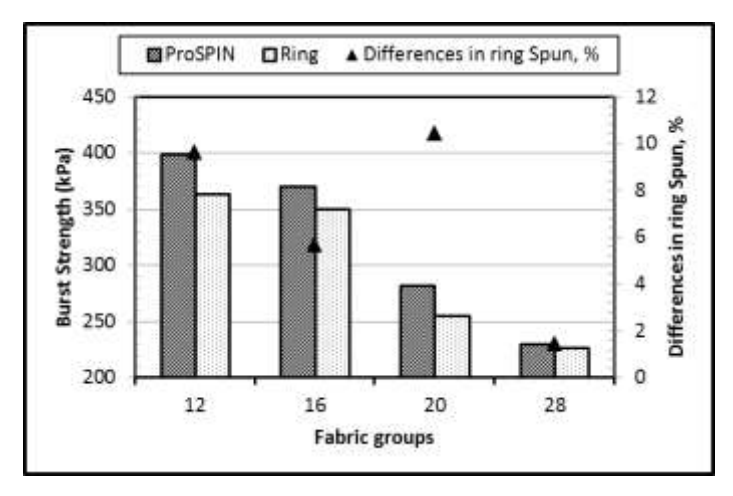


Figure 5. Burst strength values of fabrics

#### 3.2. Evaluation of abrasion resistance test results

In the determination of the abrasion resistance of the knitted fabrics produced within the scope of this study, the cycles in which the first break in the course or wale direction occurred were taken as criteria. In addition, the results were supported by including the appearance of the fabrics after 20 000 cycles. According to Figure 6, it is seen that the abrasion resistance (cycle) values of fabrics produced from ProSPIN yarns are higher than that of fabrics produced from ring yarns with the same yarn count, varying between 8.3% and 50.0%. When the abrasion resistance values are examined, there is no obvious trend of change depending on the yarn count. According to the results of the t-test analysis performed using the abrasion resistance values of raw single jersey fabrics, the differences between the abrasion resistance values of the fabrics produced from ProSPIN and ring yarns for four different fabric groups were found to be statistically significant at the level of  $\alpha = 0.05$ .

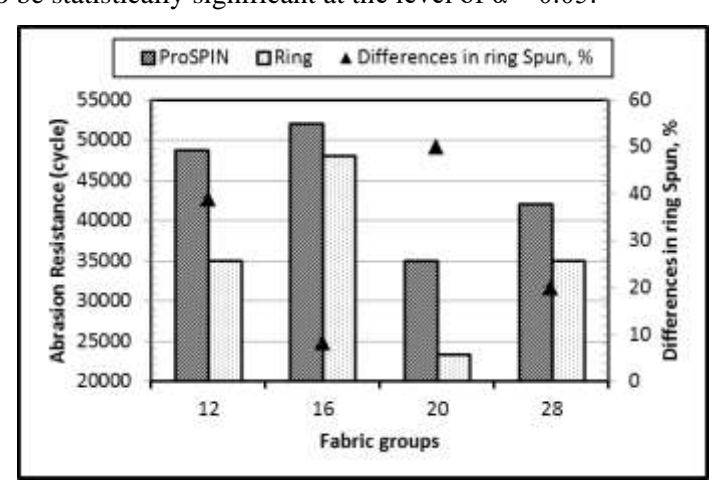


Figure 6. Abrasion resistance values of fabrics

Considering the appearance of the fabrics after the abrasion test in Figure 7, it is seen that the abrasion resistance of the fabrics knitted from ProSPIN yarns is better due to the fewer fibers protruding from the yarn body.

on Innovative Surveys in Positive Sciences

4-5 December 2022 / Full Text Book

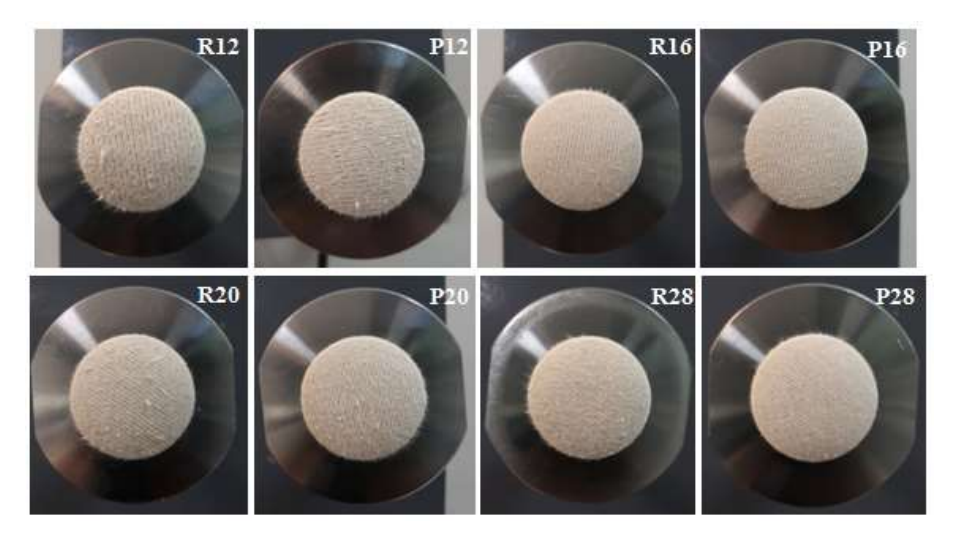


Figure 7. Images of fabrics after 20 000 cycles in the abrasion test

The abrasion resistance test results of the study are similar to the studies in the literature evaluating the abrasion resistance. In the studies conducted by Celik and Bozkurt (2005), it was stated that knitted fabrics produced from compact yarns had higher abrasion resistance. Again in parallel with this study, in the study carried out by Sun and Cheng (2000), it was observed that the abrasion resistance of knitted fabrics produced from Sirospun yarns was much better than knitted fabrics produced from conventional double-ply yarns. In the study conducted by Unal and Omeroglu (2013), it was stated that the abrasion resistance values of knitted fabrics obtained from yarns produced with compact-Siro spinning systems were higher than fabrics obtained from conventional Sirospun yarns.

#### 3.3. Evaluation of pilling resistance test results

According to the subjective evaluation results shown in Figure 8, it is seen that the fabrics produced from ProSPIN yarns have a lower pilling tendency than the fabrics produced from ring yarns, thanks to the lower hairiness values of ProSPIN yarns. When the pilling resistance values are examined, there is no obvious trend of change depending on the yarn count.

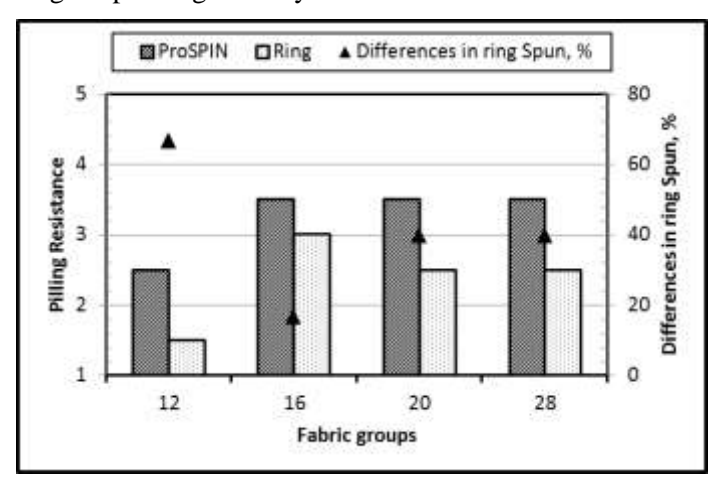


Figure 8. Pilling resistance values of fabrics

When we look at the appearance of the fabrics after the pilling test in Figure 9, it is seen that the pilling resistance of the fabrics knitted from ProSPIN yarns is higher than the fabrics knitted from ring yarns, thanks to the fact that the fibers are more tightly bound to the varn structure. With the fabric images in Figure 9, it is also clear that the courses and wales in knitted fabrics produced from ProSPIN yarns have a clearer appearance.

on Innovative Surveys in Positive Sciences 4-5 December 2022 / Full Text Book

R12 P12 R16 P16

R20 P20 R28 P28

Figure 9. Images of fabrics under the microscope after pilling

In the reviewed literature, it is stated that fabrics produced using modified ring yarns have a lower pilling tendency than fabrics produced using conventional ring yarns, and these results are in line with the results obtained from the study. In the studies conducted by Omeroglu (2005), Sezgin (2005) and Altas and Kadoglu (2009), it was stated that the pilling resistance of knitted fabrics produced from compact yarns is higher. In the study carried out by Cetin (2009), it is stated that the factors causing yarn hairiness also cause fabric pilling formation. It is also stated that if the yarn hairiness is minimized, the hairiness in the fabric will be minimized and pilling will be prevented. Again in parallel with this study, in the study carried out by Sun and Cheng (2000), it was observed that the pilling resistance of knitted fabrics produced from Sirospun yarns was higher than that of knitted fabrics produced from conventional double-ply yarns. In the study conducted by Unal and Omeroglu (2013), it was stated that the pilling resistance of knitted fabrics obtained from yarns produced with compact-Siro spinning systems was higher than fabrics obtained from conventional Sirospun yarns.

#### 4. CONCLUSIONS

In this study, in which the properties of the single jersey fabrics obtained from the yarns produced from the ProSPIN spinning system and the yarns produced from the conventional ring spinning systems were compared, it was determined that the fabrics obtained from the ProSPIN yarns had better values in burst strength, abrasion resistance and pilling resistance than the fabrics produced from the conventional ring yarns. This improvement can be explained by the individual compaction of the fiber group divided into two in a controlled manner in the ProSPIN spinning system, thus reducing the spinning triangle and incorporating the fibers on the edge of the spinning triangle into the yarn structure, as well as better placement of the fibers within the yarn structure. In the ProSPIN spinning system, the compaction process is carried out using a ceramic compactor instead of an air suction. Therefore, there is no additional energy cost during the operation of the system. Other advantages of the system include that its apparatus is inexpensive compared to other compact spinning systems and its maintenance costs are quite low. Thanks to its high tenacity and low hairiness properties, it has been observed that ProSPIN yarns show higher running performance than conventional ring yarns during knitting processes.

In the ProSPIN spinning system, since more raw material is utilized thanks to the reduced spinning triangle, ProSPIN yarns are more hairless, stronger, tighter, brighter and better looking than conventional ring yarns. In addition, thanks to the ProSPIN spinning system, since it is possible to provide a certain yarn strength value with a lower twist level than in conventional ring spinning, it is possible to obtain a higher yarn production rate. Another positive aspect of this situation is the potential of fabrics produced from ProSPIN yarns to have a softer handle than fabrics produced from ring equivalents.

Since the strength of ProSPIN yarns is higher than that of ring yarns, it is an expected result that the fabric strength will also be higher. It is also an expected result that in fabrics produced from ProSPIN yarns, it is not easy for the fibers that are firmly attached to the surface to come to the surface as a result of effects such as friction. At the same time, it can be said that fabrics produced from ProSPIN yarns have a brighter and clearer-looking surface structure.

on Innovative Surveys in Positive Sciences 4-5 December 2022 / Full Text Book

It is believed that the data, evaluation and results obtained within the scope of this study will be an important guide for researchers and it is thought that this system, as a new modified ring spinning system, can bring a new perspective to the sector.

#### **ACKNOWLEDGEMENTS**

The authors would like to thank Ozdilek Inc. (Bursa, Turkey) and Namik Kemal ISIK (the inventor of the ProSPIN system) for their assistance in the production and tests of the yarns, Basyazicioglu Textile (Bamen) Inc's. R&D Department (Kayseri, Turkey) for their assistance in the hairiness tests of the yarns and Yesim Textile Inc. (Bursa, Turkey) for their assistance in the production and tests of the fabrics.

#### REFERENCES

- 1. Akaydin, M., Can, Y., Oren, O., Ozerdogan, M. E. (2009). Ring penye ve kompakt ipliklerden orulen temel atkili orme kumaslarin patlama mukavemetleri uzerine bir arastirma. *Tekstil ve Muhendis*, 16(73/74), 16-20.
- 2. Akkis, B. (2009). Farkli iplik numaralarindan orulmus degisik orgu tiplerinin kumasin fiziksel ozelliklerine etkisi. *Yuksek Lisans Tezi*, Cukurova Universitesi Fen Bilimleri Enstitusu, Tekstil Muhendisligi Anabilim Dali, Adana.
- 3. Altas, S., Kadoglu, H. (2009). Ring ve kompakt viskon ipliklerden orulmus kumaslarin patlama, mukavemet ve boncuklanma ozelliklerinin karsilastirilmasi. *E-Journal of New World Sciences Academy Engineering Sciences*, 4(4), 538-546.
- 4. Buharali, G., Omeroglu, S. (2019a). Comparative study on carded cotton yarn properties produced by the conventional ring and new modified ring spinning system. *Fibres&Textiles in Eastern Europe*, 27(2/134), 45-51.
- 5. Buharali, G., Omeroglu S. (2019b). Konvansiyonel ring ve yeni bir modifiye ring iplik egirme sistemi kullanilarak uretilen iplik ve kumaslarin bazi ozelliklerinin karsilastirilmasi. *Uludag Universitesi Muhendislik Fakultesi Dergisi*, 24(3), 163-182.
- 6. Ceken, F., Goktepe, F. (2005). Comparison of the properties of knitted fabrics produced by conventional and compact ring-spun yarns. *Fibres&Textiles in Eastern Europe*, 13(1/49), 47-50.
- 7. Celik, A., Bozkurt, Y. (2005). Kompakt iplikler. Tekstil ve Muhendis Dergisi, 12(57), 26-38.
- 8. Cetin, E. (2009). Ring ve kompakt ipliklerde surtunme katsayisinin ve iplik tuylulugunun pilling uzerine etkisi. *Yuksek Lisans Tezi*, Marmara Universitesi Fen Bilimleri Enstitusu, Tekstil Bilimleri Anabilim Dali, Istanbul.
- 9. Demir, M., Kilic, M. (2017). Bukum iplikciligi (Siro-spun) teknolojisindeki gelismeler ve hibrit egirme teknolojileri. *Tekstil ve Muhendis*, 24(105), 31-40.
- 10. Eymen, U. E. (2007). SPSS 15.0 veri analiz yontemleri. Istatistik Merkezi Yayin, No: 1, 167 s.
- 11. Hechtl, R., (1996). Compact spinning system-An opportunity for improving the ring spinning process. *Melliand English*, 77(4), 37-38.
- 12. Kirecci, A., Kaynak, H. K., Ince, M. E. (2011). Comparative study of the quality parameters of knitted fabrics produced from Sirospun, single and two-ply yarns. *Fibres&Textiles in Eastern Europe*, 19(5/88), 82-86.
- 13. Mavruz, S., Ogulata, R. T. (2008). Ring ve kompakt iplik ozellikleri ile bu ipliklerden uretilen orme kumas ozelliklerinin istatistiksel olarak incelenmesi. *Tekstil ve Konfeksiyon*, 18(3), 197-205.

on Innovative Surveys in Positive Sciences 4-5 December 2022 / Full Text Book

- 14. Omeroglu, S. (2005). Kompakt ve ring ipliklerden elde edilmis orme kumaslarin patlama mukavemeti ve boncuklanma performansi uzerine bir arastirma. *Pamukkale Universitesi Muhendislik Bilimleri Dergisi*, 11(3), 357-360.
- 15. Sezgin, O. S. (2005). Konvansiyonel ring ve kompakt iplik egirme sistemleri ile elde edilen ipliklerin orme kumas performanslarinin karsilastirilmasi. *Yuksek Lisans Tezi*, Suleyman Demirel Universitesi Fen Bilimleri Enstitusu, Tekstil Muhendisligi Anabilim Dali, Isparta.
- 16. Stalder, H. (1995). Compact spinning- A new generation of ring spun yarns. *Melliand English*, 76(3), 29-33.
- 17. Sun, M. N., Cheng, K. P. S. (2000). The quality of fabric knitted from cotton Sirospun yarn. *International Journal of Clothing Science and Technology*, 12(5), 351-359.
- 18. Ulku, S. (2000). Ring iplikciliginde gelistirme calismalari: Kompakt iplikcilik sistemi. *Tekstil&Teknik*, 189(10), 180-184.
- 19. Unal, S., Omeroglu, S. (2013). Farkli sistemlerle direkt olarak elde edilmis cift katli iplik ozelliklerinin orme kumas ozelliklerine etkileri. *Tekstil ve Muhendis*, 20(91), 9-15.
- 20. Yilmaz, D. (2004). Farkli kompakt ring iplik egirme sistemlerinin ve elde edilen ipliklerin ozelliklerinin karsilastirilmasi. *Yuksek Lisans Tezi*, Suleyman Demirel Universitesi Fen Bilimleri Enstitusu, Tekstil Muhendisligi Anabilim Dali, Isparta.

on Innovative Surveys in Positive Sciences 4-5 December 2022 / Full Text Book

# ADVANCED TREATMENT OF SOME EMERGING MICROPOLLUTANTS BY PHOTOCATALYTIC AND MEMBRANE PROCESSES FROM RAW HOSPITAL WASTEWATER AND COST ANALYSIS

#### Gokce PEHLIVANER GUNEY<sup>1</sup>

<sup>1</sup>Dokuz Eylül University, Engineering Faculty, Environmental Engineering Department, Izmir, Turkiye.

<sup>1</sup>ORCID ID: 0000-0003-4311-5564

#### Delia Teresa SPONZA<sup>2</sup>

<sup>2</sup>Dokuz Eylül University, Engineering Faculty, Environmental Engineering Department, Izmir, Turkiye.

<sup>2</sup>ORCID ID: 0000-0002-4013-6186

#### **ABSTRACT**

A great deal of macro and micropollutants in domestic, urban, hospital and industrial wastewaters are discharged to the receiving environment. Discharge standards have not been established for micropollutants, which are still being studied on measurement techniques and their chronic effects on living organisms. The conventional wastewater treatment plants (WWTPs) are designed according to the regulations concerning on macro pollutants in wastewaters. The conventional WWTPs treat the macro pollutants (Chemical Oxygen Demand [COD], Biological Oxygen Demand [BOD], Total Suspended Solids [TSS], Total Nitrogen [TN], Total Phosphorus [TP], heavy metals, etc.) with high efficiencies, however they are insufficient to treat micropollutants due to their physicochemical properties. In this study, one of the most dangerous categories for health (neurotoxic; α-Hexabromocyclododecane [α-HBCDD], carcinogen; N-Nitrosodimethylamine [NDMA], ecotoxic; Gemfibrozil [GFZ] and endocrine disruptor; Perfluorooctanesulfonic acid [PFOS]) were selected and treatability with advanced treatment techniques (photocatalytic and membrane) were investigated. The removal efficiencies of α-HBCDD, NDMA, GFZ and PFOS were obtained as 98%, 66%, 95% and 76%, respectively at the optimum experimental conditions (nanoparticle concentration of 0.50 g L<sup>-1</sup> CeO<sub>2</sub>, irradiation time of 45 min, UV light power of 210 W, temperature of 60 °C and pH of 7.00) for the photocatalytic treatment. The removal efficiencies of α-HBCDD, NDMA, GFZ and PFOS were found as 99%, 95%, 97% and 96%, respectively at the optimum experimental conditions (permeate flux [J<sub>v</sub>] of 104.17 L m<sup>-2</sup> h<sup>-1</sup>, cross-flow velocity [CFV] of 0.10 m h<sup>-1</sup>, transmembrane pressure [TMP] of 4.75 bar, pH of 8.00, temperature of 25°C, operation time of 1 h) for the membrane treatment with RO. Cost analysis was made for both treatment alternatives and the cost of treating 1 m<sup>3</sup> of raw hospital wastewater was calculated as 5.39 € for photocatalytic treatment with CeO<sub>2</sub> and 0.67 € for RO. RO was chosen as the most feasible method to treat the studied micropollutants (α-HBCDD, NDMA, GFZ and PFOS) from raw hospital wastewater.

**Keywords:** cost, hospital wastewater, membrane, micropollutants, photocatalytic.

#### INTRODUCTION

Hospitals are one of the main sources of micropollutant emissions because of large quantities of consumption such as; medical activities performed inside, laboratory researches and drugs eliminated from the human body via excretion with urine and feces. Usually, hospital wastewaters are not treated before sending to wastewater treatment plants (WWTPs) on a global scale. The micropollutants in the hospital wastewaters are directly discharged into the sewage system in Turkey without treatment since the conventional WWTPs can only treat macropollutants such as COD, BOD, TSS, TN, TP, heavy metals, etc. Some micropollutants are not biologically removed and even decrease the biological treatment efficiency during conventional biological treatment step of the WWTPs. In

on Innovative Surveys in Positive Sciences 4-5 December 2022 / Full Text Book

Turkey, there are not any limitations for the discharge of raw hospital wastewater into sewage channels. Moreover, there are no WWTPs to treat both macro and micropollutants simultaneously in wastewater for hospitals in Turkey. The Ministry of Environment and Urbanization should take some precautions and impose some restraints about treating or pre-treating raw hospital wastewaters in Turkey. Further improvement to biological wastewater treatment can also be obtained by adopting novel treatment technologies (advanced oxidation processes, membranes, ultrasound treatment, electrochemical processes, etc.) that may prove more efficient and less time consuming. In this study, photocatalytic and membrane treatment alterntives were investigated for micropollutant removals from raw hospital wastewater. Four different micropollutants were selected from the most dangerous categories for human health (neurotoxic; α-Hexabromocyclododecane [α-HBCDD], carcinogen; N-Nitrosodimethylamine [NDMA], ecotoxic; Gemfibrozil [GFZ] and endocrine disruptor; Perfluorooctanesulfonic acid [PFOS]). After obtaining the optimum experimental conditions for the maximum micropollutant removals, a cost analysis was made both for photocatalytic and membrane experiments to determine the feasible treatment option.

#### MATERIALS AND METHODS

In the scope of this study, a university hospital (Dokuz Eylül University Hospital, Izmir, Turkiye) was selected and raw hospital wastewater samples were taken as six-hour composite samples from the sewer connection line. The raw hospital wastewater was filtered from a coarse filtration with having 0.075 mm pore sized metallic strainers by gravity to remove the big particles before the analysis.  $\alpha$ -HBCDD, PFOS, NDMA and GFZ concentrations in the raw hospital wastewater were 0.0115, 0.0180, 0.1650 and 53.30  $\mu$ g L-1, respectively.

#### Physicochemical Properties of the Studied Micropollutants (a-HBCDD, GFZ, PFOS and NDMA)

Physicochemical properties of the studied micropollutants for this study are given in Table 1.

**Table 1.** Physicochemical properties of the studied micropollutants (United States Environmental Protection Agency [EPI Suite database], 2018)

IUPAC name	CAS No	Chemical	Molecular weight (g mol <sup>-1</sup> )	Henry's Law constant (atm m³ mol <sup>-1</sup> )	Solubility in water, at 25 °C (g L <sup>-1</sup> )	Point of zero charge, pzc	Octanol/ water part. coeff.,	Molecular structure
α-Hexabromo cyclododecane ((1R,2R,5S,6R,9R,1 0S)-1,2,5,6,9,10- hexabromo cyclododecane) Abbreviation: α- HBCDD	134237- 50-6	$\mathrm{C}_{12}\mathrm{H}_{18}\mathrm{Br}_{6}$	641.70	1.72×10 <sup>-6</sup>	2.09×10 <sup>-5</sup>	7.5, 8.5	7.74	Br Br Br
Gemfibrozil (5-(2,5- dimethylphenoxy)- 2,2- dimethylpentanoic acid) Abbreviation: GFZ	25812- 30-0	$C_{15}H_{22}O_3$	250.34	1.19×10 <sup>-8</sup>	4.964×10 <sup>-3</sup>	4.75	4.77	CH <sub>3</sub> H <sub>3</sub> C CH <sub>3</sub>

on Innovative Surveys in Positive Sciences 4-5 December 2022 / Full Text Book

Perfluorooctane sulfonic acid (1,1,2,2,3,3,4,4,5,5, 6,6,7,7,8,8,8- Heptadecafluoro-1- octanesulfonic acid) Abbreviation: PFOS	1763- 23-1	$\mathrm{C_8HF_{17}O_3S}$	500.13	1.10×10 <sup>-2</sup>	0.104×10 <sup>-3</sup>	< 1.0	4.49	SOJH
N-Nitroso dimethylamine (N,N- dimethylnitrous amide) Abbreviation: NDMA	62-75-9	$\mathrm{C_2H_6N_2O}$	74.08	2.06×10 <sup>-6</sup>	4.104×10 <sup>5</sup>	3.52*	-0.57	H <sub>3</sub> C-N <sub>2</sub>

<sup>\*:</sup> Alvarez-Corena et al., 2016

#### Measurement of the Studied Micropollutants (α-HBCDD, GFZ, PFOS and NDMA)

All the studied micropollutants were extracted from raw hospital wastewater by solid phase extraction (SPE) method. The extraction procedure of  $\alpha$ -HBCDD and PFOS was taken from Chokwe et al. (2015). However, GFZ and NDMA were extracted according to Diwan et al. (2010). After the extraction process  $\alpha$ -HBCDD and PFOS concentrations were measured in LC-MS/MS. The instrumental conditions for  $\alpha$ -HBCDD and PFOS were taken from another studies performed by Zhang et al. (2016) and Sühring et al. (2015), respectively. The extracted samples of GFZ and NDMA were measured in HPLC. The instrumental conditions for GFZ and NDMA were applied according to the method given by Elsherif et al. (2013) and McDay (2010), respectively.

#### **Photocatalytic Treatment Process**

The photocatalytic experiments under Ultraviolet (UV) light were carried out in a covered stainless steel system including quartz glass reactors with a volume of 1 L and the UV light lamps having 254 nm wavelength. In this study, ten UV light lamps were used. Each of the lamps have a size of 895.0 mm× 26.0 mm and a power of 30.0 Watt (G13 Model, OSRAM). The light power required was provided by increasing or decreasing the UV lamp numbers. The distance between the UV lamps and quartz glass reactors was 15 cm. The temperature was changed using a heated magnetic stirrer in the covered stainless steel system. The raw hospital wastewater was first filtered through 0.075 mm coarse filters to remove physical impurities. After then, the studied nanoparticles was added to the filtered hospital wastewater and mixed through the photocatalytic experiments with a magnetic fish on a magnetic stirrer. The temperature of the nanoparticle added hospital wastewater was monitored regularly with a mercury thermometer. All the experiments were in batch mode and samples were analyzed immediately after the photocatalytic treatment process. All the experiments were performed in triplicate.

#### **Membrane Treatment Process**

• A reverse osmosis system was used in the membrane experiments and RO was purchased from DowDuPont, USA (FilmTec XLE-2521 model). RO was made of polyamide thin-film composite (TFC) material. Molecular weight cut-off (MWCO) value was 100 g mol<sup>-1</sup> for RO. The pores of RO with diameters varying between 0.22-0.44 nm while RO had negatively charged surfaces in the pH range of 4.50-8.50 (provided by the manufacturer). RO was operated in cross-flow mode with a total membrane area of 0.960 m<sup>2</sup>. In order to prevent clogging, a pre-filter having a pore size of 1 μm was placed before the RO. A feeding tank was placed before RO and made of high density polyethylene with a capacity of 50 L. The transmembrane pressure (TMP), permeate flux (J<sub>v</sub>), and cross-flow velocity (CFV) of RO with the removal efficiencies of studied micropollutants were evaluated and monitored during the experiments. All the experiments were in batch mode and samples were analyzed immediately after the membrane treatment process. All the experiments were performed in triplicate.

on Innovative Surveys in Positive Sciences 4-5 December 2022 / Full Text Book

#### RESULTS AND DISCUSSIONS

#### **Photocatalytic Treatment**

Preliminary experiments were carried out with five different nanoparticles (nano-SiO<sub>2</sub>, nano-ZnO, graphene, nano-TiO<sub>2</sub> and nano-CeO<sub>2</sub>) to decide which nanoparticles give higher removal efficiencies for the photocatalytic treatment of the studied micropollutants. According to the previous studies given in the literature, it was decided to use 0.25, 0.50 and 1.50 g L<sup>-1</sup> nanoparticle concentrations in this study. The experiments were carried out at a constant irradiation time (60 min), at a constant UV light power (120 W), at a constant pH (7.00) and at a constant temperature of 25 °C which was the original wastewater temperature for 100  $\mu$ g L<sup>-1</sup> initial micropollutant concentrations in a synthetic wastewater. The maximum removal efficiencies for  $\alpha$ -HBCDD, NDMA, GFZ and PFOS were obtained with 0.50 g L<sup>-1</sup> nano-CeO<sub>2</sub> (higher than 40%) and the further experiments were carried out with nano-CeO<sub>2</sub> (Data not shown). This can be attributed to the highest specific surface area of nano-CeO<sub>2</sub> (302 m<sup>2</sup> g<sup>-1</sup>) with the lowest particle size (20 nm) in the comparison with other studied nanoparticles.

The effect of nano-CeO<sub>2</sub> concentrations (0.25, 0.50, 1.00 and 1.50 g L<sup>-1</sup>) on the photocatalytic removals of all studied micropollutants were investigated at a constant irradiation time of 15 min at a constant UV light power of 120 W at a constant temperature of 25 °C and at a constant pH of 7.00. The optimum photocatalytic removals were found as 62%, 29%, 46% and 28% for α-HBCDD, PFOS, GFZ and NDMA, respectively with 0.50 g L<sup>-1</sup> nano-CeO<sub>2</sub> at the aforementioned experimental conditions (Figure 1). Increasing the amount of photocatalyst (nano-CeO<sub>2</sub>) from 0.25 to 0.50 g L<sup>-1</sup> resulted in an increase in the photocatalytic removal efficiencies of all studied micropollutants from the raw hospital wastewater (Figure 1). The nano-CeO<sub>2</sub> concentrations higher than 0.50 g L<sup>-1</sup> were slightly decreased the photocatalytic removals of all studied micropollutants (Figure 1). The increase in nanoparticle concentration increases the amount of hydroxyl (OH•) radicals to degrade the micropollutants. Also, this increase supports more binding sites for the micropollutants to adsorb onto nanoparticles (Bethi et al., 2016). However, increasing of nanoparticle concentration causes turbidity in the wastewater. The penetration of UV light through turbidity becomes difficult and the photocatalytic removal efficiencies of the micropollutants decreases (Wang et al., 2017). The optimum nano-CeO<sub>2</sub> concentration was found as 0.50 g L<sup>-1</sup> at the aforementioned experimental conditions. The ANOVA (one-way) test statistics results showed that the increasing nanoparticle concentrations from 0.25 to 0.50 g L<sup>-1</sup> had a significant effect on the photocatalytic removals of all studied micropollutants at the aforementioned experimental conditions (P = 0.038,  $\alpha = 0.05$ , F = 4.85). Any further increase in nano-CeO<sub>2</sub> concentrations (from 0.50to 1.5 g L<sup>-1</sup>) did not have a significant effect on the photocatalytic removals of all studied micropollutants at the aforementioned experimental conditions (P = 0.769,  $\alpha$  = 0.05, F = 0.09).

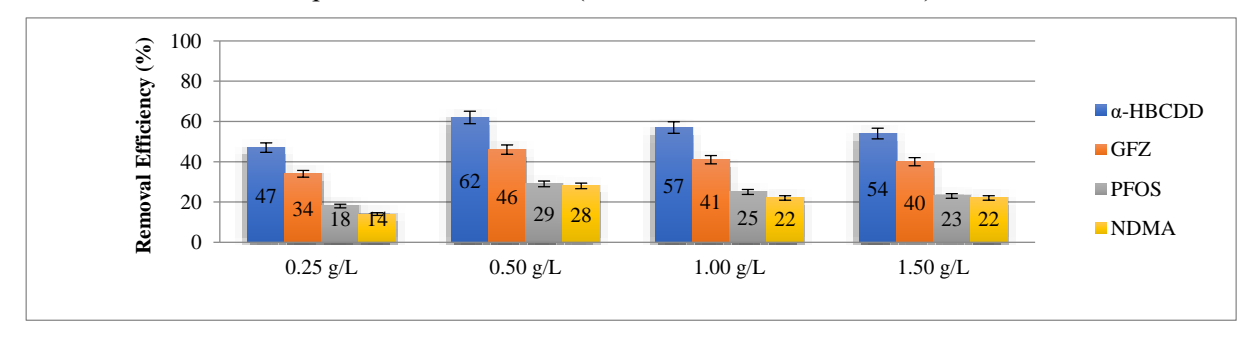


**Figure 1.** Effect of nano-CeO<sub>2</sub> concentrations (0.25, 0.50, 1.00 and 1.50 g L<sup>-1</sup>) on the photocatalytic removals of all studied micropollutants

The photocatalytic experiments at different irradiation times (15, 30, 45, 60 and 90 min) showed that 45 min was the optimum irradiation time for the maximum photocatalytic removals of α-HBCDD (85%), PFOS (48%), GFZ (72%) and NDMA (40%) with 0.50 g L<sup>-1</sup> constant nano-CeO<sub>2</sub> concentration at a constant UV light power of 120 W at a constant temperature of 25 °C and at a constant pH of 7.00 (Figure 2). OH• radicals formation increases with the increasing irradiation time and increases the micropollutant removal efficiency. If the irradiation time continues longer than the optimum irradiation time, OH• radicals formation does not increase for the constant dose of nanoparticle (Miranda-García et

on Innovative Surveys in Positive Sciences

4-5 December 2022 / Full Text Book

al., 2011). The ANOVA (one-way) test statistics showed that the increased length of time up to 45 min had a significant effect on the photocatalytic removals of all studied micropollutants at the aforementioned experimental conditions (P = 0.006,  $\alpha$  =0.05, F = 6.02). The effect of irradiation time on the photocatalytic removals of all studied micropollutants for higher than 45 min (60 and 90 min) was not significant (P = 0.792,  $\alpha = 0.05$ , F = 0.07) at the aforementioned experimental conditions.

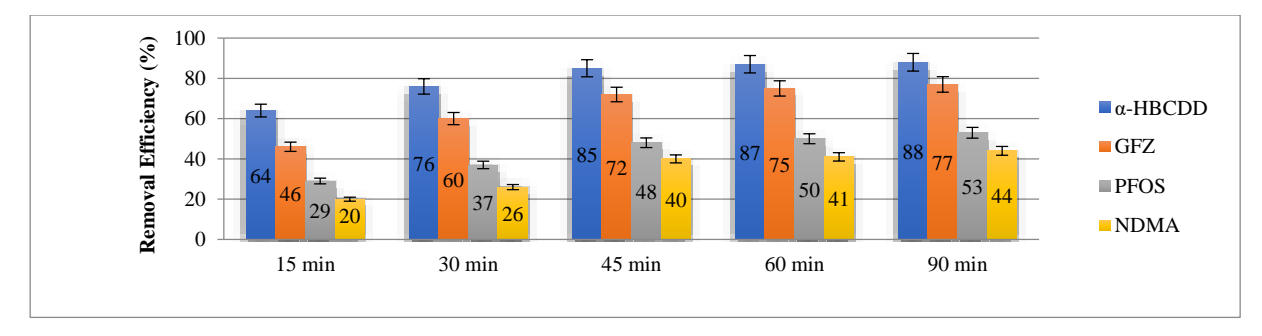


Figure 2. Effect of irradiation times (15, 30, 45, 60 and 90 min) on the photocatalytic removals of all studied micropollutants

The photocatalytic reactor system was operated at increasing UV light powers (120, 210 and 300 W) in order to determine the optimum UV light power for the maximum micropollutants removals with 0.50 g L<sup>-1</sup> constant nano-CeO<sub>2</sub> concentration at a constant irradiation time of 45 min at a constant temperature of 25 °C and at a constant pH of 7.00. The maximum photocatalytic removal efficiencies were obtained as 93%, 64%, 80% and 51% for α-HBCDD, PFOS, GFZ and NDMA, respectively at the optimum UV light power as 210 W with nano-CeO<sub>2</sub> at the aforementioned experimental conditions (Figure 3). The photocataytic removals of all studied micropollutants increased when the UV light power was increased from 120 W to 210 W with nano-CeO<sub>2</sub> (Figure 3). However, when the UV light power was increased to 300 W the photocatalytic removals of micropollutants decreased at the aforementioned experimental conditions (Figure 3). The concentrations of hydroxyl (OH•) radicals increased at increased UV light powers and they increased the photocatalytic removal efficiencies of the micropollutants. However, at too high UV light powers, the amount of photons absorbed by the nanoparticle could not be increased for the constant nanoparticle dose and sufficient hydroxyl (OH•) radicals could not be formed and causes lower photocatalytic removal efficiencies (Bai & Acharya, 2016). The optimum UV light power was found as 210 W at the aforementioned experimental conditions. The ANOVA (one-way) test statistics results showed that the increasing UV light power increased the micropollutant photocatalytic removals significantly up to 210 W UV light power at the aforementioned experimental conditions (P = 0.037,  $\alpha$ = 0.05, F = 3.64). The relationship between 300 W UV light power and the micropollutants photocatalytic removals was not significant at the aforementioned experimental conditions (P = 0.398,  $\alpha = 0.05$ , F = 0.74).

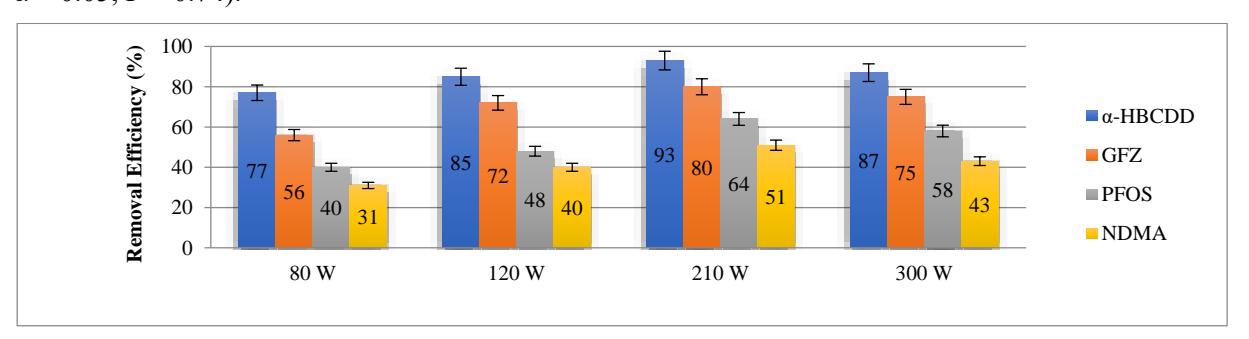
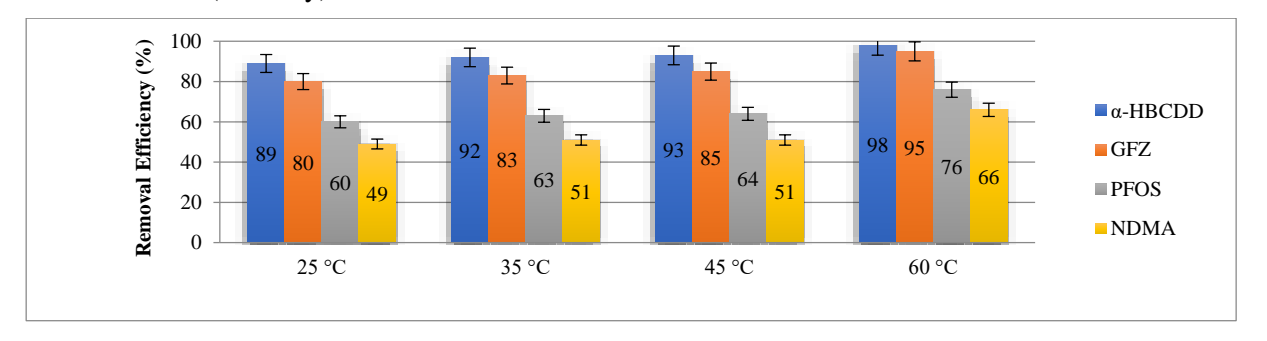


Figure 3. Effect of UV light powers (80, 120, 210 and 300 W) on the photocatalytic removals of all studied micropollutants

The results showed that 60 °C was the optimum temperature from the studied temperature range (25, 35, 45 and 60 °C) for the maximum photocatalytic removals of α-HBCDD (98%), PFOS (76%), GFZ (95%) and NDMA (66%) with 0.50 g L<sup>-1</sup> constant nano-CeO<sub>2</sub> concentration at a constant irradiation time of 45 min at a constant UV light power of 210 W and at a constant pH of 7.00 (Figure 4). Higher

on Innovative Surveys in Positive Sciences 4-5 December 2022 / Full Text Book

temperature provides higher electron transfers in valance band of the nanoparticle to higher energy levels and increases the amount of hydroxyl radicals (OH•) to degrade micropollutants (Chatila et al., 2016). The temperature affected the photocatalytic removals of all studied micropollutants significantly (P = 0.037,  $\alpha$  = 0.05, F = 4.90) for the optimum temperature of 60 °C at the aforementioned experimental conditions according to the ANOVA (one-way) test statistics results. The increase in the temperature from 25 °C to 45 °C had no significant effect on the photocatalytic removals of all studied micropollutants (P = 0.833,  $\alpha$  = 0.05, F = 0.18) at the aforementioned experimental conditions according to the ANOVA (one-way) test statistics results.



**Figure 4.** Effect of temperatures (25, 35, 45 and 60 °C) on the photocatalytic removals of all studied micropollutants

#### **Membrane Treatment**

Permeate samples were collected through 60 min of operation time from RO system. At the start-up of RO, 5 min was waited to reach steady state conditions for the stabil permeate fluxes. The removal efficiencies of  $\alpha$ -HBCDD, NDMA, GFZ and PFOS were investigated at a pH of  $8.00 \pm 0.50$  and at a temperature of  $25 \pm 2.00$  °C for RO processes. The transmembrane pressure (TMP) were determined according to Tunc et al. (2014), while permeate flux ( $J_v$ ) and cross-flow velocity (CFV) were calculated according to Bunani et al. (2015), respectively.

Preliminary experiments were carried out at increasing permeate flux  $(J_v)$  values (52.08, 69.44 and 104.17 L m<sup>-2</sup> h<sup>-1</sup>) and the optimum  $J_v$  was obtained as 104.17 L m<sup>-2</sup> h<sup>-1</sup> at 2.75 bar TMP at

0.10 m h<sup>-1</sup> of CFV for 1 h of operation time at a pH of 8.00 and at 25 °C for the highest micropollutant removal efficiencies in RO (Table 2). α-HBCDD, NDMA, GFZ and PFOS were removed 86.2%, 70.0%, 80.6% and 79.3%, respectively at the aforementioned experimental conditions (Table 2). Therefore, increased permeate flux increased the surface area over the valley regions of the ridge-and-valley structures in RO and micropollutants reached more surface area for the attachment (Tang et al., 2007).

**Table 2.**  $\alpha$ -HBCDD, NDMA, GFZ and PFOS removals at increasing permeate flux ( $J_v$ ) values (52.08, 69.44 and 104.17 L m<sup>-2</sup> h<sup>-1</sup>) in RO

	Removal efficiency (%)		
Micropollutant	$J_v = 52.08 \text{ L m}^{-2} \text{ h}^{-1}$	$J_v = 69.44 \text{ L m}^{-2} \text{ h}^{-1}$	$J_v = 104.17 \text{ L m}^{-2} \text{ h}^{-1}$
	TMP = 2.75  bar	TMP = 2.75 bar	TMP = 2.75  bar
	$CFV = 0.05 \text{ m h}^{-1}$	$CFV = 0.07 \text{ m h}^{-1}$	$CFV = 0.10 \text{ m h}^{-1}$
	V = 100 L	V = 100 L	V = 100 L
	$S = 0.96 \text{ m}^2$	$S = 0.96 \text{ m}^2$	$S = 0.96 \text{ m}^2$
	t = 2 h	t = 1.5 h	t = 1 h
α-HBCDD	$51.3 \pm 0.5$	$55.0 \pm 0.5$	$86.2 \pm 0.5$
PFOS	$47.3\pm0.5$	$50.4 \pm 0.5$	$79.3 \pm 0.5$
GFZ	$48.7 \pm 0.5$	$51.0 \pm 0.5$	$80.6 \pm 0.5$
NDMA	$38.7 \pm 0.5$	$42.4 \pm 0.5$	$70.0\pm0.5$

After then, the experiments were performed at increasing TMPs (2.75, 3.75 and 4.75 bar) at 0.10 m h<sup>-1</sup> of CFV for 1 h of operation time at a pH of 8.00 and at 25 °C for the highest micropollutant removal

on Innovative Surveys in Positive Sciences 4-5 December 2022 / Full Text Book

efficiencies in RO (Table 3). The maximum removals were observed at the highest TMP of 4.75 bar for  $\alpha$ -HBCDD (99.0%), NDMA (95.3%), GFZ (97.3%) and PFOS (96.0%) at the aforementioned experimental conditions in RO (Table 3). Higher removals are expected at higher TMPs for RO, since increasing the pressure difference affect positively the filtration driving force through the membrane (Varol et al., 2015). The higher TMP means the more rapidly saturation was achieved for the micropollutants (Causserand et al., 2005).

**Table 3.** α-HBCDD, NDMA, GFZ and PFOS removals at increasing TMPs (2.75, 3.75 and 4.75 bar) in RO

	Removal efficiency (%)		
Micropollutant	TMP = 2.75 bar	TMP = 3.75  bar	TMP = 4.75  bar
	$J_v = 104.17 \text{ L m}^{-2} \text{ h}^{-1}$	$J_v = 104.17 \text{ L m}^{-2} \text{ h}^{-1}$	$J_v = 104.17 \text{ L m}^{-2} \text{ h}^{-1}$
	$CFV = 0.10 \text{ m h}^{-1}$	$CFV = 0.10 \text{ m h}^{-1}$	$CFV = 0.10 \text{ m h}^{-1}$
	V = 100 L	V = 100 L	V = 100 L
	$S = 0.96 \text{ m}^2$	$S = 0.96 \text{ m}^2$	$S = 0.96 \text{ m}^2$
	t = 1 h	t = 1 h	t = 1 h
α-HBCDD	$86.2 \pm 0.5$	$88.0 \pm 0.5$	$99.0 \pm 0.5$
PFOS	$79.3 \pm 0.5$	$82.3\pm0.5$	$96.0 \pm 0.5$
GFZ	$80.6 \pm 0.5$	$84.1\pm0.5$	$97.3 \pm 0.5$
NDMA	$70.0 \pm 0.5$	$75.5 \pm 0.5$	$95.3 \pm 0.5$

The removals through RO processes are mainly due to size exclusion, electrostatic interaction (or charge repulsion) and hydrophobic adsorption (Narbaitz et al., 2013). The size exclusion mechanism made contribution to the removal of neutral micropollutant namely  $\alpha$ -HBCDD (pKa = pH) because the MWCO of RO (0.1 kDa – provided by the manufacturer) was lower than the molecular weights of the micropollutants ( $\approx$ 1 kDa) at the aforementioned experimental conditions in RO as reported by Khanzada et al. (2019).

In this study, the pH value of the raw hospital wastewater was kept at 8.00 which its original value. PFOS (pKa < 1.0), GFZ (pKa = 4.75) and NDMA (pKa = 3.52) exist in their anionic form (pKa < pH) in the raw hospital wastewater and the negatively charged RO surface at pH 8.00 increased its removal via the electrostatic interaction mechanism. Micropollutant separation by the electrostatic interaction mechanism arises when the electrostatic repulsive forces between the charged membrane surface and the ions of electrolyte micropollutant inhibits the ion form contacting the membrane (Narbaitz et al., 2013). Despite being quite hydrophilic micropollutant (log  $K_{\rm OW} < 3.0$ ), NDMA was removed 70% in RO, because electrostatic repulsion mechanism was effective for its removal (Table 1). Licona et al. (2018) were observed similar behaviours for the anionic hydrophilic micropollutants in RO treatment and explained that the electrostatic repulsion between the hydrophilic micropollutants and the negatively charged RO membrane surface helped to remove the hydrophilic micropollutants more effectively (Licona et al., 2018). Since pKa value of  $\alpha$ -HBCDD is between 7.5 and 8.5,  $\alpha$ -HBCDD exists in its neutral form at the operating pH value (8.00) in RO (Table 1). Therefore, the electrostatic repulsion of  $\alpha$ -HBCDD from membrane surface did not play any role for its removal mechanism.

The hydrophobic micropollutants ( $\alpha$ -HBCDD, GFZ and PFOS) have log  $K_{OW}$  values greater than 3.0 (Table 1). They adsorbed onto membrane surface and removed mainly by hydrophobic adsorption mechanism at the aforementioned experimental conditions in RO. The RO used in the experiments was made of polyamide thin-film composite (TFC) material. The polyamide thin film composite (TFC) membranes with a typical three-layer structure are considered as the most successful and commercialized membranes. It is comprised of a thin composite active layer (in the order of 100 nm thickness for RO) attached with a more open intermediate layer (about 40  $\mu$ m) and an even more open support layer. The possible reason for micropollutants removals by the membrane might be the strong interaction of organic pollutants with the membrane polymer (Hofs et al., 2013).

on Innovative Surveys in Positive Sciences 4-5 December 2022 / Full Text Book

The ANOVA (one-way) test statistics showed that removal due to hydrophobicity was significant at the aforementioned experimental conditions in RO ( $P = 5.04 \times 10^{-9}$ ,  $\alpha = 0.05$ , F = 2369.89). Secondes et al. (2014) also explained that the removal trend of micropollutants via hydrophobic adsorption were in correlation with their hydrophobic characteristics (log  $K_{OW}$  values) in membrane treatment.

# **Cost Analysis**

**Table 4.** Cost analysis for the photocatalytic and membrane treatment of all studied micropollutants from 1 m<sup>3</sup> raw hospital wastewater at the optimum experimental conditions

Inputs for photocatalytic treatment	Cost	Total cost	
UV lamps	1 UV lamp: 15 € Lifetime of 1 UV lamp: 8000 h		
•	7 UV lamp: $7 \times (1.875 \times 10^{-3})$ €/h) × (0.75 h) = $9.84 \times 10^{-3}$ €		
Investment cost (Photocatalytic reactor, isolated cabin and magnetic stirrer)	1 photocatalytic reactor: $10 \ \ \ \ \ \ \ \ \ \ \ \ \ \ \ \ \ \ \$		
Electricity consumption	1 UV lamp: 30 W power and 1 kW = 1000 W 45 min = 0.75 h and 1 kWh electricity: 0.04 $\in$ (30 W/lamp) × (7 lamps) × (1 kW/1000 W) × (0.75 h) × (0.04 $\in$ /1 kWh) = 6.30×10 <sup>-3</sup> $\in$	5.39 €	
Nanoparticles	Cerium (IV) oxide (CeO <sub>2</sub> ) nanopowder (10 kg): $120 \in$ 0.50 g nanoparticle was used for 5 cycles/L: $0.10 \text{ g/L} = 100 \text{ g/m}^3$ $100 \text{ g nano-CeO}_2$ for $1 \text{ m}^3 = 1.20 \in$		
Regeneration of nanoparticles	0.10 M HCl in ethanol = 83 mL HCl + 917 mL ethanol (83 mL HCl)×(3 $\epsilon$ /1000 mL)×(2 times/year)×(1 year) = 0.50 $\epsilon$ (917 mL ethanol)×(2 $\epsilon$ /1000 mL)×(2 times/year)×(1 year)=3.67 $\epsilon$		
Inputs for RO	Cost	Total cost	
Investment cost (membrane, feeding tank, pump, store equipments and montage)	RO membrane: $380 \in$ Lifetime of RO: 2 years = $17520 \text{ h}$ (accepted) $(0.022 \notin/\text{h}) \times (1 \text{ h}) = 0.0217 \notin$ feding tank, pump, store equipments and montage: $150 \in$ Lifetime of feding tank, pump, store equipments and montage: $10 \text{ years} = 87600 \text{ h}$ (accepted) $(0.0017 \notin/\text{h}) \times (1 \text{ h}) = 0.0017 \notin$	0.67 €	
Electricity consumption	pump: 0.25 kW power 1 kWh electricity: 0.04 $\in$ (0.25 kW) × (1 h) × (0.04 $\in$ /1 kWh) = 0.01 $\in$		

on Innovative Surveys in Positive Sciences 4-5 December 2022 / Full Text Book

Cleaning of membranes (once a month)	HNO <sub>3</sub> (0.1 N requires 6 mL HNO <sub>3</sub> /L): 2.75 €/1000 mL
	(6  mL)× $(2.75 €/1000  mL)$ × $(12  times/year)$ × $(2  years)$ =
	0.396 €
	NaOH (0.1 N requires 4 g NaOH/L): 2.5 €/1000 g
	(4  g)× $(2.5 €/1000  g)$ × $(12  times/year)$ × $(2  years) = 0.24 €$

#### CONCLUSIONS

The removal efficiencies of  $\alpha$ -HBCDD, NDMA, GFZ and PFOS were obtained as 98%, 66%, 95% and 76%, respectively with a nanoparticle concentration of 0.50 g L<sup>-1</sup> CeO<sub>2</sub>, irradiation time of 45 min, UV light power of 210 W, temperature of 60 °C and pH of 7.00 for the photocatalytic treatment. The removal efficiencies of  $\alpha$ -HBCDD, NDMA, GFZ and PFOS were found as 99%, 95%, 97% and 96%, respectively at a  $J_v$  of 104.17 L m<sup>-2</sup> h<sup>-1</sup>, CFV of 0.10 m h<sup>-1</sup>, TMP of 4.75 bar, pH of 8.00, temperature of 25°C and operation time of 1 h for RO. The cost of treating 1 m³ of raw hospital wastewater was calculated as 5.39 € for photocatalytic treatment and 0.67 € for RO. RO gave higher removal efficiencies (higher than 95% for all studied micropollutants) than the photocatalytic treatment (higher than 66% for all studied micropollutants). The most efficient and the cheapest alternative was determined as membrane treatment with RO. As a consequence, RO was chosen as the most feasible method to treat the studied micropollutants ( $\alpha$ -HBCDD, NDMA, GFZ and PFOS) from raw hospital wastewater in this study.

The conventional WWTPs are not designed to treat micropollutants, however micropollutants can reduce the biological treatment efficiency of the conventional WWTPs due to their physicochemical properties. Modifying the conventional WWTPs by placing membrane units at the end of the treatment plants can be considered in terms of providing micropollutant removals. The variety of micropollutants that can be treated and the initial investment cost of the membrane units to be used can be investigated by further studies.

#### REFERENCES

Alvarez-Corena, J. R. (2015). *Heterogeneous photocatalysis for the treatment of contaminants of emerging concern in water*. Phd Thesis, Worcester Polytechnic Institute, Massachusetts, USA.

Bai, X. & Acharya, K. (2016). Removal of trimethoprim, sulfamethoxazole, and triclosan by the green alga *Nannochloris sp. Journal of Hazardous Materials*, 315, 70–75.

Bethi, B., Sonawane, S. H., Bhanvase, B. A., & Gumfekar, S. P. (2016). Nanomaterials-based advanced oxidation processes for wastewater treatment: a review. *Chemical Engineering and Processing*, 109, 178–189.

Bunani, S., Yorukoglu, E., Yuksel, U., Kabay, N., Yuksel, M., & Sert, G. (2015). Application of reverse osmosis for reuse of secondary treated urban wastewater in agricultural irrigation. *Desalination*, *364*, 68-74.

Causserand, C., Aimar, P., Cravedi, J. P., & Singlande, E. (2005). Dichloroaniline retention by nanofiltration membranes. *Water Research*, *39*, 1594-1600.

Chatila, S., Amparo, M. R., Carvalho, L. S., Penteado, E. D., Tomita, I. N., Santos-Neto, Á. J., Gomes, P. C. F. L., & Zaiat, M. (2016). Sulfamethoxazole and ciprofloxacin removal using a horizontal-flow anaerobic immobilized biomass reactor. *Environmental Technology*, *37* (7), 847-853.

Chokwe, T. B., Okonkwo, J. O., Sibali, L. L., & Ncube, E. J. (2015). An integrated method for the simultaneous determination of alkylphenol ethoxylates and brominated flame retardants in sewage sludge samples by ultrasonic-assisted extraction, solid phase clean-up, and GC-MS analysis. *Microchemical Journal*, 123, 230-236.

Diwan, V., Tamhankar, A.J., Khandal, R.K., Sen, S., Aggarwal, M., Marothi, Y., Iyer, R.V., Sundblad-Tonderski, K., & Stalsby-Lundborg, C. (2010). Antibiotics and antibiotic-resistant bacteria in waters associated with a hospital in Ujjain, India. *BMC Public Health*, 10, 414-422.

on Innovative Surveys in Positive Sciences 4-5 December 2022 / Full Text Book

- Elsherif, Z. A., Abas, S. S., Abdelwahab, M. H., & El-Weshahy, S. (2013). Determination of gemfibrozil and fenofibrate inpharmaceuticals in presence of their degradation products. *International Journal of Pharmacy and Pharmaceutical Sciences*, 5 (3), 886–896.
- Hofs, B., Schurer, R., Harmsen, D. J. H., Ceccarelli, C., Beerendonk, E. F., & Cornelissen, E. R. (2013). Characterization and performance of a commercial thin film nanocomposite seawater reverse osmosis membrane and comparison with a thin film composite. *Journal of Membrane Science*, 446, 68–78.
- Khanzada, N. K., Farid, M. U., Kharraz, J. A., Choi, J., Tang, C. Y., Nghiem, L. D., Jang, A., & An, A. K. (2019). Removal of organic micropollutants using advanced membrane-based water and wastewater treatment: A review. *Journal of Membrane Science*, 598, 117672.
- Licona, K. P. M., Geaquinto, L. R. D. O., Nicolini, J. V., Figueiredo, N. G., Chiapetta, S. C., Habert, A. C., & Yokoyama, L. (2018). Assesing potential of nanofiltration and reverse osmosis for removal of toxic pharmaceuticals from water. *Journal of Water Process Engineering*, 25, 195-204.
- McDay, J. (2010). *Ecological method development for detecting N-nitrosodimethylamine in water using HPLC-PDAD*. Phd Thesis, Eastern Michigan University, MI, USA.
- Miranda-García, N., Suárez, S., Sánchez, B., Coronado, J. M., Malato, S., & Maldonado, M. I. (2011). Photocatalytic degradation of emerging contaminants in municipal wastewater treatment plant effluents using immobilized TiO<sub>2</sub> in a solar pilot plant. *Applied Catalysis B: Environmental*, 103, 294-301.
- Narbaitz, R. M., Rana, D., Dang, H. T., Morrissette, J., Matsuura, T., Jasim, S. Y., Tabe, S., & Yang, P. (2013). Pharmaceutical and personal care products removal from drinking water by modified cellulose acetate membrane: Field testing. *Chemical Engineering Journal*, 225, 848-856.
- Secondes, M. F. N., Naddeo, V., Belgiorno, V., & Ballesteros, F. (2014). Removal of emerging contaminants by simultaneous application of membrane ultrafiltration, activated carbon adsorption, and ultrasound irradiation. *Journal of Hazardous Materials*, 264, 342–349.
- Sühring, R., Barber, J. L., Wolschke, H., Kötke, D., & Ebinghaus, R. (2015). Fingerprint analysis of brominated flame retardants and dechloranes in North Sea sediments. *Environmental Research*, 140, 569-578.
- Tang, C. Y., Fu, Q. S., Criddle, C. S., & Leckie, J. O. (2007). Effect of flux (transmembrane pressure) and membrane properties on fouling and rejection of reverse osmosis and nanofiltration membranes treating perfluorooctane sulfonate containing wastewater. *Environmental Science & Technology, 41*, 2008-2014.
- Tunc, M. S., Yilmaz, L., Yetis, U., & Culfaz-Emecan, P. Z. (2014). Purification and concentration of caustic mercerization wastewater by membrane processes and evaporation for reuse. *Separation Science and Technology*, 49, 1968-1977.
- United States Environmental Protection Agency [EPI Suite database] (2018). Computer programme, USA.
- Varol, C., Uzal, N., Dilek, F. B., Kitis, M., & Yetis, U. (2015). Recovery of caustic from mercerizing wastewaters of a denim textile mill. *Desalination and Water Treatment*, 53 (12), 3418-3426.
- Wang, S., Yang, Q., Chen, F., Sun, J., Luo, K., Yao, F., Wang, X., Wang, D., Li, X., & Zeng, G. (2017). Photocatalytic degradation of perfluorooctanoic acid and perfluorooctane sulfonate in water: a critical review. *Chemical Engineering Journal*, 328, 927–942.
- Zhang, D., Luo, Q., Gao, B., Chiang, S. Y. D., Woodward, D., & Huang, Q. (2016). Sorption of perfluorooctanoic acid, perfluorooctane sulfonate and perfluoroheptanoic acid on granular activated carbon. *Chemosphere*, 144, 2336-2342.

on Innovative Surveys in Positive Sciences 4-5 December 2022 / Full Text Book

## ÇOK DEĞİŞKENLİ KUADRATİK KALİTE KAYIP FONKSİYONU İÇİN MAKSİMUM KAYIP VE KOŞULLU BEKLENEN DEĞER ANALİZLERİ

# MAXIMUM LOSS AND CONDITIONAL EXPECTED VALUE ANALYSES FOR THE MULTIVARIATE QUADRATIC QUALITY LOSS FUNCTION

#### Furkan Göktaş1

<sup>1</sup>Karabük Üniversitesi, İşletme Fakültesi, İşletme Bölümü, Karabük, Türkiye. <sup>1</sup>ORCID ID: 0000-0001-9291-3912

#### ÖZET

Taguchi, kuadratik kalite kayıp fonksiyonu kullanarak, kaliteyi parasal kayıpla ölçmüştür. Bu fonksiyon, Pignatiello tarafından n boyutta genelleştirilince çok değişkenli kuadratik kalite kayıp fonksiyonu elde edilmiştir. Çok değişkenli kuadratik kalite kayıp fonksiyonu için koşulsuz beklenen değer analizi yapmak oldukça kolaydır. Öte yandan sadece beklenen değere dayalı karar verme iyi bir yaklaşım değildir. Bu nedenle matematiksel modelleme yardımıyla bu fonksiyonun bir çok açıdan incelenmesi yararlı olabilir. Bu çalışmada çok değişkenli normal dağılım varsayımı altında kalite kaybının dağınıklık bileşeni ile ilgili analizler yapılmıştır. Başka bir deyişle kalite kaybının yanlılık bileşeninin sıfır olduğu varsayılmıştır. Bu varsayım, ideal bir süreç tasarımının doğal bir sonucudur. Kalite karakteristiklerinin n boyuttaki güven bölgesi elipsoit iken çok değişkenli kuadratik kalite kayıp fonksiyonunun maksimum değeri Monte Carlo Simülasyon veya Levenberg – Marquardt Algoritması ile bulunabilir. Bu çalışmada Monte Carlo Simülasyonu için kısa bir algoritma verilmiştir. Ayrıca elipsoit güven bölgesinin sınırı üzerinde kalite kaybının koşullu beklenen değeri için matematiksel ifade verilmiştir. Teorik altyapı tamamlandıktan sonra ise açıklayıcı bir örnek verilmiştir. Burada farklı güven düzeyleri için kalite kaybının koşullu beklenen değerleri ve maksimumları bulunmuştur. Elde edilen sonuçlara göre güven düzeyi arttıkça koşullu beklenen değer ve maksimum kayıp çok daha hızlı artmaktadır. Ayrıca yüksek güven düzeyleri için bu değerler, kalite kaybının koşulsuz beklenen değerinden oldukça yüksektir. Dolayısıyla uç ama olası kalite kayıplarını incelemek için bu çalışmada önerilen bu iki metrik kullanılabilir.

**Anahtar Kelimeler:** Kalite, Kuadratik Fonksiyon, Çok Değişkenli Analiz, Maksimum Kayıp, Koşullu Beklenen Değer.

#### **ABSTRACT**

Taguchi measures the quality with monetary loss by using the quadratic quality loss function. When this function is generalized to n dimensions by Pignatiello, a multivariate quadratic quality loss function is obtained. It is quite easy to perform unconditional expected value analysis for the multivariate quadratic quality loss function. On the other hand, decision making based on only expected value is not a good approach. Thus, it may be useful to examine this function from many perspectives with the help of mathematical modelling. In this study, we perform the analyses related to the dispersion component of quality loss under the assumption of multivariate normal distribution. In other words, we assume that the bias component of quality loss is equal to zero. This assumption is a natural consequence of an ideal process design. While the n-dimensional confidence region of the quality characteristics is ellipsoid, the maximum value of the multivariate quadratic quality loss function can be found with Monte Carlo Simulation or Levenberg – Marquardt Algorithm. In this study, we give a short algorithm for Monte Carlo Simulation. In addition, we give a mathematical expression for the conditional expected value of the quality loss at the boundary of the ellipsoid confidence region. After laying down the theoretical background, we also give an explanatory example. Here, we find that the conditional expected values and maximums of the quality loss for different confidence levels. According to the results obtained, as the confidence level increases, the conditional expected value and the maximum loss increase much faster. In addition, for high confidence levels, these values are considerably higher than

on Innovative Surveys in Positive Sciences 4-5 December 2022 / Full Text Book

the unconditional expected value of quality loss. Therefore, these two metric proposed in this study may be used to examine extreme but possible quality losses.

**Key Words:** Quality, Quadratic Function, Multivariate Analysis, Maximum Loss, Conditional Expected Value.

## 1. GİRİŞ

Taguchi (1986)'da kalite, kuadratik kalite kayıp fonksiyonu kullanılarak parasal kayıpla ölçülmüştür. Bu fonksiyon, Pignatiello (1993)'te n boyutta genelleştirilince çok değişkenli kuadratik kalite kayıp fonksiyonu elde edilmiştir. Çok değişkenli kuadratik kalite kayıp fonksiyonu için koşulsuz beklenen değer analizi yapmak oldukça kolaydır. Öte yandan sadece beklenen değere dayalı karar verme iyi bir yaklaşım değildir. Bu nedenle matematiksel modelleme yardımıyla bu fonksiyonun bir çok açıdan incelenmesi yararlı olabilir. Bu çalışmada çok değişkenli normal dağılım varsayımı altında kalite kaybının dağınıklık bileşeni ile ilgili analizler yapılmıştır. Başka bir deyişle kalite kaybının yanlılık bileşeninin sıfır olduğu varsayılmıştır. Bu varsayım, ideal bir süreç tasarımının doğal bir sonucudur. Kalite karakteristiklerinin n boyuttaki güven bölgesi elipsoit iken çok değişkenli kuadratik kalite kayıp fonksiyonunun maksimum değeri Monte Carlo Simülasyonu veya Levenberg – Marquardt Algoritması ile bulunabilir. Bu çalışmada Monte Carlo Simülasyonu için kısa bir algoritma verilmiştir. Ayrıca elipsoit güven bölgesinin sınırı üzerinde kalite kaybının koşullu beklenen değeri için matematiksel ifade verilmiştir ve kısa bir uygulama yapılmıştır.

#### 2. TEORİK ALTYAPI

Üretim odaklı geleneksel yaklaşımda kalite karakteristiği spesifikasyon limitleri içerisinde kaldığı sürece ürün eşit derecede iyi, bu limitlerin dışında ise eşit derecede kötüdür. Ancak tüketiciler açısından bu durum çoğunlukla doğru olmaz. Bu nedenle Taguchi kaliteye üretim sisteminin ötesinde bir anlam yüklemiştir. Ona göre kalite, ürün tamamlanıp nakliyata çıktıktan sonra toplumda oluşturduğu parasal kayıp ile ölçülür. Ayrıca kalite kaybını bu anlamın da ötesinde ürün ve süreç iyileştirmede kullanmıştır. Taguchi, parasal kalite kaybını ölçmek için sürekli kayıp fonksiyonları kullanır. Bu çalışmada olduğu gibi tam olarak istenen durumun olması istendiğinde bu fonksiyon kuadratiktir (Shilpa & Naidu, 2014). Taguchi yaklaşımının n kalite karakteristiği için genel hali olan (1) ve (2) eşitlikleri Pignatiello (1993)'te sunulmuştur. Bu çalışma boyunca kullanılan bu eşitliklerin, bir kısmı Wang vd. (2016)'da verilen birçok türevi mevcuttur.

Tek bir ürün ve n adet kalite karakteristiği için kuadratik kalite kayıp fonksiyonu aşağıdaki gibi tanımlanmıştır. Burada maliyet matrisi (C) pozitif tanımlıdır. Bu şart kalite kaybının istenen durum haricinde her zaman için pozitif olmasını sağlar.

$$L(x:\theta) = (x-\theta)^{T} C(x-\theta)$$
 (1)

Bu çalışmada kalite karakteristiklerinin n değişkenli dağılımının normal olduğu varsayılmıştır. Normal dağılım diğer birçok alanda olduğu gibi üretim yönetimi alanında da geniş bir kullanım alanına sahiptir.

Klasik yaklaşımda kalite kaybının (2)'de verilen koşulsuz beklenen değeri ile kalite analizi yapılır. Burada  $\mu$  ve  $\Sigma$  kalite karakteristiklerinin ilk iki momentini (sırasıyla ortalama vektörünü ve kovaryans matrisi) göstermektedir. "İz" fonksiyonu ise kare matrisin köşegeni üzerindeki elemanlarının toplamıdır. Görüldüğü üzere kalite kaybının iki unsuru sırasıyla yanlılık ve dağınıklıktır. Bu çalışmada varsayıldığı gibi beklenen durum, istenen duruma eşit yani  $\mu$ = $\theta$  iken ise yanlılık bileşeni sıfırdır. Bu varsayım, ideal bir süreç tasarımının doğal bir sonucudur.

$$E(L(x:\theta)) = \left[ (\mu - \theta)^T C(\mu - \theta) \right] + Iz(C\Sigma)$$
(2)

on Innovative Surveys in Positive Sciences 4-5 December 2022 / Full Text Book

#### 3. MATEMATİKSEL MODEL

Bu bölüm Studer & Lüthi (1996) ve Studer (1997) temel alınarak hazırlanmıştır. Normal dağılım ve standart normal dağılım arasındaki ilişki (3)'te verilmiştir. Burada U üst üçgen matris olmak üzere  $\sum = U^T U$ , pozitif tanımlı kovaryans matrisin Cholesky Ayrışımıdır.

$$y \square N(0,I) \Leftrightarrow \mu + U^{T} y = x \square N(\mu, \Sigma)$$
(3)

Buna göre orijinal koordinat sisteminde (1)'deki gibi olan çok değişkenli kuadratik kalite kayıp fonksiyonu, ortogonal koordinat sisteminde (4)'teki gibidir.

$$\hat{L}(y) = y^{T} \left( UCU^{T} \right) y \tag{4}$$

Bu yeni koordinat sisteminde y'nin belirlenen  $\alpha$  güven bölgesi (5)'teki gibidir. Burada P olasılık ölçüsü,  $\chi_{n,\alpha}^2$  ise n serbestlik dereceli ki kare dağılımının  $\alpha$  kantilidir.

$$P\left(y^{T} y \leq \chi_{n,\alpha}^{2}\right) = \alpha \tag{5}$$

Buna göre tek bir ürünün kalite kaybının  $\alpha$  güven düzeyinde maksimumu (6)'daki optimizasyon problemiyle bulunur. Burada "küçük eşit" yerine "eşit" ifadesinin kullanılmasının nedeni konveks fonksiyonlar için maksimum değerin güven bölgesinin sınırında olmasıdır. Bu bölge  $\mu$  merkezlidir ve 2 boyutta elips iken n boyutta elipsoittir.

Bu problem Studer (1997)'de verilen Levenberg-Marquardt algoritmasıyla nümerik olarak çözülebilir. Aşamaları aşağıda verilen Monte Carlo algoritmasıyla da bu çalışmada olduğu gibi yaklaşık bir çözüm elde edilebilir.

- 1. Standart normal dağılımda m adet rastgele vektör üretilir. Bunlar 2-normuna yani Öklid metriğinde bir vektörün orijine olan uzaklığına bölünerek standartlaştırılır. Bu vektörler her i için  $y_i$  ile gösterilsin.
- 2. Her *i* için  $\hat{L}\left(\sqrt{\chi_{n,\alpha}^2}y_i\right) = \chi_{n,\alpha}^2 \hat{L}(y_i)$  hesaplanır.
- 3. Üretilen  $\chi_{n,\alpha}^2 \hat{L}(y_i)$  değerlerinin içinden maksimumu seçilir.

Ayrıca  $\alpha$  güven bölgesinin sınırında kalite kaybının koşullu beklenen değeri (7)'deki gibidir.

$$E(\hat{L}(y)|y^{T}y = \chi_{n,\alpha}^{2}) = \frac{\chi_{n,\alpha}^{2}}{2n} \dot{I}z(UCU^{T})$$
(7)

#### 4. UYGULAMA

Kalite karakteristiklerinin ortalama vektörü ve pozitif tanımlı kovaryans matrisi ile birlikte pozitif tanımlı maliyet matrisi sırasıyla (8)'deki gibi olsun. Buna göre bunların arasındaki lineer ilişkiyi gösteren lineer korelasyon katsayısı 0.5'tir.

on Innovative Surveys in Positive Sciences

4-5 December 2022 / Full Text Book

$$\mu = \begin{vmatrix} 18 \\ 12 \end{vmatrix} \qquad \Sigma = \begin{vmatrix} 16 & 6 \\ 6 & 9 \end{vmatrix} \qquad C = \begin{vmatrix} 20 & 5 \\ 5 & 10 \end{vmatrix}$$
 (8)

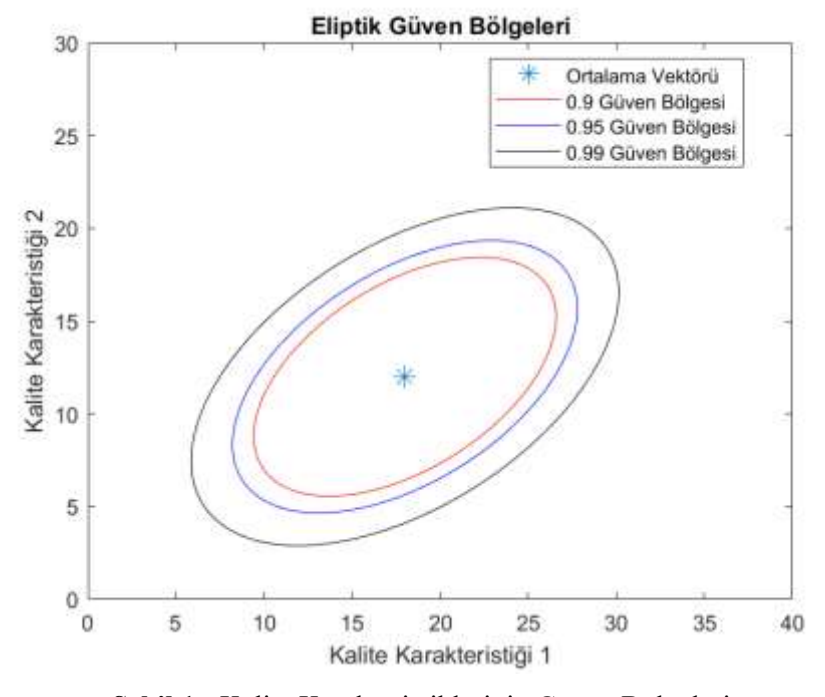
Buna göre çok değişkenli kuadratik kalite kayıp fonksiyonu (9)'daki gibi bulunur.

$$L(x:\theta=\mu) = 20(x_1 - 18)^2 + 10(x_1 - 18)(x_2 - 12) + 10(x_2 - 12)^2$$
(9)

Kalite kaybının dağınıklık bileşeninin koşulsuz beklenen değeri (10)'daki gibi bulunur.  $\mu = \theta$  varsayımı nedeniyle yanlılık bileşeni ise sıfırdır.

$$\dot{I}z(C\Sigma) = 470 \, TL \tag{10}$$

Kalite karakteristikleri için doğal alt ve üst sınırlar bulunabilir. Bu durum güven düzeyi belirlenirken dikkate alınmalıdır. Şekil 1, bu konuda bize fikir verebilir.

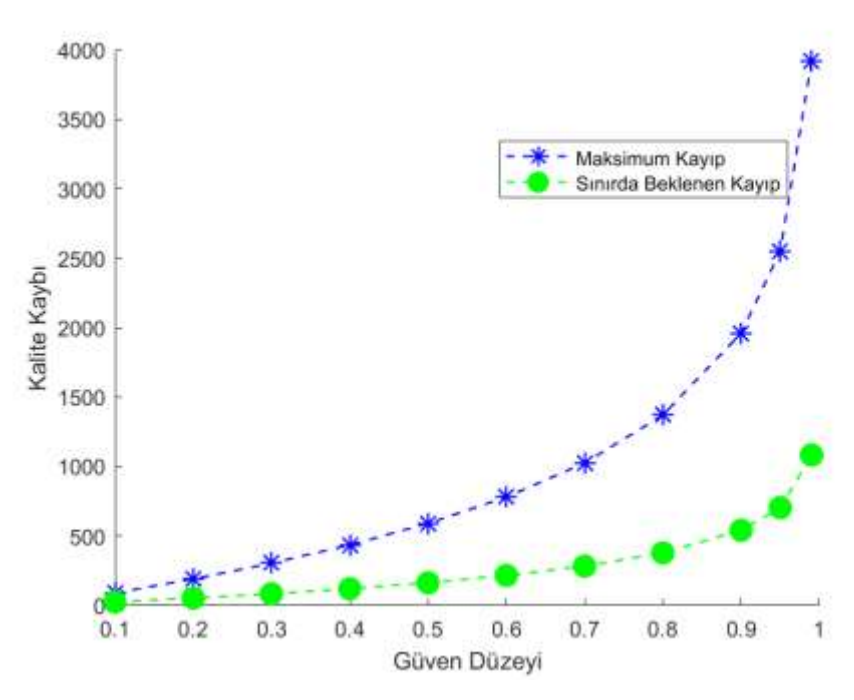


Şekil 1 : Kalite Karekteristiklerinin Güven Bölgeleri.

Güven düzeyi 0.1'den 0.99'a değişsin. Kalite kaybının dağınıklık bileşeninin maksimumu ve bu bölgenin sınırında koşullu beklenen değeri Şekil 2'de birlikte verilmiştir. Görüldüğü üzere güven düzeyi arttıkça maksimum kayıp ve bölgenin sınırında beklenen kayıp çok daha hızlı bir şekilde artmaktadır.

on Innovative Surveys in Positive Sciences

4-5 December 2022 / Full Text Book



Şekil 2 : Farklı Güven Düzeylerinde Kalite Kaybı (TL).

## 5. SONUÇ VE DEĞERLENDİRME

Her ne kadar yaygın kullanılan bir yaklaşım olsa da karar vermenin sadece beklenen değere dayalı olması, temeli itibariyle sorunludur. Bu nedenle bu çalışmada çok değişkenli normal dağılım varsayımı altında kalite kaybının dağınıklık bileşeni için iki farklı metrik önerilmiştir. Bunlardan birincisi elipsoit güven bölgesinin sınırında koşullu beklenen değer iken, diğeri bu bölgede maksimum kayıptır. Elde edilen sonuçlara göre güven düzeyi arttıkça koşullu beklenen değer ve maksimum kayıp çok daha hızlı artmaktadır. Ayrıca yüksek güven düzeyleri için bu değerler, kalite kaybının koşulsuz beklenen değerinden oldukça yüksektir. Dolayısıyla uç ama olası kalite kayıplarını incelemek için bu çalışmada önerilen bu iki metrik kullanılabilir.

#### **KAYNAKLAR**

Pignatiello Jr, J. J. (1993). Strategies for robust multiresponse quality engineering. *IIE transactions*, 25(3), 5-15.

Shilpa, M., & Naidu, N. V. R. (2014). Quantitative evaluation of quality loss for nominal-the-best quality characteristic. *Procedia Materials Science*, *5*, 2356-2362.

Studer, G. & Lüthi, (1996). *Quadratic maximum loss for risk measurement of portfolios*. Technical Report, ETH Zurich.

Studer, G. (1997). Maximum loss for measurement of market risk. PhD thesis, ETH Zurich.

Taguchi, G. (1986). *Introduction to quality engineering: Designing quality into products and processes*. Asian Productivity Organization.

Wang, J., Ma, Y., Ouyang, L., & Tu, Y. (2016). A new Bayesian approach to multi-response surface optimization integrating loss function with posterior probability. *European Journal of Operational Research*, 249(1), 231-237.

on Innovative Surveys in Positive Sciences 4-5 December 2022 / Full Text Book

### ARALIK DEĞERLİ ORTALAMA – VARYANS ANALİZİ: BİST 30 HOLDİNG HİSSELERİ ÜZERİNE BİR UYGULAMA

# INTERVAL VALUED MEAN – VARIANCE ANALYSIS: AN APPLICATION ON BIST 30 HOLDING STOCKS

#### Furkan Göktaş1

<sup>1</sup>Karabük Üniversitesi, İşletme Fakültesi, İşletme Bölümü, Karabük, Türkiye. <sup>1</sup>ORCID ID: 0000-0001-9291-3912

#### ÖZET

Markowitz'in ortalama - varyans (OV) modeli Portföy Yönetimi Teorisini derinden etkilemiştir. Örneğin, risk ve çeşitlendirme kavramları OV modelinin tanıtılmasından bu yana portföy seçiminin merkezinde olmuştur. Öte yandan parametrelerinin tahminindeki istatistiksel hatalar nedeniyle bu model uygulamada genellikle kullanılmaz. Ortalama vektörünün tahmini daha zordur ve bu nedenle daha önemli bir sorundur. Dayanıklı OV modelleri bu sorunu ortadan kaldırmak için kullanılabilir. Öte yandan bu modeller en kötü durum odaklı olduğundan genellikle tutucu yatırımcılar ve finansal kurumlar için uygundur. Bu nedenle bu çalışmada portföyde kısa pozisyon ve risksiz varlık bulunabildiği varsayımları altında aralık değerli OV analizi yapılmıştır. Burada Temel Bileşenler Analizinden yararlanılmıştır ve temel bileşenler için aralık değerli optimal çözüm elde edilmiştir. Bu çözümlerden hangisinin seçileceği yatırımcılara bırakılmıştır. OV modeli bu analizde, klasik yaklaşımda portföy seçimine karşı gelmektedir. Dayanıklı OV modeli ise kötümser yaklaşımda portföy seçimine karşı gelmektedir. Bununla birlikte iyimser yaklaşımda portföy seçimi tanımlanmıştır. Ayrıca gelecekteki getirilere bağlı olarak en iyi ve en kötü portföy seçimleri için matematiksel ifadeler elde edilmiştir. Teorik altyapı oluşturulduktan sonra, 2016 (2017) yılı eğitim (test) periyotu olmak üzere BİST 30 holding hisselerinin gerçek veri seti kullanılarak bir uygulama yapılmıştır. Yapılan uygulamada iyimser (kötümser) yaklaşımın klasik yaklaşıma göre daha iyi (daha kötü) sonuçlar verdiği görülmüştür. Ayrıca iyimser (kötümser) yaklaşımdan daha iyi (daha kötü) sonuçlar da vardır. Dolayısıyla aralık değerli OV analizi, yatırımcılara esneklik sağlar ve doğru ellerde değerli bir araç olabilir.

**Anahtar Kelimeler:** Portföy Seçimi, Ortalama – Varyans Modeli, Parametre Belirsizliği, Temel Bileşenler Analizi, Uzman Bilgisi.

#### **ABSTRACT**

The mean – variance (MV) model has had a profound influence on the Portfolio Management Theory. For example, the concepts of risk and diversification have been in the centre of the portfolio selection since the MV model was introduced. On the other hand, it is not generally used in practice due to the statistical errors in the estimation of its parameters. The mean vector's estimation is harder and thus a more important problem. Robust MV models can be used to overcome this problem. On the other hand, they are generally suitable for the financial institutions or the conservative investors due to the worstcase orientation. Thus, in this study, we perform an interval valued MV analysis under the assumption that short positioning and risk-free asset are allowed in the portfolio. Here, we use Principal Components Analysis and derive interval valued optimal solutions for the principal components. It is left to investors to selection which of these solutions. In this analysis, MV model corresponds to the portfolio selection in the classical approach. The robust MV model corresponds to the portfolio selection in the pessimistic approach. In addition, we define the portfolio selection in the optimistic approach. Furthermore, we obtain mathematical expressions for the best and worst portfolio selection based on the future returns. After laying down the theoretical background, we make an application by using the real data set of BIST 30 holding stocks where the year 2016 (2017) is the training (testing) period. In our application, we observe that the optimistic (pessimistic) approach gives better (worse) results than the classical approach. In addition, there are better (worse) results than the optimistic (pessimistic)

on Innovative Surveys in Positive Sciences 4-5 December 2022 / Full Text Book

approach. Thus, the interval valued MV analysis gives investors flexibility and may be a valuable tool in the right hands.

**Key Words:** Portfolio Selection, Mean – Variance Model, Parameter Uncertainty, Principal Components Analysis, Expert Knowledge.

### 1. GİRİŞ

Markowitz (1952)'de tanıtılan OV modeli Portföy Yönetimi Teorisini derinden etkilemiştir. Öte yandan parametrelerinin tahminindeki istatistiksel hatalar nedeniyle bu model uygulamada genellikle kullanılmaz (Goldfarb & Iyengar, 2003). Ortalama vektörünün tahmini daha zordur ve bu nedenle daha önemli bir sorundur (Garlappi vd., 2006). Dayanıklı OV modelleri bu sorunu ortadan kaldırmak için kullanılabilir. Öte yandan bu modeller en kötü durum odaklı olduğundan genellikle tutucu yatırımcılar ve finansal kurumlar için uygundur (Tütüncü & Koenig, 2004). Bu nedenle bu çalışmada portföyde kısa pozisyon ve risksiz varlık bulunabildiği varsayımları altında aralık değerli OV analizi yapılmıştır. Burada Temel Bileşenler Analizinden yararlanılmıştır ve temel bileşenler için aralık değerli optimal çözüm elde edilmiştir. Ayrıca gelecekteki getirilere bağlı olarak en iyi ve en kötü portföy seçimleri için matematiksel ifadeler elde edilmiştir. Bununla birlikte 2016 (2017) yılı eğitim (test) periyotu olmak üzere BİST 30 holding hisselerinin gerçek veri seti kullanılarak bir uygulama yapılmıştır.

#### 2. TEORİK ALTYAPI

Bu çalışmada varlıkların logaritmik getirilerinin rastgele vektörü (r) ile bunun ortalaması  $\mu$  ile kovaryans matrisi  $\Sigma$  ile gösterilmiştir. Ayrıca kovaryans matrisin yansız tahmincisine eşit olduğu varsayılmıştır. Kovaryans matrisin Temel Bileşenler Analizi,  $\Lambda$  köşegensel elemanları kovaryans matrisin özdeğerleri olan köşegen matris ve V ortogonal özvektör matrisi iken aşağıdaki gibidir. V matrisinin i. sütunu i. özdeğere karşı gelen ortonormal özvektördür ve x temel bileşen vektörüdür (Johnson & Wichern, 2007). Bu çalışmada özdeğerlerin ayrık olduğu varsayılmıştır.

$$\Sigma = V \Lambda V^T \mapsto x := V^T r \tag{1}$$

Buna göre ortogonal koordinat sisteminde lineerleştirilmiş kar fonksiyonu aşağıdaki gibidir. Burada *w* portföydeki varlıkların ağırlık vektörüdür.

$$f(x) = \tilde{w}^T x = (V^T w)^T x = w^T (Vx) = w^T r = p(r)$$
(2)

i. temel bileşenin ortalamasının c güven aralığı aşağıdaki gibidir (Johnson & Wichern, 2007). Burada  $z_c$ , standart normal dağılımın c kantilidir ve her bir varlık için getiri verisi sayısı m ile gösterilmiştir.

$$\delta_{i} := \frac{z_{(1+c)/2}}{\sqrt{m}} \sqrt{\Lambda_{i,i}}, \forall i$$

$$U = \left\{ \mu_{x} \mid \mu_{x,i}^{L} := \widehat{\mu}_{x,i} - \delta_{i} \le \mu_{x,i} \le \mu_{x,i}^{U} := \widehat{\mu}_{x,i} + \delta_{i}, \forall i \right\}$$
(3)

Göktaş & Duran (2020)'de tanıtılan dayanıklı OV modelinde i. temel bileşenin optimal ağırlığı aşağıdaki gibi bulunur. Burada sgn işaret fonksiyonudur ve  $\eta$  nonnegatif riskten kaçınma katsayısıdır.  $w_p^*(\eta,c) = V \tilde{w}_p^*(\eta,c)$  eşitliği ile riskli varlıkların optimal ağırlıkları bulunur. Risksiz varlığın ağırlığı ise riskli varlıkların ağırlıkları toplamını 1'e tamamlar.

on Innovative Surveys in Positive Sciences

4-5 December 2022 / Full Text Book

$$\widetilde{w}_{P,i}^{*}(\eta,c) = \begin{cases}
\frac{\mu_{x,i}^{L}}{\eta \Lambda_{i,i}}, \operatorname{sgn}(\mu_{x,i}^{L}) = \operatorname{sgn}(\mu_{x,i}^{U}) = 1 \\
\frac{\mu_{x,i}^{U}}{\eta \Lambda_{i,i}}, \operatorname{sgn}(\mu_{x,i}^{L}) = \operatorname{sgn}(\mu_{x,i}^{U}) = -1 \\
0, \operatorname{sgn}(\mu_{x,i}^{L}, \mu_{x,i}^{U}) \leq 0
\end{cases}$$
(4)

Markowitz'in OV modelinde ise genellikle parametreler için yansız tahminciler kullanılarak aşağıdaki çözüm elde edilir. *c*=0 iken (4) ve (5) özdeş sonuç verir (Göktaş & Duran, 2020).

$$w_M^* = \frac{\sum^{-1} \mu}{n}$$
 (5)

#### 3. MATEMATİKSEL MODEL

(4), Maks-Min probleminin sonucudur ve kötümser yaklaşıma dayanır. Bu çalışmada iyimser yaklaşım aşağıdaki Maks-Maks problemi ile tanımlanmıştır. Burada temel bileşenlerin ortalama vektörü için kutu tipi belirsizlik kümesi (U) (3)'teki gibidir.

$$\max_{\tilde{w} \in \mathbb{D}^{n}} \max_{\mu_{x} \in U} \tilde{w}^{T} \mu_{x} - 0.5 \eta \left( \tilde{w}^{T} \Lambda \tilde{w} \right)$$
 (6)

(6) için *i*. temel bileşenin optimal ağırlığı aşağıdaki gibi bulunur.  $w_O^*\left(\eta,c\right) = V\tilde{w}_O^*\left(\eta,c\right)$  eşitliği ile riskli varlıkların optimal ağırlıkları bulunur.

$$\tilde{w}_{O,i}^* \left( \eta, c \right) = \frac{\hat{\mu}_{x,i}}{\eta \Lambda_{i,i}} + \operatorname{sgn}\left( \hat{\mu}_{x,i} \right) \frac{z_{(1+c)/2}}{\eta \sqrt{m \Lambda_{i,i}}} \tag{7}$$

Kötümser yaklaşımda, eğer istatistiksel olarak anlamlı bir ortalama yoksa ilgili temel bileşende pozisyon alınmaz. Ayrıca istatistiksel olarak anlamlı ortalama olsa bile parametre belirsizliği nedeniyle alınacak pozisyon 0'a yaklaştırılır. İyimser yaklaşımda ise parametre belirsizliği nedeniyle alınacak pozisyon mutlak değerce büyütülür. Başka bir deyişle kötümser yaklaşımda, iyimser yaklaşıma göre daha yüksek oranda risksiz varlığın portföyde bulunması beklenir.

Aralık değerli OV analizinde *i.* temel bileşenin ortalaması ağırlık değerli olduğundan *i.* temel bileşenin optimal ağırlığı da aralık değerlidir.

$$\tilde{w}_{i}^{*}\left(\eta,c\right) \in \left[\frac{\hat{\mu}_{x,i}}{\eta \Lambda_{i,i}} - \frac{z_{(1+c)/2}}{\eta \sqrt{m\Lambda_{i,i}}}, \frac{\hat{\mu}_{x,i}}{\eta \Lambda_{i,i}} + \frac{z_{(1+c)/2}}{\eta \sqrt{m\Lambda_{i,i}}}\right]$$

$$\tag{8}$$

(8) sonsuz farklı çözüm verdiğinden buradan hangi çözümün seçileceği yatırımcının kararıdır. Bu kararın alınmasında istatistik, temel analiz, uzman bilgisi gibi unsurlardan yararlanabilir. Yapılabilecek en iyi ve en kötü seçim ise sırasıyla aşağıda verilmiştir. Burada i. temel bileşenin gelecekteki getirisi  $q_i$  ile gösterilmiştir. Görüldüğü üzere aralık değerli OV analizinde iyi sonuç alabilmek için kilit unsur, temel bileşenlerin gelecekteki yönünü doğru öngörmektedir.

on Innovative Surveys in Positive Sciences

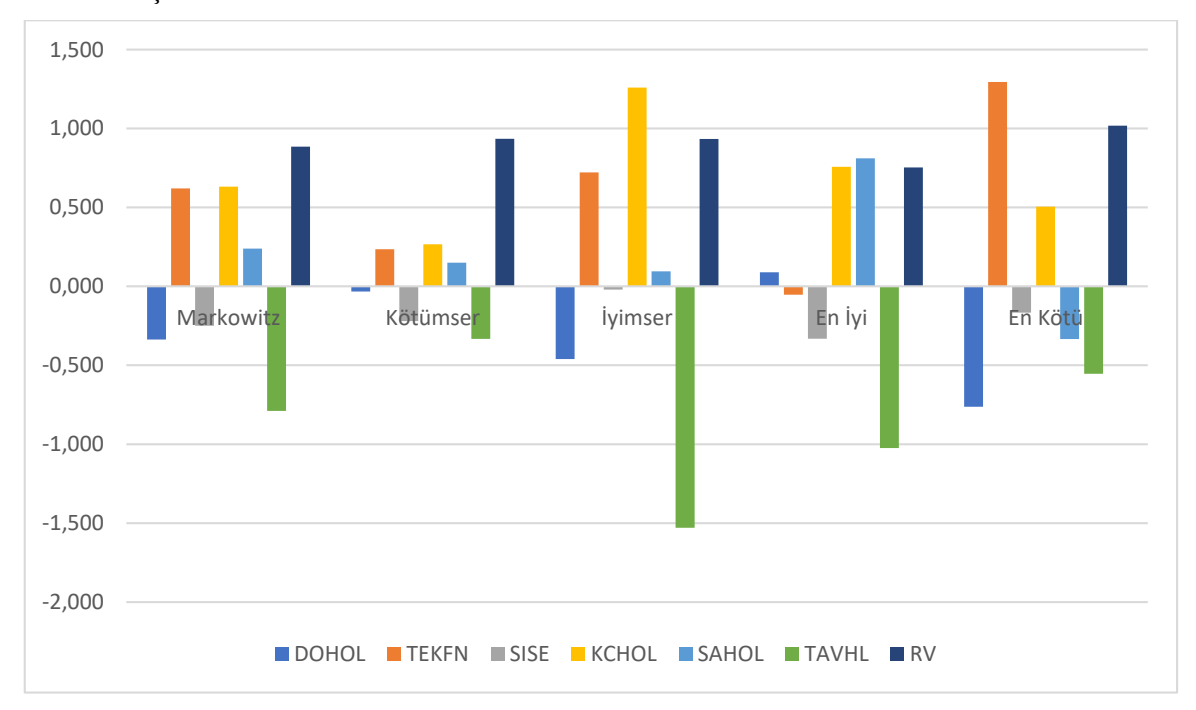
4-5 December 2022 / Full Text Book

$$MS_{i} = \frac{\widehat{\mu}_{x,i}}{\eta \Lambda_{i,i}} + \operatorname{sgn}(q_{i}) \frac{z_{(1+c)/2}}{\eta \sqrt{m\Lambda_{i,i}}}$$

$$LS_{i} = \frac{\widehat{\mu}_{x,i}}{\eta \widehat{\Lambda}_{i,i}} - \operatorname{sgn}(q_{i}) \frac{z_{(1+r)/2}}{\eta \sqrt{m\Lambda_{i,i}}}$$
(9)

#### 4. UYGULAMA

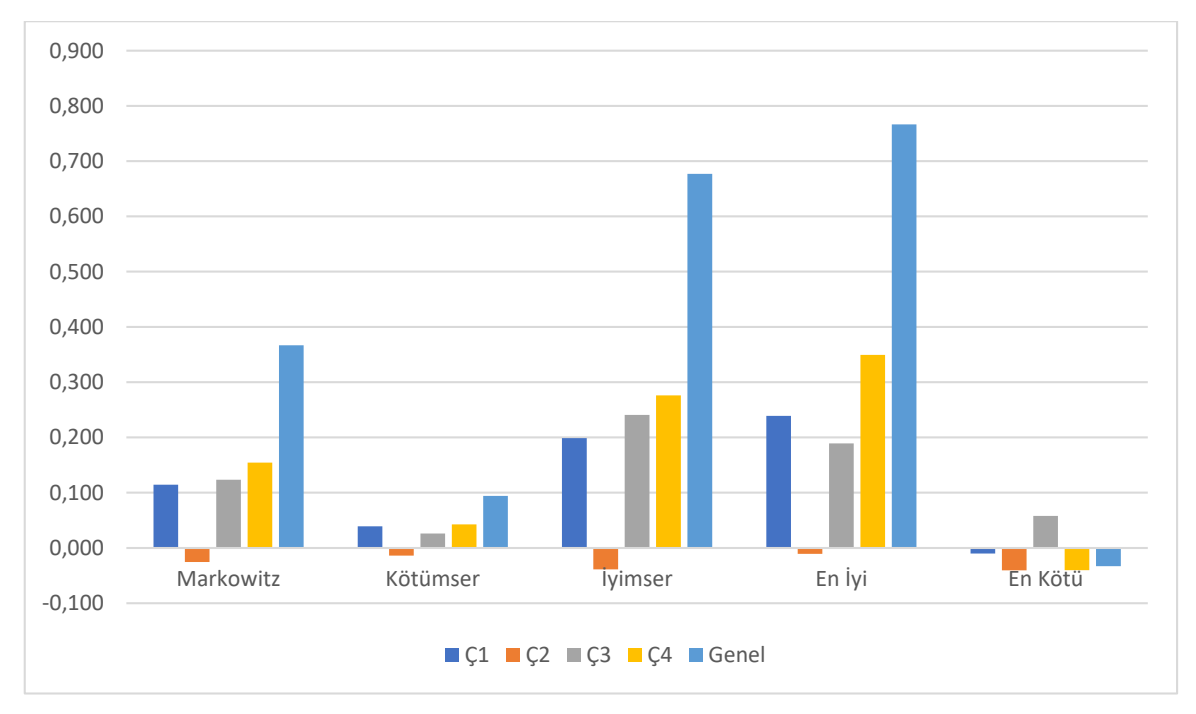
BİST 30'daki altı holding hissesi DOHOL, TEKFN, SISE, KCHOL, SAHOL ve TAVHL ile gösterilmektedir. Yapılan uygulamada bu hisselerin 2016 yılındaki, risksiz faiz oranı üzerindeki haftalık logaritmik getirileri kullanılarak optimal portföyler Şekil 1'deki gibi oluşturulmuştur. Bu çalışmada yıllık risksiz faiz oranı, Bloomberg verisine göre 0.1063 olarak alınmıştır. Ayrıca  $\eta$ =14.3890 ve c=0.8 olarak alınmıştır.



Şekil 1: Optimal vektörler.

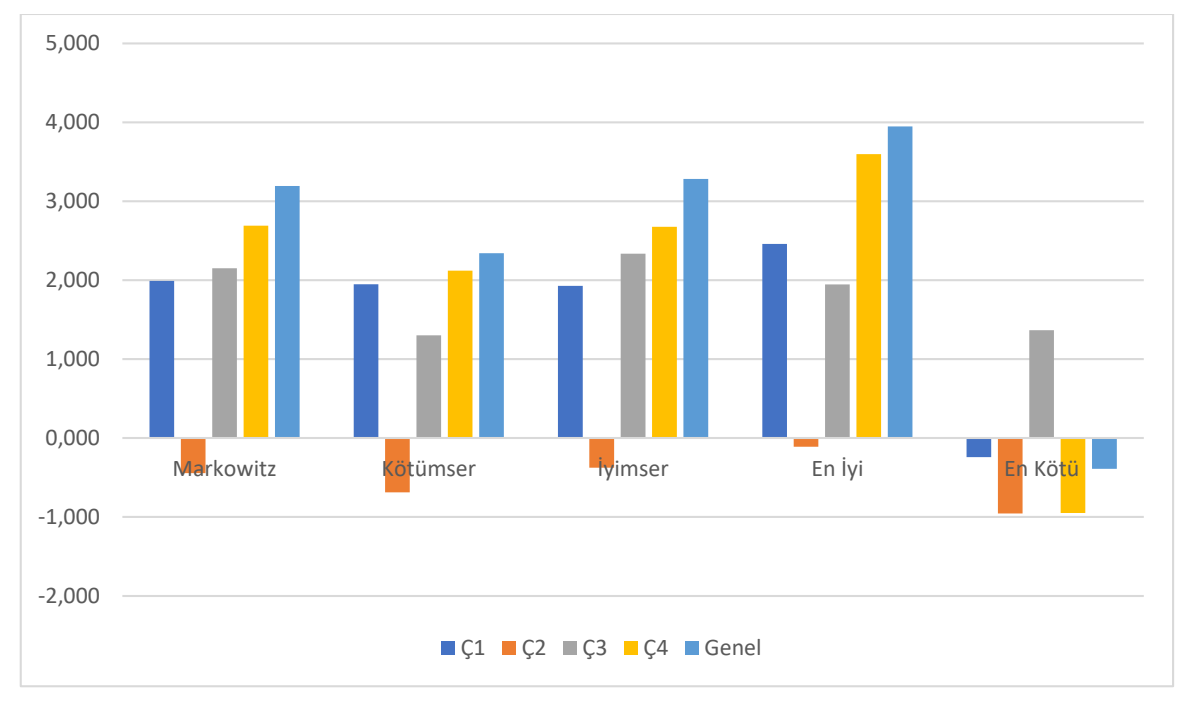
Optimal portföylerin 2017 yılında (risksiz faiz oranı üzerindeki) çeyreklik ve genel getirileri Şekil 2'de verilmiştir.

on Innovative Surveys in Positive Sciences 4-5 December 2022 / Full Text Book



Şekil 2 : Portföy getirileri.

Optimal portföylerin 2017 yılında çeyreklik ve genel Sharpe oranları Şekil 3'te verilmiştir. Negatif Sharpe oranı, risksiz faiz oranı altında getiri elde edildiğini göstermektedir ve finansal olarak anlamlı değildir. 2. çeyrekte portföylerin risksiz varlığa yenildiği görülmektedir. Aralık değerli OV analizinde en kötü seçim yapılması durumunda ise sadece 3. çeyrekte aralık değerli OV analizinin risksiz varlığı yendiği görülmektedir.



Şekil 3: Sharpe oranları.

Portföylerin 2017 yılında (risksiz faiz oranı) üzerindeki getirileri ve Sharpe oranları Tablo 1'de verilmiştir. Görüldüğü üzere iyimser (kötümser) yaklaşım Markowitz'in klasik yaklaşımına göre daha iyi sonuçlar vermiştir. Ayrıca iyimser (kötümser) yaklaşımdan daha iyi (daha kötü) sonuçlar da vardır.

on Innovative Surveys in Positive Sciences

4-5 December 2022 / Full Text Book

	Markowitz	Kötümser	İyimser	En İyi	En Kötü
Getiri	0.367	0.094	0.677	0.767	-0.033
Sharpe O.	3.193	2.341	3.282	3.947	-0.390

Tablo 1: Genel sonuçlar.

## 5. SONUÇ VE DEĞERLENDİRME

Markowitz'in OV modelinin ve dayanıklı OV modellerinin kendilerine has sorunları vardır. Bu nedenle bu çalışmada portföyde kısa pozisyon ve risksiz varlık bulunabildiği varsayımları altında aralık değerli OV analizi yapılmıştır. Aralık değerli OV analizinde sonsuz farklı optimal çözüm elde edilir. Bu çözümlerden hangisinin seçileceği yatırımcılara bırakılır. Yatırımcılar bu seçimde istatistik, temel analiz, uzman bilgisi gibi unsurlardan yararlanabilir. Bu çalışmada literatürdeki kötümser ve klasik yaklaşıma ek olarak, iyimser yaklaşım tanımlanmıştır. Ayrıca gelecekteki getirilere bağlı olarak en iyi ve en kötü portföy seçimleri tanımlanarak aralık değerli OV analizinin sınırları çizilmiştir. Bununla birlikte 2016 (2017) yılı eğitim (test) periyotu olmak üzere BİST 30 holding hisselerinin gerçek veri seti kullanılarak bir uygulama yapılmıştır. Bu uygulamada, Sharpe oranıyla ölçülen performans bazında farklar az olsa da iyimser (kötümser) yaklaşımın klasik yaklaşıma göre daha iyi (daha kötü) sonuçlar verdiği görülmüştür. Ayrıca iyimser (kötümser) yaklaşımdan daha iyi (daha kötü) sonuçlar da vardır. Dolayısıyla aralık değerli OV analizi, yatırımcılara esneklik sağlar ve doğru ellerde değerli bir araç olabilir.

#### **KAYNAKLAR**

Garlappi, L., Uppal, R. & Wang, T. (2006). Portfolio selection with parameter and model uncertainty: A multi-prior approach. *The Review of Financial Studies*, 20(1), 41–81.

Goldfarb, D., & Iyengar, G. (2003). Robust portfolio selection problems. *Mathematics of Operations Research*, 28(1), 1-38.

Göktaş, F. & Duran, A. (2020). New robust portfolio selection models based on the principal components Analysis. *Journal of Multiple Valued Logic & Soft Computing*, 34(1-2), 43-58.

Johnson, R. A. & Wichern, D. (2007). Applied Multivariate Statistical Analysis. Pearson Prentice Hall.

Markowitz, H. (1952). Portfolio selection. The Journal of Finance, 7(1), 77-91.

Tütüncü, R. H. & Koenig, M. (2004). Robust asset allocation. *Annals of Operations Research*, 132(1-4), 157-187.

on Innovative Surveys in Positive Sciences 4-5 December 2022 / Full Text Book

# RADİKÜLER KİSTLERDE EPİDERMAL BÜYÜME FAKTÖRÜ EKSPRESYONUNUN DEĞERLENDİRİLMESİ

# EVALUATION OF EPIDERMAL GROWTH FACTOR EXPRESSION IN RADICULAR CYSTS

## Dr. Öğr. Üyesi Fatih TAŞ

<sup>1</sup>Department of Histology and Embryology, Medical Faculty, Siirt University, Siirt, Turkey ORCID ID 0000-0001-9817-4241

Araş. Gör. Fırat AŞIR

<sup>2</sup>Department of Histology and Embryology, Medical Faculty, Dicle University, Diyarbakır, Turkey ORCID ID: 0000-0002-6384-9146

## Dok. Öğr. Fikri ERDEMCİ

<sup>2</sup>Department of Histology and Embryology, Medical Faculty, Dicle University, Diyarbakır, Turkey ORCID ID: 0000-0001-8083-0183

#### ÖZET

Giriş: Çenede görülen ve köken aldığı dokular dişlerle alakalı olan kist ve tümörlere, odontojenik kist veya odontojenik tümör adı verilir. Odontojenik kistler, kendi içerisinde gelişimsel ve inftamatuar odontojenik kistler olarak sınıflandırılmaktadır. Bunlardan gelişimsel odontojenik kistler; dentigeröz, keratokist, lateral periodontal ve glandüler kistler olarak sınıflandırılır. İnflamatuar odontojenik kistler ise; radiküler, paradental ve rezidüel kistler şeklinde sınıflandırılır. Çenede en çok görülen ve diş köklerinin ucunda meydana gelen inflamatuar odontojenik kistlerden bir tanesi radiküler kistlerdir. Çalışmamızda, patolojik inceleme için alınmış inflamatuar odontojenik kistlerden radiküler kistlerin immunohistokimyasal (EGF primer antikoru) olarak incelenmesi amaçlandı.

**Materyal ve Metot:** Çalışmamızda daha önce patolojik inceleme için alınmış olan inflamatuar kistlerden radiküler kistler, immunohistokimyasal inceleme için alındı. Alınan bu dokulardan elde edilen kesitler, EGF primer antikoru ile boyandı ve ışık mikroskobu altında değerlendirildi.

**Bulgular:** Çalışmamızda, radiküler kistler immunohistokimyasal olarak değerlendirildi. Epitel tabakasının yüzeyindeki hücrelerde ve bazal hücrelerde yoğun bir şekilde EGF ekspreyonu izlendi. Ayrıca damar endotelinde ve epitel tabakasının altında bulunan submukozada da yer yer EGF ekspresyonu izlendi.

**Tartışma:** Epidermal Büyüme Faktörü (EGF), EGFR'nin ana ligandlarından biridir. EGF; bağlanma, otofosforilasyon ve mitojenik sinyallerin transdüksiyonuyla sonuçlanan reseptör dimerizasyonunu indüklemektedir. EGF, gastrointestinal sisteminde dahil olduğu birçok sistemde DNA sentezi ve hücrelerin büyümesini uyaran peptitlerden bir tanesidir. Çalışmamızda, EGF eskpreyonunun yoğun olması, kistik yapılarda epitelizasyonun yüksek olduğunu ve gingival dokunun rejenerasyonu için bir marker olarak kullanılabileceğini düşündürmektedir.

Anahtar Kelimeler: Odontojenik Kist, Radiküler Kist, EGF, İmmunohistokimya

#### **ABSTRACT**

**Introduction:** Cysts and tumors that appear in the jaw and are related to the teeth, are called odontogenic cysts or odontogenic tumors. Odontogenic cysts are classified as developmental and inflammatory odontogenic cysts. Of these, developmental odontogenic cysts; are classified as dentigerous, keratocyst, lateral periodontal, and glandular cysts. Inflammatory odontogenic cysts; are classified as radicular,

on Innovative Surveys in Positive Sciences 4-5 December 2022 / Full Text Book

paradental, and residual cysts. Radicular cysts are one of the most common inflammatory odontogenic cysts that occur at the tip of the tooth roots. Our study aimed to examine radicular cysts from inflammatory odontogenic cysts taken for pathological examination by immunohistochemistry (EGF primary antibody).

**Materials and Methods:** In our study, radicular cysts, which were previously taken for pathological examination, were taken for immunohistochemical examination. Sections obtained from these tissues were stained with EGF primary antibody and evaluated under a light microscope.

**Results:** In our study, radicular cysts were evaluated immunohistochemically. Intense EGF expression was observed in cells on the surface of the epithelial layer and basal cells. In addition, EGF expression was also observed in the vascular endothelium and in the submucosa under the epithelial layer.

**Discussion:** Epidermal Growth Factor (EGF) is one of the main ligands of EGFR. The functions of EGF include binding, autophosphorylation, and receptor dimerization resulting in transduction of mitogenic signals. EGF is one of the peptides that stimulate DNA synthesis and growth of cells in many systems including the gastrointestinal tract. In our study, the intense expression of EGF suggests that epithelialization is high in cystic structures and can be used as a marker for regeneration of gingival tissue.

Keywords: Odontogenic Cyst, Radicular Cyst, EGF, Immunohistochemistry

## **GİRİŞ**

Çenelerde görülen ve köken aldığı dokular dişlerle alakalı olan kistlerle tümörler, odontojenik kist veya odontojenik tümör olarak isimlendirilmektedir. Kökenini epitelin kalıntılarından alan bu kistik yapılar, gömülü olan veya çürümüş olan dişlerle ya da kök kalıntılarıyla birlikte görülebilmektedirler. Ayrıca inflamasyonun, yaşın, oluşan mekanik travmaların, sistemik rahatsızlıkların ya da söz konusu bölgede damar oluşumunun artmasının epitelin oluşumunu tetiklediği ve bu sayede kistik yapıların ortaya çıkmasına sebebiyet verdiği düşünülmektedir (1).

Odontojenik kistler, kendi içerisinde gelişimsel ve inftamatuar odontojenik kistler olmak üzere sınıflandırılır. Bunlardan gelişimsel odontojenik kistler kendi içerisinde dentigeröz, keratokist, lateral periodontal ve glandüler kistler olarak sınıflandırılabilirken; inflamatuar odontojenik kistler de radiküler, paradental ve rezidüel kistler şeklinde sınıflandırılmaktadır (2). İnflamasyon gelişiminin bir sonucu olarak inflamatuar kistler oluşabilmektedir. Bununla birlikte gelişimsel kistlerin ortaya çıkmasına neden olan etmenler tam anlamıyla ortaya konulamamıştır. Gelişimsel kistler, ağız mukozasının epiteli ile çenede proliferasyonun oluşumunu sağlayan epitelden (Malassez epitelyum artıklarından) gelişebilmektedirler (3).

Yapılan araştırmalar en sık görülen kistlerin radiküler kistler olduğunu daha sonra ise dentigeröz kistlerin görüldüğünü ortaya koymuştur (4). Diş çürüklerinden ya da travmalara bağlı olarak devatilize bir pulpaya sahip, genel olarak dişlerin köklerinin ucundan meydana gelen inflamatuar odontojenik kistlerden bir tanesi radiküler kistlerdir (5). Bununla birlikte literatürde yapılan incelemede rezidüel kistlerin, lateral periodontal kistlerin, sürme kistlerinin ve nasopalatin kanal kistlerinin görülme oranında değişiklikler olduğu ortaya konulmuştur (4).

Epidermal büyüme faktörü reseptörü (EGFR), hücre dışı bir ligand bağlama alanı, aynı zamanda hücre içi tirozin kinaz alanı olan transmembran glikoproteinlerinden bir tanesidir. Ligandların bağlanması, EGFR dimerizasyonuyla birlikte otofosforilasyonu indükler ve böylece mitojenik sinyal transdüksiyonuna sebebiyet verir. Dokularda aşırı EGFR ekspresyonu, kötü prognoz ile ilişkilendirilmektedir. Ayrıca EGFR ekspresyon yüksekliği, bazı epitelyal kanserlerde malign transformasyonun oluşması ile de alakalıdır (6). Epidermal büyüme faktörü (EGF), EGFR'nin temel ligandlarından bir tanesidir. EGF'nin bağlanmasıyla birlikte, otofosforilasyon ve mitojenik sinyallerin transdüksiyonuyla sonuçlanan reseptör dimerizasyonu indüklenir (7). Epidermal büyüme faktörü ile Transforming büyüme faktörü (TGF-α), birbirleri ile yapısal olarak ilişkili olan ve gastrointestinal sistemin de dahil olduğu birçok sistemde, DNA'nın sentezini ve hücrelerin büyümelerini tetikleyen

on Innovative Surveys in Positive Sciences 4-5 December 2022 / Full Text Book

peptitlerdir (8). EGF hem normal hem de neoplastik hücrelerin proliferasyonunu gerek in vitro gerekse de in vivo olarak düzenleyebilen mitojenik bir hormondur (9).

Çalışmamızda, patolojik inceleme için alınmış inflamatuar odontojenik kistlerden radiküler kistlerin immunohistokimyasal (EGF primer antikoru) olarak incelenmesi amaçlanmıştır.

#### MATERYAL VE METOT

Daha önce patolojik inceleme için alınmış olan inflamatuar kistlerden radiküler kistler, EGF primer antikoru kullanılarak, immunohistokimyasal yöntemle değerlendirildi.

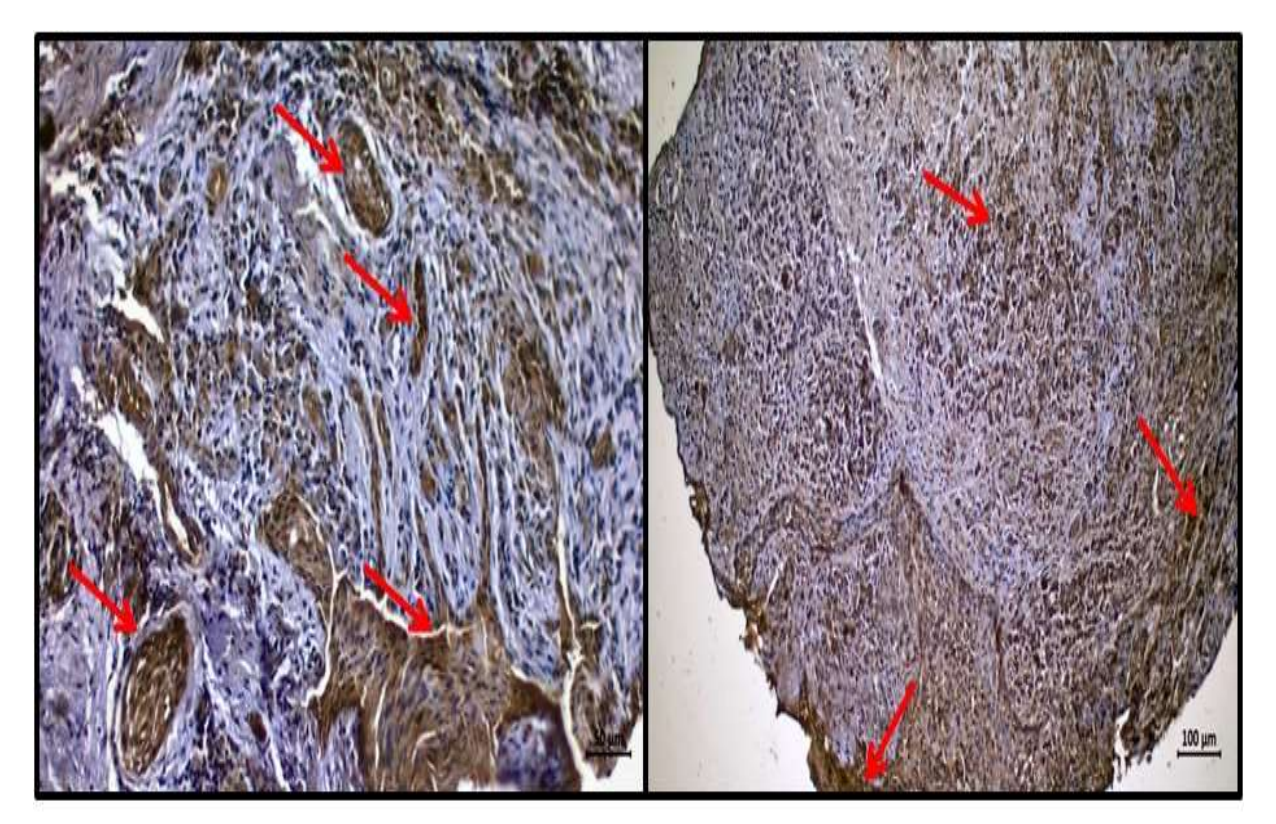
### İmmunohistokimyasal Boyama

Patolojik inceleme için alınmış olan dokulardan 4-6 µm kalınlığında kesitler alındıktan sonra 2x15 dakika süresince ksilolün içerisinde bekletildi. Ardından kesitler 8, 6 ve 4 'er dakika boyunca artan alkol dizilerinden geçirildi. Kesitler bir süre distile suyun içerisinde bekletilmelerinin ardından antijen retrevial işleminin yapılabilmesi için yaklaşık 3 dakika kadar EDTA solüsyonunun içerisine alınarak mikrodalga fırınının içerisinde bekletildi. Ardından kesitler mikrodalgadan alındı ve soğumaları için yaklaşık 15 dakika boyunca oda sıcaklığında bekletildi. 15 dakikanın ardından kesitler yeniden distile suya alındı. Daha sonra kesitler kurutularak üzerleri hidrofobik kalemle çizildi. Kesitler üzerleri cizildikten sonra immunohistokimya kutusuna alındı ve üzerlerine 3x5 dakika süresince Phosphate BufferSaline (PBS) eklendi. İmmunohistokimya kutusunun bu işlemler esnasında nemli olması gerektiğinden kutunun içerisinde daha önce hazırlanmış olan sıcak su kondu. Kesitlerin üzerinde bulunan PBS alındıktan sonra üzerlerine Hidrojen peroksit solüsyonu damlatıldı ve 20 dakika boyunca beklendi. Ardından EGF primer antikoru daha önce sınırları hidrofobik kalemle çizilmiş olan kesitlerin üzerlerine damlatıldı. Daha sonra bu kesitler +4°C'de bir gece boyunca overnight edildi. Bir sonraki gün 3x5 dakika boyunca kesitler PBS ile yıkandı, ardından biotinylated sekonder antikor damlatılarak 14 dakika boyunca bekletildi. Kesitler PBS yardımıyla 3x5 dakika boyunca yıkandı. Daha sonra kesitlere Streptavidin- peroxidase damlatıldı ve 15 dakika boyunca beklendi. PBS ile kesitler 3x5 dakika boyunca yıkandı. Bu işlemin ardından daha önce sınırları belirlenmiş olan kesitlerin üzerlerine DAB damlatılarak ortalama 10 ile 15 dakika boyunca beklendi. 3x5 dakika boyunca kesitler PBS ile yıkandı. Kesitlere Mayer hematoksilen ile yaklaşık 45 saniye zıt boyama uygulandıktan sonra, çeşme suyunun altında yaklaşık 5 dakika boyunca yıkandı. Yıkama işleminin ardından artan alkol serilerinden hızla gecirilen kesitler ksilolün icerisinde 2x15 dakika olacak sekilde bekletilerek entellan ile üzerleri kapatıldı. Preparatlar mikroskop altında incelenerek, değerlendirildi.

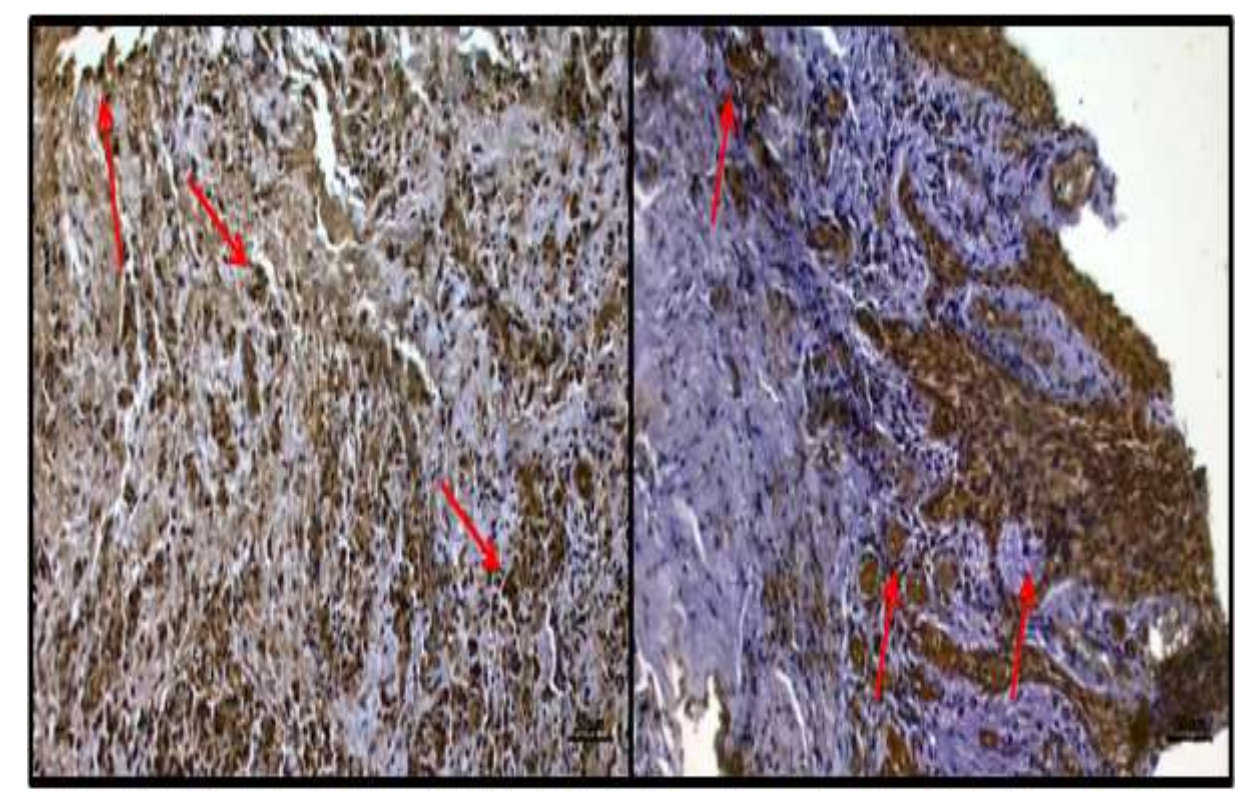
#### **BULGULAR**

Odontojenik kistlerde, epitel tabakasının yüzeyindeki hücrelerde ve bazal hücrelerde yoğun bir EGF ekspreyonu izlendi. EGF ekspreyonu, damar endotelinde ve epitelin altında bulunan submukozada da yer yer izlendi. EGF eskpreyonunun yoğun olması kistik yapılarda epitelizasyonun yüksek olduğu ve gingival dokunun rejenerasyonu için bir marker olarak kullanılabileceği şeklinde değerlendirildi (Şekil 1 ve 2).

on Innovative Surveys in Positive Sciences 4-5 December 2022 / Full Text Book



Şekil 1. Epitel yüzeyinde, bazal hücrelerde ve damar entotelinde yoğun EGF ekspresyonu



Şekil 2. Epitel yüzeyinde, bazal hücrelerde ve submukozada yoğun EGF ekspresyonu

## **TARTIŞMA**

Çalışmamızda, radiküler kistler immunohistokimyasal olarak değerlendirildi ve epitel tabakasının yüzeyindeki hücrelerde ve bazal hücrelerde yoğun bir şekilde EGF ekspreyonu gözlendi. Radiküler kistler çenenin hemen her bölgesinde görülebilmektedir. Bunun yanında bu kistlere maksilla (%60) ile

on Innovative Surveys in Positive Sciences 4-5 December 2022 / Full Text Book

birlikte anterior bölgede (%39-53) de rastlanmaktadır. Bu kistlerin büyüme eğilimleri genellikle yavaştır. Maksillada bu kistler gerek bukkal gerekse de palatal yönde büyümektedir. Mandibulada ise labia ve bukkal yönde büyürlerken, çok nadir de olsa lingual yönde de büyüme eğilimi gösterebilir (10).

Odontojenik kistlerin genel olarak maksillar bölgeden daha yoğun yerleşim göstermelerinin nedeni olarak, maksillar ve mandibular bölgelerdeki kemiklerin yapılarındaki farklılıkların bir sonucu olabileceği düşünülmektedir (11). Tortorici ve arkadaşlarının yapmış oldukları çalışmada radikuler kistlerin görülme yaşının ortalama 35.6 olduğu, erkek ve kadınlarda görülme oranının 1.15 olduğu ve literatürle uyumlu olarak maksillada daha sık görüldüğü ortaya konulmuştur (12). Boyutları aşırı bir şekilde büyümediği ve enfekte olmadıkları zaman bu kistler genel olarak herhangi bir semptom göstermezler. Bunun yanında sekonder olarak enfekte olmaları durumunda, nadir de olsa çenenin geniş bir alanında harabiyete ve patolojik kırıklara sebebiyet verebilirler (13). Radiküler kistlerde tedavi genel olarak kistin etkeni olan diş ya da dişlerin apikal rezeksiyonlarıyla beraber kistin enükleasyonunu kapsamaktadır. Kist ile alakalı dişte büyük oranda mobilitenin var olduğu durumlarda, dişin ve ilgili bölgedeki köklerin çekilmesi gerekebilir (14).

Epidermoid maligniteyle EGFR arasında bir ilişkinin var olduğu araştırmacılar tarafından ifade edilmektedir. Özellikle baş ve boyun bölgesindeki epidermoid karsinom vakkalarında, EGFR ekspresyon seviyesinin yüksekliği ortaya konulmuştur (15). Yamada ve arkadaşlarının ağız boşluğundaki epidermoid karsinom vakalarında, EGFR ekspresyonunun incelendiği çalışmada, EGFR oranı %51 oranında pozitif olarak tespit edilmiştir (16). Başka bir çalışmada ise EGFR primer antikoruyla yapılan boyanma sonucunda; keratokistlerin %90, foliküler kistlerin %60 ve radiküler kistlerin ise %50 pozitif boyanma gösterdikleri tespit edilmiştir. Özellikle inflamatuar hücrelerin yoğun olarak bulunduğu bölgelerde, genel anlamda pozitif boyanma bildirilmiştir (17).

Çalışmamızda, radiküler kistlerin epitel tabakasının yüzeyindeki hücrelerde, bazal hücrelerde, damarların endotelinde ve submukozada EGF ekspreyonu izlendi. EGFR ekspresyonu ile malignite arasındaki ilişkinin önceki çalışmalarla ortaya konulduğu düşünüldüğünde, bu durum radiküler kistlerin de ilerleyen zamanlarda malignite eğilimi gösterebileceğini düşündürmektedir.

## **SONUÇ**

Odontojenik kistlerin tanısı ve olası komplikasyonlarının neler olduğu, tedavi yönetiminin seçimi açısından son derece önemlidir. Kişilerin rutin dental kontrollerinin yapılması, radiküler kistlerin görülme insidansını azaltmada ve bu kistlerin çevre dokularda harabiyete yol açmasının önlenmesinde faydalı olabilir. Radyolojik yöntemlerle birlikte histopatolojik ve immunohistokimyasal yöntemlerin kullanılması da odontojenik kist türlerinin tesbitinde ve nasıl yaklaşılacağının anlaşılmasında yol gösterici olabilir. Ayrıca çalışmamızda, odontojenik radiküler kistlerde EGF eskpreyonunun yoğun olması, bu tarz kistik yapılarda epitelizasyonun yüksek olduğunu ve gingival dokunun rejenerasyonu açısından bir marker olarak kullanılabileceğini ortaya koymaktadır.

#### KAYNAKLAR

- 1. Leitner C, Hoffmann J, Kröber S, Reinert S. (2007), Low-grade malignant fibrosarcoma of the dental follicle of an unerupted third molar without clinical evidence of any follicular lesion. J Cranio-Maxillofacial Surg.
- 2. Regezi, Joseph, Sciubba, James, Jordan, Richard R de JE. (2012), Pathology: clinical pathologic correlations: Elsevier Health Sciences, p. 318-320.
- 3. Varinauskas V, Gervickas A, Rožnova O. (2006), Analysis of odontogenic cysts of the jaws. Medicina, 42: 201-7.
- 4. Philipsen HP. (2005), Keratocystic odontogenic tumour. In: World health organization classification of tumours: pathology and genetics of tumours of the head and neck tumours, Barnes EL, Eveson JW, Reichart P, Sidransky D eds, IARC Press, Lyon, 306-307.
- 5. lones AV, Craig GT, Franklin CD. (2006), Range and demographics of odontogenic cysts diagnosed in a UK population over a 30-year period. Oral Pathol Med, 35(8): 500-7.

on Innovative Surveys in Positive Sciences 4-5 December 2022 / Full Text Book

- 6. Foon, KA, Yang, XD, Weiner, LM, Belldegrun, AS, Figlin, RA, Crawford, J, Schwab, GM. (2004), Preclinical and clinical evaluations of ABX-EGF, a fully human anti-epidermal growth factor receptor antibody. International Journal of Radiation Oncology Biology Physics, 58(3), 984-990.
- 7. Prigent SA, Lemoine NR. (1992), The type 1 (EGFR-related) family of growth factor receptors and their ligands. Prog Growth Factor Res, 4:1–24.
- 8. Barnard JA, Beauchamp RD, Russel WE, Dubois RN, Coffey RJ. (1995), Epidermal growth factor-related peptides and their relevance to gastrointestinal pathophysiology. Gastroenterology, 108: 564–80.
- 9. Yang, XD, Jia, XC, Corvalan, JR, Wang, P, Davis, CG. (2001), Development of ABX-EGF, a fully human anti-EGF receptor monoclonal antibody, for cancer therapy. Critical reviews in oncology/hematology, 38(1): 17-23.
- 10. Shear M, Speight R. (2007), Radicular cyst and residual cyst. In: Cysts of the Oral and Maxillofacial Regions. 4th ed. Oxford: Blackwell Publishing Ltd, p.123-42.
- 11. Varinauskas V, Gervickas A, Kavoliûniene O. (2006), Analysis of odontogenic cysts of the jaws. Medicina (Kaunas), 42(3): 201-207.
- 12. Tortorici S, Amodio E, Massenti MF, Buzzanca ML, Burruano F, Vitale F. (2008), Prevalence and distribution of odontogenic cysts in Sicily: 1986-2005. J Oral Sci, 50(1): 15-18.
- 13. Delbem AC, Cunha RF, Vieira AE, Pugliesi DM. (2003), Conservative treatment of a radicular cyst in a 5- yearold child: a case report. Int J Paediatr Dent, 13(6): 447-50.
- 14. Scholl RJ, Kellett HM, Neumann DP, Lurie AG. (1999), Cysts and cystic lesions of the mandible: clinical and radiologic-histopathologic review. Radiographics, 19(5): 1107-24.
- 15. Miyaguchi M, Sakai S, Olofsson J, Kuwabara H, Sakamoto H. (1993), Prognosis significance of epidermal growth factor receptor in squamous cell carcinoma of the maxillary sinus. Eur Arch Otorhinolaryngol, 249: 478-81.
- 16. Yamada T, Takagi M, Shioda S. (1992), Evaluation of epidermal growth factor receptor in squamous cell carcinoma of the oral cavity. Oral Surg Oral Med Oral Pathol, 73: 67-70.
- 17. Gürkan, B, Özbayrak, T, Alatlı, C, Özveren, A. (1997), Epidermal Büyüme Faktörü Reseptörünün (Egfr) Ağız Boşluğunda Görülen Epidermoid Karsinom ve Odontojen Kist Epitelinde İmmunohistokimyasal Yöntemle Araştırılması. Journal of Istanbul University Faculty of Dentistry, 31(2): 130-135.

on Innovative Surveys in Positive Sciences 4-5 December 2022 / Full Text Book

# EFFECTS OF SODIUM HYDROXIDE ON THE UNCONFINED COMPRESSIVE STRENGTH OF CLAY-SAND SOILS

# KİLLİ KUM ZEMİNLERİN SERBEST BASINÇ DAYANIMI ÜZERİNDE SODYUM HİDROKSİTİN ETKİLERİ

## Tacettin GEÇKİL<sup>1</sup>

<sup>1</sup>Inonu University, Civil Engineering Department, Malatya, Turkey. <sup>1</sup>ORCID ID: 0000-0001-8070-6836

## Özge Nur ÇETKİN²

<sup>2</sup>Inonu University, Civil Engineering Department, Malatya, Turkey.

<sup>2</sup>ORCID ID: 0000-0002-0515-0337

## Ceren Beyza İNCE<sup>3</sup>

<sup>3</sup>Inonu University, Civil Engineering Department, Malatya, Turkey. <sup>3</sup>ORCID ID: 0000-0002-6385-0964

#### **ABSTRACT**

Today, due to increasing environmental problems, environmentalist projects are being tried to be realized in the field of engineering as in many other fields. In this study, a clayey-sand soil with poor bearing strength was stabilized with sodium hydroxide (NaOH) and improved, and the effects of NaOH on the unconfined compressive strength of this soil were investigated. For this purpose, the soil was first subjected to sieve analysis, hydrometer, pycnometer and consistency limit (Atterberg) tests to determine its geotechnical properties. After determining the soil properties, pure and stabilized soil samples were prepared by adding 8 Molar (M) (320 g/lt) NaOH solution to the soil in order to stabilize the soil. The prepared pure and stabilized soil samples were subjected to the standard proctor test in accordance with the ASTM D698 standard, and the maximum dry unit weights and optimum water contents of the samples were determined. Based on these values, unconfined pressure test samples were prepared in accordance with ASTM D2166 standard. The prepared test samples were subjected to unconfined pressure test after being exposed to curing times of 1 and 7 days. As a result of the experimental studies, at the end of 1 day curing, a lower value was obtained for the unconfined compressive strength values of the soil samples with the addition of NaOH compared to the unconfined compressive strength value of the pure soil. However, after 7 days of curing, it was determined that the unconfined compressive strength values of soil samples with NaOH added increased 1.79 times compared to pure soil. As a result, it was observed that the NaOH additive had a positive effect on the cohesion and internal friction resistance of the soil in the stabilization performed by the addition of NaOH.

Keywords: Soil, NaOH, Stabilization, Unconfined compressive strength, Cohesion.

### ÖZET

Günümüzde artan çevre problemleri nedeniyle birçok alanda olduğu gibi mühendislik alanında da çevreci projeler gerçekleştirilmeye çalışılmaktadır. Bu çalışmada, taşıma gücü zayıf olan killi-kumlu bir zemin, sodyum hidroksit (NaOH) ile stabilize edilerek iyileştirilmiş ve NaOH'nin bu zeminin serbest basınç dayanımı üzerindeki etkileri araştırılmıştır. Bu amaçla, zemin ilk olarak elek analizi, hidrometre, piknometre ve kıvam limit (Atterberg) deneylerine tabi tutularak geoteknik özellikleri belirlenmiştir. Zemin özelliklerinin belirlenmesinin ardından, zemini stabilize etmek amacıyla zemine 8 Molar (M) (320 g/lt) NaOH solüsyonu ilave edilerek saf ve stabilize zemin numuneleri hazırlanmıştır. Hazırlanan saf ve stabilize zemin numuneleri ASTM D698 standardına uygun olarak standart proktor deneyine tabi tutulup numunelerin maksimum kuru birim hacim ağırlıkları ile optimum su muhtevaları tespit

on Innovative Surveys in Positive Sciences 4-5 December 2022 / Full Text Book

edilmiştir. Bu değerler esas alınarak ASTM D2166 standardına uygun olarak serbest basınç deney numuneleri hazırlanmıştır. Hazırlanan deney numuneleri 1 ve 7 günlük kür sürelerine maruz bırakıldıktan sonra serbest basınç deneyine tabi tutulmuştur. Deneysel çalışmalar neticesinde, 1 günlük kürleme sonunda NaOH ilaveli zemin numunelerinin serbest basınç dayanım değerlerinin saf zemin serbest basınç dayanım değerlerinin saf zemin sonunda NaOH ilaveli zemin numunelerinin serbest basınç dayanım değerlerinin saf zemine kıyasla 1,79 kat artış gösterdiği belirlenmiştir. Sonuç olarak, zemine NaOH ilavesiyle gerçekleştirilen stabilizasyonda, NaOH katkısının zeminin kohezyonu ve içsel sürtünme direnci üzerinde olumlu bir etkiye sahip olduğu görülmüştür.

Anahtar Kelimeler: Zemin, NaOH, Stabilizasyon, Serbest basınç dayanımı, Kohezyon.

## 1. GİRİS

Son zamanlarda nüfus artışıyla birlikte yapılara olan ihtiyaç artmaktadır. Artan ihtiyaçlar doğrultusunda yapıları inşa ederken çeşitli problemler yaşanmaktadır. Yapıların üzerine inşa edileceği zeminler konusunda da sıklıkla problemler ortaya çıkmaktadır. Zeminler proje koşullarını karşılayacak özelliklere sahip olmalıdır. Ancak yapılara olan ihtiyacın artmasıyla her proje için uygun zemini temin etmek oldukça zorlaşmaktadır. Bu sebeple çeşitli yöntemler ile zemin iyileştirilmeye çalışılmaktadır. En çok tercih edilen ve çevreci olarak değerlendirilen uygulamaların başında da zemine farklı ürünler ilave ederek zemini stabilize etmek gelmektedir.

Somna vd. (2011), çalışmalarında oda sıcaklığında kürlenmiş sodyum hidroksit (NaOH) ile aktivite edilmiş uçucu kül (UK) katkılı zeminin özelliklerini araştırmışlardır. Çalışmada, alkali aktivatör olarak 4.5-16.5 Molar (M) NaOH solüsyonu kullanmışlardır. Çalışma neticesinde 4.5 M'den 14 M'a kadar karışımın mukavemetinde artış gözlenirken 14 M'den sonra düşüş yaşandığı belirlenmiştir [1]. Sukprasert vd. (2019), siltli killi zemini uçucu kül (UK) ve yüksek fırın cürufu (YFC) ile stabilize etmişlerdir. Zemin özellikleri üzerinde, UK ve YFC kombinasyonları ile NaOH aktivatörü ve kür sıcaklığının etkisi incelenmiştir. Yapılan incelemeler sonucunda UK:YFC oranının optimum değeri 20:10 olarak belirlenmiş ve kür sıcaklığının artmasıyla yüksek serbest basınç dayanım değerinin elde edildiği tespit edilmiştir [2]. Latif vd. (2018), yapmış oldukları çalışmada sodyum silikat bazlı bir sıvı katkı maddesi ile düşük plastisiteli kil ve yeşil bentonitin mühendislik özelliklerini incelemişlerdir. İncelemeler esnasında basınç dayanımı, tek boyutlu sıkıştırma ve kesme deneyleri yapılmıştır. Yapılan deneylerin sonucunda en efektif katkı oranı %6 olarak belirlenmiştir. Çalışma sonunda sodyum silikat bazlı katkı maddesi kireç çimento gibi geleneksel katkılara alternatif olarak sunulmuştur [3]. Eskişar ve Aksu (2020), kil, killi kum ve kum zeminlerde likit aktivatörle gerçekleştirilen çalışmalarda meydana gelen değisimleri incelemislerdir. Calısmalarında aktivatör oranı ve kür süresinin serbest basınc mukavemeti üzerinde meydana gelen etkilerini tespit etmislerdir. Kil zeminlerde su içeriğinin iki katı kadar aktivatör kullanılması mukavemeti artırırken killi kum ve kum zeminlerde ise optimum su oranı kadar aktivatör kullanılması yeterli olmaktadır. Kür süresi arttıkça mukavemette de artış yaşanmaktadır. Aktivatör katkılı kil zeminde serbest basınç mukavemeti 90 gün sonunda saf kil zemine kıyasla 3,54 katına çıkmıştır [4]. Hissesini vd. (2021), yapmış oldukları çalışmada sodyum hidroksit ve sodyum silikat çözeltileri ile aktivite edilen uçucu kül, metakaolin ve yüksek fırın cürufu katkılı killi zeminlerdeki iyileşme etkilerini incelemişlerdir. Çalışmada, numunelerinin 1, 7, 28 günlük kür sonunda serbest basınç mukavemet değerleri incelenmiştir. En büyük mukavemet artışı 28 günlük kür sonunda metakaolin bazlı zeminlerden elde edilmiştir [5]. Sharma vd. (2020), farklı yüzde karısımları, molarite, sıcaklık, kür süresi, aktivatör ve su/bağlayıcı oranlarının zemin üzerindeki etkilerini araştırmışlardır. Calışma sırasında %5-20 geopolimer karışımı, 25-45 °C sıcaklık, 7-28 gün kürleme, 8-12 M molarite,

1,5-2,5 aktivatör oranı ve 0,35-0,85 su/bağlayıcı parametreleri arasında iyileştirme meydana geldiği belirlenmiştir. Çalışma neticesinde geopolimer stabilizasyonu ile iyileştirme yapılabileceği gözlemlenmiştir [6].

Bu çalışmada da taşıma gücü zayıf killi-kum taban zemininin sodyum hidroksit ile stabilize edilmesi sonucu serbest basınç dayanımı üzerinde olan etkileri araştırılmıştır. Bu amaçla, zemin elek analizi, hidrometre, piknometre, kıvam limit deneylerine tabi tutulup zeminin geoteknik özellikleri tayin

on Innovative Surveys in Positive Sciences 4-5 December 2022 / Full Text Book

edilmiştir. Ardından zemine sodyum hidroksit ilave ederek saf ve stabilize zemin numuneleri hazırlanarak standart proktor ve serbest basınç deneyleri yapılmıştır.

#### 2. MATERYAL VE METOT

#### 2.1 Materyal

Çalışmada kullanılan zemin, İnönü Üniversitesi Mühendislik Fakültesi yerleşkesinden temin edilmiştir. Kullanılan zemin Birleştirilmiş Zemin Sınıflandırma Sistemine (USCS) göre killi kum (SC) olarak belirlenmiştir. Kullanılan zeminin özellikleri Tablo 1' de verilmiştir.

Tablo 1. Zeminin Fiziksel Özellikleri

Değişken Adı	Simge	Birim	Değeri
Dane birim hacim ağırlığı	γs	g/cm <sup>3</sup>	2,714
Maksimum kuru birim hacim ağırlığı	γ̃kmax	g/cm <sup>3</sup>	1,948
Optimum su içeriği	Wopt	%	14,1
Likit limit	$W_{ m L}$	%	25,87
Plastik limit	$W_p$	%	14,56
Plastisite indisi	PI	%	11,31
Sınıflandırma (Birleştirilmiş Zemin Sınıflandırma Sistemi)	-	-	SC
AASHTO Sınıflandırması	-	-	A-6

Çalışmada kullanılan NaOH solüsyonu kristal halde bulunan NaOH ve saf suyun karışımı ile elde edilmiştir. Solüsyonun molaritesi 8 Molar (M) (320 gr/lt) olarak tercih edilmiştir. Molarite seçilirken literatür [1,4] dikkate alınarak belirlenmiştir. Tablo 2'de NaOH'ın özellikleri verilmiştir [7].

Tablo 2. Sodyum Hidroksitin (NaOH) Özellikleri

Fiziksel ve Kimyasal Özellikler	Sodyum Hidroksit
Molekül formülü	NaOH
Molekül kütlesi (g/mol)	40,00
Renk	Beyaz
рН	13-14
Bağıl yoğunluk (g/cm³)	2,13

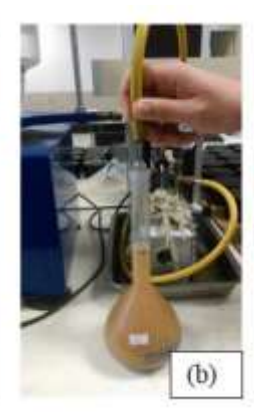
on Innovative Surveys in Positive Sciences

4-5 December 2022 / Full Text Book

#### **2.2 Metot**

Çalışmada zeminin geoteknik özelliklerini belirlemek maksadıyla elek analizi ve hidrometre (ASTM D422-63), piknometre (ASTM D854), kıvam (ASTM D4318) deneyleri yapılmıştır. Deneyler ile ilgili görüntüler Sekil 1'de verilmistir.







Sekil 1. Elek analizi (a), Piknometre (b), Kıvam (c) Deneyleri

Zeminin geoteknik özelliklerinin belirlenmesinin ardından zemine 8 M NaOH solüsyonu ilave edilerek saf (katkısız) ve NaOH katkılı stabilize zemin numuneleri hazırlanmıştır. Hazırlanan numuneler standart proktor (ASTM D698) ve serbest basınç (ASTM D2166) deneyleri ile test edilmiştir.

Standart proktor denevinde numunenin maksimum kuru birim hacim ağırlığı ile optimum su miktarı belirlenmiştir. Zeminin kuru birim hacim ağırlığı (Y<sub>k</sub>) zeminin kompaksiyon derecesini göstermektedir.  $\Upsilon_k$  değeri ne kadar fazla ise zemin o kadar sıkışmış demektir [8]. Standart proktor deneyinden elde edilen maksimum kuru birim hacim ağırlığı  $(\Upsilon_k)$  ile optimum su içeriği  $(w_{opt})$  değerleri baz alınarak serbest basınç deney numuneleri hazırlanmıştır.

Serbest basınç deneyi, kohezyonlu zeminlerde kayma mukavemetini belirlemek maksadıyla yapılmaktadır [9]. Serbest basınç deney numuneleri standarda uygun olarak hazırlanıp 1 ve 7 günlük kür sürelerini tamamlamalarının ardından serbest basınç deneyine tabi tutulmuştur. Şekil 2'de serbest basınç deney seti verilmistir.



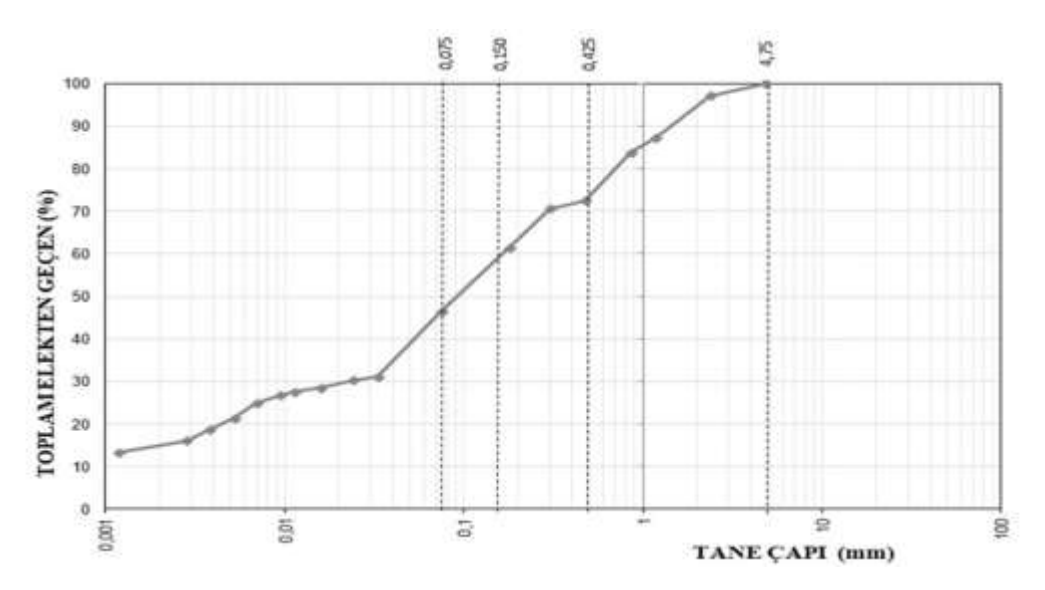
Şekil 2. Serbest Basınç Deney Seti

### 3. BULGULAR VE DEĞERLENDİRMELER

Killi zeminlerin serbest basınç dayanımı üzerinde sodyum hidroksitin (NaOH) etkilerinin incelendiği bu çalışmada ilk olarak elek analizi, hidrometre, piknometre ve kıvam deneyleri ile zeminin geoteknik özellikleri belirlenmiştir. Deneyler neticesinde elde edilen veriler doğrultusunda zeminin granülometri eğrisi Şekil 3'te verilmiştir.

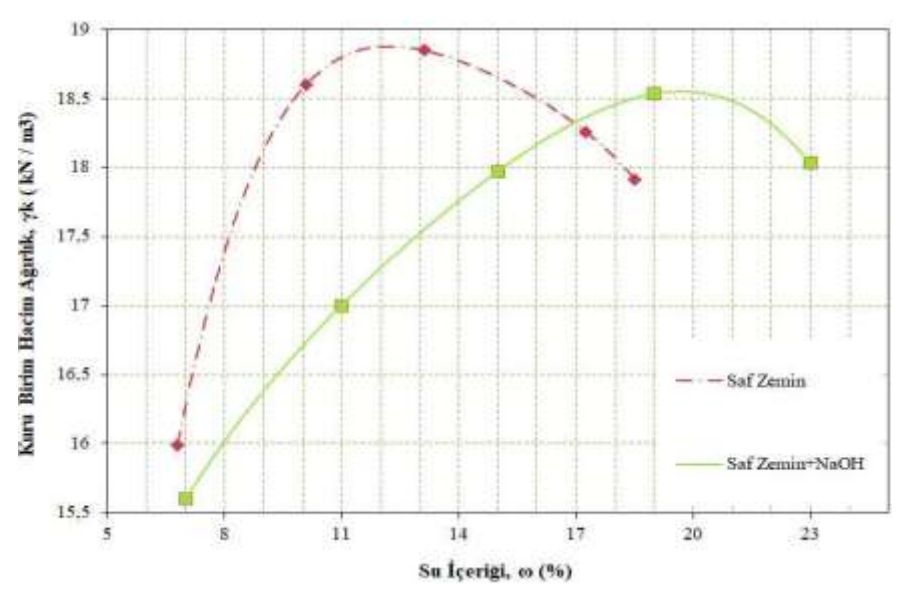
on Innovative Surveys in Positive Sciences

4-5 December 2022 / Full Text Book



Şekil 3. Zemin Granülometri Eğrisi

Zeminin geoteknik özelliklerinin tespit edilmesinin ardından zemine 8 M NaOH solüsyonu ilave edilerek saf ve stabilize zemin numuneleri hazırlanarak standart proktor testi yapılmıştır. Standart proktor testi sonunda elde edilen optimum su içeriği (w<sub>opt</sub>) ve maksimum kuru birim hacim ağırlığı (Υ<sub>k</sub>) değerleri belirlenerek kompaksiyon eğrileri çizilmiştir (Şekil 4). Yk ve wopt değerleri tablo 3'te verilmiştir.



Şekil 4. Kompaksiyon Eğrisi

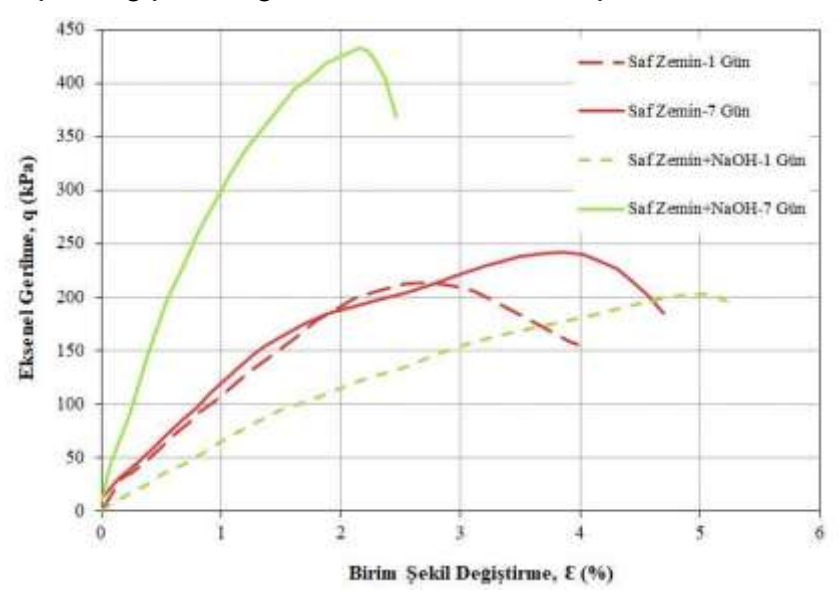
Tablo 3. Standart Proktor Deney Sonuçları

Test Numunesi	Maksimum Kuru Birim Hacim Ağırlığı Υ <sub>k</sub> (kN/m³)	Optimum Su İçeriği W <sub>opt</sub> (%)
Saf Zemin	18,88	12,00
Saf Zemin +NaOH	18,34	19,80

on Innovative Surveys in Positive Sciences 4-5 December 2022 / Full Text Book

Standart proktor deney sonuçları incelendiğinde; maksimum kuru birim hacim ağırlığının azaldığı optimum su miktarının ise arttığı gözlemlenmiştir.

Standart proktor deneyinden elde edilen  $\Upsilon_k$  ve  $w_{opt}$  değerleri baz alınarak serbest basınç deney numuneleri hazırlanmış ve numuneler 1, 7 günlük kür sürelerinin tamamlamalarının ardından numunelere serbest basınç deney uygulanmıştır. Serbest basınç deneyinde numunelerin gerilme (q) ve şekil değiştirme ( $\epsilon$ ) değerleri belirlenmiştir. Deney sonunda oluşturulan gerilme-şekil değiştirme grafiği Şekil 5'te, gerilme-şekil değiştirme değerleri ise Tablo 4'te verilmiştir.



Şekil 5. Serbest Basınç Deneyinden Elde Edilen q-E Grafiği

Tablo 4. Serbest Basınç Deneyinden Elde Edilen q-E Değerleri

Test Numunesi	Serbest Basınç Mukavemeti, (UCS), q (kPa)	Serbest Basınç Mukavemeti Değerindeki Birim Şekil Değiştirme, E (%)
Saf Zemin-1 Gün	231,46	2,76
Saf Zemin-7 Gün	242,29	3,86
Saf Zemin+NaOH-1 Gün	202,63	5,03
Saf Zemin+NaOH-7 Gün	432,65	2,16

Kür süresini tamamlayıp serbest basınç deneyi uygulanan numunelerin deney sonuçları incelendiğinde; 1 günlük saf zemin numunesinin serbest basınç mukavemet değerinin NaOH ilaveli numunenin serbest basınç mukavemet değerinden fazla olduğu, 7 günlük saf zemin serbest basınç mukavemet değerinin NaOH ilaveli numunelerin serbest basınç mukavemet değerlerinden az olduğu belirlenmiştir. Bu durum NaOH ilavesi ile gerçekleştirilen stabilizasyonda zeminin zamanla dayanım kazandığını ve numunelerin uzun dönem mukavemet değerlerinin incelenmesinin gerekliliğini göstermektedir [4].

#### 4. SONUCLAR

Killi kum zeminlerde serbest basınç dayanımı üzerinde sodyum hidroksitin etkilerinin incelendiği bu çalışmada elde edilen sonuçlar aşağıdaki gibi ifade edilmiştir.

• Standart proktor deney sonuçları incelendiğinde zemine ilave edilen NaOH ile zeminin optimum su miktarının arttığı, maksimum kuru birim hacim ağırlığının ise azaldığı gözlemlenmiştir.

on Innovative Surveys in Positive Sciences 4-5 December 2022 / Full Text Book

• Serbest basınç deney sonuçları incelendiğinde 1 günlük saf zemin numunesinin serbest basınç mukavemet değerinin NaOH ilaveli zeminin serbest basınç mukavemet değerinden fazla çıktığı ancak 7 günük saf zemin numunesinin serbest basınç mukavemet değerinin NaOH ilaveli zeminin serbest basınç mukavemet değerinden az çıktığı gözlemlenmiştir. Bu durum NaOH ilavesi ile gerçekleştirilen stabilizasyonda zeminin zamanla dayanım kazandığını göstermektedir. En yüksek serbest basınç mukavemet değerinin 7 günlük kürleme sonunda NaOH ilaveli zeminde elde edildiği ve saf zemine kıyasla NaOH ilaveli zeminin mukavemet değerinin 1,79 katına çıktığı belirlenmiştir.

Sonuç olarak sodyum hidroksit ile gerçekleştirilen zemin stabilizasyonunun serbest basınç dayanımı üzerinde kür süresinin önemli bir etkiye sahip olduğu ifade edilebilir. Aynı zamanda zemin stabilizasyonunda kullanılan çimento kireç gibi geleneksel katkılara alternatif olarak NaOH kullanılabileceği ve çevreye katkı sağlayacağı düşünülmektedir.

#### KAYNAKLAR

- [1] Somna K, Jaturapitakkul C, Kajitvichyanukul P, Chindaprasit P. (2011). NaOH-Activated Ground Fly Ash Geopolymer Cured at Ambient Temperature, Fuel, 90(6): 2118-2124.
- [2] Sukprasert S, Hoy M, Horpibulsuk S, Aruljarah A, Rashid A, Nazir R. (2018). Fly Ash Based Geopolymer Stabilization of Silty Clay/Blast Furnace Slag For Subgrade Applications, Road Materials and Pavement Design, 22(2): 357-371.
- [3] Latifi N, Vahedifard F, Ghazanfari E, Horpibulsuk S, Marto A, Williams J. (2018). Sustainable Improvement of Clays Using Low-Carbon Nontraditional Additive, International Journal of Geomechanics, 18(3): 04017162.
- [4] Eskisar T, Aksu G. (2020). Zeminlerde Tek Fazli Geopolimerizasyon Uygulamasi Ve Geopolimerizasyonun Serbest Basinç Mukavemeti Üzerindeki Etkisi, Konya Mühendislik Bilimleri Dergisi, 8(3): 466-478.
- [5] Hisseini BHA, Bennabi A, Hamzaoui R, Makki L, Blanck G. (2021). Treatment and Recovery of Clay Soils Using Geopolymerization Method, Uluslararası Geomekanik Dergisi, 21(11): 04021206.
- [6] Sharma K, Kumar A. (2020). Utilization of İndustrial Waste-Based Geopolymers As A Soil Stabilizer A Review, Innovative Infrastructure Solutions, 5: 97.
- [7] Ekinci E. (2017). Volkanik Tüf Kullanılarak Üretilen Geopolimer Betonların Bazı Mekanik Ve Fiziksel Özelliklerinin Araştırılması. Yüksek Lisans Tezi, İnönü Üniversitesi.
- [8] Geçkil T, Sarıcı T, Yıldıran ES. (2019). Kireç Katkısı ile Kil Bir Zeminin Dayanımının İyileştirilmesi, Çukurova Üniversitesi Mühendislik Mimarlık Fakültesi Dergisi, 34(4): 171-179.
- [9] Yılmaz I, Yıldırım M, Keskin İ. (2016). Zemin Mekaniği Laboratuvar Deneyleri ve Çözümlü Problemler. Seçkin Yayıncılık, 42-44.

on Innovative Surveys in Positive Sciences 4-5 December 2022 / Full Text Book

## NEW DENIAL OF SERVICE ATTACKS DETECTION APPROACH USING HYBRIDIZED NEURAL NETWORKS AND BALANCED DATASET

### Ouail MJAHED, Salah EL HADAJ, El Mahdi EL GUARMAH, Soukaina MJAHED

Faculty of Sciences and Technology, Department of Computer Sciences
L2IS, Marrakech, Morocco.

#### **ABSTRACT**

Denial of Service (DoS) intrusions are damaging cyber-attacks, and their identification is of great interest in the Intrusion Detection System (IDS). Neural Networks (NN) and Metaheuristic Algorithms typify two of the best-used approaches in the IDS research. On another side, CICIDS2017 provides an efficient dataset for the design of any IDS solution, due to the multiplicity of attacks and attributes that it encompasses. The purpose of this work is to improve a neural network-based DoS detection system by using three metaheuristic algorithms, such as Particle Swarm Optimization (PSO), Genetic Algorithm (GA) and Ant-Lion Optimizer (ALO). Thus, five DoS attack classes, including Benign, GoldenEye, Hulk, SlowHTTPTest and Slowloris, are used in a balanced ratio. For data balancing, a Synthetic Minority Oversampling Technique (SMOTE) is employed. Hybrid NN-based approaches are explored in order to select the best features and to improve detection efficiencies. In this context, the optimization of the NN input layer is achieved by only 24 features, and the NN size is reduced to five layers. Performance metrics extracted from confusion matrices, such as efficiency and purity are used. The experimental result, based on the used DoS-CICIDS2017 dataset, indicated that PSO-based NN completes promising DoS detection, providing a tested efficiency and purity of 99.92 % and 99.63 %, respectively, for both balanced and unbalanced datasets.

**Keywords:** Neural Networks, Metaheuristic Algorithm, Denial of Service, Intrusion Detection System, CICIDS2017.

#### 1. INTRODUCTION

The objective of this paper is imposed by the need to improve intrusion detection systems (IDS). The analysis of the IDS state of the art shows that the most effective methodology used is based on neural networks (NN) [1-5]. Moreover, few works are devoted to the hybridization of NNs with metaheuristic algorithms.

The proposed approach consists on the following key points.

- a) Improving the performance of NNs using metaheuristic algorithms such as Particle Swarm Optimization (PSO), Genetic Algorithm (GA) and Ant-Lion Optimizer (ALO).
- b) The use of Denial of Service (DoS) attacks from the CICIDS2017 dataset [6], to implement and validate the proposed approach.
- c) As the data is unbalanced, the use of the SMOTE [7] algorithm allows having two sets of data. This permits to better assess the results obtained.

This paper is organized as follows. Section 2 describes the used dataset and performance measure parameters. In Section 3, the experimental results of the suggested approach are presented. Finally, Section 4 ends this paper with the main conclusions.

#### 2. DATA AND METHODOLOGY

#### 2.1. Data

CICIDS2017 generated by Canadian Institute for cyber-security IDS [6], consists of 2830743 instances with 79 features, corresponding to 15 traffic classes (one normal class and 14 attack traffic classes). Five

on Innovative Surveys in Positive Sciences 4-5 December 2022 / Full Text Book

DoS attack classes, including Benign, GoldenEye, Hulk, SlowHTTPTest and Slowloris, are used in an unbalanced ratio (Dataset 1). For data balancing, a Synthetic Minority Oversampling Technique (SMOTE) is employed [7], giving Dataset 2. The data profile of Dataset 1 and 2 used is presented in Table 1, with a portion of 70% for training and 30% for testing.

Table 1. Characteristics of the used CICIDS2017 Data

		Dataset 1			Dataset 2		
Class	Class Label	$N_{Ci}$	Training	Test	$N_{\text{Ci}}$	Training	Test Set
$C_1$	Benign	227000	158900	68100	40000	28000	12000
$\mathbf{C}_2$	DoS Hulk	23000	16100	6900	10000	7000	3000
$\mathbb{C}_3$	DoS	1000	700	300	10000	7000	3000
$\mathbb{C}_4$	DoS	570	400	170	10000	7000	3000
$C_5$	DoS	530	370	160	10000	7000	3000
All		252100	176470	75630	80000	56000	24000

#### 2.2. Methodology

As previously introduced, the considered CICIDS 2017 Dos intrusions will be detected using a Back-propagation Neural Network (BPNN) [8], followed by a processing through three hybridized neural networks as described in Algorithm 1 and based on tuning parameters shown in Table 2. The purpose of this work is to improve a neural network-based DoS detection system by using three metaheuristic algorithms, such as Particle Swarm Optimization (PSO) [9], Genetic Algorithm (GA) [10] and Ant-Lion Optimizer (ALO) [11].

#### Algorithm 1: BPNN and Metaheuristic based-NN

- 1: For the BPNN approach, optimize weights and by using the training dataset
- 2: Return the results of BPNN with weights, threshold and BPNN training and Test performances (precision, sensitivity, F1-score and accuracy of classifications).
- 3: For the hybrid metaheuristic NN- based approach (GANN, PSONN and ALONN), optimize weights and thresholds according to respective metaheuristic algorithm.
- 4: Return training and test performances (precision, sensitivity, F1-score and accuracy).

Table 2. Algorithms parameters tuning

Algorithm	Parameters Tuning		
	Number of runs = 50, Maximum number of iterations = 1000,		
PSO	Number of population elements= 20-100, Inertia weight = 0.72,		
P30	Inertia weight damping ratio = 0.99, Personal learning coefficient = 1.49,		
	Global learning coefficient = 1.49		
	Number of runs = 50, Maximum number of iterations = 1000,		
GA	Number of population elements = $20-100$ , Crossover probability (pc) = $0.8$ , Mutation rate = $0.02$ , Mutation probability (pm) = $0.3$ , Selection pressure = $8$		
44.0	Number of runs = 50, Maximum number of iterations = 1000,		
ALO	Number of search agents = 1000		

on Innovative Surveys in Positive Sciences 4-5 December 2022 / Full Text Book

#### 2.3. Performance metrics

To evaluate the proposed classifiers (BPNN and hybrid-based NN), three metrics are used. For each predicted class  $C_i$ , efficiency  $\beta_i$  and purity  $\gamma_i$  are computed according to Eq. (1),  $A_{ij}$  being the value of examples of genuine class  $C_i$  classified as class  $C_j$  and  $N_i$  denote the size for class  $C_i$ .

$$\beta_i = \frac{A_{ii}}{N_i}, \ \gamma_i = \frac{A_{ii}}{\sum_i A_{ji}}$$
 (1)

Thus, the global efficiency  $\beta$  and the global purity  $\gamma$ , become as specified in Eq. (2).

$$\beta = \frac{\sum_{i} N_{i} \beta_{i}}{\sum_{i} N_{i}}, \quad \gamma = \frac{\sum_{i} N_{i} \gamma_{i}}{\sum_{i} N_{i}}$$
 (2)

#### 3. RESULTS

Starting from a 5-layer architecture, the four neural networks (BPNN, PSONN, GANN and ALONN) have been optimized to minimize fitness ( $f = 1 - \beta$ ).

The best obtained architecture, for the 4 NNs, and by using the two datasets 1 and 2, is (24, 30, 45, 30, 5), showing that the initial 79 features have been reduced to 24. Three hidden layers are enough to learn the features of the 5 DoS attack classes, with respectively, 30, 45 and 30 neurons per layer.

The results obtained during the learning and test phase are summarized in Table 3.

The experimental result, based on the used DoS-CICIDS2017 dataset, indicated that PSO-based NN completes promising DoS detection, providing a tested efficiency and purity of 99.92 % and 99.63 %, respectively. The results demonstrate that the two datasets include instances with the same properties. The SMOTE algorithm proves its usefulness here.

Table 3. Intrusion Detection Performance by using BPNN, PSONN, GANN and ALONN on Training and test Datasets

		Trainin	g Performance	Test Per	formance
Data	Method	$\beta$ (%)	γ(%)	β(%)	γ(%)
Data 1	BPNN	96.43	96.27	96.04	96.13
	<b>PSONN</b>	99.98	99.67	99.92	99.63
	GANN	99.38	99.19	99.11	99.17
	ALONN	99.53	99.46	99.45	99.32
Data 2	BPNN	96.49	96.32	96.23	96.34
	PSONN	99.99	99.68	99.93	99.62
	GANN	99.39	99.20	99.12	99.18
	ALONN	99.54	99.47	99.44	99.31

#### 4. CONCLUSION

The aim of this paper is to contribute towards improving NN-based DoS Intrusion Detection performance on CICIDS2017 Dataset, by using PSO, GA and ALO metaheuristic algorithms. A reduced unbalanced dataset and a balanced dataset have been used to achieve this approach. The metaheuristic-based NNs have greatly improved the detection of DoS intrusions in CICDS2017 dataset. The experimental result indicated that PSONN reached good performances. PSONN produces the same tested efficiency and purity. Future studies should extend the work to data reduction and IDS design by using other Machine Learning techniques.

on Innovative Surveys in Positive Sciences 4-5 December 2022 / Full Text Book

#### REFERENCES

- [1] Bindra, N., Sood, M. (2019). Detecting DDoS attacks using machine learning techniques and contemporary intrusion detection dataset. *Automatic Control and Computer Science*, *53*(5) 419–428.
- [2] Lee, J., Kim, J. Kim, I.and Han, K. (2019). Cyber threat detection based on artificial neural networks using event profiles. *IEEE Access*, 7, 165607–165626.
- [3] Kurniabudi, K., Stiawan, D., Darmawijoyo, D., Bin Idris, M. Y., Kerime, B. and Budiarto, R. (2021). Important Features of CICIDS-2017 Dataset for Anomaly Detection in High Dimension and Imbalanced Class Dataset. *Indonesian Journal of Electrical Engineering and Informatics* 9(2), 498-511.
- [4] Alrowaily, M., Alenezi, F., Lu, Z. (2019). Effectiveness of machine learning based intrusion detection systems. *Proceedings of the International Conference on Security, Privacy and Anonymity in Computation, Communication and Storage*. pp 277-288, Atlanta, GA, USA.
- [5] Panigrahi, R., Borah, S. (2018). A detailed analysis of CICIDS2017 dataset for designing intrusion detection systems. *International Journal of Engineering and Technology*, 7, 479-482.
- [6] CICIDS2017 Dataset, <a href="https://www.unb.ca/cic/datasets/ids-2017.html">https://www.unb.ca/cic/datasets/ids-2017.html</a>
- [7] Chawla, N. V., Bowyer, K.W., Hall, L.O. & Kegelmeyer, W.P., SMOTE: Synthetic Minority Over-sampling Technique, *Journal of Artificial Intelligence Research* 16 (2002) 321–357.
- [8] Haykin, S. (2009). *Neural Networks and Learning Machines*, Third Edition, Pearson Education.
- [9] Rini, P., Shamsuddin, M., & Yuhaniz. S. (2011). Particle Swarm Optimization: technique, system and challenges. *International Journal of Computer Applications* 14, 19–27.
- [10] Holland. J. H. (1975). *Adaptation in Natural and Artificial Systems*, University of Michigan Press.
- [11] Mirjalili, S. (2015). The ant lion optimizer. *Advances in Engineering Software*, 83, 80-98.

on Innovative Surveys in Positive Sciences 4-5 December 2022 / Full Text Book

### AN OPTIMIZATION-BASED VIDEO STABILIZATION APPROACH

#### Semiha Dervişoğlu<sup>1</sup>

<sup>1</sup> Iskenderun Technical University, Institute of Engineering and Natural Sciences, Department of Computer Engineering, Hatay, Turkey.

<sup>1</sup>ORCID ID: 0000-0002-3677-8792

## Mehmet Sarıgül<sup>2</sup>

<sup>2</sup> Iskenderun Technical University, Institute of Engineering and Natural Sciences, Department of Computer Engineering, Hatay, Turkey.

<sup>2</sup>ORCID ID: 0000-0001-7323-6864

#### Levent Karacan<sup>3</sup>

<sup>3</sup> Iskenderun Technical University, Institute of Engineering and Natural Sciences, Department of Computer Engineering, Hatay, Turkey.

<sup>3</sup>ORCID ID: 0000-0003-2764-5258

#### **ABSTRACT**

Nowadays, videos are ubiquitous in education, health and military fields besides daily use. However, visual instabilities such as shaking and jittering may occur in videos taken with handheld cameras. To overcome this problem, various video stabilization approaches have been proposed. Earlier in the literature, video stabilization studies were carried out with feature-based methods in which features are extracted with a feature extraction algorithm and tracked among the video frames. Then, the videos are stabilized by smoothing the feature trajectories. Recently, supervised learning-based studies have been another branch of work. In supervised learning approaches, deep learning models are trained for stabilization purposes using stable and unstable video pairs. However, obtaining those pairs is not straightforward. In recent years, interpolation-based unsupervised video stabilization methods have achieved successful results under certain conditions without the need for such data pairs. The success of these methods is directly related to the performance of the interpolation method. In addition, they can not perform well when there is a complex motion between input frames. Although these methods provide significant progress, many challenges still need to be solved to obtain successful results.

In this study, we proposed an optimization-based video stabilization method to overcome the shortcomings of the interpolation-based video stabilization strategy. In our method, we predict the warping field transforming the input unstable video frame to a stable one. Moreover, we define a new objective function to optimize a smooth warping field, so that output video does not contain unintended camera motion. Experimental results demonstrate that our proposed video stabilization algorithm achieves promising results. Our method produces up to 17.65% more successful results than the baseline interpolation-based method.

**Keywords:** Video Stabilization, Interpolation, Optimization, Warping

#### INTRODUCTION

The recent increase in video usage has increased the number of academic studies on video stabilization. The complexity of the stabilization problem has led to the development of various methods and different strategies to handle it.

In the literature, different optimization methods have been utilized for video stabilization. Digital video stabilization is performed in 3 steps: camera motion estimation, camera motion smoothing and frame synthesis. Jia *et al.* (2013) focused on smoothing the camera movement and developed a 3D rotational

on Innovative Surveys in Positive Sciences 4-5 December 2022 / Full Text Book

video stabilization method by using the manifold optimization. Their method uses a gyroscope to estimate 3D camera rotation. They considered the 3D rotation matrices as a whole and treated and formulated the smoothing problem as a regression problem. They reported better results compared to other 2D affine models. Qu et al. (2013) used an optimization based approach using L1 and L2 norms for removing unwanted camera motion. They compute smoothed camera paths by L1 constraints and utilize L2 norm of the difference between smoothed and original camera paths to retain the video information. The effect of these two norms is controlled by weight parameters. In this way, they achieved a mixed L1-L2 optimization. Wang et al. (2013) provided a solution to the parallax problem for video stabilization. In their method, each feature trajectory is treated as a Bezier curve. They integrated this reduced Bezier model into a spatial-temporal optimization problem. The Bezier model reduced the number of variables used in optimization while smoothing feature trajectories. Each optimized trajectory considers the flattened features as positional constraints. After, they perform warping of the frames with content preserving methods. In this way, they solved the parallax problem by utilizing spatial and temporal optimization. Zhao et al. Followed Wang's strategy. They extracted feature trajectories for both background and foreground. Then, a mesh was created according to the distribution of feature trajectories in each frame. After that, a two-stage optimization process was implemented by computing all transformations for all triangular grids located above the mesh. In the calculation of transformations for triangles, a constraint is applied for each triangle based on similarity to the original triangle and adjacent triangles. In this process, the close triangles become similar while others become different. This method also provides spatio-temporal consistency. After the warping operation was performed, stable images were created with the adjustable mesh method based on Delaunay triangulation of the feature trajectories (Zhao et al.2020). Yu et al proposed a CNN network for video stabilization. They claimed that an optimized network makes this non-convex highdimensional optimization problem more practical. In this way it allows to directly use a stabilization formulation based on a robust optical flow. The optimized network is used to solve the affine transformation and warping in each frame. However, due to the use of flow, the computation time is high.(Yu, et al. 2019). Yao et al. performed CNN-based optimization with a similar approach. They presented the first 3D CNN-based video stabilization method using depth maps (Lee et al. 2021). Wu et al. handle the video stabilization problem as a frame prediction problem. They conducted an extrapolation process to predict the future frames. Wu solved the challenge of predicting future frames by using a pre-trained neural network and optimizing the frame optical-flows. (Wu et al. 2022)

#### RESEARCH AND FINDINGS

#### INTERPOLATION-BASED VIDEO STABILIZATION APPROACH

With the increasing use of video stabilization for various purposes in recent years, interest and studies on the subject have increased. In the literature numerous studies aim to increase the stability of videos have been implemented. An increase in stability can be achieved by reducing large shakes in the video and making transitions smoother. There are different strategies to achieve this, one of them being the interpolation-based approach. DIFRINT eliminates low-level vibrations using frame interpolation techniques without cropping the image size. In addition, the idea of using iterative interpolations also strengthened the increase in the stabilization score (Choi, *et al.* 2020). In the light of this information, we tested the use of ABME and VFIformer interpolation techniques (Park, *et al.* 2021, Lu *et al.* 2022), which are the recently developed interpolation methods with a similar strategy. We examined the stability scores of the obtained results. In Figure 1, we give the videos we tested taken from the NUS dataset (Liu, *et al.*2013). We compare performance of interpolation methods ABME and VFIformer with DIFRINT. Number of the frames, cropping ratios, distortion values and stability scores are given in Table 1. The results are very close to each other. However, the iteration-based DIFRINT approach still has a better stability score than other studies. To surpass performance of DIFRINT and to eliminate the need for iterations we proposed an optimization method using PWC-Net (Sun, *et al.* 2018).

on Innovative Surveys in Positive Sciences 4-5 December 2022 / Full Text Book



Fig:1 Comparison with 6 publicly available videos (NUS) in terms of three metrics (Liu,2013).

3 ITERATION		3 ITERATION VFIFORMER RESULTS				
VID_NO/FR AME_NUM	CROP(AVG,MIN)	DIST	STAB(AVG,TRANS,R OT)	CROP(AVG,M IN)	DIST	STABILITY(AVG,TR ANS, ROT)
1/246	1.0000, 0.9954	0.9956	0.8258 0.8183 0.8332	1.0000  0.9951	0.9950	0.8273 0.8181  0.8366
2/431	1.0000, 0.9871	0.9926	0.7765 0.7175 0.8355	1.0000  0.9875	0.9916	0.7847 0.7430  0.8265
3/446	0.9999, 0.9941	0.9902	0.6245 0.5927 0.6563	1.0000  0.9945	0.9897	0.6230 0.5521  0.6938
4/387	1.0000, 0.9952	0.9919	0.7306 0.5724 0.8888	1.0000  0.9952	0.9921	0.7300 0.5713  0.8887
5/627	1.0000, 0.9892	0.9753	0.6765 0.4559 0.8971	1.0000  0.9893	0.9735	0.6682 0.4411  0.8952
6/877	0.9999, 0.9946	0.9916	0.8345 0.8950 0.7740	0.9999  0.9936	0.9909	0.8290 0.8946  0.7634

**Table 1:** ABME and VFIformer stability score table in 3 iterations

#### USING OPTIMIZATION IN VIDEO STABILIZATION

In this study, we developed an optimization-based video stabilization method to increase the stability scores and at the same time to reduce blur caused by iterations applied in interpolation-based methods. Let xt be an unstable frame in the video at time t. ABME model is represented by A that we used as a pre-trained interpolation model.

In this study, we aim to warp unstable frame (xt) onto the stable plane by optimizing optical-flows for each frame (Ft). Thus, a smoother motion will be obtained. For this reason, we optimize Ft for iiteration. The output image of our optimized flow can be shown as  $\hat{l}i = warp(xt, Fti)$  where the warp function is PWC-net (Sun, et al 2018). We also utilize softsplat operation for forward warping. The softsplat process called S is applied to the resulting warp frame (Niklaus, et al. 2020). It is shown as  $soft(i) = S(\hat{l}i, Fti)$ . Softsplat is used to improve image quality affecting stability score of optimized frames. First, with  $\hat{A} = \sum_{i=1}^{4} A(xt - j, xt + j)$ , interpolation frames  $\hat{A}1, \hat{A}2, \hat{A}3, \hat{A}4$  with different time intervals are produced. The initial flow to be optimized is taken as  $Ft1 = (xt, \hat{A}1t)$ . Initial optical flow values are optimized for a number of iterations for each unstable frame. We utilize various loss functions in our optimization-based work. The first loss function  $Lint = (|\hat{l}i - \hat{A}1| + |\hat{l}i - \hat{A}2| + |\hat{l}i - \hat{A}3| + |\hat{l}i - \hat{A}3|)$  $|\hat{i}i - \hat{A}4|$ )/4 makes the next frame resemble interpolations sampled from various frame intervals so that it can be optimized to a suitable location for the video stream.  $Lcons = \sum_{i=1}^{n} (|xt - soft(i)|)$  is defined to reduce the blur of the image. Ltemp =  $\sum_{i=1}^{n} (|\hat{l}i - \hat{l}i - 1|)$  defines a loss function that enforces the backward accuracy of the same stream so that the stream produced for the image with Ltemp is consistent. Ltemp2 =  $\sum_{i=1}^{n} (|\hat{l}i - 1 - A(\hat{l}i - 2, \hat{l}i)|)$  forces the next frame produced as a result of optimization with Ltemp2 to also resemble the previous generated frame so that it contains less distortion. We get the result of interpolation of Îi-2, Îi frames with ABME model. Then, we define its similarity to the previous frame as a loss function. We are optimizing our work with these losses by using ADAM optimizer.

#### RESULTS AND DISCUSSION

In Table 2, we give stability scores for each iteration using the interpolation-based video stabilization method for a shaky video using ABME interpolation. For the same video, in Table 3, we reported the effectiveness of the losses we added to our flow optimization approach. In our first experiment, we run 4000 iterations and use only MSE loss with interpolation frames obtained by using ABME. In our second experiment, we used *Lint* loss and *Lcons* loss. In our results, we observed that the quality of the images, therefore, our distortion and stabilization score increased. In our third experiment, we

on Innovative Surveys in Positive Sciences 4-5 December 2022 / Full Text Book

additionally used *Ltemp*, which forces the current frames we created to be similar to the one we produced before. In the experiments we performed at four, five and six steps, we examined the effect of the newly created restriction on the total loss with the coefficients we gave. In our seventh experiment, with the frame we created by optimizing the flow at that moment, we ensured the interpolation result of the frame we created 2 steps ago to be similar to the frame we created one step ago, with *Ltemp2*. In our last experiment, we measured the effect with different coefficients. In this study, we reported that we passed the basic model with experiment eight. We report the stability scores step by step in Table 3.

ITERATI	CROPPING_RATIO	DISTORTION_V	STABILITY_SCORE(AVG,TR
ON _NO	(AVG,MIN)	ALUE	ANS,ROT)
1	1.0000   0.9892	0.9898	0.5721   0.6412   0.5029
2	1.0000   0.9825	0.9874	0.6276   0.6892   0.5660
3	1.0000   0.9759	0.9855	0.6672   0.7171   0.6173

**Table 2:** The number of iterations and stability scores for the video produced using ABME

TEST	CROPPING	DISTORTIO	STABILITY(AVG,	RESULTS
NO	(AVG, MIN)	N	TRANS, ROT)	
1	1.0000	0.9613	0.4119  0.5056	Using mse loss
	0.9497		0.3181	
2	1.0000	0.9896	0.5163   0.5655	Using Lint and Lcons
	0.9872		0.4671	
3	1.0000	0,9428	0.5547  0.5797	Using Lint and Lcons and
	0.9508		0.5298	Ltemp
4	0.9991	0.9772	0.4467  0.5164	Using Lint and Lcons and
	0.9687		0.3769	Ltemp*05
5	1.0000	0,9146	0.5892  0.6927	Using Lint and Lcons and
	0.8786		0.4856	Ltemp*10
6	0.9913	0.0246	0.6306  0.6557	Using Lint and Lcons and
	0.0235		0.6056	Ltemp*100
7	1.0000	0.9527	0.5977  0.6161	Using Lint and Lcons and
	0.9443		0.5792	Ltemp*100, Ltemp2*50
8	1.0000	0.9631	0.7850  0.8200	Using Lint and Lcons and
	0.9775		0.7500	Ltemp*100, Ltemp2*100

**Table 3:** Results of different utilized loss functions

#### **CONCLUSION**

In this paper, we proposed a novel optimization-based video stabilization approach. Unlike previous iteration-based studies, we aimed to use an interpolation method in video stabilization without the need of iterations. In the light of this motivation, we reported that our novel optimizing approach that finds intermediate frames using optimization increases the stability scores of the generated video. In our study, we also surpass the results of the baseline iteration-based study. The limitation of our method is that it has to process each video frame separately, therefore takes a longer runtime compared to alternatives. In our future work, we will try to make our approach to work in real-time.

#### REFERENCES

- 1) Park, J., Lee, C., & Kim, C. S. (2021). Asymmetric bilateral motion estimation for video frame interpolation. In *Proceedings of the IEEE/CVF International Conference on Computer Vision* (pp. 14539-14548).
- **2)** Lu, L., Wu, R., Lin, H., Lu, J., & Jia, J. (2022). Video Frame Interpolation with Transformer. In *Proceedings of the IEEE/CVF Conference on Computer Vision and Pattern Recognition* (pp. 3532-3542).

on Innovative Surveys in Positive Sciences 4-5 December 2022 / Full Text Book

- **3)** Choi, J., & Kweon, I. S. (2020). Deep iterative frame interpolation for full-frame video stabilization. *ACM Transactions on Graphics (TOG)*, 39(1), 1-9.
- **4)** Wu, Y., Wen, Q., & Chen, Q. (2022). Optimizing Video Prediction via Video Frame Interpolation. In *Proceedings of the IEEE/CVF Conference on Computer Vision and Pattern Recognition* (pp. 17814-17823).
- 5) Sun, D., Yang, X., Liu, M. Y., & Kautz, J. (2018). Pwc-net: Cnns for optical flow using pyramid, warping, and cost volume. In *Proceedings of the IEEE conference on computer vision and pattern recognition* (pp. 8934-8943).
- Niklaus, S., & Liu, F. (2020). Softmax splatting for video frame interpolation. In *Proceedings* of the IEEE/CVF Conference on Computer Vision and Pattern Recognition (pp. 5437-5446).
- **7)** Lee, Y. C., Tseng, K. W., Chen, Y. T., Chen, C. C., Chen, C. S., & Hung, Y. P. (2021). 3D Video Stabilization with Depth Estimation by CNN-based Optimization. In *Proceedings of the IEEE/CVF Conference on Computer Vision and Pattern Recognition* (pp. 10621-10630).
- **8)** Qu, H., & Song, L. (2013, September). Video stabilization with L1–L2 optimization. In *2013 IEEE International Conference on Image Processing* (pp. 29-33). IEEE.
- **9)** Wang, Y. S., Liu, F., Hsu, P. S., & Lee, T. Y. (2013). Spatially and temporally optimized video stabilization. *IEEE transactions on visualization and computer graphics*, 19(8), 1354-1361.
- **10)** Jia, C., & Evans, B. L. (2013, May). 3D rotational video stabilization using manifold optimization. In 2013 IEEE International Conference on Acoustics, Speech and Signal Processing (pp. 2493-2497). IEEE.
- **11)** Zhao, M., & Ling, Q. (2020). Adaptively meshed video stabilization. *IEEE Transactions on Circuits and Systems for Video Technology*, 31(9), 3504-3517.
- **12)** Yu, J., & Ramamoorthi, R. (2019). Robust video stabilization by optimization in cnn weight space. In *Proceedings of the IEEE/CVF Conference on Computer Vision and Pattern Recognition* (pp. 3800-3808).
- **13)** Huang, Z., Zhang, T., Heng, W., Shi, B., & Zhou, S. (2022). Real-time intermediate flow estimation for video frame interpolation. In *European Conference on Computer Vision* (pp. 624-642). Springer, Cham.
- **14)** Liu, S., Yuan, L., Tan, P., & Sun, J. (2013). Bundled camera paths for video stabilization. *ACM Transactions on Graphics (TOG)*, 32(4), 1-10.
- **15)** Liu, S., Tan, P., Yuan, L., Sun, J., & Zeng, B. (2016, October). Meshflow: Minimum latency online video stabilization. In *European Conference on Computer Vision* (pp. 800-815). Springer, Cham.

on Innovative Surveys in Positive Sciences 4-5 December 2022 / Full Text Book

## STRATEJİK KARAR VERME YAKLAŞIMIYLA DÖKME GEMİ SEÇİMİNDE YAKIT TÜKETİMİNİ ETKİLEYEN FAKTÖRLERİN BULANIK ANALİTİK HİYERARŞİ PROSESİ YÖNTEMİYLE SIRALANMASI

WITH A STRATEGIC DECISION-MAKING APPROACH, ORDERING THE FACTORS AFFECTING FUEL CONSUMPTION IN BULK CARRIER VESSEL SELECTION BY USING FUZZY ANALYTICAL HIERARCHY PROCESS METHOD

## Dilek Gedik<sup>1</sup>

<sup>1</sup>Arş. Gör., Karadeniz Teknik Üniversitesi, Sürmene Deniz Bilimleri Fakültesi, Deniz Ulaştırma İşletme Mühendisliği, Trabzon, Türkiye

## Ünal Özdemir 1002

<sup>2</sup>Doç. Dr., Mersin Üniversitesi, Denizcilik Fakültesi, Denizcilik Işletmeleri Yönetimi Bölümü, Mersin, Türkiye

## Devran Yazır 101

<sup>1</sup>Dr. Öğr. Üyesi, Karadeniz Teknik Üniversitesi, Sürmene Deniz Bilimleri Fakültesi, Deniz Ulaştırma İşletme Mühendisliği, Trabzon, Türkiye

## Yunus Emre Nazlıgül<sup>1</sup>

<sup>1</sup>Arş. Gör., Karadeniz Teknik Üniversitesi, Sürmene Deniz Bilimleri Fakültesi, Deniz Ulaştırma İşletme Mühendisliği, Trabzon, Türkiye

#### ÖZET

Ticaretin gelişmesi ile beraber deniz yoluyla taşıma faaliyetleri de doğru orantılı olarak artmaktadır. Deniz yoluyla yapılan taşımacılıkta geminin hızı, kullanılan yakıt tipi, otomasyon sistemleri, geminin makinesi, atık ısıdan geri dönüşüm, pervane çeşidi, geminin yükü, karina temizliği, baş/kıç iterler ve geminin detveyt tonajı gibi unsurlar geminin yakıt tüketimini etkileyen en önemli parametrelerdir.

Bu çalışmada uzman görüşleri alınarak belirlenen on kriterin bulanık AHP yöntemi kullanılarak sıralaması yapılmıştır. Bu sıralama geminin makinesi > geminin detveyt tonajı > geminin yükü > karina temizliği > geminin hızı > kullanılan yakıt tipi > atık ısıdan geri dönüşüm > baş/kıç iterler > pervane çeşidi > otomasyon sistemler şeklindedir.

Anahtar Kelimeler: Gemi seçimi, Yakıt tipi, Bulanık AHP, Karar verme

#### **ABSTRACT**

With the development of trade, transportation activities by seas also increase in direct proportion. Factors such as the ship's speed, the type of fuel used, the automation systems, the ship's machinery, waste heat recycling, the propeller type, the cargo type, the cleaning of the hull, the bow/stern thrusters and the deadweight tonnage of the ship are the most important parameters affecting the fuel consumption of the ship.

In this study, ten criteria determined by taking expert opinions were ranked by using fuzzy AHP method. This order is as follows: ship's machine > deadweight tonnage > cargo type > hull cleaning > ship's speed > fuel type used > waste heat recycling > bow/stern thrusters > propeller type > automation systems.

**Keywords:** Vessel selection, Type of fuel, Fuzzy AHP, Decision making

on Innovative Surveys in Positive Sciences 4-5 December 2022 / Full Text Book

## **GİRİŞ**

Deniz yolu ile yapılan taşımacılık faaliyetleri, artan insan/kaynak gereksinimlerini karşılamak için, yer ve zaman faydası sağlayacak biçimde, var olan kaynakların en etkili ve edam ettirilebilir şekilde kullanımına olanak tanımaktadır ve ekonominin ürün ve hizmet üretim sığasının arrtırılmasına katkı sağlamaktadır. (Bayraktutan ve Özbilgin, 2015).

Taşımacılık; insan, eşya gibi ihtiyaçların çeşitli vasıtalar kullanılarak bir noktadan başka noktaya ulaştırılması işidir. (Albayrak, 2011). Başka bir deyiş ile taşımacılık; alıcı ihtiyaçlarını gidermek amacıyla satılan ürünlerin, ihtiyaç duyulan kesimlere ve satış merkezlerine ulaştırılması işlemidir. (Quayle ve Bryan, 1993). Uluslararası alanda, kargo ve insan taşımak için kullanılan beş yöntem bulunmaktadır. Bunlar denizyolu, karayolu, demiryolu, havayolu, boru hattı taşımacılığıdır (Albayrak, 2011). Ulaştırma türlerinin, taşıma süresi ve maliyet açısından avantajları çeşitlilik göstermektedir. En hızlı taşımacılık türü havayolu, en yavaş taşıma türü denizyoludur. (Bayraktutan ve Özbilgin, 2015).

Şirketler kargoların tesliminde kullanılacak ulaştırma yöntemini kargonun özelliklerini, sahip olunan taşıma olanaklarını ve maliyeti göz önünde bulundurarak seçmektedirler. Bu bağlamda deniz vasıtalarının kargo ve yolcu taşıma sığasının yüksek oluşu, yol yapım ve yenileme maliyetlerinin olmayışı, kıtalararası alım ve satımın kolay olması sebebiyle denizyolu taşımacılığı yüksek ölçekli malların az maliyetle bir yerden diğer bir yere iletilmesine imkân sağlayarak diğer ulaştırma araçları arasında öne çıkmaktadır (Albayrak, 2011).

Taşımanın şeklini; kargonun fiziksel yapısı, sahip olunan taşıma imkanları, süre, taşıma maliyeti ve emniyeti belirlemektedir. Denizyolu taşımacılığı, kargonun su yolu ile bir noktadan başka bir noktaya kadar gemiler ile taşınmasıdır (Deniz, 2003). Deniz yolu taşımacılığı iki türde olmaktadır. Bunlar, Liner taşımacılık, düzenli ve sürekli biçimde hizmet sunan taşımacılık şeklidir. Bu hizmet türünde en kısa sürede en etkin taşıma esastır. İkinci olarak Tramp taşımacılık limandan limana şeklinde yapılan yük taşıma hizmeti şeklidir. Liner taşımacılıkta esas olan süre iken, tramp taşımacılıkta esas olan yüktür (Kayserilioğlu, 2004).

Günümüzde denizyolu taşımacılığındaki temel amaç deniz vasıtalarının limanda daha kısa süre harcayarak daha verimli bir şekilde kullanılmasıdır. Taşıma maliyetlerini azaltıp maksimum fayda sağlanması ise diğer amaçtır (Yeşilbağ,1999).

Yakıt giderleri, yükleme ve tahliye giderleri, limandaki giderler, kanal geçiş ücretleri, personel giderleri, gemi sigorta giderleri, yüke ait sigorta bedelleri, gemi denetim bedelleri, gemi bakım ve onarım harcamaları, kumanya ve yedek parça giderleri gibi giderler geminin temel harcamaları oluşturan maliyetlerdir (Özdemir 2009).

Yakıt giderleri, gemi sefere çıkmadığı zamanlarda minimumdadır. Ancak her zaman bir yakıt tüketimi mevcuttur. Gemilerin demirde veya limanda beklediği süre zarfında elektrik üretimi, havalandırma yapılması, ısıtma veya soğutma gibi gündelik operasyonların devamlılığı için yardımcı makinelerin çalışır durumda olması yakıt giderlerini ortaya çıkarmaktadır. Yakıt giderlerinin hesabı yapılırken, geminin yapacağı sefer ile ilgili olarak kullanım miktarının işlendiği yağ-yakıt defteri bulunmaktadır ve buraya kaydedilen yağ, su ve yakıt tüketimi ölçülerek değerlendirilmeye alınmaktadır (Saban ve Güğerçin, 2009).

Yakıt ve yağ tüketim miktarı denizyolu ile yapılan taşımacılıkta gemilerin türlerine göre değişiklikler göstermektedir, bu maliyetler bunker maliyetleri olarak da adlandırılır. Gemi yaşı, ana makinelerinin tipi, gücü ve kullanılmakta olan yakıt cinsi yakıt maliyetini etkilemektedir. Gemi seyirdeyken yakıt harcaması, gemi hızına, çevre koşullarına, makinelerin yaşına, geminin bakımına ve kaptanın, baş mühendisin ve diğer mürettebatın tecrübelerine bağlıdır. Fakat bu faktörler içerisindeki en önemli etken gemi hızıdır (Çetinkaya, 2002).

#### ARAŞTIRMA VE BULGULAR

Bir gemi tasarlanırken, gemi inşa mühendisleri tekne iskelet şekli ve makine boyutlarına bağlı olarak en uygun hızı belirler. Belirlenen bu hız, belirli bir sürede (genelde yıllık olarak) geminin hız/yakıt tüketimi verimliliğini optimum hale getiren hızdır. Bu hızın düşük veya yüksek süratle seyir yapıldığında yıllık verimlilik oranı düsecektir. Gemi yüksek hızda seyrederse, gemi karinasına deniz suyu

on Innovative Surveys in Positive Sciences 4-5 December 2022 / Full Text Book

tarafından daha fazla sürtünme uygulanacağından dolayı yakıt tüketimi artar. Çalışan bir geminin genel maliyetleri içerisinde yakıt masraflarının %32 ile %45 arasında değişiklik göstermektedir. Bu durum yakıt tüketiminde tasarrufun önemini öne çıkartır. (Stopford, 1997).

Yük gemileri, kargoya göre, sıvı yük ve kuru yük gemileri şeklinde tasarlanmaktadır (Rodrigue vd. 2006). Dökme haldeki yüklerin taşımacılığı fosfat, kömür, hurda, buğday, gübre, tuz, şeker, maden cevheri gibi kargoların taşındığı taşımacılık şeklidir. Bu gemi türleri her seferinde tüm gemi kapasitelerinde yük alabilmektedir. Dökme haldeki yüklerin taşınması, yükleme ve tahliye operasyon giderlerini en düşük seviyede tutmaktadır (Özdemir, 2009).

Gemilerin işletilebilmesi için gereken maliyetler çeşitlendirilmektedir ve bu giderlerin bir kısmı azaltılabilir bir kısmı ise sabittir. Bu amaçla gemi giderlerindeki en büyük paya sahip olan yakıt maliyetinin düşürülmesi gemi işletmecilerinin ve gemi sahiplerinin temel amaçları arasındadır.

Çalışmada yakıt tüketimini doğrudan etkileyen kriterlerin kıyaslanması amaçlanmıştır. Elde edilen literatür çalışmaları ve uzman görüşleri göz önüne alınarak yakıt tüketimini etkileyen faktörleri şu şekilde belirtilebilir; karina temizliği, geminin hızı, geminin detveyt tonajı, geminin yükü, kullanılan yakıt tipi, geminin makinesi, atık ısıdan geri dönüşüm, pervane çeşidi, baş iter, otomasyon sistemleridir.

23 uzmanın online ortamda katıldığı anketler vasıtasıyla yakıt tüketimini etkileyen 10 kriterin bulanık AHP yöntemiyle uzmanların karşılıklı olarak kıyaslanması istenmiştir. Tutarlı olarak kabul edilen 18 anket cevabının geometrik ortalaması alınarak tek bir karar verme matrisi oluşturulmuştur. Daha sonra her bir kriterin bulanık ağırlıkları hesaplanarak elde edilen kriter ağırlıkları en yüksekten en düşüğe doğru sıralanmıştır.

### **Bulanık AHP (BAHP)**

İnsanların kararlarında genellikle somut kavramlarla birlikte soyut kavramlar da etkilidir. Bu durum ortaya belirsizlikleri çıkartmaktadır. Bu belirsizlik durumunda sonuca varmak zorunda kalan kişi birçok yönteme başvurmuştur ve bulanık mantığı ileri sürmüştür. Bulanık mantık kişinin lojiğine daha yakın olması sebebiyle, bulanık mantığı üzerinde duran yöntemler uygulanarak verilen seçimler daha doğru sonuçlar ortaya çıkarmaktadır. Analitik hiyerarşik prosesi belirsizlik durumlarında karar vermek için yeteri kadar uygun olmadığı için, bulanık mantık ve AHP birleştirilerek bulanık analitik hiyerarşi prosesi ileri sürülmüştür. Karar verici genellikle kesin değerler içeren değerlendirme yapmaz ve aralıklı değerlendirme yapmayı daha güvenilir bulmaktadır (Göksu ve Güngör, 2008).

**Tablo:1** Üçgensel Bulanık Sayılar (Chan ve Kumar, 2007)

GERÇEK SAYI	ÜÇGENSEL	ÜÇGENSEL
	BULANIK SAYI	BULANIK
		SAYILARIN TERSİ
1	(1, 1, 1)	(1, 1, 1)
2	(1, 2, 3)	(1/3, 1/2, 1)
3	(2, 3, 4)	(1/4, 1/3, 1/2)
4	(3, 4, 5)	(1/5, 1/4, 1/3)
5	(4, 5, 6)	(1/6, 1/5, 1/4)
6	(5, 6, 7)	(1/7, 1/6, 1/5)
7	(6, 7, 8)	(1/8, 1/7, 1/6)
8	(7, 8, 9)	(1/9, 1/8, 1/7)
9	(8, 9, 9)	(1/9, 1/9, 1/8)

on Innovative Surveys in Positive Sciences 4-5 December 2022 / Full Text Book

#### Buckley Yaklaşımı (1985)

Buckley bu yaklaşımda bulanık ağırlıkları ve performans skorlarını ortaya çıkarabilmek için geometrik toplama metodunu kullanmıştır (Yacan, 2016). Bu metodun kullanılma amacı bulanık durumların rahatlıkla genelleştirilmesi ve karşılaştırma matrislerinde tek çözüm elde edilmesidir (Dayanandan ve Kalimuthu, 2018). Geometrik ortalama metodu ile birden fazla katılımcının olduğu anket sonuçlarını tek bir matrise indirgenmesini sağlar.

Bulanık AHP yönteminin adımları:

1.Katılımcılara ait karar matrisleri üçgensel bulanık sayılara göre hazırlandı.

$$\widetilde{A}^{k} = \begin{bmatrix} 1 & \widetilde{A}_{12} & \widetilde{A}_{1y} \\ \widetilde{A}_{21} & 1 & \widetilde{A}_{2y} \\ \vdots & \vdots & \vdots \\ \widetilde{A}_{y_{1}} & \widetilde{A}_{y_{2}} & 1 \end{bmatrix}$$

$$(1)$$

2.Ardından katılımcıların cevaplarından elde edilen tüm veriler aşağıda verilen ağırlıklı ortalama formülü ile düzenlenir (Kafalı, 2014).

$$\widetilde{A}_{xy} = \frac{z_1 A_{xy}^1 + z_2 A_{xy}^2 \cdots z_k A_{xy}^k}{z_1 + z_1 + \cdots + z_k} \tag{2}$$

3.Karar matrislerini oluşturduktan sonra her bir katılımcıya ait olan kriter ağırlıkları geometrik toplama yöntemi ile teke indirgendi.

$$\widetilde{b_1} = \left(\widetilde{a_{l1}} \otimes \widetilde{a_{l2}} \otimes \cdots \otimes \widetilde{a_{ly}}\right)^{1/y} \tag{3}$$

4.Daha sonra bulanık sayıların karşılık geldiği mutlak değerlere dönüştürülmesi ve tüm kriterler arasındaki bağıl aralıkların hesaplanması gerekir.

$$B = \frac{b_1 + b_2 + b_3}{3} \tag{4}$$

5. Elde edilen değerlerin daha iyi değerlendirilebilmesi için normalizasyon işlemi uygulandı.

$$\left(w_i^R\right)^N = \frac{w_i^N}{\sum_{i=1}^n w_i^N} \tag{5}$$

## **SONUÇ**

Gemilerin yakıt tüketimini etkileyen birçok faktör vardır ve bu faktörlerin değerlendirilmesine yönelik literatürde birçok çalışma mevcuttur. Bu çalışmada, yakıt tüketimini doğrudan etkileyen kriterlerin kıyaslanması amaçlanmıştır. Elde edilen literatür çalışmaları ve uzman görüşleri göz önüne alınarak yakıt tüketimini etkileyen faktörleri şu şekilde belirtilebilir; Karina temizliği, Geminin hızı, Geminin detveyt tonajı, Geminin yükü, Kullanılan yakıt tipi, Geminin makinesi, Atık ısıdan geri dönüşüm, Pervane çeşidi, Baş iter, Otomasyon Sistemleri. 23 uzmanın online ortamda katıldığı anketler vasıtasıyla yakıt tüketimini etkileyen 10 kriterin bulanık AHP yöntemiyle uzmanların karşılıklı olarak kıyaslanması istenmiştir. Tutarlı olarak kabul edilen 18 anket cevabının geometrik ortalaması alınarak tek bir karar verme matrisi oluşturulmuştur. Daha sonra her bir kriterin bulanık ağırlıkları hesaplanarak elde edilen kriter ağırlıkları en yüksekten en düşüğe doğru sıralanmıştır. Kriter ağırlıklarının sıralaması; Geminin makinesi (K6)> Geminin detveyt tonajı (K3)> Geminin yükü (K4)> Karina temizliği (K1)> Geminin hızı (K2)> Kullanılan yakıt tipi (K5)> Atık ısıdan geri dönüşüm (K7)> Baş iter (K9)> Pervane çeşidi (K8)> Otomasyon sistemler (K10) elde edilmiştir.

#### **KAYNAKÇA**

Albayrak, B. (2011). Denizyolu taşımacılığında muhasebe düzeni ve yük taşıma maliyetlerinin muhasebeleştirilmesi, (Yüksek Lisans Tezi). Marmara Üniversitesi Sosyal Bilimler Enstitüsü, İstanbul.

on Innovative Surveys in Positive Sciences 4-5 December 2022 / Full Text Book

Bayraktutan, Y. ve Özbilgin, M. (2015). Uluslararası ve yurtiçi ticarette taşıma türlerinin payı: bir analitik hiyerarşi prosesi (ahp) uygulaması. *Çankırı Karatekin Üniversitesi Sosyal Bilimler Enstitüsü Dergisi*, 6(2): 405-436.

Chan, F.T.S. and Kumar, N. (2007). Global supplier development considering risk factors using fuzzy extended AHP-based approach. *OMEGA 35*, 417–431.

Çetinkaya, Ö. (2002). *Tanker İşletmeciliğinde Sefer Maliyet Analizi*. (Bitirme Projesi). İstanbul Üniversitesi, Mühendislik Fakültesi, Deniz Ulaştırma İşletme Mühendisliği, İstanbul.

Dayanandan, U. and Kalimuthu, V. (2018). Software architectural quality assessment model

for security analysis using fuzzy analytical hierarchy process (FAHP) method. 3D Research Center, 9(31), 1-14.

Deniz, R. (2003). Gemi işletmeciliği, acentelik, brokerlik, İstanbul: Akademi Denizcilik, s.452.

Göksu, A. ve Güngör, G. (2008). Türkiye'de eğitimin finansmanı ve ülkelerarası bir karşılaştırma, *Celal Bayar Üniversitesi İ.İ.B.F. dergisi*, 20(1), 59-72.

Kafalı, M. (2014). *Gemi inşa sanayinde bulanık karar verme uygulamaları*, (Yüksek Lisans Tezi), Karadeniz Teknik Üniversitesi, Fen Bilimleri Enstitüsü, Trabzon.

Kayserilioğlu, E. (2004). Deniz taşımacılığı sektör profili. İstanbul: İstanbul Ticaret Odası Yayınları.

Özdemir, Ö. (2009). *Denizyolu yük taşımacılığında maliyetler ve bir uygulama*, (Doktora Tezi). İstanbul Üniversitesi, Sosyal Bilimler Enstitüsü, İşletme Anabilim Dalı Muhasebe Bilim Dalı, İstanbul.

Quayle R.M. ve Bryan J. (1993), Logistics: an integrated apporach, *Newcastle: Tudorbusiness Publishing*, s.87.

Rodrigue, J.J., Slack, B. and Comtois, C. (2006). *The geography of transport systems*, New York: Routledge.

Saban, M. ve Güğerçin, G. (2009). Deniz taşımacılığı işletmelerinde maliyetleri etkileyen faktörler ve sefer maliyetleri. *DEÜ Denizcilik Dergisi*, *Cilt.1*, *Sayı.1*.

Stopford, M. (1997). Maritime Economics. London: Routledge.

Yeşilbağ, L., Akdoğan, A.İ. ve Ünsan Y. (1999). Ro-Ro taşımacılığının ülkemiz deniz ulaştırma sektöründeki yeri, Gemi İnşaatı ve Deniz Teknolojisi Teknik Kongresi 99-Bildiri Kitabı, İstanbul: *Yaklaşım*, 1999, s.411.

Yacan, İ. (2016). Eğitim kalitesinin belirlenmesinde etkili olan faktörlerin bulanık AHP ve bulanık TOPSIS yöntemi ile değerlendirilmesi, (Yüksek Lisans Tezi), Pamukkale Üniversitesi, Sosyal Bilimler Enstitüsü, Denizli, Türkiye.

on Innovative Surveys in Positive Sciences 4-5 December 2022 / Full Text Book

## DENİZCİLİK EĞİTİMİNDE OYUNLAŞTIRMA METODOLOJİSİNİN KULLANIMI ÜZERİNE DOĞAL DİL İŞLEME (NLP) TEKNİKLERİYLE BİR LİTERATÜR TARAMASI ÖRNEĞİ

AN EXAMPLE OF LITERATURE REVIEW WITH NATURAL LANGUAGE PROCESSING (NLP) TECHNIQUES ON THE USE OF GAMIFICATION METHODOLOGY IN MARITIME EDUCATION

## Emin Serkan ERDÖNMEZ<sup>1</sup>

<sup>1</sup>Dokuz Eylül Üniversitesi, Denizcilik Fakültesi, İzmir, Türkiye <sup>1</sup>ORCID ID: 0000-0003-3200-1561

## Cenk ŞAKAR<sup>2</sup>

<sup>2</sup>Dokuz Eylül Üniversitesi, Denizcilik Fakültesi, İzmir, Türkiye <sup>2</sup>ORCID ID: 0000-0001-5821-6312

#### ÖZET

Günümüzde teknolojinin gelişmesi, eğitim ve öğretim sürecine dair farklı tekniklerin kullanılmasına ön ayak olmuştur. Denizcilik eğitiminde verimliliği artırmaya yönelik çalışmalar kapsamında son dönemde yenilikçi oyunlaştırma tekniklerinin ağırlık kazandığı görülmektedir. Oyunlaştırma, eğitim motivasyonu üzerindeki etkisinin fark edilmesi ile daha da önemli hale gelmiştir. Yenilikçi oyunlaştırma araçları olarak simülatörler, sanal ve artırılmış gerçeklik teknolojileri örnek gösterilebilir. Bu çalışmada "Maritime Education" ve "Gamification" anahtar kelimeleriyle literatür taraması yapılmış ve son 5 yılda yazılmış 20 makale rastgele seçilmiştir. Daha sonra seçilen 20 makale üzerinde Doğal Dil İşleme (NLP) teknikleri uygulanmıştır. Doğal Dil İşleme, bilgisayarların dili insanlara benzer şekilde kullanılmasına yönelik çalışmaların yürütüldüğü ve dil bilimi, bilgisayar bilimi gibi disiplinlerin bir arada çalıştığı yapay zekanın bir alt alanıdır. Temel amacı, çalışılan dilin bağlamsal nüansları da dahil olmak üzere, belgelerin içeriğini anlayabilen bir bilgisayar yazılımı ortaya koymaktır. Makalelerin analizinde ise konu modelleme yöntemi kullanılmıştır. Konu modelleme, büyük verileri otomatik olarak organize etmek, anlamak, aramak, özetlemek ve kesfedilen temalara göre sınıflandırmak için kullanılmaktadır. Özellikle büyük hacimli metinlerden gizli konuları çıkarmak için oldukça sık kullanılan bir tekniktir. Konu modelleme algoritmalarından bir olan Latent Dirichlet Allocation (LDA) algoritması, Türkçe'siyle "Gizli Dirichlet Ayırımı" (GDA) algoritması, konu modelleme algoritmaları arasında sadeliği ve kullanım kolaylığı yönünden öne çıkmaktadır. Doğal dil işlemede GDA, "Naive Bayes" teoremini esas alan ve hangi kelimenin hangi dokümanda hangi konuyu temsil ettiğini tahmin etmeye calısan bir denetimsiz sınıflandırma modelidir. Kısaca gözlemlenmeyen gruplar aracılığıyla bir dizi gözlemi açıklayan üretken bir istatistiksel algoritmadır. Belirlenen makaleler ilk aşamada GDA Algoritması kullanılarak kendi içinde incelenmiş ve makalenin içeriği otomatik olarak tespit edilmiştir. Sonraki süreçte seçilen bütün makaleler bir arada yorumlanarak denizcilik eğitiminde oyunlaştırma ile ilgili yapılan araştırmaların ne yönde eğilimi olduğu ile ilgili değerlendirmelerde bulunulmuştur.

**Anahtar Kelimeler:** Denizcilik Eğitimi, Oyunlaştırma, Doğal Dil İşleme, Gizli Dirichlet Ayırımı, Konu Modelleme

#### **ABSTRACT**

Today, the development of technology has led to the use of different techniques in the education and training process. Within the scope of efforts to increase efficiency in maritime education, it's seen that innovative gamification techniques have gained weight recently. Gamification has become even more important with the realization of its effect on educational motivation. Simulators and virtual and augmented reality technologies can be given as examples of innovative gamification tools. In this study,

on Innovative Surveys in Positive Sciences 4-5 December 2022 / Full Text Book

a literature review was conducted with the keywords "Maritime Education" and "Gamification" and 20 articles written in the last 5 years were randomly selected. Then, Natural Language Processing (NLP) techniques were applied to 20 selected articles. Natural Language Processing is a sub-field of artificial intelligence in which studies are carried out for computers to use language in a similar way to humans and disciplines such as linguistics and computer science work together. Its main purpose is to produce computer software that can understand the content of documents, including the contextual nuances of the studied language. The subject modeling method was used in the analysis of the articles.. Topic modeling is used to automatically organize, understand, search, summarize and categorize big data according to the themes discovered. It is a very common technique to extract hidden topics, especially from big datas. The Latent Dirichlet Allocation (LDA) algorithm, which is one of the topic modeling algorithms, stands out among the topic modeling algorithms in terms of simplicity and ease of use. In Natural Language Processing, LDA is an unsupervised classification model that is based on the "Naive Bayes" theorem and tries to predict which word represents which subject in which document. In short, it is a generative statistical algorithm that describes a set of observations through unobserved groups. The determined articles were examined in themselves using the GDA Algorithm at the first stage and the content of the article was determined automatically. In the next process, all the selected articles were interpreted together and evaluations were made about the tendency of the research on gamification in maritime education.

**Keywords:** Maritime Education, Gamification, Natural Language Processing, Latent Dirichlet Allocation, Topic Modeling

## 1. GİRİŞ

Değişen ekonomik, küresel, teknolojik ve işgücü piyasası sorunlarıyla karşı karşıya kalan günümüz eğitim kurumları, işgücünü eğitmek, ilham vermek, motivasyonu artırmak ve sürdürmek için etkili ve verimli eğitim programları ve araçları geliştirmek gibi zorlu bir görevle karşı karşıyadırlar.

Eğitim kurumları bu sorunları aşmak adına çeşitli adımlar atmakta ve genel olarak dijital çözümlere başvurmaktadırlar. Günümüzde eğitim sürecinde kullanılan geleneksel araçlar belirli bir seviyede kabul görmüş ve halihazırda kullanılmaktadır. Fakat yeni teknolojilerin ortaya çıkışı ve rekabetçi toplum şartları gibi ana etmenler, eğitim sürecine de doğrudan etki etmekte ve olumlu katkılar sağlamaktadır. Bu kapsamda günümüzde kendini kabul ettirmiş veya ettirmekte olan eğitsel teknolojilere örnek olarak bilgisayarlar, simülatörler, akıllı tahtalar ve projektörler gösterilebilir. Bunlara ek olarak nispeten daha yeni olan sanal ve artırılmış gerçeklik teknolojileri de örnek gösterilebilir.

Dijital eğitim çözümleri birçok avantajı beraberinde getirmektedir. Örneğin yeni yeni kendine yer edinmeye başlayan sanal gerçeklik (VR) ve artırılmış gerçeklik (AR) gibi eğitsel araçlar, denizci öğrencilerin bir dizi senaryoyu gerçek gemi şartlarına benzer şekilde uygulayabilecekleri ve anında geri bildirim alarak hatalarından ders çıkarabilecekleri etkileşimli ve deneyimsel bir eğitime izin verir. Ayrıca, zaman ve yer kısıtlamalarını ortadan kaldırarak öğrenmeyi herkes için, her yerde ve her zaman mümkün kılar.

Öğrencilerin ders çalışma motivasyonunu artırma ve sürdürülebilir olmasını sağlamak adına birçok araştırma yapılmış ve birçok girişimde bulunulmuştur. Kendini kanıtlamış modern motivasyon araçlarından biri de oyunlaştırmadır teknikleridir. Oyunlaştırma yaklaşımı, öğretme ve öğrenmeyi daha ilginç ve etkili hale getirmek için oyun öğelerini kullanma fikrini ön planda tutmaktadır. Oyun uygulamalarının ve mekanizmalarının oyun dışı bir bağlamda kullanarak öğrencileri problem çözümüne dahil edilir.

Bu çalışmada öncelikle denizcilik eğitimindeki trendlerden ve oyunlaştırma kavramından bahsedilmiş ve bu iki husus ile ilgili son 5 yılda yapılan çalışmalar baz alınarak bir literatür taraması yapılmıştır. Daha sonra belirli kriterlere göre elde edilen toplam 20 adet araştırma makalesi elde edilmiştir. Bu 20 makale üzerinde doğal dil işleme teknikleri ile, otomasyon olacak şekilde bir yazılım vasıtasıyla konu analizi yapılmıştır. Elde edilen sonuçlara göre denizcilik eğitiminde oyunlaştırma yöntemlerinin ne gibi kullanım alanları olduğu, nasıl bir ağırlığa sahip olduğu ve denizcilik eğitiminde yönelimlerin hangi yönde olduğu gibi konulara cevap aranmıştır.

on Innovative Surveys in Positive Sciences 4-5 December 2022 / Full Text Book

## 2. ARAŞTIRMA VE BULGULAR

Çalışmamızın temel amacı, oyunlaştırma yaklaşımı temelinde denizcilik eğitiminde kullanılan yöntemleri belirlemek ve bu konudaki yönelimleri yakalamaktır. Denizcilik eğitiminde oyunlaştırma metodolojisinin ne oranda ve ne amaçlarıyla kullanıldığına dair bilimsel veri elde edilmesi maksadıyla literatür taraması yapılmıştır. Daha sonra elde edilen araştırma makaleleri doğal dil işleme (NLP) teknikleri incelenmiştir. Programlama Dili olarak Python kullanılmıştır.

Literatür taramasında ise sistematik derleme yöntemi tercih edilmiştir. Sistematik derleme, belli bir konuda hazırlanmış araştırma sorusuna yanıt bulmak için, belirlenmiş kriterlere uygun olarak o alanda yayınlanmış orijinal çalışmaların sistemli ve yan tutmadan taranması, bulunan çalışmaların geçerliğinin değerlendirilmesi ve sentezlenerek birleştirilmesidir. Bu maksatla alanında uzman olan kişiler tarafından, önceden belirlenen bir yöntemi kullanan çok sayıda araştırma incelenerek kapsamlı bir sentezi yapılır.

Sistematik derlemenin aşamaları şu şekilde sıralanır. Konunun belirlenmesi, önceden belirlenmiş kaynaklardan tarama yapılması, elde edilen makalelerin değerlendirilmesi ve analizi, sonuçların özetlenmesi ve derlenmesi ve son olarak da yayın kısmından oluşmaktadır (Karaçam, 2013).

Bu duruma uygun olarak literatür taraması için kullanılacak öncelikle konu belirlenmiş ve müteakiben Scopus Veri Tabanı, kullanılacak platform olarak seçilmiştir. Bu veri tabanı üzerinde "Maritime Education" ve "Gamification" / "Game" olmak üzere seçilen 2 anahtar kelimenin bütün kombinasyonları ile tarama yapılmış ve 20 adet yayın seçilmiştir. Tablo-1'de seçilen yayınlar ve yayın tarihi beraber gösterilmiştir.

Tablo 1. Seçilen Makaleler ve Yayın Tarihleri.

Makale	Makale Adı	Yayın
Nu		Tarihi
1	The Use Of Digital Escape Room in Educational Electronic Environment Of	2020
	Maritime Higher Education Institutions	
2	A Preliminary Design Of A 3d Maritime Gamified Mentoring Platform To	2022
	Support Tanker Pre-Vetting Inspection Training: 'Maritime Gamentor'	
3	Human Factors Assessment in VR-based Firefighting Training in Maritime: A	2020
	Pilot Study	
4	Preconceptions Towards Gamifying Work A Thematic Analysis Of Responses	2021
	Of A Maritime Logistics Organization	
5	Finger Tracking And Hand Recognition Technologies İn Virtual Reality	2020
	Maritime Safety Training Applications	
6	Gamification In Freight Transportation: Extant Corpus And Future Agenda	2021
7	Experimental Research On The Formation Of Future Ship Engineers'	2020
	Communicative Competence Based On Gamification Approach	
8	Maritime Safety Edcuation With VR Technology (MarSEVR)	2019
9	Virtual Reality Enhances Safety Training İn The Maritime İndustry: An	2022
	Organizational Training Experiment With A Non-Weird Sample	
10	The Continuum Of Simulator-Based Maritime Training And Education	2021
11	Impact of Simulation Fidelity on Student Self-Efficacy and Perceived Skill	2019
	Development in Maritime Training	
12	Computerized Adaptive Testing İn Educational Electronic Environment Of	2020
	Maritime Higher Education Institutions	
13	Rethinking Maritime Education, Training, and Operations in the Digital Era:	2019
	Applications for Emerging Immersive Technologies	
14	Simulation-Based Training with Gamified Components for Augmented Border	2022
	Protection	

on Innovative Surveys in Positive Sciences 4-5 December 2022 / Full Text Book

15	Neural Network Driven Eye Tracking Metrics and Data Visualization in	2022
	Metaverse and Virtual Reality Maritime Safety Training	
16	Application Of VR Technologies İn Building Future Maritime Specialists'	2021
	Professional Competences	
17	An Analytical Game For Knowledge Acquisition for Maritime Behavioral	2020
	Analysis Systems	
18	Future Of Maritime Education And Training: Blending Hard And Soft Skills	2020
19	Augmented Reality Model Framework for Maritime Education to Alleviate the	2020
	Factors Affecting Learning Experience	
20	Maritime Technology and the Industrial Revolution	2020

Seçilen araştırma makalelerinde Latent Dirichlet Allocation (LDA), Türkçe'si ile Gizli Dirichlet Ayrımı kullanılarak konu modellemesi (topic modelling) yapılmıştır. Konu modelleme bir metnin içerisindeki konu (topic) olarak geçen kelime gruplarını bulmak için kullanılan gözetimsiz bir makine öğrenmesi algoritmasıdır (Xing ve Croft, 2006). Gözetimsiz bir yöntem olduğundan etiketli verilere ihtiyaç duymaz. Bu durumda modeller doğrudan metinlere uygulanabilir.

Belirtilen bu kelime grupları, sıklıkla beraber kullanılan ve genellikle ortak bir temayı paylaşan kelimelerden oluşmaktadır. Konular, bir metni açıklayan ve tanımlayabilen anahtar kelimeler olarak düşünülebilir. Konu modelleme kümelemeye benzer şekilde, sayısal metrik hesaplamaları (Öklid, Manhattan vb.) kullanarak bir metin içeriğinde yer alan doğal konu gruplarını bulan ve bir araya getiren istatistiksel algoritmalardır.

Kısacası konu modelleme metinlerin içeriğindeki saklı anlamsal bağları araştıran istatistiksel bir metin madenciliği yöntemidir. Bu yönüyle büyük metinlerin organizasyonu, basite indirgenmesi ve özetlenmesi maksadıyla sık sık kullanılmakta ve önemi de gün geçtikçe artmaktadır.

Konu modelleme ve konu sınıflandırma farklı kavramlardır. Konu sınıflandırması gözetimli bir öğrenme algoritması iken konu modellemesi gözetimsiz bir öğrenme algoritmasıdır. Literatürde sık olarak kullanılan konu modelleme tekniklerinden bazıları sunlardır.

- Gizli Anlamsal Analiz (Latent Semantic Analysis LSA)
- Olasılıksal Gizli Anlamsal Analiz (Probabilistic Latent Semantic Analysis PLSA)
- Gizli Dirichlet Ayrımı (Latent Dirichlet Allocation LDA)
- İlişkisel Konu Modeli (Correlated Topic Model CTM)
- Yapısal Konu Modeli (Structural Topic Model STM)

Gizli Dirichlet Ayrımı'nda, her konunun altta yatan bir kelime kümesinin bir karışımı olduğunu ve her belgenin bir dizi konu olasılığının bir karışımı olduğunu varsayan üretken bir olasılık modelidir.

Belirli kriterlere göre elde edilen araştırma makaleleri otomasyon olacak şekilde aşağıdaki 6 aşamadan geçmiştir:

- Araştırma makalesinin uygun formatta programa yüklenmesi
- Araştırma makalesinin özetten başlayacak şekilde ve kaynakça yer almadan sadece sonuç kısmını kapsayacak şekilde kırpılması ve düz metin haline getirilmesi
- Düz metnin Doğal Dil İşleme teknikleri ile işlenmesi
- Keşifsel Veri Analizi ile metnin ön analizi
- Metnin Gizli Dirichlet Ayırımı (Latent Dirichlet Allocation LDA) analizi için uygun formata sokulması
- LDA modelinin eğitimi ve metnin modele sokulması

Tablo-1'de yer alan araştırma makaleleri sırası ile yukarıda belirtilen aşamaları içeren yazılıma sokulduğunda 3 farklı çıktı verecektir. Örnek olarak Tablo-1'de ilk sırada yer alan arastırma

on Innovative Surveys in Positive Sciences 4-5 December 2022 / Full Text Book

makalesinin çıktıları aşağıdaki gibi olacaktır. İlk olarak araştırma makalesinin kaç sayfadan ibaret olduğu çıktı olarak alınır.

• Total number of pages: 13

Daha sonra her bir makaleyi açıklayan 10 konu ve bu 10 konuyu en iyi açıklayan 15 adet kelime grubu önem sırasına göre çıktı alınır.

- (0, '0.060\*"use" + 0.049\*"professional" + 0.043\*"gamification" + 0.031\*"technology" + 0.027\*"competence" + 0.027\*"education" + 0.024\*"competency" + 0.024\*"environment" + 0.019\*"module" + 0.019\*"information" + 0.019\*"electronic" + 0.019\*"learning" + 0.019\*"game" + 0.018\*"development" + 0.018\*"english"')
- (1, '0.034\*"educational" + 0.034\*"possibility" + 0.018\*"place" + 0.018\*"fig" + 0.018\*"using" + 0.018\*"formation" + 0.018\*"analysis" + 0.018\*"create" + 0.018\*"see" + 0.018\*"possible" + 0.018\*"list" + 0.018\*"image" + 0.018\*"consider" + 0.018\*"received" + 0.018\*"multiple")
- (2, '0.047\*"educational" + 0.035\*"gamification" + 0.029\*"education" + 0.029\*"using" + 0.024\*"method" + 0.024\*"modern" + 0.024\*"content" + 0.023\*"higher" + 0.022\*"technology" + 0.021\*"maritime" + 0.018\*"material" + 0.018\*"electronic" + 0.017\*"virtual" + 0.012\*"year" + 0.012\*"research")
- (3, '0.071\*"virtual" + 0.055\*"educational" + 0.053\*"process" + 0.038\*"use" + 0.037\*"world" + 0.037\*"environment" + 0.036\*"reality" + 0.034\*"allow" + 0.020\*"task" + 0.020\*"answer" + 0.020\*"create" + 0.020\*"short" + 0.020\*"type" + 0.020\*"question" + 0.020\*"onto"')
- (4, '0.040\*"learning" + 0.034\*"moodle" + 0.034\*"task" + 0.027\*"lm" + 0.027\*"educational" + 0.021\*"using" + 0.021\*"process" + 0.021\*"type" + 0.021\*"electronic" + 0.020\*"gamification" + 0.020\*"activity" + 0.014\*"ship" + 0.014\*"allows" + 0.014\*"level" + 0.014\*"study")
- (5, '0.041\*"fig" + 0.041\*"education" + 0.041\*"higher" + 0.033\*"question" + 0.028\*"increase" + 0.028\*"competence" + 0.028\*"marine" + 0.028\*"level" + 0.018\*"type" + 0.014\*"wa" + 0.014\*"first" + 0.014\*"according" + 0.014\*"time" + 0.014\*"communicative" + 0.014\*"one")
- $\bullet \qquad (6, \ '0.040*"task" \ + \ 0.034*"room" \ + \ 0.034*"escape" \ + \ 0.027*"process" \ + \ 0.027*"ship" \ + \ 0.021*"information" \ + \ 0.021*"knowledge" \ + \ 0.021*"quality" \ + \ 0.021*"result" \ + \ 0.021*"cadet" \ + \ 0.021*"solving" \ + \ 0.021*"crossword" \ + \ 0.019*"one" \ + \ 0.016*"moodle" \ + \ 0.016*"lm"')$
- $\bullet \qquad (8, \ '0.061*"room" \ + \ 0.047*"escape" \ + \ 0.040*"professional" \ + \ 0.040*"maritime" \ + \ 0.023*"quest" \ + \ 0.023*"competence" \ + \ 0.019*"form" \ + \ 0.016*"code" \ + \ 0.016*"competency" \ + \ 0.016*"example" \ + \ 0.016*"future" \ + \ 0.016*"security" \ + \ 0.016*"wa" \ + \ 0.014*"activity" \ + \ 0.012*"learning"')$
- $\bullet \qquad (9, \ '0.059*"drop" + 0.051*"drag" + 0.049*"task" + 0.034*"room" + 0.034*"text" + 0.034*"image" + 0.026*"escape" + 0.026*"testing" + 0.024*"type" + 0.022*"question" + 0.017*"allows" + 0.017*"result" + 0.017*"emergency" + 0.017*"use" + 0.017*"taken")$

Nihai olarak araştırma makalesini en iyi tanımlayan konuların indeks numarası ve metni açıklama yüzdesi çıktı olarak alınır.

• [(0, 0.19892353), (2, 0.15165219), (3, 0.011904528), (4, 0.12152975), (5, 0.011683416), (6, 0.12372445), (7, 0.034983397), (8, 0.25028265), (9, 0.087492906)]

Elde edilen sonuçlara göre bu araştırma makalesini tanımlayan en iyi kelime grupları yaklaşık %25 ağırlığı ile 8 numaralı indeks grubu ve yaklaşık %20 ağırlığı ile 0 numaralı indeks grubudur. Bahse konu bu gruplarda yer alan kelimeler incelendiğinde araştırma makalesinin içeriği ile genel olarak bir fikir

on Innovative Surveys in Positive Sciences 4-5 December 2022 / Full Text Book

elde edilebilir. Nitekim ilgili kelimeler incelendiğinde bu araştırma makalesinin denizcilik eğitiminde profesyonel kaçış odalarının kullanımıyla ilgili bir içeriğe sahip olduğu anlaşılabilir.

Şekil-1'de belirtilen bu kelime gruplarının görselleştirmesi bulunmaktadır. Örnek olarak seçilen 1 numaralı konunun içerdiği kelimelerin önem sırasına göre dizilimi görülmektedir. Şeklin sol tarafında bulunan panel konu dağılımını içerir. Bu konular baloncuklar şeklinde temsil edilir. Balon ne kadar büyük olursa, belgelerdeki konu o kadar sık olur. Az sayıda konuya sahip bir konu modelinde, grafik boyunca dağılmış, üst üste binmeyen büyük baloncuklar bulunurken, çok sayıda konuya sahip konu modelinde, grafikte kümelenmiş, üst üste binen birçok küçük boyutlu baloncuk olacaktır. Konular arasındaki mesafe, konular arasındaki anlamsal ilişkinin bir tahminidir. Şekil-1'in sağ tarafındaki kelime sırasında mavi renkler konulardaki kelimelerin sıklık dağılımını gösterir. Kırmızı renkler ise bir konu verilen her kelimenin sıklığını tanımlar.

**Şekil 1.** 1 numaralı konu ve kelimelerinin ilgi düzeylerine göre sıralanması.

Yukarıda belirtilen şekilde toplam 20 adet araştırma makalesinin her biri incelenmiştir. Araştırma makaleleri ve bu makaleleri en iyi temsil eden kelime grupları Tablo-2'de gösterilmiştir.

Tablo 2. Seçilen Makaleleri Açıklayan En İyi Kelimeler.

Makale Nu	Makaleyi Açıklayan Kelime Grupları
1	room, escape, professional, maritime, quest, competence, form, code, competency, example, future, security, activity, learning, use, professional, gamification, technology, education, environment, modüle, information, electronic, learning, game, development, english
2	design, maritime, game, modüle, serious, ship, gamentor, tanker, study, preliminary, sire, training, model, group, platform, domain, development, literatüre, methodology, sgdm, educational

on Innovative Surveys in Positive Sciences 4-5 December 2022 / Full Text Book

3	system, vr, evaluation, paid, attention, task, training, user, emotion, experience, questionnaire, performance, feedback, induced, stress, trainee, real, world, situation, fire, demanding, event, similar, hypothesized
4	work, gamification, mindtrek, employee, gamifying, preconception, study, aim, towards, motivating, interviewee, task, affordances, gamification, motivation, expressed, research, example, related, organizational
5	technology, tracking, recognition, hand, finger, vr, reality, virtual, marsevr, maritime, computer, eye, research, safety, training, ocean, strategy, safety, learning, immersive, development, green, cost, environmental, sea
6	game, perceived, point, challenge, currency, virtual, experience, roleplay, cooperation, positive, outcome, narrative, result, reality, learning, transportation, freight, research, study, gamified, gamification, intervention, affordances, motivational, literatüre, practical, search, area
7	communicative, competence, gamification, english, approach, language, purpose, education, ship, formation, engineer, model, future, seafarer, problem, maritime, professional, forming, foreign, collision, technology, modern, skill, practice
8	training, industry, safety, shipping, technology, trainee, challenge, practice, simulator, education, simulation, maritime, system, method, change, effective, operation, marsevr, simulation, watch, procedure, simulator
9	vr, training, simulation, learning, personal, trainer, safety, study, reflection, group, risk, significantly, maritime, vrbased, nonweird, research, value, related, realistic, standard, sample, according
10	training, maritime, trainee, practice, skill, simulator, assessment, education, use, regarding, covid, learning, simulatorbased, instructor, bridge, analysis, type, cloudbased, well, physical, vr, learning, ship, reality
11	simulator, vr, fidelity, study, concept, training, high, room, desktop, immersion, education, found, engine, student, traditional, skill, based, immersive, perceived, task, development, participant, using
12	testing, adaptive, control, student, question, knowledge, test, learning, method, level, use, new, process, result, figure, ship, future, engineer, approach, competence, method, communicative, modern, teaching, professional, generalization, theoretical, scientific, analysis, data
13	technology, ar, mr, vr, training, operation, student, learning, simulator, new, maritime, met, industry, application, method, traditional, facility, technology, instructor, economic, maritime, seafarer, ship, throughout, including
14	training, system, project, event, user, scenario, developed, aresibo, based, message, capability, solution, end, cmre, gamified, game, serious, modüle, feature, gamification, simulation, train, simulator, trial, developed
15	eye, cognitive, data, metric, visualization, tracking, task, load, training, workload, imotions, vr, analysis, virtual, tracking, reality, eye, technology, science, safety, cognitive, movement, training, hand, metaverse, network, neural, data
16	maritime, training, education, specialist, future, international, technology, new, simulatorbased, course, group, method, develop, based, professional, competence, vr, environment, simulator, building, simulation, result, skill, potential, state
17	game, knowledge, maritime, acquisition, marisa, network, bayesian, surveillance, used, analytical, analysis, design, use, behavioral, probability, iqr, network, probability, expert, subdimension, experiment, structure, stated, support, result
18	knowledge, skill, need, teaching, triangle, method, maritime, demand, party, process, different, within, system, development, traditional, process, learning, set, problem, critical, related, research, allows, professional, decisionmaking, effective

on Innovative Surveys in Positive Sciences 4-5 December 2022 / Full Text Book

19	strategy, multimedia, preferred, learning, simulation, handson, denotes, simulator, material, platform, better, mean, course, show, questionnaire, student, ar, course, use, knowledge, session, every, time, make, need, different
20	ai, data, iot, innovation, artificial, thing, intelligence, technology, example, mariner, machine, learning, empower, computer, explore, innovation, utilizing, ship, thing, framework, internet, industry, information, industrial, advance, sailor, automation, part, checking

Tablo-2 genel olarak incelendiğinde "maritime", "training", "education", "gamification" ve "game" ve türevleri kelimelerin sıklıkla tabloda geçtiği görülmektedir. "Maritime Education" ve "Gamification" anahtar kelimeleri ile araştırma makalelerini seçtiğimiz göz önünde bulundurulursa bu durumun normal olduğu kabul edilebilir. Ayrıca bir makaledeki anahtar kelimeleri o makaleyi temsil ettiği düşünüldüğünde yazılımın bu anahtar kelimeleri otomatik olarak bulması bir başarı kriteri olarak değerlendirilebilir.

Bir başka husus ise yazılım toplam 20 araştırma makalesinin 10'unda "vr", "reality", "virtual", "ar" ve "mr" gibi birbirleriyle ilişkili kelimeler geçmektedir. Artırılmış Gerçeklik (AR), Sanal Gerçeklik (VR) ve Karma Gerçeklik (MR) teknolojileri gün geçtikçe hayatımızda yer edinmekte ve günlük yaşantımızdaki araçlara adapte olmaktadırlar. Bir dakika içinde yazılımın 20 araştırma makalesini analiz edip bu trendi yakalamış olması bilgisayarların önemini göz önüne sermektedir.

Ek olarak her bir makalenin temasına göre kelimelerin yakalandığı görülmektedir. Örneğin 20. makale kısaca denizcilikteki gelişmeler ve endüstri 4.0'ın etkilerini incelemektedir. Oluşturulan yazılım da bu duruma paralel olarak yazılımda kelime grupları bulmuştur. Yine aynı şekilde 15 numaralı makalede yapay sinir ağı ve sanal gerçeklik destekli deniz güvenliği eğitimleri hakkında bilgi vermektedir. Kullandığımız yazılımda bu duruma uygun kelimeler türetmiştir.

## 3. SONUÇ

Büyük veri kavramının hayatımıza girmesi ve yer edinmesi ile büyük veriyi hızlı ve etkili bir şekilde anlama çalışmaları da hızlanmıştır. Bu çalışmada nispeten toplu olarak büyük veri sayılabilecek 20 adet araştırma makalesinin doğal dil işleme teknikleri konu modelleme için uygun formata sokulmuştur. Daha sonra yazılım sayesinde bir dakikadan kısa süre içerisinde analizi yapılmıştır. Elde edilen bulguların yüksek doğruluk oranı, hacimli metinlerin içeriğini yansız bir şekilde anlamayı kolaylaştırmıştır.

Gizli Dirichlet Ayrımı, konu modelleme için en sık kullanılan yöntemlerden biridir. GDA genel konu modelleme görevleri için çok uygun olsa da, daha gelişmiş veri ilişkilerini modelleme yeteneğine sahip değildir. Ayrıca metinler yeterli uzunlukta olmadığında düşük performans göstermektedir. Bu durum araştırmalar için bir kısıtlama oluşturmaktadır. Örneğin 2-3 cümleden oluşan bir metnin GDA ile analizi doğru sonuçlar vermeyecektir.

Büyük verinin her geçen gün çeşitlenmesi ve öneminin artmasına paralel olarak yeni konu modelleme tekniklerinin ortaya çıkması ve var olan tekniklerin çeşitli genişletilmiş sürümleri ortaya çıkmıştır. Metin madenciliği, biyomedikal araştırma, duygu analizi, konuşma teknolojisi, görüntü işleme, gibi birçok alanda konu modellemesi teknikleri kullanılmakta ve ileride de artan önemine binaen daha fazla kullanılm alanı bulacağı değerlendirilmektedir.

#### 4. KAYNAKÇA

Voloshynov, S. A., Popova, H. V., Yurzhenko, A. Y., & Shmeltser, E. O. (2020). The Use Of Digital Escape Room In Educational Electronic Environment Of Maritime Higher Education Institutions.

Gürbüz, S. C. & Çelik M. (2022): A Preliminary Design of a 3D Maritime Gamified Mentoring Platform to Support Tanker Prevetting Inspection Training: 'Maritime Gamentor', *Ships and Offshore Structures*, DOI: 10.1080/17445302.2022.2133878

on Innovative Surveys in Positive Sciences 4-5 December 2022 / Full Text Book

Y. Liu et al., "Human Factors Assessment in VR-Based Firefighting Training in Maritime: A Pilot Study," 2020 International Conference on Cyberworlds (CW), 2020, pp. 157-163, doi: 10.1109/CW49994.2020.00034.

Wallius E., Klock A. C. T., Eronen V., and Hamari J. (2021). Preconceptions Towards Gamifying Work: A Thematic Analysis of Responses of a Maritime Logistics Organization. *24th International Academic Mindtrek Conference (Academic Mindtrek '21)*, 128–133. https://doi.org/10.1145/3464327.3464368

E. Markopoulos, P. Markopoulos, N. Laivuori, C. Moridis and M. Luimula, "Finger tracking and hand recognition technologies in virtual reality maritime safety training applications," (2020) 11th IEEE International Conference on Cognitive Infocommunications (CogInfoCom), 2020, pp. 000251-000258, doi: 10.1109/CogInfoCom50765.2020.9237915.

Klock, A. C. T., Wallius, E., & Hamari, J. (2021). Gamification in freight transportation: extant corpus and future agenda. *International Journal of Physical Distribution & Logistics Management*, *51*(7), 685-710.

Sherman, M., & Yurzhenko, A. (2020). Experimental research on the formation of future ship engineers' communicative competence based on gamification approach. *Educational Dimension*, *55*(3), 251–266. https://doi.org/10.31812/educdim.v55i0.3939

Markopoulos, Evangelos & Lauronen, Jenny & Luimula, Mika & Lehto, Pihla & Laukkanen, Sami. (2019). Maritime Safety Education with VR Technology (MarSEVR). https://doi.org/10.1109/CogInfoCom47531.2019.9089997.

Makransky, Guido & Klingenberg, Sara. (2022). Virtual Reality Enhances Safety Training in the Maritime Industry: An Organizational Training Experiment with a non-WEIRD sample. *Journal of Computer Assisted Learning*. https://doi.org/38. 10.1111/jcal.12670.

Kim, Te., Sharma, A., Bustgaard, M. et al. (2021). The continuum of simulator-based maritime training and education. *WMU J Marit Affairs* 20, 135–150 https://doi.org/10.1007/s13437-021-00242-2

Renganayagalu, S. K., Mallam, S., Nazir, S., Ernstsen, J., Hogström, P. (2019). Impact of Simulation Fidelity on Student Self-efficacy and Perceived Skill Development in Maritime Training. *TransNav, the International Journal on Marine Navigation and Safety of Sea Transportation*. *13*. https://doi.org/663-669. 10.12716/1001.13.03.25.

Diahyleva, O. S., Gritsuk, I. V., Kononova, O. Y., & Yurzhenko, A. Y. (2021). Computerized adaptive testing in educational electronic environment of maritime higher education institutions. CEUR Workshop Proceedings.

Mallam, S. C., Nazir, S., & Renganayagalu, S. K. (2019). Rethinking Maritime Education, Training, and Operations in the Digital Era: Applications for Emerging Immersive Technologies. *Journal of Marine Science and Engineering*, 7(12), 428. https://doi.org/10.3390/jmse7120428

Paliokas, I., Patenidis, A. T., Mitsopoulou, E. E., Tsita, C., Pehlivanides, G., Karyati, E., Tsafaras, S., Stathopoulos, E. A., Kokkalas, A., Diplaris, S., Meditskos, G., Vrochidis, S., Tasiopoulou, E., Riggas, C., Votis, K., Kompatsiaris, I., & Tzovaras, D. (2020). A Gamified Augmented Reality Application for Digital Heritage and Tourism. *Applied Sciences*, *10*(21), 7868. https://doi.org/10.3390/app10217868

Markopoulos, E., Luimula, M., Calbureanu-Popescu, C., Markopoulos, P., Ranttila, P., Laukkanen, S., Laivuori, N., Ravyse, W., Saarinen, J., & Nghia, T. (2021). Neural Network Driven Eye Tracking Metrics and Data Visualization in Virtual Reality Maritime Safety Training.

Renganayagalu, S. K. (2019). Virtual Reality as a future training medium for seafarers: potential and challenges.

de Rosa, F., & De Gloria, A. (2020). An Analytical Game for Knowledge Acquisition for Maritime Behavioral Analysis Systems. *Applied Sciences*, 10(2), 591. https://doi.org/10.3390/app10020591

de Água, P. M. G. B., da Silva Frias, A. D., Carrasqueira, M. D. J., & Daniel, J. M. M. (2020). Future of maritime education and training: blending hard and soft skills. *Pomorstvo*, 34(2), 345-353.

on Innovative Surveys in Positive Sciences 4-5 December 2022 / Full Text Book

Balcita, R. & Palaoag, T. (2020). Augmented Reality Model Framework for Maritime Education to Alleviate the Factors Affecting Learning Experience. International Journal of Information and Education Technology. 10. https://doi.org/603-607. 10.18178/ijiet.2020.10.8.1431.

Reni, A., Hidayat, S., Bhawika, G. W., Ratnawati, E., & Nguyen, P. T. (2020). Maritime technology and the Industrial Revolution. *Journal of Environmental Treatment Techniques*, 8(1), 250-253.

Hu, Y., Boyd-Graber, J., Satinoff, B. *et al.* Interactive topic modeling. *Mach Learn* 95, 423–469 (2014). https://doi.org/10.1007/s10994-013-5413-0

Karaçam, Z. (2013). Sistematik Derleme Metodolojisi: Sistematik Derleme Hazırlamak İçin Bir Rehber . *Dokuz Eylül Üniversitesi Hemşirelik Fakültesi Elektronik Dergisi* , *6 (1)*, *26-33*. Retrieved from https://dergipark.org.tr/tr/pub/deuhfed/issue/46815/587078

Xing W. & W. B. C. (2006). LDA-Based Document Models For Ad-Hoc Retrieval. *Annual International ACM SIGIR Conference On Research And Development In Information Retrieval (SIGIR '06)*. Association for Computing Machinery, New York, NY, USA, 178–185. https://doi.org/10.1145/1148170.1148204

Kaya, A., & GÜLBANDILAR, E. (2022). Konu Modelleme Yöntemlerinin Karşılaştırılması. *Eskişehir Türk Dünyası Uygulama ve Araştırma Merkezi Bilişim Dergisi*, *3*(2), 46-53.

Duğan, Ö. (2022). Dijital Çağda Öğrenme Aracı Olarak Oyunlaştırmanın Sağlık Okuryazarlığı Üzerindeki Rolü . *TRT Akademi*, 7 (14) , 262-285 . DOI: 10.37679/trta.960815

Aydın, S. C. & Baştuğ, S. (2021). Denizcilik Eğitiminde Oyunlaştırma Üzerine Derleme Türünde Literatür Çalışması . *Journal of Maritime Transport and Logistics*, 2 (1) , 28-35 . Retrieved from https://dergipark.org.tr/tr/pub/mtl/issue/60384/810368

on Innovative Surveys in Positive Sciences 4-5 December 2022 / Full Text Book

# HISTOMORPHOMETRIC EVALUATION OF THE EFFECTS OF CAPSAICIN APPLICATION ON SMALL INTESTINE OF RATS

## KAPSAİCİN UYGULAMASININ SIÇANLARIN İNCE BAĞIRSAK DOKUSUNA ETKİLERİNİN HİSTOMORFOMETRİK DEĞERLENDİRİLMESİ

#### Buket Bakır

Assoc. Prof. Dr., Tekirdag Namik Kemal University, Faculty of Veterinary Medicine, Department of Histology and Embriyology

ORCID ID: 0000-0003-3637-3688

#### Ebru Karadağ Sarı

Prof. Dr., Kafkas University, Faculty of Veterinary Medicine, Department of Histology and Embriyology

The present study was summarized from a PhD thesis.

#### ABSTRACT

Hot pepper, which has a very old history and is used as a spice. It has started to be used in the field of medicine today. Capsaicin is colorless, odorless, hydrophobic and is the active ingredient that gives hot pepper its bitterness. In studies conducted with capsaicin today, it has been shown that the effect of capsaicin varies according to the application dose, organ and duration of use. In this study, it was aimed to histomorphometrically evaluate PDGF-C (Platelet Derived Growth Factor-C) and PDGFR- $\alpha$  (Platelet Derived Growth Factor receptor- $\alpha$ ) immunoreaction intensities and villus length/crypt depth ratio between groups in intestinal tissues of rats treated with Capsaicin.

Thirty Spraque dawley female rats were divided into 3 groups with 10 in each group. Group 1 (subcutaneous drug administration) were injected subcutaneously daily by adding 1 mg/kg capsaicin, dissolved in 10% ethanol, and then adding 1% Tween 20 and 80% distilled water. Group 2 (oral drug administration), 1 mg/kg capsaicin was added to the rats' water. Group 3 (subcutaneous sham administration); The mixture containing 10% ethanol, 1% Tween 20 and 80% distilled water was injected subcutaneously every day for a week with the help of an insulin injector according to the weight of the animal.Intensity of PDGF-C and PDGFR- $\alpha$  immunoreactivity and the ratio of villus length/crypt depth in per unit area were compared histomorphometrically between the groups. Streptavidin-Biotin-Peroxidase Complex Method was used to compare the PDGF-C and PDGFR- $\alpha$  immunoreaction intensities in the small intestine. Crossman's triple staining was applied to the ratio of villus length to crypt depth.

As a result of statistical analysis, it was determined that capsaicin increased intensities of immunoreaction of PDGF-C and PDGFR- $\alpha$  in duodenum, jejunum, ileum and villus length/crypt depth. From this study, it can be concluded that capsaicin can increase the absorption of nutrients and has positive effects on growth.

**Key words:** Capsaicin, PDGF-C, PDGFR-α, Small Intestine

\*Doktora tezinden üretilmiştir.

#### ÖZET

Çok eski geçmişe sahip olan ve baharat olarak kullanılan acı biber günümüzde tıp alanında da kullanılmaya başlanmıştır. Kapsaisin, renksiz, kokusuz, hidrofobik özellikte olup acı bibere acılığını

on Innovative Surveys in Positive Sciences 4-5 December 2022 / Full Text Book

veren etken maddesidir. Günümüzde kapsaisinle yapılan çalışmalarda kapsaisinin etkisinin uygulama dozuna, organa ve kullanım süresine göre değiştiği bildirilmiştir. Bu çalışmada Kapsaisin uygulanan sıçanların bağırsak dokularında PDGF-C (Platelet Kaynaklı büyüme Faktörü-C) ve PDGFR-α (Platelet Kaynaklı Büyüme Faktörü reseptörü- α) immunoreaksiyon şiddetleri ve gruplar arasında villus uzunluğu/kript derinliği oranı histomorfometrik olarak değerlendirilmesi amaçlanmıştır.

30 adet Spraque dawley ırkı dişi sıçanlar her grupta 10 adet olacak şekilde 3 gruba ayrıldı. Grup 1'de (subkutan uygulama yapılan) bulunan sıçanlara 1 mg/kg kapsaicin, % 10 ethanol içinde çözdürüldükten sonra % 1 Tween 20 ve % 80 distile su ilave edilerek günlük olarak subkutan yolla enjekte edildi. Grup 2 (oral yolla uygulama yapılan), 1 mg/kg kapsaisin sıçanların içtikleri suya ilave edildi. Grup 3 (subkutan sham); % 10 ethanol, % 1 Tween 20 ve % 80 distile su içeren karışım hayvanın ağırlığına göre insulin enjektörü yardımıyla bir hafta süre ile her gün subkutan yolla enjekte edildi. Birim alanda gruplar arasında PDGF-C ve PDGFR-α salınım şiddeti ve villus uzunluğunun/kript derinliğine oranı histomorfometrik olarak karşılaştırıldı. İnce bağırsak dokusunda PDGF-C ve PDGFR-α immunoreaksiyon şiddetlerinin karşılaştırması amacıyla immünohistokimyasal (Streptavidin-Biotin Peroxidase Complex) boyama ve villus uzunluğunun/kript derinliğine oranı için Crossman'nın üçlü boyama yöntemi uygulandı.

İstatistiksel analizler sonucunda, kapsaisin uygulamasının duodenum, jejenum ve ileumda PDGF-C ve PDGFR-α salınım şiddetlerini ve villus uzunluğu/kript derinliğini arttırdığı tespit edildi. Bu çalışmadan kapsaisinin besinlerin emilimini arttırabildiği ve büyüme üzerinde olumlu etkilere sahip olduğu sonucuna varılabilir.

**Anahtar kelimeler:** Kapsaicin, PDGF-C, PDGFR-α, İnce bağırsak

#### INTRODUCTION

Capsaicin is the active principle in hot peppers Capsicum, and as such it is an important ingredient of the spicy foods typical of tropical regions. Capsicum fruits contain about 0.1 to 1% of capsaicin. Capsaicin forms colorless platelets which have an intensely burning taste (threshold - 10 ppm), melt at 63 to 65°C, and boil at 210 to 220°C (Monsereenusorn et al., 1982). Capsaicin and other members of the group of Capsaicinoids produce a large number of physiological and pharmacological effects such as effects on the gastrointestinal system (Surh and Lee, 1995).

The PDGF family is probably one of the best studied growth factor systems. The PDGF family consists of five members; PDGFAA, PDGF-BB, PDGF-AB, PDGF-CC, and PDGF-DD (Li et al., 2001). PDGF-C has significant functions such as in cell reproduction, wound healing, organ remodeling, and development of both embryonic and adult tissues (Deuel F.,1987). Platelet-derived growth factor receptor- $\alpha$  (PDGFR- $\alpha$ ) is a member of the PDGF receptor family (Heldin and Westermark 1999).

Actually the crypt-villus is the main functional unit of absorption in the rat's small intestine. All of the absorptive and also a part of the digestive capacity of the small intestine occur around and near villi and crypts (Kitt et al., 2001). Histomorphometric analysis is greatly used in studies about gastrointestinal systems. The availability of animal models and using morphometric analysis as a quantitative assessment have facilitated evaluating the morphological alterations of intestinal mucosa under various experimental conditions such as special diets and drugs (Gulbinowicz et al., 2004).

#### MATERIALS AND METHODS

#### **Animals**

All experiments were approved by the Kafkas University Institutional Animal Care and Use Committee protocol (KAÜ-HADYEK 11.06.2009/04). Thirty (50-day-old) female Sprague Dawley rats were randomly divided into three groups: group 1 (n = 10) (subcutaneous drug administration), group 2 (n = 10) (oral drug administration), and group 3 (n = 10) (subcutaneous sham administration). Rats were housed in a continuously ventilated room at a mean temperature of  $22 \pm 2$  °C with a lighting period of 12 h dark and 12 h light. Animals were fed standard rodent chow (Bayramoğlu, Erzurum, Turkey) and water ad libitum. The amount of capsaicin used in our study was based on studies conducted by Moran

on Innovative Surveys in Positive Sciences 4-5 December 2022 / Full Text Book

et al 2003., and Tütüncü, 2009. For the rats in group 1, 1 mg/kg capsaicin (cat no. M 2028, Sigma-Aldrich, Germany) was dissolved in 10% ethanol and mixed with 1% Tween 20 (cat no. M 8170772100, Merck, USA) and 80% distilled water.

## **Experimental design**

Capsaicin solution was freshly prepared according to daily body weights of the rats and injected subcutaneously with an insulin injector at the same time every day for a week.

For the rats in group 1 (n = 10) (subcutaneous drug administration), 1 mg/kg capsaicin (cat no. M 2028, Sigma-Aldrich, Germany) was dissolved in 10% ethanol and mixed with 1% Tween 20 (cat no. M 8170772100, Merck, USA) and 80% distilled water. Capsaicin solution was freshly prepared according to daily body weights of the rats and injected subcutaneously with an insulin injector at the same time every day for a week. For the rats in group 2 (n = 10) (oral drug administration), 1 mg/kg capsaicin was dissolved in 10% ethanol and mixed with 1% Tween 20 and 80% distilled water. Capsaicin solution was freshly prepared according to daily body weights of the rats and added to their drinking water. For the rats in group 3 (subcutaneous sham administration), a solution of 10% ethanol, 1% Tween, and 80% distilled water was injected subcutaneously as described previously.

All rats were weighted daily before injection and oral administration of solutions. After 1 week, all rats were sacrificed under diethyl ether anesthesia and small intestine samples (duodenum, jejunum, and ileum) were taken.

## Histological procedure

Samples were fixed in 10% formalin for 24 h, and then routine procedures were applied and samples were embedded in paraffin. Serial sections of 5  $\mu$ m thick were sliced from paraffin-embedded blocks and Crossman's triple staining method was used to demonstrate them general structure of the small intestine.

#### Immunohistochemical method

The streptavidin biotin peroxidase complex (strepABC) method was applied to investigate PDGF-C and PDGFR-α immunoreactivity in the small intestine. Sections of 5 μm thickness were collected on adhesive slides. Sections were processed in citrate buffer solution (ph 6.0) for 10 min in a microwave oven at 700 watts. Then, tissues incubated in 3% hydrogen peroxide (H<sub>2</sub>O<sub>2</sub>) for 10 min. Sections were incubated with polyclonal goat anti-PDGF-C antibody (sc-18228, Santa Cruz Laboratories, Santa Cruz, CA, USA) diluted 1:50 in PBS and polyclonal rabbit anti-PDGFR-α antibody (sc-338, Santa Cruz Laboratories) diluted 1:400 in PBS. Sections were incubated with biotinylated goat antirabbit and rabbit antigoat IgG for 30 min and peroxidaseconjugated streptavidin (1:300) (P0397; Dako Corp., Carpinteria, CA, USA) for 30 min. 3,3'-Diaminobenzidine tetrahydrochloride (0.5 mg/mL; Dako Corp.) was used as chromogen followed by hematoxylin counterstaining. Sections were mounted with ImmunoMount and examined by light microscope (Olympus BX51, Tokyo, Japan). Rabbit serum without primer antibody served as the negative control. Immunostaining intensity of PDGF-C and PDGFR-α immunoreactive cells were evaluated in four different cross-sections and by two different researchers.

#### **Histomorphometric evaluations**

Villus height, crypt depth were determined in five villi chosen randomly from six sections taken serially from the duodenum, jejunum, and ileum of each animal. Villus height was measured from the tip of the villus to the villus-crypt junction by using  $10\times$  objective, crypt depth was determined by measuring the distance between edges of crypts with  $10\times$  objective (Bakir and Karadag Sari, 2015). The intensity of immunohistochemical staining was examined using light microscopy at X400 magnification. Semiquantitative scoring was performed to determine the intensity of the reaction of cells (-) negative, (+) very slight, (++) slight, (+++) moderate, (++++) intensive, or (+++++) very intensive immunolabeling. PDGF-C and PDGFR- $\alpha$  immunoreactivity were analysed according to graded the intensity of the reaction in five sections chosen from 20 villi, cyrpt and goblet cells in doudenum.

## **Statistical Analysis**

on Innovative Surveys in Positive Sciences 4-5 December 2022 / Full Text Book

Statistical analyses were performed with SPSS (Version 20.0; Chicago, IL). Data were examined for normality distribution and variance homogeneity assumptions (Shapiro-wilk test). If normally distributed, a One-way ANOVA test was applied, and the differences between groups were analyzed with the post-hoc Tukey's test. The differences were considered significant at P < 0.05, and the means and standard errors were calculated. In the study, nonparametric tests were used as the data did not provide normal assumptions. Therefore, the differences between the groups were analyzed with Kruskal Wallis and Mann Whitney U tests. Additionally, the differences were considered significant at p < 0.05, and the median values (minimum - maximum) were calculated.

#### **RESULTS**

## Villus height to crypt depth ratio

According to our findings, villus height to crypt depth ratio was increased significantly in group 1 and 2 as compared to group 3 in the duodenum, jejenum and ileum (p < 0.05). When compared the villus height to crypt depth ratio was increased in group 1 compared to the group 2 and also the villus height to crypt depth ratio was the greatest group 1 compared with all groups. All data are shown in Figure 1.

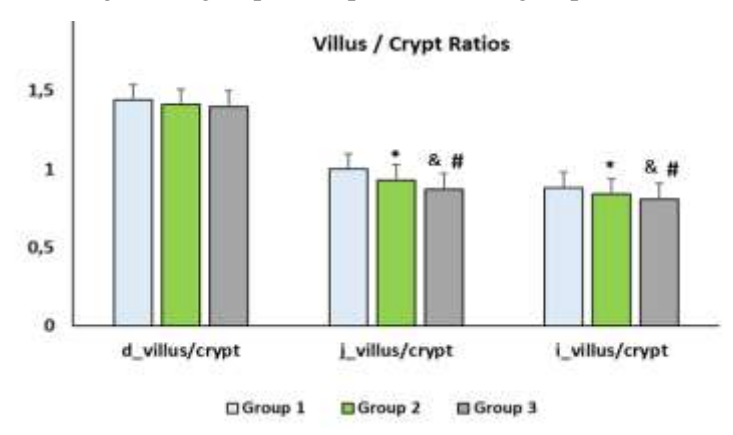


**Figure 1.** The villus height /crypt depth ratios in duodenum (d), jejenum (j) and ileum (i) in all groups. \* P < 0.05; Group 2 versus Group 1, # P < 0.05; Group 3 versus Group 1, & P < 0.05; Group 3 versus Group 2

#### **Intensity of PDGF-C immunoreactivity**

It was observed that intensity of PDGF-C immunoreactivity in goblet cells significant increased in group 1 and group 2 compared with group 3 (P < 0.05) but not significant in villus and crypts cells in duodenum. When all groups were compared in terms of intensity of PDGF-C in jejenum and ileum, an increase in villus, crypts and goblet cells were observed in group 1 and 2 compared to group 3. When all groups were compared there was a significant increase in group 1 compared to others (P < 0.05). All data of PDGF-C intensity are shown in Figure 2.

on Innovative Surveys in Positive Sciences

4-5 December 2022 / Full Text Book

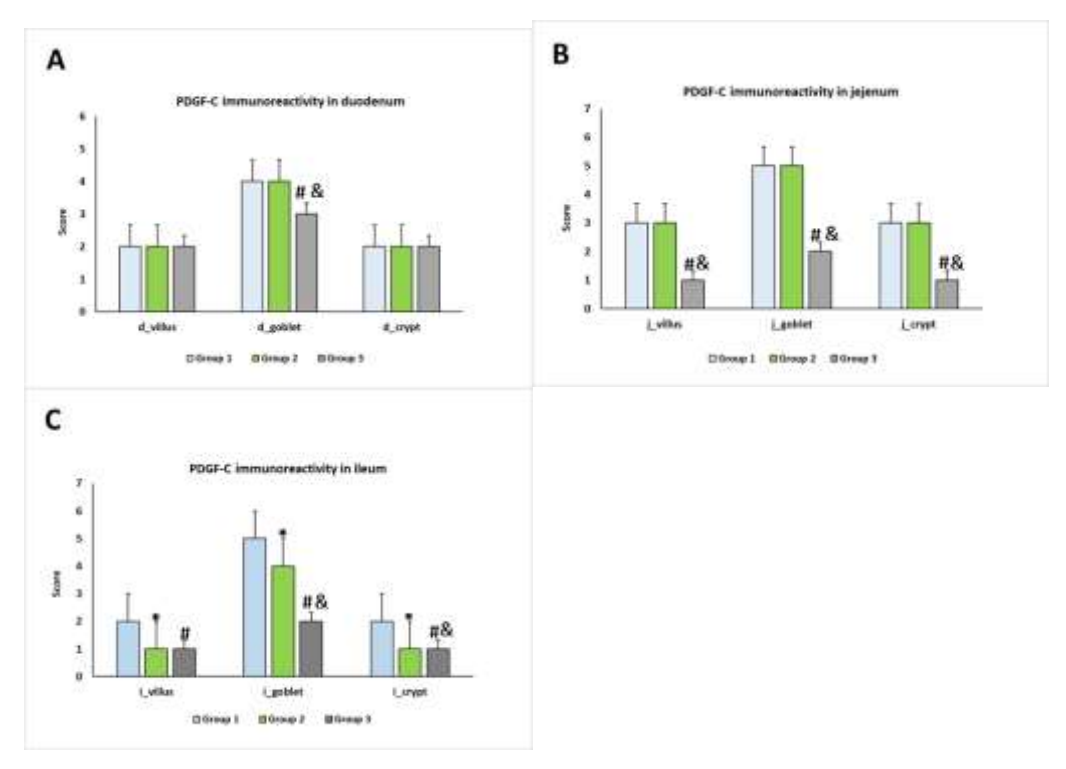
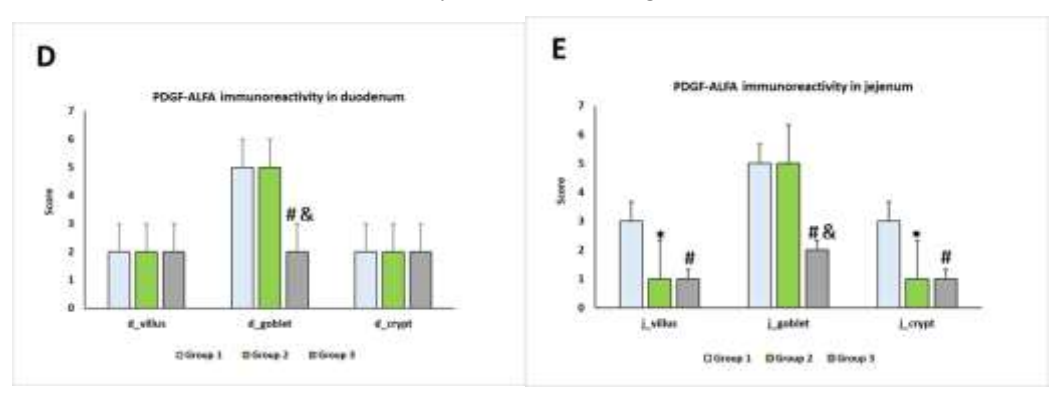


**Figure 2.** Intensity of PDGF-C immunoreactivity scores in duodenum (A), jejenum (B) and ileum (C) in all groups. PDGF-C immunreactivity All data are presented as the median (min-max). (\*): P < 0.05; group 2 versus group 1, (#): P < 0.05; Group 3 versus group 1, (&): P < 0.05; Group 3 versus Group 2.

## Intensity of PDGFR-a immunoreactivity

When all groups were compared in terms of intensity of PDGFR- $\alpha$  immunoreactivity in doudenum, it was observed a significant increase intensity in goblet cells of group 1 and 2 (P<0.05). But it was determined similar intensity of PDGFR- $\alpha$  in villus and crypts cells of all groups. It was observed that intensity of PDGFR- $\alpha$  increased the most in group 1 in villus, goblet and crypts cells of jejenum and ileum. All data of PDGFR- $\alpha$  intensity are shown in Figures 3.



on Innovative Surveys in Positive Sciences 4-5 December 2022 / Full Text Book

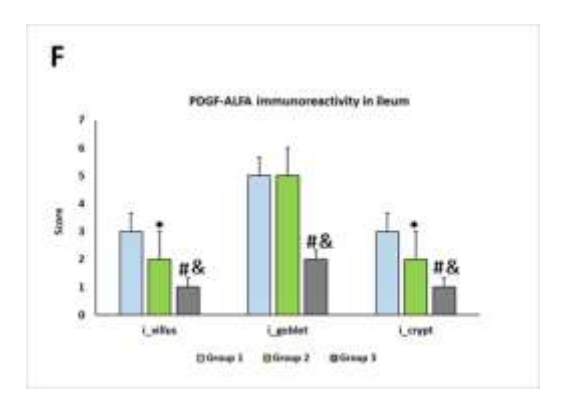


**Figure 3.** Intensity of PDGFR- $\alpha$  immunoreactivity scores in duodenum (A), jejenum (B) and ileum (C) in all groups. All data are presented as the median (min-max). (\*): P < 0.05; group 2 versus group 1, (#): P < 0.05; Group 3 versus group 1, (&): P < 0.05; Group 3 versus Group 2.

#### DISCUSSION

In this study, we set out to investigate the effect of capsaicin, which is known to have a long-standing history and a wide area of use, especially spices and the medical field, on the distribution of PDGF-C and PDGFR- $\alpha$  in the small intestines.

The morphology of small intestine is considered as the main indicator of normal gut histology. A part of the functional status of the small intestine is defined by villus height and crypt depth (Laudadio et al., 2012). A higher villus height to crypt depth ratio results in a decreased turnover of the intestinal mucosa. A slower turnover rate of the intestinal epithelium leads to a lower maintenance requirement and finally can result in a higher growth efficiency of the animal (Van et al., 2005). Overall it can be said that villus height, crypt depth and the ratio of villus height to crypt depth are considered as a criterion to reflect the small intestine morphology and absorption capacity (Montagne et al., 2003). Therefore, an increase in villus height, villus height to crypt depth ratio or decrease in the crypt depth is correlated with an improvement in the digestion and absorption of nutrients. In our study, the villus height to crypt depth ratio was significantly increased in subcutaneous capsaicin administration group (group 1) and oral capsaicin administration group (group 2) compared to sham group. Since the duodenum, jejunum and ileum are the most important absorptive parts, it may be concluded that the capsaicin has a better effect on the absorption of the nutrients.

Platelet-derived growth factor (PDGF) was identified more than three decades ago. The currently known PDGF genes and polypeptides belong to a family of structurally and functionally related growth factors including also the vascular endothelial growth factors (VEGFs) (Fredriksson et al., 2004). PDGFR- $\alpha$  is expressed in mesenchymal cells. Particularly strong expression of PDGFR- $\alpha$  has been noticed in subtypes of mesenchymal progenitors in lung, skin, and intestine and in oligodendrocyte progenitors (Kaetzel D.M.2003).

It was reported that both PDGF-A and PDGFR- $\alpha$  were necessary for development of the gastrointestinal system, and release of these factors was necessary in villus and crypt epithelial cells, the submucosa, and muscles. Even though expression details of PDGF/PDGFR- $\alpha$  signals could not be explained in adult gastrointestinal tissue (Chan et al., 2010). PDGF-C and PDGFR- $\alpha$  immunoreactivity was present in villus and crypt epithelial cells, goblet cells, vascular endothelial cells, and smooth muscle cells in the tissue of the small intestine (Bakir and Karadag Sari, 2015). In the study conducted the intensity of PDGF-C and PDGFR- $\alpha$  release increased more in the capsaicin-administered groups compared to the sham group.

The present study concluded that capsaicin administration increased the ratio of villus height to crypt depth and showed an increasing effect on growth by increasing intensity of PDGF-C and PDGFR- $\alpha$  release villus and crypt and goblet cells.

#### Acknowledgment

The present study was summarized from a PhD thesis.

on Innovative Surveys in Positive Sciences 4-5 December 2022 / Full Text Book

#### REFERENCES

Bakir B., Karadag Sari E., (2015). Immunohistochemical distribution of platelet-derived growth factor-C and plateletderived growth factor receptor- $\alpha$  in small intestine of rats treated with capsaicin. Turk J Vet Anim Sci., 39: 160-167.

Chan F., Liu Y., Sun H., Li X., Shang H., Fan D., An J., Zhou D., (2010).Distribution and possible role of PDGF-AA and PDGFR-α in the gastrointestinal tract of adult guinea pigs. Virchows Arch 457: 381–388.

Deuel F., (1987). Polypeptide growth factors: roles in normal. Annu Rev Cell Biol., 3: 443-492.

Eriksson U., (2000). PDGF-C is a new protease-activated ligand for the PDGF alpha-receptor Nat. Cell Biol., 2 (5):302-309.

Fredriksson L., Li H., Eriksson U., (2004). The PDGF family: Four gene products form five dimeric isoforms. Cytokine Growth Factor Rev. 15:197–204.

Gulbinowicz M., Berdel B., Wójcik S., et al., (2004). Morphometric analysis of the small intestine in wild type mice C57BL/6L — a developmental study. Folia Morphol. 63(4): 423–430.

Heldin CH., Westermark B., (1999). Mechanism of action and in vivo role of platelet-derived growth factor. Physiol Rev 79: 1283–1316.

Kaetzel D.M., (2003). Transcription of the platelet-derived growth factor A-chain gene. Cytokine Growth Factor Rev.14:427–446.

Kitt SJ., Miller PS., Lewis AJ., (2001). Factors affecting small intestine development in weanling pigs. Nebraska Swine Report. 33–35.

Laudadio V., Passantino L., Perillo A., et al., (2012). Productive performance and histological features of intestinal mucosa of broiler chickens fed different dietary protein levels. Poult Sci. 91(1): 265-270,

Li X., Ponten A., Aase K., Karlsson L., Abramsson A., Uutela M., Backstrom G., Hellstrom M., Bostrom H., Li H., Soriano P., Betsholtz C., Heldin C.H., Alitalo K., Ostman A., Kitt SJ., Miller PS., Lewis AJ., (2001). Factors affecting small intestine development in weanling pigs. Nebraska Swine Report., 33–35.

Monsereenusorn Y., Kongsamut S., Pezalla P.D., (1982). CAPSAICIN - A LITERATURE SURVEY. CRC Critical Reviews in Toxicology. 10:321-339.

Montagne L., Pluske JR., Hampson DJ., (2003). A review of interactions between dietary fibre and the intestinal mucosa, and their consequences on digestive health in young non-ruminant animals. Anim Feed Sci Technol. 108(1-4): 95–117

Moran C., Morales L., Razo RS., Apolonio J., Quiroz U., Chavira R., Dominguez R., (2003). Effects of sensorial denervation induced by capsaicin injection at birth or on day three of life, on puberty, induced ovulation and pregnancy. Life Sci., 73: 2113–2125.

Surh YJ., Lee SS., (1995). Capsaicin, double-edged sword: toxicity, metabolism, and chemo preventive potential. Life Sci. 56: 1845–1855.

Tütüncü S., (2009). Immunohistochemical expression of VR1 in ovaries of capsaicin treated rats during development. PhD, Uludağı University, Bursa, Turkey.

Van Nevel CJ., Decuypere JA., Dierick NA., et al., (2005). Incorporation of galactomannans in the diet of newly weaned piglets: effect on bacteriological and some morphological characteristics of the small intestine. Arch Anim Nutr. 59(2): 123–138, d

on Innovative Surveys in Positive Sciences 4-5 December 2022 / Full Text Book

## ECONOMIC ANALYSIS OF SOLAR POWER PLANT FOR MERSİN PROVINCE MERSİN İLİ İÇİN GES SANTRALİNİN EKONOMİKLİK ANALİZİ

## Seren Geçgel<sup>1</sup>

<sup>1</sup>Mersin University, Engineerin Faculty, Mechanical Engineering, Turkiye, Mersin. <sup>1</sup>ORCID ID: 0000-0001-7277-7650

#### Fatih Ünal<sup>2</sup>

<sup>2</sup> Mersin University, Engineerin Faculty, Mechanical Engineering, Turkiye, Mersin.

<sup>2</sup> ORCID ID: 0000-0001-6660-9984

## **ABSTRACT**

Nowadays, a large part of the energy used to meet the increasing living standards and the energy needs of the increasing population; fossil resources such as coal, oil and natural gas. Fossil fuels used with increasing energy demand cause air pollution, global warming and acid rain. Fossil fuels used today are getting depleted and replaced by renewable energy. There are renewable energy sources that can be used as an alternative to fossil fuels to meet the world's energy needs. These renewable energy sources are cleaner, cheaper and harmless than fossil fuels. Solar energy is one of the renewable energy sources. Turkey is a country that meets most of its energy needs from fossil fuels and is dependent on foreign sources for energy supply. For this reason, the country should reduce its dependence on fossil fuels by turning to renewable energy sources to protect its economic and strategic interests and meet its increasing energy needs. Turkey is in a geographically advantageous position to benefit from solar energy, which is renewable energy. Turkey's current potential position should be evaluated very well for renewable energy. In this context, in this study the annual energy yield of the solar power plant established in Mersin Tarsus District, which is located in the Mediterranean region and receives a high amount of solar radiation annually, and the cost and economic analysis of the solar power plant were examined.

**Keywords:** Solar energy, Renewable energy, Solar Power Plant, Mersin

#### ÖZET

Günümüzde artan yaşam standartları ve artan nüfusun enerji ihtiyacını karşılamak için kullanılan enerjinin büyük bir kısmını; fosil kaynaklar olan kömür, petrol ve doğalgaz oluşturmaktadır. Artan enerji ihtiyacı ile kullanılan fosil yakıtlar hava kirliliği, küresel ve ısınma asit yağmurlarına sebep olmaktadır. Günümüzde kullanılan fosil yakıtlar giderek tükenmekte ve yerini yenilenebilir enerjiye bırakmaktadır. Dünyanın enerji ihtiyacının karşılanabilmesi için fosil yakıtlara alternatif olarak başvurulacak yenilenebilir enerji kaynakları bulunmaktadır. Bu yenilenebilir enerji kaynakları fosil yakıtlara göre daha temiz, ucuz ve zararsızdır. Güneş enerjisi yenilenebilir enerji kaynaklarından biridir. Türkiye, enerji ihtiyacının büyük bir kısmını fosil yakıtlardan karşılayan ve enerji arzında dışa bağımlı bir ülkedir. Bu nedenle ülkenin ekonomik ve stratejik çıkarlarını korumak ve artan enerji ihtiyaçlarını karşılamak için fosil yakıtlara olan bağımlılığını yenilenebilir enerji kaynaklarına yönelerek azaltması gerekmektedir. Türkiye, yenilenebilir enerji olan güneş enerjisinden yararlanmak için coğrafı olarak avantajlı bir konumdadır. Türkiye'nin mevcut potansiyel konumu yenilenebilir enerji için çok iyi değerlendirilmelidir. Bu bağlamda, yapılan çalışmada Akdeniz bölgesinde yer alan ve yıllık olarak yüksek miktarda güneş radyasyonu alan Mersin Tarsus İlçesinde kurulan GES santralinin yıllık enerji kazanımı ile GES santralinin maliyet ve ekonomik analizi incelenmistir.

Anahtar Kelime: Güneş enerjisi, Yenilenebilir enerji, GES Santrali, Mersin,

on Innovative Surveys in Positive Sciences 4-5 December 2022 / Full Text Book

#### 1. INTRODUCTION

Energy consumption is the most important parameter used to determine the level of development of countries, both technologically and economically. Today, the consumption of fossil fuels used in the energy sector and the emission of toxic gases pose a serious environmental problem [1]. Fossil fuels cause global warming, air pollution, acid rain, ozone depletion and the destruction of forests [2]. While electrical energy production was 17,450,00 terawatt hours in the world in 2004, electricity consumption is expected to increase to 31,657,00 terawatt hours in 2030. Thousands of new power plants are needed to meet this electrical energy need [3]. Today, a large part of the energy is used to meet the increasing living standards and the energy needs of the increasing population; fossil resources such as coal, oil and natural gas. Due to the limited fossil resources in the world and the resulting oil crises, many countries have started to search for different energy sources. For this reason, a trend towards cleaner and cheaper renewable energy sources has been achieved. Solar energy is one of these renewable energy sources. Due to its increasing energy consumption, Turkey has increased its orientation towards renewable energy sources to maintain its economic and strategic power. Located between 26°—45° east meridians and 36°—42° north parallels, Turkey is one of the countries in a geographically good position to use renewable energy, solar energy. Measurement results on sunshine duration and radiation intensity for Turkey show that the solar energy potential is high. Similar to this study, there are various studies in the literature. Kwaśniewski et al. (2020) investigated in their study to make an economic analysis of photovoltaic (PV) installations and utilization possibilities in farms. The research was conducted on 15 farms located in the Malopolskie Province. In the initial calculations, they found that the payback period ranged from 5.5 to 7 years for the 40% government support option and 9 to 11 years without government support [4]. Karaagac et al. (2020) investigated the design and cost analysis of the solar energy system in their study on the poultry farm. They stated that the farm's monthly average electricity consumption is 2,778.00 kWh, and the monthly average electricity consumption cost is 1,290 TL, with a total annual energy consumption cost of 15,480,00 TL. They calculated that the payback period of the solar panels is 6 years when the solar panel system to be installed on the farm roof is strong enough to meet all the electrical energy of the farm [5]. Dagli (2018) evaluated the investment data of a solar power plant with financial analysis methods in his study. In addition, his work includes methods such as net present value, internal rate of return, regulations and laws related to solar power plants. In the study, the development of solar energy in the country and the change in investment cost in the process from the past to the present [6]. Ozdemir (2013) made examinations by selecting the regions where the installation is appropriate to investigate the applicability of SPP systems for financial investment techniques and to make financial analyses. In the study, he investigated how many panels are needed for the amount of energy to be produced depending on the sunshine hour and radiation rate of the selected region. As a result of the study, cost, depreciation and efficiency calculations for each region were compared using financial cost techniques [7].

When the studies in the literature are examined, it is seen that solar energy, which is renewable energy, can be used to meet future energy needs and reduce foreign dependency. In this study, the economic contribution of solar energy to the SPP system installed in the Berdan Civata of Mersin Province, located in the Mediterranean region, was investigated.

## 2. MATERIAL and METHOD

Turkey has an area of 783,562.00 km<sup>2</sup> and is located in the orange zone, which is geographically called the sunbelt in Figure 1.

on Innovative Surveys in Positive Sciences 4-5 December 2022 / Full Text Book

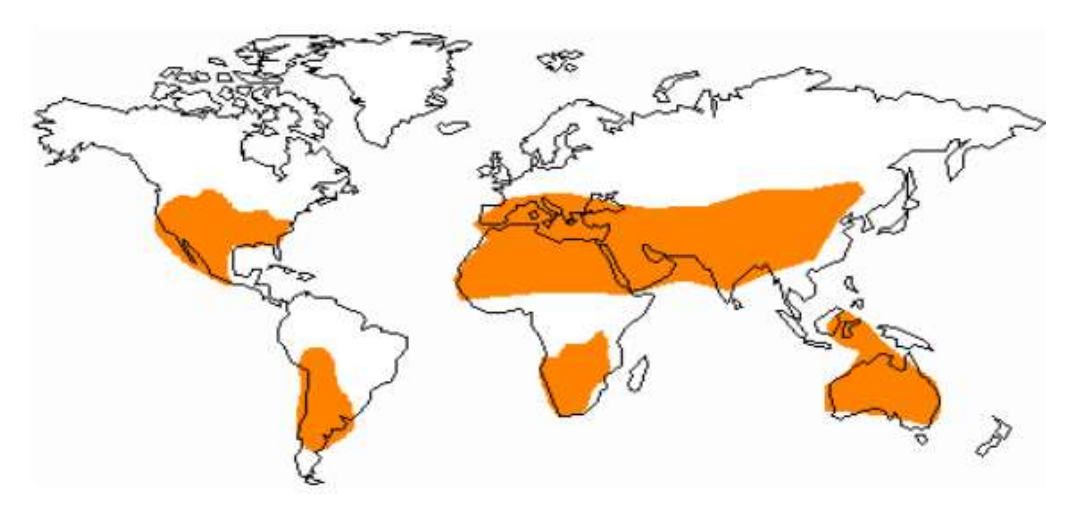


Figure 1. Countries with the Most Solar Radiation Worldwide [8].

Although Turkey is located in a region rich in solar energy, it does not use solar energy enough for energy. With the depletion of fossil fuels in the future, solar energy will be needed more. Figure 2. shows the radiation values at which provinces in Turkey can benefit from solar energy at the maximum level.

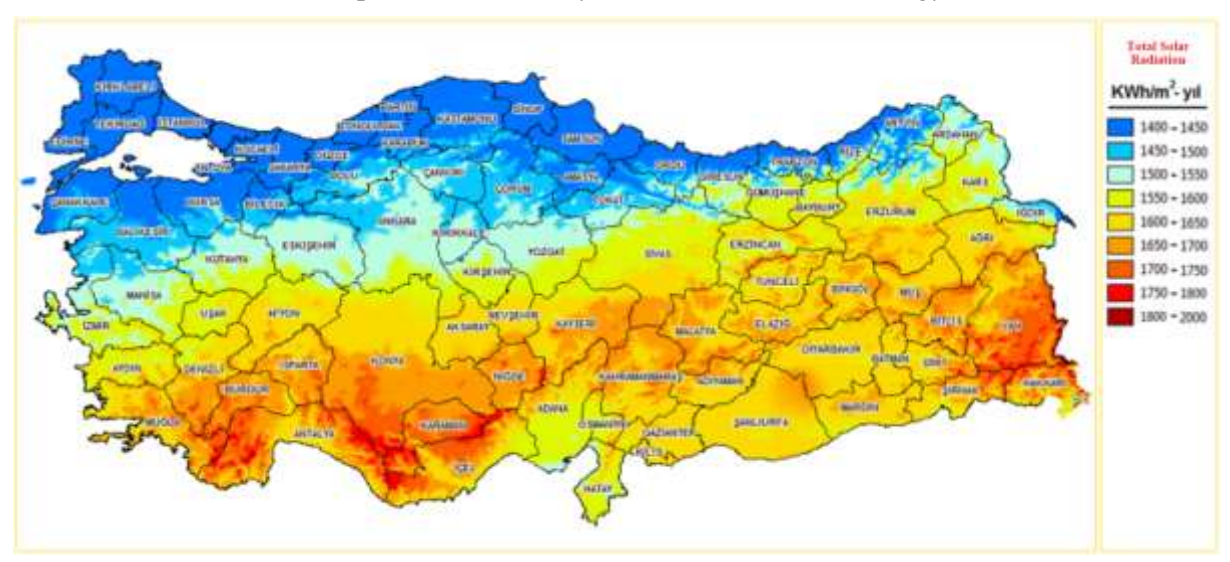
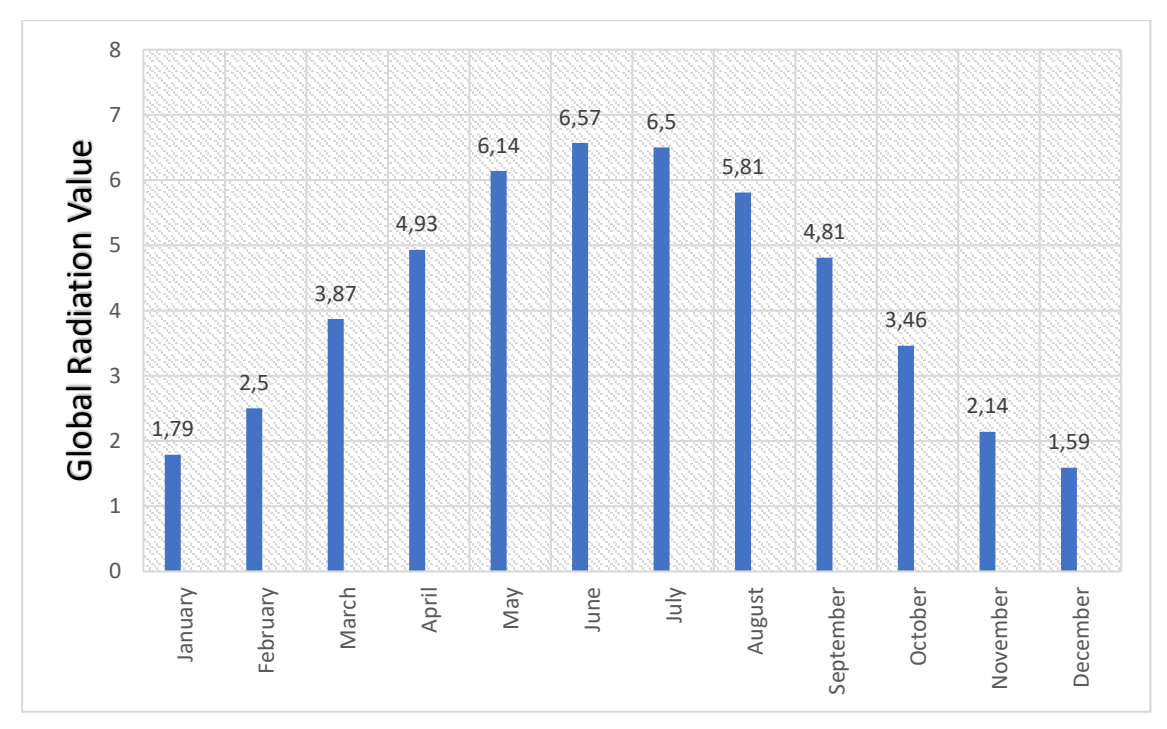


Figure 2. Turkey Solar Energy Potential Atlas [11]

In Figure 3, Turkey's average daily global radiation values on a monthly basis are given. When the average daily global radiation values are examined monthly, while the global radiation value is the highest in June, the global radiation value is the lowest in December [11].

on Innovative Surveys in Positive Sciences

4-5 December 2022 / Full Text Book



**Figure 3.** Turkey Global Radiation Values (kWh/m<sup>2</sup>—day) [11]

In Figure 4. Turkey's sunshine durations are given hourly. When the figure is examined, the months with the maximum sunshine duration are June and July, and the months with the minimum are December and January. Turkey's average daily sunshine duration monthly is 7.49 hours—days. In this context, the annual average total sunshine duration is found as 7.49 (hours) x 365 (days) = 2736.00 (hours x years).

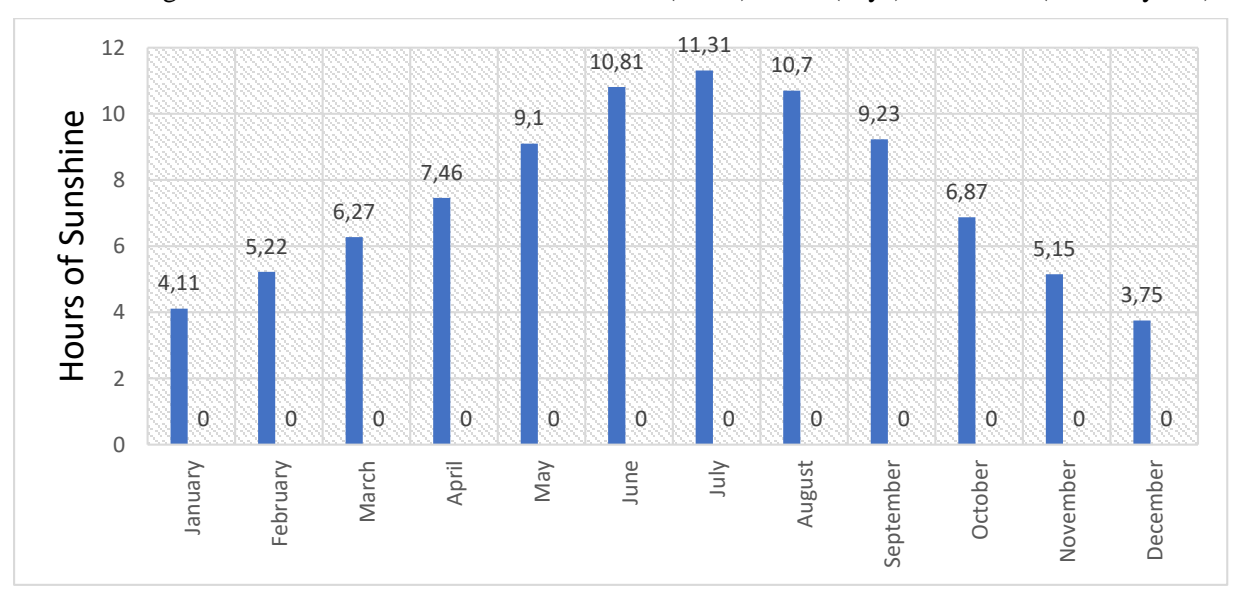


**Figure 4.** Turkey Sunshine Durations (Hours) [11]

Table 1 shows the distribution of Turkey's solar energy potential and sunshine duration values by region [10]. Looking at the table, it is seen that the highest values are in the South-eastern Anatolia Region and the Mediterranean Region, and the lowest values are in the Black Sea Region and the Marmara Region. Mersin Province, where the solar power plant to be investigated is located, is located in the Mediterranean Region, which is one of the regions with the highest solar energy potential and sunshine duration values.

**Table 1.** Distribution of Turkey's Solar Energy Potential by Regions [10]

on Innovative Surveys in Positive Sciences 4-5 December 2022 / Full Text Book

ZONE	TOTAL SOLAR POWER (kWh/m² x year)	SUNSHINE DURATIONS Hour/Year		
South-eastern Anatolia	1460	2993		
Mediterrenian	1390	2956		
Eastern Anatolia	1365	2664		
Central Anatolia	1314	2628		
Aegean	1304	2738		
Marmara	1168	2409		
Black Sea	1120	1971		

#### 3. FINDINGS

Mersin is located in the Mediterranean Region of Turkey between 36—37° north latitude and 33—35° east longitude. The surface area of Mersin is 15,853,00 km² [9]. The Mediterranean region is one of the regions where Turkey receives the most solar radiation. Mersin province is one of the most irradiated provinces in the Mediterranean Region. In Figure 5, the solar energy potential atlas of Mersin province is given. When Figure 5 is examined, it is seen that the average solar radiation of the districts of Mersin is between 1,600-1,800 kWh/m²-year. The longest sunshine duration takes place in July with 11.45 (hours). The minimum amount of sunshine duration is 4.64 (hours) in December.

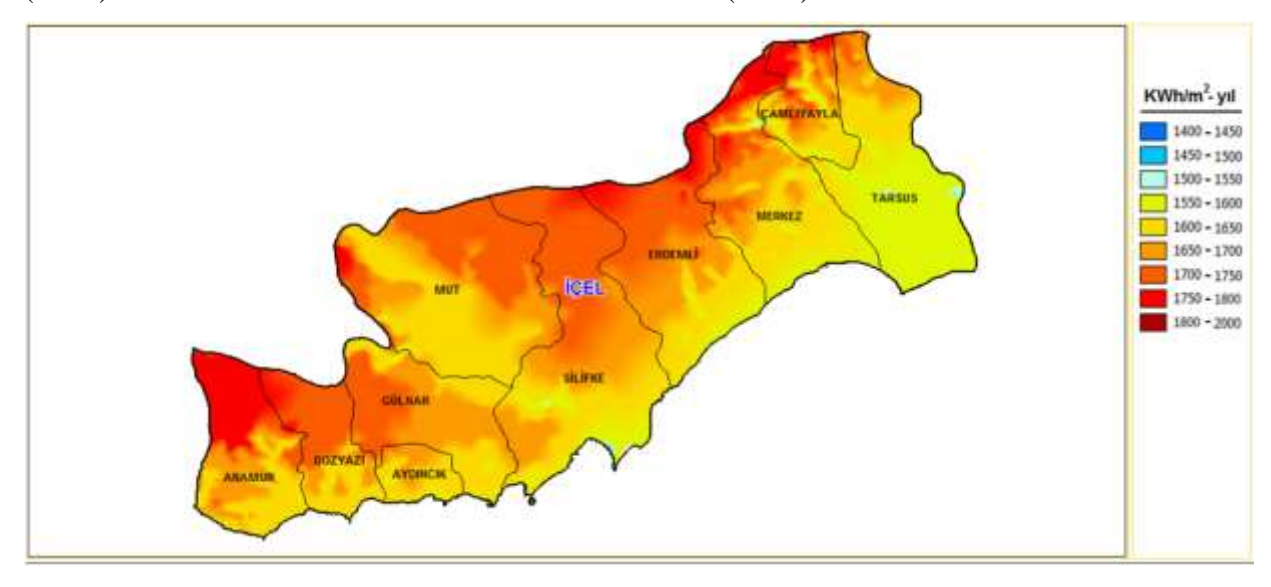


Figure 5. Solar Energy Potential Atlas of Mersin Province [11]

The research, which is the subject of the study, was carried out in the solar power plant belonging to the Berdan Civata. The related Solar Power Plant is located in the Tarsus District of Mersin Province. In Table 2, the global radiation values of the Tarsus district of Mersin province are given.

on Innovative Surveys in Positive Sciences 4-5 December 2022 / Full Text Book

**Table 2.** Global radiation values of Tarsus district of Mersin province [11]

SOLAR RADIATION INTENSITY (kWh/m2-day)	JANUARY	FEBRUARY	MARCH	APRIL	MAY	JUNE	JULY	AUGUST	SEPTEMBER	OCTOBER	NOVEMBER	DECEMBER	MEAN	
TARSUS	2	2,45	4,15	5,02	6,06	6,69	6,44	5,96	4,89	3,8	2,37	1,83	4,31	

The data and annual production of the solar power plant system of the Berdan Civata in Tarsus, where the research was carried out, are given in Table 3 and Table 4.

 Table 3. Berdan Civata Solar Power Plant Monthly Recovery Amount

MONTHS	PRODUCTION (kWh)	PRICE (TL)	PRICE (USD)
JANUARY	80.018,00 kWh	38.152,58 TL	5.204,99 \$
FEBRUARY	106.675,00 kWh	49.923,90 TL	6.764,76 \$
MARCH	131.058,00 kWh	69.434,53 TL	8.325,48 \$
APRİL	149.629,00 kWh	83.582,76 TL	10.131,24 \$
MAY	163.092,00 kWh	95.979,65 TL	11.278,45 \$
JUNE	147.764,00 kWh	89.825,74 TL	10.324,80 \$
JULY	153.532,00 kWh	103.680,16 TL	12.298,95 \$
AUGUST	186.210,00 kWh	133.736,02 TL	16.074,04 \$
SEPTEMBER	143.313,00 kWh	91.691,65 TL	10.314,02 \$
OCTOBER	102.286,00 kWh	87.618,19 TL	9.222,97 \$
NOVEMBER	66.782,00 kWh	62.514,63 TL	4.823,66 \$
DECEMBER	47.813,00 kWh	58.432,27 TL	4.423,34 \$
TOTAL	1.478.172,00 kWh	964.572,08 TL	109.186,70 \$

**Table 4.** Berdan Civata Solar Power Plant Monthly Recovery Amount

	OSB (Kwh)	GES (Kwh)	TOPLAM (Kwh)	GES (%)
<b>LAL</b>	6.018.949,00	1.478.172,00	7.497.121,00	19,72%
TO	kWh/year	kWh /year	kWh /year	,,-

The measurements in the study are the data of the Solar Power Plant System of Berdan Civata Company located in the Mersin-Tarsus Organized Industrial Zone of Tarsus Province, which has the lowest radiation intensity average as a result of 2021. It has been observed that Berdan Civata Company has achieved high profits with the Solar Power Plant System. Considering these results, it has been found

on Innovative Surveys in Positive Sciences 4-5 December 2022 / Full Text Book

that the investment cost of the power plant installed at Berdan Civata Company can pay for itself in 8 years according to the calculations made at the end of 2021.

#### 4. RESULTS and DISCUSSIONS

With the increase in population, technological developments and continuous development of the industry, more and more energy needs are needed day by day. The fossil fuels being used will be sufficient for a while. However, due to developing technology and increasing population density, fossil fuels will run out after a while. Since fossil fuels are limited, it is necessary to resort to energy sources that constantly renew themselves. Renewable energy sources should be used not only because fossil fuels will run out, but also to provide clean energy to the environment. The current geographical location of Turkey is quite suitable for generating electricity with solar energy.

In this study, the solar energy potential of Tarsus District, where the solar radiation of Mersin province is the lowest, was investigated. Mersin province is a province with high sunshine duration in the Mediterranean region. Looking at the data of Mersin province, it is seen that even the district with the lowest solar radiation, receives high efficiency from Solar Power Plants. With this efficiency, it is seen that power plants, which have high installation costs, can amortize themselves over time. When these data are evaluated, it is understood that the high installation cost seen at the beginning is a profitable investment in the future. According to the calculation made according to the end of 2021, it has been learned that the power plant can amortize itself in 8 years. However, when we look at the increasing electricity bills in today's conditions, it is seen that this amortization period is getting shorter. It is expected that solar energy will be preferred more soon, as it is a profitable energy in terms of the amount of energy it provides.

#### REFERENCES

- 1. Čeřovský, Z., Mindl, P.: "Hybrid Electric Cars, Combustion Engine driven cars and their Impact on Environment", SPEEDAM 2008 International Symposium on Power Electronics, Electrical Drives, Automation and Motion, pp. 739 743.
- 2. Wai, R., J., Wang, W., H., Lin, C., Y.: "HighPerformance Stand—Alone Photovoltaic Generation System", IEEE Transactions On Industrial Electronics, 55, (1), January 2008.
- 3. Güler, Ö.: "Wind energy status in electrical energy production of Turkey", Renewable and Sustainable Energy Reviews, 13, (2), February 2009, pp. 473—478.
- 4. Kwaśniewski, D., Akdeniz, C., Durmaz, F. ve Kömekçi, F., 2020, Economic analysis of the photovoltaic installation use possibilities in farms, Agricultural Engineering,
- 5. Karaağaç, M. O., Oğul, H. ve Bardak, S., 2020, Design and cost calculation of solar energy system for poultry farm, Düzce University Journal of Science and Technology
- 6. Dağlı, E., 2018. Evaluation of 1MW Solar Power Plant Using Economic Analysis Methods, Osmaniye Korkut Ata University, Institute of Science and Technology, Master Thesis, 9—25s, Osmaniye.
- 7. Özdemir, G., 2013. Investment Analysis of Solar Energy Systems. Bahçeşehir University, Graduate School of Natural and Applied Sciences, Master Thesis, Istanbul.
- 8. Altuntop, N., Erdemir, D., 2013 Developments in Solar Energy in the World and in Turkey
- 9. https://mersin.ktb.gov.tr/
- 10. TMMOB Makina Mühendisleri Odası. 2014. "Türkiye'nin Enerji Görünümü," Yayın No: MMO/2014/616, Ankara
- 11. https://gepa.enerji.gov.tr/MyCalculator/pages/33.aspx

on Innovative Surveys in Positive Sciences 4-5 December 2022 / Full Text Book

# EFFECTS of HAWTHORN VINEGAR on CD4 and CD8 T LYMPHOCYTES EXPRESSION in SPLEEN of RATS

## ALIÇ SİRKE UYGULAMASININ SIÇANLARIN DALAĞINDA CD4 VE CD8 T LENFOSİTLERİNİN EKSPRESYONU ÜZERİNE ETKİLERİ

#### Buket Bakır

Assoc. Prof. Dr., Tekirdag Namik Kemal University, Faculty of Veterinary Medicine, Department of Histology and Embriyology

ORCID ID: 0000-0003-3637-3688

Assoc. Prof. Nilay SEYİDOĞLU

Assoc. Prof. Dr., Tekirdag Namik Kemal University, Faculty of Veterinary Medicine, Department of Physiology

ORCID ID: 0000-0002-2817-5131

#### **ABSTRACT**

The immune system is a defense process in a response of antigen. Imunomodulators are compounds affecting the immune response by increasing the immune system and suppressing abnormal. Natural products are known to contain bioactive compounds such as antioxidant and antiinflammatory that can be used as immunomodulator. The purpose of this study was to examine the effect of natural content of hawthorn vinegar administration immunohistochemically on CD4 and CD8 release in the spleen tissue of rats.

Hawthorn vinegar was obtained by three methods. 1. classical fermentation method 2. The sample obtained in a jar in a water bath at 65 0C for 30 minutes by thermal pasteurization. 3. The sample to be created by trading with the Response Surface Method and Ultrasound. The experimental groups as follows: Control (C) (untreated group), KAS (Fermentation, oral gavage 1 ml/kg hawthorn vinegar), PAS (thermal pasteurization, oral gavage 1 ml/kg), UAS (ultrasound method, oral gavage, 1 ml/kg). Crossman's Triple staining was performed in order to examine spleen tissue histologically. The streptavidin-Biotin Peroxidase Complex method was used for CD4 and CD8 expression in the spleen. Statistical measurements were analized in order to determine whether there was a difference between groups of weight of spleen tissue.

As a results, application of hawthorn vinegar increased CD4 and CD8 expression. It was remarkabled that the most intense reaction was seemed in the UAS group. It was not seemed difference weight of spleen tissue between all groups. In conclusion, It can be concluded that hawthorn vinegar increase the immune response by activating immune cells.

Key words: CD4, CD8, Hawthorn, Spleen

## ÖZET

Bağışıklık sistemi, antijene yanıt olarak bir savunma sürecidir. İmmünomodülatörler, bağışıklık sistemini artırarak ve anormallikleri baskılayarak bağışıklık tepkisini etkileyen bileşiklerdir. Doğal ürünlerin, immünomodülatör olarak kullanılabilecek antioksidan ve antiinflamatuvar gibi biyoaktif bileşikler içerdiği bilinmektedir. Bu çalışmanın amacı, doğal içeriye sahip olan alıç sirkesi uygulamasının sıçanların dalak dokusunda CD4 ve CD8 salınımı üzerine etkilerinin immünohistokimyasal yöntemle incelenmesidir.

Alıç sirkesi üç yöntemle elde edildi: 1. Klasik fermantasyon yöntemi 2. Termal pastörizasyon ile 65 0C'de 30 dakika su banyosunda kavanozda elde edilen numune. 3. Tepki Yüzey Metodu ve Ultrason ile işlem yapılarak oluşturulan numune. Deney grupları: Kontrol (C) (tedavi uygulanmayan grup), KAS

on Innovative Surveys in Positive Sciences 4-5 December 2022 / Full Text Book

(Fermantasyon, oral gavaj 1 ml/kg alıç sirkesi), PAS (termal pastörizasyon, oral gavaj 1 ml/kg ), UAS (ultrasound yöntemi, oral gavaj, 1 ml/kg). Dalak dokusunun histolojik olarak incelenmesi için Crossman'nın Üçlü boyaması yapıldı. Dalakta CD4 ve CD8 ekspresyonu için streptavidin-Biotin Peroxidase Complex yöntemi kullanıldı. Gruplar arasında dalak dokusu ağırlığı açısından fark olup olmadığını belirlemek için istatistiksel ölçümler yapıldı.

Sonuç olarak alıç sirkesi uygulaması CD4 ve CD8 ekspresyonunu arttırdı. En yoğun tepkinin ise UAS grubunda olduğu dikkat çekti. Tüm gruplar arasında dalak dokusu ağırlığı bakımından fark olmadığı görüldü. Sonuç olarak, alıç sirkesinin bağışıklık hücrelerini aktive ederek immün yanıtı arttırabileceği sonucuna varılabilir.

Anahtar kelimeler: CD4, CD8, Alıç, Dalak

#### **INTRODUCTION**

As the largest peripheral immune organ, spleen is an important immunorespons. There are various of immunocytes in spleen, including T lymphocytes, B lymphocytes, dendritic cells, macrophages, natural killer cells, and monocytes, that involve in variety of immunoresponses (Lee et al., 2015). Spleen is the locality for T lymphocytes residing and responding immunoreactions, and has an important role in innate and adaptive immunity. Study showed that the amount of T lymphocytes in spleen had the positive correlation with immune responses (Lim et al., 2014). T lymphocytes can be grouped into subpopulations according to surface antigen expression, CD4 subgroup and CD8 subgroup, which is the key regulation in immune reaction (de Leeuw et al., 2013). The imbalance ratio of the two subgroups will result different disease (Marin et al., 2015).

Hawthorn (Crataegus sp.) belong to Rosacaea family, known as "safety (GRAS)" and "traditional herbal medicine" by European Medicines Agency and European Pharmacopoeia (EMA 2016; EP 2017). Hawthorn has rich in vitamin, organic acids, carotene which can improve the activity of digestive and gastric enzymes (Leilei and Zhipeng, 2011). It was also reported that hawthorn contains several bioactive compunds with a large pharmacological activity, such has pectin, phenolic contents, flavonoids, polyphenol, triterpenoids and etc. (Wang et al 2007; Liu et al., 2020; Li et al., 2022). Alongside of the compounds of hawthorn, researchers have been studied the antioxidant, anti inflammatory, antihyperlipidemic, antidiabetic, anticancer and immune activities in recent years (Wang et al., 2007; Vanden Berghe 2012; Kadas et al., 2014; Li et al., 2022).

Healthy and balanced nutrition is important throughout the World, especially natural foods, herbs and extracts. Hawthorn is an important fruit that interested in nutrition in recent years. In this study, Our aimed to deeply understand how hawthorn vinegar changes CD4 and CD8 T lymphocytes subgroup in the spleen.

## **MATERIALS and METHODS**

## **Ethical approval**

The study protocol was approved by The Ethical Committee of Tekirdag Namik Kemal University Chair of Experimental Medicine Research and Application Center (2022-11-09/1).

## Animals

Thirty two female, healthy Wistar albino rats aged about 6-7 months old with an average body weight (230-260g) were used in this study. The animals were housed under standard laboratory conditions (22  $\pm$  10C; 55  $\pm$  10% humidity) in clear, standard cages, with stainless steel feed hoppers. Rats were given ad libitum access to a standard rat pellet diet and tap water.

## **Hawthorn Vineagar preperation**

5 kg of hawthorn from Turkey/Bursa was used as raw material for the production of hawthorn vinegar. Vinegar was produced by modifying the previous method (Yıkmış, 2019). The resulting vinegar was undergo 3 processes:

on Innovative Surveys in Positive Sciences 4-5 December 2022 / Full Text Book

- 1. Fermentation (coded as KAS).
- 2. The sample obtained in a jar in a water bath at 65 °C for 30 minutes by thermal pasteurization (coded as PAS).
- 3. The sample to be created by treatment with the Response Surface Method and Ultrasound, and the application of temperature and time with the best bioactive components as a result of optimization (coded as UAS).

Hawthorn vinegar obtained by three methods (1 ml/kg ca) for each vinegar, were given to the animals daily and orally by oral gavage (Moon and Cha, 2008; De Dios Lozano et al., 2012)

## **Experimental Design and Treatment Process**

The rats were divided into 4 groups and each group was included eight animals. The total experiment protocol was maintained for 45 days. The experimental groups as follows: (C) (control, untreated), KAS (Fermantation, oral gavage 1 ml/kg hawthorn vinegar), PAS (thermal pasteurization, oral gavage 1 ml/kg), UAS (ultrasound method, oral gavage, 1 ml/kg).

## Histological procedure

Tissue samples were fixed in 10% formalin for 24 h at room temperature. After fixation, the samples were dehydrated ethanol, cleared with xylene and embedded in paraffin. The sections taken at 5  $\mu$ m were deparaffinized in xylene, rehydrated through decreasing concentrations of ethanol and stained with Crossman's triple staining for histological examination (Crossman, 1937).

#### Immunohistochemical method

The streptavidin biotin peroxidase complex (strepABC) method was applied to investigate CD4 and CD8 T lymphocytes immunoreactivity in the spleen. Sections of 5 µm thickness were collected on adhesive slides. Sections were processed in citrate buffer solution (ph 6.0) for 10 min in a microwave oven at 700 watts. Then, tissues incubated in 3% hydrogen peroxide (H<sub>2</sub>O<sub>2</sub>) for 10 min. Sections were incubated with anti-CD4 antibody (ab237722) diluted 1:150 in PBS and anti-CD8 alpha antibody [OX-8] (ab33786) diluted 1:100 in PBS. Sections were incubated with biotinylated goat antirabbit and rabbit antigoat IgG for 30 min and peroxidase conjugated streptavidin (1:300) (P0397; Dako Corp., Carpinteria, CA, USA) for 10 min. 3,3'-Diaminobenzidine tetrahydrochloride (DAB, 0.5 mg/mL; Dako Corp.) was used as chromogen followed by hematoxylin counterstaining. Sections were mounted with ImmunoMount and examined by light microscope (Olympus BX51, Tokyo, Japan). Rabbit serum without primer antibody served as the negative control. Immunostaining intensity of CD4 and CD8 immunoreactive cells were evaluated by two different researchers. Immunoreactive cells were categorized as having negative, slight, moderate, and intensive.

## Relative spleen weight

Fresh spleen from sacrificed rats were subsequently weighted. Absolute spleen weights were recorded to the nearest 0.1 mg using an electric balance. To obtain a more precise measure of the change in organ weights.

## **Statistical Assessment**

Statistical analyses were performed with SPSS (Version 17.0; Chicago, IL). Data were examined for normality distribution and variance homogeneity assumptions (Shapiro-wilk test). If normally distributed, One-way ANOVA test was applied, and the differences between groups were analyzed by the post hoc Tukey test. The differences were considered significant at P< 0.05, and the means and standard errors were calculated. In the study, nonparametric tests were used as the data did not provide normal assumptions. So, the differences between groups were analyzed by Kruskal Wallis, and Mann Whitney U test was used between groups. Also, the differences were considered significant at p<0.05, and the median values (minimum - maximum) were calculated.

on Innovative Surveys in Positive Sciences 4-5 December 2022 / Full Text Book

#### RESULTS

## **Histological results**

Normal histological results were obtained and no difference was observed in the histological structure of rats in all groups. The tissue was surrounded by a capsule from the outside. Trabeculae separated from the capsule extended to the parenchyma of the organ. Spleen consisted of separated lymphoid follicles (white pulp), the white pulp was formed of marginal zones and surrounded by highly vascular matrix (red pulp) (Figure 1).

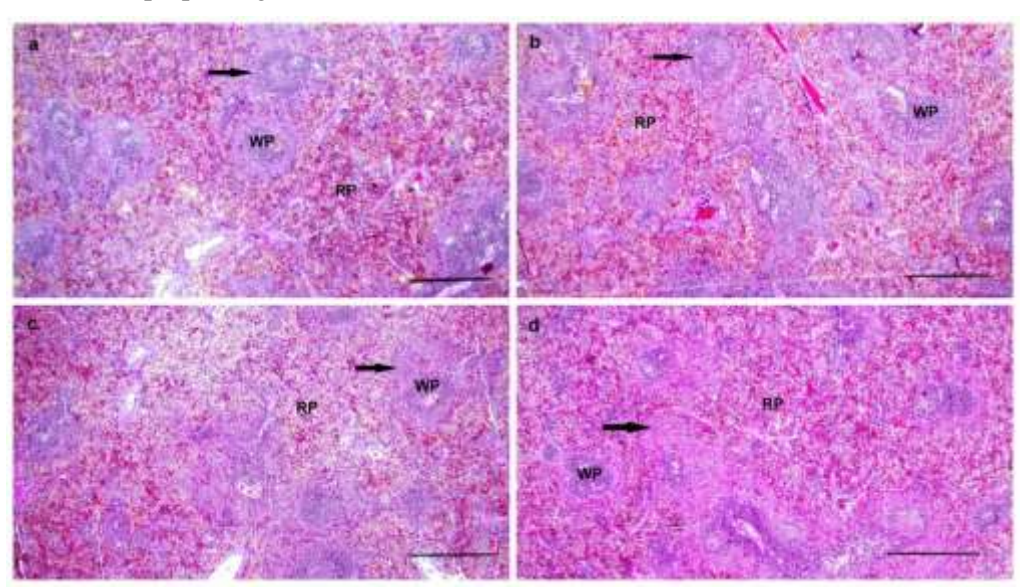


**Figure 1.** Histological structure of spleen tissue. Control (a), KAS (b), PAS (c), UAS (d). Red pulp (RP), White pulp (WP), marginal zones (arrow). Triple staining. Bar=100 μm.

## **Immunohistochemical results**

Specific CD4 and CD8 reactions were observed in spleen of all groups. While intensive reaction was observed mostly in the red pulp and few positive cells in the white pulp of group UAS (figure 5), moderate reaction was remarkabled in KAS (figure 3) and PAS (figure 4). Also, slight CD4 and CD8 reaction was observed in control group (figure 2). It was remerkabled that CD4 and CD8 lymphocytes subtypes in spleen were localized only the red pulp in control, KAS, and PAS groups.

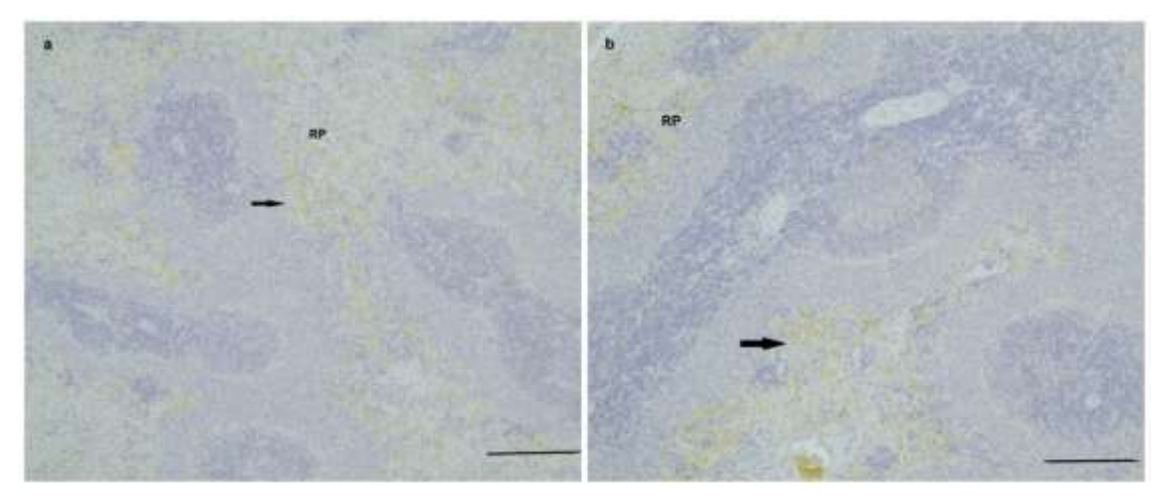


**Figure 2.** CD4 and CD8 expression in spleen tissue of control group. CD4 (a), CD8 (b), Red pulp (RP), slight CD4 and CD8 reaction in control group (arrow). Immunohistochemical staining. Bar=100 μm.

on Innovative Surveys in Positive Sciences 4-5 December 2022 / Full Text Book

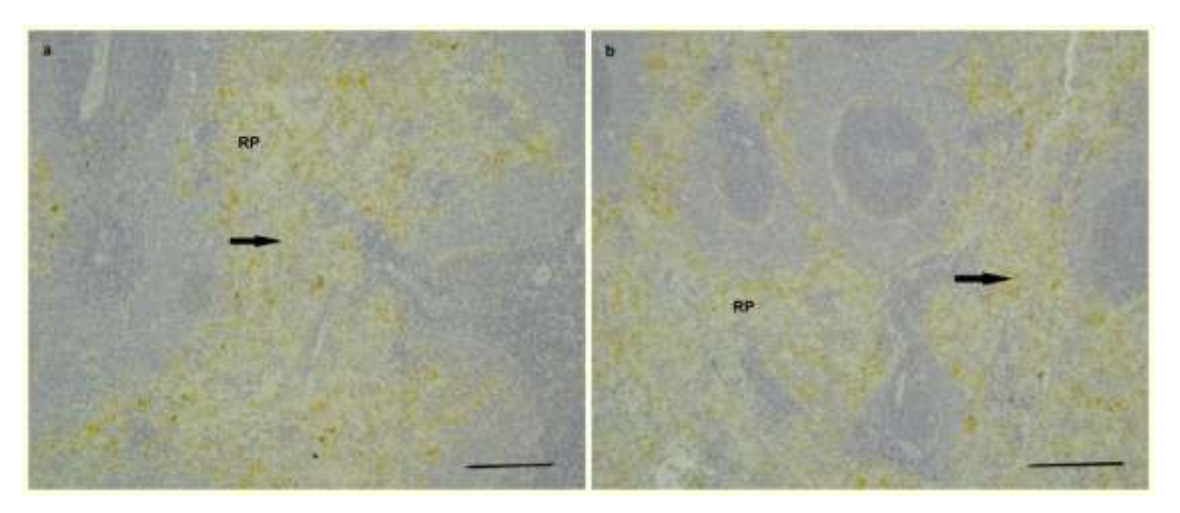


**Figure 3.** CD4 and CD8 expression in spleen tissue of KAS group. CD4 (a), CD8 (b), Red pulp (RP), moderate CD4 and CD8 reaction in KAS group (arrow). Immunohistochemical staining. Bar=100 μm.

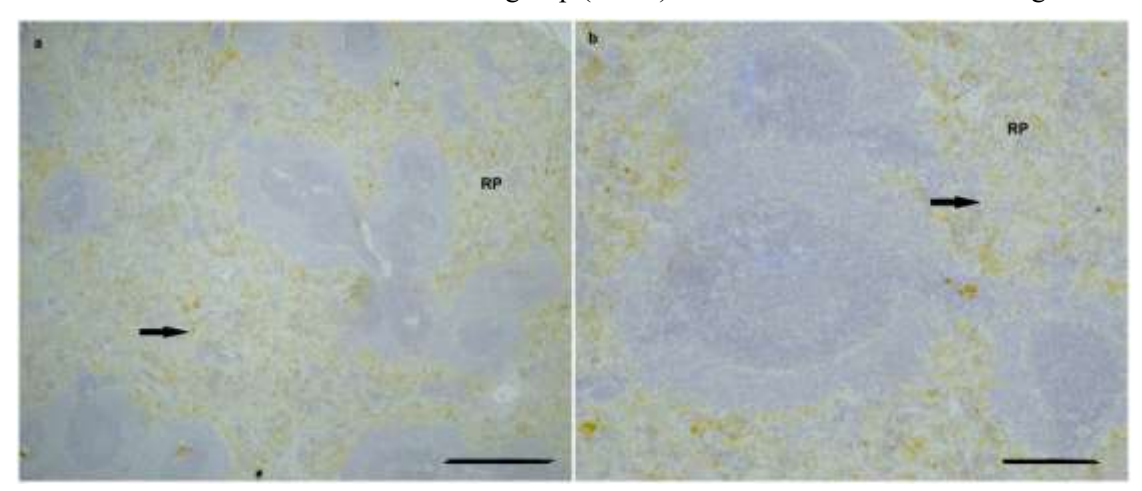


**Figure 4.** CD4 and CD8 expression in spleen tissue of PAS group. CD4 (a), CD8 (b), Red pulp (RP), moderate CD4 and CD8 reaction in PAS group (arrow). Immunohistochemical staining. Bar=100 μm.

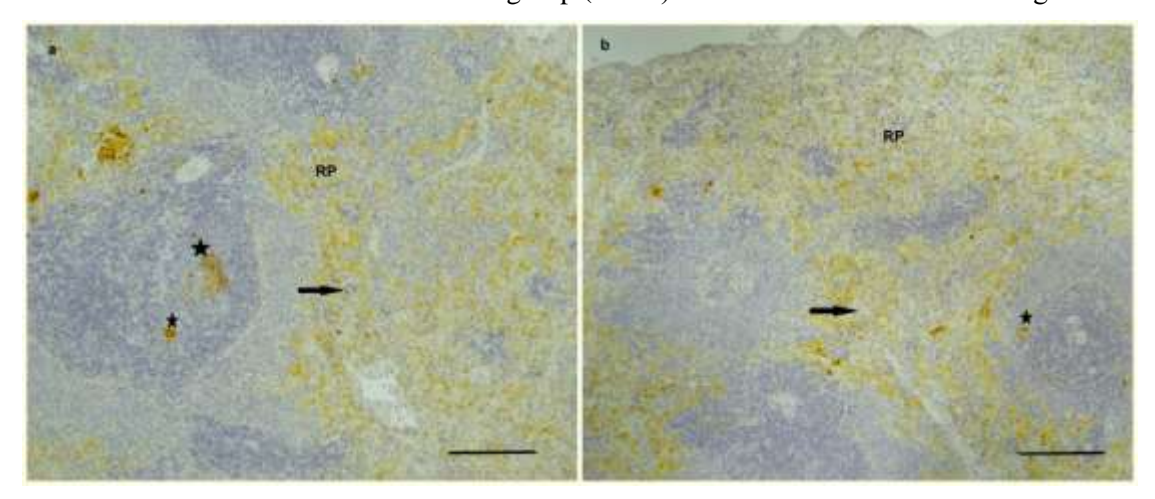


**Figure 5.** CD4 and CD8 expression in spleen tissue of UAS group. CD4 (a), CD8 (b), Red pulp (RP), CD4 and CD8 reaction in the white pulp (star), intensive CD4 and CD8 reaction in UAS group (arrow). Immunohistochemical staining. Bar= $100 \mu m$ .

#### **Statistical results (spleen weight)**

When all the groups were compared in terms of spleen weight, there was no significant difference among them (P>0.05) (figure 6).

on Innovative Surveys in Positive Sciences 4-5 December 2022 / Full Text Book

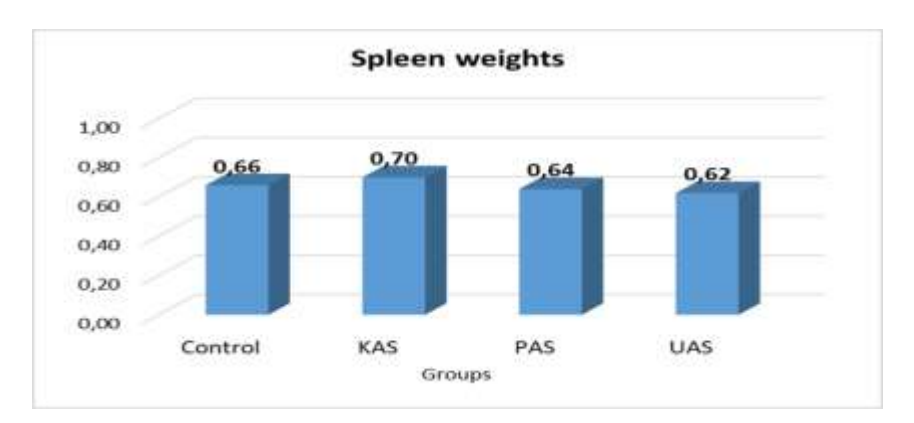


Figure 6. Comparison of mean values of spleen weight among the groups.

#### **DISCUSSION**

Evaluating the reaction of the immune system is seemingly complex because it that embraces various organs ranges from the peripherally located lymph nodes to the more centrally placed thymus and spleen, gut-associated lymphoid tissue, and interconnecting lymphatic and vascular channels. In addition, the antigenicity of the material being tested as well as its route of administration and dose affect local and systemic immune responses (Shyh-Jou et al., 2014).

Spleen is directly involved in cellular immunity and regulates. Spleen plays important role on immunity and inflammatory responses in organism (Bronte and Pittet 2013). Several vital functions such as filtering blood, maintaining immune response and recycling iron are interested by researchers. It also known secondary lymhoid organ of organism (Bronte and Pittet 2013). There have been some natural supplements, herbs or foods used for strengthening the spleen (Barrea et al., 2018). Appropriate dieatry including vitamins (vitamin D), micronutrients (magnesium), vegetables herbs, herbal teas and etc. have a high role on spleen health. According to literature, it was reported that ethanol extract of hawthorn can promote digestion by refreshing spleen and effect on gastric dysfunction (Yu and Duan 2016). Also, it was evaluated that oral 50, 100 and 200 mg/kg hawthorn (Crataegus monogyna) phenolic extract application modulated the lymphocyte subsets in rats (Lis et al., 2020). However, there is no study about the hawthorn vinegar and its efficiency on spleen. In our study, it was seen that hawthorn vinegar increased CD4 and CD8 expression.

Natural antioxidants have rich contents which are effectable on growth, immunity and protection of health. There are several vinegars known as natural antioxidant used for this purpose (Aydin and Seyidoglu 2021). It was reported that vinegar produced by different fruits or herbs, has antioxidant, anticarcinogenic, antidiabetic and health protection effects. Also, vinegar has been used for pharmaceticul industry (FDA, 1989; WHO 2013; Karabiyikli and Sengün 2017). The most popular contents of vinegar are phenolics, fructooligosaccarids, amino acids, minerals and vitamins (Verzelloni et al, 2010; Tagliazucchi er al., 2010). However, it was reported that all these bioactive compounds can be changed by the raw materials and production prossess (Ho et al., 2017). The beneficial effects of hawthorn were rewieved by researchers (Li et al., 2022). Through the literatures, hawthorn application could accelerate the metabolism, increase the lipid elimination and improves the cholesterol metabolism. The possible antioxidant mechanism of hawthorn in vivo may be correlated by increasing endogenous antioxidant enzymesIn our study, hawthorn vinegar was obtained by three different methods. It was examined the effects of all three vinegars on the immune response through the release of CD4 and CD8 T lymphocyte subtypes in the spleen (Kadas et al., 2014).

Organ weight has also been suggested as a method to gauge pathological condition and disease (Schulte et al., 2002). Especially, lymphoid organs such as spleen is highly sensitive to various stresses, and exposure to disease causes splenic atrophy (Khayal et al., 2022). We compared the weight of the spleen at the end of the experiment with the study and we did not found no differentitation between spleen weights in all groups.

on Innovative Surveys in Positive Sciences 4-5 December 2022 / Full Text Book

In this study, it was seen that hawthorn vinegar produced with different techniques and administered orally could increase the immune response by activating CD4 and CD8 T lymphocyte subtypes in the spleen tissue of rats.

#### **ACKNOWLEDGEMENT**

This study was financially supported by a grant from Scientific Research Fund of Tekirdag Namik Kemal University (Grant number: NKUBAP.10.GA.18.147).

#### REFERENCES

Aydin, C., Seyidoglu, N. (2021). Natural Antioxidants to the Rescue? in Antioxidants. [Online First], IntechOpen press, London. Available from:

Barrea, L, Di Somma C, Muscogiuri G, Tarantino G, Tenore GC, Orio F, Colao A, Savastano S. (2018). Nutrition, inflammation and liver-spleen axis, Critical Reviews in Food Science and Nutrition, 58:18, 3141-3158

Bronte, V., and M. J. Pittet. (2013). The spleen in local and systemic regulation of immunity. Immunity, 39:806–18.

Crossman, G. (1937). A modification of Mallory's connective tissue stain with a discussion of the principles involved. Anat. Rec., 6, 33–38.

De Dios Lozano, J., Juarez-Flores, B. I., Pinos-Rodriguez, J. M., Aguirte-Rivera, J. ve Alvarez-Fuentez, G. (2012). Supplementary effects of vinegar on body weight and blood metabolites in healthy rats fed conventional diets and obese rats fed high-caloric diets. J. Med. Plants Res., 6, 4135–41.

deLeeuw RJ, Kost SE, Kakal JA and Nelson BH. (2012). The prognostic value of FoxP3+ tumor-infiltrating lymphocytes in cancer: a critical review of the literature. Clin Cancer Res, 18: 3022-3029

European Medicines Agency. ( (2016). Herbal medicine: summary for the public: Hawthorn leaf and flower. Erişim adresi: https://www.ema.europa.eu/en/documents/herbal-summary/hawthorn-leaf-flower-summary-public\_en-0.pdf.

European Pharmacopoeia. (2017). European Union herbal monograph on Crataegus spp.,folium cum flore. https://www.ema.europa.eu/en/documents/herbal-monograph/final-european-union-herbal-monograph-crataegus-spp-folium-cum-flore\_en.pdf.

Food and Drug Administration, FDA. (1989). Acetic acid - use in foods - labeling of foods inwhichused.https://www.fda.gov/iceci/compliancemanuals/compliancepolicyguidancemanu l/ucm074577.htm.

Ho, C.W., Lazim, A.M., Fazry, S., Zaki, U.K.H.H. ve Lim, S.J. (2017). Varieties, production, composition and health benefits of vinegars: A review. Food Chem., 221, 1621–1630.

Lee S, Khang D and Kim SH. (2015). High dispersity of carbon nanotubes diminishes immunotoxicity in spleen. Int J Nanomedicine.,10: 2697-2710.

Leilei Wu, Zhipeng He (2011). Effects of Hawthorn water extract on 5-HT and 5-HT3R expression in colonic mucosa of rats with irritable bowel syndrome [J]. Journal of mudanjiang medical college, 32(04):6-9.

Li T, Fu S, Huang X, Zhang X, Cui Y, Zhang Z, Ma Y, Zhang X, Yu Q, Yang S, Li S. (2022). Biological properties and potential application of hawthorn and its major functional components: A review. Journal of Functional Foods, 90. 104988.

Lim MA, Lee J, Park JS, Jhun JY, Moon YM, Cho ML and Kim HY., (2014). Increased Th17 differentiation in aged mice is significantly associated with high IL-1beta level and low IL-2 expression. Exp Gerontol., 49: 55-62

Lis M, Szczypka M, Susko-Pawlowska A, Sokół-Łętowska A, Kucharska A, Obmińska-Mrukowicz B. (2020). Hawthorn (Crataegus monogyna) Phenolic Extract Modulates Lymphocyte Subsets and Humoral Immune Response in Mice. Planta Med., 86(02): 160-168

on Innovative Surveys in Positive Sciences 4-5 December 2022 / Full Text Book

Liu, F., Zhang, X. S., & Ji, Y. (2020). Total flavonoid extract from hawthorn (Crataegus pinnatifida) improves inflammatory cytokines-evoked epithelial barrier deficit. Medical Science Monitor, 26, e920170.

Kadas, Z., Akdemir Evrendilek, G. ve Heper, G.(2014). The metabolic effects of hawthorn vinegar in patients with high cardiovascular risk group. Journal of Food and Nutrition Res., 2(9):539-545.

Karabiyikli, S. ve Sengun, I. Y. (2017). Beneficial Effects of Acetic Acid Bacteria and Their Food Products, in Acetic Acid Bacteria: Fundamentals and Food Applications, Boca Raton: CRC Press, Taylor & Francis Group, 221-242.

EES, Alabiad MA, Elkholy MR, Shalaby AM, Nosery Y, El-Sheikh AA. (2022). The immune modulatory role of marjoram extract on imidacloprid induced toxic effects in thymus and spleen of adult rats. Toxicol., 471.

Marin AC, Gisbert JP and Chaparro M. (2015). Immunogenicity and mechanisms impairing the response to vaccines in inflammatory bowel disease. World J Gastroenterol. 21: 11273-11281.

Moon, Y. J. and Cha, Y. S. (2008). Effects of persimmon-vinegar on lipid metabolism and alcohol clearance in chronic alcohol-fed rats. J. Med. Food., 11:38–45

Schulte A, Althoff J, Ewe S, et al. (2002). Two immunotoxicity ring studies according to OECD TG 407-comparison of data on cyclosporin A and hexachlorobenzene. Regul Toxicol Pharmacol., 36:12–21.

de Leeuw S, Thirugnanabalan B, Varsani H, Warden F, Makengo N, Lewis J, Pesenacker A, Wedderburn L. (2013). PReS-FINAL-1004: Can the cd4/cd8b ratio be used as a predictive biomarker in extended-tobe oligoarticular JIA? Pediatric Rheumatology, 11:2,2

Shyh-Jou Shieh, Prashanth Varkey,Po-Yang Chen, Su-Ya Chang, Lynn L.H. Huang (2014). Counting CD4+ and CD8+ T cells in the spleen: a novel in vivo method for assessing biomaterial immunotoxicity. 1(1):11–16.

Tagliazucchi, D., Verzelloni, E. ve Conte, A. (2010). Contribution of melanoidins to the antioxidant activity of traditional balsamic vinegar during aging. Journal Food Biochemistry, 34, 1061-1078.

Vanden Berghe, W. (2012). Epigenetic impact of dietary polyphenols in cancerchemoprevention: Lifelong remodeling of our epigenomes. Pharmacological Research, 65(6):565–576.

Verzelloni, E., Tagliazucchi, D. ve Conte, A. (2010). From balsamic to healthy: Traditional balsamic vinegar melanoidins inhibit lipid peroxidation during simulated gastric digestion of meat. Food and Chemical Toxicology, 48:2097-2102.

Wang, N., Zhang, C. Y., Qi, Y. D., & Li, T. P. (2007). Extraction and food chemical characterizations of haw pectins. Science and Technology of Food Industry, 28(11):87–92.

World Health Organization-WHO, (2013). WHO Traditional Medicine Strategy,

https://www.who.int/health-topics/traditional-complementary-and-integrative

## medicine#tab=tab 1.

Yıkmış, S. (2019). Optimization of Uruset Apple Vinegar Production Using Response Surface Methodology for the Enhanced Extraction of Bioactive Substances. Foods, 8:107.

Yu Q, and Duan Z-H. 2016. Research Progress in the Processing and Exploitation of Hawthorn. Joint International Conference on Social Science and Environmental Science (SSES 2016) and International Conference on Food Science and Engineering (ICFSE 2016). 395-403

on Innovative Surveys in Positive Sciences 4-5 December 2022 / Full Text Book

# USING OF GREEN SPACES IN HEALTHCARE FACILITIES AND ITS IMPACT ON HUMAN HEALTH

Parween Karim<sup>a</sup>, Dedar S. Khoshnaw<sup>b,c,d</sup>, Zana F. Ali<sup>e,f</sup>

<sup>a,</sup> Consultant Architect, Directorate of Health – Erbil, Kurdistan Region, Iraq

b. Marcel Breuer Doctoral School, University of Pécs, Boszorkány u. 2, 7624 Pecs, Hungary

<sup>c</sup>Department of Architectural Engineering, Faculty of Engineering, Koya University, Erbil, Kurdistan Region, Iraq

<sup>d,</sup> Energia Design Building Technology Research Group, Szentágothai Research Centre, Ifjúság útja 20, 7624 Pecs, Hungary

<sup>e,</sup> Doctoral School of Earth Sciences, University of Pécs, Ifjúság Str 6, H-7624 Pécs, Hungary

f. Department of Geography, Faculty of Education, Koya University, Kurdistan Region, Iraq

#### **ABSTRACT**

Recently, many scientific papers discussed the importance of green spaces in designing hospitals and its impact on mental and physical well-being of hospital attenders. The natural environment around hospitals plays an important role in boosting the psychological well-being of patients and staff. The current study attempts to examine the impact of green spaces by providing a case study of evaluating and assessing outdoor and indoor gardens and their impact on patient outcomes and staff performance in Shar hospital in Sulaymaniyah, Iraq. In order to assess the green spaces in Shar hospital, the research adopted a qualitative and quantitative approach enhanced with field observation. The approach is oriented towards hospital attendees and their personal observations. In addition, the study concentrates on analyzing and assessing different key areas in Shar Hospital; outdoor gardens, main reception hall, waiting area, corridors, doctor rooms and patient rooms and wards. Then the important findings were derived in the design of outdoor and indoor greenery and its effects on hospital occupants. The research finds that gardens and plants have positive effects in reducing negative effects such as stress and fatigue on patients and staff. The research also finds that greenery beneficial in creating a healthy environment, and recommends that interior and outdoor green spaces should be designed and operated as therapeutic and healing spaces for all hospital occupants.

**Keywords:** greenery in hospitals and healthcare facilities, benefits of green spaces, positive effects of gardens on patients and staff, natural environment improves physiological and psychological effects.

#### INTRODUCTION

Human health has been affected both positively and negatively by social changes and city planning in the past 200 years. There have been substantial reductions in communicable diseases due to vaccination and improvements in living standards and living environments -such as better hygiene, housing, and access to recreation areas. The conviction that gardens and green spaces are important for patients in health facilities is more than one thousand years old, and the conviction first started in Asia and Western Cultures (Ulrich and Parsons, 1992; Ulrich, 2002). Modern hospitals and other healthcare settings are designed based on scientific researches that reported that certain factors contribute to quicker patient recovery. A growing number of studies have been conducted on the benefits of green spaces in hospitals and healthcare settings in recent years (Wendelboe-Nelson, 2019; Rugel, 2015; Dadvand, 2012). The reason for this is the growing understanding of the value of nature as well as the positive effects of its benefits on both patients and staff. As a crucial tool for sustainable development, green spaces are an integral part of sustainable healthcare.

Although green spaces have been linked to a variety of health benefits, studies on impact of greenery on mental health in Kurdistan Regions are scarce. Particularly, in Iraq, including those of

on Innovative Surveys in Positive Sciences 4-5 December 2022 / Full Text Book

the Kurdistan region, hospital designs were not studied to understand if the green spaces in Iraqi hospitals are sufficient enough to contribute to the well-being of hospital attenders. Hospital designers face this problem in their daily work whether decreasing green space or sometimes changing gardens to the building. Additionally, indoor gardens are neglected or hospitals have a lack of inner greenery, in addition that green roofs and green walls have no existence.

Therefore, the current research attempts to study green spaces in Shar hospital to showcase if the green spaces of the hospital are contributing to mental and physical well-being of hospital attenders.

## RESEARCH QUESTIONS AND METHODOLOGY

Current research aims at answering two questions about green spaces in hospital. The research tries to understand what is the role of gardens and plants in hospital and healthcare setting designs? And why is it crucial to focus exclusively on greenery in healthcare facilities? To answer these questions, the research relies on mixed method. Qualitative approach allows deep insight and provides knowledge about the topic under scrutiny. In addition to that, the quantitative approach focuses more on statistics and numbers. In addition to field visits and accessing original maps, the researchers employed a twenty five questions questionnaire, appendix (1). The questionnaire was administered by researchers. Moreover, the questionnaire was partially close-ended and partially open-ended. The questions of the questionnaire were designed to understand the personality of the person, then, to understand why the person attends the hospital and finally, to understand the experience of the hospital attendee. Concerning the sampling, 30 patients and 10 permanent staff were recruited. Furthermore, the research illustrate the components of Shar hospital, and also provides a related literature.

#### LITERATURE REVIEW

Health benefits associated with urban green spaces, but detailed studies on the impact of green spaces on mental health are rare in Iraqi and Kurdistan Region health facilities. The benefits of greenery for patients and staff have been demonstrated in numerous studies which are reported in the next sections according to different connections, as the followings;

## Nature connection and the benefit access to greenspace.

In recent years, due to COVID 19 break out, maintaining wilderness and nature gained popularity. The National Institute for Health and Care Excellence (NICE) recommends that greenery ought to be considered in designing health facilities to accommodate healthy and smooth recovery (NICE, 2019). Evidence shows that closeness of health facilities to nature gives hospital attenders greater connection to nature and generates satisfaction emotions (Richardson, 2019, and Capaldi CA, 2014). Also, One study showed that in Chicago tenants expressed stronger sense of community and stronger feelings of unity with neighbours whenever there are trees around their buildings, which improves mental health and quality of life (Wisconsin DNR forestry news, Healthcare facilities using green spaces to help in healing, 2017),outdoor spaces contributes to enhance social communication between residents, it also promotes a healthy lifestyle as it encourages residents to engage in some sort of fancy farming (Baiz et al., 2017). Several studies consistently showed that simply looking at the certain types of natural plants and gardens significantly ameliorates stress within five minutes or less (Grinde & Patil, 2009; De Vries et al, 2013). Moreover, other researchers also reported that looking at nature for longer periods not only helps to create serenity, but can also promote improvement in clinical outcomes such as reducing pain, motivates medication intake and shortening hospital stays (Ulrich, 2002). Furthermore, Dijkstra, Pieterse, and Pruyn (2008) reported that indoor plants enhance pain tolerance and have a positive effect on health and well-being.

#### THE IMPACT OF GREENERY DESIGN ON CLINICAL OUTCOMES

The connection between greenery and clinical outcomes is a topic of many studies.

Greenspaces that are well designed and maintained can reduce antisocial behaviours, while those that are poorly designed or neglected tend to have the opposite effect (Brink 2016).

Studies show that it is very critical that patients have adequate welcoming spaces during their hospitalization process (Douglas and Calbert, 2004). Other studies show the importance of creating a

on Innovative Surveys in Positive Sciences 4-5 December 2022 / Full Text Book

relaxation area by combining indoor space with the exterior green space, healing gardens, courtyards, and green elements that provide a healing environment for patients, the goal of the Healing Environment is to turn the hospital setting into a place to support families in the physical, emotional, and spiritual healing process (Sandra Whitehouse, 2001). On the other hand, Ulrich et al, (2004; 21) showed that physiological changes, such as a decrease in blood pressure and heart activity, have been shown to occur as a result of viewing nature in laboratory and clinical studies. Also, studies found that patients with a view of trees and greenery from their window recover more quickly and need fewer painkillers than patients without a view of green space (Ulrich, 1984). Additionally, some hospitals take new treatment procedures into account, such as some hospitals treat cancer patients, especially chemotherapy patients, in outdoor gardens and the results showed that it is more effective than the traditional procedures (Ulrich, 1984). Moreover, some studies show that a well-designed hospital garden is playing vital and indirect role in positive clinical outcomes and it elevates the level of positive feelings, and provides an opportunity to escape from negative psychological and emotional stresses such as fear, anger, and sadness (Cooper-Marcus and Barnes 1995; Marcus and Barnes 1999; Ulrich 1999, 2000c; Rodiek 2009; Carr 2011). Therefore, healing gardens and plants reduce stress and psychological disorder factors and promote healthy well-being.

#### BENEFITS OF PLANTS AND GARDENS FOR STAFF

The mental well-being of hospital staff and adequate space for hospital staff lead to quality performance in health facilities. Some studies reported that the decline of job satisfaction contributes to shortages of qualified staff which jeopardizes the quality of care that patients receive (Ulrich, 2002). Also, evidence emphasized that hospital gardens increase job satisfaction which may help in maintaining staff qualifications (Whitehouse et al., 2001). In addition, reports showed that nurse and staff rooms with view over the greenery increase the workplace staff satisfaction and leads to well performance (Sadler, 2001). Moreover, studies showed that sufficient green spaces improve social cohesion leading to reduction of feelings of loneliness and isolation (Cooper-Marcus and Barnes, 1995), which enables the staff to build a strong network connection between themselves and the patients.

#### CASE STUDY DESCRIPTION

Shar Hospital is a general hospital in the Sulaymaniyah governorate of the Iraqi Kurdistan Region, it is located in the northeast of Suleimani province, on the longitude and latitude line (35°34'53.5"N 45°26'33.9"E), (Zakaria et al., 2013) see Figure (1). The current study paper studies a case study to illustrate and evaluate the quality of green space design of Shar Hospital. They study, by referring to original design and the execution, demonstrates the green spaces inside and outside the hospital.

Shar General Hospital 400 Bed

Location: Sulaymaniyah, Iraq

Client: World Health Organization

Design Consultant: Associated Consulting Engineers International ACE

Sub-Consultant: VDO international Group

Date completed: 2013 Plot Area: 45,911m2

Future extension from east side: 23,184m2 Future extension from west side: 23,380m2

Build-up area: 15,934m2 Open area: 29,977m2

Outdoor garden area: 5226m2 Figure (2)

Inner green areas (10 courtyards): 828m2 Figure (3)

Floors: 6 floors

on Innovative Surveys in Positive Sciences 4-5 December 2022 / Full Text Book

Hight: +28.20

THE  $\pm 0.00$  finished floor level, corresponds to +77.00 on the site elevation.

Site plan: hilly site the highest point 102.50m from the east side and the lowest point 45m from the west side. Figure (4)



Figure 1: Geographical Location of Study area (Sahr hospital) on Iraqi Map.

Source: Google Earth by Using Arc GIS 10.8



Figure 2: Shar hospital indicating the area of outdoor greenery compare

to the size of the hospital as a general

Source: Engineering and Technical Services S.P.A.



Figure 3: indoor plants

Source: Author (2021)

on Innovative Surveys in Positive Sciences 4-5 December 2022 / Full Text Book



Figure 4: contour lines and site plan of Shar hospital

Source: Sulaimaniyah General Directorate of Health (2022)

The following departments are located at Shar hospital:

Ground floor: congregation area, autopsy/post-mortem examination, workshops, laundry, services, store packing material, ultrasound scan, x-Ray diagnostics general, control room, angiography, extracorporeal shock wave lithotripsy, mammography, stores, computed tomography, dark room, kitchen, daylight film processing, meeting conference room, demonstration room, doctors office, medical records office, catheterization, archive medical records, dining area, staff changing dress, seminar room, lecture hall, teaching and library, prayer room, drug store, and laboratories.

First Floor: parking area, main entrance, main waiting area, lift lobby, scintigraphy procedure room, thyroid uptake room, needlework and handicrafts hall, urology examination room, dermatology radiation room, cardio-tomography room, laboratory dermatology hall, laboratories-all departments, plastic surgery examination room, children's playroom, medical records room, consultation room, gift shops, pharmacy, personal administration office, medical director office, financial director office, nursing services director office, purchasing office, reference archive hall, typing pool, technical manager room, accounts office, cashier office, patient admission venue, doctors on duty room, first aid room, waiting area ambulant patients, shock room, stretcher bay, emergency entrance, police office, emergency ambulance parking, medicine bathroom, massage room, gymnasium room, hydro therapist room, cafeteria, egometry/ stress test laboratory, ultrasound section, echocardiography room, electrocardiography room, laboratory blood bank, laboratory clinical chemistry, all department of laboratories.

**Second floor:** doctors' office, general surgeries of all types, delivery rooms, ultrasound room, maternity department, endoscopy gastroscopy room, operation rooms, day-care rooms, consultation rooms, nurse station, 10 courtyards, and bed rooms.

**Third floor:** nurse offices, doctor on call, UPS room, transformer room, MV room, housekeeping central store, electrical, doctor office, examination room, kitchen, prayer room, day room visitors, equipment store, and bed rooms.

**Fourth floor:** discharge area, housekeeping central store, central pantry, electrical office, main lobby, service lobby, nurse offices, doctor offices, examination room, equipment store, kitchen, dayroom visitors, staff restroom, waiting room, and bed rooms.

**Fifth floor:** discharge area, housekeeping, central pantry, electrical office, mechanical shaft office, clean contamination room, reception, nurse offices, doctor offices, examination room, tea-break room, bathroom, dirty contamination room, staff restroom, patient shower, waiting area, nurse station, children playroom, and paediatrics bedroom.

Sixth floor: stairs, lobby, AGSS.

#### ANALYSIS AND DISCUSSION

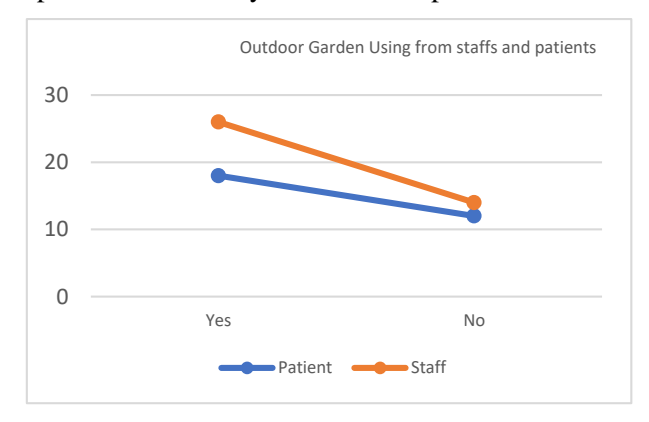
The analysis concentrates on the themes clarified via case study, observation and the questionnaires collected. The two themes discussed are outdoor and indoor green spaces in and around the Shar hospital. The responses of the questionnaire are analysed based on if the respondent is a patient, or a staff. Furthermore, the analysis is backed up by studying the original designing of the facility and site visit.

on Innovative Surveys in Positive Sciences 4-5 December 2022 / Full Text Book

Concerning the sampling, 40 participants, ten staff and thirty patients, were recruited randomly. In addition, both samples were carefully designed to include staff who are from different backgrounds and different profession levels, e.g., doctors, nurses, front desk, administrative. On the other hand, the patient samples were also from different ages, attending hospital for different types of diseases and from different backgrounds. Moreover, in both samples, gender balance was respected, appendix (1).

#### Theme 1:

**Outdoor garden;** the questionnaire was designed to understand the outdoor gardens' impact on the patients and staff. The questions were designed in a way to see if patients and staff can realize the greenery space they are exposed to when they visit Shar hospital.



Fogure 5: Chart shows the utilizing outdoor garden from patients and staffs

Figure (5) shows the utilizing outdoor garden from patients and staff according to their questionnaire response. The label illustrates the percentage of patients and staff participants. The label also shows that the garden is used by staff and patients with a staff using it a bit higher. This is because the staff spend more time in the hospital than patients. The responses from the questionnaire showed that staff take a walk, get fresh air and also use the waiting area to wait for surgery frequently. Simultaneously, the respondents who do not use green areas because they don't have enough time to use it, they just look at outdoor gardens through windows. Moreover, fewer responses indicated that they were not able to access the green spaces because they are not familiar with the different parts of the facility or the access to these green spaces were not easy.

Researchers observed that there are two main reasons behind avoiding visiting green spaces in Shar hospital, firstly, as Figure 5 indicated, amount of gardens and green spaces in Shar hospital is relatively small if compared to the overall size of the facility, secondly, it is observed that the garden designed to be more like a barrier between the hospital and highway, rather than being designed for a place to be used for walking.

The observation also indicated that the main obstacle behind inaccessibility of outdoor gardens. The research found that there are not clearly-indicating-signs to show pedestrians how to access the outdoor gardens. In addition to that, the research found that there are no, or little, outdoor events in Shar hospital. These barriers also de-motivates the social interaction, culture cohesion. Kim and Kaplan (2004) reported that outdoor events and activities in hospitals lead to social involvement and formulates the sense of belonging to a community, which could not be observed or achieved in Shar hospital.

Despite the fact that the hospital lacks seats, a rain/sun sheltering place, the hospital also lacks places for physical activities and recreation equipment, and there is no place for children to play in the garden as well. Braubach, Matthias, et al, 2017 cited in (Barton and Pretty 2010; Bodin and Hartig 2003), showed that there is a strong relationship between physical activity and the natural environment, and physical activity in green areas, green exercise, is more effective and beneficial to health than physical activity in non-green areas.

#### Theme 2:

Exposure to plants by the hospital users;

on Innovative Surveys in Positive Sciences 4-5 December 2022 / Full Text Book

The research focused on different areas in Shar hospital; waiting area, main reception hall, patient rooms, ward and staff workplaces. The purpose of the case study and the questionnaire are to investigate how the interior atmosphere and outdoor gardens, in terms of natural plants and greenery, affect patients and staff.

Main Reception, Corridors, and Waiting Area; the study tried to understand to what extent indoor plants have affected staff work environment and patients healing. The questionnaire was designed to understand how and when hospital visitors and staff are looking at plants. It is observed that a large reception hall is situated in the middle of the hospital with wide windows overlooking the garden, indoor plants and greenery. The windows are designed to attract people's attention who work daily or are waiting or walking there. The questionnaire responses indicated that 70% of staff and patients felt positive about the existing natural elements and watching the landscape, and believed that it reduced their stress level. There is no doubt that plants and flowers enhance positive physiological responses of patients and also contribute to lowering anxiety and fatigue levels. Also, it has a significant positive impact on the quality of work of staff which leaves a direct and positive impact on the quality of patient care, figure (6). The site visits showed, potentially due to availability of plants, that the number of patients waiting in the reception hall, where there are no seats, is far more than those who are waiting in the waiting area.



Figure 6: Main reception hall of Shar hospital

Source: Author (2021)

The responses concerning the emergency section, where the plants are scarce and there is no access to outdoor gardens, showed similar negative feeling rates. The data also showed that over-crowding and large numbers of patients are also contributing to the high negative feeling rates. Negative feelings vary according to the different parts of Shar hospital and different respondents. While some expressed their negative feelings towards the patient wards because of situating many beds in a relatively small hall where the access to nature is limited, some others indicated that they believe the worst part of the hospital is the consultant rooms as the queue is long and the atmosphere is not friendly. Others stated that the worst part of the hospital is the service area as there is no hot water supply. The respondents indicated that they are feeling comfy with having one bad room with access to an outdoor garden. The questionnaire also showed that surgical, laboratory, and the x-ray are the best parts of the hospital because they have appropriate waiting areas and attractive art works on the walls with live TV showing the queue, as shown in figure (7).

on Innovative Surveys in Positive Sciences

4-5 December 2022 / Full Text Book



Figure 7: Waiting area of Shar hospital

Source: Author (2021)

Figure 8 and 9 demonstrated number of participants and the general description of some places in the hospital from patient's and staff's perspectives. The figures showed that there are contradictory feelings from patients and staff responses, for instance, the charts showed that the highest number of the staff participants and the lowest number of the patient participants thought that the corridors are well designed. Also, figure 10 and 11 confirm that the corridors are well designed with adequate lighting, artificial or natural light, and the pathway widths are planned accordingly. Furthermore, it connects different parts of the hospital without complexions. The site visit revealed that the patients' negative feeling about the corridors, especially those corridors that pass through the patient wards, is caused by the shape of the corridors which goes through the patients' wards without adding a window and the angles. The corridor is oblique which make patient uncomfortable and confused as they struggle to find different departments and sections effortlessly.

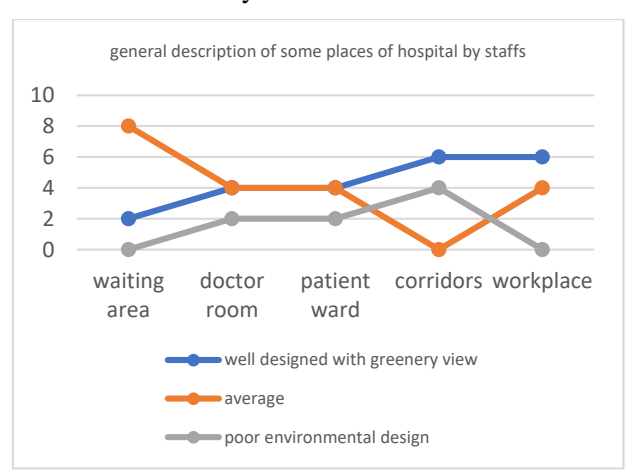
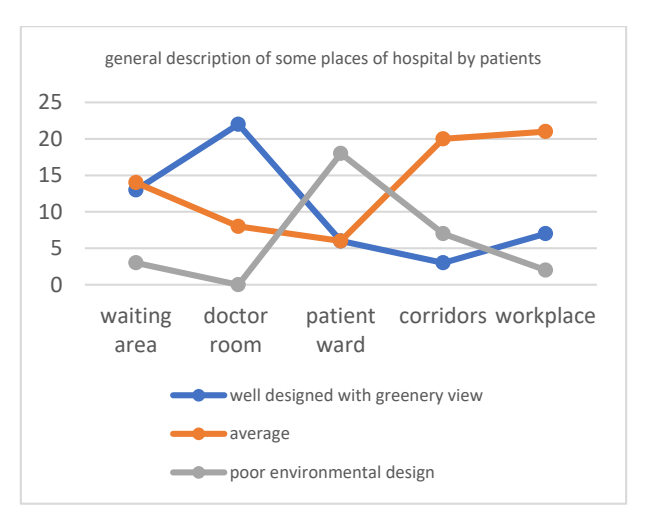


Figure 8: Chart shows the general description of some places of hospital by staffs

on Innovative Surveys in Positive Sciences

4-5 December 2022 / Full Text Book



Fogure 9: Chart shows the general description of some places of hospital by patients

Figure (8) and (9) showed patient's and staff's descriptions for the waiting area. The charts showed that about 80% of participants stated that waiting-area is not well-designed, especially without greenery view. About 20% of participants from both charts expressed that the waiting area is situated in an unsuitable area. The observation of the researchers confirms the dissatisfied responders as Shar hospital has no main waiting area, but each department has a waiting area of their own which are almost identical in design and arrangement. Moreover, the waiting-area has no wide windows, no natural views and no indoor plants; it closed in three sides of wall figure (11).



Figure 10: workplace and corridors with an oblique angle

Source: Author (2021)

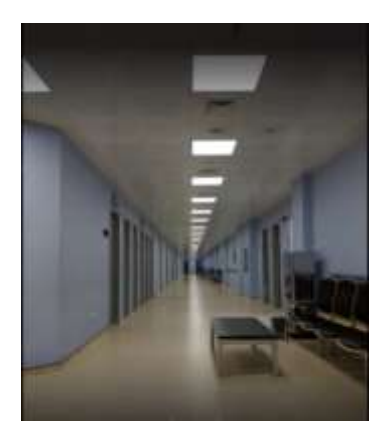


Figure 11: corridors and waiting area

Source: Muhammad Fatih (2018)

**Patient Room and Ward;** Shar hospital has 400 beds. All beds are placed in second, third, fourth, and fifth floors. There are same number of beds in each floor. Figures (12),(13) and(14) demonstrate the

on Innovative Surveys in Positive Sciences 4-5 December 2022 / Full Text Book

patient's wards. The patient's beds are well designed, furnished, and half of them have access to the nature view of Goizha and Ezmer Mountains, the other half are located at the opposite side of the hospital construction site. The beds are well organized and the rooms have access to a natural light. While, still in each hall, there are eight beds surrounded with curtains, patients are stay in their beds at least 12 hours. They felt anxiety, fatigue and bored inside curtain-covered sides except 2 beds from each ward feeling well and fresh which located in front of the window figure (13).



Figure 12: Patient ward has access view to Ezmer and Goizha Mountain

Source: Author (2021)



Figure 13: patient ward with 10 beds in each room

Source: Author (2021)



Figure 14: Patient ward has access view to the opposite side of the Shar hospital

Source: Author (2021)

#### Doctor Rooms, Work places, and Nurse Station & Laboratories

The questionnaire's from both staffs and patients for the Doctor rooms show another contradictory answer, patients thought that doctor room are well environmental designed with greenery view, reverse to the staff description the highest contributors said the doctor rooms are well designed but without greenery view. site visit showed that the doctor's rooms are well designed but without greenery access. Figure (15) shows that doctor's rooms are well designed, fully furnished but there is no greenery view

on Innovative Surveys in Positive Sciences 4-5 December 2022 / Full Text Book

from inside or outside. In addition, the workplaces in Shar hospital are designed and appropriately furnished. The study selected two workplaces for examination and questionnaire; laboratories and nursing station. Laboratories in the hospital are located in the ground and first floors. The workspace is designed to allow natural light, natural ventilation and natural view to penetrate the spacious of windows. Moreover, staff and patients can work and move easily because of the good arrangement and connection with the other departments. Furthermore, the nurse station is also well designed with having adequate natural lighting and greenery view from the station.



Figure 15: Doctor room

Source: Ameer Bahaddin (2022)



Figure 16: laboratories with natural elements

Source: Author (2021)

#### **FINDINGS**

Responses from the patients and staffs in four questions from the questionnaire clearly illustrated the prominence of utilizing natural resources inside and outside of the hospital for the people. The responses of the four greenery-related questions, from staff and patients perspectives, indicated the importance and the mental and physical impact of adequate greenery in designing health facilities. For the first question, how do you feel when you see greenery inside and outside the hospital? All participants expressed the sense of comfort and joy when they are exposed to green spaces inside or outside of the health facilities. Secondly, when you have stress do you think greenery reduce it? The responses indicated that there is no doubt about the reduction of mental stresses when exposed to greenery. Thirdly, the recruited participants were asked; would you like to increase or decrease green spaces outside and the greenery inside the hospital? All participants expressed that, with no hesitation, increasing green spaces and greenery inside and outside of the hospital is helpful. Fourthly, in an open question, the participants were asked; is there anything you would like to tell me about the greenery design in the outdoor and interior space? All responses recommended increasing the green spaces in hospital.

The Shar hospital staff stated that they are feeling happy and satisfied working in the hospital. They also expressed that the existing green spaces inside and outside the hospital is considerably contributing to improving their haunting stress and annoyed mood. The overall staff' responses indicated that they are

on Innovative Surveys in Positive Sciences 4-5 December 2022 / Full Text Book

happy with greenery in Shar hospital. on the other hand, As 60% of patients believed that patient's ward is not well designed and lacks access to green spaces, and 40% of patients believed the otherwise, 80% of staff' responses indicated that the patient ward is well designed and the green spaces is almost adequate, however, 20% of staff agreed with patients in matters of design and green spaces in the patients ward.

Concerning the outdoor green spaces around Shar hospital, Participants, both staff and patients, expressed different feelings towards the selected areas. Despite the fact that the participants used the outdoor gardens, they are not happy about it and felt dissatisfied because the gardens are not well designed. In addition, the outdoor spaces are occupied with invasive herbs and grasses and lacks modern greenery design. In addition, there is no clear pathway to access the outdoor green spaces. Moreover, the lack of modern designed garden, makes arranging outdoor events and activities almost impossible and the records show that there are no outdoor activities in Shar hospital outdoor gardens. Consequently, the lack of social cohesion is apparent.

Although a large number of the participants expressed positive feelings about indoor green spaces, such as pots or exposing to outdoor gardens through windows, but considerable portion of patients and staff felt relaxed and comfortable even when there are no natural view and plants. The site visit revealed that one of the factors behind this is existence of art pieces, availability of plenty of daylight, artificial light and attractive furniture. Parween Karim (2016) stated that physical environment design such as daylighting, colour, natural view and art are playing an important role in psychological healing in healthcare building design. However, some participants showed that they are dissatisfied with poor design wards without access to the greenery view, they believed that these factors might increase their stressed and fatigued. Moreover, the lack of clearly-indicating navigating pathway prevent patients in the corridors to reach the desired department, is also increasing the stress levels.

#### RECOMMENDATIONS

Based on the results and discussions, the research recommends the followings;

- Designing healing gardens and courtyards as treatment, such as chemo gardens, or green physiotherapy, exercise places.
- Designing a noise-free gardens for walking and relaxation.
- Designing and providing places where staff, elderly and ambulatory patients can go for walk to boost their recovery process.
- Designing a modern green roofs and green facades in hospital buildings.
- Designing indoor gardens inside healthcare buildings such as in waiting areas which contributes to reduction of anxiety and pain and largely prevents indoor air pollutants.
- Planting vegetation around patient wards and rooms to shorten hospital stays.
- .• Providing greenery accessibility through the windows. Patient's rooms should be windows oriented to grant the access to outdoor natural views.
- Designing attractive and pleasant landscapes around hospitals including gardens, trees and green borders.

#### **CONCLUSION**

The current study attempted to understand the importance of green spaces, indoor and outdoor, impact on the way hospital visitors relating their experiences. In addition, the research was trying to investigate which part of the hospital is designed to adequately showcase green spaces. Through analysing different areas of the hospital, the research found that designing an attractive gardens and landscapes are important for patients and staff to reduce their stress and anxiety. Generally, Staff and patients feel positive when they are exposed to greenery inside the hospital, whether from indoor plants or from outdoor gardens through the windows. Employees in workplaces, such as nursery and laboratory, also felt positive and satisfied with their job due to seeing green spaces through windows with having a good sufficient plants in the rooms. Moreover, hospital's visitors also felt positive in the main

on Innovative Surveys in Positive Sciences 4-5 December 2022 / Full Text Book

reception hall because of existing plants and overlooking windows to the gardens. In contrast, patients felt stressful in the patient rooms and wards because of lack windows that overlook the nature.

From the review of scientific literature and the analysis of the questionnaire as previously stated, the study found that green spaces in hospitals are playing important role. The research also found that it is crucial to consider the green spaces in designing health facilities. In addition, the data showed that designing gardens and landscapes in hospitals enhance physical health through stress reduction, relaxation and other psychological effects. And, the physical activities in the green space is contributing to blood pressure reduction, lowering stress levels, fear and anger. Therefore, designing therapeutic gardens for patients and places for physical exercise, walking and relaxing is essential tool for promoting psychological well-being. Furthermore, the research found that outdoor gardens and natural environment enhance social cohesion and community engagement.

#### REFERENCES

Ameer Bahaddin, (2022), "Shar Hospital Gallery" [online] last access 15th of Jul. 2022 at Shar Hospital - Hospital in Sulaymaniyah (business.site)

Baiz, W. H., Khoshnaw, D. S., & Byze, A. H. (2017). High-Rise Buildings Aspects and Significant Impacts in Urban Areas. *International Journal of Engineering Research and Applications*, 06(10), 20–26. <a href="https://doi.org/10.9790/9622-0610012026">https://doi.org/10.9790/9622-0610012026</a>

Braubach, M., Egorov, A., Mudu, P., Wolf, T., Ward Thompson, C., & Martuzzi, M. (2017). Effects of urban green space on environmental health, equity and resilience. In *Nature-based solutions to climate change adaptation in urban areas* (pp. 187-205). Springer, Cham.

Capaldi, C. A., Dopko, R. L., & Zelenski, J. M. (2014). The relationship between nature connectedness and happiness: A meta-analysis. *Frontiers in psychology*, 976.

Centre for Sustainable Healthcare. (2020), Green Space for Health: "Green Health Routs". [Online] last access 8<sup>th</sup> of Jun. 2022 at <a href="https://sustainablehealthcare.org.uk/what-we-do/green-spacehealth?fbclid=IwAR07vdiW64VA3AQ4GcKVBiCXVsb-MHoBC7WkzEaSp0wbMo5y7W2J8P7cl4A">https://sustainablehealthcare.org.uk/what-we-do/green-spacehealth?fbclid=IwAR07vdiW64VA3AQ4GcKVBiCXVsb-MHoBC7WkzEaSp0wbMo5y7W2J8P7cl4A</a>

Dadvand, P., De Nazelle, A., Figueras, F., Basagaña, X., Su, J., Amoly, E., & Nieuwenhuijsen, M. J. (2012). Green Space, Health Inequality and Pregnancy. *Environment International*, 40, 110-115.

De Vries, S., Van Dillen, S. M., Groenewegen, P. P., & Spreeuwenberg, P. (2013). Streetscape Greenery and Health: Stress, Social Cohesion and Physical Activity as Mediators. *Social Science & Medicine*, *94*, 26-33.

Dijkstra, K., Pieterse, M. E., & Pruyn, A. (2008). Stress-reducing effects of indoor plants in the built healthcare environment: The mediating role of perceived attractiveness. *Preventive medicine*, 47(3), 279-283.

Douglas, C. H., & Douglas, M. R. (2004). Patient-Friendly Hospital Environments: Exploring the Patients' Perspective. *Health Expectations*, 7(1), 61-73.

Ellen C., (2017), "Healthcare facilities using green spaces to help in healing" Wisconsin DNR Forestry News, [Online] last access 10th of Aug. 2022 at <a href="https://forestrynews.blogs.govdelivery.com/2017/11/15/healthcare-facilities-using-green-spaces-to-help-in-healing/">https://forestrynews.blogs.govdelivery.com/2017/11/15/healthcare-facilities-using-green-spaces-to-help-in-healing/</a>

Engineering and Technical Services S.P.A. [online] last acces 5<sup>th</sup> of Feb. 2022 at <u>Shar Hospital - ETS</u> <u>Engineering and Technical Services SPA</u>

Grinde, B., & Patil, G. G. (2009). Biophilia: Does Visual Contact With Nature Impact On Health And Well-Being? *International Journal of Environmental Research and Public Health*, 6(9), 2332-2343.

Hiemstra, J. A., de Vries, S., & Spijker, J. H. (2017). Green and Healthcare: A summary of the positive effects of greenery on well-being in recovery environments. Wageningen University & Research.

on Innovative Surveys in Positive Sciences 4-5 December 2022 / Full Text Book

Jiang, S., Allison, D., & Duchowski, A. T. (2022). Hospital Greenspaces and the Impacts on Wayfinding and Spatial Experience: An Explorative Experiment through Immersive Virtual Environment (IVE) Techniques. *HERD: Health Environments Research & Design Journal*, 19375867211067539.

Jinguang Zhang et al., (2020), "Links between green space and public health: a bibliometric review of global research trends and future prospects from 1901 to 2019 "Environ. Res. Lett. 15 063001 [online] last access 10<sup>th</sup> of Jul. 2022 at <a href="https://iopscience.iop.org/article/10.1088/1748-9326/ab7f64/pdf">https://iopscience.iop.org/article/10.1088/1748-9326/ab7f64/pdf</a>

Karanikola, P., Andrea, V., Tampakis, S., & Tsolakidou, A. (2020). Indoor and Outdoor Design in Healthcare Environments: The Employees' Views in the General University Hospital of Alexandroupolis, Greece. *Environments*, 7(8), 61.

Karim, P. (2016). *An Investigation into How the Design of Health Centres Can Promote Psychological Healing*. Author House.

Kim, J., & Kaplan, R. (2004). Physical and psychological factors in sense of community: New urbanist Kentlands and nearby Orchard Village. *Environment and behavior*, *36*(3), 313-340.

Kondo, M. C., Fluehr, J. M., McKeon, T., & Branas, C. C. (2018). Urban green space and its impact on human health. *International journal of environmental research and public health*, 15(3), 445.

Muhammad Fatih, (2018), "Shar Hospital Gallery" [online] last access 15<sup>th</sup> of Jul. 2022 at <u>Shar Hospital</u> - <u>Hospital in Sulaymaniyah (business.site)</u>

National Institute for Health and Care Excellence (NICE). (2019). Physical Activity: Encouraging Activity in the Community. Quality Standard QS183.

Richardson, M., Hunt, A., Hinds, J., Bragg, R., Fido, D., Petronzi, D., & White, M. (2019). A measure of nature connectedness for children and adults: Validation, performance, and insights. *Sustainability*, 11(12), 3250.

Ridgley, H., Hands, A., Lovell, R., Petrokofsky, C., Stimpson, A., Feeley, A., & Brannan, M. (2020). Improving access to greenspace A new review for 2020. *Public Health England*.

Rugel, E. (2015). *Green Space and Mental Health: Pathways, Impacts, and Gaps.* Vancouver, BC: National Collaborating Centre for Environmental Health.

Salonen, H., Lahtinen, M., Lappalainen, S., Nevala, N., Knibbs, L. D., Morawska, L., & Reijula, K. (2013). Design approaches for promoting beneficial indoor environments in healthcare facilities: A review. *Intelligent Buildings International*, *5*(1), 26-50.

Sulaimaniyah General Directorate of Health(2022), Ministry of Health Krg, Projects Department.

Ten Brink, P., Mutafoglu, K., Schweitzer, J. P., Kettunen, M., Twigger-Ross, C., Baker, J., & Dekker, S. (2016). The health and social benefits of nature and biodiversity protection. *A report for the European Commission (ENV. B. 3/ETU/2014/0039)*. London/Brussels: Institute for European Environmental Policy.

Ulrich, R. S. (2002). Health benefits of gardens in hospitals. *International Exhibition Floriade* (Vol. 17, No. 5, p. 2010).

Wendelboe-Nelson, C., Kelly, S., Kennedy, M., & Cherrie, J. W. (2019). A Scoping Review Mapping Research on Green Space and Associated Mental Health Benefits. *International Journal of Environmental Research and Public Health*, 16(12), 2081.

West Virginia University. (2022, February 18). Seeing 'green' can ease confusion, anger in navigating hospitals. *ScienceDaily*. Retrieved August 25, 2022 from <a href="https://www.sciencedaily.com/releases/2022/02/220218172312.htm">www.sciencedaily.com/releases/2022/02/220218172312.htm</a>

Whitehouse, S., Varni, J. W., Seid, M., Cooper-Marcus, C., Ensberg, M. J., Jacobs, J. R., & Mehlenbeck, R. S. (2001). Evaluating a children's hospital garden environment: Utilization and consumer satisfaction. *Journal of environmental psychology*, 21(3), 301-314.

Zakaria, S., Mustafa, Y. T., Mohammed, D. A., Ali, S. S., Al-Ansari, N., & Knutsson, S. (2013).

on Innovative Surveys in Positive Sciences 4-5 December 2022 / Full Text Book

Estimation of annual harvested runoff at Sulaymaniyah Governorate, Kurdistan region of Iraq. *Natural Science*, 05(12), 1272–1283. <a href="https://doi.org/10.4236/ns.2013.512155">https://doi.org/10.4236/ns.2013.512155</a>

#### Appendix 1,

### Questionnaire

This questionnaire is part of our research paper at Shar Hospital in Sulaymaniyah city. It aims at exploring the perception of patients and the staffs of Shar hospital about their experience concerning the existing greenery and its impact on reducing their pains and stress. By completing this survey, you will provide helpful data. Please remember that this is not a test, so there is no right or wrong answers and you do not need write your name on it. Your responses will be confidential.

- 1. Gender (Male or Female)
- 2. Age Range (15-20, 21-30, 31-40, 41-50, 51-60, 61-70 71-80, <8)
- 3. Would you mind let me know if you are (A visitor, Patient who is in the hospital, coming here for the outpatient (test, checking up, appointment, x ray, etc), Medical staff, Working at the hospital, Staff or employee, Other (specify) ......)
- 4. Would you mind let me know what is the type of your disease (Heart disease, Blood pressure, Diabetes, Chronic respiratory disease, Cancer disease, Blood disease, Chronic kidney disease, Disease of the nervous and psychological, Other (specify)......)
- 5. Why you choose this hospital (staff and patients).....
- 6. How often do you come here? (Everyday, Several times a day, 2-3 days a week, Once a week, Once a month, Occasionally or sometimes, My first time)
- 7. When you come how long do you stay here?(15-30 minutes, More than an hour, Few hours, One day or more than a day, One week, More than a week, less than a month, Other (specify time)......)
- 8. How do you feel when you, wait here? (Relaxing, have coffee, talking with friends, read, stroll, etc.)
- 9. Describe this place, generally? (Waiting area, Doctor room, Patient ward, Patient room, Corridors, Working place, Well designed with greenery view, Average, Poor environmental design)
- 10. Describe behavior or mood of people in this place (Very Relaxing (very good), Good, Average, Panic (poor), Not in the moody (very poor))
- 11. Describe your feeling in this place, (Waiting area, Doctor room, Patient ward, Patient room, Corridors, Working place) (Very good, Good, Average, Poor, Very bad)
- 12. When you come here do you feel better (patients)? (Yes, No)
- 13. When you work here how do you feel? (staff)(Very good, Good, Average, Poor, Very poor)
- 14. Where do you feel best in this hospital? Why?
- 15. Where do you feel bad in this hospital? Why?
- 16. Do you feel anything different or strange in this place when you spent time of staying or working here?
- 17. What is the reason you still working here (staff)? Or coming here again (patients)?
- 18. Is there anything that prevents you from coming here next time?
- 19. Do you use outdoor gardens? Why? (Yes, No)
- 20. How do you feel when you see greenery inside and outside the hospital? (Very good, Good, Average, Nothing)

on Innovative Surveys in Positive Sciences 4-5 December 2022 / Full Text Book

- 21. When you have stress do you think greenery reduce it? (Yes, No)
- 22. When and where do you feel breathtaking or relaxing in the hospital?
- 23. Would you like to increase or decrease green spaces outside and the greenery inside the hospital?
- 24. Is there anything you would like to change or add in the design of this place?
- 25. Is there anything you would like to tell me about the greenery design in the outdoor and interior spaces?

on Innovative Surveys in Positive Sciences 4-5 December 2022 / Full Text Book

# EXPERIMENTAL STUDY ON THE EFFECT OF GRAPHENE IN FLAT-PLATE COLLECTORS

#### Gamze GENÇ

Erciyes Üniversitesi Mühendislik Fakültesi Enerji Sistemleri Mühendisliği Bölümü ORCID ID: 0000-0002-1133-2161

#### Rumeysa URAL

Erciyes Üniversitesi Mühendislik Fakültesi Enerji Sistemleri Mühendisliği Bölümü

#### Merve ATİK

Erciyes Üniversitesi Mühendislik Fakültesi Enerji Sistemleri Mühendisliği Bölümü

#### Hilal DOĞAN

Erciyes Üniversitesi Mühendislik Fakültesi Enerji Sistemleri Mühendisliği Bölümü

#### **ABSTRACT**

Solar energy is commonly used to a large degree through solar flat plate collectors in Turkey which have high solar energy potential. However, the thermal efficiency of this collector is limited by the absorption properties of the water for these collectors. Nanofluids are mixed with water to enhance the collector's thermal efficiency nowadays. The presented study is aimed to perform an experimental study for the effect of nanofluid on the performance of a flat-plate collector. For this aim, graphene having a higher thermal conductivity parameter than water is used as nano-fluid. In addition, the effect of natural and forced circulation are also investigated. In the study, measurements were done at different times by using a mixture of water and graphene in three different ratios and time-dependent temperature graphs were obtained. Increasing the density of graphene allowed more heat to be absorbed in the fluid. Thus, the efficiency was increased. Moreover, it was observed that higher efficiency was obtained from forced circulation between the forced and natural circulation system by using water in the system.

Keywords: Solar energy, Nanofluid, Graphene, Flat-plate collector

### **INTRODUCTION**

Countries have sought to quickly integrate themselves into renewable production processes as well as fossil fuels in order to meet the needs of people with the continuous increase in the global population and the effective use of resources [1]. Solar energy is an energy source that comes from the sun and has no operating costs. In Turkey, which has a high solar energy potential, solar energy is mostly utilized through solar collectors. Hot water systems are among the most economical and common solar energy systems. The annual hot water requirement is covered by solar energy to the extent of 60–75% by planar collectors, which are typically installed on the south side of the roof. Solar collectors absorb solar energy and turn it into heat, which is then transferred to a working fluid such as water or solar fluid. Thus, solar rays are used to heat buildings, swimming pools, heating and cooling systems [2]. Some of the reasons for the common use of solar energy in hot water systems are as follows [3]:

- The change in the energy required for the hot water requirement is very low during the year compared to the months.
- Due to low energy requirements and low needed temperatures, a large collecting surface is not necessary. Therefore, the placement of the collectors is not a problem.
- The system is easy to construct, has few auxiliary elements, and is simple to control.
- Hot water is not required to be available every day. If necessary, a certain period of time can be waited according to the sun's condition.

Two systems are used in planar solar collectors. These are natural and forced circulation systems.

on Innovative Surveys in Positive Sciences 4-5 December 2022 / Full Text Book

Natural circulation systems are among the most widely used hot water systems. System consists of flat collectors and an insulated tank. Forced circulation systems are systems in which the heat transfer fluid is circulated in the system with a pump [4]. Recently, nanofluids with high thermal conductivity coefficient have been used. Nanofluids are formed by dispersing solid particles of nanometric size (1-100 nm) in a basic fluid. The purpose of creating such a structure is to increase the thermal conductivity of the fluid by mixing a nanomaterial (metal, metal oxide or high surface area carbonic structures) with a higher thermal conductivity than the base fluid [5]. Abu-Hamdeh et al. [6] used graphene fluid in Flat Plate Solar Collectors. The experimental/numerical results obtained have led to the optimization of the use of nanofluids in heating systems and to reduce the cost of using flat plate solar collectors in buildings. Graphene nanofluid showed good thermal performance. Vakili et al. [7] conducted an experiment on Graphene nanoplatelets / deionized water nanofluid, a volumetric solar collector for domestic hot water systems. Graphene nanoplatelets/deionized water nanofluid is thought to increase the efficiency of volumetric solar collector, which has applicability for domestic hot water systems. For this purpose, nanofluids of 0.0005%, 0.001 and 0.005% by weight were prepared and the effect of using graphene nanoplatelet nanofluid as an absorbing medium in a direct absorption solar collector was investigated. In conclusion, solar energy absorption experiments show that graphene nanoplatelets/deionized water nanofluids have good absorbing ability for solar energy and can improve the efficiency of volumetric solar collector. Therefore, this nanofluid can be applied to solar thermal energy system for residential applications. Sani et al. [8] prepared nanofluids consisting of graphene nanoplatelets for thermal solar collectors. If graphene-based nanoparticles are used in solar collectors, their performance will increase. Even at low concentrations, the addition of nanoparticles results in significantly increased sunlight absorption compared to pure liquid (0.005% and 0.05% by weight). The effect of graphene nanoplatelets on the performance of flat plate solar collectors was investigated experimentally and theoretically. Adding Gnp to deionized water can significantly increase the temperature and absorbed energy of the kettle. The fact that the outlet temperature of the water heater reaches 67.5 °C and 71 °C for 0.01% and 0.02% by weight Gnp, respectively, indicates that the system is suitable for domestic consumption. The theoretical thermal efficiency of flat plate solar collector was calculated and compared with the experimental one, and the results reveal that Gnp can effectively improve the performance of solar water heating systems [9].

In this study, graphene fluid, which has a higher thermal conductivity coefficient than water, was used instead of fluid water used in solar energy systems. The yield difference between natural and forced convection systems was researched

#### EXPERIMENTAL SETUP

The collector prototype case is made of glass wool for insulation, thin sheet metal and glass coated with black color, and a plastic water bottle is used for the water tank. The system consists of two solar collector prototypes for simultaneous measurements. Solar collectors are 21x29 cm2 in size. Pipe selection was made in accordance with the dimensions. The view of the collector is given and The inlet and outlet pipes were connected to the tank as shown in Figure 1.

In the first stage, it was aimed to examine the efficiency difference by using the thermal conductivity coefficient of graphene and water. For the first experiment, water was circulated in the first collector and a graphene-water mixture was circulated in the second collector. A mixture of 150 ml of water was placed in the first tank, 140 ml of water and 10 ml of graphene were placed in the second tank. For the second experiment, 200 ml of water was put into the first tank, 190 ml of water and 10 ml of graphene mixture were put into the second tank. For the third experiment, 200 ml of water was put into the first tank, 180 ml of water and 20 ml of graphene mixture were put into the second tank.

on Innovative Surveys in Positive Sciences 4-5 December 2022 / Full Text Book



Figure 1. Prototype view of solar and Connection of solar collectors to the tank.

# **RESULTS and DISCUSSIONS**

The result of the third experiment is shared as follows.

In the first experiment, the air temperature is 24 °C and the wind speed is 18 km/h. Due to the adverse conditions caused by external factors, sufficient yield could not be obtained. Experiment-related data are given in Table 1 and Figure 2.

**Table 1. Data of the first experiment** 

Time	Temprature of Water	Temprature of Water + Graphene						
	150 ml water	140 ml water 10 ml graphene						
14:17	25	25						
14:23	34	35						
14:39	38	39.5						
14:45	41.5	43						
15:51	44	47						
15:56	46	48						
16:00	46	47						

on Innovative Surveys in Positive Sciences

4-5 December 2022 / Full Text Book

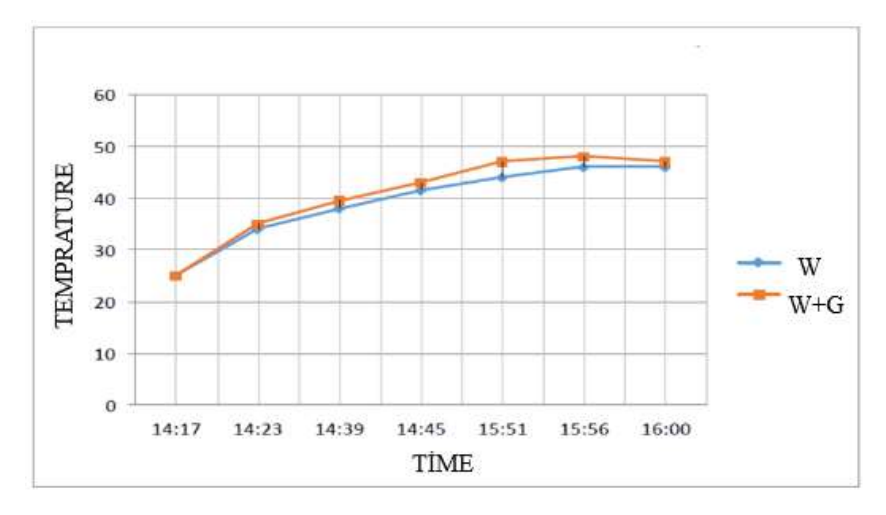


Figure 2. Time dependent temperature change according to the results of the first experiment.

In the second experiment, the day when the air temperature was 26 °C and the wind speed was 5 km/h was chosen. The yield we obtained in this experiment is higher than the second experiment, as expected. Experiment-related data are given in Table 2 and Figure 3.

Table 2. Data of the second experiment

Time	Temperature of water	Temperature of graphene
	200 ml water	190 ml water 10 ml graphene
12:13	20	20
12:18	24	28
12:23	33	37
12:33	38.5	42
12:39	43	47
12:44	46	51
12:51	48	55
12:58	50	55.5
13:05	51	57
13:11	51.5	58
13:18	53	59

on Innovative Surveys in Positive Sciences 4-5 December 2022 / Full Text Book

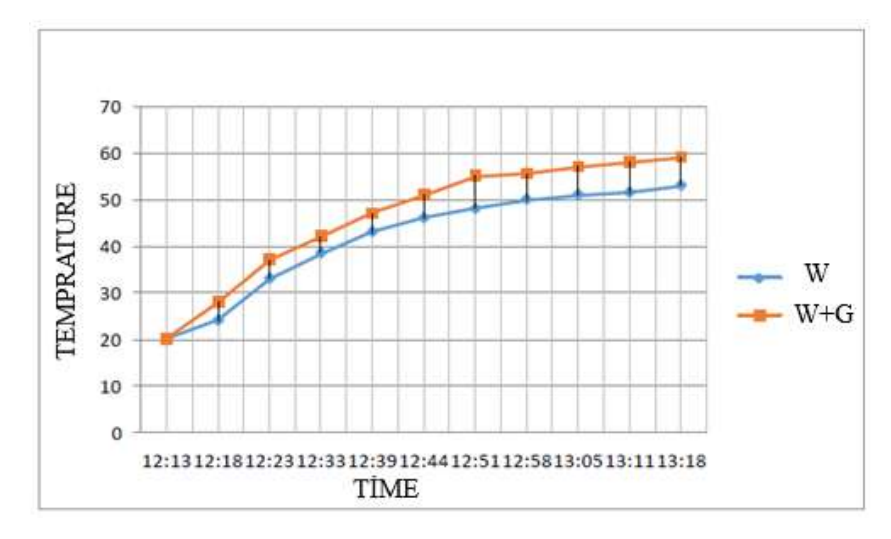


Figure 3. Time dependent temperature change according to the results of the second experiment.

In the third experiment, the graphene density was increased in the graphene-water mixture. Increasing the density of graphene enabled more heat to be absorbed in the fluid, since graphene has a high thermal conductivity coefficient. Thus, the efficiency was increased. Experiment-related data are given in Table 3 and Figure 4.

Table 3. Data of the third experiment

Time	Temprature of Water	Temprature of Water + Graphene							
	200 ml water	180 ml water 20 ml graphene							
11:45	20	20							
11:50	23	32							
11:55	32.5	40.5							
12:00	37	43							
12:05	41	49							
12:10	44.5	52.5							
12:15	46	55							
12:20	47.5	58.5							
12:25	49	61.5							
12:30	50	63							
12:35	50.5	63.5							

on Innovative Surveys in Positive Sciences 4-5 December 2022 / Full Text Book

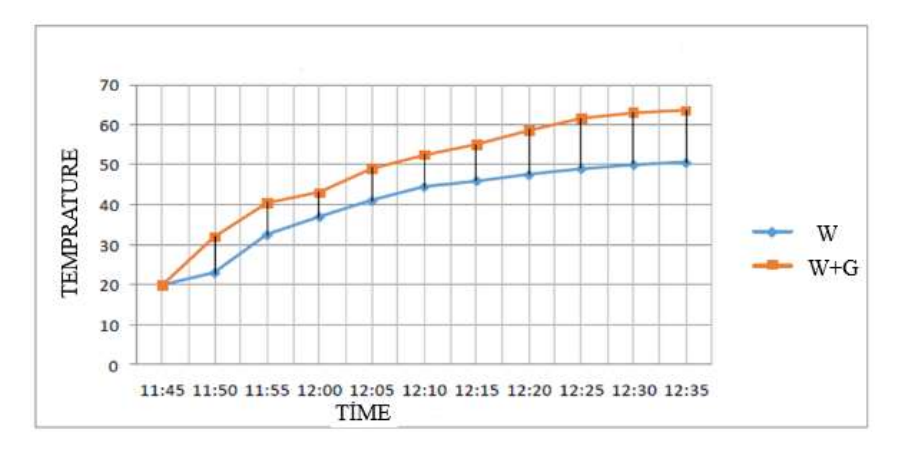


Figure 4. Time dependent temperature change according to the results of the third experiment.

In the fourth experiment, a different method was followed and a study was carried out to increase efficiency. The pump was used to indicate the effect of forced circulation on heat transfer. Although there was no significant difference, forced circulation was observed to be more efficient than natural circulation. Experiment-related data are given in Table 3 and Figure 4.

Table 4. Data of the fourth experiment

Time	Natural circulating water temperature	Forced Circulating Water Temperature						
	600 ml water	600 ml water						
14:03	22	22						
14:10	24	27						
14:17	31	33						
14:24	36	39						
14:31	40	44						
14:38	44.5	48.5						
14:45	48	52						
14:52	49.5	53						
14:59	51	54.4						
15:06	52	55						

on Innovative Surveys in Positive Sciences 4-5 December 2022 / Full Text Book

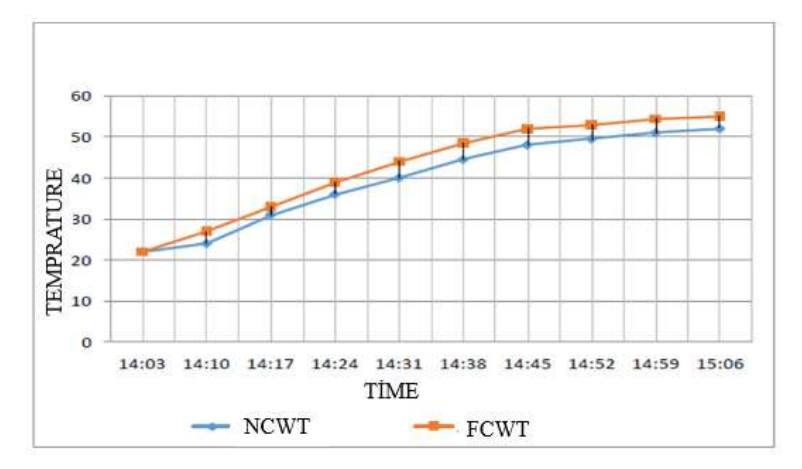


Figure 5. Time dependent temperature change according to the results of the fourth experiment.

#### **CONSLUSIONS**

As a result of different experiments, increasing the density of graphene enabled more heat to be absorbed in the fluid, since graphene has a high thermal conductivity coefficient. So the efficiency was increased. It was also observed that forced circulation was more efficient than natural circulation.

#### REFERENCES

- [1] Gielen, D., Boshell, F., Saygin, D., Bazilian, M. D., Wagner, N., & Gorini, R. (2019). The role of renewable energy in the global energy transformation. Energy Strategy Reviews, 24, 38-50.
- [2] Kumar, R., Verma, S. K., & Singh, M. (2022). Performance evaluation of cerium oxide/water nanofluid based FPSC: An experimental analysis. Materials Today: Proceedings, 56, 1659-1667.
- [3] Sibel, A. Ğ. I., & Günerhan, H. Sıvılı Düzlemsel Güneş Kolektörlerinde Verim Artırma Olanakları.
- [4] Kılıç, A. Güneş Enerjili Sıcak Su Sistemlerinin Seçimi Tasarımı Ve İşletilmesi.
- [5] Atmaca, İ., Koçak Soylu, S., Özdemir, O. S., & Asiltürk, M. (2019). Nanoakışkanlar ve güneş enerjili sıcak su sistemlerinde kullanımı.
- [6] Abu-Hamdeh, N. H., Khoshaim, A., Alzahrani, M. A., & Hatamleh, R. I. (2022). Study of the flat plate solar collector's efficiency for sustainable and renewable energy management in a building by a phase change material: Containing paraffin-wax/Graphene and Paraffin-wax/graphene oxide carbon-based fluids. Journal of Building Engineering, 57, 104804.
- [7] Vakili, M., Hosseinalipour, S. M., Delfani, S., Khosrojerdi, S., & Karami, M. (2016). Experimental investigation of graphene nanoplatelets nanofluid-based volumetric solar collector for domestic hot water systems. Solar Energy, 131, 119-130.
- [8] Sani, E., Vallejo, J. P., Cabaleiro, D., & Lugo, L. (2018). Functionalized graphene nanoplatelet-nanofluids for solar thermal collectors. Solar Energy Materials and Solar Cells, 185, 205-209.
- [9] Ahmadi, A., Ganji, D. D., & Jafarkazemi, F. (2016). Analysis of utilizing Graphene nanoplatelets to enhance thermal performance of flat plate solar collectors. Energy Conversion and Management, 126, 1-11.

on Innovative Surveys in Positive Sciences 4-5 December 2022 / Full Text Book

# KAYSERİ'DEKİ MANEVA ATIKLARININ BİYOGAZ ÜRETİMİNDE DEĞERLENDİRİLMESİ

#### Gamze GENÇ

Erciyes Üniversitesi Mühendislik Fakültesi Enerji Sistemleri Mühendisliği Bölümü ORCID ID: 0000-0002-1133-2161

#### Hatice Büşra PEKER

Erciyes Üniversitesi Mühendislik Fakültesi Enerji Sistemleri Mühendisliği Bölümü

#### Hilal DOĞAN

Erciyes Üniversitesi Mühendislik Fakültesi Enerji Sistemleri Mühendisliği Bölümü

#### ÖZET

Her gün milyonlarca ton meyve ve sebze atığı tüm dünyada çöp olarak atılıyor. Meyve sebze reyonunda deforme olmuş ve tercih edilmeyen ürünlere çıkma ürünler denilmektedir. Bu atıklar biyogaz üretiminde kullanılarak yeniden kullanılabilir. Ancak atıkların en düşük karbon emisyonu ile üretim noktasına taşınması büyük önem taşımaktadır. Bu yaklaşımda bir çalışma yapabilmek için Kayseri ilinde bir örnek olay çalışması yapılmıştır. Veriler Kayseri ilindeki 109 büyük marketten toplanmıştır. Çöpe atılan miktar yılda yaklaşık 13873.450 ton gibi çok büyük bir rakama tekabül etmektedir. İlk olarak bakkallar K-means algoritması ile kümelere ayrılmıştır. Agregasyon ağı oluşturulurken CitySurf ve Google map kullanarak işaretleyip bölgelere ayırdığımız dijital haritamız üzerinde CBS tabanlı bir yazılım olan arcGIS kullanılarak etkin ve verimli bir sistem tasarımı için yöneylem araştırması teknikleri kullanılarak yönlendirme yapılmıştır. Toplama noktası için tüm noktaları ve her bölgeyi kapsayan optimum rota belirlenir. Matematiksel bir model bir çözücü (CPLEX) kullanılarak yazılmış ve çözülmüştür. İkinci olarak, biyogaz üretimi iki farklı atık durumu için incelenmiştir, birinci durum %100 meyve ve sebze atığı (MSA) ve ikinci durum %17 inek gübresi (BHG) + %17 tavuk gübresi (TG) + 67 karışımıdır.

Anahtar Kelimeler: Enerji, Biyogaz üretimi, Atık değerlendirmesi.

# **ABSTRACT**

Every day, millions of tons of fruit and vegetable waste are released as garbage all over the world. The deformed and unpreferred products in the fruit and vegetable aisle are called extruded products. These wastes can be reused by using them in biogas production. These wastes can be reused by using them in biogas production. However, It is of great importance that the wastes are transported to the production point with the lowest carbon emission. In order to conduct a study in this approach, a case study was conducted in the Kayseri province. Data were collected from 109 large grocery stores in Kayseri. The amount thrown away corresponds to a very large figure, approximately 13873,450 tons per year. Firstly, grocery stores were divided into clusters with the K-means algorithm. While creating the aggregation network, routing was done by using operations research techniques for an effective and efficient system design by using arcGIS, a GIS-based software, on our digital map, which we marked and divided into zones using CitySurf and Google map. The optimum route covering all points for the collection point and each region is established. A mathematical model was written and solved using a solver (CPLEX). Secondly, biogas production was investigated for two different waste situations, the first case being 100% fruit and vegetable waste (MSA) and the second case being a mixture of 17% cow manure (BHG) + 17% chicken manure (TG) + 67% fruit and vegetable waste.

**Keywords:** Energy, Biogas production, Waste evaluation.

on Innovative Surveys in Positive Sciences 4-5 December 2022 / Full Text Book

# 1. GİRİŞ

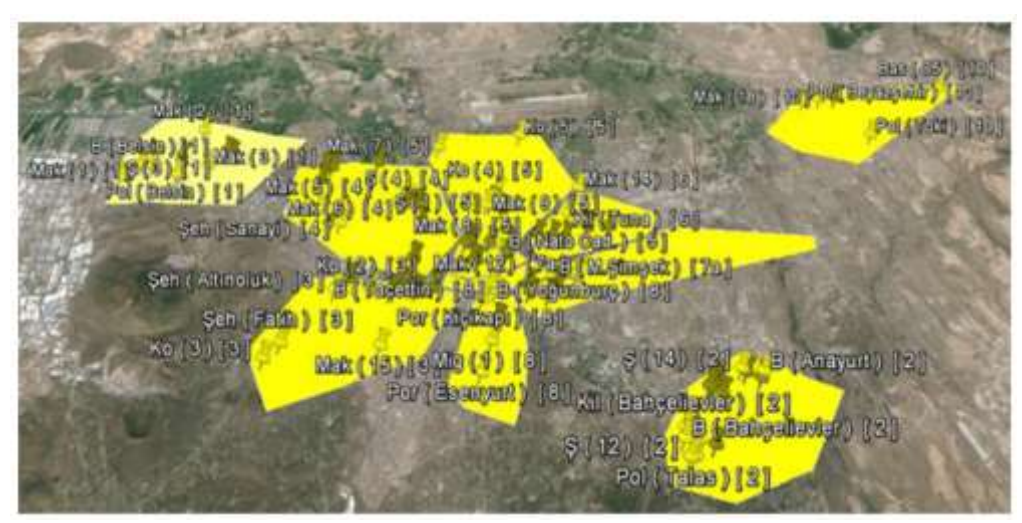
Sürdürülebilir kalkınma, doğaya, ekosistemlere ve biyolojik çeşitliliğe zarar verilmeyen veya zararın telafi edildiği bir kalkınma stratejisidir [1]. Bu strateji kapsamında fosil yakıtlar yerine yenilenebilir enerji kaynaklarının geliştirilmesine önem verilmiştir [2]. Biyogaz önemli özelliklere sahip yenilenebilir bir enerji kaynağıdır. Biyogaz, organik atıkların kontrollü koşullarda depolanmasını sağlaması, arıtıcı etkiye sahip olması, organik atıkların neden olduğu koku sorununu büyük ölçüde çözmesi ve organik toprak düzenleyicilerin tarımda kullanımını kolaylaştırması gibi önemli özelliklere sahiptir [3]. Ayrıca organik maddenin biyogaza dönüşümünün birçok avantajı vardır. Bunlar; enerji kaynağı olması, çürütülmüş atığın toprak iyileştirici olarak kullanılabilmesi, atık giderme problemlerinin giderilmesi, prosesin oksijene ihtiyaç duymaması, fosil yakıtların kullanımını azaltarak atmosferdeki sera gazı emisyonlarını azaltmasıdır. Biyogaz organik atıkların oksijensiz ortamda fermantasyona uğraması sonucu oluşan bir gaz karışımıdır. Organik bazlı atık/artıkların oksijensiz ortamda (anaerobik) fermantasyonu sonucu ortaya çıkan gazın %40-70 metan, %30-60 karbondioksit, %0-3 hidrojen sülfür ile çok az miktarda azot ve hidrojenden oluşmaktadır. Organik atıklar anaerobik olarak ayrıştırılabilir. Anaerobik arıtmada polimerik bileşiklerden metan gazı oluşumuna kadar bir süreç vardır [4].

Atık potansiyeli yüksek sektörlerden biri de manavlardır. Birçok ürün satılmadığı için yıllarca reyonlarda çürüyor. Meyve sebze reyonunda deforme olmuş ve tercih edilmeyen ürünlere ekstrüde ürünler denilmektedir. Bu isimle kilolarca ürün çöpe atılıyor. Kayseri ilinde bir vaka çalışması yapılmıştır. Veriler Kayseri ilinde bulunan 109 büyük marketten toplanmıştır. Bu çalışmada Kayseri ilinde bulunan 109 farklı marketin manav reyonundan elde edilen meyve/sebze atık potansiyeli belirlenmiştir.

- Büyük ve Küçük Kapasiteli Biyogaz Tesisi Güzergahları
- Atıklardan biyogaz üretimi
- Biyogazdan Metan Gazı Elde Edilmesi
- Metan Gazından Elektrik Üretiminin Hesaplanması
- Kayseri Büyük ve Küçük Kapasiteli Biyogaz tesisi için Maliyet Analizi yapılmıştır.

#### 2. KAYSERİ MANAV ATIKLARININ DEĞERLENDİRİLMESİ

Yaygınlıkları ve büyüklüklerine göre seçilen 109 market CBS tabanlı Citysurf ve Google Map programlarını kullanarak noktalar dijital harita üzerinde işaretlendi. K-means algoritmasıyla kümelere ayrıldı. Kümeleme yapılırken merkez nokta belirlendi, merkez noktaya uzaklıklarına göre tüm noktalar kendilerine en yakın kümeye yerleşir ve yeni merkez noktaları oluşturuldu. Dışarda kalan noktalar en yakın kümeye dahil edildi. Şekil 1'de dijital harita üzerinde işaretlenen bölgeler verilmiştir



Şekil 1. Dijital harita üzerinde marketlerin bölgelere ayrılması

on Innovative Surveys in Positive Sciences

4-5 December 2022 / Full Text Book

Kümeleme yapıldıktan sonra bölgelere göre yıllık fire oranları belirlenmiştir. Sonuçlar Tablo 1 ve Şekil 2'de verilmiştir.

	BÖLGE 1	BÖLGE 2	BÖLGE 3	BÖLGE 4	BÖLGE 5	BÖLGE 6	BÖLGE7 A	BÖLGE7 B	BÖLGE 8	BÖLGE9 A	BÖLGE9 B	BÖLGE1 0
Ocak	34,10	64,24	13,24	64,53	5,02	29,70	93,56	84,31	19,05	76,17	61,57	4,14
Şubat	72,02	61,55	10,76	66,65	65,39	59,12	68,42	61,66	111,46	78,73	63,64	23,66
Mart	57,34	65,61	6,42	4,41	54,98	42,05	24,00	21,62	33,76	56,49	45,66	25,65
Nisan	83,74	97,95	1,31	94,65	15,64	66,63	10,85	9,78	17,94	25,96	20,99	26,06
Mayıs	72,08	108,36	5,14	12,06	20,37	66,28	37,96	34,21	74,80	56,04	45,30	27,45
Haziran	101,57	224,48	63,76	112,47	328,32	71,45	136,05	122,60	453,21	341,62	276,14	39,98
Temmu z	59,61	102,85	9,89	75,14	153,64	56,53	48,64	43,83	52,97	49,41	39,94	12,38
Ağustos	70,82	58,95	46,10	68,61	208,71	51,31	619,62	558,36	65,69	589,17	476,24	19,89
Eylül	99,89	121,27	31,74	89,15	29,47	57,24	51,04	46,00	16,27	175,05	141,50	32,70
Ekim	79,63	88,82	19,53	92,49	328,38	44,26	297,56	268,15	118,96	112,45	90,89	20,61
Kasım	55,67	84,91	9,54	79,08	52,98	55,08	364,36	328,34	154,78	219,87	177,73	34,50
Aralık	44,34	96,97	14,47	92,36	113,39	54,22	176,43	158,98	112,62	131,49	106,28	21,37

Tablo 1. Bölgelere göre fire miktarları (ton) (1 yıllık ay bazında)



Şekil 2. Yıllık çıkma meyve sebze atık miktarının değişimi

Her market için aylık %10 -%20 arasında değişen fire oranları ve toplam yıllık 13873,5 ton çıkma ürün bulunmaktadır. Çıkma ürünlerin en yoğun olduğu ayların Haziran ve Ağustos en az olduğu ayların ise mart ve nisan olduğu Şekil 2'de görülmektedir.

# 2.1. KAYSERİ'DE MEYVE SEBZE ATIKLARI İÇİN TOPLAMA AĞI OLUŞTURULMASİ

Toplama ağı oluştururken etkin ve verimli bir sistem tasarımı için yöneylem araştırması teknikleri kullanılarak rotalama yapılmıştır. Toplama noktası ve her bir bölge için tüm noktaları kapsayan optimum (en kısa mesafeli) rota oluşturulmuştur. Bunun için bir matematiksel model yazılmış ve bir çözücü (CPLEX) kullanılarak çözülmüştür. Rotalar oluşturulurken öncelikle CitySurf ve Google map kullanarak işaretlediğimiz ve bölgelere ayırdığımız dijital haritamızı CBS tabanlı bir yazılım olan arcGIS kullanarak uzaklık matrisleri çıkarıldı. Uzaklık matrisi bir rotayı oluşturacak noktalar için nxn boyutunda bir matristir. Örneğin, Tablo 2'de verildiği üzere BÖLGE1'da ana toplama merkezi (ATN) hariç 10 marketten manav çıkma firesi toplanacaktır. Ancak marketler hangi sıra ile ziyaret edilirse en kısa mesafe (en az yakıt) kat edileceği önemli bir yöneylem araştırması problemidir. Bu problem literatürde araç rotalama problemi olarak bilinmektedir ve çok fazla seçenek olduğu için çözmesi zor bir problemdir. Bunun için bir yöneylem tekniği olan matematiksel model kurma ve onu

on Innovative Surveys in Positive Sciences 4-5 December 2022 / Full Text Book

uygun bir teknikle çözme yöntemi seçilmiştir. Harita bölgelere ayrılarak kapsanacak nokta sayısı azaltılmış problem araç rotalama probleminden gezgin satıcı problemine indirgenmiştir. Bölgelerin mesafe matrislerini ve gezgin satıcı matematiksel modelini CPLEX optimizasyon yazılımını kullanarak toplama aracının alacağı en kısa mesafeler ve sıra ile geçeceği noktalar elde edilmiştir

UID B(Belsin) B(byz) [1] Pol(Belsin) Kil(Belsin) [1Kil(Şeker) Mak(1) [1Mak(2) [ Mak(3) [1Bel(3) [1] (3) [1] 0 8344.47378 9450.671399 9029.71025 9090.7612502 9617.82519 8076.1568 38472.2684 39390.6260 8637.8822 78051.43976 ATN 0 1859.033747 730.302630 807.54528442 1964.93071 313.22334 01601.2909 21382.9218 5764.59380 6785.283846 8 (Belsin) [1] 9450.67139 1859.03374 0 1353.36577 1283.5596056 167.547540 2140.7387 997.44527 3626.67865 91119.6712 42640.07526 B(byz)[1] 0[83.742239817[1414.42781]1040.56786[1513.3130]763.818801[617.79695][1402.98318 Pol (Belsin) [1] 9029.71029.730.302630.1353.365771 9090.76125 807.545284 1283.559605 83.74223981 0 1339.71428 1119.0836 11490.6665 3686.03065 3619.84497 11486.7163 Kil (Belsin) [1] 9617.82519 1964.93071 167.5475404 1414.42781 11339.7142861 0 2254,5463 5 1164,0284 0 658, 299 9 7 3 1 2 4 3, 7 4 3 4 8 2 7 3 9, 8 9 1 2 1 Kil (Şeker) [1] 8076.15683 313.223340 2140.738796 1040.56786 1119.0836130 2254.54635 0 1777.043491689.220041026.23809558.683296 Mak(1)[1] 8472 26843 1601 29093 997 4452734 1513 31301 41490 6665386 1164 02840 1777 04345 0 1207 38575 929 24610 0 2335 3903 Mak(2) [1] 9390.62606 1382.92185 626.6786594 763.818801 686.03065385 658.299973 1689.22004 1207.38575 Mak(3)[1] 8637.88227,764.5938061119.671243,617.796951,619.84497147,1243.74348,1026.23805929.246100,772.009296 Bel(3)[1]

**Tablo 2: Mesafe matrisi (metre)** 

# 2.2. BÜYÜK VE KÜÇÜK KAPASİTELİ BİYOGAZ TESİSİ İÇİN ROTALAR

Harita bölgelere ayrılarak kapsanacak nokta sayısı azaltılmış problem araç rotalama probleminden gezgin satıcı problemine indirgenmiştir. Bölgelerin mesafe matrislerini ve gezgin satıcı matematiksel modelini CPLEX optimizasyon yazılımını kullanarak toplama aracının alacağı en kısa mesafeler ve sıra ile geçeceği noktalar elde edilmiştir. En kısa mesafeli rotalar büyük kapasiteli ve küçük kapasiteli tesisler için Tablo 3 ve Tablo 4'te verilmiştir.

8051 43976 785 283849 2640 075264 1402 983 184 1486 71633 75 2739 8912 1 558 6832 962 335 3903 32 132 3981 31548 8005 2

BÖLGE	EN KI	SA   ROTA
İSMİ	MESAFE	
BÖLGE1	21,371 km	1 (ATN)-8-3-6-9-5-4-10-2-7-11-
		1(ATN)
BÖLGE2	50,527 km	1-13-6-3-14-11-2-15-9-7-5-12-4-8-
		10-1
BÖLGE3	36,350 km	1-4-5-11-8-6-7-2-10-9-3-12-1
BÖLGE4	32,577 km	1-10-11-2-7-14-15-5-9-13-6-12-8-
		4-3-1
BÖLGE5	36,893 km	1-4-10-9-3-7-6-8-2-5-1
BÖLGE6	3,942 km	1-5-2-8-3-4-6-7-1
BÖLGE7A	19,89 km	1-7-2-3-8-5-4-6-1
BÖLGE7B	21,728 km	1-2-8-5-4-7-3-6-1
BÖLGE8	38,334 km	1-2-5-6-3-4-8-7-1

1-3-7-8-6-5-2-4-1

1-2-4-5-3-8-7-6-1

1-5-6-2-3-4-1

Tablo 3. En Kısa Mesafeli Rotalar Büyük Kapasiteli Tesis için

BÖLGE9A

BÖLGE9B

BÖLGE10

17,373 km

18,250 km

54.589 km

5(3)[1]

on Innovative Surveys in Positive Sciences 4-5 December 2022 / Full Text Book

En kısa mesafeli rotaların büyük kapasiteli tesis için bir günlük kat edilmesi beklenen yol miktarı 386,7 km dir.

Tablo 4. En Kısa Mesafeli Rotalar Küçük Kapasiteli Tesisler için

BÖLGE İSMİ	EN KISA MESAFE	ROTA					
BÖLGE1	5,371 km	8-3-6-9-5-4-10-2-7-11-8					
BÖLGE2	20,527 km	13-6-3-14-11-2-15-9-7-5-12-4-8- 10-13					
BÖLGE3	16,350 km	4-5-11-8-6-7-2-10-9-3-12-4					
BÖLGE4	22,577 km	10-11-2-7-14-15-5-9-13-6-12-8-4- 3-10					
BÖLGE5	16,893 km	4-10-9-3-7-6-8-2-5-4					
BÖLGE6	3,942 km	5-2-8-3-4-6-7-5					
BÖLGE7A	9,89 km	7-2-3-8-5-4-6-7					
BÖLGE7B	11,728 km	2-8-5-4-7-3-6-2					
BÖLGE8	18,334 km	2-5-6-3-4-8-7-2					
BÖLGE9A	7,373 km	3-7-8-6-5-2-4-3					
BÖLGE9B	8,250 km	2-4-5-3-8-7-6-2					
BÖLGE10	24,589 km	5-6-2-3-4-5					

En kısa mesafeli rotaların küçük kapasiteli tesisler için bir günlük kat edilmesi beklenen yol miktarı 165,7 km dir.

# 2.3. KAYSERİ İLİ İÇİN MEYVE ATIKLARINDAN BİYOGAZ ÜRETİM POTANSİYELİ (BÜYÜK KAPASİTELİ TESİS KURULUMU)

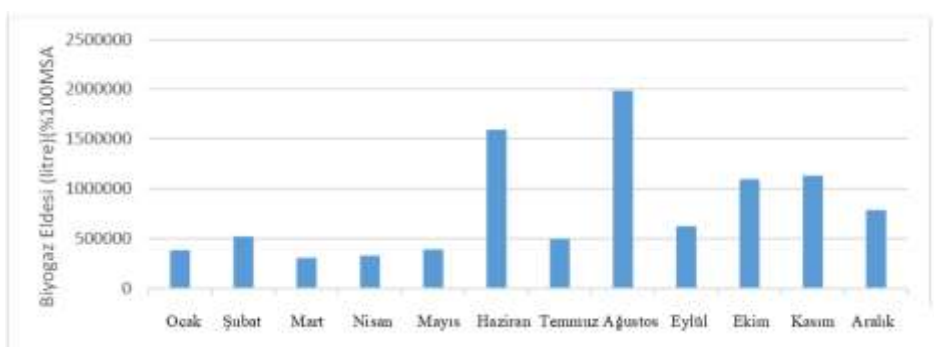
Çalışmada iki durum ele alınmıştır. Bunlardan birincisi %100 meyve sebze atığı (MSA) kullanılması ve ikinci durum ise %17 büyükbaş hayvan gübresi (BHG) %17 tavuk gübresi (TG) % 67 meyve sebze atığı karışımı kullanılmasıdır. Her bir durum için ne kadar biyogaz üretildiği incelenmiştir. İki durum için sırasıyla aylık bölgesel biyogaz üretim miktarlarının değişimi Tablo 5 ve Tablo 6'da sırasıyla verilmiştir. Ayrıca, toplam şehir bazında üretilen biyogaz miktarının aylık değişimi ise Şekil 3 ve Şekil 4'te verilmiştir. %100 meyve sebze atığı (MSA) kullanıldığında elde edilen biyogaz eldesi diğer karışımlara oranla oldukça düşük olmasına karşın Tablo 5 ve Şekil 3'te gösterildiği gibidir. En fazla biyogaz %17 büyükbaş hayvan gübresi (BHG) %17 tavuk gübresi (TG) % 67 meyve sebze atığı karışımı kullanıldığında elde edebilmektedir. Bu karışımlarda elde edilen biyogaz miktarı Tablo 6 ve Şekil 4'te gösterilmiştir. Sadece MSA atıklarıyla kullanılarak analiz ve %67 MSA, %17 BHG,%17 TG ile karışım halinde yapılan analizle kıyaslamış ve sonuç Şekil 5'te verilmiştir. Bu sonuca göre karışım halinde olan atıkların MSA'dan çok daha yüksek oranda biyogaz elde edildiği görülmüştür.

on Innovative Surveys in Positive Sciences

4-5 December 2022 / Full Text Book

Tablo 5. Biyogaz eldesi (litre) (%100 MSA)

	BÖLGE1	BÖLGE2	BÖLGE3	BÖLGE4	BÖLGE5	BÖLGE6	BÖLGE7A	BÖLGE7B	BÖLGE8	BÖLGE9A	BÖLGE9B	BÖLGE10
Ocak	23942,2591	45107,23	9298,824	45314,39	3527,963	20855,99	65697,08	59202,23	13377,33	53488,25	43235,81	2909,306
Şubat	50571,2196	43219,66	7558,015	46799,59	45914,79	41516,07	48047,43	43297,6	78270,37	55283,83	44687,3	16611,06
Mart	40266,8139	46072,08	4508,967	3096,799	38606,06	29527,03	16850,52	15184,15	23703,5	39670,63	32066,27	18011,99
Nisan	58802,6658	68784,75	922,0175	66465,31	10985,56	46786,95	7617,002	6864,22	12600,67	18231,09	14736,83	18299,91
Mayıs	50614,7573	76090,67	3605,91	8468,797	14302,16	46540,47	26654,24	24019,5	52522,69	39353,22	31809,95	19276,7
Haziran	71326,7952	157632	44772,97	78978,91	230550,7	50174,46	95536,6	86091,71	318254	239892,4	193909,5	28074,13
Temmuz	41855,9423	72220,72	6947,784	52761,45	107892,2	39695,91	34153,27	30776,99	37198,81	34697,49	28046,75	8693,508
Ağustos	49733,4687	41395,99	32374,54	48179,45	146558,6	36030,31	435108,7	392094,1	46130,37	413728,8	334424,1	13965,09
Eylül	70143,5511	85157,06	22287,12	62599,58	20695,89	40195,19	35844,22	32300,11	11425,15	122925,4	99363,01	22959,15
Ekim	55917,9379	62369,95	13712,99	64948,51	230595,7	31081,75	208954,6	188298	83537,73	78964,16	63827,77	14473,5
Kasım	39091,9965	59623,56	6695,687	55531,72	37205,83	38678,39	255859,5	230565,5	108689,2	154398,3	124803,1	24223,85
Aralık	31137,2257	68095,87	10160,45	64853,71	79621,44	38071,67	123889,5	111642,1	79080,73	92333,06	74634,96	15005,78

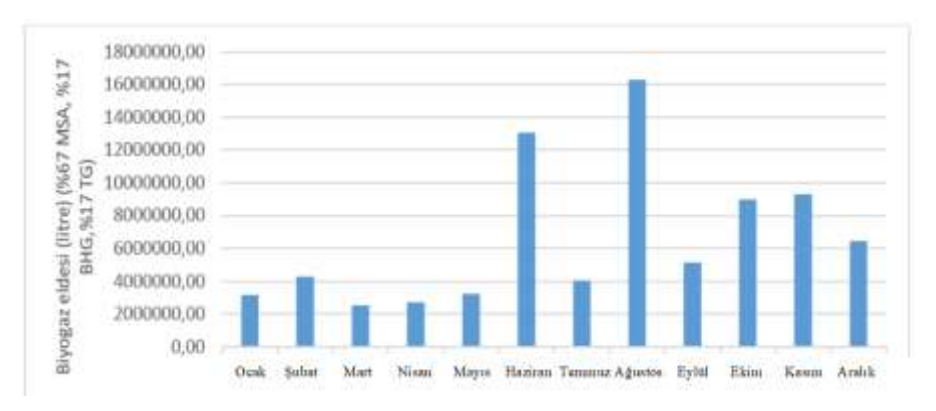


Şekil 3. Biyogaz Eldesi (litre) (%100MSA grafiği Tablo 6. Biyogaz eldesi (litre) (%67 MSA, %17 BHG, %17 TG)

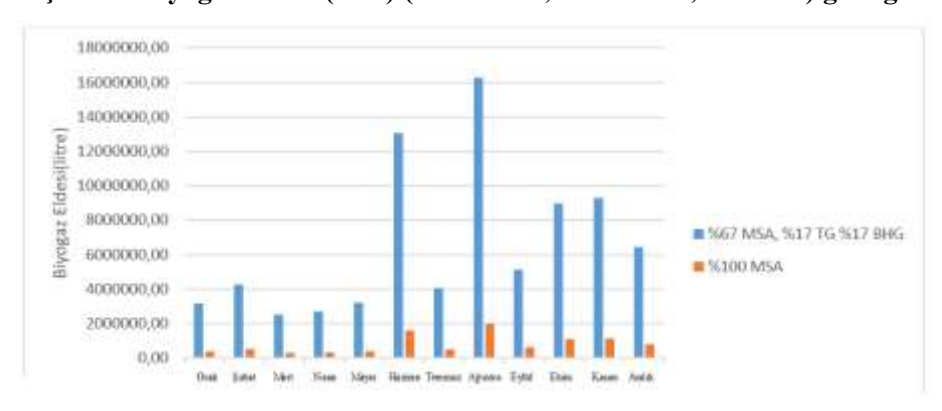
	BÖLGEI	BÖLGE2	BÖLGE3	BÖLGE4	BÖLGE5	BÖLGE6	BÖLGE7A	BÖLGE7B	BÖLGE8	BÖLGE9A	BÖLGE9B	BÖLGE10
Ocak	195783,04	368855,36	76039,27	370549,33	28849,21	170545,72	537224,75	484114,40	109390,43	437389,47	353552,18	23790,27
Şubat	413536,04	353420,11	61804,16	382694,25	375458,98	339489,34	392898,28	354057,50	640040,27	452072,48	365421,47	135833,63
Mart	329273,82	376745,25	36871,18	25323,45	315693,33	241451,39	137791,75	124165,32	193830,66	324398,62	262215,47	147289,48
Nisan	480847,04	562473,55	7539,61	543506,80	89832,23	382590,89	62286,51	56130,79	103039,47	149081,07	120507,49	149643,82
Mayıs	413892,06	622216,23	29486,61	69251,90	116953,02	380575,35	217959,72	196414,69	429493,83	321803,11	260119,54	157631,33
Haziran	583260,61	1289004,05	366122,03	645834,23	1885282,40	410291,65	781231,45	703997,79	2602458,72	1961671,95	1585655,97	229570,61
Temmuz	342268,60	590570,53	56814,12	431446,21	882266,87	324605,35	279281,53	251672,65	304185,80	283731,80	229346,66	71089,43
Ağustos	406685,50	338507,41	264736,33	393977,83	1198454,03	294630,64	3558014,31	3206270,95	377221,86	3383184,85	2734686,20	114196,72
Eylül	573584,86	696354,81	182248,48	511895,55	169236,48	328688,11	293108,94	264127,65	93426,90	1005197,60	812521,14	187743,84
Ekim	457257,76	510017,83	112135,24	531103,48	1885649,91	254164,80	1708684,32	1539769,41	683113,11	645713,64	521938,80	118354,13
Kasım	319666,99	487559,77	54752,64	454099,50	304243,22	316284,78	2092239,91	1885402,99	888784,36	1262560,85	1020552,46	198085,69
Aralık	254618,44	556840,38	83085,05	530328,27	651088,42	311323,45	1013081,75	912930,64	646666,86	755035,17	610312,49	122706,78

on Innovative Surveys in Positive Sciences

4-5 December 2022 / Full Text Book



Şekil 4. Biyogaz eldesi (litre) (%67 MSA, %17 BHG,%17 TG) grafiği



Şekil 5. İki farklı Karışım Yüzdesi İçin Kıyaslı Grafik

# 2.4. KAYSERİ İLİ İÇİN MEYVE ATIKLARINDAN METAN GAZI VE ELEKTRİK ÜRETİM POTANSİYELİ (BÜYÜK KAPASİTELİ TESİS KURULUMU)

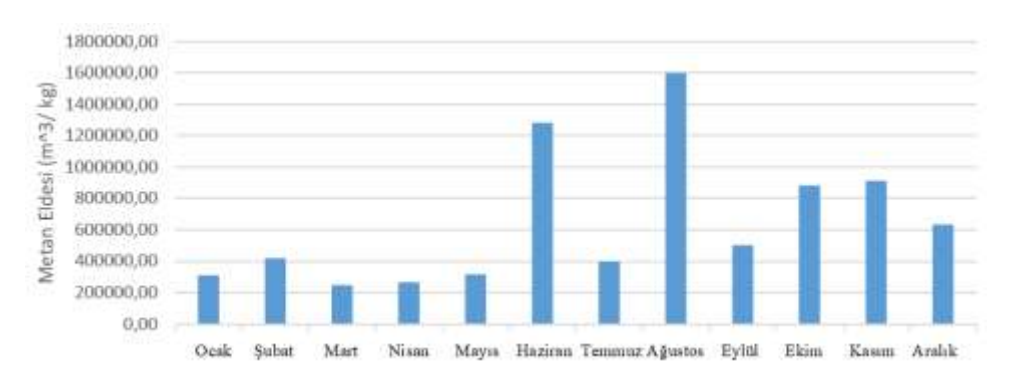
Biyogazdan metan gazı eldesi verileri Tablo 7 ve Şekil 6'da verilmiştir. Verilere göre ay bazında değerlendirildiğinde en yüksek metan üretiminin ağustos ayında 1600000,00 m³/kg ile üretilebileceği görülmektedir.

Tablo 7. Metan Eldesi (m³/kg) (30 gün, T=35°C)

	BÖLGE1	BÖLGE2	BÖLGE3	BÖLGE4	BÖLGE5	BÖLGE6	BÖLGE7A	BÖLGE7B	BÖLGE8	BÖLGE9A	BÖLGE9B	BÖLGE10
Ocak	19248,33	36263,87	7475,77	36430,41	2836,30	16767,14	52817,04	47595,52	10754,68	43001,77	34759,34	2338,93
Şubat	40656,63	34746,36	6076,25	37624,43	36913,10	33376,76	38627,64	34809,02	62925,31	44445,33	35926,27	13354,43
Mart	32372,43	37039,56	3624,98	2489,67	31037,27	23738,20	13546,94	12207,26	19056,39	31893,12	25779,61	14480,71
Nisan	47274,29	55299,37	741,25	53434,66	8831,82	37614,27	6123,67	5518,48	10130,29	14656,85	11847,65	14712,17
Mayıs	40691,63	61172,94	2898,96	6808,47	11498,19	37416,12	21428,62	19310,43	42225,52	31637,95	25573,55	15497,46
Haziran	57343,04	126727,93	35995,14	63494,94	185350,80	40337,66	76806,46	69213,27	255859,71	192861,01	155893,14	22570,14
Temmuz	33650,00	58061,71	5585,66	42417,46	86739,72	31913,45	27457,45	24743,10	29905,91	27894,98	22548,13	6989,13
Ağustos	39983,12	33280,22	26027,45	38733,78	117825,54	28966,50	349804,78	315223,27	37086,42	332616,49	268859,60	11227,21
Eylül	56391,77	68461,85	17917,69	50326,81	16638,42	32314,84	28816,89	25967,61	9185,23	98825,61	79882,70	18457,96
Ekim	44955,12	50142,20	11024,53	52215,23	185386,93	24988,11	167988,63	151381,82	67160,00	63483,08	51314,21	11635,94
Kasım	31427,93	47934,25	5382,98	44644,61	29911,55	31095,41	205697,74	185362,65	87380,48	124128,17	100335,21	19474,72
Aralık	25032,71	54745,54	8168,47	52139,02	64011,50	30607,64	99600,73	89754,42	63576,80	74230,99	60002,63	12063,87

on Innovative Surveys in Positive Sciences

4-5 December 2022 / Full Text Book

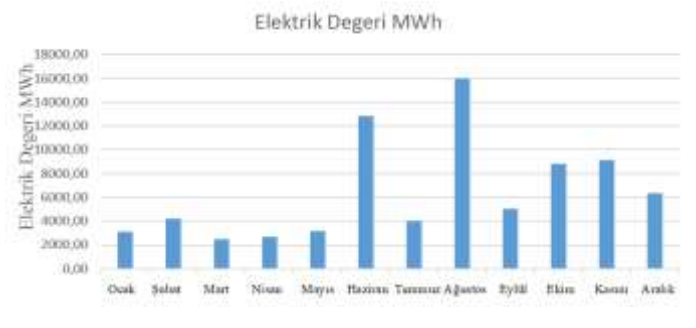


Şekil 6 Metan Eldesi (m³/kg) (30 gün, T=35°C) grafiği

1m³ metan gazı 10kWh enerjidir. Metan gazından ay bazında kaç kWh elektrik elde edilme hesabı yapılmış ve veriler Tablo 8 ile Şekil 9'da paylaşılmıştır.

	BÖLGEI	BÖLGE2	BÖLGE3	BÖLGE4	BÖLGE5	BÖLGE6	BÖLGE7A	BÖLGE7B	BÖLGE8	BÖLGE9A	BÖLGE9B	BÖLGE10
Ocak	192483,32	362638,69	74757,71	364304,12	28362,99	167671,35	528170,40	475955,17	107546,78	430017,74	347593,44	23389,31
Şubat	406566,33	347463,59	60762,52	376244,35	369131,02	333767,61	386276,40	348090,24	629253,08	444453,28	359262,68	133544,30
Mart	323724,26	370395,61	36249,76	24896,66	310372,65	237381,98	135469,42	122072,65	190563,85	318931,23	257796,11	144807,08
Nisan	472742,88	552993,66	7412,54	534346,58	88318,20	376142,73	61236,74	55184,76	101302,85	146568,47	118476,46	147121,73
Mayıs	406916,35	611729,44	28989,64	68084,73	114981,90	374161,16	214286,24	193104,33	422255,17	316379,47	255735,50	154974,62
Haziran	573430,37	1267279,26	359951,43	634949,39	1853507,98	403376,62	768064,63	692132,65	2558597,06	1928610,06	1558931,43	225701,44
Temmuz	336500,03	580617,09	55856,58	424174,64	867397,20	319134,47	274574,54	247430,97	299059,07	278949,80	225481,27	69891,29
Ağustos	399831,25	332802,23	260274,49	387337,76	1178255,37	289664,96	3498047,77	3152232,67	370864,19	3326164,88	2688595,98	112272,06
Eylül	563917,70	684618,49	179176,88	503268,10	166384,18	323148,42	288168,90	259676,06	91852,29	988256,07	798826,96	184579,62
Ekim	449551,17	501422,02	110245,32	522152,30	1853869,29	249881,12	1679886,27	1513818,24	671599,97	634830,83	513142,08	116359,40
Kasım	314279,34	479342,47	53829,84	446446,14	299115,53	310954,14	2056977,44	1853626,53	873804,84	1241281,73	1003352,13	194747,17
Aralık	250327,12	547455,43	81684,74	521390,15	640115,02	306076,43	996007,34	897544,17	635767,98	742309,86	600026,32	120638,69

Tablo 8. Elektrik değeri (kWh)/ay



Şekil 7. Elektrik değeri (kWh)/ay

Elektrik üretimi verilerine bakıldığı zaman en yüksek değerin ağustos ayında 16000,00 MWh olduğu Şekil 7'de görülmektedir. Ayrıca saatlik, günlük ve yıllık değerler hesaplanıp Tablo 9'da verilmiştir.

on Innovative Surveys in Positive Sciences 4-5 December 2022 / Full Text Book

Tablo 9. Metan gazından saatlik, günlük ve yıllık üretilen elektrik miktarı (MWh)

Yıllık değer	Günlük değer	Saatlik değer
77709,4889(MWh)	212,902709(MWh)	8,87094622(MWh)

# 2.5. KAYSERİ İLİ İÇİN MEYVE ATIKLARINDAN BİYOGAZ ÜRETİM POTANSİYELİ (KÜÇÜK KAPASİTELİ TESİS KURULUMU)

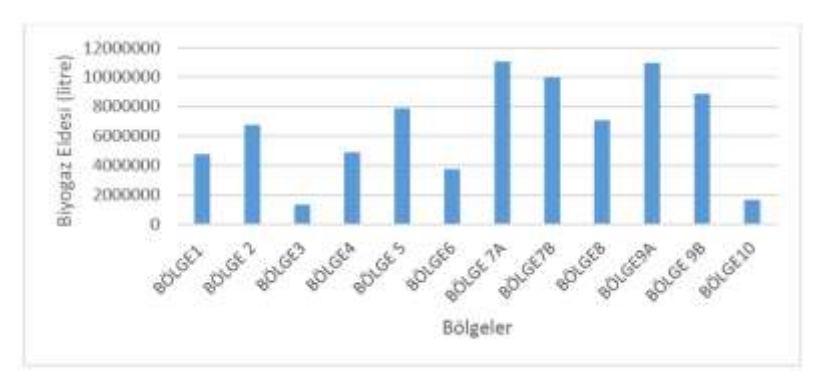
Büyük kapasiteli tesisler için yapılan benzer hesaplar küçük kapasiteli tesisler içinde yapılmıştır. Atıklardan en yüksek biyogaz eldesi BÖLGE 7A olarak 11073803,23 litredir. Tablo 10 ve Şekil 8'de ayrıntılı olarak veriler paylaşılmıştır.

Tablo 10. Biyogaz eldesi (litre) (%67 MSA, %17 BHG, %17 TG) (yıllık)

	Biyogaz Eldesi (litre)
BÖLGE1	4770674,739
BÖLGE 2	6752565,259
BÖLGE 3	1331634,732
BÖLGE 4	4890010,802
BÖLGE 5	7903008,088
BÖLGE 6	3754641,459
BÖLGE 7A	11073803,23
BÖLGE 7B	9979054,772
BÖLGE 8	7071652,274
BÖLGE 9A	10981840,61
BÖLGE 9B	8876829,868
BÖLGE 10	1655935,737

on Innovative Surveys in Positive Sciences

4-5 December 2022 / Full Text Book



Şekil 8. Bölgelerden Elde Edilen Biyogaz Miktarı Grafiği

# 2.6. KAYSERİ İLİ İÇİN MEYVE ATIKLARINDAN METAN GAZI VE ELEKTRİK ÜRETİM POTANSİYELİ (KÜÇÜK KAPASİTELİ TESİS KURULUMU)

Biyogazdan metan eldesi sonuçlarına bakıldığında en yüksek oranın 7B bölgesinde olduğu görülmektedir. 1m³ metan gazı 10 kWh enerjidir. Tablo 12'ye göre ay bazında en yüksek üretilen elektrik Bölge 7A ile 10887166 kWh'dır.

Tablo 11. Metan Gazı ve Elektrik Üretim Değerleri (30 gün, T=35°C)

	Metan eldesi (m³ / kg)	Elektrik değeri (kWh) / ay
BÖLGE1	565066,00	4690270,1
BÖLGE 2	763560,09	6638758
BÖLGE 3	425120,26	1309191,5
BÖLGE 4	429795,87	4807594,9
BÖLGE 5	530455,13	7769811,3
BÖLGE 6	2380835,50	3691361
BÖLGE 7A	704101,68	10887166
BÖLGE 7B	3126005,37	9810868,5
BÖLGE 8	881521,11	6952467,1
BÖLGE 9A	1668254,28	10796753
BÖLGE 9B	1746189,28	8727220,4
BÖLGE 10	1188090,39	1628026,7

# 2.6. KAYSERİ İLİ İÇİN MEYVE ATIKLARINDAN BİYOGAZ ÜRETİM TESİSİNİN MALİYET ANALİZİ

Kayseri'de bulunan büyük ve küçük ölçekli tesisler için yaklaşık maliyet hesabı oluşturulmuştur. Hesaplanan eriler Tablo 12 ve Tablo 13'te verilmiştir.

on Innovative Surveys in Positive Sciences 4-5 December 2022 / Full Text Book

Tablo 12. Büyük Kapasiteli Biyogaz Tesisi için Maliyet Analizi

TESİS BİLEŞENİ	HESAPLAMA YÖNTEMİ	ÖRNEK	FİYAT	BİRİM
Kurulum Maliyeti	Yerleşik Kapasite (kWh) x Yatırım			
	gideri (£/kWh)	10000 kWh x 4000 £	40000000	£
GİDERLER				
Fermenterin Kullanımı ve	(Toplan yatırım gideri- kojenerasyon	(40000000£-	1188000	£/yıl
Bakımı	ünitesi yatırım gideri) x %3	400000£) x 0.03		
Kojenerasyon ünitesinin	Çalışma saati /yıl x (0.8-1.1) £/h	8000 h/y x 0.95 £/h	7600	£/yıl
Kullanım ve Bakımı				
Sigorta ve vergiler	Toplam Yatırım gideri x %0.05 - 0.1	40000000 x 0.05	2000000	£/yıl
İş gücü	Kişi x 12 ay x 1000£	30 x 12 x 1000	360000	£/yıl
Hammadde ve taşıma giderleri (MSA)	Günlük km x 365 x 1.02£	386 x 365 x 1.02	143707,8	£/yıl
Hammadde ve taşıma	3520.1 (yıllık ihtiyaç) x 45.3 (ton fiyat)	3520.1 x 45.3	159460,53	£/yıl
giderleri (BHG) Hammadde ve taşıma	3520.1 (yıllık ihtiyaç) x 45.3 (ton fiyat)	3520.1x45.3	159460,53	£/yıl
giderleri (TG)	3320.1 (yınık intiyaç) x 43.3 (toli fiyat)	3320.1X43.3	139400,33	L/yII
Yıllık Toplam gider			4018228,86	£/yıl
GELİRLER				
Elektrik Satışı	Yerleşik Kapasite (kWh) x Çalışma saati x elektik fiyatı	10000 kWh x 8000 x 0.133£	10640000	£/yıl
Karbon Ticareti (TC İçin henüz etkin değil)	Yerleşik Kapasite (kWh) x Çalışma saati x (-0.05) x yeşil sertifika ücreti	10000x8000 x (- 0.05) x 0.02£/h Wh	0	£/yıl
Kullanılan Isı	Kojenerasyon ısısı (kWh) x çalışma saati x 0.03£/kWh	10000 kW x 8000 x 0.03 £/kWh	2400000	£/yıl
Yıllık toplam gelir			13040000	£/yıl
Yıllık kar	(Gelir-gider) / yıl	14640000-3694229	9021771,14	£/yıl
Geri ödeme süresi yıl	Toplam Yatırım gideri / yıllık kar	4000000/10945771	4,43371921	Yıl

Tablo 14. Küçük Kapasiteli Biyogaz Tesisi için Maliyet Analizi

	HESAPLAMA			l
TESİS BİLEŞENİ	YÖNTEMİ	ÖRNEK	FİYAT	BİRİM
Kurulum Maliyeti	Powertainer x Gerekli adet	2000000£ x 17	34000000	£
GİDERLER				
Sigorta ve vergiler	Toplam Yatırım gideri x % 0.05- 0.1	34000000 x 0.05	1700000	£/yıl
İş gücü	Kişi x 12 ay x 1000£	30 x 17 x 1000	360000	£/yıl
Hammadde ve taşıma giderleri Günlük km x 365 x 1.02£ (MSA)		165 x 365 x 1.02	61429,5	£/yıl
Hammadde ve taşıma giderleri (BHG)	3520.1 (yıllık ihtiyaç) x 45.3 (ton fiyat)	3520.1 x 45.3	159460,53	£/yıl
Hammadde ve taşıma giderleri (TG)	3520.1 (yıllık ihtiyaç) x 45.3 (ton fiyat)	3520.1 x 45.3	159460,53	£/yıl
Yıllık Toplam gider			2440350,56	£/yıl
GELİRLER				
Elektrik Satışı	Yerleşik Kapasite (kWh) x Çalışma saati x elektik fiyatı	77709489 x 0.133£	10335362,04	£/yıl
Karbon Ticareti (TC için henüz etkin değil)	Yerleşik Kapasite (kWh) x Çalışma saati x (- 0.05) x yeşil sertifika ücreti	10000x8000 x (-0.05) x 0.02 £/hWh	0	£/yıl
Kullanılan Isı	Kojenerasyon ısısı (kWh) x çalışma Saati x 0.03 £/kWh	200 Kw x 8000 x 0.03 £/kWh x 17	816000	£/yıl
Yıllık toplam gelir			11151362,04	£/yıl
Yıllık kar	(Gelir-gider) / yıl	11151362 - 2440350	8711011,477	£/yıl
Geri ödeme süresi yıl	Toplam Yatırım gideri / yıllık kar	34000000 / 10945771	3,903105867	Yıl

on Innovative Surveys in Positive Sciences 4-5 December 2022 / Full Text Book

#### 3. SONUÇ

109 farklı marketin manav reyonundan elde edilen atıklardan büyük ve küçük kapasiteli biyogaz tesisleri için manav atıklarından biyogaz, biyogazdan metan gazı üretimi, metan gazından elektrik üretimi potansiyeli araştırılmış ve tesisler için yaklaşık maliyet analizi yapılmıştır.

Meyve sebze reyonunda deforme olmuş ve tercih edilmeyen ürünler doğaya atılmaktadır ve bu atıkların katma değeri yüksek bir ürün olan biyogaz üretiminde değerlendirilerek yeniden kullanılması önerilmektedir.

#### **KAYNAKLAR**

- [1] Demirayak, F. (2002). Biyolojik çeşitlilik-doğa koruma ve sürdürülebilir kalkınma. TÜBİTAK vizyon, 2023, 1-30.
- [2] Emeksiz, C., & FINDIK, M. M. (2021). Sürdürülebilir Kalkınma İçin Yenilenebilir Enerji Kaynaklarının Türkiye Ölçeğinde Değerlendirilmesi. Avrupa Bilim ve Teknoloji Dergisi, (26), 155-164.
- [3] Igoni, A. H., Ayotamuno, M. J., Eze, C. L., Ogaji, S. O. T., & Probert, S. D. (2008). Designs of anaerobic digesters for producing biogas from municipal solid waste. Applied energy, 85(6), 430-438.
- [4] Kankılıç, T., & Topal, H. (2015). Belediye Atıklarından Düzenli Depolama Sahalarında Biyogaz Ve Enerji Üretimi. Mühendis Ve Makina, 56(669), 58-69.

on Innovative Surveys in Positive Sciences 4-5 December 2022 / Full Text Book

#### FLOW CHARACTERISTICS ON NACA2415 AIRFOIL AT LOW REYNOLDS NUMBER

Mustafa ÖZDEN<sup>1,2</sup>, Mustafa Serdar GENÇ<sup>1,3,4</sup>, Halil Hakan AÇIKEL<sup>1</sup>, Kemal KOCA<sup>1,5</sup>

<sup>1</sup>Wind Engineering and Aerodynamic Research Laboratory, Department of Energy Systems Engineering, Erciyes University, 38039, Kayseri, Turkey

<sup>2</sup>Scientific Research Projects Unit of Erciyes University, Erciyes University, 38039, Kayseri, Turkey

<sup>3</sup>Energy Conversion Research and Application Center, Erciyes University, 38039, Kayseri, Turkey

<sup>4</sup>MSG Teknoloji Ltd. Şti, Erciyes Teknopark Tekno-1 Binası, 61/20, 38039, Kayseri, Turkey

<sup>5</sup>Department of Mechanical Engineering, Abdullah Gül University, 38080, Kayseri, Turkey

#### **ABSTRACT**

In the aviation and energy sectors, aircrafts and airfoils which is a component of aircrafts may be studied in twofold, including experimental investigation and numerical simulation. In this study, NACA2415 airfoil which was suitable for wind turbine blades and unmanned air vehicles was investigated. ANSYS Fluent software was utilized for the flow analysis and the boundary conditions were taken as a reference. Analysis was performed at  $0^{\circ} \le \alpha \le 26^{\circ}$  and Reynolds number of  $0.5 \times 10^{5}$ . The power coefficients were ensured at the end of the analysis. The obtained data ensured by numerical analysis was compared with the experimental data in the literature. Velocity profiles were provided to understand and visualize some flow phenomena including flow separation and laminar separation bubble. The result showed that the force coefficient result obtained by numerical simulation was consistent with the experimental data.

#### 1 Introduction

Many factors are dependent on airfoil design in the shape of wings, which determines the amount of lift generated and the drag force. There are a lot of types of airfoils. The lift coefficient by an uncambered airfoil is typically different from that of a cambered airfoil [1-3].

Genç at al. [4] visualized the transition on the NACA 2415 airfoil with oil flow visualization test. The flow direction is shown in Figure 1 as being from right to left. The leading edge of the wing is on right, while the trailing edge is on left. Lines indicate where the flow separation and reattachment in the Figure 1. The regions where the oil accumulate with presence of adverse pressure gradients (APGs) are the regions of flow separation and reattachment. In the boundary layer of in this region, flow movement is relatively less. On the airfoil, this is known as a laminar separation bubble (LSB). LSB on the wing has a negative impact on airfoil performance [5, 6].

on Innovative Surveys in Positive Sciences 4-5 December 2022 / Full Text Book

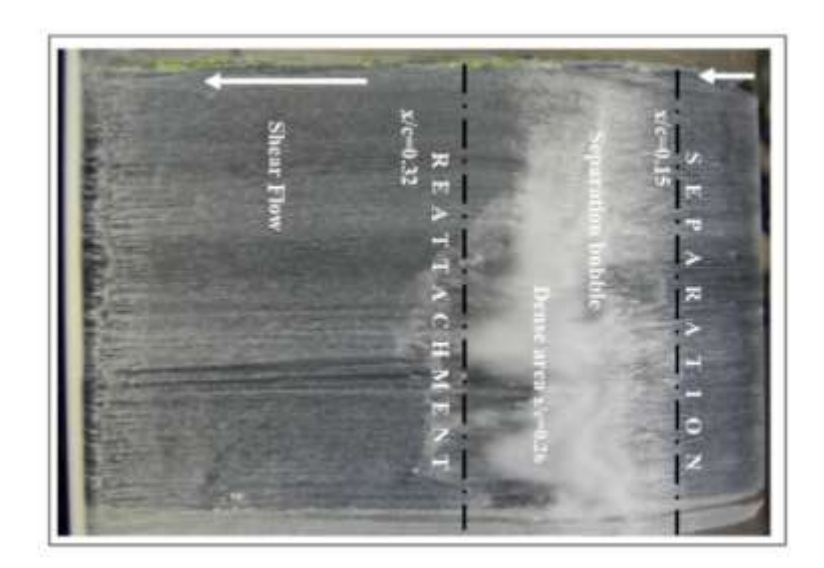


Figure 1. Oil flow visualization over the NACA 2415 airfoil at AoA =  $8^{\circ}$  [5, 6]

#### 2 Numerical Model

ANSYS Workbench software was utilized for numerical modelling in this study. Geometry was created by using Spaceclaim software. The dimensions of domain were set as multiples of the chord length accepted in the literature [7-9]. Domain, flow direction, boundary conditions and dimensions were ensured as illustrated in Figure 2.

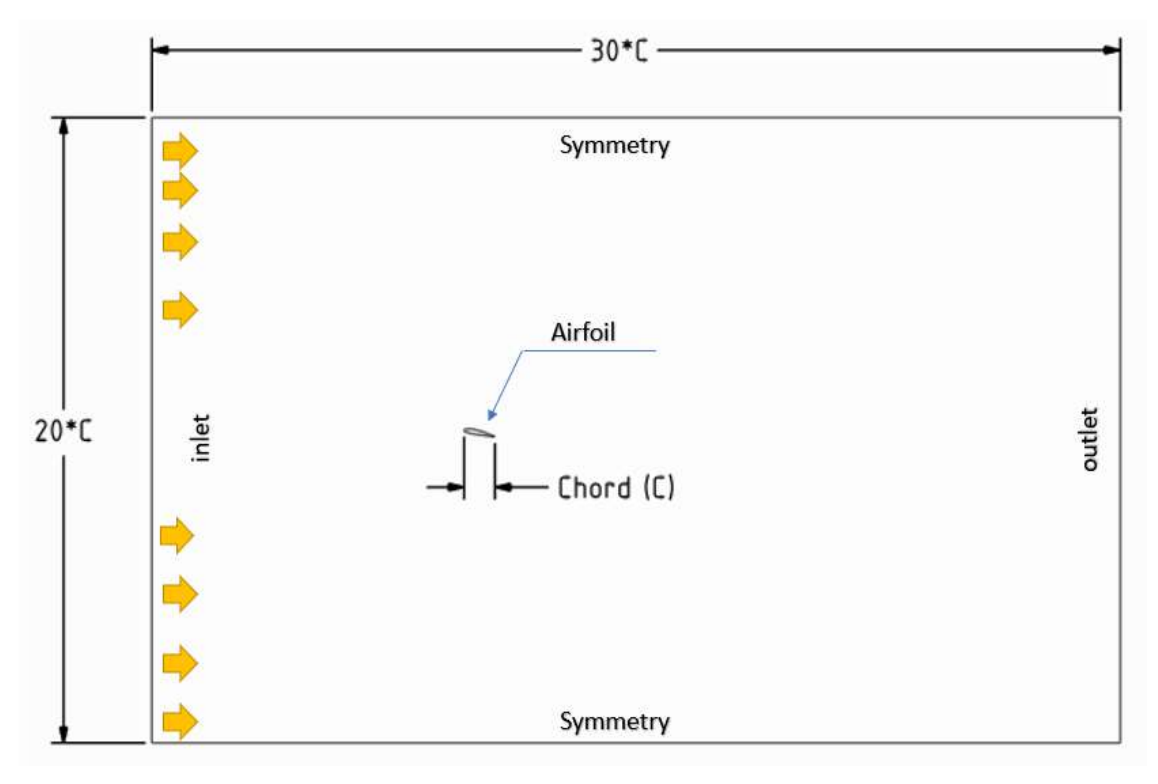


Figure 2. Flow domain and boundary conditions

One of the most important parameters in the sensitivity and accuracy of the numerical analysis is mesh structure. The boundary layer mesh is also crucial in resolving the flow on examined model. On the airfoil, the boundary layer mesh with 20 layers was created. Mesh structures were given in Figure 3.

on Innovative Surveys in Positive Sciences 4-5 December 2022 / Full Text Book

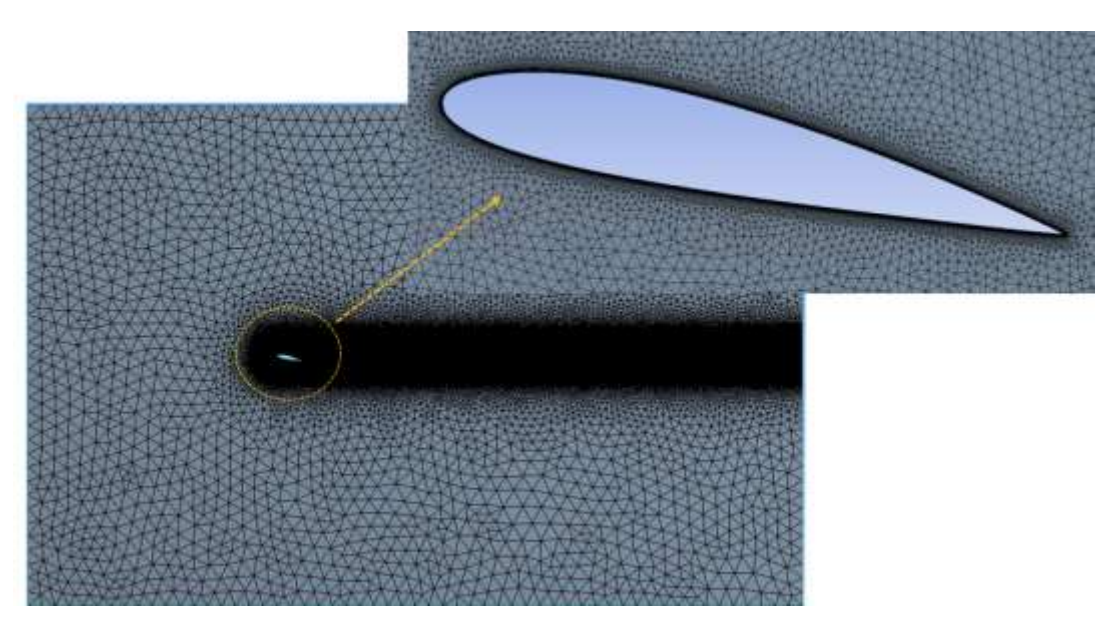


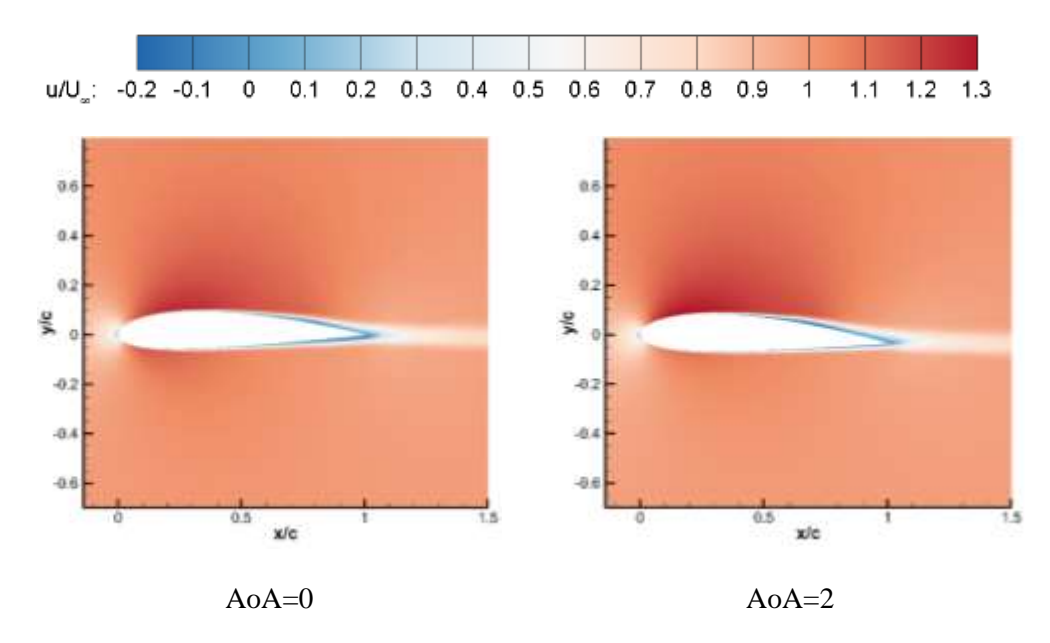
Figure 3. Mesh structure of domain and boundary mesh

#### 3 Numerical Results and Experimental Dataset

The subject of this study is simulated the flow behavior formed on NACA2415 airfoil. The results obtained from the numerical studies was presented in this section. Experimental data were taken from studies in the literature [1].

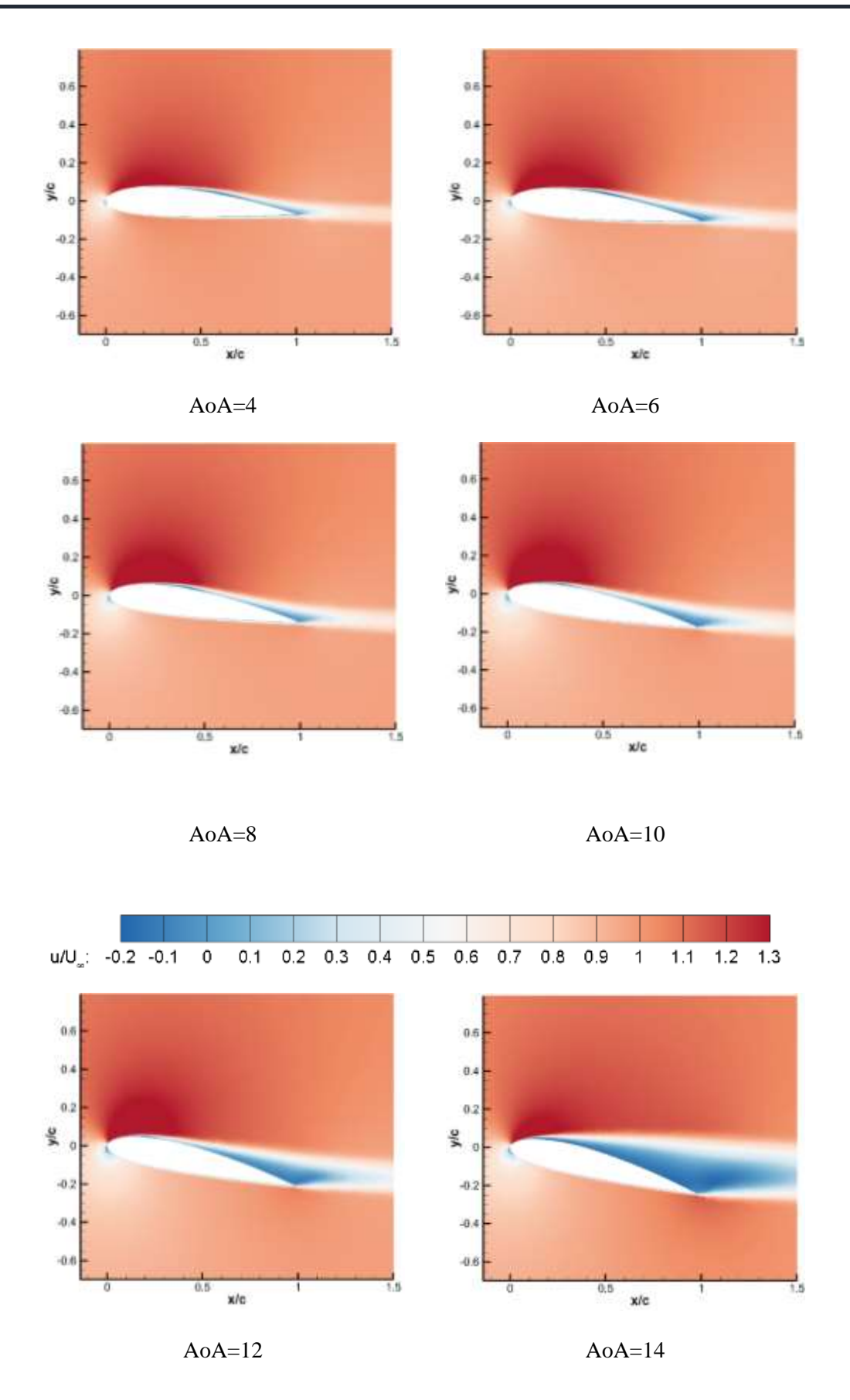
#### 3.1 Numerical results

Force coefficient as well as velocity contours at different angles of attack were provided at the end of numerical simulation. The velocity contours were divided by freestream velocity and  $u_x/U_\infty$  was obtained. As denoted in Figure 4, the velocity shown in red color indicate the maximum, while the blue color indicates minimum speed. The negative values shown at the minimum speed represent speed's direction. As clearly pointed out from the Figure, the separated shear layer was thinner at the lower angles of attacks. As expected, shear layer was much bigger when angle of attack increased and the effects of APGs played the dominant role in the boundary layer. Additionally, massive separation occurred lower angle of attack, resulting in existing the wider wake region at the airfoil. This led the drag force to be higher than those occurred at lower angle of attack.



on Innovative Surveys in Positive Sciences

4-5 December 2022 / Full Text Book



on Innovative Surveys in Positive Sciences 4-5 December 2022 / Full Text Book

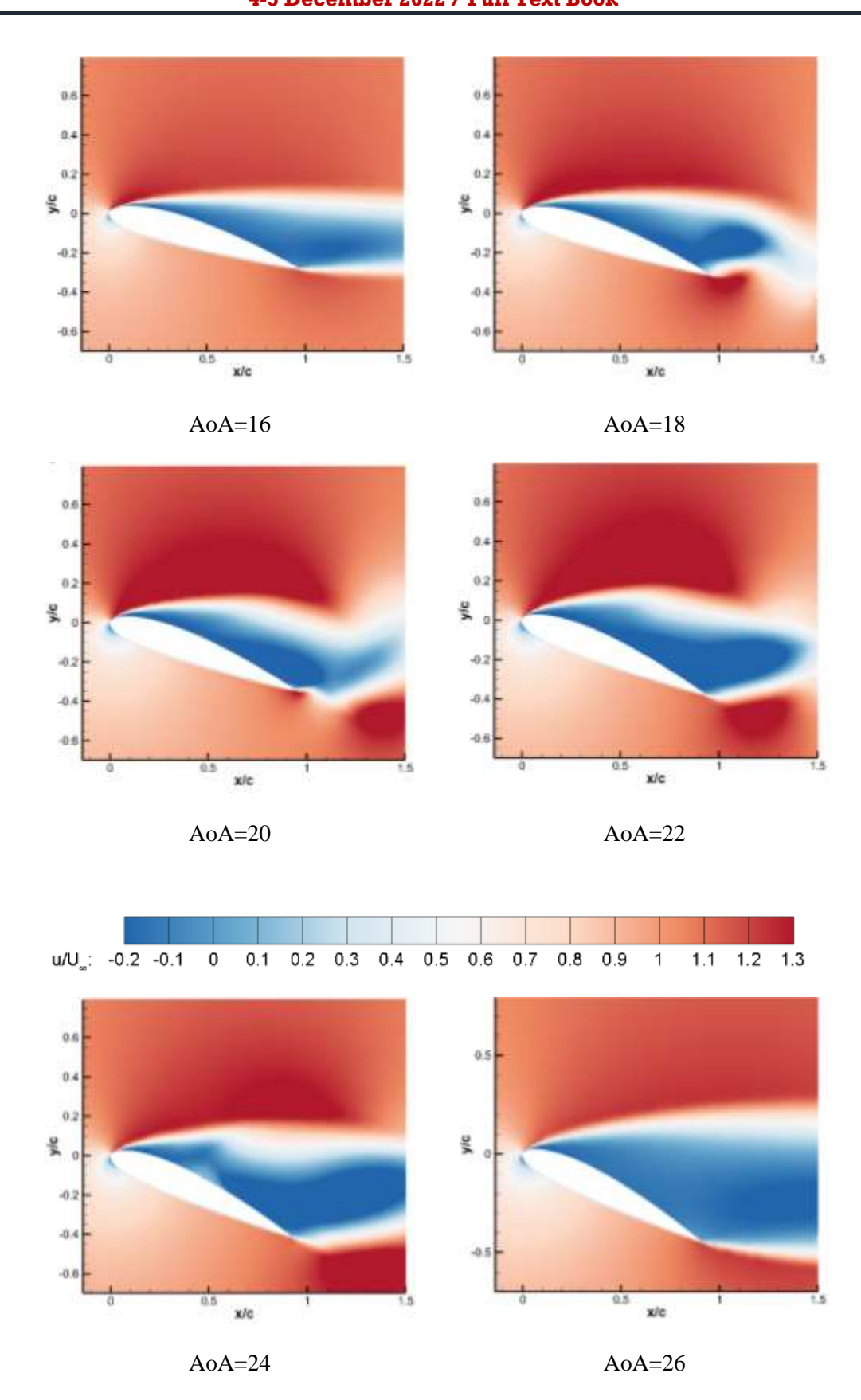


Figure 4. Results of velocity contour on NACA 2415 Airfoil

on Innovative Surveys in Positive Sciences 4-5 December 2022 / Full Text Book

#### 3.2. Comparisons between numerical results and experimental dataset

#### 3.2.1. Aerodynamics force coefficients

In the study where experimental data were obtained (in Figure 5), researchers carried out experiments in the wind tunnel. In spite of some discrepancy of the curves obtained from numerical and experimental investigations, the stall angle and graph trends are relatively similar. The stall angle was 12°. While the maximum lift coefficient in experimental data was 1.1, the maximum lift coefficient in the numerical research was 0.95. It was clearly indicated that abrupt stall occurred in the experimental investigation, whereas the mild stall existed in the numerical simulation. In the numerical and experimental studies, the drag force coefficient is close at low angles of attack, but the disparity between the number grows as the angle of attack increases.

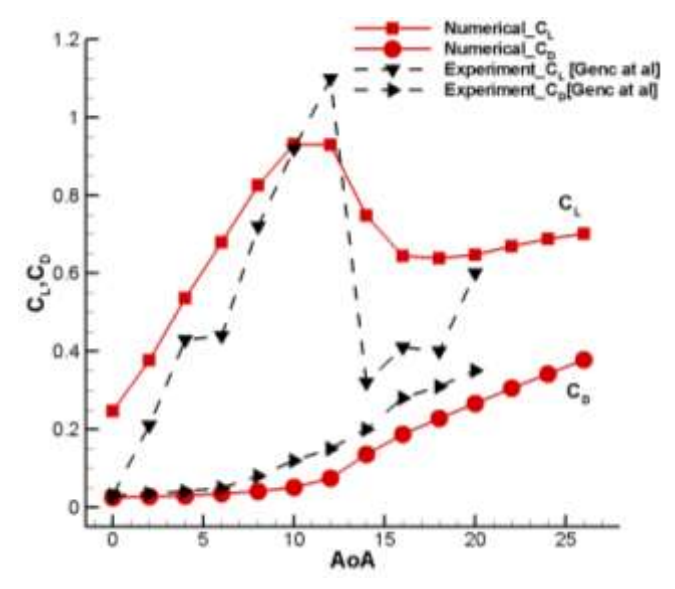


Figure 5. Force coefficient with experimental data

# **4 Conclusion**

In this study, the flow over NACA2415 airfoil investigated numerically and the numerical results compared experimental data. The mesh grid of numerical model was constructed by ANSYS Mechanical Modules. Fluid analyzes were performed with ANSYS Fluent. Force coefficients and velocity contour were obtained from analysis. The numerical results of this study were compared with experimental studies of Genç et al. The velocity results showed that the flow is relatively steady at lower angles of attack and shear layer is therefore thinner. However, it was clearly seen that massive flow separation occurred when angle of attack increased, resulting in presence of chaotic region in the massive separation. Moreover, this flow separation caused the wake region to be wider than those lower angle of attack. Hence, drag forces played dominant role at higher angles of attack. Additionally, force coefficients obtained from both numerical simulation and experimental investigation agreed well coherence between each other.

# Acknowledgments

The authors would like to acknowledge funding from the Scientific Research Projects Unit of Erciyes University under the contract no: FDS-2022-11532.

### References

- 1. Genç, M. S., Karasu, İ., & Açıkel, H. H. (2012). An experimental study on aerodynamics of NACA2415 aerofoil at low Re numbers. *Experimental Thermal and Fluid Science*, *39*, 252-264.
- 2. Shaha, S. N., & Pachapuri, M. S. A. (2015). NACA 2415-Finding Lift Coefficient Using CFD, Theoretical and Javafoil. *International Journal of Research in Engineering and Technology04*, 7, 444-49

on Innovative Surveys in Positive Sciences 4-5 December 2022 / Full Text Book

- 3. Radhakrishnan, P. M., & Dheepthi, M. (2019). CFD Analysis of NACA 2415 and 23012 Airfoil. *International Journal of Research in Aeronautical and Mechanical Engineering*, 7, 11-17.
- 4. Genç, M. S., Kaynak, Ü., & Yapici, H. (2011). Performance of transition model for predicting low Re aerofoil flows without/with single and simultaneous blowing and suction. European Journal of Mechanics-B/Fluids, 30(2), 218-235.
- 5. M.S. Genç, Ü. Kaynak, G. Lock, Flow over an aerofoil without and with leadingedge slat at a transitional Reynolds number, Proc. Inst. Mech. Eng. G 223 (G3) (2009) 217–231.
- 6. M.S. Genç, 2009, Control of Low Reynolds Number Flow over Aerofoils and Investigation of Aerodynamic Performance (in Turkish), PhD Thesis, Graduate School of Natural and Applied Sciences, Erciyes University, Kayseri, TURKEY.
- 7. Jain, R., Jain, M. S., & Bajpai, M. L. (2016). Investigation on 3-D Wing of commercial Aeroplane with Aerofoil NACA 2415 Using CFD Fluent. *IRJET*, *3*(6), 243-249.
- 8. Rahman, M. W. U., Rashid, F., Jahangir, S. B., & Anam, I. (2020, August). Design and Fabrication of a Turbine having NACA 2415 Blades and Feasibility Study of its Application in Cooling Tower. In *IOP Conference Series: Materials Science and Engineering* (Vol. 912, No. 4, p. 042034). IOP Publishing.
- 9. Islam, N., Islam, M. M., & Mashud, M. Experimental Study on NACA 2415 Airfoil with Rotating Cylinder at Leading Edge.

on Innovative Surveys in Positive Sciences 4-5 December 2022 / Full Text Book

#### TRANSITION MODELLING

# Mustafa Serdar GENÇ<sup>1,2</sup>

<sup>1</sup> Energy Systems Engineering", Erciyes University ,38039, Kayseri, Turkey

<sup>2</sup> "Wind Engineering ve Aerodynamic Research Group", Erciyes University, 38039, Kayseri, Turkey

#### **ABSTRACT**

Low Re number flows involving stochastic and three-dimensional unstable processes and the transition to turbulence is still not fully understood. Measuring, modeling, and predicting the transition to laminar separation bubbles and turbulence are still challenging tasks. In addition, there is a knowledge gap in determining turbulence and transition to turbulence in fluid mechanics, these are defined as the most important unsolved problems in classical physics. To address this shortcoming in predicting the separated flow transition, studies on turbulent transition models have been conducted in the last 20 years and a modification has been made to the well-known k-w SST turbulence model by Langtry and Menter (2005). The turbulent kinetic energy (k) was allowed to grow rapidly when the laminar boundary layer was separated. The main idea behind the split-induced transition fix is; is to allow the local intermittency (y - intermittency) to exceed 1 when the laminar boundary layer separates. The size of the laminar separation bubble can be controlled by one or more constants. A mixing function change is disabled when the viscosity ratio is large enough to cause re-adhesion. Such a transition model, also used in commercial computational fluid dynamics (CFD) software, is considered an experimental transition model combined with two-equation shear stress transport (SST) models. It also provides two additional transport equations for the discontinuity (y) and the momentum thickness Re number  $(Re_{\theta})$  to predict the transition flow. In the k-k<sub>L</sub>-w transition model, which is another turbulent transition model developed by Walters and Stork (2002), a three-equation turbulent viscosity model is solved for the transition flow simulation. It includes the terms of the turbulent kinetic energy per unit mass, k, and the laminar kinetic energy per unit mass, k<sub>L</sub>, and the specific dispersion ratio (ω) terms. Although these differential equations include turbulent generation, bypass transition, natural transition, near-wall damping terms, viscous damping function, intermittent damping function, wall turbulence length scale, turbulent viscosity coefficient, the necessary terms or functions for separated transition and laminar separation bubble do not include. This deficiency should be brought to both the literature and CFD models as a result of the correlations to be obtained with new studies.

**Keywords:** Transition, boundary layer, CFD

# 1. Introduction

The amount of experimental work needed to produce data is extremely significant. The complexity of the flow makes the simulation difficult in order to obtain finer measurements for sensitive and smaller-scale flows. Experimental tests in such circumstances for a variety of parameters will inevitably be expensive. As a result, numerical studies using a variety of CFD techniques, such as Reynolds Averaged Navier-Stokes (RANS), Direct Numerical, and/or Large Eddy Simulation (DNS/LES) methods, emerge as effective substitutes for experimentation. In terms of the higher-order theoretical approaches, You and Moin [1] carried out a large-eddy simulation (LES) of turbulent flow separation over a NACA0015 aerofoil at Re= 896,000 and looked at the efficacy of artificial jets. The large-eddy simulation for this flow showed that synthetic-jet actuation might successfully postpone the beginning of flow separation and result in a significant boost in the lift coefficient. Utilizing vortex generators, pulsed jets, and blown jets, Shan et al. [2,3] and Deng et al. [4] studied the flow separation and control of the separation over a NACA0012 aerofoil. Segawa et al. [5] investigated the performance of a jet actuator array that alternated between suction and blowing for a range of Reynolds numbers between 3.8×10<sup>5</sup> to 5.7×10<sup>5</sup>. Roberts and Yaras [6] considered LES modelling in the transition process over a flat plate under low freestream turbulence conditions.

on Innovative Surveys in Positive Sciences 4-5 December 2022 / Full Text Book

For design purposes, the RANS-based approaches are the most effective of all numerical techniques because DNS/LES calculation costs are very expensive. Today, transitional and turbulent flows are able to simulate using RANS-based CFD techniques because of high-performance computing capabilities. Modern RANS solvers usually contain useful one- or two-equation turbulence closure models [7] for computations involving totally turbulent flows. The e<sup>N</sup> technique [8-9], two-equation low Re–number turbulence models [10], and certain early [11] and contemporary [12-13] methods based on experimental correlations have all advanced transition predictions concurrently.

The e<sup>N</sup> technique has been applied extremely well and is now essentially the industry standard [8]. Due to their use of integral (or global) boundary layer parameters, the so-called correlation-based models [13–15] have developed into useful tools for industry. In order to avoid certain difficult steps in the early methods, transport equation models [14-17] that rely on (local) information have recently been presented. In addition to the fundamental turbulence models, these transport equation models also solve a number of "transport" partial differential equations for different transition quantities. Several commercial CFD codes have made some of these models available [14, 16]. Various authors have also evaluated transport equation models, including through the application of various user-dependent transition correlations.

Performance evaluations of transition-sensitive, single-point eddy viscosity models are necessary because they are still relatively new. This study's goal is to inform how well transition and turbulence models are in RANS-based CFD.

#### 2. Numerical Modelling

To simulate the low Reynolds number flow, a variety of different RANS-based turbulence or transition models are employed. Among the models, it is demonstrated that the recently created k-k<sub>L</sub>-w transition model accurately predicts the location and size of the separation bubble found through experiment [17-22]. To mimic the single or simultaneous blowing and suction effect, single and multiple jets were positioned on the airfoil's upper surface [20].

### 3.2 Turbulence models

The computational fluid dynamics (CFD) codes include a number of two-equation eddy-viscosity type turbulent transport models. k-w model and the k- $\square$  turbulence model are utilized as the baseline models. For simulation of low Reynolds number flow, k- $\square$  turbulence model may be selected. The k- $\square$  RNG theory offers an effective viscosity that compensates for low Reynolds number effects, whereas the traditional k- $\square$  model is a high Reynolds number model. The k-w SST model may be used to simulate low Reynolds number flow, and this is a hybrid type and the k-w model (in the near-wall region) and the standard k- $\square$  model (in the far-field region) are blended together in this model, which is essentially a turbulence model that couples the standard and Wilcox k-w models with low Reynolds number effects. The model also incorporates the modeling of shear stress transport (SST) through a modified definition of turbulent viscosity.

#### 3.3. Transition models

Current RANS-based solvers have benefited from the incorporation of some benchmark experimental data that were expressed in terms of global boundary layer parameters thanks to the recent introduction of the so-called "transport equation models," which are essentially newer variants of the early correlation models. Suzen and Huang's intermittency transport equation models [12–13] and the correlation-based k- $\omega$  SST transition model of Menter et al. [14-15] are two examples of these models. The k-k<sub>L</sub>-w transition model of Walters and Leylek [16], which effectively does away with the necessity for intermittency, and a version of the SST model known as the k- $\omega$ - $\gamma$  model of Fu and Wang [17] are examples of true single-point RANS techniques that have been developed more recently. As they solve extra transport equations for forecasting transition events that rely just on local information, as opposed to the global information employed in the early approaches, these models are suited for simple implementation within RANS methods.

The transition onset momentum thickness Reynolds number ( $Re_{\theta t}$  - equation), which is compelled to follow experimentally known correlations with some lag, and an intermittency equation ( $\gamma$  - equation),

on Innovative Surveys in Positive Sciences

4-5 December 2022 / Full Text Book

which is utilized to initiate the transition process, form the foundation of the k-w SST transition model. By linking the transition model with the k-w SST turbulence model, the Shear Stress Transport (SST) component of this model is connected to the transition model [15]. User-dependent data from benchmark tests conducted at several laboratories are transition correlations.

$$\begin{split} \frac{\partial(\rho Re_{\theta t})}{\partial t} + \frac{\partial(\rho U_j Re_{\theta t})}{\partial x_j} &= P_{\theta t} + \frac{\partial}{\partial x_j} \left[ \sigma_{\theta t} (\mu + \mu_t) \frac{\partial Re_{\theta t}}{\partial x_j} \right] \\ P_{\theta t} &= c_{\theta t} \frac{\rho}{t} (\text{Re}_{\theta t} - \tilde{R}e_{\theta t}) (1 - F_{\theta t}) \\ F_{\theta t} &= \min \left( maks \left( F_{wake} e^{-\left(\frac{y}{\delta}\right)^4}, 1.0 - \left(\frac{\gamma - 1/c_{e2}}{1 - 1/c_{e2}}\right)^2 \right), 1.0 \right) \\ \theta_{BL} &= \frac{\tilde{R}e_{\theta t}\mu}{\rho U} \quad \delta_{BL} = \frac{15}{2} \theta_{BL} \quad \delta = \frac{50\Omega y}{U} \delta_{BL} \quad t = \frac{500\mu}{\rho U^2} \\ F_{wake} &= e^{-\left(\frac{Re_{\omega}}{1E + \delta}\right)^2} \quad \text{Re}_{\omega} = \frac{\rho \omega y^2}{\mu} \\ \frac{\partial(\rho \gamma)}{\partial t} + \frac{\partial(\rho U_j \gamma)}{\partial x_j} &= P_{\gamma 1} - E_{\gamma 1} + P_{\gamma 2} - E_{\gamma 2} + \frac{\partial}{\partial x_j} \left[ \left(\mu + \frac{\mu_t}{\sigma_{\gamma}}\right) \frac{\partial \gamma}{\partial x_j} \right] \\ P_{\gamma 1} &= F_{length} c_{a1} \rho S \left[ \gamma F_{onset} \right]^{c_{\alpha}} \\ E_{\gamma 1} &= c_{a2} \rho \Omega \gamma F_{turb} \\ E_{\gamma 1} &= c_{e2} P_{\gamma 2} \gamma \end{split}$$

The k-k<sub>L</sub>-w model [16], which comprises transport equations for turbulent kinetic energy (k), laminar kinetic energy (k<sub>L</sub>), and specific dissipation rate (w), is thought to be a three-equation eddy-viscosity type. But, the k<sub>L</sub> is more like a pre-transitional kinetic energy, and it was named as pre-transitional kinetic energy term by Genc et al [20]. The advantages of the earlier correlation methods are combined with this model, which is essentially a single-point strategy, and intermittency is no longer necessary. This model makes the assumption that the turbulent energy in the vicinity of the wall is divided into two types: small-scale turbulent energy, which directly contributes to the production of turbulence, and large-scale turbulent energy, which contributes to the production of laminar kinetic energy via the splat mechanism [16]. According to Walters and Leylek [16], the transition begins when the laminar streamwise fluctuations are transported a predetermined distance from the wall, where the predetermined distance is based on the free stream's energy content and kinematic viscosity.

$$\begin{split} \frac{Dk_T}{D_t} &= P_{K_T} + R + R_{NAT} - \omega k_T - D_T + \frac{\partial}{\partial x_j} \left[ \left( \nu + \frac{\alpha_T}{\alpha_k} \right) \frac{\partial k_T}{\partial x_j} \right] \\ & \frac{Dk_L}{D_t} = P_{K_L} + R + R_{NAT} - D_L + \frac{\partial}{\partial x_j} \left[ \nu \frac{\partial k_L}{\partial x_j} \right] \\ & \frac{D_\omega}{D_t} = C_{\omega 1} \frac{\omega}{k_T} P_{k_T} + \left( \frac{C_{\omega R}}{f_W} - 1 \right) \frac{\omega}{k_T} \left( R + R_{NAT} \right) - C_{\omega 2} \omega^2 \\ & + C_{\omega 3} f_\omega \alpha_T f_W^2 \frac{\sqrt{k_T}}{d^3} + \frac{\partial}{\partial x_j} \left[ \left( \nu + \frac{\alpha_T}{\alpha_\omega} \right) \frac{\partial \omega}{\partial x_j} \right] \end{split}$$

on Innovative Surveys in Positive Sciences 4-5 December 2022 / Full Text Book

Since the broad framework of these studies has been published without providing a thorough explanation of the fundamental mathematical expressions, scholars have worked on the building or alternatives of these correlations [23–27]. The full specifications of the initial  $\gamma$ -Re<sub> $\theta$ </sub> model, including all correlations, were made public at the end of 2009 [28]. In numerous industrial applications, including aerodynamics, turbomachinery, and wind turbine flows, this model is frequently utilized. The  $\gamma$ -Re $_{\theta}$  model was modified and attempts were made to decrease the auxiliary equations in the investigations that followed. By adding a parameter that is akin to the shape function, Coder and Maughmer [29] have simplified their work so that they can take into account the effect of the pressure gradient locally within the boundary layer. This approach does not automatically account for the effect of turbulence density, which limits the applicability of the models to aerodynamic external flows with known and essentially constant free-flow turbulence levels. The disadvantage of this approach is that the shape parameter, like the original  $\gamma$ -Re $_{\theta}$  model, uses local velocity with respect to the wall and is therefore not Galilean invariant. The same parameter was most recently utilized by the same authors in the creation of a transition model [29], which roughly tracks the expansion of Tollmien-Schlichting waves in a setting based on local transport equations. Dassler et al. [30] conducted another test of the  $\gamma$ -Re $_{\theta}$  model by including the effects of wall roughness. These experiments show the flexibility of the model to include almost any transitional effects for which relations can be defined.

Durbin [31] and Ge et al [32] have recently presented another intriguing transition model based on a single discreteness transport equation employing only local variables. The fundamental structure of this model is comparable to that of the original model and is for bypass transition, which they observed can be modeled using diffusion processes for the amounts of turbulence and the discontinuity equations. It does not take into account low levels of free-flow turbulence. This model produced accurate predictions for a wide number of skip turbulent transition instances for penetration into the boundary layer. Although an empirical calibration input for a laminar boundary layer upstream of the turbulent transition is included in the model, external data correlations are not.

Using the diffusion process alone is inappropriate for predicting migration in separated boundary layers and through natural migration and cross-flow instabilities [33]. The transition length is taken into account by a special relation called  $F_{length}$  in the original  $\gamma$ -Re $_{\theta}$  model; however, in the one-equation model recently developed by Menter et al. [33], the transition length correlation has been removed for simplicity, and  $F_{length}$  is now a constant instead of a correlation. Similar to the -Re model, the model is entirely dependent on local variables and maintains the key characteristics of formulations based on local expressions, which combine traditional transport equations with empirical expressions (correlations). For aerodynamic exterior flows with minimal turbulence and appropriate pressure gradients, for which no test cases have yet been estimated with the new model, the transition model needs to be altered and fine-tuned [33].

# 4. Conclusion

The evaluation of transition patterns available in commercial CFD software is being studied by different researchers. Evaluation studies have shown that newly developed transition models are more successful than turbulence models in predicting low Re number flows, but they do not yet have sufficient accuracy and experimental data are required for new equations, and some researchers have suggested that the laminar separation bubble is more accurate than the original k-kL-w transition model. Modifications of different model coefficients have been proposed to predict. Existing transition models converge with models based on the transport equation, which take longer to solve, but show a stronger sensitivity to network resolution downstream than transport models. However, this estimation is still not fully accurate, and empirical experimental data are still needed to model turbulent transition flows, and separation-induced transition.

#### References

- [1] You D., Moin P., 2008, "Active control of flow separation over an aerofoil using synthetic jets", J Fluid Struct, Vol. 24, pp.1349-1357.
- [2] Shan H, Jiang L. and Liu C., 2005, "Direct Numerical Simulation of Flow Separation around a NACA 0012 Aerofoil", Comput Fluids, Vol. 34, pp.1096-114.

on Innovative Surveys in Positive Sciences 4-5 December 2022 / Full Text Book

- [3] Shan H., Jiang L., Liu C., Love M. and Maines B., 2008, "Numerical Study of Passive and Active Flow Separation Control over a NACA0012 Aerofoil", Comput Fluids, Vol. 37, pp. 975-992.
- [4] Deng S., Jiang L. and Liu C., 2007, "DNS for Flow Separation Control around an Aerofoil by Pulsed Jets", Comput Fluids, Vol. 36, pp. 1040-1060.
- [5] Segawa T., Mizunuma H., Murakami K., Li F.C. and Yoshida H., 2007, "Turbulent Drag Reduction by means of Alternating Suction and Blowing Jets", Fluid Dyn Res, Vol. 39, pp. 552-568.
- [6] Roberts S.K. and Yaras M.I., 2006, "Large-Eddy Simulation of Transition in a Separation Bubble", J Fluid Eng T ASME, Vol. 128, pp. 232-238.
- [7] Wilcox, D.C., 1998, *Turbulence Modeling for CFD*, 2nd ed, DCW Industries Inc., La Canada, California.
- [8] Cebeci, T., Mosinskis, G.J. and Smith A.M.O. 1972, "Calculation of Separation Points in Incompressible Turbulent Flows", J Aircraft, Vol. 9, pp. 618-624.
- [9] Drela, M. and Giles, M.B., 1987, "Viscous-inviscid Analysis of Transonic and Low Reynolds Number Aerofoils" AIAA J, Vol. 25, pp. 1347-1355.
- [10] Wilcox, D.C., 1994, "Simulation of Transition with a Two-equation Turbulence Model" AIAA J, Vol. 32, pp. 247-255.
- [11] Abu-Ghannam, B.J. and Shaw, R., 1980, "Natural Transition of Boundary Layers-The Effect of Turbulence, Pressure Gradient and Flow History" J Mech Eng Sci, Vol. 22, pp. 213-228.
- [12] Suzen, Y. B. and Huang, P.G., 2000, "Modeling of Flow Transition using an Intermittency Transport Equation" J Fluid Eng T ASME, Vol. 122, pp. 273-284.
- [13] Suzen, Y. B. and Huang, P.G., 2003, "Predictions of Separated and Transitional Boundary Layers under Low-Pressure Turbine Aerofoil Conditions using an Intermittency Transport Equation" J Turbomach, Vol. 125, pp. 455-464.
- [14] Menter, F.R., Langtry, R.B., Likki, S.R., Suzen, Y.B., Huang, P.G. and Völker, S., 2004, "A Correlation Based Transition Model Using Local Variables: Part I-Model Formulation", Proceedings of ASME Turbo Expo 2004, Vienna, Austria, ASME-GT2004-53452, pp. 57-67.
- [15] Langtry, R.B. and Menter, F.R., 2005, "Transition Modeling for General CFD Applications in Aeronautics", AIAA Paper 2005-0522.
- [16] Walters D.K. and Leylek, J. H., 2004, "A New Model for Boundary Layer Transition Using a Single-Point RANS Approach", J Turbomach, Vol. 126, pp. 193-202.
- [17] Fu S. and Wang L., 2008, "Modelling the Flow Transition in Supersonic Boundary Layer with a New k-ω-γ Transition/Turbulence Model", 7th International Symposium on Engineering Turbulence Modelling and Measurements-ETMM7, Limassol, Cyprus, 4-6 June.
- [18] Genç M.S., Kaynak U., Gary D. Lock, Flow over an Aerofoil without and with Leading Edge Slat at a Transitional Reynolds Number, Proc IMechE, Part G- Journal of Aerospace Engineering, vol. 223(G3) 217-231, 2009.
- [19] Genç M.S., Numerical Simulation of Flow over an Thin Aerofoil at High Reynolds Number using a Transition Model, Proc IMechE, Part C- Journal of Mechanical Engineering Science, Vol 224 (10), pp. 2155 2164, 2010.
- [20] Genç M.S., Kaynak U., Yapici H., Performance of Transition Model for Predicting Low Re Aerofoil Flows without/with Single and Simultaneous Blowing and Suction, European Journal of Mechanics B/Fluids, vol 30 (2), pp. 218-235, 2011.
- [21] Karasu İ., Genç M.S., Açıkel H.H., Numerical Study on Low Reynolds Number Flows over an aerofoil, Journal of Applied Mechanical Engineering, 2:131, 2013.

on Innovative Surveys in Positive Sciences 4-5 December 2022 / Full Text Book

- [22] Karasu İ., Özden M., Genç M.S., Performance Assessment of Transition Models for 3D flow over NACA4412 wings at low Reynolds numbers, Journal of Fluids Engineering-Transactions of The ASME, vol.140 (12), pp.121102-1-121102-15, 2018.
- [23] Content, C., Houdeville, R. (2010) Application of the  $\gamma$ -Re $\theta$  Laminar-Turbulent Transition Model in Navier-Stokes Computations AIAA Paper 2010-4445
- [24] Suluksna, K., Juntasaro, V., Juntasaro, E.: Capability Assessment of Intermittency Transport Equations for Modeling Flow Transition. In: Proc. 19 Conference of Mechanical Engineering Network of Thailand, Phuket, Thailand (2005)
- [25] Malan, P., Suluksna, K., Juntasaro, E.: Calibrating the  $\gamma$  Re $\theta$  Transition Model for Commercial CFD. AIAA Paper 2009-1142 (2009)
- [26] Misaka, T., Obayashi, S. Application of local correlation-based transition model to flows around wings. 44th AIAA Aerospace Sciences Meeting and Exhibit. 2006.
- [27] Piotrowski, W., Elsner, W., Drobniak, S.: Transition Prediction on Turbine Blade Profile with Intermittency Transport Equation. ASME J. of Turbomach 132(1) (2009)
- [28] Langtry, R.B., Menter, F.R.: Correlation-Based Transition Modeling for Unstructured Parallelized Computational Fluid Dynamics Codes. AIAA J. 47(12), 2984-2906 (2009)
- [29] Coder, J.M., Maughmer M. D. (2014) Computational Fluid Dynamics Compatible Transition Modelling using an Amplification Factor Transport Equation. AIAA J. doi:10.2514/1.J052905.
- [30] Dassler, P., Kozulovic, D., Fiala, (2012) A Transport Equation for Roughness Effects on Laminar-Turbulent Transition. Proc. Conference on Modelling Fluid Flow CMFF 2012, Budapest, Hungary.
- [31] Durbin, P.A. (2012) An intermittency model for bypass transition. Int. J. Heat Fluid Flow 36, pp. 1–6.
- [32] Ge, X., Arolla, S., Durbin, P. (2014) A Bypass Transition Model Based on the Intermittency Function. Flow Turbulence and Combustion, 93, pp. 37–61.
- [33] Menter F., Smirnov P.E., Liu T., Avancha R., (2015) A One-Equation Local Correlation-Based Transition Model, Flow Turbulence Combust, 95, pp. 583–619.